Universidad de Las Palmas de Gran Canaria

Año 1999

# Coleccion de Separatas

N.P.

BIBLIOTECA UNIVERSITARIA
LAS PALMAS DE G. CANARIA
N.º Documento 219535
N.º Copia 622968

BIBLIOTECA GENERAL

Facultad de Ciencias del Mar
Biblioteca de Ciencias Básicas

© Del documento, los autores. Digitalización realizada por ULPGC. Biblioteca Universitaria, 2009

Depósito Legal: G.C. 912-2000
ISBN 84-699-2551-2
Imprime: Servicio de Reprografía de la U.L.P.G.C.
http://www.ccbb.ulpgc.es/ccmar

© Del documento, los autores. Digitalización realizada por ULPGC. Biblioteca Universitaria, 2009

# INDICE

Almunia, J.; Basterretxea, G.; Arístegui, J.; Ulanowicz, R. E. : Benthic-pelagic switching in a coastal subtropical lagoon. **Estuarine, Coastal and Shelf Science**, 1999, vol.49, p. 363-384

Barry, A. R.y Luque, A. : Ecology and distribution of the genus "Tamarix" L. (Tamaricales: Tamaricaceae) on the island of Gran Canaria. **Boletim do Museu Municipal do Funchal,** 1998, sup.no. 5, p. 47-58

Basterretxea, Gotzon y Arístegui, Javier. : Phytoplankton biomass and production during late austral spring (1991) and summer (1993) in the Bransfield strait. **Polar Biology,** 1999, vol. 21, p. 11-22

Bessonart, M; Izquierdo, M. S.; Salhi, M.; Hernández Cruz, C. M.; González, M. M., Fernández Palacios, H. : Effect of dietary arachidonic acid levels on growth and survival of gilthead sea bream ( "Sparus aurata" L.) larvae. **Aquaculture,** 1999, vol. 179, p. 265-275

Both, R. A.; Palero, F. J.; Arribas, A.; Boyce, A. y Mangas, J. : Metallogenesis of lead-zinc deposits of the Alcudia Valley, Spain. **Mineral deposits: processes to processing**, Stanley et al. , 1999, p. 817-820

Caballero, Catalina y Castro, José J. : Effect of residence and size asymmetries upon the agonistic interactions between juvenile white-seabream ("Diplodus sargus cadenati" de la Paz, Bauchot and Daget, 1974). **Agressive behaviour**, 1999, vol. 25, p. 297-303

Carracedo, Juan Carlos; Day, Simon J.; Guillou, Hervé and Pérez Torrado, Francisco J. : Giant quaternary landslides in the evolution of La Palma and El Hierro, Canary Islands. **Journal of Volcanology and Geothermal Research**, 1999, vol. 94, p. 169-190

Castro, J. J.; Santiago, J. A.; Hernández García, V. y Pla, C. : Growth and reproduction of the dolphinfish ("Coryphaena equiselis" and "Coryphaena hippurus") in the Canary Islands, Central-East Atlantic (preliminary results). **Scientia Marina**, 1999, vol. 63, no. 3-4, p. 317-325

Castro, J. J.; Santiago, J. A. y Hernández García, V. : Fish associated with fish aggregation devices off the Canary Islands (Central-East Atlantic). **Scientia Marina**, 1999, vol.63, no. 3-4, p. 191-198

© Del documento, los autores. Digitalización realizada por ULPGC. Biblioteca Universitaria, 2009

Davenport, R.; Neuer, S.; Hernández Guerra, A.; Rueda, M. J.; Llinas, O.; Fischer, G. and Wefer, G. : Seasonal and interannual pigment concentration in the Canary Islands region from CZCS data and comparison with observations from the ESTOC. **International Journal of Remote Sensing,** 1999, vol. 20, no. 7, p. 1419-1433 191379

Eiguren Fernández, A. ; Sosa Ferrera, Z. ; Santana Rodríguez, J. J. : Application of cloud-point methodology to the determination of polychlorinated dibenzofurans in sea water by high-~~performace~~ performance liquid chromatography. **The Analyst,** 1999, vol. 124, p. 487-491 203608

García Jiménez, P.; Marian, F. D.; Rodrigo, M. and Robaina, R. R. : Sporulation and sterilization method for axenic culture of "Gelidium canariensis". **Journal of Biotechnology**, 1999,vol. 70, p. 227-229 190972

Hernández Cruz, C. M.; Salhi, M.; Bessonart, M.; Izquierdo, M. S.; González, M. M. y Fernández Palacios, H. : Rearing techniques for red porgy ("Pagrus pagrus") during larval development. **Aquaculture,** 1999, vol. 179, p. 489-497 191425

Hernández León, Santiago; Postel, Lutz; Arístegui, Javier; Gómez, May; Montero, María Fernanda; Torres, Santiago; Almeida, Carlos; Kühner, Eugen; Brenning, Ullrich and Hagen, Eberhard. : Large scale and mesoscale distribution of plankton biomass and metabolic activity in the northeastern central Atlantic. **Journal of Oceanography**, 1999, vol.55, p. 471-482 191414

Hernández León, S.; Torres, S.; Gómez, M. and Montero, I. : Biomass and metabolism of zooplankton in the Bransfield strait (Antartic peninsula) during austral spring. **Polar Biology**, 1999, vol.21, p. 214-219 191389

Ivanova, A. P.; Robaina, R. R.; Martín, J. y Stefanov, K. L. : Effect of glycerol on the lipids in the red alga "Gratelupia doryphora". **Grasas y aceites,** 1999, vol. 50, fasc. 6, p. 469-471 191433

Lorenzo, José M. y Pajuelo, José G. : Biology of a deep benthopelagic fish, roudi escolar "Promethichthys prometheus" (Gempylidae), off the Canary Islands. **Fishery Bulletin**, 1999, vol. 97, p. 92-99 191439

Martínez, Antonio; Pérez, Esther y Bruno, Miguel. : Variation of the tidal properties around Gran Canaria. **Oceanologica Acta**, 1999, vol. 22, no. 1, p.19-30 191447

© Del documento, los autores. Digitalización realizada por ULPGC. Biblioteca Universitaria, 2009

Medina, L.; García Jiménez, P.; Luque, A. y Robaina, R. : The community structure of phytoplankton as indicator of coastal water quality in the tourist area. **Boletim do Museu Municipal do Funchal**, 1998, vol. 50, no. 288, p. 91-106 191454

Mendoza, H.; Martel, A.; Jiménez del Rio, M. y García Reina, G. : Oleic acid is the main fatty acid related with carotenogenesis in "Dunaliella salina". **Journal of Applied Phycology**, 1999, vol. 11, p. 15-19 191457

Montero, D.; Marrero, M.; Izquierdo, M. S.; Robaina, L.; Vergara, J. M. y Tort, L. : Effect of vitamin E and C dietary supplementation on some immune parameters of gilthead seabream ("Sparus aurata") juveniles subjected to crowding stress. **Aquaculture**, 1999, vol. 171, p. 269-278 191794

Montero, D.; Izquierdo, M. S.; Tort, L.; Robaina, L. y Vergara, J. M. : High stocking density produces crowding stress altering some physiological and biochemical parameters in gilthead seabream, "Sparus aurata", juveniles. **Fish Physiology and Biochemistry**, 1999, vol. 20, p. 53-60 191891

Pacheco, M. M. y Hernández Guerra, A. : Seasonal variability of recurrent phytoplankton pigment in the Canary Islands area. **International Journal of Remote Sensing**, 1999, vol. 20, no. 7, p. 1405-1418 191940

Rodríguez J. M.; Hernández León, S. and Barton, E.D. : Mesoscale distribution of fish larvae in relation to an upwelling filament off northwest Africa. **Deep-sea Research I**, 1999, vol.46, p. 1969-1984 191946

Rodríguez Santana, A.; Pelegrí, J. L.; Sangrá, P. y Marrero Díaz, A. : Diapycnal mixing in Gulf Stream meanders. **Journal of Geophysical Research**, 1999, vol. 104, no. C11, p. 25.891-25.912 191951

Roo, F. J.; Socorro, J.; Izquierdo, M. S., Caballero, M. J.; Hernández Cruz, C. M.; Fernández, A. y Fernández Palacios, H. : Development of red porgy "Pagrus pagrus" visual systems in relation with changes in the digestive tract and larval feeding habits. **Aquaculture**, 1999, vol. 179, p. 499-512 191960

Salhi, M.; Hernández Cruz, C. M.; Bessonart, M.; Izquierdo, M. S. y Fernández Palacios, H. : Effect of different dietary polar lipid levels and different n-3 HUFA content in polar lipids on gut and liver histological structure of gilthead seabream ("Sparus aurata") larvae. **Aquaculture**, 1999, vol. 179, p. 253-263 191978

© Del documento, los autores. Digitalización realizada por ULPGC. Biblioteca Universitaria, 2009

Santana Rodríguez, J. J. : Fluorescent study of organic compounds of environmental interest in organized molecular systems. Analytical applications. **Third Conference on Fluorescence Microscopy and Fluorescent Probes**, 1999, p. 179-192 191987

Sosa Henríquez, Pedro. : El acceso a los recursos genéticos en el Convenio sobre Diversidad Biológica. **Medio ambiente Canarias**, 1999, no. 13, p. 21-23 192005

Sosa, Pedro A. y Lindstrom, Sandra C. : Isozymes in macroalgae (seaweeds): genetic differentiation, genetic variability and applications in systematics. **European Journal of Phycology**, 1999, vol. 34, p. 427-442 190759

Urgeles, Roger; Canals, Miquel; Roberts, John and SNV "Las Palmas" Shipboard Party. : Fluid flow pore pressure measurements off La Palma, Canary Islands. **Journal of Volcanology and Geothermal Research**, 1999, vol.94, p. 305-321 192094

Vergara, J. M.; López Calero, G.; Robaina, L.; Caballero, M. J.; Montero, D.; Izquierdo, M. S. y Aksnes, A. : Growth, feed utilization and body lipid content of gilthead seabream ("Sparus aurata") fed increasing lipid levels and fish meals of different quality. **Aquaculture**, 1999, vol.179, p. 35-44 192009

© Del documento, los autores. Digitalización realizada por ULPGC. Biblioteca Universitaria, 2009

*Estuarine, Coastal and Shelf Science* (1999) 49, 363–384
Article No. ecss.1999.0503, available online at http://www.idealibrary.com on IDEAL®

# Benthic-Pelagic Switching in a Coastal Subtropical Lagoon

**J. Almunia[a], G. Basterretxea[a], J. Arístegui[a] and R. E. Ulanowicz[b]**

[a]*Facultad de Ciencias del Mar, Universidad de Las Palmas de Gran Canaria, P.O. Box 550, 35017 Las Palmas de Gran Canaria, Spain*
[b]*University of Maryland Center for Environmental Science, Chesapeake Biological Laboratory, P.O. Box 38, Solomons, Maryland 20688-0038, U.S.A.*

*Received 22 June 1998 and accepted in revised form 8 February 1999*

The structure of the ecosystem fluxes occurring in the Maspalomas coastal lagoon (Canary Islands) were investigated for three successive stages using estimates of the food webs that typify each interval. The first stage was representative of a benthic producer-dominated system and the third typified a pelagic-dominated system. The second phase was taken as the transient stage between these endpoints. The standing stocks and fluxes pertaining to each compartment and the overall trophic structure of the system were quantified as a network model. This food web budget was subjected to network analysis to assess the status of the system at each stage. The ensuing trophic analysis indicated that detritivory increases in passing from the first to the third stage (ratio of detritivory to herbivory 13·19, 7·57 and 20·32 respectively) and there is a concomitant drop in the average trophic efficiency. Cycle analysis revealed an increase in the amount of matter being cycled during the third stage (percentages of cycled matter 17·7%, 22·6% and 41·8% respectively), mostly via short, fast loops, which suggest that the third stage is representative of an immature ecosystem. Finally, the analysis of topological system-level indices reveals a dramatic increase in organization during the last stage, due primarily to the inflation of the total system throughput (TST). From a global point of view, results show a significant decline in the benthic subsystem, which represents a major perturbation to the ecosystem and renders it vulnerable to the subsequent invasion by pelagic elements. Although conditions in the third stage may seem typical of a eutrophic system, no appreciable resources are being added to the system from the outside. Therefore, the process is more accurately described as a shift in resources from one subsystem (the benthic) to another (the pelagic). © 1999 Academic Press

**Keywords:** modelling; ecosystems; eutrophication; coastal lagoons; Canary Islands

## Introduction

Maspalomas lagoon is a small subtropical coastal lagoon that is subject to periodical anoxic crises (Almunia, 1998). The system is representative of shallow eutrophic lagoons characterized by high throughput rates and as a consequence, structural changes become evident over relatively short periods of time (weeks) (Llinás *et al.*, 1986; Basterretxea & Van Lenning, 1995). Inputs to the system are rapidly transferred and dissipated among its components, resulting in dramatic changes in the structure and function of the ecosystem (Almunia, 1998). One way of providing insight into the fundamental structure and behaviour of an ecosystem is to measure the energy and material fluxes taking place within the system and to estimate the efficiencies of transfer among the different compartments (Longhurst, 1984; Ulanowicz & Platt, 1985; Ulanowicz, 1986; Baird *et al.*, 1991; Baird & Ulanowicz, 1993). Accordingly, these tasks became the priorities for a research programme carried out in Maspalomas; further detail concerning sampling protocols and results can be found in Almunia (1998).

The study employed network analysis on the ecosystem to reveal several of its properties, such as its structural complexity, cycling behaviour and trophic relationships among compartments of the system. This type of analysis uses available data to quantify the material and energetic interactions within the community, which are believe to condition the self-organizing and self-regulating behaviour of the system (Odum, 1971; Ulanowicz, 1986; Ulanowicz & Norden, 1990). From a practical standpoint, the separation into distinct components allows an investigator to focus on a particular section of the network and to identify the key processes controlling the functioning of the overall system (Ulanowicz & Norden, 1990).

Self-organization of ecosystems generally occurs over an interval of decades but the changes addressed in this work transpire over the span of a single year.

0272–7714/99/090363+22 $30.00/0 © 1999 Academic Press

© Del documento, los autores. Digitalización realizada por ULPGC. Biblioteca Universitaria, 2009

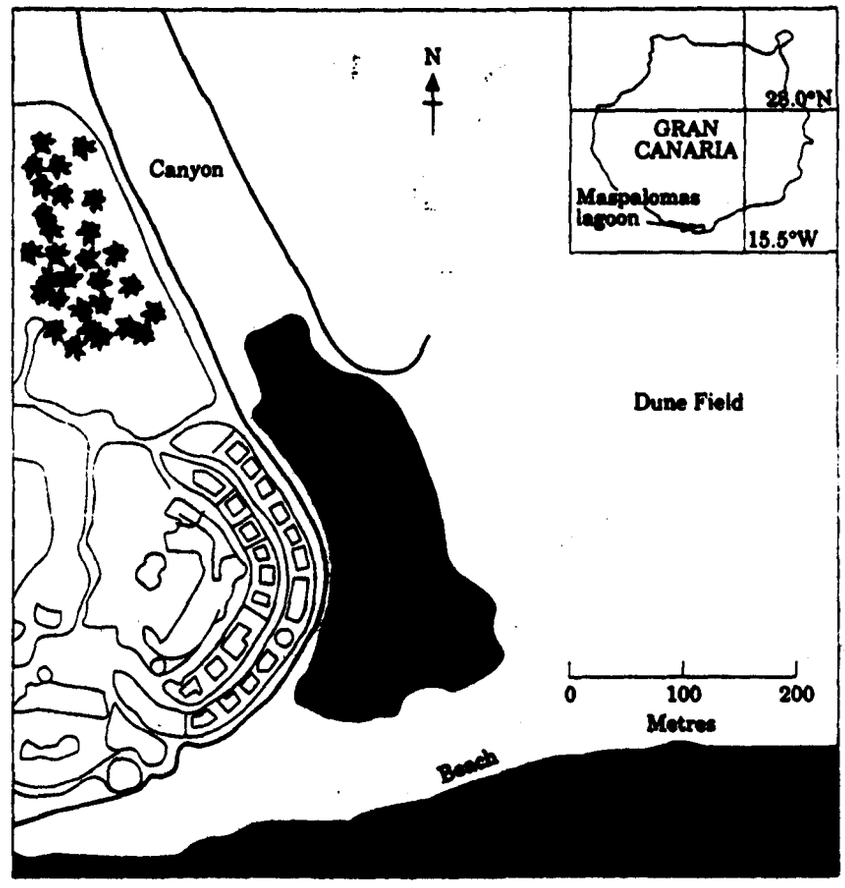


FIGURE 1. Location of Maspalomas lagoon.

Thus, it would be more appropriate to refer to any organizational behaviour as self-regulation, rather than self-organization. The differences between the dynamics of self-organization and self-regulation are discussed in some detail in Gafiychuk and Ulanowicz (1996) and Ulanowicz (in press). Whereas self-organization evolves over longer times and is mediated primarily by positive feedbacks, the much more rapid phenomenon of self-regulation involves mostly negative feedback responses by the system. Nevertheless, it remains a useful exercise to focus upon correspondences in the overall structure and function of the intra-annual stages of the system (Margalef, 1982), utilizing the same system-level indices that have proven useful for interpreting system changes over longer periods (e.g. Ulanowicz, 1984).

The aim of this work is to conceptualize, quantify and analyse the trophic schematic of the ecosystem of Maspalomas lagoon at three different stages of its transition from a benthic-dominated system, with a low, stable pelagic biomass, to a highly-variable pelagic-dominated configuration, from which benthic producers have virtually disappeared.

## Study location

The 'Charca de Maspalomas' (Figure 1) is a small (*c.* 3·5 ha), shallow 1–2 m subtropical coastal lagoon, located on the southern coast of Gran Canaria (Canary Islands). The lagoon is the result of groundwater water seepage from the landward side and infiltrations of seawater through the sand bar. The water temperature in the lagoon ranges from 30 °C in summer to 15 °C in winter. During heavy rains, water runs through the arroyo, producing very rapid increases in water level. Alternatively, seawater can enter the lagoon during spring tides or during storm surges, thereby repleting the existing fish communities, composed mainly of *Liza aurata*, *Dicentrarchus punctatus* and *Diplodus sargus* (T. Moreno, 1997). Although different species of coastal and inland birds inhabit the proximity of the lagoon (wading birds, ducks, etc.), the most representative species of waterfowl is the moorhen (*Gallinula chloropus*).

The bottom of the lagoon is muddy, with the exception of the southern end, where sand from the nearby beach and dune fields dominates. The

© Del documento, los autores. Digitalización realizada por ULPGC. Biblioteca Universitaria, 2009

phanerogam *Ruppia maritima* and the algae *Cladophora* sp. and *Chara globularis* (episodically), dominate the muddy beds. The few sandy areas are practically free of bottom vegetation. As *R. maritima* is the major benthic producer in Maspalomas lagoon, its life cycle drives the major ecosystem changes. *Ruppia maritima* begins growing in early spring, reaching its maximum density in mid-summer and then decreases rapidly at the end of summer. The lagoon suffers from recurrent anoxic crises during the intervals when *R. maritima* is not visible, probably due to the lack of wind mixing in combination with high rates of community respiration. During hypoxic events water becomes extremely turbid, sharply curtailing light penetration to the bottom and promoting benthic algal decay. At these times *R. maritima* is restricted to the shallowest margins of the lagoon (Almunia, 1998).

As hypoxic conditions are related to the disappearance of the phanerogam, it was decided to study the changes induced in the ecosystem by the annual dieoff of *R. maritima*. For the purposes of this study, three stages have been selected when the Maspalomas lagoon ecosystem occurs an ecosystem with (1) low dissolved nutrients, low phytoplankton standing stocks, well-developed bottom algae and low water turbidity, (2) a transient stage with diminished benthic production and a burgeoning plankton community and finally (3) a community without benthic producers, but with high dissolved nutrients and a high density of phytoplankton; all representative of the anoxic conditions leading to fish kills.

## Estimates, methods and assumptions

A carbon flow model was constructed for each of the stages described above (Figure 2, 3 and 4). In order to estimate the network model one needs the magnitude of biomass in each component, as well as the intensities of flows between compartments and exchanges between the system and its surroundings. Standing stocks are expressed in mg C $m^{-2}$ and flows between the compartments in mg C $m^{-2}$ $d^{-1}$. Due to a lack of historical studies on Maspalomas, the magnitudes of standing stocks of living and non-living constituents required by the model (Table 1) had to be obtained in most cases by direct measurement.

The food web is comprised of 17 compartments (14 in the third stage, due to the disappearance of benthic primary producers), including three non-living constituents. Living compartments were chosen to be resolved as closely to the species level as available data and sampling strategy would allow (Baird & Ulanowicz, 1989). Of course, identification to the species level occurred mainly at the higher levels of the network.

Carbon budgets were constructed for each compartment according to the balance:

$$C = P + R + E + Ex$$

where $C$=consumption, $P$=production, $R$=respiration, $E$=egestion and $Ex$=excretion or exudation (Crisp, 1971; Baird & Ulanowicz, 1989). Exudation by primary producers was considered to be the largest source of dissolved organic carbon (DOC) (Valiela, 1984; Baird & Ulanowicz, 1993).

The structures of trophic levels and cycling for each network were analysed and system properties were calculated using algorithms described by Ulanowicz (1983, 1986*a*) and Kay *et al.* (1989). Briefly, the relationships between any arbitrary pair of components are assessed by the total flow calculation predicated on the Leontief inverse (Leontief, 1936; 1951) as applied to ecological systems (Hannon, 1973; Szyrmer & Ulanowicz, 1987). This analysis and the ones that follow, all require the input of biomasses to each compartment, the inputs from and outputs to the surroundings, an estimation of the energy dissipation (respiration) by each component, and the matrix of fluxes between the compartments themselves.

The study is comprised of four different analyses:

(1) The input-output analysis (IOA) (Hannon, 1973), which measures the importance of each particular entity and the bilateral influences that each pair of taxa have on each other. It is in this section of the algorithm that the total contribution coefficient (TCC) and the total dependency coefficient (TDC) are calculated for each compartment (Szyrmer & Ulanowicz, 1987). The TCC is the fraction of what leaves compartment *i* that eventually enters compartment *j*, and the TDC is the fraction of the total ingestion by *j* which passed through compartment *i* along its way to *j*.

(2) A second analysis interprets the network according to the trophic concepts of Lindeman (1942)), but without relegating each group to a unique trophic level (Ulanowicz & Kemp, 1979; Levine, 1980; Ulanowicz, 1995). Rather, each taxon is apportioned among a series of integer trophic levels according to how much reaches the taxon in question over pathways of different lengths. Using this partitioning, an equivalent straight chain of trophic transfers can be assembled and used to track the trophic status of the ecosystem as it changes.

© Del documento, los autores. Digitalización realizada por ULPGC. Biblioteca Universitaria, 2009

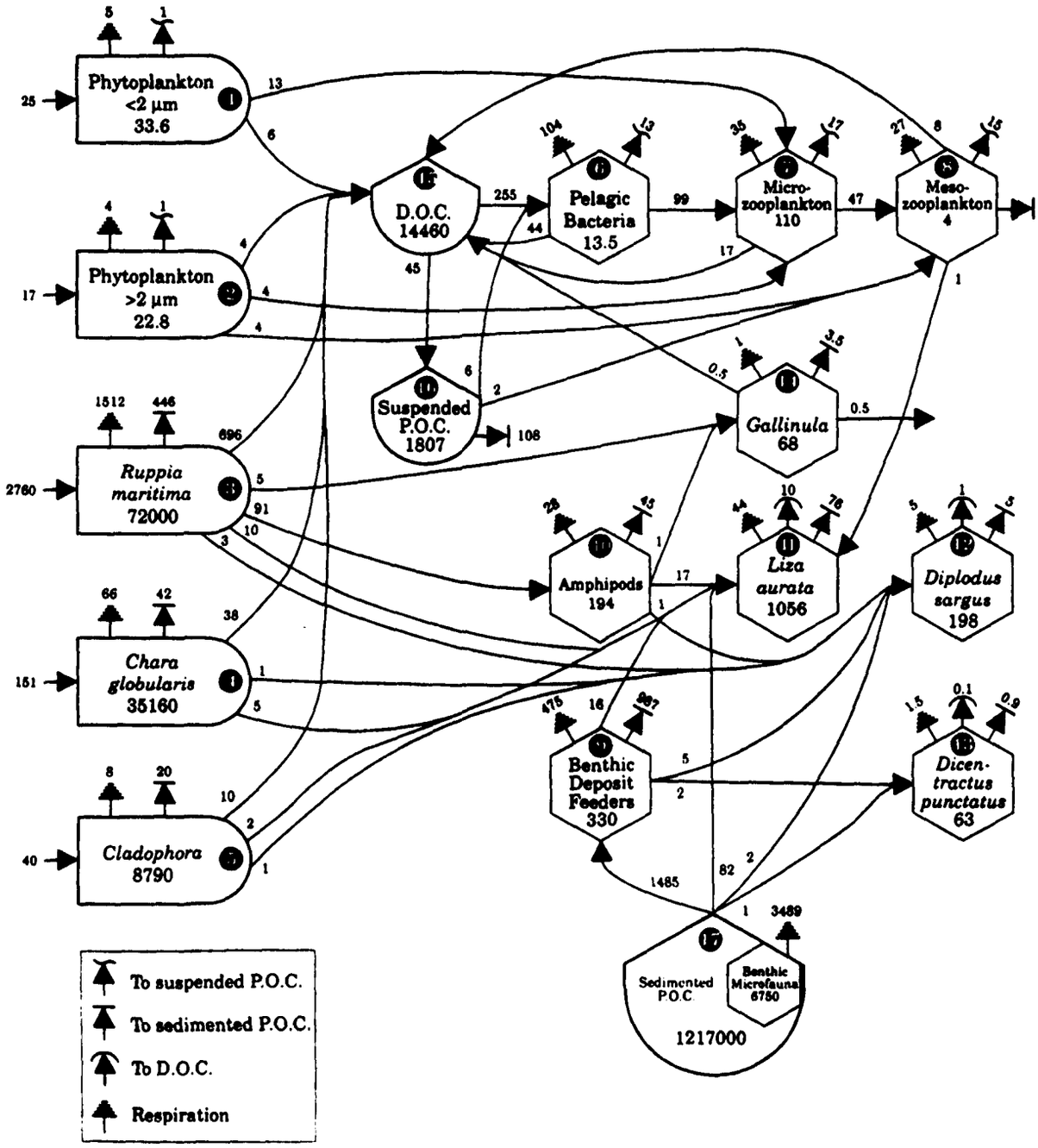


FIGURE 2. Energy flow network for stage 1 (biomass C in mg m $^{-2}$; carbon flows in mg m $^{-2}$ day $^{-1}$; rounded rectangles—autotrophs; hexagons—heterotrophs; rounded triangles—detritus).

(3) A third segment of the algorithm enumerates the biogeochemical cycles and outlines the complexity of cycling in the system in terms of the number and length of cycles and the percentage of total system activity devoted to cycling matter (Finn, 1976). A high fraction of cycled flow could indicate a mature and less disturbed system (Odum, 1969), if the matter is cycling through long-slow cycles, but if the matter is circulating rapidly around short loops, a high fraction could be indicative of a stressed ecosystem (Ulanowicz, 1984).

(4) Finally, the topological structure of the network (Hirata & Ulanowicz, 1984; Ulanowicz, 1986; Ulanowicz & Norden, 1990) is quantified by several indices: ascendency (Ulanowicz, 1986*a*)

© Del documento, los autores. Digitalización realizada por ULPGC. Biblioteca Universitaria, 2009

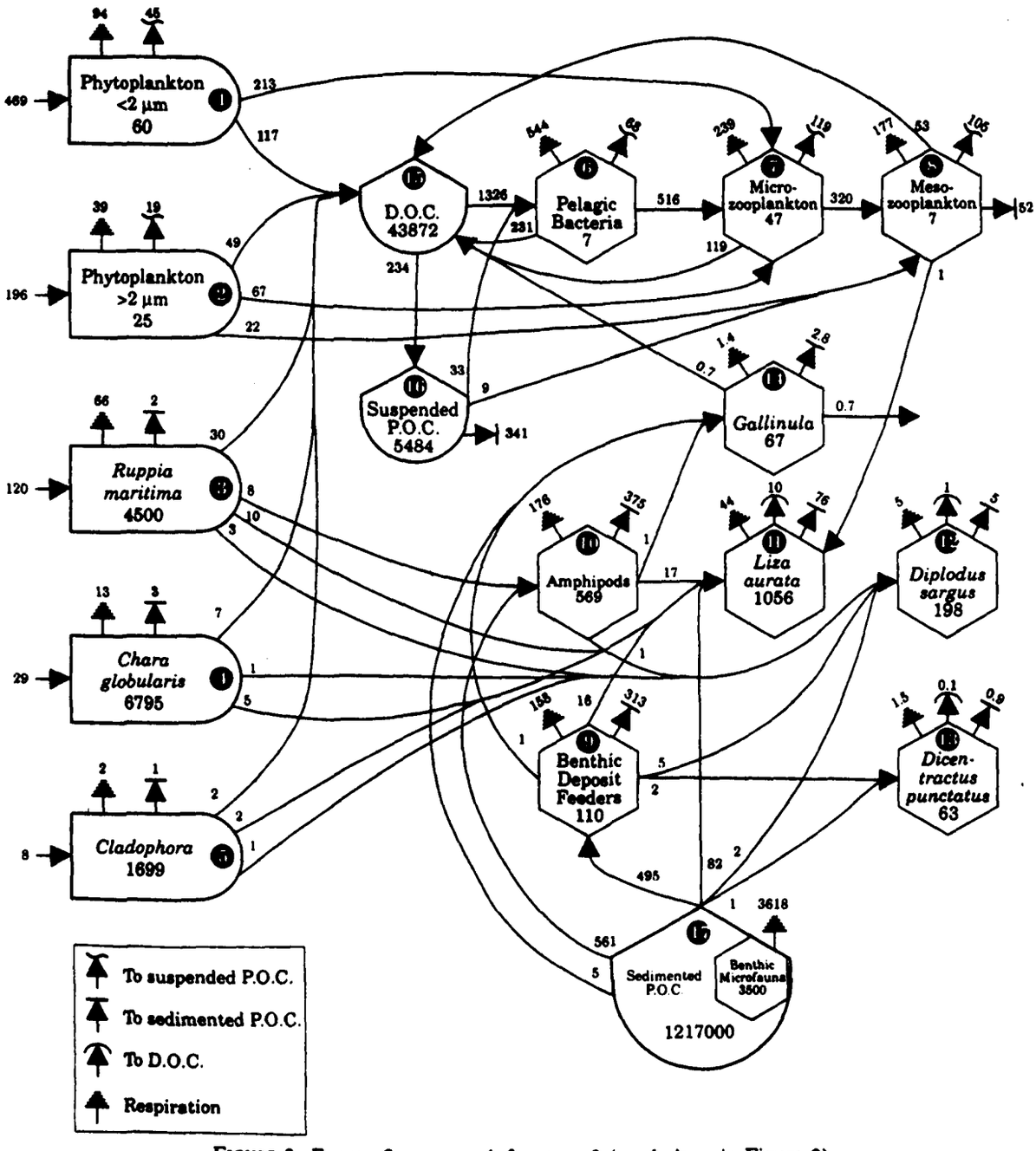


FIGURE 3. Energy flow network for stage 2 (symbols as in Figure 2).

measures in a single index both the system size and the organization inherent in its flow structure. Development capacity (Rutledge *et al.*, 1976; Ulanowicz, 1986*a*) is an upper bound on the ascendency, i.e. a measure of the network's potential for competitive advantage over other virtual network configurations. Overhead (Ulanowicz & Norden, 1990) is the difference between the magnitudes of the realized structure and its upper boundary. Whereas ascendency gauges the performance of a system in terms of how efficiently and with what definitiveness transfers are made, the overhead is complementary in that it quantifies how inefficiently and with what ambiguity the system is acting, on average. Redundancies or parallel flows in the imports, exports, dissipations and internal exchanges all contribute to the total overhead.

© Del documento, los autores. Digitalización realizada por ULPGC. Biblioteca Universitaria, 2009

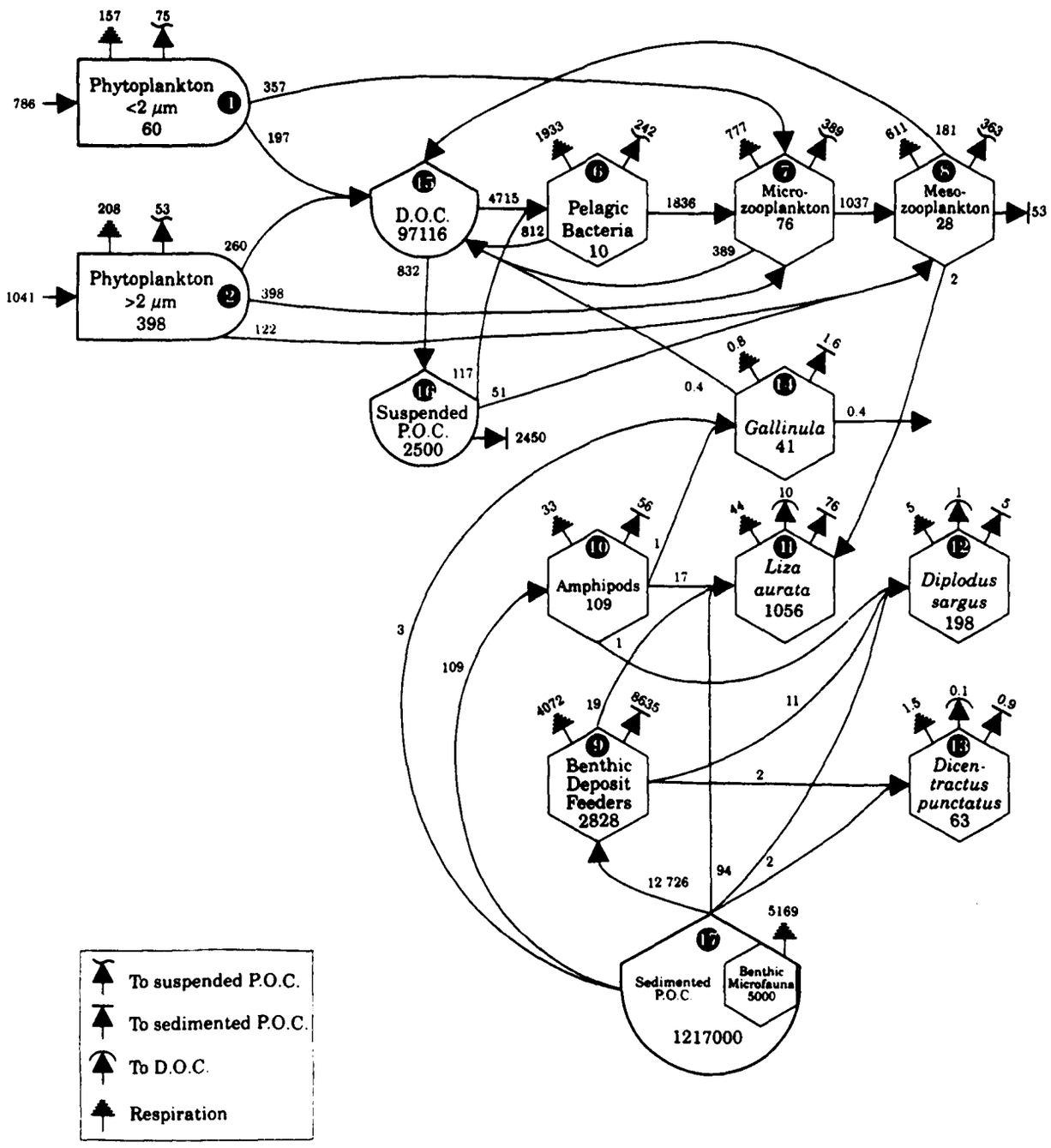


FIGURE 4. Energy flow network for stage 3 (symbols as in Figure 2).

Because the network was constructed primarily with direct measurements and supplemented with data from the literature, the final network was slightly unbalanced (by about 10% of total system throughput.) Final balance was achieved using the automated balancing routine, DATBAL (Ulanowicz, 1996). Since differences in the analyses carried out with NETWRK (Ulanowicz & Kay, 1991) for balanced and unbalanced data were minimal, the complete analysis was based on unbalanced data.

### *Phytoplankton*

Phytoplankton was divided into two compartments, picoplankton (<2μm) and phytoplankton (>2μm). Both are grazed by microzooplankton, but

© Del documento, los autores. Digitalización realizada por ULPGC. Biblioteca Universitaria, 2009

TABLE 1. Model data sources

| Compartment | Parameter | Source |
|---|---|---|
| Pelagic primary producers | Biomass | Measurements of chlorophyll |
| | Production | % of net planktonic production (O2 method) |
| | Respiration | % of planktonic respiration (O2 method) |
| | Exudation | Baird and Ulanowicz (1989) |
| | Death | Jorgensen *et al.* (1991) |
| Benthic primary producers | Biomass | Direct observations and Edwards (1978), Verhoeven (1980), Harrison (1982), Flores-Verdugo *et al.* (1988) and Betancort (1993) |
| | Production | Congdon *et al* (1979), Pentecost (1984), Evans *et al.* (1986) and Menendez and Peñuelas (1993) |
| | Respiration and Exudation | Edwards (1978) |
| Pelagic bacteria | Biomass | Bacteria counts (epifluorescence) |
| | Assimilation | Calculated from planktonic respiration data |
| | Respiration | Hobbie and Williams (1984) |
| Microzooplankton | Biomass | Direct counts (epifluorescence) |
| | Grazing on phytoplankton, grazing on bacteria, respiration and excretion | Fenchel (1982) |
| Mesozooplankton | Biomass | Dry weight and CHN |
| | Grazing, respiration and excretion | Margalef (1983), Hobbie and Williams (1984) and Jorgensen *et al.* (1991) |
| Benthic microfauna | Biomass and respiration | Margalef (1983 |
| Benthic deposit feeders | Biomass | Dry weight and CHN |
| | Assimilation, respiration and excretion | Moreno (1996) |
| Fish | Biomass | Fresh weight |
| | Diet, consumption and Assimilation | Moreno (1996) |
| | Respiration, excretion and egestion | Moreno (1996) and Wootton (1992) |
| Waterfowl | Biomass | Census |
| | Diet | Direct observation |
| | Respiration, excretion and egestion | Gibbons (1989) |
| DOC | Concentration | Total organic carbon analyzer measurements |
| Suspended POC | Concentration | CHN measurements |
| | Sedimentation and aggregation | Peterson (1984) |
| Sedimented POC | Concentration | CHN measurements |

phytoplankton can also be eaten by mesozooplankton. Phytoplankton chlorophyll was determined fluorometrically (Holm-Hansen *et al.*, 1965) in a Turner Designs fluorometer that was calibrated with pure chlorophyll *a*. Triplicate samples were taken from the centre of the lagoon and subsamples were filtered onto Whatman GF/F filters (assumed to retain the total phytoplankton biomass) and onto Nuclepore 2μm pore size polycarbonate filters. The fraction <2μm was estimated by difference between the two measurements. A wide range of carbon to chlorophyll ratios (25 to 145) can be found in the literature (Strickland, 1960; Antia *et al.*, 1963; Parsons *et al.*, 1984; Jorgensen *et al.*, 1991) to estimate the biomass in carbon units from chlorophyll measurements. The 30 carbon/chlorophyll ratio suggested by Strickland (1960) was used, because it was closer to the values reported for healthy, actively growing phytoplankton.

Phytoplankton primary production was estimated by the differences in oxygen measurements taken in light and dark bottles, respectively. Six light and six dark bottles were incubated *in situ* at approximately 0·5 m depth from dawn to noon. The oxygen in each bottle was measured by an automated microwinkler titrator (Williams & Jenkinson, 1982); the coefficient of variation on the measures were always below 1%. Due to the lack of fractionated production measurements, estimates were divided up proportionally between the two phytoplankton compartments. Photosynthetic quotients (PQs) in the literature range from 1·1 to 1·3 (Parsons *et al.*, 1984). A PQ of 1·2 was used in this study to convert oxygen into carbon.

Literature on phytoplankton exudation showed values anywhere from 0·2 to 62% (Valiela, 1984; Baird & Ulanowicz, 1989; Jorgensen *et al.*, 1991) of primary production. The index was assumed to be

© Del documento, los autores. Digitalización realizada por ULPGC. Biblioteca Universitaria, 2009

25% of primary production (Baird & Ulanowicz, 1989). The flux of phytoplankton to suspended detritus was calculated assuming a mean death rate equal to 9·6% of primary production (Jorgensen *et al.*, 1991).

*Benthic primary producers*

Benthic primary producers are composed mainly of the phanerogam *R. maritima* and the algae *C. globularis* and *Cladophora* sp. *Ruppia maritima* is grazed by amphipods (Verhoeven, 1980*b*), moorhens and some fishes (as deduced from stomach contents.) The algae were considered to be grazed only by herbivorous fishes.

To calculate the amount of *R. maritima* carbon per square metre, the percentage of area covered by the plant at each stage was estimated, and applied density values for *Ruppia* sp. in different reservoirs, as found in the literature (Edwards, 1978; Verhoeven, 1980*b*; Harrison, 1982; Flores-Verdugo *et al.*, 1988). Corresponding literature values were also used to calculate production (Congdon & McComb, 1979; Evans *et al.*, 1986; Menendez & Peñuelas, 1993), respiration and exudation (Edwards, 1978).

The same procedure was used to calculate algal biomass (Patronato de la Charca de Maspalomas, 1993), production, respiration (Pentecost, 1984) and exudation (25% of primary production, as in phytoplankton and *R. maritima*) for each stage.

*Bacteria*

Bacteria were assumed to be free-living heterotrophs suspended in the water column that use DOC and POC as their food source. They are grazed mainly by microzooplankton and occasionally by mesozooplankton.

Bacterial biomass was estimated by acridine orange staining and epifluorescence counts (Porter & Feig, 1980). A conversion factor of $2 \times 10^{-14}$ g C cell$^{-1}$ (Baird & Ulanowicz, 1989; Ballesteros, 1994) was used to estimate carbon biomass.

Although bacterial assimilation was not able to be measured directly, we were aware of the importance of estimating this parameter accurately. Therefore, planktonic respiration was calculated first, using metabolic coefficients from the literature. Then assimilation values were calculated that yielded figures for overall respiration equal to the pelagic respiration as measured in each phase using the dark bottle method.

We used ratios taken from the literature to calculate respiration, excretion and death of pelagic bacteria (Hobbie & Williams, 1984).

Respiration values by benthic bacteria were estimated from literature data for eutrophic lakes (Margalef, 1983) and were assigned to the POC compartment under the assumption that, from a trophic point of view, it is not necessary to distinguish between POC and bacterial carbon.

*Microzooplankton (heterotrophic flagellates and ciliates)*

The microzooplankton compartment represents the heterotrophic flagellates, which graze on pelagic bacteria and phytoplankton <2μm and are eaten by mesozooplankton.

Microzooplankton biomass was estimated by direct epifluorescence counts of heterotrophic flagellates after proflavine staining (Haas, 1982). Ratios for converting cells to carbon and rates of respiration and excretion were estimated from the literature (Fenchel, 1982).

Experiments with microzooplankton grazing on nutrient-enriched natural phytoplankton were carried out as in Landry and Hasset (1982). The grazing rate estimated in this manner was used as a maximum potential value, against which to check if microzooplankton were able to crop the existing production figures for phytoplankton and bacteria.

*Mesozooplankton*

The mesozooplankton compartment represents planktonic organisms >100 μm. In the second stage these consisted mainly of copepods and in the third stage, rotifers. Mesozooplankton were assumed to graze on phytoplankton >2 μm, microzooplankton and suspended POC. Due to the absence of any benthic plankton feeders or planktivorous fishes, it was considered that the mesozooplankton biomass flows primarily to the sediment POC and only a small amount is grazed by *L. aurata*.

Mesozooplankton were sampled by horizontal hauls of a WP2 (UNESCO 1968) 100 μm net. Biomass was estimated as dry weight (Lovegrove, 1966), using a 40% dry weight to carbon ratio, obtained from a CHN analysis of the dry biomass.

Grazing on phytoplankton was calculated under the same assumptions that were applied to microzooplankton and metabolic rates were taken from the literature (Margalef, 1983; Hobbie & Williams, 1984; Jorgensen, 1991).

*Benthic deposit feeders*

During each stage several sediment samples (1000 cm$^3$) were fractionated through 1000, 500 and

© Del documento, los autores. Digitalización realizada por ULPGC. Biblioteca Universitaria, 2009

100 µm sieves. The results revealed that, as regards trophic habits, benthic organisms can be separated into either benthic deposit feeders (mainly worms and some chironomids) or herbivores (amphipods).

Benthic deposit feeders were separated from the sample and their dry weight was determined as in Lovegrove (1966). Biomass as carbon was calculated using an assumed carbon to dry weight ratio of 40%. Ingestion, respiration, excretion and death were calculated using indices from the literature (Moreno, 1996).

### *Amphipods*

Amphipods have been frequently observed grazing on *Ruppia* sp. stands (Verhoeven, 1980; Menendez & Comín, 1990), so it was assumed that amphipods in Maspalomas graze exclusively on *R. maritima* and detritus, and that they are eaten by all predators that either graze on *R. maritima* or feed on detritus. Although epiphytic algae may also be part of the amphipods' diet, this item has not been considered in the present model. Amphipod biomass was calculated as for the benthic deposit feeders and the amounts of macrophytes consumed by animal populations in different seasons were taken from literature (Menendez & Comín, 1990).

### *Fish*

The fish species found in Maspalomas exhibit different feeding behaviour. *Liza aurata* feed principally on detritus, however, mosquito larvae, benthic organisms and algae are also included in their diet. *Diplodus sargus* is an herbivorous fish feeding on the existing algal communities. Finally, *D. punctatus* is a carnivorous feeder with a high assimilation rate (Moreno, 1996).

Fish biomasses were calculated using abundance data from systematic samplings (Moreno, 1996), and carbon to freshweight indices from the literature (Parsons *et al.*, 1984). Diets were determined from an analysis of stomach contents, in conjunction with consumption to biomass indices taken from the literature (*L. aurata*: 5%, *D. punctatus*: 0·5%; and *D. sargus*: 2·75%; Wootton, 1992; Moreno, 1996). Indices from the literature also were used to calculate production, respiration, excretion and egestion for each species (Wootton, 1992).

### Gallinula chloropus

The Viceconsejeria de Medio Ambiente carried out visual censuses of waterfowl during recent years (R. Gallo, pers. comm.). Whereas other populations of waterfowl use Maspalomas opportunistically, *G. chloropus* appears to use this aquatic ecosystem as its primary habitat.

Unfortunately, due to the laws protecting the waterfowl, no stomach content analysis could be undertaken. The Moorhen's diet was assumed from observations on its behaviour made during each stage. Anatomic and metabolic parameters from the literature were also used (Gibbons, 1989).

### *POC and DOC*

Both forms of organic carbon result from excretion, lysis and mortality or organisms, and become available to bacteria. Suspended POC can be filtered by mesozooplankton (no benthic filter-feeders were found in the ecosystem), whereas sedimented POC is ingested by benthic deposit feeders, fishes and moorhens.

Water samples of from 50 to 200 ml were filtered onto Whatman GF/F filters, acidified and stored frozen until measured in a Perkin-Elmer CHN Analyzer to calculate the suspended POC concentration. Phytoplanktonic carbon was subtracted from the result to calculate the concentration of detrital carbon. POC concentrations in the first 5 cm of sediment (Baird & Ulanowicz, 1989) were measured from several sediment samples taken from the muddy and sandy areas of the pond.

DOC concentrations were measured in a Shimadzu TOC Analyzer after acidification of the sample (UNESCO, 1994). Literature data were used to calculate POC sedimentation and DOC aggregation rates (Peterson, 1984).

## Results

The total contribution coefficients (TCC) for each compartment do not show marked differences over the three stages (Table 2). The most relevant changes are the increments from first to second stage in almost all the contribution coefficients from pelagic bacteria, and in those from the benthic deposit feeders during the third. The total dependency coefficient (TDC) indicates overall decreased dependency on the benthic producers in successive stages (Table 3). This effect is compensated by corresponding increases in the dependencies on detritus. Both effects are to be expected from the observed development of the ecosystem; as benthic producers disappear, organisms are forced to change their diets and contributions from the detrital pool increase as a result.

The diagonal elements of the total dependency matrix indicate the amounts by which each species is

© Del documento, los autores. Digitalización realizada por ULPGC. Biblioteca Universitaria, 2009

TABLE 2. Total contribution coefficients (TCC) matrix (percentage). Compartments are indicated by their number

Stage 1

| | 6 | 7 | 8 | 9 | 10 | 11 | 12 | 13 | 14 | 15 | 16 | 17 |
|---|---|---|---|---|---|---|---|---|---|---|---|---|
| 1 | 12 | 55 | 23 | 7 | 0 | 1 | 0 | 0 | 0 | 35 | 21 | 23 |
| 2 | 11 | 27 | 35 | 7 | 0 | 1 | 0 | 0 | 0 | 32 | 21 | 25 |
| 3 | 8 | 3 | 1 | 6 | 3 | 1 | 0 | 0 | 0 | 25 | 3 | 21 |
| 4 | 8 | 3 | 1 | 10 | 0 | 4 | 1 | 0 | 0 | 25 | 3 | 33 |
| 5 | 8 | 3 | 1 | 16 | 0 | 6 | 3 | 0 | 0 | 25 | 3 | 55 |
| 6 | 8 | 40 | 17 | 5 | 0 | 1 | 0 | 0 | 0 | 25 | 17 | 18 |
| 7 | 8 | 3 | 42 | 9 | 0 | 1 | 0 | 0 | 0 | 21 | 27 | 31 |
| 8 | 6 | 2 | 1 | 12 | 0 | 3 | 0 | 0 | 0 | 14 | 27 | 39 |
| 9 | 0 | 0 | 0 | 20 | 0 | 3 | 1 | 0 | 0 | 0 | 0 | 67 |
| 10 | 0 | 0 | 0 | 18 | 0 | 20 | 0 | 0 | 1 | 2 | 0 | 61 |
| 11 | 3 | 1 | 0 | 17 | 0 | 1 | 0 | 0 | 0 | 8 | 1 | 58 |
| 12 | 3 | 1 | 0 | 12 | 0 | 1 | 0 | 0 | 0 | 8 | 1 | 39 |
| 13 | 1 | 0 | 0 | 9 | 0 | 1 | 0 | 0 | 0 | 3 | 0 | 30 |
| 14 | 3 | 1 | 0 | 18 | 0 | 1 | 0 | 0 | 0 | 8 | 1 | 59 |
| 15 | 31 | 12 | 5 | 3 | 0 | 0 | 0 | 0 | 0 | 8 | 11 | 11 |
| 16 | 6 | 2 | 3 | 28 | 0 | 2 | 0 | 0 | 0 | 2 | 1 | 95 |
| 17 | 0 | 0 | 0 | 30 | 0 | 2 | 0 | 0 | 0 | 0 | 0 | 21 |

Stage 2

| | 6 | 7 | 8 | 9 | 10 | 11 | 12 | 13 | 14 | 15 | 16 | 17 |
|---|---|---|---|---|---|---|---|---|---|---|---|---|
| 1 | 31 | 55 | 24 | 3 | 4 | 1 | 0 | 0 | 0 | 35 | 24 | 30 |
| 2 | 30 | 45 | 30 | 3 | 4 | 1 | 0 | 0 | 0 | 34 | 26 | 31 |
| 3 | 22 | 10 | 4 | 2 | 9 | 9 | 3 | 0 | 0 | 26 | 7 | 20 |
| 4 | 22 | 10 | 4 | 3 | 4 | 18 | 4 | 0 | 0 | 26 | 7 | 29 |
| 5 | 24 | 11 | 5 | 4 | 5 | 26 | 13 | 0 | 0 | 28 | 8 | 40 |
| 6 | 22 | 45 | 19 | 2 | 3 | 1 | 0 | 0 | 0 | 25 | 16 | 2 |
| 7 | 18 | 8 | 43 | 4 | 4 | 1 | 0 | 0 | 0 | 21 | 17 | 35 |
| 8 | 14 | 6 | 3 | 4 | 5 | 1 | 0 | 0 | 0 | 14 | 31 | 38 |
| 9 | 0 | 0 | 0 | 7 | 8 | 5 | 1 | 0 | 0 | 1 | 0 | 66 |
| 10 | 0 | 0 | 0 | 7 | 8 | 5 | 0 | 0 | 0 | 0 | 0 | 68 |
| 11 | 7 | 3 | 1 | 7 | 7 | 2 | 0 | 0 | 0 | 8 | 2 | 59 |
| 12 | 7 | 3 | 1 | 5 | 5 | 1 | 0 | 0 | 0 | 8 | 2 | 41 |
| 13 | 3 | 1 | 1 | 3 | 4 | 1 | 0 | 0 | 0 | 0 | 1 | 31 |
| 14 | 9 | 4 | 2 | 5 | 5 | 1 | 0 | 0 | 0 | 10 | 3 | 43 |
| 15 | 86 | 39 | 17 | 3 | 4 | 1 | 0 | 0 | 0 | 22 | 29 | 30 |
| 16 | 7 | 3 | 3 | 8 | 10 | 2 | 0 | 0 | 0 | 2 | 2 | 75 |
| 17 | 0 | 0 | 0 | 11 | 12 | 3 | 0 | 0 | 0 | 0 | 0 | 15 |

Stage 3

| | 6 | 7 | 8 | 9 | 10 | 11 | 12 | 13 | 14 | 15 | 16 | 17 |
|---|---|---|---|---|---|---|---|---|---|---|---|---|
| 1 | 31 | 55 | 24 | 24 | 0 | 1 | 0 | 0 | 0 | 35 | 34 | 34 |
| 2 | 31 | 49 | 33 | 22 | 0 | 0 | 0 | 0 | 0 | 35 | 31 | 31 |
| 6 | 22 | 45 | 19 | 17 | 0 | 0 | 0 | 0 | 0 | 25 | 24 | 24 |
| 7 | 19 | 9 | 43 | 25 | 0 | 1 | 0 | 0 | 0 | 21 | 35 | 35 |
| 8 | 14 | 6 | 3 | 27 | 0 | 1 | 0 | 0 | 0 | 15 | 35 | 38 |
| 9 | 0 | 0 | 0 | 48 | 1 | 1 | 0 | 0 | 0 | 0 | 0 | 68 |
| 10 | 1 | 1 | 0 | 44 | 1 | 18 | 1 | 0 | 1 | 2 | 1 | 62 |
| 11 | 6 | 3 | 1 | 42 | 1 | 1 | 0 | 0 | 0 | 8 | 3 | 60 |
| 12 | 6 | 3 | 1 | 27 | 0 | 1 | 0 | 0 | 0 | 7 | 3 | 38 |
| 13 | 3 | 1 | 0 | 22 | 0 | 0 | 0 | 0 | 0 | 3 | 1 | 31 |
| 14 | 9 | 4 | 2 | 31 | 1 | 1 | 0 | 0 | 0 | 10 | 4 | 44 |
| 15 | 86 | 38 | 17 | 25 | 0 | 1 | 0 | 0 | 0 | 22 | 35 | 35 |
| 16 | 5 | 2 | 3 | 68 | 1 | 1 | 0 | 0 | 0 | 2 | 2 | 95 |
| 17 | 0 | 0 | 0 | 71 | 1 | 1 | 0 | 0 | 0 | 0 | 0 | 48 |

TABLE 3. Total dependency coefficients (TDC) matrix (percentage). Compartments are indicated by their number

Stage 1

| | 6 | 7 | 8 | 9 | 10 | 11 | 12 | 13 | 14 | 15 | 16 | 17 |
|---|---|---|---|---|---|---|---|---|---|---|---|---|
| 1 | 1 | 12 | 10 | 0 | 0 | 0 | 0 | 0 | 0 | 1 | 5 | 0 |
| 2 | 1 | 4 | 10 | 0 | 0 | 0 | 0 | 0 | 0 | 1 | 3 | 0 |
| 3 | 90 | 77 | 65 | 15 | 99 | 31 | 39 | 15 | 100 | 91 | 65 | 15 |
| 4 | 5 | 4 | 4 | 1 | 0 | 5 | 8 | 1 | 0 | 5 | 4 | 1 |
| 5 | 1 | 1 | 1 | 1 | 0 | 2 | 8 | 1 | 0 | 1 | 1 | 1 |
| 6 | 8 | 85 | 70 | 1 | 0 | 1 | 1 | 1 | 0 | 8 | 36 | 1 |
| 7 | 4 | 3 | 82 | 1 | 0 | 1 | 0 | 1 | 0 | 3 | 27 | 1 |
| 8 | 1 | 1 | 1 | 1 | 0 | 1 | 0 | 1 | 0 | 1 | 14 | 1 |
| 9 | 0 | 0 | 0 | 20 | 0 | 24 | 42 | 73 | 0 | 0 | 0 | 20 |
| 10 | 0 | 0 | 0 | 1 | 0 | 14 | 8 | 1 | 17 | 0 | 0 | 1 |
| 11 | 1 | 1 | 1 | 2 | 0 | 1 | 1 | 2 | 0 | 1 | 1 | 2 |
| 12 | 0 | 0 | 0 | 0 | 0 | 0 | 0 | 0 | 0 | 0 | 0 | 0 |
| 13 | 0 | 0 | 0 | 0 | 0 | 0 | 0 | 0 | 0 | 0 | 0 | 0 |
| 14 | 0 | 0 | 0 | 0 | 0 | 0 | 0 | 0 | 0 | 0 | 0 | 0 |
| 15 | 99 | 85 | 71 | 2 | 0 | 2 | 1 | 2 | 0 | 8 | 72 | 2 |
| 16 | 3 | 2 | 5 | 3 | 0 | 2 | 1 | 3 | 0 | 0 | 1 | 3 |
| 17 | 1 | 1 | 1 | 100 | 0 | 74 | 54 | 100 | 0 | 1 | 1 | 21 |

Stage 2

| | 6 | 7 | 8 | 9 | 10 | 11 | 12 | 13 | 14 | 15 | 16 | 17 |
|---|---|---|---|---|---|---|---|---|---|---|---|---|
| 1 | 14 | 36 | 30 | 3 | 3 | 3 | 2 | 3 | 3 | 13 | 25 | 3 |
| 2 | 6 | 12 | 16 | 1 | 1 | 14 | 1 | 1 | 1 | 5 | 11 | 1 |
| 3 | 3 | 2 | 14 | 1 | 2 | 8 | 24 | 1 | 1 | 3 | 2 | 1 |
| 4 | 1 | 0 | 0 | 0 | 0 | 4 | 8 | 0 | 0 | 1 | 0 | 0 |
| 5 | 0 | 0 | 0 | 0 | 0 | 2 | 8 | 0 | 0 | 0 | 0 | 0 |
| 6 | 22 | 65 | 54 | 6 | 6 | 5 | 3 | 6 | 6 | 22 | 37 | 6 |
| 7 | 13 | 8 | 83 | 6 | 6 | 6 | 4 | 6 | 6 | 12 | 27 | 6 |
| 8 | 5 | 3 | 3 | 3 | 3 | 4 | 2 | 3 | 3 | 4 | 25 | 3 |
| 9 | 0 | 0 | 0 | 7 | 7 | 17 | 40 | 69 | 20 | 0 | 0 | 7 |
| 10 | 0 | 0 | 0 | 9 | 8 | 19 | 12 | 9 | 22 | 0 | 0 | 9 |
| 11 | 1 | 1 | 0 | 2 | 2 | 2 | 1 | 2 | 2 | 1 | 1 | 2 |
| 12 | 0 | 0 | 0 | 0 | 0 | 0 | 0 | 0 | 0 | 0 | 0 | 0 |
| 13 | 0 | 0 | 0 | 0 | 0 | 0 | 0 | 0 | 0 | 0 | 0 | 0 |
| 14 | 0 | 0 | 0 | 0 | 0 | 0 | 0 | 0 | 0 | 0 | 0 | 0 |
| 15 | 99 | 64 | 55 | 9 | 9 | 8 | 8 | 9 | 9 | 22 | 76 | 9 |
| 16 | 3 | 2 | 4 | 8 | 8 | 7 | 7 | 8 | 8 | 1 | 2 | 8 |
| 17 | 1 | 1 | 0 | 1 | 98 | 86 | 86 | 100 | 100 | 1 | 1 | 15 |

Stage 3

| | 6 | 7 | 8 | 9 | 10 | 11 | 12 | 13 | 14 | 15 | 16 | 17 |
|---|---|---|---|---|---|---|---|---|---|---|---|---|
| 1 | 6 | 18 | 16 | 3 | 3 | 3 | 3 | 3 | 3 | 6 | 10 | 3 |
| 2 | 8 | 21 | 30 | 3 | 3 | 4 | 3 | 3 | 3 | 8 | 13 | 3 |
| 6 | 22 | 71 | 62 | 10 | 10 | 10 | 10 | 10 | 10 | 22 | 35 | 10 |
| 7 | 12 | 9 | 87 | 9 | 9 | 10 | 9 | 9 | 9 | 12 | 32 | 9 |
| 8 | 4 | 3 | 3 | 5 | 5 | 6 | 5 | 5 | 5 | 4 | 16 | 5 |
| 9 | 0 | 0 | 0 | 48 | 48 | 55 | 89 | 83 | 48 | 0 | 0 | 48 |
| 10 | 0 | 0 | 0 | 0 | 1 | 19 | 8 | 1 | 26 | 0 | 0 | 1 |
| 11 | 0 | 0 | 0 | 0 | 1 | 1 | 1 | 1 | 1 | 0 | 0 | 1 |
| 12 | 0 | 0 | 0 | 0 | 0 | 0 | 0 | 0 | 0 | 0 | 0 | 0 |
| 13 | 0 | 0 | 0 | 0 | 0 | 0 | 0 | 0 | 0 | 0 | 0 | 0 |
| 14 | 0 | 0 | 0 | 0 | 0 | 0 | 0 | 0 | 0 | 0 | 0 | 0 |
| 15 | 99 | 70 | 63 | 16 | 16 | 17 | 16 | 16 | 16 | 22 | 60 | 16 |
| 16 | 3 | 2 | 6 | 26 | 26 | 26 | 26 | 26 | 26 | 1 | 2 | 26 |
| 17 | 0 | 0 | 0 | 100 | 99 | 98 | 100 | 100 | 100 | 0 | 0 | 48 |

© Del documento, los autores. Digitalización realizada por ULPGC. Biblioteca Universitaria, 2009

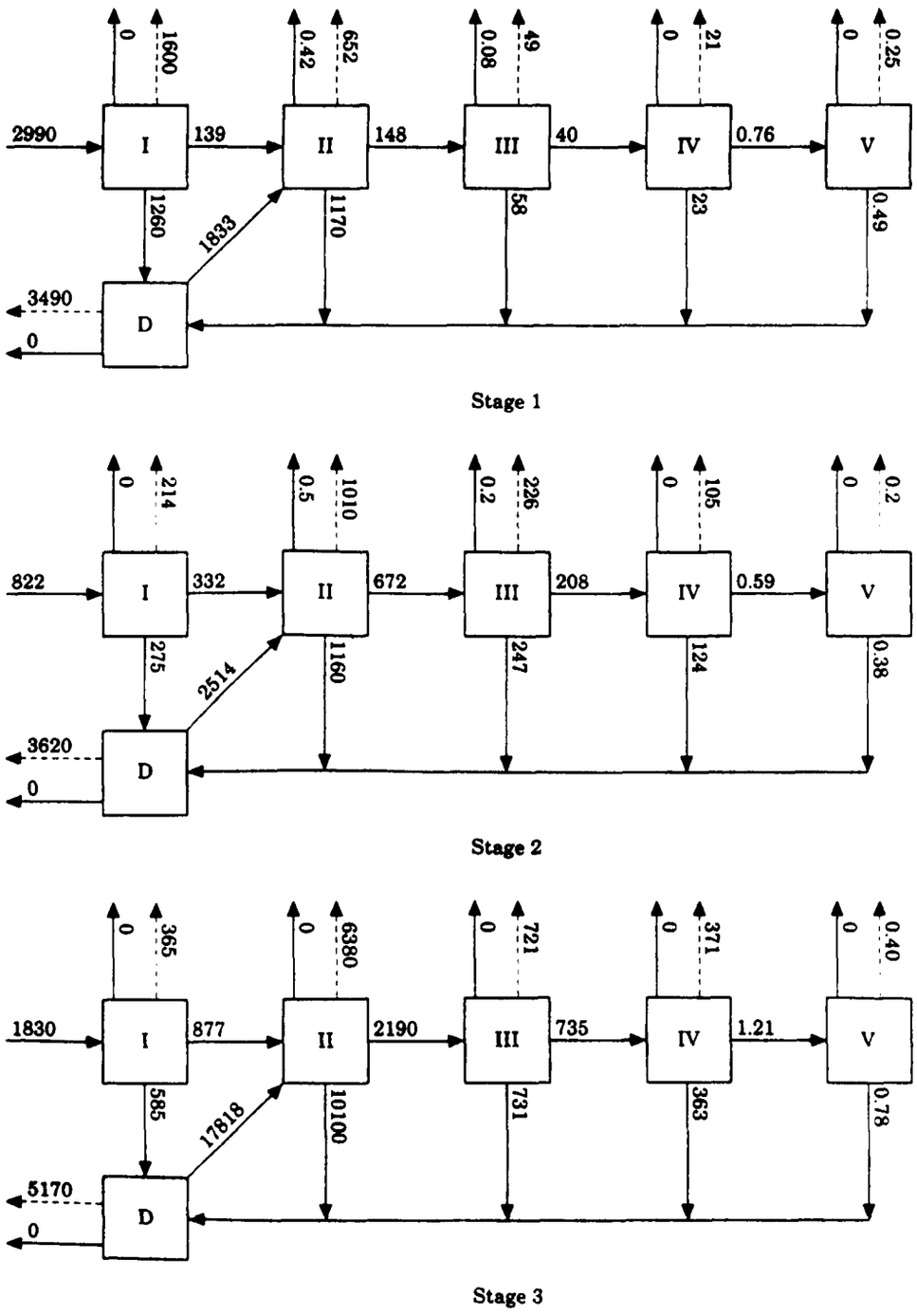


FIGURE 5. Aggregation of the flow web into a concatenated chain representing the discrete tropic levels and detritus (solid lines—carbon flows; broken lines—respiration; flows in mg $m^{-2}$ $day^{-1}$).

dependent upon its own production via cycling pathways. These diagonal fractions generally are quite low, with only a few values equal or greater than 20% (benthic deposit feeders 20% and sedimented POC 21% in the first stage, pelagic bacteria 22%, and DOC 22% in the second and pelagic bacteria 22%, benthic deposit feeders 48%, DOC 22% and sedimented POC 48% in the third). The 48% recycling via the benthic deposit feeders and the sedimented POC is an unusually high figure. In fact, it is the largest percentage recycle of carbon ever reported. These figures provide evidence that detritivory progressively increases with each successive stages. The same evidence is provided by the successive dependencies of

© Del documento, los autores. Digitalización realizada por ULPGC. Biblioteca Universitaria, 2009

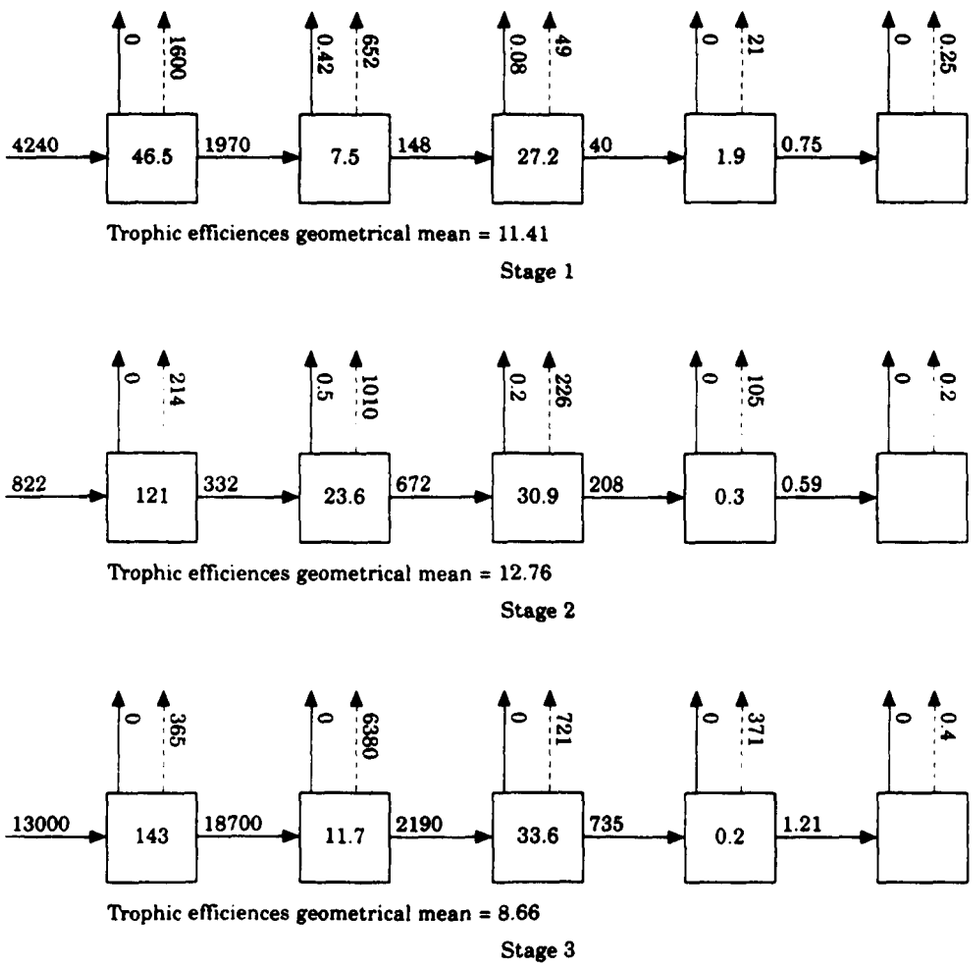


FIGURE 6. Aggregation of the flow web into a concatenated chain representing the discrete trophic levels, assuming detritus in the first level (symbols as in Figure 5).

the three detritic compartments upon themselves (DOC 2%, 9% and 16%, suspended POC 3%, 8% and 26%, and sedimented POC 21%, 15%, and 48%).

Any web of ecosystem interactions can be apportioned into a straight chain of discrete transfers (Ulanowicz, 1995) called the ' Lindeman spine '. For example, if a population obtains 25% of its food from plants, 60% as a carnivore and 15% as a secondary carnivore, then its activity would be apportioned over levels 2, 3 and 4 of the Lindeman spine in the proportions 5:12:3, respectively. The Lindeman spines for the three stages all possess the same number of trophic levels (Figure 5).

Alternatively, one could weight the various pathways over which sustenance reaches a given predator by the number of trophic links in that pathway to obtain a non-integer ' average trophic position ' (Levine, 1980). The predator used as an example in the last paragraph would feed at trophic level 2·9 (=(0·25 × 2)+(0·60 × 3)+(0·15 × 4)). The highest average trophic level for any taxon is 3·64 for mesozooplankton, despite the fact that some fishes eat mesozooplankton. Fish diet is primarily based on detritus and primary producers (first trophic level) and only marginally on mesozooplankton (third trophic level). As a result, their average trophic positions fall substantially below 4.

The highest primary production values are found at the first stage, which is also when the lowest detritivory values were measured. The highest detritivory was registered in the third stage. The ratio of detritivory to herbivory was intermediate in the first stage (13·19), lowest in the second (7·57) and highest in the third (20·32). Precisely the opposite order was revealed in the geometric mean of the trophic efficiencies (Figure 6). Trophic efficiencies were moderate in the first stage (11·4), highest in the second (12·8) and lowest in the third (8·66). Trophic aggregation analysis confirms our expectation that

© Del documento, los autores. Digitalización realizada por ULPGC. Biblioteca Universitaria, 2009

detritivory would be highest in the third stage, a circumstance which considerably reduces the averaged trophic efficiency at that stage.

The evolution in the pattern of recycling over the three ecosystem stages consists of an increase of the number of simple cycles from the first stage (99) to the second and third stages (159 and 155). Furthermore, the Finn Cycling Index increases as well (17·7%, 22·6% and 41·8%, respectively), indicating that the percentage of cycled matter increases as switching occurs. Odum (1969) suggested that mature ecosystems recycle a greater percentage of material and energy than do pioneer or disturbed communities. Viewed in this way, the progressive increase in the Finn Cycling Index would suggest a maturation of the ecosystem. Ulanowicz (1984), however, has remarked that perturbed systems also often exhibit greater degrees of recycling. Ulanowicz and Wulff (1991) hypothesize that such augmented cycling in disturbed systems is a homeostatic response that maintains in circulation resources that before the perturbation had been stored as biomass in the higher organisms. Looking deeper into the cycling structure, it can be seen that in all the stages, carbon cycles along short and fast loops. The average path-lengths of the system in all three stages are low (2·18, 2·42 and 2·14 respectively), and the percentage of matter cycled over loops of various trophic lengths (Table 4) reveals that in stage 3, proportionately more matter is cycling over the shortest cycles, despite the increase in the Finn Index at that stage (Table 4). This observation supports the previous indications that the system is stressed at all three stages and is not maturing.

The evolution of total system throughput (TST) begins with a smooth decrease between the first and second stage, followed by a dramatic increase in the third stage (Table 5). These changes in TST modulate the variation in development capacity (DC), the network's *potential* for competitive advantage (Ulanowicz & Norden, 1990), which increases at each stage, although the informational factor (in bits) does not change as dramatically. Much the same pattern of change can be seen in the Ascendency (a unitary measure of activity and organization), which increases markedly toward the third stage, due mostly to the precipitous rise in TST. The positive evolution of these indices, fuelled as it is by a burgeoning TST does not, however, reveal ecosystem maturation, but rather indicates what often happens after the invasion of a new spatial domain following a major perturbation (Golley, 1974; Ulanowicz, 1997), a scenario that is consistent with the previous results outlined above.

The degree to which a system realizes its potential for growth, organization and development is given by the ratio A/C (Ulanowicz & Mann, 1981). Highly organized systems exhibit the tendency to internalize most of their activity, and thereby to become relatively independent of exchanges with the external world. Hence, the ratio of the indices $A_i$ and $C_i$ (Internal Ascendancy and Internal Capacity, calculated using internal exchanges only) is considered to be representative of a system's developmental status (Field *et al.*, 1989; Mann *et al.*, 1989; Baird *et al.*, 1991). This ratio is almost unchanged in the two first stages and rises in the third, suggesting that the last stage is a better organized system possessing more internal stability, which makes it difficult to change its basic structure via external influences (Table 5).

TABLE 4. Cycle normalized distributions (percentage of matter cycled through different cycle length)

| Cycle length | Stage 1 | Stage 2 | Stage 3 |
|---|---|---|---|
| 1 | 0 | 0 | 0 |
| 2 | 16·1 | 16 | 37 |
| 3 | 0·83 | 3·92 | 2·78 |
| 4 | 0·31 | 2·21 | 1·64 |
| 5 | 0·07 | 0·24 | 0·08 |
| 6 | 0·28 | 0·09 | 0·02 |
| 7 | 0·08 | 0·06 | 0·02 |
| Total (Finn Index) | 17·7 | 22·6 | 41·8 |

## Conclusions

The ecological study of the disappearance of benthic producers from Maspalomas lagoon, describes not merely the senescence of an ecosystem, but also the development of a new pelagic structure emerges as a result of the crisis that befalls the benthos.

Part of the trophic development is an increment in overall detritivory, presumably as a homeostatic response of the system to retain the organic carbon released from the previous ecosystem structure. This large amount of matter is circulated over fast, short loops in the new structure and in combination with an increment in pelagic primary production, results in a high total system throughput. This pattern of behaviour is consistent with the hypothesis that, at the beginning, immediately after a system has undergone a major destructive perturbation, or when it is invading a new spatial domain, the initial response of the system is to augment its activities and biomass at the fastest rate possible (Golley, 1974). This increase in system activity, reflected in the significant rise in TST, also augments the development capacity and Ascendency, even though no such intense changes are

© Del documento, los autores. Digitalización realizada por ULPGC. Biblioteca Universitaria, 2009

TABLE 5. Information indices. Where TST, DC, A, Overheads, R, Ci and Ai are expressed in mg C $m^{-2}$ $day^{-1}$, between brackets are percentages of the development capacity, finally A/C and Ai/Ci are adimensional indices

| Index | Stage 1 | Stage 2 | Stage 3 |
|---|---|---|---|
| Total system throughput (TST) | 13 626 | 12 264 | 51 544 |
| Development capacity (DC) | 47 840 | 52 359 | 192 750 |
| Development capacity (Bits) | 3·51 | 4·27 | 3·74 |
| Ascendancy (A) | 19 349 (40·4%) | 19 854 (37·9%) | 87·047 (45·2%) |
| Overhead on imports | 1522 (3·2%) | 1312 (2·5%) | 1801 (0·9%) |
| Overhead on exports | 2 (0%) | 785 (1·5%) | 6 (0%) |
| Dissipative overhead | 13 923 (29·1%) | 12 932 (24·7%) | 49 389 (25·6%) |
| Redundancy (R) | 13 044 (27·3%) | 17 476 (33·4%) | 54 327 (28·2%) |
| Internal capacity (Ci) | 23 136 | 31 436 | 128 260 |
| Internal Ascendancy (Ai) | 10 091 | 13 960 | 73 935 |
| A/C | 0·404 | 0·379 | 0·452 |
| A/TST (Bits) | 1·42 | 1·62 | 1·69 |
| Ai/Ci | 0·436 | 0·444 | 0·576 |

evident in the normalized versions of these indices. (The ratio internal Ascendancy/internal capacity does, however, indicate an increase in the developmental status during the third stage.)

The drastic changes in the system from stage 1 to stage 3 appear outwardly to portray the process of eutrophication, but the changes in whole system indices do not confirm this conclusion. Ulanowicz (1986*b*) has defined eutrophication as ' any increase in system Ascendency due to a rise in total system throughput that more than compensates for a concomitant fall in the mutual information of the flow network. ' Although, the TST does increase drastically during phase 3, the average mutual information (A/TST) of the system does not decrease. It actually increases from 1·42 bits in stage 1 to 1·69 bits in stage 3.

The most likely explanation of this phenomenon is a shift in resources from one subsystem (the benthic) to another (the pelagic) within Maspalomas. No appreciable resources are being added to the system from the outside. If one wanted to make the case for eutrophication, one would have to confine the analysis strictly to a comparison of the pelagic subsystem between stages 1 and 3. Overall, however, resources are simply being transferred from the benthic subsystem, with its attendant redundancies, to the more streamlined pelagic subsystem. Eventually, the system reverses itself and reconstructs the more intricate benthic community.

The entire cycle is reminiscent of Holling's (1986) ' figure–8 ' scenario for ecosystem development. Holling identifies ' creative destruction ' as an element of almost all ecosystem behaviours. Although conditions in stage 3 are not aesthetically pleasing and do indicate that the process of eutrophication may have occurred over a number of decades, the transition from stages 1 to 3 is not in itself an example of eutrophication and the indices confirm this conclusion. In order to establish that the Charca is a eutrophic ecosystem, it would be necessary to compare an annual network (that could be elaborated with seasonal data presented here) with one that which existed several decades ago.

## Acknowledgements

The study was supported in part by Grant No. PN95 18028274 from the Ministerio de Educación y Ciencia. Field work was partially supported by the Viceconsejeria de Medio Ambiente del Gobierno de Canarias.

The authors wish to thank Teresa Moreno for her willingness to share her data on fish and for her useful comments. They thank also Raquel Arriaga, Isidoro Falcón, Pedro Cazorla, Ramón Gallo, Mercedes García and Diego Ponce for their enthusiastic help with the field work. Cristina Bondavalli provided helpful comments on a draft of the manuscript.

## References

Almunia, J. 1998 *Estudio de las características tróficas y modelización del ecosistema de la Charca de maspalomas*. Unpublished doctoral dissertation. University of Las Palmas de Gran Canaria, Spain, 242 pp.

Antia, N. J., McAllister, C. D., Parsons, T. R., Stephens, K. & Strickland, J. D. H. 1963 Further measurements of primary production using a large-volume plastic sphere. *Limnology and Oceanography* **8**, 166–183.

© Del documento, los autores. Digitalización realizada por ULPGC. Bibliotecas Universitaria, 2009

Baird, D. & Ulanowicz, R. E. 1989 The seasonal dynamics of the Chesapeake Bay ecosystem. *Ecological Monographs* **59**, 329–364.

Baird, D. & Ulanowicz, R. E. 1993 Comparative study of the trophic structure, cycling and ecosystem properties of four tidal estuaries. *Marine Ecology Progress Series* **99**, 221–237.

Baird, D., MacGlade, J. M. & Ulanowicz, R. E. 1991 The comparative ecology of six marine ecosystems. *Philosophical Transactions of the Royal Society of London* **333**, 15–29.

Ballesteros, S. 1994 *Influencia de las estructuras mesoescalares sobre la distribución y abundancia de bacterias y cianobacterias en aguas de Canarias*. Unpublished doctoral dissertation. University of Las Palmas de Gran Canaria, Spain, pp. 114.

Basterretxea, G. & Van Lenning, K. 1995 Estudio planctonico de la Charca de Maspalomas. Informe Preliminar. *Report to the Environmental Agency of Canary Islands Government*, Las Palmas de Gran Canaria.

Bannerman, D. A. 1963 *Birds of the Atlantic Islands* Vol. 1, A history of the birds of the Canary Islands and of the Salvages. Oliver & Boyd, Edimburg.

Betancort, M. J. 1993 Informe de vegetación de las actividades realizadas en la Charca de Maspalomas. *Report to the Environmental Agency of Canary Islands Government*, Las Palmas de Gran Canaria.

Congdon, R. A. & McComb, A. J. 1979 Productivity of *Ruppia*: seasonal changes and dependence on light in an Australia estuary. *Aquatic Botany* **6**, 121–132.

Crisp, D. J. 1971 Energy flow measurements. In *Methods for the Study of Marine Benthos* (Holure, N. A. & McIntyne A. D., eds). International Biological Programme Handbook N16, Blackwell Scientific, Oxford, pp. 197–279.

Edwards, R. R. C. 1978 Ecology of a coastal lagoon complex in Mexico. *Estuarine and Coastal Marine Science* **6**, 75–92.

Evans, A. S., Webb, K. L. & Penhale, P. A. 1986 Photosynthetic temperature acclimatation in two coexisting seagrasses *Zostera marina* L. and *Ruppia maritima* L. *Aquatic Botany* **24**, 185–197.

Fenchel, T. 1982 Ecology of heterotrophic microflagellates. II. Bioenergetics and growth. *Marine Ecology Progress Series* **8**, 225–231.

Field, J. C., Moloney, C. L. & Attwood, C. G. 1989 Network analysis of simulated succession after an upwelling event. In *Network Analysis in Marine Ecology: Methods and Applications* (Wulff, F. W., Field, J. G. & Mann, K. H. eds). Springer Verlag, Berlin pp. 132–158.

Finn, J. T. 1976 Measures of ecosystem structure and function derived from analysis of flows. *Journal of Theoretical Biology* **41**, 535–546.

Flores-Verdugo, F. J., Day, J. W. Jr., Mee, L. & Briseño-Dueñas, R.1988 Phytoplankton production and seasonal biomass variation of seagrass, *Ruppia maritima* L. in a tropical lagoon with an ephemeral inlet. *Estuaries* **11**, 51–56.

Gafiychuk, V. V. & Ulanowicz, R. E. 1996 Self-development and distributed self-regulation in dissipative networks. Ref. No. CBL 96-010, Chesapeake Biological Laboratory, Solomons, Maryland.

Gibbons, D. W. 1989 Seasonal reproductive success of the moorhen *Gallinula chloropus*: the importance of the male weight. *Ibis* **131**, 57–68.

Golley, F. B. 1974 Structural and functional properties as they influence ecosystem stability. In *Proceedings of the First International Congress of Ecology*. (Cave, A. J., ed.) Centre for agricultural Publishing and Documentation, Wageningen, Netherlands.

Haas, L. W. 1982 Improved epifluorescence microscopy for observing planktonic micro-organisms. *Annales de l'Institute Oceanographique, Paris* **58**, 261–266.

Hannon, B. 1973 The structure of ecosystems *Journal of Theoretical Biology* **41**, 535–546.

Harrison, P. G. 1982 Seasonal and year-to-year variations in mixed intertidal populations of *Zostera japonica* Ashers. & Graeb. and *Ruppia maritima*. *Aquatic Botany* **14**, 357–371.

Hirata, H. & Ulanowicz, R. E. 1984 Information theoretical analysis of ecological network. *International Journal Systems Science* **5**, 261–270.

Hobbie, J. E. & Williams, P. J. leB. (eds) 1984 *Heterotrophic Activity in the Sea*. Plenum Press, New York.

Holling, C. S. 1986 The resilience of terrestrial ecosystems: Local surprise and global change. In *Sustainable Development of the Biosphere* (Clark, W. C. & Munn, R. E., eds). Cambridge University Press, Cambridge, pp.292–317.

Holm-Hansen, O., Lorenzen, C. J., Holmes, R. W. & Strickland, J. D. H. 1965 Fluorimetric determination of chlorophyll. *Journal du Conseil International pour l'Exploration de la Mer* **30**, 3–15.

Jorgensen, S. E., Nielsen, S. N. & Jorgensen, L. A. 1991 *Handbook of Ecological parameters and Ecotoxicology*. Elsevier.

Kay, J. J., Graham, L. A. & Ulanowicz, R. E. 1989 A detailed guide to network analysis. In *Network Analysis in Marine Ecosystems: Methods and Applications* (Wulff, F., Field, J. G., & Mann K. H. eds). Springer-Verlag, Heidelberg, pp. 15–61.

Landry, M. R. & Hasset, R. P. 1982 Estimating the grazing impact of marine micro-zooplankton.*Marine Biology* **67**, 283–288.

Leontief, W. W.1936 Quantitative input-output relations in the economic system of the United States. *Review of Economics and Statistics* **18**, 105–125.

Leontief, W. W. 1951 *The structure of American Economy 1919–1939*. Oxford University Press, New York, pp. 257.

Levine, S. H.1980 Several measures of trophic structure applicable to complex food webs. *Journal of Theoretical Biology* **83**, 195–207.

Lindeman, R. L. 1942 The trophic-dynamic aspect of ecology. *Ecology* **23**, 399–418.

Llinàs, O., Ojeda, A. & O'Shanahan, L. 1986 Breve informe sobre la Charca de Maspalomas. *Report to the Environmental Agency of Canary Islands Government*, Las Palmas de Gran Canaria.

Longhurst, A. R. 1984 The importance of measuring rates and fluxes in marine ecosystems. In *Flows of Energy and Material in Marine Ecosystems: Theory and Practice* (Fasham, M. R. J., ed.). Plenum Press, New York, pp. 1–32.

Lovegrove, T. 1966 The determination of dry weight of plankton and the effect of various factors on the values obtained. In *Some Contemporary Studies in Marine Sciences* (Barnes, H. ed.). George Allen & Unwin Ltd., London, pp. 429–467.

Mann, K. H., Field, J. G. & Wulff, F. 1989 Network analysis in marine ecology: an assessment. In *Network Analysis in Marine Ecology and Applications* (Wulff, F., Field, J. G. & Mann, K. H. eds). Springer-Verlag, Heidelberg, pp. 259–282.

Margalef, R. 1982 *Ecologia*. Omega, Barcelona.

Margalef, R. 1983 *Limnologia*. Omega, Barcelona.

Menendez, M. & Comin, F. A. 1990 Consumption of macrophytes by invertebrates in Tancada lagoon (NE Spain). *Scientia Marina* **54**, 139–144.

Menendez, M. & Peñuelas, J. 1993 Seasonal photosynthetic and respiratory responses of *Ruppia cirrhosa* (Pentagna) Grande to changes in light and temperature. *Archive fur Hydrobiologie* **129**, 221–230.

Moreno, M. T. 1996 *Estructura trófica de la comunidad de peces de la Charca de Maspalomas (Gran Canaria, Islas Canarias), un ecosistema de aguas salobres regenerado*. Unpublished master thesis. University of Las Palmas de Gran Canaria, Spain.

Odum, H. T. 1969 The strategy of ecosystem development. *Science* **164**, 262–270.

Odum, H. T. 1971 *Environment, Power and Society*. Wiley, New York.

Parsons, T. R., Takahashi, M. & Hargrave, B. 1984 *Biological Oceanographic Processes*. Pergamon Press.

Patronato de la Charca de Maspalomas 1993 Informe de vegetacion de las actividades realizadas en la Charca de Maspalomas. *Report to the Environmental Agency of Canary Islands Government*, Las Palmas de Gran Canaria.

Pentecost, A. 1984 The growth of *Chara globularis* and its relationship to calcium carbonate deposition in Malham Tarn. *Field Studies* **6**, 53–58.


© Del documento, los autores. Digitalización realizada por ULPGC. Biblioteca Universitaria, 2009

Peterson, B. J. 1984 Synthesis of carbon stocks and flows in the open ocean mixed layer. In *Heterotrophic Activity in the Sea*. (Hobbie, J. E. & Williams, P. J. leB., eds). Plenum Press, New York, pp. 547–555.

Porter, K. G. & Feig, Y. S. 1980 The use of DAPI for identifying and counting aquatic microflora. *Limnology and Oceanography* **25**, 943–948.

Rutledge, R. W., Basore, B. L. & Mulholland, R. J. 1976 Ecological stability: an information theory viewpoint. *Journal of Theoretical Biology* **57**, 355–371.

Strickland, J. D. H. 1960 Measuring the production of marine phytoplankton. *Fisheries Research Board of Canada Bulletin* **122**, 172.

Szyrmer, J. & Ulanowicz, R. E. 1987 Total flows in ecosystems. *Ecological Modelling* **35**, 123–136.

Ulanowicz, R. E. (in press) Life after Newton: An ecological metaphysic. *Biosystems*.

Ulanowicz, R. E. 1983 Identifying the structure of cycling ecosystems. *Mathematical Bioscience* **65**, 219–237.

Ulanowicz, R. E. 1984 Community measures of marine food networks and their possible applications. In *Flows of Energy and Materials in Marine Ecosystems* (Fasham M. R. J., ed.) Plenum Press, New York, pp. 23–47.

Ulanowicz, R. E. 1986*a* *Growth and Development: Ecosystems Phenomenology*. Springer-Verlag, New York, pp. 203.

Ulanowicz, R. E. 1986*b* A phenomenological perspective of ecological development. In *Aquatic Toxicology and Environmental Fate* Vol. 9. (Poston, T. M. & Purdy, R., eds) ASTM STP 921, American Society for Testing and Materials, Philadelphia, USA, pp. 73–81.

Ulanowicz, R. E. 1995 Ecosystem trophic foundations: *Lindeman exonerata*. In *Complex Ecology: The part-Whole Relation in Ecosystems* (Patten, B. C. & Jorgensen, S. E., eds). Prentice Hall PTR, New Jersey, pp. 549–567.

Ulanowicz, R. E. 1996 *DATBAL [Computer Software]*. Solomons, MD.

Ulanowicz, R. E. 1997 *Ecology, the Ascendent Perspective*. Columbia University Press, New York, pp. 201.

Ulanowicz, R. E. & Kay, J. J. 1991 A package for the analysis of ecosystem flow networks. *Environmental Software* **6**, 131–142.

Ulanowicz, R. E. & Kemp, W. M. 1979 Toward canonical trophic aggregations. *American Naturalist* **114**, 871–883.

Ulanowicz, R. E. & Mann, K. H. 1981 Ecosystem stress. In *Mathematical Models in Biological Oceanography* (Platt, T., Mann, K. H., & Ulanowicz, R., eds). UNESCO Press, Paris, pp. 133–137.

Ulanowicz, R. E. & Norden, J. S. 1990 Symmetrical overhead in flow networks. *International Journal Systems Science* **21**, 429–437.

Ulanowicz, R. E. & Platt, T. 1985 Ecosystem theory for biological oceanography. *Canadian Journal of Fisheries and Aquatic Science* **213**, 1–260.

Ulanowicz, R. E. & Wulff, F. 1991 Comparing ecosystem structures: The Chesapeake Bay and the Baltic Sea. In *Comparative Analyses of Ecosystems* (Cole, J., Lovett, G. & Findlay, S., eds). Springer-Verlag, New York.

UNESCO 1968 Zooplankton sampling. *Monography of Oceanographical Methods* **2**, 1–174.

UNESCO 1994 *Protocols for the Joint Global Ocean Flux Study (JGOFS) Core Measurements*. Manual and Guides Vol. 29.

Valiela, I. 1984 *Marine Ecological Processes*. Springer-Verlag, New York.

Verhoeven, J. T. A. 1980*a* The ecology of *Ruppia*-dominated communities in Western Europe. 2. Synecological classification. Structure and dynamics of the macroflora and macrofauna communities. *Aquatic Botany* **8**, 1–85.

Verhoeven, J. T. A. 1980*b* The ecology of *Ruppia*-dominated communities in western Europe. 3. Aspects of production, consumption and descomposition. *Aquatic Botany* **8**, 209–253.

Williams, P. J. LeB. & Jenkinson, N. W. 1982 A transportable microprocessor-controlled precise Winkler titration suitable for field station and shipboard use *Limnology and Oceanography* **27**, 576–584.

Wootton, R. J. 1992 *Fish Ecology*. Chapman & Hall, New York.

© Del documento, los autores. Digitalización realizada por ULPGC. Biblioteca Universitaria, 2009

## Appendix

| Compartment | Flux | Stage | Magnitude mg C $m^{-2}$ $day^{-1}$ | Source or estimation |
|---|---|---|---|---|
| Phytoplankton<2 μm | Primary production | First | 25 | Primary production measured by oxygen changes (μmol $O_2 l^{-1} hr^{-1}$) in *in situ* incubated BOD bottles (Microwinkler titration). Per unit biomass rates are multiplied by the chlorophyll in <2μm fraction. The flux is expressed as mg C $m^{-2}$ $day^{-1}$ considering a photosynthetic quotient of 1·2 (Parsons *et al.*, 1984), a mean depth of 1 m and the sunlight hours at each stage. |
| | | Second | 469 | |
| | | Third | 785 | |
| | Respiration | First | 5 | 20% of primary production (Moshkina, 1961; Parsons *et al.*, 1984; Williams, 1984; Sakshaug *et al.*, 1989; and Baird & Ulanowicz, 1989). |
| | | Second | 94 | |
| | | Third | 157 | |
| | Exudation 1→15 | First | 6 | 25% of primary production (Valiela, 1984; Baird & Ulanowicz, 1989; and Jorgensen *et al.*, 1991). |
| | | Second | 117 | |
| | | Third | 197 | |
| | Death 1→16 | First | 1 | Death rate is assumed to be 9·6% of primary production (Jorgensen *et al.*, 1991). |
| | | Second | 45 | |
| | | Third | 75 | |
| | 1→7 | First | 13 | By difference, assuming a balanced compartment. |
| | | Second | 213 | |
| | | Third | 357 | |
| Phytoplankton>2μm | Primary production | First | 17 | Same as for <2 μm phytoplankton, but multiplying by the chlorophyll in >2 μm fraction. |
| | | Second | 196 | |
| | | Third | 1041 | |
| | Respiration | First | 4 | Assumed to be 20% of primary production (Moshkina,1961; Parsons *et al.*, 1984; Williams, 1984; Sakshaug *et al.*, 1989 and Baird & Ulanowicz, 1989). |
| | | Second | 39 | |
| | | Third | 208 | |
| | Exudation 2→15 | First | 4 | 25% of primary production (Valiela, 1984; Baird & Ulanowicz, 1989, and Jorgensen *et al.*, 1991). |
| | | Second | 49 | |
| | | Third | 260 | |
| | Death 2→16 | First | 1 | Assumed to be 9·6% of primary production (Jorgensen *et al.*, 1991). |
| | | Second | 19 | |
| | | Third | 53 | |
| | 2→7 | First | 4 | Chlorophyll consumption rate was measured by grazing experiments (Landry y Hasset, 1982) and transformed to carbon units using a C:Chl *a* ratio of 30 (Antia *et al.*, 1963; Parsons *et al.*, 1984; and Jorgensen *et al.*, 1991). |
| | | Second | 67 | |
| | | Third | 398 | |
| | 2→8 | First | 4 | By difference, assuming a balanced compartment. |
| | | Second | 22 | |
| | | Third | 122 | |
| *Ruppia maritima* | Primary production | First | 2760 | Primary production estimations (mg $O_2$ g $dw^{-1}$ $h^{-1}$) for different coastal lagoons were used (Congdon & McComb, 1979; Evans *et al.*, 1986; and Menendez & Peñuelas, 1993). mg C $m^{-2}$ $day^{-1}$ were calculated on the basis of biomass estimations, sunlight hours in each sampling and a photosynthetic quotient of 1. |
| | | Second | 120 | |
| | | Third | 0 | |
| | Respiration | First | 1512 | *R* is calculated using respiration rates measured for *R. maritima* (mg $O_2$ g $dw^{-1}$ $h^{-1}$) at different production rates (Edwards, 1978). mg C $m^{-2}$ $day^{-1}$ were calculated from the estimated biomass, a respiratory quotient = 1 and an homogeneous 24 hour respiration cycle. |
| | | Second | 66 | |
| | | Third | 0 | |
| | Exudation 3→15 | First | 696 | Using net production data for *R. maritima* from Edwards (1978) an exudation rate of 25·2% of gross production is calculated. |
| | | Second | 30 | |
| | | Third | 0 | |

© Del documento, los autores. Digitalización realizada por ULPGC. Biblioteca Universitaria, 2009

**Appendix *continued***

| Compartment | Flux | Stage | Magnitude mg C m$^{-2}$ day$^{-1}$ | Source or estimation |
|---|---|---|---|---|
| *Ruppia maritima* continued | 3→10 | First | 91 | Calculated from consumption to biomass indices for *Gammarus* sp. feeding on *R. maritima* (Menendez & Comin, 1990). Biomass of anphypods from direct measurements. |
| | | Second | 8 | |
| | | Third | 0 | |
| | 3→11 | First | 10 | Calculated from a 5% diel consumption to biomass index (Wootton, 1992). *Liza aurata* biomass was estimated by Moreno (1996). |
| | | Second | 10 | Stomach content analysis (Moreno, 1996) showed that benthic producers were 10% of *Liza aurata* diet. Ingestion was apportioned between the benthic producers based on their abundance. |
| | | Third | 0 | |
| | 3→12 | First | 3 | Calculated from a 2·8% diel consumption to biomass index (Wootton, 1992). Benthic producers represent 34% of *D. sargus* diet (Moreno 1996). Ingestion is apportioned between the benthic producers based on their abundance. |
| | | Second | 3 | |
| | | Third | 0 | |
| | 3→4 | First | 5 | Calculated from a 9% diel consumption to biomass index (Gibbons, 1989). Biomass estimated from visual census. *R. maritima* is considered to represent 85% of *G. chloropus* diet. |
| | | Second | 0 | |
| | | Third | 0 | |
| | Death 3→17 | First | 446 | By difference. |
| | | Second | 2 | |
| | | Third | 0 | |
| *Chara globularis* | Primary production | First | 151 | Calculated multiplying production (μ C g dw$^{-1}$ h$^{-1}$) data from the literature (Pentecost, 1984) by historical biomass data (Betancort, 1993) and sunlight hours at each sampling. |
| | | Second | 29 | |
| | | Third | 0 | |
| | Respiration | First | 66 | 44% of primary production (Haniffa & Pandian, 1978). |
| | | Second | 13 | |
| | | Third | 0 | |
| | Exudation 4→15 | First | 38 | 25% of primary production (Valiela, 1984; Baird & Ulanowicz, 1989; and Jorgensen *et al.*, 1991). |
| | | Second | 7 | |
| | | Third | 0 | |
| | 4→1 | First | 5 | Calculated from a 5% diel consumption to biomass index (Wootton, 1992). *Liza aurata* biomass estimated by Moreno (1996). Stomach contents (Moreno, 1996) show that benthic producers represent 10% of *L. aurata* diet. Ingestion is apportioned between the benthic producers based on their abundance. |
| | | Second | 5 | |
| | | Third | 0 | |
| | 4→12 | First | 1 | Calculated from a 2·8% diel consumption to biomass index (Wootton, 1992). *Diplodus sargus* biomass estimated by Moreno (1996). Stomach contents (Moreno, 1996) show that benthic producers represent 34 of *D Sargus* diet. Ingestion is apportioned between the benthic producers based on their abundance. |
| | | Second | 1 | |
| | | Third | 0 | |
| | Death 4→17 | First | 42 | By difference. |
| | | Second | 3 | |
| | | Third | 0 | |
| Cladophora | Primary production | First | 40 | Calculated multiplying production (μg C g dw$^{-1}$ h$^{-1}$) data from the literature (Gordon *et al.*, 1980; Lester *et al.*, 1988 and Dodds & Gudder, 1992) by the biomass and the sunlight hours in each sampling. |
| | | Second | 8 | |
| | | Third | 0 | |

© Del documento, los autores. Digitalización realizada por ULPGC. Biblioteca Universitaria, 2009

**Appendix *continued***

| Compartment | Flux | Stage | Magnitude mg C m$^{-2}$ day$^{-1}$ | Source or estimation |
|---|---|---|---|---|
| Cladophora continued | Respiration | First | 8 | 20% of primary production (Dodds & Gudder, 1992). |
| | | Second | 2 | |
| | | Third | 0 | |
| | Exudation 5→15 | First | 10 | 25% of primary production (Valiela, 1984; Baird & Ulanowicz, 1989; and Jorgensen *et al.*, 1991). |
| | | Second | 2 | |
| | | Third | 0 | |
| | 5→11 | First | 2 | Calculated from a 5% diel consumption to biomass index (Wootton, 1992). *Liza aurata* biomass estimated by Moreno (1996). Stomach contents (Moreno, 1996) show that benthic producers represents 10% of *L. aurata* diet. Ingestion is apportioned between the benthic producers based on their abundance. |
| | | Second | 2 | |
| | | Third | 0 | |
| | 5→12 | First | 1 | Calculated from a 2·8% diel consumption to biomass index (Wootton, 1992), by *D. sargus* biomass estimated by Moreno (1996). Stomach contents (Moreno, 1996) show that benthic producers represent 34% of *D. sargus* diet. Ingestion is apportioned between the benthic producers based on their abundance. |
| | | Second | 1 | |
| | | Third | 0 | |
| | Death 5→17 | First | 20 | By difference. |
| | | Second | 1 | |
| | | Third | 0 | |
| Pelagic Bacteria | DOC assimilation | First | 255 | DOC assimilation was estimated using community respiration measured in oxygen *in situ* incubations. Respiration coefficients for planktonic organisms were obtained from literature. Bacteria assimilation was adjusted to equal plankton respiration at the measured respiration rates. |
| | | Second | 1326 | |
| | | Third | 4715 | |
| | POC assimilation | First | 6 | Was assumed to be 2·5% of DOC assimilation. |
| | | Second | 33 | |
| | | Third | 117 | |
| Pelagic Bacteria | Respiration | First | 104 | Obtained from the planktonic community respiration estimations. |
| | | Second | 544 | |
| | | Third | 1933 | |
| | 6→7 | First | 99 | By difference, assuming a balanced compartment. Results were always below maximum grazing capability calculated from grazing experiments performed as in Landry and Hasset (1982). Carbon units were obtained using a C:Chl *a* ratio of 30 (Antia *et al.*, 1963; Parsons *et al.*, 1984; and Jorgensen *et al.*, 1991). |
| | | Second | 516 | |
| | | Third | 1836 | |
| | 6→15 | First | 44 | 17% of assimilation (Peterson, 1984). |
| | | Second | 231 | |
| | | Third | 812 | |
| | Death 6→16 | First | 13 | 5% of assimilation (Peterson, 1984). |
| | | Second | 68 | |
| | | Third | 242 | |
| Microzooplankton | Respiration | First | 35 | 30% of ingestion (Fenchel, 1982; Peterson, 1984). |
| | | Second | 239 | |
| | | Third | 777 | |
| | Excretion 7→15 | First | 17 | 15% of ingestion (Fenchel, 1982; Peterson, 1984). |
| | | Second | 119 | |
| | | Third | 389 | |

© Del documento, los autores. Digitalización realizada por ULPGC. Biblioteca Universitaria, 2008

**Appendix *continued***

| Compartment | Flux | Stage | Magnitude mg C m$^{-2}$ day$^{-1}$ | Source or estimation |
|---|---|---|---|---|
| Microzooplankton continued | 7→8 | First | 47 | By difference, assuming a balanced prey compartment. Results were below maximum grazing capability calculated from grazing experiments performed as in Landry and Hasset (1982). Carbon units were obtained using a C:Chl *a* ratio of 30 (Antia *et al.*, 1963; Parsons *et al.*, 1984; and Jorgensen *et al.*, 1991). |
| | | Second | 320 | |
| | | Third | 1037 | |
| | Death 7→16 | First | 17 | By difference |
| | | Second | 119 | |
| | | Third | 389 | |
| Mesozooplankton | Respiration | First | 27 | 50·5% of ingestion (Margalef, 1983). |
| | | Second | 177 | |
| | | Third | 611 | |
| | Egestion 8→16 | First | 15 | 30% of ingestion (Jorgensen *et al.*, 1991). |
| | | Second | 105 | |
| | | Third | 363 | |
| | 8+1 | First | 1 | Due to the absence of zooplankton in the stomach contents studies (Moreno, 1996) a minimum consumption was assumed since ingestion studies were carried out during low zooplankton abundance periods. |
| | | Second | 1 | |
| | | Third | 2 | |
| Mesozooplankton | 8→15 | First | 8 | 15% of ingestion (Jorgensen *et al.*, 1991). |
| | | Second | 53 | |
| | | Third | 181 | |
| | Death 8→17 | First | 7 | By difference |
| | | Second | 52 | |
| | | Third | 53 | |
| Benthic deposit feeders | Respiration | First | 475 | 32% of ingestion (Moreno, 1996). |
| | | Second | 158 | |
| | | Third | 4072 | |
| | 9→11 | First | 16 | Calculated from a 5% diel consumption to biomass index (Wootton 1992). *Liza aurata* biomass estimated by Moreno (1996). Stomach contents (Moreno, 1996) show that benthic producers represent 10% of *L. aurata* diet. Ingestion is apportioned between the benthic producers based on their abundance. |
| | | Second | 16 | |
| | | Third | 19 | |
| | 9→12 | First | 5 | Calculated from a 2·8% diel consumption to biomass index (Wootton 1992). Biomass estimated by Moreno (1996). Stomach contents (Moreno 1996) show that benthic producers represent 34% of *Diplodus sargus* diet. Ingestion is apportioned between the benthic producers based on their abundance. |
| | | Second | 5 | |
| | | Third | 11 | |
| | 9→13 | First | 2 | Calculated from a 0·5% diel consumption to biomass index (Wootton, 1992). *Dicentrarchus punctatus* biomass estimated by Moreno (1996). Stomach contents (Moreno, 1996) show that benthic deposit feeders represent 59% of *D. punctatus* diet. |
| | | Second | 2 | |
| | | Third | 2 | |
| | Egestion and death 9→17 | First | 987 | By difference. |
| | | Second | 313 | |
| | | Third | 8635 | |
| Anphypods | Respiration | First | 28 | 30% of ingestion (Verhoeven, 1980*a*). |
| | | Second | 176 | |
| | | Third | 33 | |

© Del documento, los autores. Digitalización realizada por ULPGC. Biblioteca Universitaria, 2009

**Appendix *continued***

| Compartment | Flux | Stage | Magnitude mg C m$^{-2}$ day$^{-1}$ | Source or estimation |
|---|---|---|---|---|
| Anphypods continued | 10→11 | First | 17 | Calculated from a 5% diel consumption to biomass index (Wootton, 1992). Stomach contents (Moreno, 1996) show that anphypods represent 10% of *L. aurata* diet. |
| | | Second | 17 | |
| | | Third | 19 | |
| | 10→12 | First | 1 | Calculated from a 2·8% diel consumption to biomass index (Wootton, 1992). Stomach contents (Moreno, 1996) show that anphypods represent 14% of *D. sargus* diet. |
| | | Second | 1 | |
| | | Third | 1 | |
| | 10→14 | First | 1 | Calculated from a 9% diel consumption to biomass index (Gibbons, 1989). *Gallinula chloropus* biomass estimated from visual census. It is considered that anphypods represent 15% of *G. chloropus* diet. |
| | | Second | 1 | |
| | | Third | 1 | |
| | Death | First | 45 | By difference. |
| | 10→17 | Second | 375 | |
| | | Third | 56 | |
| *Liza aurata* | Respiration | First | 44 | 30% of ingestion (Wootton, 1992). |
| | | Second | 44 | |
| | | Third | 44 | |
| | Excretion | First | 10 | 7·5% of ingestion (Wootton, 1992). |
| | 11→15 | Second | 10 | |
| | | Third | 10 | |
| | Egestion | First | 76 | 52% of ingestion (Wootton, 1992). |
| | 11→17 | Second | 76 | |
| | | Third | 76 | |
| *Diplodus sargus* | Respiration | First | 5 | 44% of ingestion (Wootton, 1992). |
| | | Second | 5 | |
| | | Third | 5 | |
| | Excretion | First | 1 | 7·5% of ingestion (Wootton 1992) |
| | 12→15 | Second | 1 | |
| | | Third | 1 | |
| | Egestion | First | 5 | 38% of ingestion (Wootton, 1992). |
| | 12→17 | Second | 5 | |
| | | Third | 5 | |
| *Dicentrarchus punctatus* | Respiration | First | 1·5 | 37% of ingestion (Wootton, 1992). |
| | | Second | 1·5 | |
| | | Third | 1·5 | |
| | Excretion | First | 0·1 | 7·5% of ingestion (Wootton, 1992). |
| | 13→15 | Second | 0·1 | |
| | | Third | 0·1 | |
| | Egestion | First | 0·9 | 22·5% of ingestion (Wootton, 1992). |
| | 13→17 | Second | 0·9 | |
| | | Third | 0·9 | |
| *Gallinula chloropus* | Respiration | First | 1 | 0·534 $W^{0.723}$, where W is the *G. chloropus* biomass (Gibbons, 1989). |
| | | Second | 1·4 | |
| | | Third | 0·8 | |
| *Gallinula chloropus* | Excretion | First | 3·5 | 8% of ingestion (Gibbons, 1989). |
| | 14→5 | Second | 2·8 | |
| | | Third | 1·1 | |
| | Egestion | First | 0·5 | 50% of ingestion (Gibbons, 1989). |
| | 14→17 | Second | 0·7 | |
| | | Third | 0·4 | |
| | Exports | First | 0·5 | 8% of ingestion (Gibbons, 1989). |
| | | Second | 0·7 | |
| | | Third | 0·4 | |

© Del documento, los autores. Digitalización realizada por ULPGC. Biblioteca Universitaria, 2009

**Appendix *continued***

| Compartment | Flux | Stage | Magnitude mg C m$^{-2}$ day$^{-1}$ | Source or estimation |
|---|---|---|---|---|
| DOC | Bacterial assimilation 15→6 | First | 255 | DOC assimilation was estimated using community respiration measured in oxygen *in situ* incubations. Respiration coefficients for planktonic organisms were obtained from literature. Bacteria assimilation was adjusted to equal plankton respiration at the measured respiration rates. |
| | | Second | 1326 | |
| | | Third | 4715 | |
| | Aggregation 15→16 | First | 45 | 15% of the DOC concentration y$^{-1}$ (Peterson, 1984). |
| | | Second | 234 | |
| | | Third | 832 | |
| POC | Bacterial assimilation 16→6 | First | 6 | Was assumed to be 2·5% of DOC assimilation. |
| | | Second | 33 | |
| | | Third | 117 | |
| | 16→8 | First | 2 | Is calculated from the total zooplankton grazing and the relative abundance of POC compared to the other food resources. |
| | | Second | 9 | |
| | | Third | 51 | |
| | Sedimentation 16→7 | First | 108 | 30% of all POC inlets (Peterson, 1984; Jorgensen *et al.*, 1991). |
| | | Second | 341 | |
| | | Third | 2450 | |
| Sedimented Organic Carbon | Respiration | First | 700 | Calculated from subtracting to the total ecosystem respiration, which was calculated from diel oxygen cycles (Fast *et al.*, 1988), the estimated respiration for all other compartments. |
| | | Second | 700 | |
| | | Third | 2661 | |
| | 17→9 | First | 1485 | Calculated using a consumption:biomass ratio of 450% (Moreno, 1996). Benthic deposit feeder carbon concentration was obtained from sediment samples. |
| | | Second | 495 | |
| | | Third | 12 726 | |
| | 17→10 | First | 0 | Calculated from *Gammarus* sp. average consumption demand (Menendez & Comin 1990). It is assumed that *Gammarus* sp. preferably feeds on *R. maritima* and diet is compleated by sediment ingestion. |
| | | Second | 561 | |
| | | Third | 109 | |
| Sediment | 17→11 | First | 82 | Calculated from a 5% diel consumption to biomass index (Wootton, 1992). Stomach contents (Moreno, 1996) show that detritus can represent 70% of *L. aurata* diet. Only if other resources are not available the demand is compensated with detritus ingestion. |
| | | Second | 82 | |
| | | Third | 94 | |
| | 17→12 | First | 2 | Calculated from a 2·8% diel consumption to biomass index (Wootton, 1992). Stomach contents (Moreno, 1996) show that detritus may represent 18% of *D. sargus* diet. Only if other resources are not available the demand is compensated with detritus ingestion. |
| | | Second | 2 | |
| | | Third | 2 | |
| | 17→13 | First | 1 | Calculated from a 0·5% diel consumption to biomass index (Wootton, 1992). Stomach contents (Moreno, 1996) show that detritus may represent 41% of *D. punctatus*. |
| | | Second | 1 | |
| | | Third | 1 | |
| | 17→14 | First | 0 | By difference between *R. maritima* availability and *G. chloropus* consumption demand. |
| | | Second | 5 | |
| | | Third | 3 | |

© Del documento, los autores. Digitalización realizada por ULPGC. Biblioteca Universitaria, 2009

# ECOLOGY AND DISTRIBUTION OF THE GENUS *TAMARIX* L. (TAMARICALES: TAMARICACEAE) ON THE ISLAND OF GRAN CANARIA

By A.R. BARRY * & A. LUQUE *

With 1 plate

*ABSTRACT.* The genus *Tamarix* L. (Tamaricaceae) presents a complex taxonomy due to the polymorphic characteristics and that even the smallest morphological differences are used in its classification.

The aim of this work is to study the present distribution in Gran Canaria of the different species of the *Tamarix* L. in relation to the characteristics of their habitat (i.e. altitude, temperature, soil, humidity, etc.) and to investigate their ancient distribution to best aid the taxonomy of their species and know the abundance and the ecologic interest in appointment to their level of protection.

## INTRODUCTION

### The species

Currently, there are two recognized non-endemic species of the *Tamarix* LINNE, 1753, genus in the Canary Islands, *Tamarix canariensis* Willdenow, 1816, and *Tamarix africana* POIRET, 1789.

*T. canariensis* Willd. has been mentioned for all the islands, while *T. africana* Poir. is only found in Lanzarote, Fuerteventura, Gran Canaria and Tenerife (HANSEN & SUNDING, 1993). Both species have also been recorded as existing in the other islands of the Macaronesia. *T. canariensis* Willd. also grows on some of the Cape Verde Islands, *T. africana* Poir. in some of islands of the Azores and on the Madeira island only *Tamarix gallica* LINNE, 1753, is found (HANSEN & SUNDING, 1993). *T. gallica* L. is not found living on Madeira island because they are confounded with *T. canariensis* WILLD. (BAUM 1978), and *T. canariensis* WILLD. From Cape Verde islands is possibly confounded with *T. senegalensis* DE CONDOLLE, 1828.

* Grupo de Ecología Litoral. Departamento de Biología, Universidad de Las Palmas de Gran Canaria. 35017, Las Palmas, Islas Canarias, España

**Bol. Mus. Mun. Funchal,** Sup. no. 5: 47-58, 1998 ISSN 0870-3876

© Del documento, los autores. Digitalización realizada por ULPGC. Biblioteca Universitaria, 2009

The world distribution of *T. canariensis* Willd. is also distributed to north Africa, south Spain, Corsica and Sardinia while *T. africana* Poir. it is in the same locations and also at the south France and Italy (BAUM, 1978).

On a systematic level, the wild Canarian species represent two Sections and two Series in the islands (BAUM, 1978).

Gen. *Tamarix* L.
- Sec. *Tamarix*
  - Ser. *Leptostachyae* (Bge.) Baum
    - Sp. *T. canariensis* Willd.
- Sec. *Oligadenia* (Ehremb.) Endl.
  - Ser. *Anisandrae* Bge.
    - Sp. *T. africana* Poir.

According to some authors (RIVAS CEMBELLIN et al., 1990), there are some specimens which are difficult to determine at a specific level as they possess intermediate characteristics between *T. gallica* L. and T. *canariensis* Willd., and which have for now been included as *Tamarix* grex *gallica*, without excluding the possible presence of *T. gallica* L., all to be subject to future investigations. We for now at present us will remit to the two recognized species.

Both species of *Tamarix* L. in the Canary Islands are protected under the Law of 20th February, 1991, on the "Protection of Species of Wild Vascular Flora" (BOC, nº 35, 18th March 1991). This fact has been the cause of controversy due to differing opinions about of their ecologic and environmental value on the part of the farmers and the scientific community respectively.

Therefore the principal objective of this study is to clarify the degree of interest that these species arouse by studying:

- The possible naturalization of the species.
- The degree of abundance of the species.
- Areas and ways of distribution.
- Determining factors influencing the distribution.
- Localization in protected areas.

Another specie found cultivated in gardens on the Gran Canaria island is *Tamarix ramosissima* Ledebour, 1829, (BAUM 1978) legitim name of *Tamarix pentandra* Pallas, 1788, mentioned by some authors as BRANWELL & BRANWELL, 1985.

This representation of the genus is thus sparse in the Canary Islands, since the total world number of species from the genus is fifty- four (BAUM, 1978).

**Identification of the species**

The different characteristics used in the determination of both species are very selected

© Del documento, los autores. Digitalización realizada por ULPGC. Biblioteca Universitaria, 2009

due to the high incidence of polymorphy exhibited by individual specimens, with seasonal and sometimes local variations (OZENDA, 1983), and there may even be variations in the flower clusters in the same individual specimen.

One of the key characteristics for the identification of the taxons present in the islands is the presence or absence of a pinnacle on the anthers (RIVAS CEMBELLIN et al, 1990). While *T. canariensis* Willd. has the pinnacle, it is not present in *T. africana* Poir.

KUNKEL (1968) pointed out what the main differents are the colour of the cortex, the size of the racime and the kind of sepals and petals.

In general, the two species show very few morphological variations.

**Antiquity in the Islands**

Without doubt, at least one of the species of *Tamarix* L. has appeared in abundance and spontaneously in the lower areas of the Canarian Archipelago, or at least in the eastern islands, since it is reflected in many place names. Always, this names are referring to "tarajal" or "tarahal" since is in this manner populary known the *Tamarix* L. genus in the Canary islands.

The oldest records of this can be found in the "Le Canarien", written from the year 1404, in which the chronicle relates how in the area of Betancuria (Fuerteventura) "Gadifer de la Salle's men had constructed the tower of Valtarajal", a name which seems to refer to the "Tarajales Valley" (HERNANDEZ RUBIO, 1991).

We can find real evidence of ancient places with the presence of "tarajales" in the toponymy in old maps. TORRIANI (1590) places the beach or port of Taraalejo in the island of Fuerteventura. Furthermore, he presents us with a curious map representing the extreme south of Gran Canaria, from Arguineguín to Maspalomas, which shows groups of trees at the entrance of and along the course of both of these ravines; from their situation, they could be the predecessors of the small woods of "tarajales" which currently exist in these areas of Gran Canaria.

Later on, the existing cartography continues to indicate several similar examples, all of them situated along the east coast of Fuerteventura: Taratalo (SANSON, 1734) Tarajalejo and Gran Tarajal (MACHADO FIESCO, 1762), Gran Tarajalero (TRINIDAD DE HERRERA, 1786), with this type of toponymy continuing growing in number until the present day (LOPEZ, 1986 and TOUS, 1994, 1995 ).

In his "Diccionario de Historia Natural de las Islas Canarias", VIERA Y CLAVIJO (1869) states, "They are numerous in Canaria and Fuerteventura where due to the lack of mountain trees, not only the old inhabitants of Fuerteventura, but also the primitive settlers who came from Europe, made use of them".

According to CACERES & SALAS (1992) in "Nombres de Plantas Canarias", the word "tarahal" is arabic in origin and could have come directly from the north of Africa, where it is called "tara'al", or from the Spanish Mainland with the name "taray", which also comes from Arabic and has been consolidated as "tarahal" and "tarajal" in the islands.

© Del documento, los autores. Digitalización realizada por ULPGC. Biblioteca Universitaria, 2009

A observation which stands out in their plants is the popular tendency of the farmers in the north to call them mostly by the name of "tarahal", while "tarajal" seems more common in the south, and this fact coincides with the oldest place names of the islands and could by relates to *T. canariensis* Willd. and *T. africana* Poir. respectively. Or it could merely open up possibilities about the semantic origin of the word which could in later investigations reflect the origin of these species.

**Uses and exploitation**

Apparently, the aborigines in Fuerteventura used to use "tarajal" wood in the building of their huts as beams superimposed on top of other stronger and sturdier wood. In the same way, the first settlers of the same island also used this wood for beams in their primitive houses (HERNANDEZ RUBIO, 1991).

Medicinally speaking, both species possess astringent properties. Its skin is appetisizing and diuretic (VIERA Y CLAVIJO, 1869). It is a hepatic tonic, especially useful in cases of oppilattions and obstructions in the liver and spleen (JAEN, 1984). It is also effective against dropsy (PEREZ DE PAZ, 1988).

Its seeds or pips possess coloring substances which were used by the ancient dyers as black dye instead of oak apples (VIERA Y CLAVIJO, 1869).

Many *Tamarix* L. possess a sickly sweet substance which has come to be interpreted in many instances as the "manna" of the jews described in the Bible (MOLDENKE, 1952, in BAUM, 1978). LEONCIO RODRIGUEZ (1942) said "in the Canary Islands the tarhais or tarajales distilled a gum as salt, white and beautiful", since they possess glands in the leaves, rachis, bracts and calyx which secrete a sticky substance, causing the unpleasant feel they have to the touch and the impregnation in the soil as well as its salty nature. However, these nectar-like substances in the flowers are very appetising for insects.

The lexivial salt which is extracted from the ashes of the "tarajal" is of the same type as the well-known salt called "glauber", belonging to *Pentandra triginia* (VIERA Y CLAVIJO, 1869).

The "tarajal" is also very effective in the fixing of soil, due to its capacity for taking root in loose ground thus avoiding erosion. It has been used to fix land in the "sorribas" or remove of land carried out along the length and the sides of ravines, avoiding the eroding away of walls and land by rushing water down the ravines.

They have been planted since the beginning of the century along the edges of roads built by the Ministry of Public Works, due to their ground-fixing character, and later they were introduced as ornamental plants, serving in addition as wind-breaks.

A final use which is of great interest and which is fairly widespread so much inside as outside the islands is its use as wood for ribs in the building of small boats, due to its high resistance to salt (SANTOS, 1979).

© Del documento, los autores. Digitalización realizada por ULPGC. Biblioteca Universitaria, 2009

### Habitat of the species

Both species are halophytic plants which tolerate salt spray very well, absorbing it during the day in order to excrete it at night and especially at dawn in the form of dew, as confirmed by certain farmers in the north of the island of Gran Canaria. Several shepherds in the south of the island commented that when the "tarajales" weep at sunset during certain summer months (June-July) it is because we are going to have a rainy winter.

They can lead to the desalinization of the deeper layers of the soil and increase the salinity of the surface layers (BAUM, 1978). The soil's surface is covered every year by a litter or layer of discarded and saline twigs (BAUM, 1978).

The "tarajal" posed grand capacity for taking root in loose ground. They are very good for fixing soil in sandy, desert conditions and good for holding dunes in sandy, coastal areas as to The Maspalomas Dunes where they are spreading widely after an official protection policy came into force.

## MATERIALS AND METHOD

### The zone of study

Gran Canaria is an island situated approximately between 27° 44' and 28° 11' latitude North and 15° 22' and 15° 50' longitude West.

It is more or less conical in shape and has a maximum diameter of 48 km, reaching its maximum height above sea level of 1949 m in the central area (Pico de las Nieves). The surface area above sea level is 1532 km2.

The island has been greatly excavated due to a dense arterial drainage network. A line which goes from the north-west (Agaete) to the south-east (Juan Grande) divides the island into two clear geological halves: the "Paleocanarian" south-west which is of a fundamentally sialic nature and the "Neocanarian" north-east, where the most recent volcanic material of the most basic composition appears on the surface (SANTANA & NARANJO, 1992).

The differences caused by the altitude and orientation make up a mountainous environment of marked contrasts. The altitude which the island reaches creates a facade effect with a slope which is directly exposed to the almost constant influence of the trade winds, called "Alisiocanaria", and another sheltered by it called "Xerocanaria". This dichotomy creates a marked contrast in the distribution of rainfall with a north-eastern half where the rainfall is greater than the annual average of 1,000 mm and the other southwestern half which hardly reaches 600 mm. On the other hand, we find the appearance of the "sea of clouds" produced by the thermal reversal of the trade wind frequently affected by an altitudinal ridge which goes from 600 m to 1500 m, situated between the ravines of Agaete and Telde, generating an additional contribution of water and an increase in relative humidity by means

© Del documento, los autores. Digitalización realizada por ULPGC. Biblioteca Universitaria, 2009

of the phenomenon of "horizontal precipitation". Consequently, we end up with a subhumid facade and a semiarid one.

The island has a population of 750,000 inhabitants spread among numerous population nuclei. The rest of the island's surface is principally used for crops, which are found up to 300 m. with tomatoes, bananas, tobacco and garden vegetables out of season, irrigated crops and ornamental plants in greenhouses. Mediterranean dry crops can be found between 300 m. and 900 m. and above 900 m forest exploitation and livestock raising is carried out.

## Cartography

The work plan consisted of drawing up maps of the units of vegetation on a scale of 1:25,000 using maps edited by the Army Geographical Service corresponding to different years (1976 to 1993). The UTM (Universal Transverse Mercator) coordinates of projection and the level curves for altitude were used as a starting point. The degree of abundance of the species in ravines was studied on quadrilled divided into square kilometers.

On drawing up the maps two types of graphs were made: on the one hand, graphs referring to the existing species in the ravines, which were then transferred to the map both the isolated ones and those found in communities, and on the other hand, graphs showing those situated outside the ravines (generally cultivated), only registering those communities with more than five individuals, discounting isolated species, unless they were large specimens, which were then also charted. Simultaneously, descriptions were recorded in a notebook of the plant landscape along with a floral inventory and other information of interest.

Once all the information had been compiled, it was reworked, specifying the limits, completing altitude data, highlighting the orientation, the situation of meanders and so on.

We have not taken into account oral statements in the drawing up of the map, but they have been of great help in the search for communities as well as for finding other information about the species.

## Expeditions

The prior data which we had at our disposition for the localization of the species was the maximum height above sea level of 400 m. (KUNKEL, 1977), and the preference of the species for coastal areas and ravines. Therefore, we decided to make an exhaustive study of all the ravines by penetrating them from the coast up to 400 m., or on occasions more if we were able to observe some indication of a continuing of the species.

Daily expeditions were made during a period of three months using the hours of daylight to a maximum. Sometimes it was necessary to spend the night in those more remote areas which were key centers on the route, like for example Maspalomas (the south), Veneguera (south-west), Tejeda (the basin and ravine of La Aldea) and Los Berrazales (the

© Del documento, los autores. Digitalización realizada por ULPGC. Biblioteca Universitaria, 2009

north-west). The rest was carried out from the city of Las Palmas.The coastal zones which are inaccessible by land were reached by sea (Güi-Güi).

For the determination of the species we used a lens count-threads, observing the presence of the pinnacle on the anthers of *T. canariensis* WILLD.

## RESULTS

The maximum limit of altitude found for the naturalized species of *T. canariensis* Willd. is 200 m, although the best specimens are found below that at an altitude of around 100 m. The occasional ascent found above this level in some ravines is related to forced plantations and in the same way the relatively abundant presence of his species towards the interior of the island is linked exclusively to plantations, generally on the edges of farms and roads. In low areas out of ravines they also were planted.

The maximum altitude found for the naturalized species of *T. africana* Poir. was observed to be around 350 m (basin of Tejeda and ravine of La Aldea), with possibilities of being found up to 400 m following the banks of the ravines as far as the reservoirs situated on these altitude levels. The optimum of this species is observed to be between 150 m and 250 m in altitude.

With regard to the ecological characteristics observed, we can say that the two species of *Tamarix* L. studied are highly conditioned by edafic factors, with a clear difference between *T. canariensis* Willd., which prefers loose, salines or sandy soil, especially that which is well turned over and impoverished, and *T. africana* Poir, which exclusively seeks detrital-sedimentary alluvial soil on the ravine banks and without too much salt.

Another decisive factor is temperature, although it has more influence in the general geographical distribution than in the local distribution, since we find *T. africana* Poir. towards the south and the west in semi-arid areas of high sunshine, unlike *T. canariensis* Willd. which is best localized in the north up to a height of 200 m or in the coastal regions of the south, but with a clear influence of the temperate zones.

A well-known important factor is the degree of resistance to salt, which is observed to be more marked in *T. canariensis* Willd than in *T. africana* Poir., with the former being found much more developed in estuary areas while the latter is rarely observed in these areas, since generally it is localized up the ravine banks.

The search for aquiferous zones is another important factor, but it is greatly conditioned by temperature and altitude. In this case, while *T. canariensis* Willd. prefers salt and residual water, settling in river beds, meanders, low-lying reservoirs etc., which have briny filtration, irrigation waters etc., *T. africana* Poir. seeks purer waters up the ravine, even getting as far as reservoirs at a higher altitude on an alluvial bank water table.

The distribution of *T. canariensis* is widely localized in many ravines on the north slope, and less in the south, not being found much from the ravine of Moya to the ravine of

© Del documento, los autores. Digitalización realizada por ULPGC. Biblioteca Universitaria, 2009

Agaete (except in a small water-bed near Agaete), although it is observed planted in adjoining land. In the south and west it can be seen in ravines which were intensely cultivated like Maspalomas, Arguineguín, Mogán, La Aldea, El Risco, etc., but only in estuary areas or near them, being widespread in the protected area of the Nature Reserve of the Dunes of Maspalomas. One must think that *T. canariensis* Willd. seems to have an invading character and can turn out to be harmful or disturbing for other plants in the area, as it competes for their habitats and above all it can cause impoverishing of springs and reserves of water.

*T. africana* Poir., is localized exclusively in the south and west of the island, in alluvial soil on the banks of ravines like Fataga, Chamoriscán, Ayagaures, Arguineguín, Mogán, La Aldea (as far as the basin of Tejeda), El Risco (below Tirma) and Guayedra, strictly following the banks,. This species, apart from the natural determining factors of its situation, seems to be situated in those ravines where there were aboriginal settlements.

The most natural appearance of the communities of "tarajales" seems to be found on the banks of ravines following the course of the water near drains, irrigation channels, wells or reservoirs etc. but with a low altitude.

The spontaneous distribution of the species offers clear differences between both. *T. africana* Poir. does not seem to offer any doubt to its natural manner, and can be defined as a native species. *T. canariensis* Willd., however, shows very natural features in areas around the mouths of ravines, but it offers large doubts in the rest. The coastal areas like the Nature Reserve of the Maspalomas Dunes, the ravines of Veneguera and El Risco, the beach of La Aldea etc, according to the data compiled from the area in relation to the existing crops there seem to point to their introduction by man, although rather long ago. Undoubtedly, the Nature Reserve of "Las Dunas de Maspalomas" offers an ecosystem of great beauty which deserves its name, and it may perhaps be the site of the natural introduction of the species, but we must not forget the plantations which existed on the hill of the "Morro de Maspalomas", the "Campo de Golf" and "Campo International" zones, etc.

In the north, the most spontaneous species of *T. canariensis* WILLD. are located in the ravines of Tenoya, El Cardón, Pagador, Cabo Verde etc, but like the rest, they are situated near the crops and appear as large communities lined up in chain formation, bordering the banana plants along the ravine bank, which scarcely leaves any doubt to their anthropic origins.

This non-spontaneous appearance is very heightened in *T. canariensis* Willd. which also seems to have more of an invading nature than *T. africana* Poir, which appears to be wilder and less abundant.

One must detach that *T. canariensis* Willd. is the invading character with a good cutting reproduction, like by power to aid to confirm the before sketch. On the other hand, many ravines have a total absence of both species, although they still have crop plantations nearby on their edges, a fact which could be attributed to the volcanic nature of the soil, to the non-anthropogenic action of the area and the considerable impoverishing of many of them.

The naturalization of *T. canariensis* Willd. in the ravines seems to be relatively

© Del documento, los autores. Digitalización realizada por ULPGC. Biblioteca Universitaria, 2009

recent, since it shows itself to be strongly linked to the presence of crop plantations, where there are species planted along the edges or to fix ground remove of "sorribas" on the sides and banks of ravines so they are not swept away. Possibly *T. canariensis* Willd. brought about as a result of old, destroyed "tarajales" (CEBALLOS & ORTUÑO, 1976). This is not the case with *T. africana* Poir., which is more localized and less widespread, and which could be the real "tarajal" of the guanche aborigines.

So much as we have previously mentioned, the naturalization of the species may not be only due to introductions but to re-introductions of our own species which try to recover the ground that was snatched away from them.

The species *T. ramossima* Ledeb. which is found in some gardens and farm vegetable gardens does not seem to grow wild, at least in the areas under study. This latter species together with the possible group *Tamarix* grex *gallica* is pending future investigation.

**Distribution of the naturalized species of *Tamarix* L. genus in Gran Canaria island**

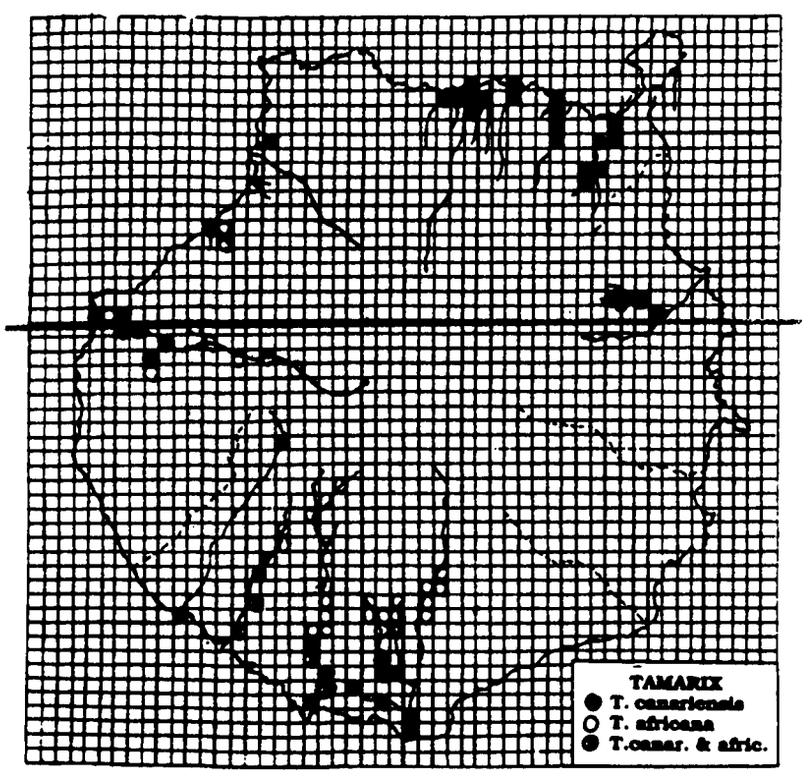


* The symbols of the two species, and both together, have been representated over square of 1 km².

© Del documento, los autores. Digitalización realizada por ULPGC. Biblioteca Universitaria, 2009

## REFERENCES

BAUM, B.R.:

1967. Introduced and Naturalized Tamarisk in the Unites States and Canadá (Tamaricaceae). *Bayleya*, **15**: 19-25.

1978. *The Genus Tamarix*. The Israel Academy of Sciences and Humanities, Jerusalem, pp. 209.

BOC (Official Canarian Bulletin):

1991. Orden 20 de febrero de 1991 sobre Protección de Especies de la Flora Vascular Silvestre de la Comunidad Autónoma Canaria. *Boletin Oficial de Canarias*, **35**: 1324-1334.

BRAMWELL, D. & Z. BRAMWELL:

1985. *Jardines de Canarias III. Plantas Utiles*. Ed. Rueda, Madrid, pp.133.

1990. *Flores Silvestres de las Islas Canarias*. Ed. Rueda, Madrid, pp. 375.

CACERES, M.T. & M. SALAS:

1995. *Los Nombres de las Plantas Canarias*. Excmo. Cabildo Insular de Gran Canaria, Las Palmas de Gran Canaria, pp.161.

CEBALLOS, L. & F. ORTUÑO:

1976. *Estudio Sobre la Vegetación y la Flora Forestal de las Canarias Occidentales*. Excmo. Cabildo Insular deTenerife, Santa Cruz de Tenerife, pp. 433.

CORRALES, C., D. CORBELLA & M.A. ALVAREZ:

1992. *Tesoro Lexicográfico del Español de Canarias*. Real Academia Española de la Lengua y Consejería de Educación Cultura y Deportes del Gobierno de Canarias, Madrid, pp. 972.

FARR, E.R., J.A. LEUSSINK & F.A. STAFLEU:

1979. Tamarix. *Index Nominum Genericorum (Plantarum)*, **3**: 1.721.

HANSEN, A., SANTANA, A. & PEREZ CHACON, E.:

1990. *Mapa de las formas del relieve de Gran Canaria. E. 1:100.000*. Excmo. Cabildo Insular de Gran Canaria, Las Palmas de Gran Canaria, pp. 1.

HANSEN, A. & SUNDING, P.:

1993. Flora of Macaronesia Checklist of Vascular Plant. *Sommerfeltia*, **1**: 1-167.

HERNANDEZ-RUBIO, J.M.:

1991. *Fuerteventura. Hasta la Abolición de los Señorios (1477-1837)*. Excmo. Cabildo Insular

© Del documento, los autores. Digitalización realizada por ULPGC. Biblioteca Universitaria, 2009

de Fuerteventura, Santa Cruz de Tenerife, pp. 648.

JAEN, J.:

1984. *Nuestras Hierbas Medicinales*. Caja Insular de Ahorros de Canarias, Las Palmas de Gran Canaria, pp. 82.

KUNKEL, G.:

1968. Bibliografía Botánica. *Cuadernos de Botánica Canaria*, **3**: 59

1977. Endemismos Canarios. Inventario de las Plantas Vasculares Endémicas de la Provincia de Las Palmas. *ICONA Monografías*, **15**: 436.

LOPEZ, T.:

1986. *Mapa de la Isla de Gran Canaria. Año 1780*. Ser. Geográfico del Ejército, Madrid, pp.1.

OZENDA, P.:

1958. *Flore du Sahara*. Editions du Centre National Recherche Scientifique, Paris, pp. 344-349.

PEREZ DE PAZ, P.L. & I. MEDINA:

1988. *Catálogo de las Plantas Medicinales de la Flora Canaria. Aplicaciones Populares*. Instituto de Estudios Canarios y Viceconsejería de Cultura y Deportes del Gobierno de Canarias, Sta. Cruz de Tenerife, pp. 132

RIVAS CEMBELLIN M.M., M.C. LEON ARENCIBIA & W. WILDPRET DE LA TORRE:

1990. El género *Tamarix* L. (Tamaricaceae): Consideraciones acerca de los taxones presentes en Canarias. *Vieraea*, **19**: 29-44.

RODRIGUEZ, L.:

1982. *Los Arboles Históricos y Tradicionales de Canarias*. Excmo. Cabildo Insular de Tenerife & I. B. Viera y Clavijo, Santa Cruz de Tenerife, pp. 79.

SANTANA, A. & A. NARANJO:

1992. *El Relieve de Gran Canaria*. Ed. Nogal, Las Palmas de Gran Canaria, pp. 108.

SANTOS. A.:

1979. *Arboles de Canarias*. Flora de Canarias I. Ed. Interinsular Canaria, Sta. Cruz de Tenerife, pp. 47.

TOUS, J.:

1994. *Plano de las Yslas de Canaria por don F. Machado Fiesco. Año de 1762*. Museo Militar

© Del documento, los autores. Digitalización realizada por ULPGC. Biblioteca Universitaria, 2009

Regional de Canarias, Santa Cruz de Tenerife, pp. 26

1995. *El primer Mapa Impreso en las Islas Canarias. Mapa con Plano y Vistas de las Yslas de Canaria* por *Josef Trinidad de Herrera*. Museo Militar Regional de Canarias, Santa Cruz de Tenerife, pp. 1

VIERA Y CLAVIJO, J.:

1982. *Diccionario de Historia Natural de las Islas Canarias*. Excma. Mancomunidad de Cabildos de Las Palmas, Madrid, pp. 467.

© Del documento, los autores. Digitalización realizada por ULPGC. Biblioteca Universitaria, 2008

Polar Biol (1999) 21: 11–22 © Springer-Verlag 1999

ORIGINAL PAPER

Gotzon Basterretxea · Javier Aristegui

# Phytoplankton biomass and production during late austral spring (1991) and summer (1993) in the Bransfield Strait

Accepted: 5 July 1998

**Abstract** Phytoplankton biomass and productivity were measured during two cruises in the Bransfield Strait in December 1991 (D91) and January/February 1993 (J93). Strong seasonal variability in productivity values was observed due to differences in the physiological response of phytoplankton. However, although the photosynthetic capacity of phytoplankton was markedly lower in D91 [$P^B_m = 0.61 \pm 0.25$ mg C (mg Chla)$^{-1}$ h$^{-1}$] than in J93 [$P^B_m = 2.18 \pm 0.91$ mg C (mg Chla)$^{-1}$ h$^{-1}$], average water column chlorophyll values in different areas of the strait were approximately similar in D91 (49–78 mg Chla m$^{-2}$) and J93 (22–76 mg Chla m$^{-2}$). The spatial distribution of chlorophyll was patchy and generally associated with the influence of the different water masses that meet together in the Bransfield Strait. No correlation was found between the mixed layer depth and either the integrated chlorophyll or the productivity. Our results suggest that major phytoplankton blooms in the Bransfield Strait are advected from the nearby Gerlache Strait or Bellingshausen Sea following the main eastward surface currents.

## Introduction

Inshore waters west of the Antarctic Peninsula form one of the most productive areas of the Antarctic Ocean (El-Sayed 1968a; Comiso et al. 1990; Sullivan et al. 1993). However, phytoplankton distribution in this region is very patchy in space and time (Holm-Hansen and Mitchell 1991; Priddle et al. 1994). Although inorganic macronutrient concentrations are generally high (Le Jehan and Tréguer 1985) and rarely limit algal growth in the Southern Ocean (Holm-Hansen 1985; Smith 1987), vast areas present high macronutrient and low chlorophyll concentrations (HNLC). It has been suggested that low concentrations of oligoelements like iron may limit phytoplankton growth (Martin et al. 1989; Martin et al. 1990; Baar et al. 1995). The so-called "iron hypothesis" is controversial since factors other than iron availability can be invoked to explain HNLC waters (e.g. Smetacek et al. 1997). In coastal areas like the Antarctic Peninsula, iron concentrations are above limiting levels. Experiments conducted in this region (Nolting et al. 1991; Westerlund and Ohman 1991) show that the Antarctic Peninsula supplies iron to the nearby neritic areas and that the enrichment can reach as far as to the Scotia/Weddell Confluence (Baar 1994).

Phytoplankton blooms in the Southern Ocean are frequently isolated phenomena associated with coastal sheltered areas (Holm-Hansen and Mitchell 1991), island mass effects (El-Sayed et al. 1964; El-Sayed and Jitts 1973; Nast and Gieskes 1986), particular hydrographic features like fronts (Bidigare et al. 1986; Nelson et al. 1987; Laubscher et al. 1993) and eddies (Heywood and Priddle 1987), or shallow mixed layers caused by ice melting (Alexander and Niebauer 1981; Smith and Nelson 1985; Sullivan et al. 1988). Water column stability has traditionally been considered as one of the main factors controlling phytoplankton blooms in the Antarctic Ocean (e.g. Hart 1934; Sakshaug and Holm-Hansen 1984; Lutjeharms et al. 1985; Perissinotto et al. 1990; Mitchell and Holm-Hansen 1991). Density stratification in the upper layers enhances vertical stability reducing the mixed layer and causing retention of phytoplankton inside the euphotic zone. This allows *in situ* growth and accumulation of algal cells at the surface. Some studies (e.g. Lipski and Rakusa-Suszczewski 1990) have related chlorophyll distribution to vertical stability of the water column. Nevertheless, the relationship between the upper mixed layer (UML) and phytoplankton biomass is not always consistent (e.g. Priddle et al. 1986, 1994). In a study carried out around Prince Edward Archipelago, Perissinotto et al. (1990) found that a rel-

G. Basterretxea (✉) · J. Aristegui
Facultad de Ciencias del Mar,
Universidad de Las Palmas de Gran Canaria,
E-35017 Las Palmas de Gran Canaria, Spain
e-mail:gotzon.basterretxea@biologia.ulpgc.es, Fax: + 34-28-452922

© Del documento, los autores. Digitalización realizada por ULPGC. Biblioteca Universitaria, 2009

atively low percentage of total biomass variance was accounted for by the degree of vertical stability of the water column. They hypothesized that mesoscale variations in chlorophyll would be the result of physical processes affecting the vertical structure of the water column which produce accumulation and dissipation of algal cells rather than *in situ* growth.

Advection of phytoplankton-rich waters in areas of intense hydrology can be a mechanism for increasing chlorophyll concentrations without necessarily increasing primary production. One such potential area is the Bransfield Strait, where horizontal advection of organic carbon may dominate vertical carbon fluxes (Huntley et al. 1991). The Bransfield Strait can be described as a complex mosaic of water masses generated in the Antarctic Peninsula and adjacent seas which converge in this semi-enclosed region (Clowes 1934; Gordon and Nowlin 1978; Grelowski and Tokarczyc 1985; Heywood 1985; Grelowski et al. 1986; Stein 1988; Niiler et al. 1991; Garcia et al. 1994). The geographical position of the fronts between these water masses varies frequently due to local shifts in the atmospheric forcing (Anonymous 1990; Stein and Heywood 1994). Several studies have been carried out to date to study different aspects of the phytoplankton biomass distribution and productivity in this region. Nevertheless, these studies either concentrated solely on the phytoplankton distribution (e.g. Priddle et al. 1994) or covered a small area of the strait (Bodungen et al. 1986; Bölter et al. 1988; Holm-Hansen and Mitchell 1991; Kang and Lee 1995).

During December 1991 (D91) and January/February 1993 (J93), we conducted intensive sampling along the Bransfield Strait. Our purpose was to study the physical and biological factors causing spatial and temporal differences in biomass and primary production in an area where complex hydrography suggests great variations in phytoplankton biomass and productivity. The survey was carried out in 2 consecutive years in which climatic conditions differed significantly (Smith et al. 1995).

## Materials and methods

Samples for this study were collected as part of the BIOANTAR program in the Bransfield Strait on board the B.I.O. Hespérides. A grid of 36 stations in 1991 and 78 biological stations in 1993 were sampled along the strait (Fig. 1). Continuous vertical CTD profiles were obtained at each station using a SeaBird SB-19 and a Neil Brown Mk III CTD, respectively. Temperature and conductivity values from the CTD sensors were calibrated against reversing thermometer readings and water bottle salinity samples. Photosynthetically available radiation (PAR) profiles were obtained in the first 100 m of the water column by means of a scalar QSP-200 light sensor (Biospherical Inst.) lowered at the end of the CTD casts.

The depth of the mixed layer was assumed to be where a density change of 0.03 kg $m^{-3}$ occurred within 10 m (Priddle et al. 1986; Perissinotto et al. 1990)

Chlorophyll *a* and phaeopigments were measured at 6–8 depths within the upper 100 m of the water column, following the acidification method of Holm-Hansen et al. (1965). Samples (50–500 ml) were filtered through Whatman GF/F filters and extracted overnight in 10 ml 90% acetone at 4°C in the dark. Fluorescence was measured before and after acidification with a Turner Designs fluorometer, calibrated with pure chlorophyll *a* (Sigma Chemical).

**Fig. 1** Maps of the Bransfield Strait showing the sampling stations during D91 and J93. Only stations referring to other figures or tables are labelled. *Triangles* mark the stations where P-I experiments were carried out. The region of study is divided into characteristic zones (*WW* Weddell Water zone, *BW* Bransfield Water zone, *GW* Gerlache Water zone, *BGW* Bellingshausen Water zone). *Arrows* indicate the flow of the major surface currents (adapted from Clowes 1934; Heywood 1985; Grelowski and Tokarczyk (1985); Grelowski et al. 1986; Niiler et al. 1991; Stein and Heywood 1994)

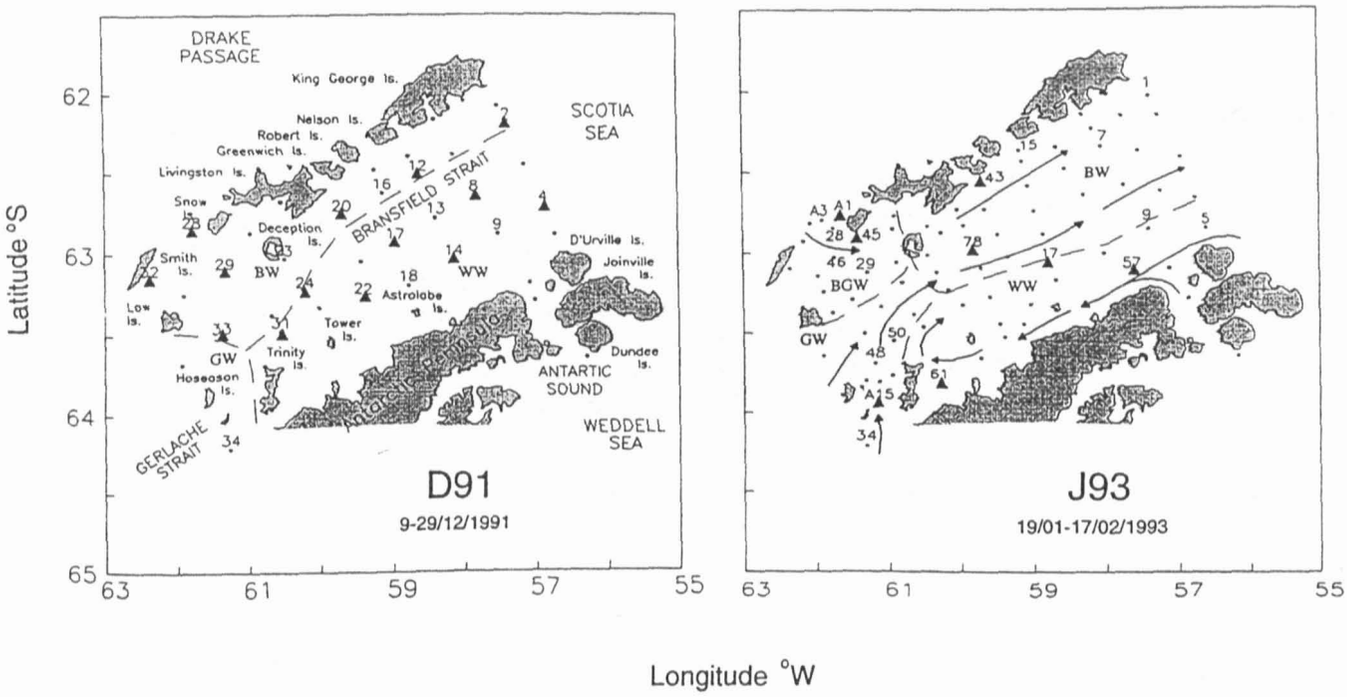


© Del documento, los autores. Digitalización realizada por ULPGC. Biblioteca Universitaria, 2009

Estimations of primary production were carried out around local 12 noon using near-surface water. Shortly after sampling, photosynthesis-irradiance (P-I) experiments were performed in an on-deck incubator containing ten 125-ml bottles in the first cruise and twenty-five 80-ml bottles in the second. Light gradients of up to ~200 μE $m^{-2}$ $s^{-1}$ in the first cruise and ~680 μE $m^{-2}$ $s^{-1}$ in the second cruise were created inside the incubator, interposing neutral density filters in the light path of a slide projector. Irradiance in each bottle was measured with a quantum scalar irradiance meter QSL-100 (Biospherical Inst.). An amount of 7–14 μCi of $^{14}C$-labelled sodium bicarbonate solution was added to each bottle. *In situ* temperatures were reproduced inside the incubator with a cooling bath to within ±0.1°C. The added activity was estimated at the beginning of the incubation by counting 1 ml of solution in a vial with Protosol (NEN) and scintillation cocktail. After 3 h of incubation, samples were filtered onto glass fibre filters (Whatman GF F, 25 mm) and acidified with 1 ml HCl (10%) for 18 h to drive off inorganic carbon. Radioactivity was counted in a Beckman scintillation counter using Aquasol-II cocktail. An external standard was used for quench correction. The photosynthesis-irradiance curve parameters $\alpha^B$ and $P^B_m$ were estimated by non-linear regression fitting of the expression of Webb et al. (1974):

$$P^B_{z,t}(I) = P^B_m\left[1 - \exp(-\alpha I_{z,t}/P^B_m)\right]$$

where $P^B_{z,t}$ is the instantaneous rate of primary production per unit chlorophyll at certain depth [mg C (mg Chla)$^{-1}$ h$^{-1}$]. $P^B_m$ is the primary production per unit chlorophyll at saturating irradiance (same units). $\alpha^B$ is the slope of the curve at light-limiting levels [mg C (mg Chla)$^{-1}$ h$^{-1}$ (μE $m^{-2}$ $s^{-1}$)$^{-1}$] and $I_{z,t}$ is the depth ($z$) and time ($t$) dependent irradiance in μE $m^{-2}$ $s^{-1}$. The adaptative parameter of the P-I curve, $I_k$ (μE $m^{-2}$ $s^{-1}$), was calculated from $I_k = P^B_m/\alpha^B$.

Daily production rates were obtained from surface irradiance ($I_{0,t}$) values calculated for local latitude and date of the cruise according to Platt et al. (1990). Reflectance at sea surface was estimated by interpolation of tabulated values of Austin (1974) for winds of 4 m $s^{-1}$. Integrated production values (0–50 m) were estimated assuming a homogeneous chlorophyll distribution. The light attenuation coefficient $K$ ($m^{-1}$) in terms of pigment concentration was obtained by the regression between $K$ (obtained from the exponential decrease of observed irradiances) and pigment concentration. Rates calculated are potential because no attempt was made to account for cloud covering. Daily production rates in the first 50 m ($P_{z,T}$) were derived from:

$$P_{z,T} = \int_0^D \int_0^{50} B_z P_{z,t}\, dz\, dt$$

where $D$ is the daylength in hours and $B$ is the phytoplankton biomass expressed as chlorophyll.

## Results

### Hydrography

During the two sampling periods, the general distribution of surface water masses was consistent with previous descriptions of the region. A well-defined surface thermohaline front separated colder and saltier Weddell Sea water inflowing through the Antarctic Sound from the warmer and fresher Central Bransfield water (Fig. 2). Although the spatial resolution in the two samplings was not the same and therefore interpolation biases could occur, the front seemed to vary in position and strength, being placed in J93 further southeast than in D91.

In the two cruises, the warmest surface temperatures (>1°C) and lowest salinities (<36.7 psu) were measured in southwestern Bransfield, in the water from Gerlache Strait. Warm surface water (>1°C), presumably advected from the Bellingshausen Sea into the strait, was also observed near Smith and Snow Islands in J93. Near-surface temperatures showed clear variations in absolute values between cruises (Fig. 2). In D91 temperatures were generally below 0°C. Only one station placed in the Gerlache Strait reached higher values. In contrast, in J93 near-surface temperatures were generally above 0°C. Although samplings were carried out in different months, temperature differences could be enhanced by interannual changes. Monthly averaged meteorological records at Palmer Station show that atmospheric temperatures in D91 were almost 2°C lower than in the same period in 1992.

Composite T-S diagrams at several representative stations illustrate the different water masses found during D91 and J93 (Fig. 3). The boundaries between surface water masses are difficult to define due to the complex circulation patterns in the area, that cause interleaving and mixing between different layers, and due to changes produced by local conditions, like ice melting. For our purpose, we divided the surveyed area into four zones, which adequately define the general surface physical structure and the distribution patterns of the biological characteristics observed during the sampling periods: (1) Weddell water zone (WW). This zone includes cold (<−0.4°C in D91 and <0.6°C in J93) and salty (>34.2 psu in D91 and >34.1 psu in J93) water from the Weddell Sea spread along the Antarctic Peninsula shelf. Chlorophyll profiles generally show a homogeneous distribution due to the presence of a deep mixed layer. (2) Gerlache water zone (GW). This zone includes modified Bellingshausen Sea water, warm and highly stratified, with surface salinities <34.0 psu and surface chlorophyll values >1 mg $m^{-3}$. (3) Bellingshausen water zone (BGW). This zone is affected by Bellingshausen Sea water entering into the strait between Smith and Snow Islands. Sea surface water presents temperatures of >1.4°C and chlorophyll values >2 mg $m^{-3}$. (4) Bransfield water zone (BW). The water mass composition in this zone presents the characteristics of Weddell water at depth and a mixture of waters of different origin near the surface. Chlorophyll values are generally <1 mg $m^{-3}$.

### Chlorophyll distribution

The distribution of chlorophyll *a* at the surface was closely related ($r = 0.83$, $P < 0.001$) to the integrated chlorophyll from the upper water column (0–50 m) in the two cruises (Fig. 4). Therefore, water column biomass estimations can be derived from surface chlorophyll samples.

The depth of the mixed layer varied widely in the two surveys and did not show a consistent relationship with the integrated chlorophyll concentration (see also Mura et al. 1995). Figures 5 and 6 illustrate the vertical dis-

© Del documento, los autores. Digitalización realizada por ULPGC. Biblioteca Universitaria, 2009

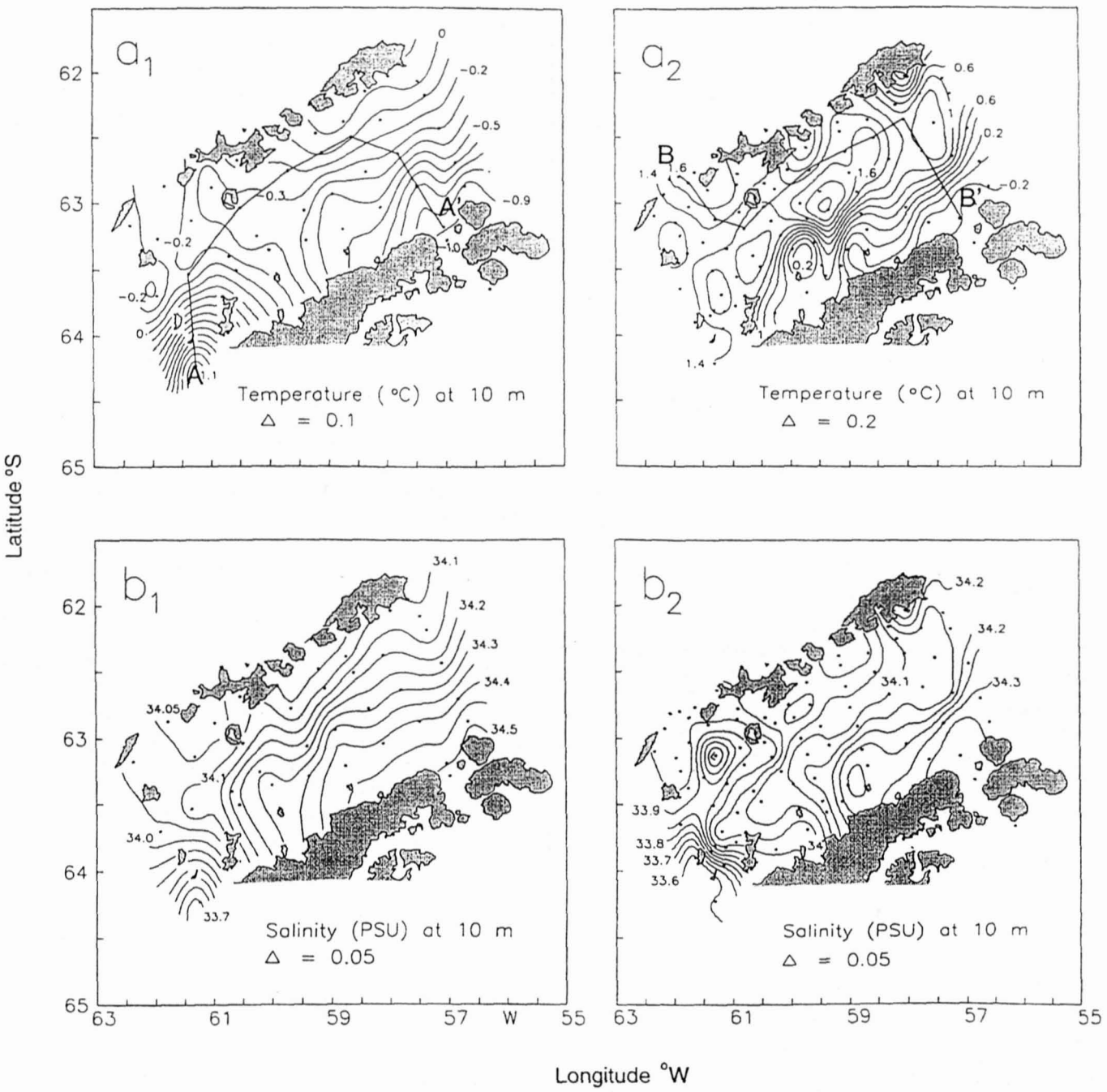


**Fig. 2a1–b2** Surface temperature and salinity distributions during D91 ($a_1$, $b_1$) and J93 ($a_2$, $b_2$)

tribution of chlorophyll and density at different stations during the two cruises. At several stations where chlorophyll is high there is a lack of correlation between the chlorophyll content and the depth of the mixed layer. In particular, station 18 from WW in D91 and stations 28 and A3 from BGW in J93 show low stratification but high chlorophyll values. An exception is station 34 (from GW) in D91 where an intense surface bloom is clearly related to the presence of a shallow pycnocline.

The surface distribution of chlorophyll during the two cruises (Fig. 7) provides evidence of the relationship between phytoplankton abundance and water mass structure in the surface waters of the Bransfield Strait. In D91, two areas of increased phytoplankton biomass concentrations (>2 mg Chla $m^{-3}$) were observed, one in southwestern Bransfield and the other close to Astrolabe Island (Fig. 6). The first area was characterized by the influence of fresher and warmer surface Gerlache Strait water (Fig. 2), with phytoplankton restricted to the upper few meters in the presence of a strong pycnocline (Fig. 6). In contrast, the chlorophyll enhancement in the vicinity of Astrolabe Island extended from the surface to the bottom (~90 m depth), suggesting that a coastal bloom was sinking (Fig. 5).

© Del documento, los autores. Digitalización realizada por ULPGC. Biblioteca Universitaria, 2009

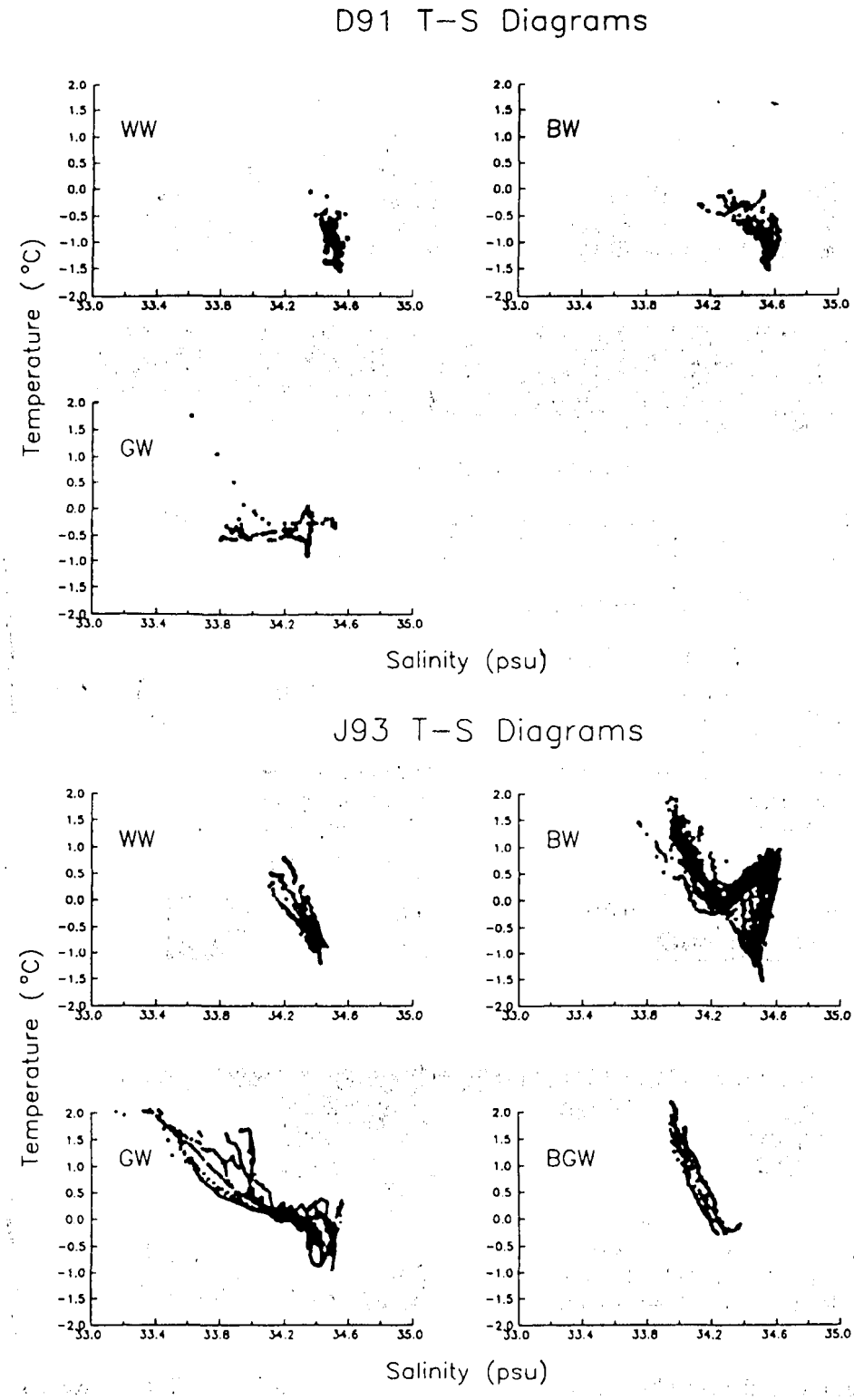


**Fig. 3** Representative T-S diagrams of each zone during D91 and J93

In J93 mean surface chlorophyll concentrations in stations in Central Bransfield (0.7 ± 0.5 mg $m^{-3}$) were approximately the same as in D91 (1.1 ± 0.4 mg $m^{-3}$). Relatively high chlorophyll values (> 1 mg $m^{-3}$) were again evident at the entrance of Gerlache Strait, decreasing towards the Bransfield Strait (Fig. 6). To the north, close to Smith and Snow Islands, a second and more intense surface bloom contributed chlorophyll concentrations of up to 5 mg $m^{-3}$. This biomass accumulation presumably proceeded from the intrusion of surface Bellingshausen water into the Bransfield Strait. In contrast to the above-mentioned blooms, it was not related to coastal or shelf processes, since depths in the canyon connecting Drake Passage and western Bransfield exceed 500 m.

© Del documento, los autores. Digitalización realizada por ULPGC. Biblioteca Universitaria, 2009

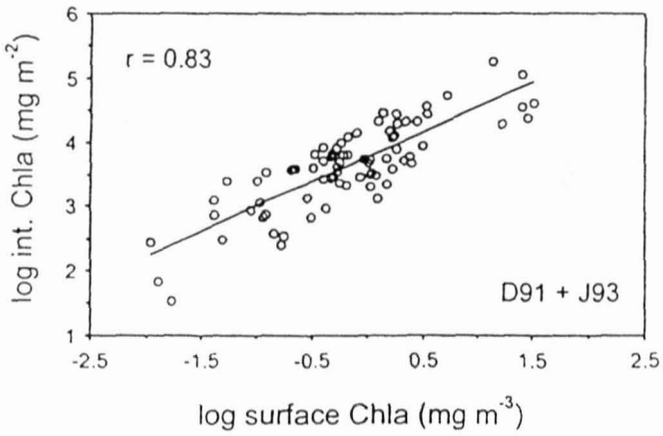


**Fig. 4** Relationship between surface and integrated (0–50 m) chlorophyll *a* in the two cruises

## Light and primary production

The photosynthetic parameters obtained from the P-I experiments showed marked differences between the two surveys. Values of $\alpha^B$ and $P^B_m$ in D91 were consistently lower than in J93 (Fig. 8; Table 1). A wider variability in the photosynthetic parameters was observed in J93 compared with D91. No significant photoinhibition was observed in any of the samples for the light range measured. Light-limited photosynthesis ($\alpha^B$) averaged 0.012 ± 0.006 mg C (mg Chla)$^{-1}$ h$^{-1}$ (μE m$^{-2}$ s$^{-1}$)$^{-1}$ for D91 and 0.040 ± 0.016 for J93, while assimilation numbers averaged 0.61 ± 0.25 mg C (mg Chla)$^{-1}$ h$^{-1}$ for D91 and 2.18 ± 0.91 for J93. Maximum $P^B_m$ values were measured in the vicinity of Smith and Snow Islands (stations 28, 32) in D91 and in the western Bransfield Strait (station A15) in J93. $I_k$ (irradiance approximating onset of saturation) was remarkably stable and similar in the two cruises (55 ± 29 and 58 ± 17 μE m$^{-2}$ s$^{-1}$), probably due to the high co-variation of $\alpha^B$ and $P^B_m$ ($r = 0.90$, $P < 0.001$) (Fig. 9).

In nearly all J93 stations where light attenuation was measured, the 1% light level was close to the top of the pycnocline when this existed. Exceptions included some stations with high phytoplankton biomass, or stations where a pycnocline was not fully developed. The euphotic zone depth ranged between 30 and 60 m. The regression equation obtained between the light attenuation coefficient ($K$) and the pigment concentration for J93 was:

$$K = 0.045 + 0.015 \quad [\text{Chla} + \text{Phaeopigments}] \quad (r^2 = 0.87,\ n = 108,\ P < 0.001).$$

The 0.045 (m$^{-1}$) constant is similar to the value obtained by Figueiras et al. (1994) for the Weddell-Scotia Sea. The specific attenuation coefficient of chlorophyll ($k_c$ = 0.015 m$^2$ mgChla + Phaeo$^{-1}$) is however closer to the value obtained by Mitchell and Holm-Hansen (1991) in the Gerlache Strait and western Bransfield. The few $K$-pigment pairs obtained during the D91 cruise fit well into the above relationship.

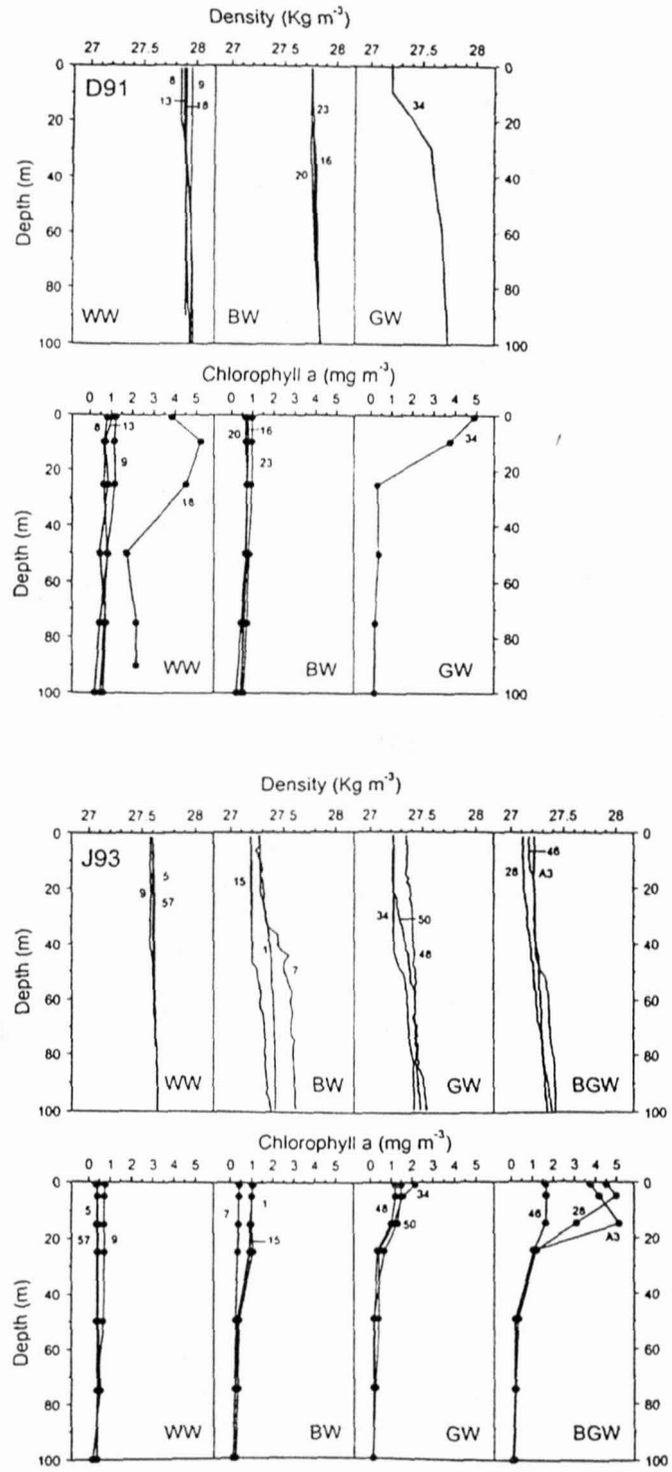


**Fig. 5** Vertical profiles of density and chlorophyll *a* at selected stations in the different areas of study during D91 and J93 (see Fig 1). *Station numbers* are provided in each graph

Integrated values of primary production in D91 averaged 333 ± 125 mg C m$^{-2}$ day$^{-1}$ and showed small spatial variation (Table 2). Conversely, high variability in primary production was found during J93 (423–3913 mg C m$^{-2}$ day$^{-1}$). In this case, the close correlation between integrated production and chlorophyll

© Del documento, los autores. Digitalización realizada por ULPGC. Biblioteca Universitaria, 2009

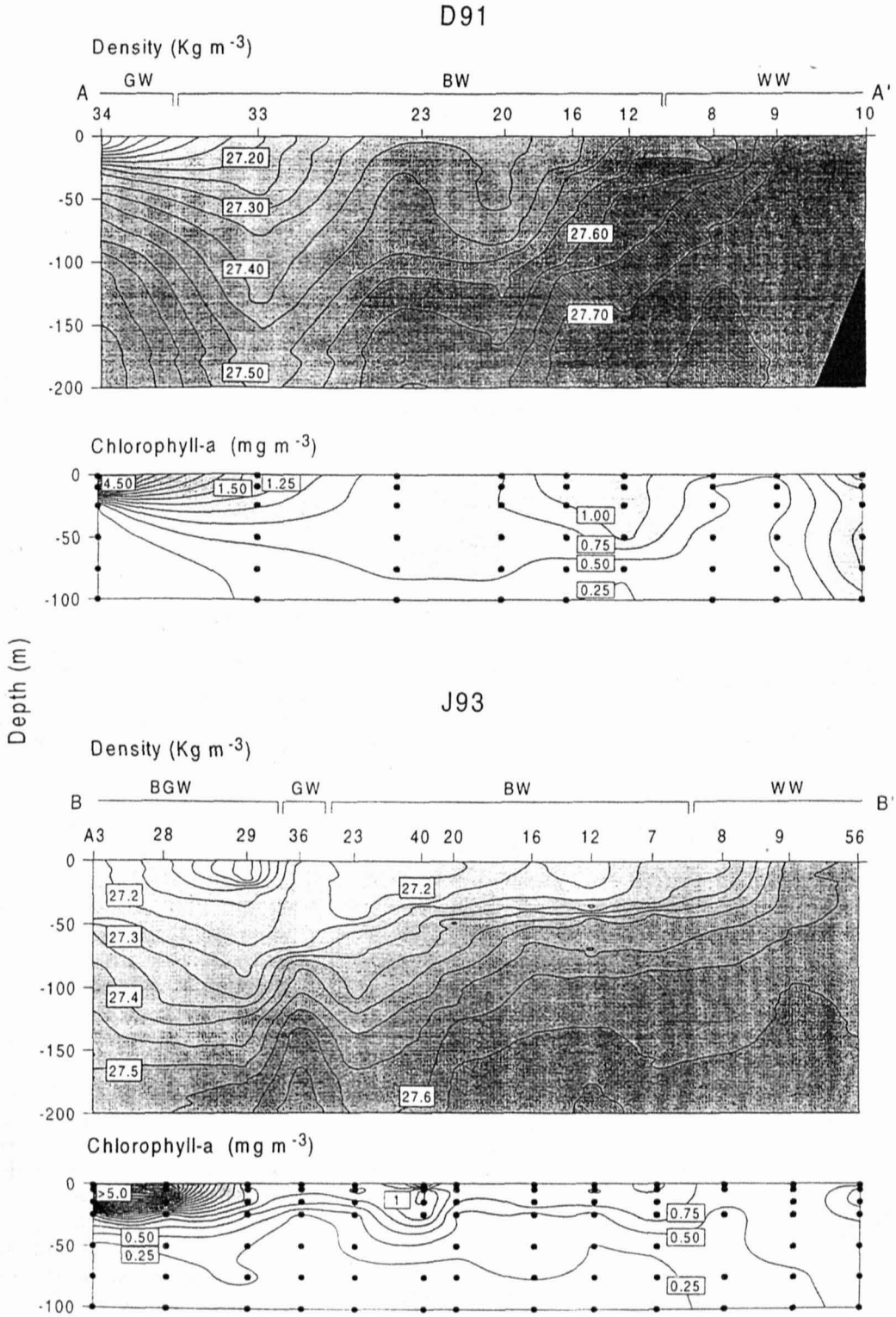


**Fig. 6** Vertical density and chlorophyll *a* distribution along transect AA' (D91) and BB' (J93). Position of the transects is shown in Fig. 2

($r = 0.95$, $n = 8$, $P < 0.001$) suggests that most of the variability was due to differences in phytoplankton biomass and ultimately to the distribution of water masses. Integrated production estimations agreed well ($r = 0.94$ $n = 30$) with *in situ* production measurements (see Aristegui et al. 1996).

## Discussion

The complex distribution of water masses in the Bransfield Strait makes the understanding of the processes that control plankton productivity and distribu-

© Del documento, los autores. Digitalización realizada por ULPGC. Biblioteca Universitaria, 2009

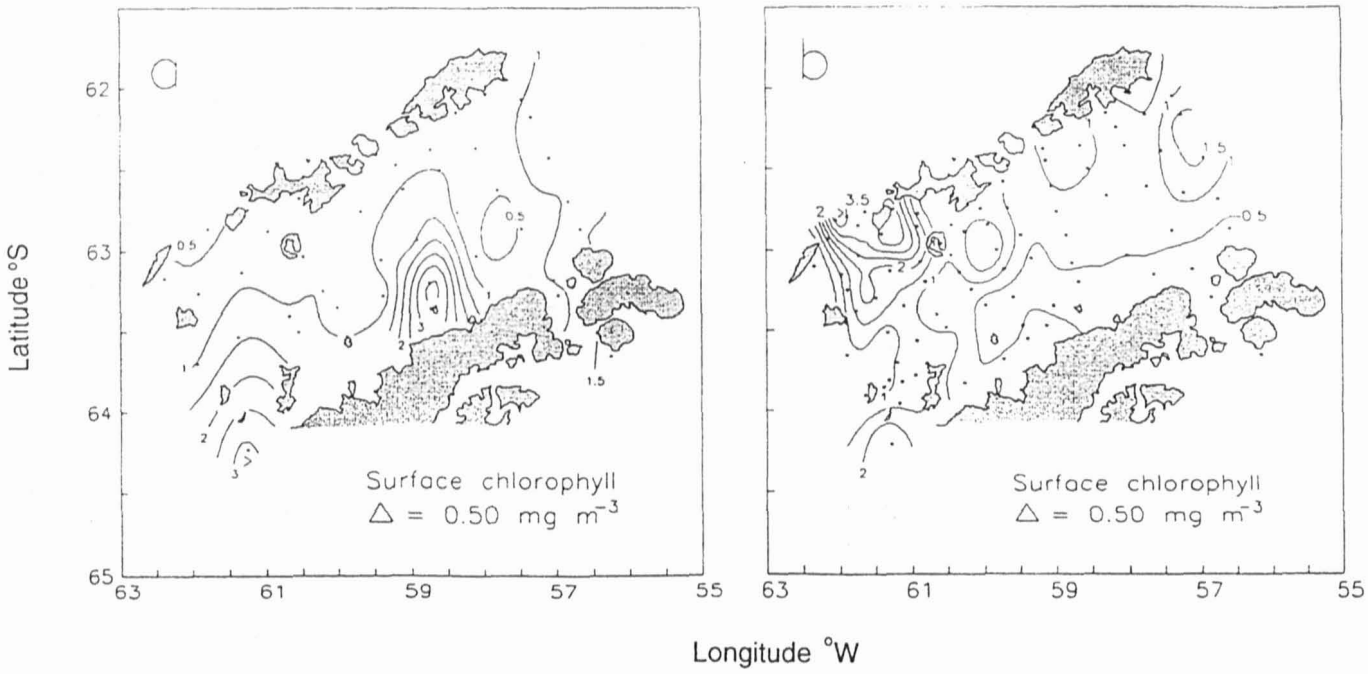


**Fig. 7a,b** Distribution of surface chlorophyll *a* during D91 (**a**) and J93 (**b**)

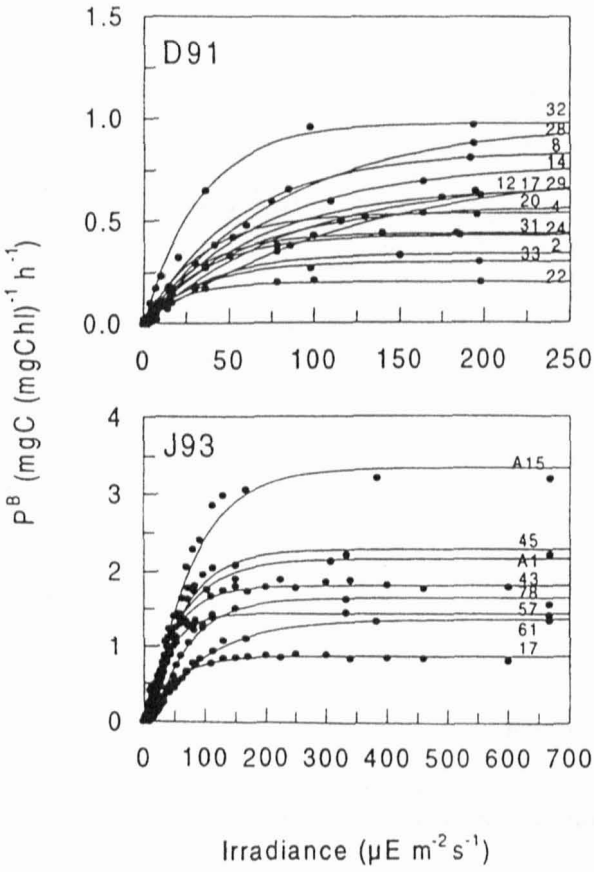


**Fig. 8** Photosynthesis versus irradiance curves in D91 and J93. *Labels* indicate station numbers. Note the different *scales* in the axes

tion difficult. Several studies have partitioned this region on the basis of water mass distribution (Makarov et al. 1988; Priddle et al. 1994; Helbling et al. 1995). Our results show that the basic distribution of surface water masses did not vary greatly during the two sampling periods, although the position of their boundaries changed. The movement of these boundaries has been attributed to atmospheric forcing (Anonymous 1990).

Stratification, warming, and phytoplankton biomass content change seasonally and interannually, and consequently the contribution of each zone to the carbon budget of the strait is altered. In our study, a major interannual difference was caused by the intrusion of Bellingshausen water during J93, presumably as a result of the meandering of the Circumpolar Current close to Smith and Snow Islands (Clowes 1934; Amos 1987; Capella et al. 1992). During strong northerly winds, southeast Pacific basin surface water may penetrate along the deep channel between Snow and Low Islands, blocking the Bellingshausen water that enters into the strait from the southwest (Anonymous 1990). Bellingshausen water advected into the Bransfield Strait during J93 transported high amounts of phytoplankton, presumably developed in the Bellingshausen ice edge, and the main source of chlorophyll enhancement in the strait. Blooms in the Bellingshausen Sea may persist for several weeks before they vanish (Weeks et al. 1995). Lipski (1985) also reported high chlorophyll values in northwestern Bransfield, associated with the entrance of Bellingshausen water, as well as chlorophyll enhancements in the vicinity of the entrances to the Antarctic Sound and Gerlache Strait.

The Gerlache Strait seems to be the most permanent input of high-chlorophyll waters into the Bransfield Strait. In D91, surface chlorophyll levels at the station in GW exceeded 4.5 mg m$^{-3}$, dropping sharply towards

© Del documento, los autores. Digitalización realizada por ULPGC. Biblioteca Universitaria, 2009

**Table 1** Parameters describing the photosynthesis versus irradiance curves, *in situ* temperature and integrated chlorophyll ($Chl_{int}$); $\alpha^B$ is in units of mgC mgChla$^{-1}$ h$^{-1}$ (µE m$^{-2}$ s$^{-1}$)$^{-1}$; $P^B_m$ in mgC mgChla$^{-1}$ h$^{-1}$, $I_k$ in µE m$^{-2}$ s$^{-1}$, temperature in °C and $Chl_{int}$ in mgChla m$^{-2}$

| Cruise | Station | Lat. S | Lon. W | $\alpha^B$ | $P^B_m$ | $I_k$ | Temp. | $Chl_{int}$ |
|---|---|---|---|---|---|---|---|---|
| D91 | 2 | 62°11′ | 57°21′ | 0.009 ± 0.001 | 0.34 ± 0.01 | 38 | −0.09 | 76 |
| | 4 | 62°42′ | 56°50′ | 0.010 ± 0.001 | 0.57 ± 0.03 | 57 | −0.48 | 44 |
| | 8 | 62°37′ | 57°47′ | 0.015 ± 0.0004 | 0.84 ± 0.01 | 56 | −0.28 | 37 |
| | 12 | 62°30′ | 58°36′ | 0.008 ± 0.001 | 0.70 ± 0.06 | 87 | −0.07 | 76 |
| | 14 | 63°02′ | 58°05′ | 0.011 ± 0.0002 | 0.78 ± 0.01 | 71 | −0.52 | 36 |
| | 17 | 62°55′ | 58°55′ | 0.010 ± 0.001 | 0.67 ± 0.04 | 67 | −0.56 | 76 |
| | 20 | 62°45′ | 59°40′ | 0.016 ± 0.001 | 0.54 ± 0.01 | 33 | −0.30 | 46 |
| | 22 | 63°22′ | 59°21′ | 0.009 ± 0.001 | 0.20 ± 0.01 | 22 | −0.44 | 46 |
| | 24 | 63°15′ | 60°12′ | 0.014 ± 0.002 | 0.44 ± 0.03 | 31 | −0.43 | 64 |
| | 28 | 62°52′ | 61°47′ | 0.012 ± 0.001 | 0.97 ± 0.04 | 80 | −0.07 | 53 |
| | 29 | 63°08′ | 61°19′ | 0.006 ± 0.001 | 0.78 ± 0.01 | 130 | −0.25 | 73 |
| | 31 | 63°30′ | 60°33′ | 0.012 ± 0.001 | 0.43 ± 0.01 | 35 | −0.08 | 48 |
| | 32 | 63°32′ | 62°21′ | 0.030 ± 0.001 | 0.98 ± 0.02 | 32 | −0.27 | 85 |
| | 33 | 63°32′ | 61°21′ | 0.009 ± 0.0004 | 0.30 ± 0.01 | 33 | −0.39 | 89 |
| J93 | 17 | 62°55′ | 58°54′ | 0.018 ± 0.001 | 0.90 ± 0.02 | 50 | 2.0 | 33 |
| | 43 | 62°35′ | 59°46′ | 0.040 ± 0.003 | 1.86 ± 0.04 | 47 | 0.6 | 33 |
| | 45 | 62°54′ | 61°26′ | 0.053 ± 0.004 | 2.85 ± 0.07 | 54 | 2.0 | 158 |
| | 57 | 63°09′ | 57°42′ | 0.055 ± 0.006 | 1.86 ± 0.07 | 34 | −0.3 | 19 |
| | 61 | 63°50′ | 60°18′ | 0.017 ± 0.001 | 1.56 ± 0.03 | 92 | 0.9 | 37 |
| | 78 | 63°00′ | 59°52′ | 0.038 ± 0.003 | 2.23 ± 0.06 | 59 | 1.9 | 129 |
| | A1 | 62°46′ | 61°39′ | 0.038 ± 0.002 | 2.25 ± 0.04 | 59 | 1.6 | 60 |
| | A15 | 63°57′ | 61°11′ | 0.058 ± 0.003 | 3.93 ± 0.01 | 68 | 2.0 | 32 |

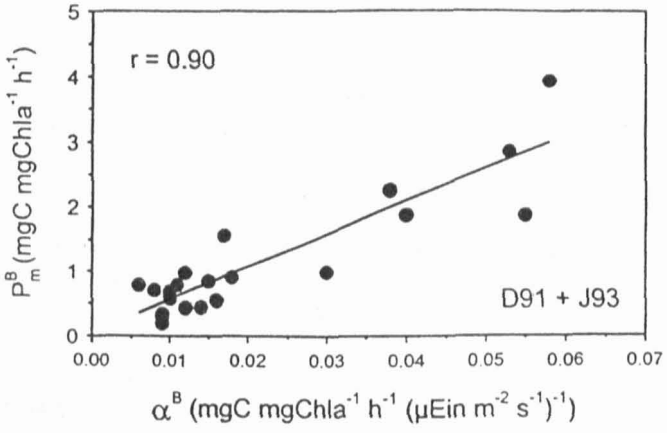


**Fig. 9** Relationship between the photosynthetic parameters $\alpha^B$ and $P^B_m$ in the two cruises

eastern Bransfield Strait. High primary production rates and chlorophyll concentrations have been reported from shelf waters in the Gerlache Strait (El-Sayed 1968b; Lipski 1985; Holm-Hansen and Vernet 1990; Holm-Hansen and Mitchell 1991) where pigment concentrations can exceed 20 mg m$^{-3}$ (Mitchell and Holm-Hansen 1991). Intensive blooms in this area are closely associated with the increase in vertical stability of the water column. Meltwater stabilization promotes the development of a shallow (< 50 m) pycnocline favoring phytoplankton biomass accumulation at the surface (Mitchell and Holm-Hansen 1991). The phytoplankton bloom sinking near Astrolabe Island in D91 could also have originated by meltwater stabilization before mixing of the water column. The general situation in the Bransfield Strait differs, however, from the Gerlache Strait since high chlorophyll concentrations are not regularly related to the presence of a shallow pycnocline.

A well-established pycnocline at depths shallower than 100 m is a conspicuous feature of most of the central and eastern Bransfield Strait. It originates by isopycnal sinking of the continental shelf Weddell water (Whitworth et al. 1994). Nevertheless, this water column stabilization does not seem to be a critical factor for bloom formation as in other regions. In our study, no correlation was obtained between biomass and stability.

**Table 2** Mean(±SD) integrated (0–50 m) chlorophyll ($Chl_{int}$) and primary production ($Prod_{int}$) values for different areas in Bransfield Strait (see Fig. 1). $Chl_{int}$ is in mgChla m$^{-2}$ and $Prod_{int}$ in mgC m$^{-2}$ day$^{-1}$ ($n$ = number of data)

| | D91 | | J93 | |
|---|---|---|---|---|
| | $Chl_{int}$ | $Prod_{int}$ | $Chl_{int}$ | $Prod_{int}$ |
| WW | 67 ± 28 ($n$ = 17) | 335 ± 55 ($n$ = 7) | 22 ± 8 ($n$ = 16) | 595 ± 243 ($n$ = 3) |
| BW | 49 ± 14 ($n$ = 16) | 330 ± 43 ($n$ = 7) | 35 ± 6 ($n$ = 10) | 843 ± 321 ($n$ = 2) |
| BGW | | | 76 ± 31 ($n$ = 8) | 2673 ± 1754 ($n$ = 2) |
| GW | 78.08 ($n$ = 1) | | 38 ± 12 ($n$ = 8) | 1524 ($n$ = 1) |

© Del documento, los autores. Digitalización realizada por ULPGC. Biblioteca Universitaria, 2009

Our maximum pigment values were, however, lower than in the intensive blooms reported for other areas, where the relationship between stability and chlorophyll may work better. Perissinotto et al. (1990) pointed out that phytoplankton biomass may not be a suitable variable for use in mesoscale analysis on the relationships between local phytoplankton variations and the vertical structure of the upper ocean. These authors suggested, from a study carried out at the Prince Edward Islands, that the physical structure of the water column was, however, the dominant source of variation responsible for the observed differences in local phytoplankton photosynthesis.

During D91 and J93 the variability in the photosynthetic parameters showed no regular trend along the Bransfield Strait. Conversely, the surface chlorophyll distribution provided a clear indication of a decreasing west-east gradient in phytoplankton biomass along the strait. This may indicate that much of the phytoplankton observed in the Bransfield Strait originated in adjacent areas like the Gerlache Strait and Bellingshausen Sea, being subsequently advected into the Bransfield Strait. According to studies carried out during the RACER program (Holm-Hansen and Mitchell 1991; Karl et al. 1991 Niiler et al. 1991), one of the main mechanisms to explain the demise of phytoplankton blooms in the Gerlache Strait is lateral advection of water towards the Bransfield Strait. This advective transport of organic material would explain the high microplankton respiration rates observed by Aristegui and Montero (1995) in the path of the northeasterly Bransfield Current during the D91 survey. Advection may thus be a major process controlling the distribution of plankton in this region.

The photosynthetic capacity of phytoplankton was significantly lower in D91 than in J93. In D91, $\alpha^B$ and $P^B_m$ did not vary substantially among the different water masses. Tilzer et al. (1985) and Bodungen et al. (1986) found also no basic differences in the photosynthetic capacity among plankton populations in western Bransfield in a study carried out during November and December.

The stability of the $I_k$ values in the two cruises suggests adaptation of phytoplankton to their light regime. Simultaneous increases in light-saturated and light-limited photosynthetic rates in Antarctic phytoplankton incubated at different temperatures were observed by Tilzer et al. (1986). They found that at extremely low temperatures some temperature-dependent reactions control photosynthesis at any given photon flux density. Our data do not allow us to draw any specific conclusion on the effect of temperature on productivity rates, but they do show that at subzero temperatures (D91) $\alpha^B$ and $P^B_m$ were significantly lower than at temperatures above zero (J93). The low $I_k$ values indicate adaptation to low light intensities while the absence of photoinhibition indicates that cells stand high irradiances without losing their photosynthetic efficiency. Harrison and Platt (1986) observed that, under low irradiance conditions, phytoplankton populations tend to be more susceptible to photoinhibition. However, during summer in polar seas, cells are not constantly exposed to low irradiances but to highly varying conditions.

Despite the photosynthetic parameters being higher in J93, water column chlorophyll values averaged per zone were as high or higher in D91 than in J93, excepting the stations in BGW (Table 2). One argument to explain the discrepancy between chlorophyll and productivity values is grazing pressure. Protozoans are reported to contribute significantly to maintenance of low phytoplankton biomass in open-ocean Antarctic ecosystems, like the Weddell Sea (Bjørnsen and Kuparinen 1991; Smetacek et al. 1997), where nanoflagellate/protozoan-dominated systems are the most characteristic communities of the pelagial (Smetacek et al. 1990). In coastal Antarctic waters, however, the grazing impact of protozoans on phytoplankton assemblages is poorly known and low biomass of microzooplankton has been observed in the Bransfield Strait (Alder and Boltovskoy 1991). In our two cruises, mesozooplankton biomass was very low (at the lower range of previous estimations for Antarctic waters) and constant (S. Hernández-León, personal communication). Therefore, differences in copepod grazing pressure would not explain phytoplankton abundances. However, although krill populations are known to attain maximum concentrations during January and February in the Bransfield Strait (Rakusa-Suszczewski 1982; Brinton 1991; Huntley and Escritor 1991), samples collected by means of Bongo and Bioness nets during the two cruises did not give evidence of a higher abundance of krill populations during J93 (I. Moreno, personal communication).

As stated before, the variability in chlorophyll concentrations inside the Bransfield Strait seems to be related to the distribution of water masses rather than to the grazing pressure. Our results show that primary production in the Bransfield Strait presents strong seasonal variability in the physiological response of phytoplankton. However, the spatial distribution of chlorophyll is patchy and generally associated with the influence of blooms generated in the Gerlache Strait and Bellingshausen Sea, which are transported by local currents into the Bransfield Strait. These intrusions of water join the Bransfield Current (Stein 1988; Niiler et al. 1991), transporting organic material from west to east along the Bransfield Strait. Additionally, chlorophyll-rich shelf waters from the north-west Weddell Sea spread into the eastern Bransfield Strait, part of them being later transported to the Weddell-Scotia Sea (e.g. Whitworth et al. 1994). These waters could contribute to the formation of biomass maxima at the Weddell-Scotia Confluence (Schloss and Estrada 1994).

**Acknowledgements** We thank M. Garcia for CTD data from J93. This work was supported by projects "Oceanografía del Estrecho de Bransfield, 1991" and "Oceanografía dinámica y productividad en el Estrecho de Bransfield durante el verano austral, 1993" (CICYT). Data from the Palmer LTER data archive were supported by Office of Polar Programs, NSF (OPP-96-32763).

© Del documento, los autores. Digitalización realizada por ULPGC. Biblioteca Universitaria, 2009

## References


Alder VA, Boltovskoy D (1991) Microplanktonic distributional patterns west of the Antarctic Peninsula, with special emphasis on the tintinnids. Polar Biol 11:103–112

Alexander V, Niebauer HJ (1981) Oceanography of the eastern Bering Sea ice-edge in spring. Limnol Oceanogr 26:1111–1125

Amos AF (1987) RACER: physical oceanography of the western Bransfield Strait. Antarct J US 22:137–140

Anonymous (1990) SIBEX Physical Oceanography Workshop. Cambridge, 9–27 March 1987. BIOMASS Rep Ser 62:1–38

Aristegui J, Montero MF (1995) Plankton community respiration in Bransfield Strait (Antarctic Ocean) during austral spring. J Plankton Res 17:1647–1659

Aristegui J, Montero MF, Ballesteros S, Basterretxea G, Lenning K van (1996) Planktonic primary production and microbial respiration measured by 14°C assimilation and dissolved oxygen changes in coastal waters of the Antarctic Peninsula during austral summer: implications for carbon flux studies. Mar Ecol Prog Ser 132:191–2010

Austin RW (1974) The remote sensing of spectral radiance from below the ocean surface. In: Jerlov NG, Nielsen ES (eds) Optical aspects of oceanography. Academic Press, San Diego, pp 317–344

Baar HJW de (1994) von Liebig's Law of the Minimum and plankton ecology (1899–1991). Prog Oceanogr 33:347–386

Baar HJW de, Jong JTM de, Bakker DCE, Löscher BM, Veth C, Bathmann U, Smetacek V (1995) Importance of iron for plankton blooms and carbon dioxide drawdown in the Southern Ocean. Nature 373:412–415

Bidigare RR, Frank TJ, Zastrow C, Brooks JM (1986) The distribution of algal chlorophylls and their degradation products in the Southern Ocean. Deep Sea Res 33:923–937

Bjørnsen PK, Kuparinen J (1991) Determination of bacterioplankton biomass, net production and growth efficiency in the Southern Ocean. Mar Ecol Prog Ser 71:185–194

Bodungen B von, Smetacek VS, Tilzer MM, Zeitzschel B (1986) Primary production and sedimentation during spring in the Antarctic Peninsula region. Deep Sea Res 33:177–194

Bölter M, Bodungen B von, Liebezeit G, Meyer M (1988) The pelagic ecosystem of the Bransfield Strait Antarctica: an analysis of microbiological, planktological and chemical characteristics by multivariate analyses. In: Sahrhage D (ed) Antarctic Ocean and resources variability. Springer, Berlin Heidelberg New York, pp 160–166

Brinton E (1991) Distribution and population structures of immature and adult *Euphausia superba* in the western Bransfield Strait region during the 1986–87 summer. Deep Sea Res 38:1169–1193

Capella JE, Ross RM, Quentin LB, Hofmann EE (1992) A note on the thermal structure of the upper ocean in the Bransfield Strait-South Shetland Islands region. Deep Sea Res 39:1221–1229

Clowes AJ (1934) Hydrology of the Bransfield Strait. Discovery Rep 9:1–64

Comiso JC, Maynard NG, Smith WO Jr, Sullivan CW (1990) Satellite ocean color studies of Antarctic ice edges in summer and autumn. J Geophys Res 95:9481–9496

El-Sayed SZ (1968a) On the productivity of the southwest Atlantic Ocean and the waters of the Antarctic Peninsula. Antarct Res Ser 11:15–47

El-Sayed SZ (1968b) Primary productivity of the Antarctic and Subantarctic. In: Bushnell V (ed) Primary productivity and benthic marine algae of the Antarctic and Subantarctic. Folio 10. Antarct Map Folio Ser. American Geographic Society New York, pp 1–6

El-Sayed SZ, Jitts H (1973) Phytoplankton production in the Southwestern Indian Ocean. Proc Symp Univ Kiel, March 31–April 6 1971. Springer, Berlin Heidelberg New York, pp 131–544

El-Sayed SZ, Mandelli EF, Sugimura Y (1964) Primary organic production in the Drake Passage and Bransfield Strait. In: Lee O (ed) Biology of the Antarctic Seas I, vol 1. American Geophysical Union, Washington, DC, pp 1–110

Figueiras FG, Pérez FF, Pazos Y, Rios AF (1994) Light and primary productivity of Antarctic phytoplankton during austral summer in an ice edge region in the Weddell-Scotia Sea. J Plankton Res 16:233–253

Garcia MA, López O, Sospedra J, Espino M, Gracia V, Morrison G, Rojas P, Figa J, Puigdefàbregas J, Arcilla AS (1994) Mesoscale variability in the Bransfield Strait Region (Antarctica) during austral summer. Ann Geophys 12:856–867

Gordon AL, Nowlin WD Jr (1978) The basin waters of the Bransfield Strait. J Phys Oceanogr 8:258–264

Grelowski A, Tokarczyk R (1985) Hydrological conditions in the region of Bransfield Strait and southern part of Drake Passage in the period from December 10 1983 and January 8 1984 (BIOMASS-SIBEX). Pol Polar Res 6:23–41

Grelowski A, Majewicz A, Pastuzak M (1986) Mesoscale hydrodynamic processes in the region of the Bransfield Strait and the southern part of Drake Passage during BIOMASS-SIBEX 1983/1984. Pol Polar Res 7:353–369

Harrison WG, Platt T (1986) Photosynthesis-irradiance relationships in polar and temperate phytoplankton populations. Polar Biol 5:153–164

Hart TJ (1934) On the phytoplankton of the South-West Atlantic and the Bellingshausen Sea 1929–31. Discovery Rep 21:261–356

Helbling EW, Villafañe VE, Holm-Hansen O (1995) Variability of phytoplankton distribution and primary production around Elephant Island, Antarctica during 1990–1993. Polar Biol 15:233–246

Heywood RB (1985) Environmental conditions in the Antarctic Peninsula area of the Southern Ocean during the Anglo-German Joint Biological expedition, February 1982. Meeresforschung 30:220–239

Heywood RB, Priddle J (1987) Retention of phytoplankton by an eddy. Cont Shelf Res 7:937–955

Holm-Hansen O (1985) Nutrient cycles in Antarctic marine ecosystems. In: Siegfried WR, Condy PR, Laws RM (eds) Antarctic nutrient cycles and food webs. Springer, Berlin Heidelberg New York, pp 6–11

Holm-Hansen O, Mitchell BG (1991) Spatial and temporal distribution of phytoplankton and primary production in the western Bransfield Strait region. Deep Sea Res 38:961–980

Holm-Hansen O, Vernet M (1990) RACER: phytoplankton distribution and rates of primary production during the austral spring bloom. Antarct J US 25:141–144

Holm-Hansen O, Lorenzen CJ, Holmes RW, Strickland JDH (1965) Fluorometric determination of chlorophyll. J Cons Perm Int Explor Mer 30:3–15

Huntley M, Escritor F (1991) Dynamics of *Calanoides acutus* (Copepoda: Calanoida) in Antarctic coastal waters. Deep Sea Res 38:1145–1167

Huntley M, Karl DM, Niiler P, Holm-Hansen O (1991) Research on Antarctic Coastal Ecosystem Rates (RACER): an interdisciplinary field experiment. Deep Sea Res 38:911–941

Kang S-H, Lee SH (1995) Antarctic phytoplankton assemblage in the western Bransfield Strait region February 1993: composition biomass and mesoscale distributions. Mar Ecol Prog Ser 129:253–267

Karl DM, Tilbrook BD, Tien G (1991) Seasonal coupling of organic matter production and particle flux in the western Bransfield Strait Antarctica. Deep Sea Res 38:1097–1126

Laubscher RK, Perissinotto R, McQuaid DC (1993) Phytoplankton production and biomass at frontal zones in the Atlantic sector of the Southern Ocean. Polar Biol 13:471–481

Le Jehan S, Tréguer P (1985) The distribution of inorganic nitrogen phosphorous and dissolved organic matter in the surface and deep waters of the Southern Ocean. In: Siegfried WR, Condy PR, Laws RM (eds) Antarctic nutrient cycles and food webs. Springer, Berlin Heidelberg New York, pp 22–29


© Del documento, los autores. Digitalización realizada por ULPGC. Biblioteca Universitaria, 2009

Lipski M (1985) Chlorophyll *a* in the Bransfield Strait and the southern part of Drake Passage during BIOMASS-SIBEX (December 1983–January 1984). Pol Polar Res 6:21-30

Lipski M, Rakusa-Suszczewski S (1990) Early summer pattern of vertical distribution of chlorophyll *a* (Bransfield Strait Antarctica November 1986). Pol Arch Hydrobiol 37:287-293

Lutjeharms JRE, Walters NM, Allanson BR (1985) Oceanic frontal systems and biological enhancement. In: Siegfried WR, Condy PR, Laws RM (eds) Antarctic nutrient cycles and food webs. Springer, Berlin Heidelberg New York, pp 11-21

Makarov RR, Maslennikov VV, Solyankin EV, Spiridonov VA, Yakolev VN (1988) Variability in population density of Antarctic krill in the Western Scotia Sea in relation to hydrological conditions. In: Sahrhage D (ed) Antarctic Ocean and resources variability. Springer, Berlin Heidelberg New York, pp 231-236

Martin JH, Gordon RM, Fitzwater S, Broenkow W (1989) VERTEX: phytoplankton/iron studies in the Gulf of Alaska. Deep Sea Res 36:649-680

Martin JH, Fitzwater S, Gordon RM (1990) Iron deficiency limits growth in Antarctic waters. Global Biogeochem Cycles 4:5-12

Mitchell BG, Holm-Hansen O (1991) Observations and modeling of the Antarctic phytoplankton crop in relation to mixing depth. Deep Sea Res 38:981–1007

Mura MP, Satta MP, Agusti S (1995) Water-mass influences on summer Antarctic phytoplankton biomass and community structure. Polar Biol 15:15–20

Nast F, Gieskes W (1986) Phytoplankton observations relative to krill abundance around Elephant Island in November 1983. Arch Fischereiweiss 37:73–94

Nelson DM, Smith WO Jr, Gordon LI, Huber B (1987) Spring distributions of density, nutrients, and phytoplankton biomass in the ice-edge zone of the Weddell-Scotia Sea. J Geophys Res 92:7181–7190

Niiler PP, Amos A, Hu J (1991) Water masses and 200 m relative geostrophic circulation in the western Bransfield Strait region. Deep Sea Res 38:943–959

Nolting RF, Baar HJW de, Bennekom AJ van, Masson A (1991) Cadmium, copper and iron in the Scotia Sea, Weddell Sea and Weddell/Scotia Confluence (Antarctica). Mar Chem 35:219–243

Perissinotto R, Duncombe Rae CM, Boden BP, Allanson BR (1990) Vertical stability as a controlling factor of the marine phytoplankton production at the Prince Edward Archipelago (Southern Ocean). Mar Ecol Prog Ser 60:205–209

Platt T, Sathyendranath S, Ravindran P (1990) Primary production by phytoplankton: analytic solutions for daily rates per unit area of water surface. Proc R Soc Lond B 241:101–111

Priddle J, Hawes I, Ellis-Evans JC, Smith TJ (1986) Antarctic aquatic ecosystems as habitats for phytoplankton. Biol Rev 61:199–238

Priddle J, Brandini F, Lipski M, Thorley MR (1994) Pattern of variability of phytoplankton biomass in the Antarctic Peninsula region: an assessment of the BIOMASS cruises. In: El-Sayed SZ (ed) Southern Ocean ecology. Cambridge University Press, Cambridge, pp 49–61

Rakusa-Suszczewski S (1982) Feeding of *Euphausia superba* Dana under natural conditions. Pol Polar Res 3:289–297

Sakshaug E, Holm-Hansen O (1984) Factors governing pelagic production in polar oceans. In: Holm-Hansen O (ed) Lecture notes on coastal and estuarine studies. Springer, Berlin Heidelberg, New York, pp 1–18

Schloss I, Estrada M (1994) Phytoplankton composition in the Weddell-Scotia confluence area during austral spring in relation to hydrography. Polar Biol 14:77–90

Smetacek V, Baar HJW de, Bathmann UV, Lochte K, Rutgers Loeff MM van der (1997) Ecology and biogeochemistry of the Antarctic Circumpolar Current during austral spring: a summary of Southern Ocean JGOFS cruise ANT X 6 of R.V. Polarstern. Deep Sea Res 44:1–21

Smetacek V, Scharek R, Nöthig EM (1990) Seasonal and reginal variation in the pelagial and its relationship to the life history cycle of krill. In: Kerry KR, Hempel G (eds) Antarctic ecosystems. Ecological change and conservation. Springer, Berlin Heidelberg New York, pp 103–114

Smith RC, Baker KS, Fraser WR, Hofmann EE, Karl DM, Klinck JM, Quentin LB, Prézelin BB, Ross RM, Trivelpiece WZ, Vernet M (1995) The Palmer LTER: a long-term ecological research program at Palmer station Antarctica. Oceanography 8:77–86

Smith WO (1987) Phytoplankton dynamics in the marginal ice zones. Oceanogr Mar Biol A Rev 25:11–38

Smith WO, Nelson DM (1985) Phytoplankton bloom produced by a receding ice edge in the Ross Sea: spatial coherence with a density field. Science 227:163–166

Stein M (1988) Variation of geostrophic circulation off the Antarctic Peninsula and in the southwest Scotia Sea 1975–1985. In: Sahrhage D (ed) Antarctic Ocean and resources variability. Springer, Berlin Heidelberg New York, pp 81-91

Stein M, Heywood RB (1994) Antarctic environment - physical oceanography: the Antarctic Peninsula and Southwest Atlantic region of the Southern Ocean. In: El-Sayed SZ (ed) Southern Ocean ecology. Cambridge University Press, Cambridge, pp 11–24

Sullivan CW, McClain CR, Comiso JC, Smith WO Jr (1988) Phytoplankton standing crops within an Antarctic ice edge assessed by satellite remote sensing. J Geophys Res 93:12487–12498

Sullivan CW, Arrigo KR, McClain CR, Comiso JC, Firestone J (1993) Distributions of phytoplankton blooms in the Southern Ocean. Science 262:1832–1837

Tilzer MM, Bodungen B von, Smetacek V (1985) Light-dependence of phytoplankton photosynthesis in the Antarctic Ocean: implications for regulating productivity. In: Siegfried WR, Condy PR, Laws RM (eds) Antarctic nutrient cycles and food webs. Springer, Berlin Heidelberg New York, pp 60–69

Tilzer MM, Elbrächter M, Gieskes WW, Beese B (1986) Light-temperature interactions in the control oh photosynthesis in Antarctic phytoplankton. Polar Biol 5:105–111

Webb WL, Newton M, Starr D (1974) Carbon dioxide exchange of *Alnus rubra*: a mathematical model. Oecologia 17:281–291

Weeks AR, Griffiths G, Roe H, Moore G, Robinson IS, Atkinson A, Shreeve R (1995) The distribution of acoustic backscatter from zooplankton compared with physical structure, phytoplankton and radiance during the spring bloom in the Bellingshausen Sea. Deep Sea Res 42:997–1019

Westerlund S, Ohman P (1991) Iron in the water column of the Weddell Sea. Mar Chem 35:199–217

Whitworth T III, Nowlin WD Jr, Orsi AH, Locarnini RA, Smith SG (1994) Weddell Sea shelf water in the Bransfield Strait and Weddell-Scotia Confluence. Deep Sea Res 41:629–641

© Del documento, los autores. Digitalización realizada por ULPGC. Biblioteca Universitaria, 2009

ELSEVIER

Aquaculture 179 (1999) 265–275

Aquaculture

# Effect of dietary arachidonic acid levels on growth and survival of gilthead sea bream (*Sparus aurata* L.) larvae

M. Bessonart [a,*], M.S. Izquierdo [b], M. Salhi [c], C.M. Hernández-Cruz [b], M.M. González [c], H. Fernández-Palacios [c]

[a] *Departamento de Zoología Vertebrados, Facultad de Ciencias, Universidad de la República, Iguá 4225, 11400 Montevideo, Uruguay*

[b] *Departamento de Biología, Universidad de Las Palmas de Gran Canaria, 35017 Las Palmas, Spain*

[c] *Instituto Canario de Ciencias Marinas, P.O. Box 56, 35200 Telde, Spain*

**Abstract**

In order to determine the effect of different levels of arachidonic acid (AA) in microdiets on growth and survival of gilthead seabream larvae, two experiments were carried out. In the first experiment, 17-day old larvae were fed microdiets for 14 days. In this trial, we tested four diets with a similar docosahexaenoic acid (DHA)/eicosapentaenoic acid (EPA) ratio and AA in the range of 0.1%–1.8% dry weight (d.w.) and a fifth diet with 1.0% d.w. of AA and a different DHA/EPA ratio. In the second experiment, 16-day old larvae were fed for 21 days on two microdiets with levels of 0.1% and 1.0% d.w. AA. All diets in the two experiments had the same total $n-3$ HUFA level. Growth was measured by total length and dry body weight of larvae. Larval lipids were extracted and fatty acid compositions of total neutral lipid (NL) and total polar lipid (PL) fractions were determined by gas chromatography. In the first experiment, the diet containing 1.8% d.w. of AA showed the best survival ($P < 0.05$) but did not improve growth rate. In the second experiment, an increase in the AA dietary level from 0.1% to 1.0% d.w. significantly improved ($P < 0.05$) larval growth. EPA accumulation in the PLs of the larvae was negatively affected by the inclusion of dietary AA. When working with a fixed dietary $n-3$ HUFA level (2.2% d.w.), the effect of dietary AA on larval growth was masked by that of the dietary DHA/EPA ratio. However, when DHA/EPA ratio in diet was unchanged (~ 1.8), it was

* Corresponding author. Tel.: +598-2-5258618; fax: +598-2-525-8617; E-mail: martinb@fcien.edu.uy

0044-8486/99/$ - see front matter © 1999 Elsevier Science B.V. All rights reserved.
PII: S0044-8486(99)00164-7

© Del documento, los autores. Digitalización realizada por ULPGC. Biblioteca Universitaria, 2009

possible to improve larval growth by supplementing the diet with 1.0 d.w. of AA. The negative effect produced by the increment of dietary AA on the EPA incorporation into the larval PLs may be related to a competition interaction. © 1999 Elsevier Science B.V. All rights reserved.

*Keywords:* *Sparus aurata* larvae; Arachidonic acid; Growth; DHA/EPA ratio

## 1. Introduction

It has been demonstrated that marine fish larvae require $n-3$ highly unsaturated fatty acids ($n-3$ HUFA), mainly eicosapentaenoic (EPA, 20:5 $n-3$) and docosahexaenoic (DHA, 22:6 $n-3$) acids, for normal development and survival (Izquierdo et al., 1989; Koven et al., 1989, 1992; Mourente et al., 1993; Rodríguez et al., 1993; Watanabe, 1993; Rodríguez, 1994; Salhi et al., 1994; Izquierdo, 1996; Furuita et al., 1996). The essentiality of this fatty acids is based on the important structural role they play as membrane phospholipid components, together with the inability of marine fish to synthesize EPA and DHA from linolenic acid (18:3 $n-3$).

Despite the same limitation in the conversion of linoleic acid (18:2 $n-6$) to $n-6$ highly unsaturated fatty acids ($n-6$ HUFA) (Sargent et al., 1994), $n-6$ fatty acids (other than 18:2 $n-6$) have received little attention in feeding studies in marine fish nutrition (Castell et al., 1994; Bell et al., 1995; Zheng et al., 1996). Among $n-6$ HUFA, several studies have pointed out the importance of arachidonic acid (AA, 20:4 $n-6$) in fish metabolism since it is known to be the main precursor fatty acid of eicosanoids in fish (Henderson and Sargent, 1985; Henderson et al., 1985; Bell et al., 1994; Sargent et al., 1994) and it is also one of the main components of phosphatidylinositol (PI) (Bell and Dick, 1990; Bell et al., 1983), where it is incorporated more specifically than into any other lipid class (Linares and Henderson, 1991).

AA is released from membrane phospholipids in response to hormone stimulation in different tissues, and can act as a second messenger in activating protein kinase C (Mc Phail et al., 1984) or can be converted to any number of compounds including prostaglandins, thromboxanes, hidroxyeicosatetraenoic acids and leukotrienes (Smith, 1989). All these molecules are very active even at low physiological concentrations and play an important role during larval development. Nevertheless, despite having important functions as components of cell membranes and being a precursor of these substances, AA is present in very limited amounts in fish tissues, making it difficult to determine quantitative requirements for this fatty acid.

The aim of the present work was to study the effects of different levels of AA in microdiets on growth, survival and biochemical composition of gilthead seabream larvae.

## 2. Materials and methods

Two trials were carried out feeding *Sparus aurata* larvae squid meal-based experimental microdiets (Salhi et al., 1994) differing only in their fatty acid composition. To

© Del documento, los autores. Digitalización realizada por ULPGC. Biblioteca Universitaria, 2009

obtain the desired fatty acid profile, squid meal was previously defatted three times with chloroform. Fish oils, EPA 28 and DHA 27 (Nippon Chemical Feed, Tokyo, Japan) were used as sources of EPA and DHA, respectively. AA was obtained from Sigma, St. Louis, USA. Lipid and fatty acid composition of microdiets are shown in Table 1. In the first trial, 17-day old larvae were fed microdiets for 14 days. In this trial, five diets were tested, four with AA content from 0.1% to 1.8% d.w. and similar DHA and EPA contents (DHA/EPA = 1.8) and a fifth diet with 1.0% d.w. of AA and DHA/EPA ratio of 0.7 (Table 1) included to observe AA effect under different EPA contents in the diet. In the second experiment, 16-day old larvae were fed for 21 days two microdiets with levels of 0.1%–1.0% d.w. AA and DHA/EPA ratio around 1.8. In both experiments, all diets had the same total $n-3$ HUFA level.

Gilthead seabream larvae were obtained from natural spawning of the broodstock of the Instituto Canario de Ciencias Marinas. Larvae were reared in 100 l cylindrical tanks filled with seawater filtered with 50 μm net. Tanks were provided with central constant aeration and the water flow was 450 ml $min^{-1}$ (around 6.5 water exchanges per day). Larvae were fed microdiets at a rate of 1.5–2.0 g $day^{-1}$. The diet was supplied by automatic feeders for 12 h $day^{-1}$. Rotifers (*Brachionus plicatilis*) fed baker's yeast, which had no HUFA content, were added twice a day to keep a density of 3.5 ind. $ml^{-1}$. Microalgae were no added to experimental tanks. A photoperiod of 12 h artificial light was maintained during the experiments. A total of 2700 and 3000 larvae per tank (individually counted) were used in the first and second experiment, respectively. Water temperature was 17°–19°C in experiment I and 19°–21°C in experiment II.

Table 1
Crude lipid and selected fatty acid content of TL of the experimental diets (% d.w.). tr.: traces

| Fatty acids | Experiment I | | | | | Experiment II | |
|---|---|---|---|---|---|---|---|
| | 1A | 1B | 1C | 1D | 1E | 2A | 2B |
| 16:0 | 1.3 | 1.5 | 1.4 | 1.4 | 1.1 | 1.6 | 1.5 |
| 18:0 | 0.3 | 0.3 | 0.3 | 0.3 | 0.2 | 0.3 | 0.3 |
| 18:1$n-9$ | 4.7 | 5.0 | 4.3 | 3.1 | 4.7 | 5.3 | 4.3 |
| 18:2$n-6$ | 1.5 | 1.7 | 1.6 | 1.6 | 1.6 | 1.8 | 1.7 |
| 20:2$n-6$ | tr. | tr. | tr. | tr. | tr. | tr. | tr. |
| 20:4$n-6$ | 0.1 | 0.2 | 1.0 | 1.8 | 1.1 | 0.1 | 1.0 |
| 20:4$n-3$ | tr. | tr. | tr. | tr. | tr. | tr. | tr. |
| 20:5$n-3$ | 0.7 | 0.7 | 0.7 | 0.7 | 1.1 | 0.8 | 0.8 |
| 22:5$n-6$ | tr. | tr. | tr. | tr. | tr. | 0.1 | 0.1 |
| 22:5$n-3$ | 0.1 | 0.1 | 0.1 | 0.1 | 0.1 | 0.1 | 0.1 |
| 22:6$n-3$ | 1.2 | 1.3 | 1.3 | 1.3 | 0.8 | 1.4 | 1.4 |
| Saturated | 2.0 | 2.2 | 2.1 | 2.1 | 1.7 | 2.3 | 2.2 |
| Monoenoic | 5.6 | 6.1 | 5.3 | 4.3 | 5.7 | 6.4 | 5.2 |
| $\Sigma n-3$ | 2.3 | 2.6 | 2.6 | 2.5 | 2.6 | 2.8 | 2.7 |
| $\Sigma n-6$ | 1.7 | 2.0 | 2.7 | 3.5 | 2.7 | 2.0 | 2.7 |
| $\Sigma n-9$ | 4.8 | 5.1 | 4.4 | 3.2 | 4.8 | 5.4 | 4.4 |
| $\Sigma n-3$ HUFA | 2.0 | 2.2 | 2.1 | 2.1 | 2.1 | 2.4 | 2.3 |
| DHA/EPA | 1.8 | 1.8 | 1.8 | 1.8 | 0.7 | 1.8 | 1.8 |
| EPA/AA | 7.0 | 3.5 | 0.7 | 0.4 | 1.0 | 8.0 | 0.8 |
| TL | 15.7 | 15.6 | 16.6 | 18.8 | 17.2 | 17.4 | 16.6 |

© Del documento, los autores. Digitalización realizada por ULPGC. Biblioteca Universitaria, 2009

Treatments were tested in triplicate. Survival was calculated by individual counting of all the surveying larvae at the beginning and the end of the experiments. Larval growth was determined by measuring at least 30 larvae of each tank, at the beginning, the middle and the end of the feeding trials, by a profile projector (Nikon V-12 A).

Samples of diets, larvae and rotifers were frozen at −80°C for biochemical analysis. Total lipids (TLs) were extracted according to Folch et al. (1957), polar lipid (PL) and neutral lipid (NL) were separated by adsorption chromatography on silica cartridges (Juaneda and Rocquelin, 1985). For fatty acid analysis, heneicosanoic acid (21:0) was added to the crude lipid as an internal standard, lipids were methylated by transesterification with $H_2SO_4$ in methanol solution (Christie, 1982) and purified on $NH_2$ silica cartridges (Sep-Pak®, Van RC, Waters, Milford MA, USA) (Fox, 1990). Fatty acid methyl esters were analyzed using a Shimadzu GC-14A gas chromatograph (Shimadzu, Kyoto, Japan) with flame ionization detector and a Supelcowax-10 fused-silica capillary column (30 m × 0.32 mm I.D., Supelco, Bellefonte, PA, USA) using helium as carrier gas. Column temperature was 180°C during 10 min, increasing afterwards to 215°C at a rate of 2.5°C $min^{-1}$ and maintained at 215°C for 15 min. Fatty acids were identified by reference to a well-characterized fish oil.

The statistical analyses were conducted using a one way analysis of variance (ANOVA) and Tukey test for multiple comparison of means (Sokal and Rohlf, 1981). Linear regression analyses were performed on several diet-larvae parameters.

## 3. Results

In experiment I, 31-day old larvae fed the different AA content microdiets (diet 1A to 1D) did not show significant differences in growth after 14 days of experiment. Larvae

Table 2
Growth and survival of larvae fed microdiets containing different AA levels. Values having the same superscript letter within each column and experiment are not significantly different ($P < 0.05$)

| Experiment I | Diet | Larval age (days) | 17 | 31 | 17 | 31 | 31 |
|---|---|---|---|---|---|---|---|
| | | | Total length (mm) | | Dry body weight (μg) | | Survival (%) |
| | 1A | | 5.03 | 5.76[a] | 86 | 110 | 8.7[a] |
| | 1B | | 5.03 | 5.71[a] | 86 | 112 | 10.0[a] |
| | 1C | | 5.03 | 5.86[a] | 86 | 128 | 19.0[ab] |
| | 1D | | 5.03 | 5.80[a] | 86 | 124 | 31.6[b] |
| | 1E | | 5.03 | 5.54[b] | 86 | 102 | 11.6[a] |
| Experiment II | | Larval age (days) | 16 | 37 | 16 | 37 | 37 |
| | 2A | | 5.33 | 7.30[a] | 122 | 302 | 31.2 |
| | 2B | | 5.33 | 7.48[b] | 122 | 318 | 35.6 |

© Del documento, los autores. Digitalización realizada por ULPGC. Biblioteca Universitaria, 2009

Table 3
Crude lipid and selected fatty acid content of TLs of the larvae (% of total fatty acids). (*) % d.w. tr.: traces

| Fatty acid | Initial | Treatment | | | | | Initial | Treatment | |
|---|---|---|---|---|---|---|---|---|---|
| | | 1A | 1B | 1C | 1D | 1E | | 2A | 2B |
| 16:0 | 18.0 | 14.5±0.9 | 13.4±0.4 | 14.5±0.2 | 13.3±0.6 | 13.6±0.4 | 17.7 | 15.0±0.7 | 14.9±0.2 |
| 16:1$n-7$ | 3.5 | 9.1±1.0 | 10.3±0.7 | 9.6±1.0 | 10.3±0.6 | 9.1±0.2 | 3.6 | 12.4±0.4 | 12.4±0.3 |
| 18:0 | 10.6 | 10.9±0.3 | 10.8±0.2 | 11.0±0.3 | 10.9±0.1 | 11.4±0.1 | 9.0 | 9.3±0.2 | 9.2±0.0 |
| 18:1$n-9$ | 12.6 | 14.4±0.2 | 15.6±0.5 | 15.3±0.6 | 14.8±0.9 | 14.0±0.2 | 13.8 | 21.2±0.4 | 21.1±0.3 |
| 18:2$n-6$ | 1.8 | 2.7±0.2 | 2.4±0.0 | 2.4±0.1 | 2.2±0.1 | 2.4±0.3 | 2.5 | 2.5±0.1 | 2.3±0.1 |
| 20:1$n-9$ | 0.7 | 3.0±0.2 | 1.9±0.1 | 2.1±0.3 | 2.5±0.6 | 2.7±0.4 | 0.7 | 0.4±0.1 | 0.3±0.0 |
| 20:2$n-6$ | 1.5 | 1.2±0.2 | 1.0±0.1 | 0.9±0.1 | 1.1±0.2 | 1.4±0.0 | 2.4 | 1.6±0.9 | 0.6±0.1 |
| 20:4$n-6$ | 3.9 | 3.7±0.4 | 4.1±0.5 | 4.8±0.2 | 5.7±0.2 | 5.1±0.0 | 4.4 | 2.0±0.1 | 3.4±0.1 |
| 20:5$n-3$ | 8.8 | 2.7±0.1 | 3.2±0.2 | 2.9±0.2 | 2.6±0.1 | 2.9±0.2 | 2.7 | 2.6±0.0 | 2.4±0.1 |
| 22:1 | tr. | 1.9±0.4 | 1.0±0.1 | 1.2±0.2 | 1.6±0.5 | 1.8±0.4 | 0.3 | 0.5±0.1 | 0.3±0.0 |
| 22:4$n-9$ | 0.3 | 1.7±0.4 | 0.9±0.0 | 1.1±0.2 | 1.3±0.4 | 1.4±0.3 | 0.4 | tr. | 0.3±0.1 |
| 22:5$n-3$ | 5.1 | 1.5±0.0 | 1.8±0.1 | 1.6±0.1 | 1.7±0.2 | 1.7±0.1 | 10.0 | 1.2±0.1 | 1.3±0.0 |
| 22:6$n-3$ | 21.8 | 7.8±0.2 | 9.1±0.8 | 8.5±0.5 | 7.9±0.2 | 7.2±0.5 | 16.8 | 8.2±0.2 | 8.2±0.3 |
| 24:1 | 0.3 | 1.4±0.1 | 1.4±0.0 | 1.4±0.1 | 1.9±0.5 | 1.7±0.2 | 0.5 | 1.2±0.1 | 1.2±0.1 |
| Saturated | 31.1 | 29.6±0.9 | 27.0±0.2 | 28.1±0.6 | 26.9±0.6 | 28.8±0.4 | 29.1 | 26.3±0.9 | 26.0±0.3 |
| Monoenoic | 19.1 | 37.2±0.5 | 39.4±1.5 | 38.2±1.2 | 39.3±0.6 | 37.2±1.2 | 21.3 | 45.5±0.7 | 45.1±0.7 |
| $\Sigma n-3$ | 39.9 | 12.9±0.3 | 14.9±1.0 | 13.9±0.8 | 13.0±0.7 | 12.5±0.8 | 34.2 | 12.8±0.1 | 12.8±0.4 |
| $\Sigma n-6$ | 8.1 | 8.7±0.5 | 8.5±0.6 | 9.0±0.2 | 10.2±0.2 | 9.8±0.2 | 10.3 | 6.7±0.8 | 6.9±0.1 |
| $\Sigma n-9$ | 10.7 | 19.6±0.4 | 19.0±0.6 | 19.3±0.4 | 19.2±0.2 | 18.5±0.8 | 11.8 | 22.9±0.1 | 22.8±0.2 |
| $\Sigma n-3$ HUPA | 36.1 | 12.1±0.3 | 14.2±1.0 | 13.1±0.9 | 12.3±0.5 | 12.0±0.8 | 33.5 | 12.1±0.1 | 12.0±0.4 |
| EPA/AA | 2.5 | 0.7±0.1 | 0.8±0.1 | 0.6±0.0 | 0.5±0.0 | 0.6±0.0 | 1.8 | 1.3±0.1 | 0.7±0.0 |
| DHA/EPA | 2.3 | 2.9±0.2 | 2.8±0.1 | 3.0±0.1 | 3.1±0.1 | 2.5±0.0 | 2.3 | 3.1±0.1 | 3.4±0.1 |
| TLs (*) | | 19.5 | 20.1 | 22.3 | 18.9 | 23.0 | | 16.2 | 16.5 |
| NLs (*) | | 11.2 | 9.7 | 11.4 | 10.1 | 13.3 | | 7.6 | 6.9 |
| PLs (*) | | 8.3 | 10.4 | 12.9 | 8.8 | 9.7 | | 8.7 | 9.6 |

© Del documento, los autores. Digitalización realizada por ULPGC. Biblioteca Universitaria, 2009

Table 4
Selected fatty acid content of PLs of the larvae (% total fatty acids). n.d.: non-detected. tr.: traces

| Fatty acid | Treatment | | | | | | |
|---|---|---|---|---|---|---|---|
| | 1A | 1B | 1C | 1D | 1E | 2A | 2B |
| 16:0 | 17.4±0.5 | 16.8±0.7 | 17.3±0.3 | 17.3±0.2 | 17.0±0.4 | 18.4±0.6 | 18.1±0.2 |
| 16:1*n*−7 | 8.3±0.9 | 8.7±0.6 | 8.8±0.5 | 9.2±0.7 | 8.0±0.2 | 9.6±0.3 | 9.2±0.4 |
| 18:0 | 11.0±0.3 | 10.9±0.4 | 10.9±0.1 | 10.7±0.3 | 11.4±0.3 | 9.6±0.2 | 9.8±0.0 |
| 18:1*n*−9 | 15.9±0.3 | 15.9±0.7 | 15.9±0.3 | 15.5±0.3 | 15.7±0.4 | 20.6±0.4 | 20.1±0.4 |
| 18:2*n*−6 | 2.9±0.3 | 2.5±0.1 | 2.5±0.2 | 2.1±0.1 | 2.2±0.1 | 2.7±0.1 | 2.5±0.1 |
| 20:1*n*−9 | 1.0±0.0 | 0.91±0.0 | 1.0±0.0 | 0.9±0.0 | 0.9±0.1 | 1.0±0.1 | 1.1±0.0 |
| 20:2*n*−6 | 0.5±0.0 | 0.5±0.0 | 0.5±0.0 | 0.5±0.0 | 0.5±0.0 | 0.8±0.0 | 0.7±0.0 |
| 20:4*n*−6 | 2.7±0.1 | 3.0±0.2 | 4.2±0.3 | 5.2±0.4 | 4.0±0.0 | 2.0±0.2 | 3.8±0.1 |
| 20:4*n*−3 | 0.3±0.0 | 0.3±0.0 | 0.2±0.0 | 0.2±0.0 | 0.3±0.0 | n.d. | tr. |
| 20:5*n*−3 | 4.1±0.1 | 4.1±0.3 | 3.6±0.2 | 3.4±0.0 | 4.2±0.1 | 3.3±0.1 | 3.1±0.0 |
| 22:4*n*−9 | 0.3±0.0 | 0.3±0.0 | 0.3±0.0 | 0.4±0.0 | 0.3±0.0 | n.d. | tr. |
| 22:5*n*−3 | 2.3±0.1 | 2.2±0.1 | 2.1±0.0 | 2.1±0.0 | 2.4±0.1 | 1.7±0.1 | 1.8±0.0 |
| 22:6*n*−3 | 11.8±0.6 | 11.7±1.4 | 10.9±0.2 | 10.5±0.6 | 10.4±0.4 | 11.2±0.6 | 10.8±0.5 |
| 24:1 | 0.5±0.0 | 0.5±0.1 | 0.5±0.1 | 0.5±0.0 | 0.4±0.1 | 0.6±0.0 | 0.6±0.0 |
| Saturated | 31.1±0.5 | 30.0±0.2 | 30.5±0.6 | 30.2±0.3 | 30.9±0.8 | 29.9±0.3 | 29.8±0.3 |
| Monoenoic | 34.5±0.7 | 35.2±1.5 | 35.0±0.1 | 35.4±1.2 | 34.7±0.8 | 38.9±0.8 | 38.1±1.0 |
| Σ*n*−3 | 19.7±0.6 | 19.6±1.9 | 18.2±0.2 | 17.5±0.6 | 18.4±0.4 | 17.4±0.6 | 17.0±0.6 |
| Σ*n*−6 | 7.0±0.3 | 7.0±0.3 | 8.1±0.3 | 8.7±0.5 | 7.7±0.1 | 6.0±0.1 | 7.7±0.2 |
| Σ*n*−9 | 17.9±0.2 | 17.8±0.7 | 17.9±0.3 | 17.6±0.3 | 17.7±0.4 | 22.1±0.5 | 21.5±0.4 |
| Σ*n*−3 | 18.4±0.6 | 18.3±1.8 | 16.9±0.2 | 16.2±0.7 | 17.2±0.5 | 16.2±0.6 | 15.8±0.6 |
| HUFA | | | | | | | |
| EPA/AA | 1.6±0.1 | 1.4±0.1 | 0.9±0.1 | 0.6±0.0 | 1.0±0.0 | 1.6±0.2 | 0.8±0.0 |
| DHA/EPA | 2.9±0.1 | 2.8±0.2 | 3.0±0.2 | 3.1±0.2 | 2.5±0.0 | 3.4±0.2 | 3.5±0.2 |

© Del documento, los autores. Digitalización realizada por ULPGC. Biblioteca Universitaria, 2009

Table 5
Selected fatty acid content of NLs of the larvae (% total fatty acids)

| Fatty acid | Treatment | | | | | | |
|---|---|---|---|---|---|---|---|
| | 1A | 1B | 1C | 1D | 1E | 2A | 2B |
| 16:0 | 12.4±1.7 | 9.8±0.3 | 10.7±0.3 | 9.8±1.0 | 11.1±0.4 | 11.1±0.9 | 10.5±0.1 |
| 16:1$n-7$ | 9.7±1.9 | 12.0±0.9 | 10.8±1.9 | 11.3±1.3 | 9.8±0.5 | 15.6±1.0 | 16.7±0.2 |
| 18:0 | 10.9±0.8 | 10.7±0.0 | 11.2±0.7 | 11.1±0.2 | 11.4±0.3 | 8.8±0.7 | 8.4±0.0 |
| 18:1$n-9$ | 13.2±0.5 | 15.2±0.6 | 14.5±1.2 | 14.2±1.8 | 12.8±0.1 | 21.8±0.8 | 22.6±0.1 |
| 18:2$n-6$ | 2.6±0.1 | 2.2±0.0 | 2.3±0.1 | 2.3±0.2 | 2.5±0.4 | 2.2±0.1 | 1.9±0.1 |
| 20:1$n-9$ | 4.5±0.5 | 2.9±0.1 | 3.8±0.6 | 3.8±1.2 | 4.0±0.7 | 0.9±0.2 | 0.8±0.1 |
| 20:2$n-6$ | 1.6±0.5 | 1.4±0.2 | 1.5±0.3 | 1.7±0.3 | 2.0±0.0 | 2.6±1.9 | 0.4±0.2 |
| 20:4$n-6$ | 4.5±0.9 | 5.3±1.0 | 5.6±0.8 | 6.1±0.4 | 5.8±0.0 | 1.9±0.1 | 2.8±0.0 |
| 20:5$n-3$ | 1.7±0.3 | 2.2±0.0 | 1.9±0.4 | 1.9±0.2 | 2.0±0.2 | 1.8±0.1 | 1.6±0.1 |
| 22:1 | 3.3±0.8 | 2.1±0.2 | 2.8±0.5 | 2.9±0.9 | 3.1±0.7 | 1.1±0.2 | 0.8±0.1 |
| 22:4$n-9$ | 2.7±0.9 | 1.6±0.0 | 2.1±0.4 | 2.2±0.8 | 2.1±0.5 | 0.5±0.1 | 0.5±0.0 |
| 22:5$n-3$ | 0.8±0.0 | 1.3±0.1 | 0.9±0.3 | 1.3±0.4 | 1.2±0.1 | 0.6±0.1 | 0.6±0.0 |
| 22:6$n-3$ | 4.9±0.1 | 6.3±0.3 | 5.1±1.4 | 5.7±0.5 | 5.0±0.7 | 4.7±0.2 | 4.5±0.0 |
| 24:1 | 2.0±0.2 | 2.4±0.0 | 2.7±0.3 | 3.0±0.9 | 2.7±0.5 | 2.0±0.3 | 2.0±0.2 |
| Saturated | 29.0±1.4 | 24.2±0.5 | 25.6±1.0 | 24.5±0.8 | 27.5±0.1 | 22.7±1.5 | 21.6±0.4 |
| Monoenoic | 39.2±1.1 | 43.9±2.2 | 42.5±2.9 | 42.6±0.9 | 39.0±1.4 | 53.0±1.9 | 55.0±0.6 |
| $\Sigma n-3$ | 7.8±0.3 | 9.8±0.4 | 8.0±1.9 | 9.1±1.2 | 8.2±1.0 | 7.4±0.5 | 6.9±0.1 |
| $\Sigma n-6$ | 10.0±1.2 | 10.0±1.2 | 10.3±0.9 | 11.5±0.3 | 11.3±0.3 | 7.5±1.7 | 5.9±0.2 |
| $\Sigma n-9$ | 20.9±0.8 | 20.3±0.8 | 21.1±1.0 | 20.5±0.1 | 19.1±1.1 | 23.8±0.5 | 24.7±0.0 |
| $\Sigma n-3$ HUFA | 7.4±0.4 | 9.8±0.4 | 7.8±2.0 | 8.9±1.0 | 8.2±1.0 | 7.3±0.5 | 6.8±0.0 |
| EPA/AA | 0.4±0.0 | 0.4±0.1 | 0.3±0.0 | 0.3±0.0 | 0.3±0.0 | 1.0±0.0 | 0.6±0.0 |
| DHA/EPA | 3.0±0.4 | 2.8±0.1 | 2.7±0.2 | 3.0±0.0 | 2.5±0.0 | 2.5±0.0 | 2.9±0.2 |

© Del documento, los autores. Digitalización realizada por ULPGC. Biblioteca Universitaria, 2009

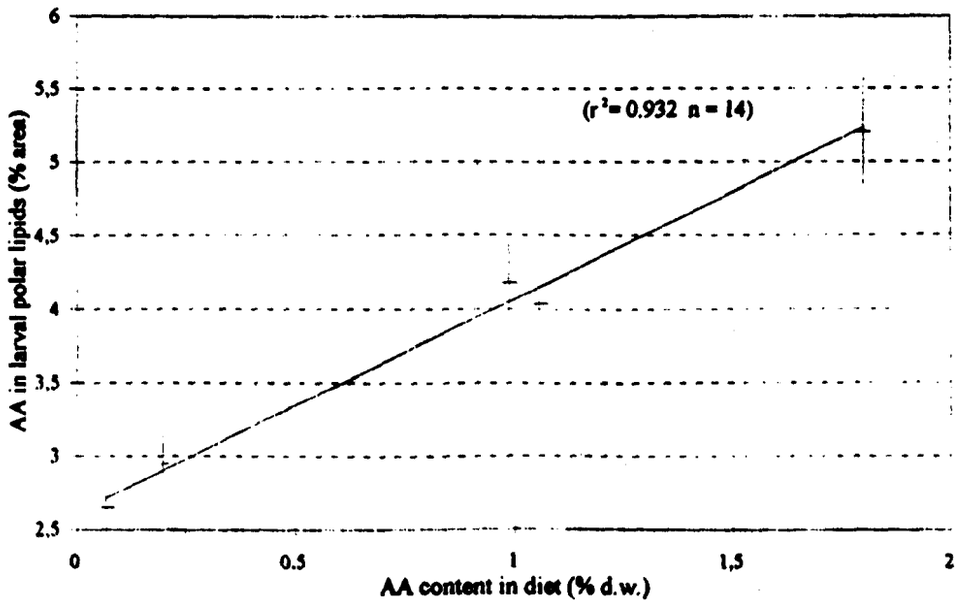


Fig. 1. Effect of different dietary AA levels on AA accumulation in larval PLs.

fed diet 1E, with 1% d.w. of AA but with a lower DHA/EPA ratio (0.7) than the other diets (1.8), presented the smallest ($P < 0.05$) size at the end of the experiment (Table 2). Larvae fed diet 1D containing 1.8% d.w. of AA showed a better survival than those fed diets 1A or 1B, with 0.1% and 0.2% d.w. of AA, respectively (Table 2).

In the second, and longer experiment, an increase in the AA level in the diets from 0.1% to 1.0% d.w. significantly improved ($P < 0.05$) larval growth after 21 days of feeding the microdiets.

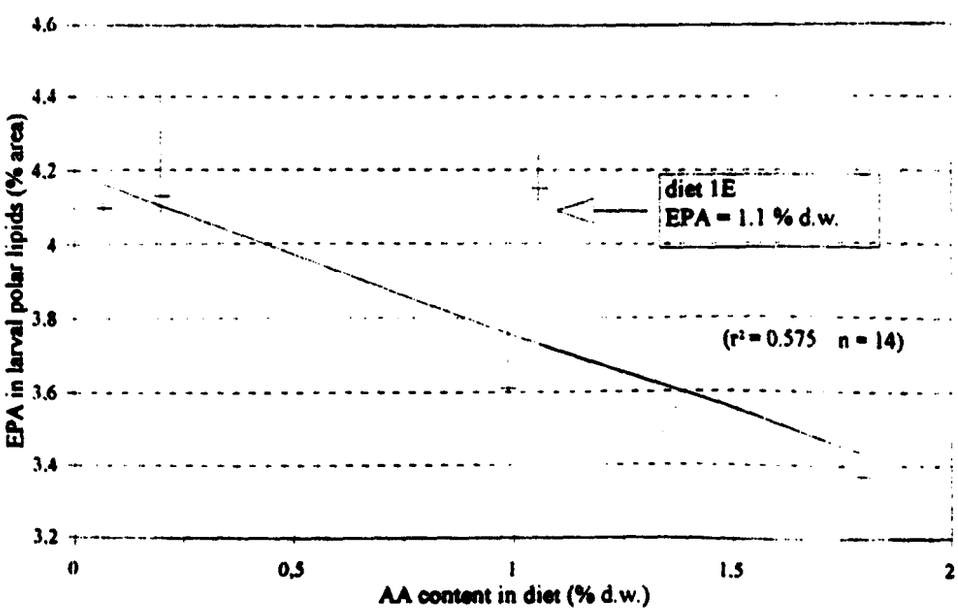


Fig. 2. Effect of different dietary AA levels on EPA accumulation in larval PLs.

© Del documento, los autores. Digitalización realizada por ULPGC. Biblioteca Universitaria, 2009

Izquierdo, M.S., 1996. Essential fatty acid requirements of cultured marine fish larvae. Review article. Aquacult. Nutr. 2, 183–191.

Izquierdo, M.S., Watanabe, T., Takeuchi, T., Arakawa, T., Kitajima, C., 1989. Requirement of larval red seabream *Pagrus major* for essential fatty acids. Nippon Suisan Gakkaishi 55, 859–867.

Juaneda, P., Rocquelin, G., 1985. Rapid and convenient separation of phospholipids from rat heart using silica cartridges. Lipids 20, 40–41.

Koven, W.M., Kissil, G.W., Tandler, A., 1989. Lipid and $\bar{\omega}$-3 requirements of *Sparus aurata* larvae during starvation and feeding. Aquaculture 79, 185–191.

Koven, W.M., Tandler, A., Kissil, G.W., Sklam, D., 1992. The importance of $n-3$ highly unsaturated fatty acids for growth in larval *Sparus aurata* and their effect on survival, lipid composition and size distribution. Aquaculture 104, 91–104.

Linares, F., Henderson, R.J., 1991. Incorporation of $^{14}$C-labeled polyunsaturated fatty acids by juvenile turbot, *Scophthalmus maximus* (L.) in vivo. J. Fish Biol. 38, 335–348.

Mc Phail, L.C., Clayton, C.C., Snyderman, R., 1984. A potential second messenger role for unsaturated fatty acids: activation of $Ca^{2+}$ dependent protein kinase C. Science 224, 622–625.

Mourente, G., Rodríguez, A., Tocher, D.R., Sargent, J.R., 1993. Effects of dietary docosahexaenoic acid (DHA; 22:6 $n-3$) on lipid and fatty acid compositions and growth in gilthead sea bream (*Sparus aurata* L.) larvae during first feeding. Aquaculture 112, 79–98.

Reitan, K.I., Rainuzzo, J., Olsen, Y., 1994. Influence of lipid composition of live feed on growth, survival and pigmentation of turbot larvae. Aquacult. Int. 2, 23–48.

Rodríguez, C., 1994. Estudio de los requerimientos de ácidos grasos esenciales de la dorada europea (*Sparus aurata*, L.) durante las dos primeras semanas de alimentación. PhD Thesis, University of La Laguna, Spain.

Rodríguez, C., Pérez, J.A., Izquierdo, M.S., Mora, J., Lorenzo, A., Fernández-Palacios, H., 1993. Essential fatty acid requirements for larval gilthead sea bream (*S. aurata*). Aquacult. Fish. Manage. 24, 295–304.

Rodríguez, C., Pérez, J.A., Díaz, M., Izquierdo, M.S., Fernández-Palacios, H., Lorenza, A., 1997. Influence of the EPA/DHA ratio in rotifers on gilthead seabream (*Sparus aurata*) larval development. Aquaculture 150, 77–89.

Salhi, M., Izquierdo, M.S., Hernández-Cruz, C.M., González, M., Fernández-Palacios, H., 1994. Effect of lipid and $n-3$ HUFA levels in microdiets on growth survival and fatty acid composition of larval gilthead seabream (*Sparus aurata*). Aquaculture 124, 275–282.

Sargent, J.R., Bell, J.G., Bell, M.V., Henderson, R.J., Tocher, D.R., 1994. The metabolism of phospholipids and polyunsaturated fatty acids in fish. In: Lahlou, B., Vitiello, P. (Eds.), Aquaculture: Fundamental and Applied Research. American Geophysical Union, pp. 103–113.

Smith, W.L., 1989. The eicosanoids and their biochemical mechanism of action. Biochem. J. 259, 315–324.

Sokal, R.R., Rohlf, F.J., 1981. Biometry. The Principles and Practices of Statistics in Biological Research. 2nd edn. Freeman, New York, 859 pp.

Tocher, D.R., Sargent, J.R., 1986. Incorporation of [1–14C] arachidonic and [1–14C] eicosapentaenoic acid into the phospholipids of peripheral blood neutrophils from the plaice *Pleuronectes platessa* L. Biochim. Biophys. Acta 876, 592–600.

Watanabe, T., 1993. The importance of docosahexaenoic acid in marine larval fish. J. World Aquacult. Soc. 24, 152–161.

Zheng, F., Takeuchi, T., Yosheda, K., Kobayashi, M., Hirokawa, J., Watanabe, T., 1996. Requirement of larval cod for arachidonic acid, eicosapentaenoic acid and docosahexaenoic acid using by their enriched *Artemia* nauplii. Nippon Suisan Gakkaishi 62, 669–676, In Japanese.

© Del documento, los autores. Digitalización realizada por ULPGC. Biblioteca Universitaria, 2009

1997). The results showed that, at least for larval growth and survival, the possible effect of AA could be masked by the influence of dietary DHA/EPA ratio.

AA has been described as one of the main components of certain phospholipids, specifically PI (Bell and Tocher, 1989; Bell and Dick, 1990; Bell et al., 1983). In larval gilthead seabream, the AA content in the PL fraction of the larvae was increased by the increase in dietary AA level, in agreement with the data reported by Bell et al. (1995). The EPA incorporation in the PL fraction of the larvae has also been related to the EPA content in the diet (Reitan et al., 1994). Looking for possible interaction between dietary EPA and AA values on larval composition, we observed that EPA incorporation in the PL fraction of the larvae was negatively affected by dietary AA content. Competition between EPA and AA during phospholipid esterification has been suggested to occur in fish (Tocher and Sargent, 1986; Bell et al., 1995), particularly in PI where both fatty acids are major components. The results of the present study are consistent with the competition between the two fatty acids for incorporation into PLs. Since both AA and EPA released from PI by phospholipase $A_2$ action are precursors of eicosanoids (Henderson et al., 1985), their respective incorporation into such PL fractions may have an influence on the synthesis of different types of eicosanoids.

## References

Bell, M.V., Dick, J.R., 1990. Molecular species composition of phosphatidylinositol from brain, retina, liver and muscle of cod (*Gadus morhua*). Lipids 25, 691–694.

Bell, M.V., Tocher, D.R., 1989. Molecular species composition of the major phospholipids in brain and retina from rainbow trout (*Salmo gardnieri*). Biochem. J. 264, 909–915.

Bell, M.V., Simpson, C.M.F., Sargent, J.R., 1983. ($n-3$) and ($n-6$) polyunsaturated fatty acids in the phosphoglycerides of salt-secreting epithelia from two marine fish species. Lipids 18, 720–725.

Bell, J.G., Tocher, D.R., Sargent, J.R., 1994. Effects of supplementation with 20:3 ($n-6$), 20:4 ($n-6$) and 20:5 ($n-3$) on the production of the prostaglandins E and F of the 1-, 2- and 3-series in turbot (*Scophthalmus maximus* L.) brain astroglial cells in primary culture. Biochim. Biophys. Acta 1211, 335–342.

Bell, J.G., Castell, J., Tocher, D.R., MacDonald, F.M., Sargent, J.R., 1995. Effects of different dietary arachidonic acid: dosahexaenoic acid ratios on phospholipid fatty acid compositions and prostaglandin production in juvenile turbot (*Scophthalmus maximus* L.). Fish Physiol. Biochem. 14, 139–151.

Castell, J.D., Bell, J.G., Tocher, D.R., Sargent, J.R., 1994. Effect of purified diets containing different combinations of arachidonic and docosahexaenoic acid on survival, growth and fatty acid composition of juvenile turbot. Aquaculture 128, 315–333.

Christie, W.W., 1982. Lipid Analysis. Pergamon, Oxford, UK.

Folch, J., Lees, M., Stanley, G.H.S., 1957. A simple method for the isolation and purification of total lipids from animal tissues. J. Biol. Chem. 226, 497–509.

Fox, C., 1990. Studies on polyunsaturated fatty acid nutrition in the larvae of a marine fish — the herring, *Clupea harengus* L. PhD Thesis, University of Stirling, Scotland.

Furuita, H., Takeuchi, T., Toyota, M., Watanabe, T., 1996. EPA and DHA requirements in early juvenile red seabream using HUFA enriched *Artemia* nauplii. Fish. Sci. 62, 246–251.

Henderson, R.J., Sargent, J.R., 1985. Fatty acid metabolism in fish. In: Cowey, C.B., Mackie, A.M., Bell, J.G. (Eds.), Nutrition and Feeding in Fish. Academic Press, London, pp. 349–364.

Henderson, R.J., Bell, M.V., Sargent, J.R., 1985. The conversion of polyunsaturated fatty acids to prostaglandins by tissue homogenates of the turbot, *Scophthalmus maximus* (L.). J. Exp. Mar. Biol. Ecol. 85, 93–99.

© Del documento, los autores. Digitalización realizada por ULPGC. Biblioteca Universitaria, 2009

Larval TL content and fatty acid composition are presented in Table 3. In the first experiment, a significant correlation ($P < 0.05$) was found between AA levels of the diet and the AA content in the larval TL. In experiment II, larvae fed diet 2B (AA = 1.0% d.w.) showed higher AA levels ($P < 0.05$) in TL than larvae fed diet 2A (AA = 0.1% d.w.).

The fatty acid composition of the PL and NL fractions are shown in Tables 4 and 5, respectively. As observed in the TL, AA contents of the NL and PL reflected those of the diets, being positively correlated ($P < 0.05$) with the dietary values (Fig. 1).

The larval EPA content was negatively affected by the AA level of the diet. In experiment I, a decrease in the EPA amount in larval PL was observed when the AA level in the diet was increased, the EPA level was negatively correlated ($P < 0.05$) with the amount of AA in the diet (Fig. 2). In experiment II, larvae fed diet 2B (1.0% d.w. AA) presented significantly lower amounts of EPA in PL than those fed diet 2A (0.1% d.w. AA). The amount of AA in larval PL did not seem to be affected when the EPA content in the diet was increased from 0.7% to 1.1% d.w.

## 4. Discussion

Investigations on marine fish nutrition conducted to determine the effect of AA on fish growth and survival are scarce. Zheng et al. (1996) reported that cod larvae fed enriched *Artemia* with different AA levels (3.7%–7.6% d.w.) showed poorer survival and slower growth than those larvae fed *Artemia* with less than 0.5 d.w. AA level. Castell et al. (1994) fed juvenile turbot for 11 weeks and found a rapid response to dietary supplementation with AA during the first 2 weeks. However, a compensatory growth response was observed during the rest of the feeding trial, because they did not observe differences in growth with fish fed a non-AA supplemented diet at the end of the experiment, suggesting that the fish were deficient in this fatty acid at the beginning of the experiment.

A growth promoting effect of AA was observed in the present study after 3 weeks feeding the experimental microdiets. In experiment I, the increase in AA level from 0.1% to 1.0% d.w. after 14 days feeding slightly increased growth rate but not significantly, perhaps suggesting that a longer feeding period could show an effect of AA acid supplementation on growth. Thus, a 3-week feeding trial was conducted, and the increase in the AA level from 0.1% to 1.0% d.w. significantly improved larval growth. Since all the diets had a similar $n-3$ HUFA content and the same DHA/EPA ratios (with the exception of diet 1E that showed the lowest growth), the consistently good survival of fish fed diet 1D and the bad performance of those fed diets 1A and 1B, and the better growth observed in larvae fed diet 2B (high AA) than 2A, confirms the importance of AA for gilthead seabream larvae.

Besides the importance of dietary AA, the importance of dietary DHA/EPA ratio was also marked, since larvae fed diet 1E showed the lowest growth in experiment I, in spite of the high dietary AA content (1.0% d.w.). The significance of the DHA/EPA ratio in diets for gilthead seabream larvae has already been reported (Rodríguez et al.,

© Del documento, los autores. Digitalización realizada por ULPGC. Biblioteca Universitaria, 2009

*Mineral Deposits: Processes to Processing, Stanley et al. (eds) © 1999 Balkema, Rotterdam, ISBN 90 5809 068 X*

# Metallogenesis of lead-zinc deposits of the Alcudia Valley, Spain

**R.A. Both** – *Department of Geology and Geophysics, University of Adelaide, S.A., Australia*

**F.J. Palero** – *Departamento de Geología, Minas de Almadén y Arrayanes, Spain*

**A. Arribas** – *Escuela Técnica Superior de Ingenieros de Minas, Madrid, Spain*

**A. Boyce** – *Scottish Universities Research and Reactor Centre, East Kilbride, UK*

**J. Mangas** – *Departamento de Física, Universidad de Las Palmas de Gran Canaria, Spain*

ABSTRACT: Neoproterozoic and Palaeozoic sedimentary rocks in the Alcudia Valley, Spain, host a large number of Pb-Zn(-Ag-Cu) deposits which can be classified into five types. With the exception of the minor syn-diagenetic stratabound type V mineralisation, other deposits occupy fractures generated during the Hercynian Orogeny. Types I, II and III are syn-tectonic veins whereas the most abundant deposits, type IV, are post-tectonic veins showing a spatial relationship with late Hercynian granite intrusions.

## 1 INTRODUCTION

The Alcudia Valley in the eastern Sierra Morena, Ciudad Real Province, Spain (Figure 1) has been mined since Roman times and was an important mining field in the last quarter of the 19th century and the early part of the 20th century. This district, along with the neighbouring Linares and La Carolina fields, made Spain one of the leading Pb-producing countries during that period. The district is remarkable for the intensity of mineralisation, with a total of 484 mines and prospects hosted by Neoproterozoic and Palaeozoic sedimentary rocks in an area of approximately 2500 km$^2$ (Palero 1991). The deposits are dominantly Pb-Zn veins with significant contents, but irregular distribution, of Ag and Cu.

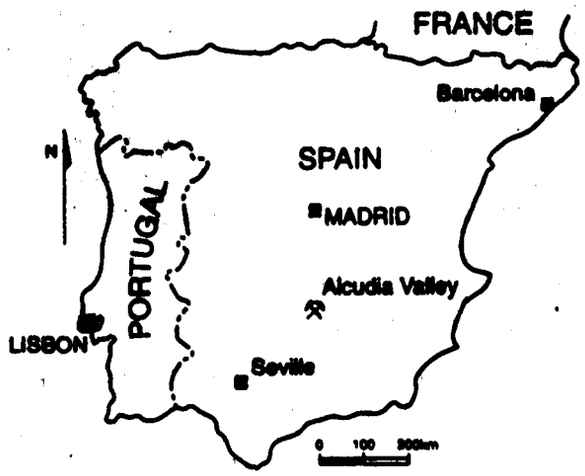


Figure 1. Location of the Alcudia Valley mineral field

## 2 GEOLOGICAL SETTING

The Alcudia Valley lies within the southern sector of the Central Iberian Zone of the Iberian Massif. A prominent feature of the geology is a series of major WNW-ESE trending anticlines and synclines formed during the Hercynian Orogeny.

The Neoproterozoic rocks, generally referred to as "Alcudiense" (Tamain 1972), are equivalent to the schist-graywacke complex that forms a broad zone in the central and western parts of the Iberian Peninsula. The "Lower Alcudiense" unit is a monotonous sequence of shales and graywackes, and is overlain unconformably by the more heterogeneous "Upper Alcudiense" unit consisting of sandstones, shales, graywackes, conglomerates and limestones. The contact between the "Upper Alcudiense" and Lower Palaeozoic rocks is marked by a disconformity. The Ordovician-Devonian sequence is almost continuous from Tremadocian to Gedinnian and consists of alternating orthoquartzites, shales and sandstones.

Lower Carboniferous rocks crop out in a wide belt in the southern part of the area and form a characteristic unit known as "Culm de Los Pedroches" consisting of a monotonous sequence of shales and sandstones, with some intercalated lenses of conglomerate. Deposition of the "Culm" was followed by the Hercynian Orogeny and the post-orogenic sediments of the Puertollano coal basin of Stephanian age.



© Del documento, los autores. Digitalización realizada por ULPGC. Biblioteca Universitaria, 2009

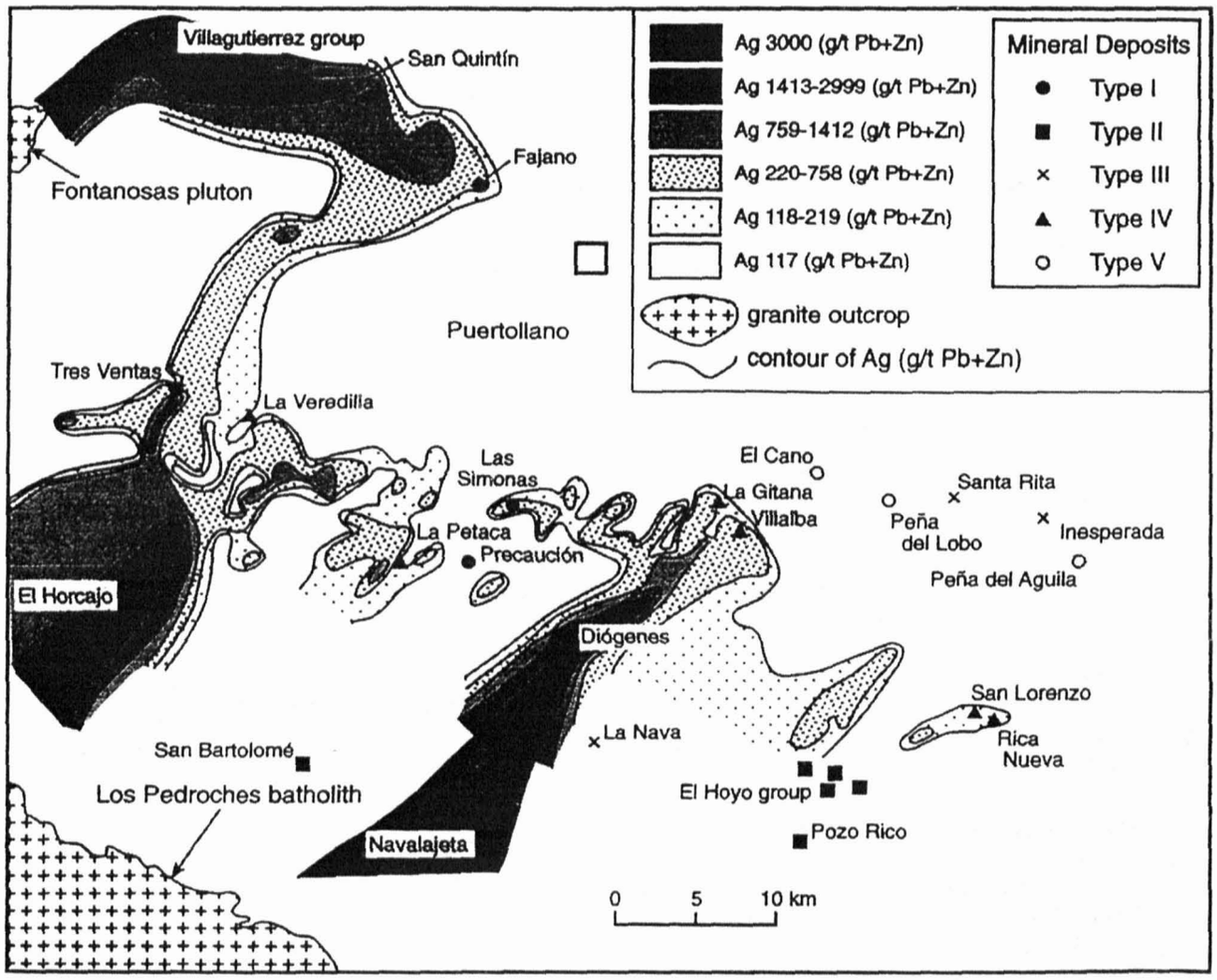


Figure 2. Location of the major examples of the five types of Pb-Zn deposits in the Alcudia Valley and contours of Ag grades of type IV deposits

The rocks of the Alcudia Valley have been subjected to several phases of deformation. Two pre Ordovician deformation events affected the Precambrian rocks; the first folded the "Lower Alcudiense" rocks whereas the second followed deposition of the "Upper Alcudiense" sediments and involved vertical displacement of blocks controlled by major NW-SE fractures. The most important deformation took place during the Hercynian Orogeny, with two phases that affected almost the entire Precambrian and Palaeozoic sequence. The first phase ($H_{D1}$) was responsible for the major WNW-ESE trending folds and longitudinal fractures parallel to fold axes. $H_{D1}$ post-dated deposition of the "Culm" but preceded Stephanian sedimentation. The second phase of Hercynian deformation ($H_{D2}$) produced ductile-brittle shear zones, the majority of which are sinistral, trending NE-SW, with some dextral, trending NW-SE. The impact of these shear zones on $H_{D1}$ structures resulted in interference folds and fractures in which most of the Pb-Zn veins of the Alcudia Valley were deposited.

Magmatic activity in the region is represented by Palaeozoic and Tertiary-Quaternary volcanism and both pre- and syn-Hercynian granite intrusions. Volcanic rocks, mainly pyroclastics, are found interbedded with sediments at several stratigraphic levels in the Palaeozoic sequence. Pre-Hercynian intrusive rocks are found in the northwestern part of the district, and consist of small stocks of calcalkaline porphyries. Of much greater significance are the Hercynian granites which crop out in the northwest and southwest of the area as the Fontanosas stock and Los Pedroches batholith (Figure 2). Two distinct facies are present in these intrusive bodies: a biotite granodiorite with enclaves and a porphyritic cordierite monzogranite with feldspar megacrysts. Recent investigations on equivalent granites in nearby areas have shown that the granodiorites were emplaced either during the interval between the two



© Del documento, los autores. Digitalización realizada por ULPGC. Biblioteca Universitaria, 2009

Hercynian deformations ($H_{D1}$ and $H_{D2}$) or at the beginning of $H_{D2}$, whereas the monzogranites clearly post-dated $H_{D2}$ (Palero, Zuazo & Fernández-Carrasco, unpubl.).

## 3. MINERALISATION

### 3.1 *Mineral deposit types*

Five distinct types of deposits (Figure 2) have been recognised on the basis of morphology, host rocks, structural setting and mineral assemblages (Palero 1991). Type I deposits (e.g. Tres Ventas) are Zn-Pb veins in $H_{D2}$ shear fractures in Neoproterozoic rocks. Type II deposits (e.g. El Hoyo group) are strongly deformed Zn-Pb-Cu veins in $H_{D1}$ fractures in Ordovician rocks. Type III deposits (e.g. La Nava) are Zn-Pb veins exhibiting a greater variation in morphology and degree of deformation compared with other types, and are found in both $H_{D1}$ and $H_{D2}$ fractures in Late Ordovician and Early Silurian rocks. Type IV deposits (e.g. San Quintín) are the most abundant and economically most important type. These are Pb-Ag-Zn veins occupying $H_{D2}$ fractures and are widely distributed through the district in rocks ranging from Neoproterozoic to Late Ordovician, although most common in Neoproterozoic host rocks. Type IV veins are characterised by complex mineralogy and paragenetic sequence and show a spatial relationship with porphyritic monzogranites emplaced at around 290 Ma (Penha & Arribas 1974). Ag grades of these deposits show a zonation in three "corridors" extending out from post-$H_{D2}$ intrusions (Figure 2). The zonation also correlates with a trend from early stage minerals close to granite contacts to later stage minerals further out. Type V (e.g. Peña del Aguila) is a minor type of stratabound Zn-Pb mineralisation occurring as disseminations and small veins in Late Ordovician limestone.

### 3.2 *Metallogenesis*

Deposition of Type V mineralisation preceded the Hercynian Orogeny. A syn-diagenetic origin is suggested by the limited stratigraphic distribution of the mineralisation and anomalous base metal contents of Late Ordovician-Early Silurian black shales overlying the mineralised limestone (Palero & Martín-Izard 1988). $\delta^{34}S$ values of 8.3 to 13.6‰ are compatible with bacteriogenic reduction of Late Ordovician-Early Silurian seawater sulphate. Minor remobilisation of disseminated sulphides into veins took place during late diagenesis or early Hercynian deformation.

The origins of the other four types of deposits are intimately related to the Hercynian Orogeny. Type II deposits were syn-$H_{D1}$ veins. Fluid inclusions in quartz are mainly aqueous and rarely aqueo-carbonic, with mean homogenisation temperatures (Th) of 176°C and 344°C, respectively. The mean salinity of each fluid inclusion type is approximately 3.5 wt. % NaCl equivalent. $\delta^{34}S$ values of sulphides are -0.7 to 17.0‰ and calculated $\delta^{18}O_{H_2O}$ values are approximately -1 to 2.5‰. Lithogeochemical studies (Delgado et al. 1988) have shown depletion in metal contents of host rocks adjacent to the veins of El Hoyo group, suggesting a lateral secretion process involving mobilisation of metals by a surface-derived fluid, either seawater or meteoric water. The former is more likely on the basis of $\delta^{34}S$ data, which may be explained by thermochemical or inorganic reduction of seawater sulphate. The aqueo-carbonic fluid inclusions may represent a minor influx of metamorphic fluid.

Type III veins formed during both $H_{D1}$ and $H_{D2}$ in localised hydrothermal systems. Fluid inclusions in quartz are aqueous with a mean Th of 206°C and mean salinity of 6.2 wt % NaCl equivalent. The stratigraphic distribution and $\delta^{34}S$ values of sulphides (7.3 to 13.3‰) are similar to type V deposits, suggesting an origin involving either remobilisation of syn-diagenetic type V mineralisation or derivation of metals from the same source (viz. Late Ordovician-Early Silurian black shales). $\delta^{13}C$ values of carbonates (-7.5 to -7.1‰) are within the possible range for dissolution of limestone (Ohmoto 1986) but an organic-derived component is also probable. Calculated $\delta^{18}O_{H_2O}$ values are approximately 5 to 7‰, in keeping with formation waters.

Type I deposits were syn-$H_{D2}$ veins. Fluid inclusions in quartz contain a higher temperature aqueo-carbonic fluid (mean Th of 270°C and salinity up to 8 wt % NaCl equivalent) and a lower temperature aqueous fluid (mean Th of 228°C and mean salinity of 9 wt % NaCl equivalent), and may represent mixing of a metamorphic fluid with formation water. Calculated $\delta^{18}O_{H_2O}$ values are approximately 2 to 7‰. $\delta^{34}S$ values of sulphides of -12.7 to 4.7‰ and $\delta^{13}C$ values of carbonates of -12.5 to -9.3‰ are in keeping with black shales of the Neoproterozoic sequence as the major source of sulphur and a partial source of carbon.

Fluid inclusions in ankerite in type IV veins record relatively low temperatures (Th values from 89° to 145°C) and a wide range of salinities (12 to 41 wt % NaCl equivalent), typical of basinal brines (e.g. Munoz et al. 1994, Wilkinson et al. 1995). Calculated $\delta^{18}O_{H_2O}$ values are approximately 0 to 4‰. The veins are located in $H_{D2}$ fractures and the spatial relationship to monzogranite outcrops indicates that late Hercynian magmatism was the source of heat driving fluid migration through the fracture system. Reaction of the fluid with black shales of the Neoproterozoic sequence is suggested by $\delta^{34}S$ values of sulphides (-10.0 to -2.7‰) and $\delta^{13}C$ values of carbonates (-11.8 to -8.2‰) of the main



© Del documento, los autores. Digitalización realizada por ULPGC. Biblioteca Universitaria, 2009

stages of the paragenetic sequence. The final paragenetic stage consists of barite ($\delta^{34}S$ = 13.4 to 19.0‰), with calcite and pyrite (single $\delta^{34}S$ value = -23.8‰). In the adjacent Linares and La Carolina fields, barite veins associated with Pb veins similar to the Alcudia type IV deposits reach, and are hosted by, the lower part of the Triassic sequence overlying the Palaeozoic sedimentary rocks and granites (Azcárate et al. 1971). This suggests that the final stage of the Alcudia type IV veins may have been deposited during a later hydrothermal event than minerals of the main stages.

## 4 CONCLUSIONS

The Pb-Zn(-Ag-Cu) deposits of the Alcudia Valley represent a sequence of mineralising events over a time span of at least 200 Ma, commencing with syn-diagenetic type V mineralisation in Late Ordovician sediments. Syn-tectonic mineralisation was deposited during both major phases of Hercynian deformation, with type II deposits syn-$H_{D1}$, type I syn-$H_{D2}$ and type III deposited during both $H_{D1}$ and $H_{D2}$. The economically most important mineralisation event was post-tectonic, when deposition of the main stages of type IV veins was associated with the emplacement of late Hercynian granites. The final stage of type IV mineralisation was apparently deposited during the Triassic.

## REFERENCES


Azcárate, J.E., A.Vergara & A.Argüelles 1971. Carácteres metalogénicos de los distritos mineros de Linares - La Carolina. *Congr. Hispano - Luso - Americano de Geologia Económica, Madrid.* 1:3-14.

Delgado, J. C., A. Martín-Izard & F.J. Palero 1988. Litogeoquímica de la Formación Estratos Pochico (Ordovícico Inferior) y su relación metalogénica con algunos yacimientos filonianos de Pb-Zn de Sierra Morena Oriental. *Geociencias*, 3: 333-350.

Munoz, M., A.J. Boyce, P. Courjault-Rade, A.E. Fallick & F. Tollon 1994. Multi-stage fluid incursion in the Palaeozoic basement-hosted Saint-Salvy ore deposit (NW Montagne Noire, southern France). *Appl. Geochem.* 9: 609-626.

Ohmoto, H. 1986. Stable isotope geochemistry of ore deposits. In J.W. Valley, H.P. Taylor Jr. & J.R. O'Neil (eds.), *Stable Isotopes in High Temperature Geological Processes*. Reviews in Mineralogy, 16: 491-559. Min. Soc. Amer.

Palero, F.J. 1991. Evolución geotectónica y yacimientos minerales de la Región del Valle de Alcudia, (Sector Meridional de la Zona Centroibérica). Unpubl. doctoral thesis, Univ. de Salamanca.

Palero, F.J. & A. Martín-Izard 1988. Las mineralizaciones estratoides de Zn-Pb en la Caliza Urbana del paraje de Peña del Aguila, Calzada de Calatrava (Ciudad Real). *Bol. Soc. Esp. de Mineralogía*, 11: 179-189.

Penha, M. H., and Arribas, A. 1974, Datacion geocronológica de algunos granitos uraníferos españoles. *Bol. Geol. y Min.*, LXXXV: 271-273.

Tamain, G. 1972, Recherches geologiques et minieres en Sierra Morena Orientale, Espagne: Unpubl. These 3ème cycle, Univ. de Paris Sud. Centre d'Orsay.

Wilkinson, J.J., G.R.T. Jenkin, A.E. Fallick & R.P. Foster 1995. Oxygen and hydrogen isotope evolution of Variscan crustal fluids, south Cornwall, U.K. *Chem. Geol.* 123:239-254.




© Del documento, los autores. Digitalización realizada por ULPGC. Biblioteca Universitaria, 2009

AGGRESSIVE BEHAVIOR
Volume 25, pages 297–303 (1999)

# Effect of Residence and Size Asymmetries Upon the Agonistic Interactions Between Juvenile White-Seabream (*Diplodus sargus cadenati* de la Paz, Bauchot and Daget, 1974)

**Catalina Caballero and José J. Castro***

*Departamento de Biología, Universidad de Las Palmas de Gran Canaria, Las Palmas de Gran Canaria, Canary Islands, Spain*

**The behavioural patterns of juvenile white-seabream suggest that asymmetry in residence is an important factor governing the outcome of contest between individuals of this species. Asymmetries due to resident status had strong effects on agonistic behaviour, with asymmetries in body sizes producing weaker effects. Resident fish won all the combats against intruders of lower or similar length. However, when the intruder was larger than the residents (higher than 5% in length and 20% in weight), the percentage of combats won by the residents decreased to 85.7%. There was a significant correlation between fight intensity and size asymmetry in favour of the resident fish. The resident fish was more aggressive and persistent in attacks, and contests were more intense when the size of the intruder was greater. During agonistic interactions, the frontal attacks and lateral displays were more frequent when the intruders were similar or larger than residents. Attacks to the flanks and chases were more frequent in pairs where the intruders were smaller. Aggr. Behav. 25:297–303, 1999.** © 1999 Wiley-Liss, Inc.

**Key words:** *Diplodus sargus cadenati*; sparidae; agonistic territorial behaviour; asymmetrical contest; prior residency effect

## INTRODUCTION

Maynard-Smith [1976] added a conditional strategy to the Hawks-Doves model called "bourgeoids" to deal with the case where one individual already owns the resource or occupies the area, which leads to home-field advantage. These individuals play a hawk

*Correspondence to: José J. Castro, Departamento de Biología, Universidad de las Palmas de Gran Canaria, Apdo. 550, Las Palmas de Gran Canaria, Canary Islands, Spain. E-mail: JOSEJUAN.CASTRO@BIOLOGIA.ULPGC.ES

Received 7 November 1997; amended version accepted 29 April 1998.

© 1999 Wiley-Liss, Inc.

© Del documento, los autores. Digitalización realizada por ULPGC. Biblioteca Universitaria, 2009

strategy if they are on home ground (or already own the resource in dispute) but act like a dove if they are in someone else's territory. Assuming that there are no other asymmetries, bourgeoids turns out to be a purely evolutionary stable strategy. The model of the "war of attrition" [Maynard-Smith, 1974] predicts that fights will be longest when individuals are of similar size (or weight) and also when the resource is of greatest value to the resident. Residence may be considered to be a kind of payoff asymmetry when individuals differ in the net gain or loss from escalating contests [Maynard-Smith and Parker, 1976].

The observation that owners tend to win contests vs. intruders does not mean that the bourgeoid strategy is being adopted. According to Krebs and Davies [1993], owners may win for at least three reasons: (1) they are better fighters, (2) owners value the resource more than intruders (i.e., they know the feeding value of the resource), and (3) arbitrary asymmetry of ownership settles the contest. Krebs's [1982] and Tobias's [1997] data on great tits and European robins, respectively, support the second reason.

Several studies on asymmetries in fighting abilities and information with respect to resource value have been carried out. Riechert [1984], working with the females of funnel-web spiders, found that residence was usually unimportant in determining the outcome of the contest and that competitors estimated their relative weights early on in the contest. Subsequent behaviour depended on the results of this assessment. If a spider had a large weight advantage, it immediately escalated the fight, whereas the smaller spider, even when it was resident, tended to retreat. If they were the same size, then the resident won. Similar results were obtained in bowl and doily spiders [Austad, 1982, 1983], water mites [Edwards and Dimock, 1991], dungflies [Sigurjònsdòttir and Parker, 1981], prawns [Evan and Shehadi-Moacdieh, 1988], red swamp crayfish [Figler et al., 1995], and swordtail fish [Beaugrand and Beaugrand, 1991]. On the contrary, asymmetries due to resident status had strong effects on agonistic behaviour of flies [Englund and Otto, 1991; Gribbin and Thompson, 1991], fiddler crabs [Jennions and Blackwell, 1996], cichlid fish [Turner, 1994], salamanders [Smith and Pough, 1994; Wiltenmuth, 1996], gulls [Pierotti and Annett, 1994], and elephant seals [Haley, 1994], being asymmetries in body size of weaker effects.

Size asymmetries can outweigh residence advantages [Beaugrand et al., 1996; Figler et al., 1995; Turner, 1994; Wagner, 1989; Wazlavek and Figler, 1989]. The effects of body size on behaviour may occur at two levels: First, disposition to fight—larger individuals may possess greater vigour, agility, or energy reserves that can be used in aggressive acts (in the case of fish, body size [Enquist et al., 1987], ferocity [Huntingford et al., 1990], and/or standard metabolic rate [Metcalfe et al., 1995] indicate the resource holding potential or fighting ability of an individual). Second, differences in size between contenders may affect their behavioural interactions [Wiltenmuth, 1996]. Individuals of similar size are expected to interact more frequently or with greater intensity than individuals differing in size [Enquist et al., 1987; Evan and Shehadi-Moacdieh, 1988; Leimar and Enquist, 1984; Parker, 1974].

The aim of this study was to examine the effects of asymmetries in residence and body size on agonistic behaviour of juvenile white-seabream. We tested the importance of residence and relative size in determining the outcome in contest between two fish (the resident and an intruder). The hypothesis to check was that residence has stronger effects in determining the outcome of the contest between fish than the differences in their relative size whenever differences in size were under 20%.

© Del documento, los autores. Digitalización realizada por ULPGC. Biblioteca Universitaria, 2009

White-seabream were selected for this study since juvenile of this coastal and schooling species inhabit rocky bottoms, and sometimes they shelter in cracks where they behave much the same as territorial species. The results obtained could be of potential application in the aquaculture industry of sparids.

## METHODS

Juvenile white-seabream (*Diplodus sargus cadenati*) were collected from tide pools along the north coast of the island of Gran Canaria, Spain (28°10' N, 15°40' W) in July, 1996. Fish were transported to the laboratory and housed in a 180-litre aquarium with recirculating seawater at 20–24°C for 1 month. Twelve of them were selected by chance and individually housed in 90-litre aquaria. All fish were measured at the beginning of the experiment and returned to the wild at the end of it. Each tank had three opaque sides and a glass front used for observation. The bottom of each tank was covered with gravel.

Fish were fed fast-sinking pelletised food dispersed over the water surface several times a day. However, in the aquaria containing isolated fish, food was delivered always at the same location through a plastic pipe.

Isolated fish were identified by their natural body marks (e.g., the size and shape of the saddle-like dark blotch on the caudal peduncle). During a week, we allowed isolated fish to become accustomed to the characteristics of their aquarium (location of the feeding places, refuges, etc.) and to establish a territory (in accordance with Drickamer et al. [1996], the territory was an area aggressively defended by the fish against other individuals). We call them "resident fish."

After this, we confronted these fish with an intruder, but only one per trial. Immediately prior to behavioural interactions, we disturbed the resident to equalize possible effects of handling on behaviour of introduced fish. We monitored the aggressive interaction between them, the type of agonistic interaction (chases, attacks, and lateral displays), and which fish won or lost the bouts after 10 min of exposure. Each resident fish was confronted with 10 or 11 intruders of different sizes, with a lapse of time of over half an hour between each intruder. No re-used fish ever met an opponent that it had previously encountered in testing.

We considered that contender fish were similar in size when length differences were equal to or lower than 5% [Wazlavek and Figler, 1989], which is the equivalent to under 20% difference in weight. Enquist et al. [1987] found that when the weight of the smaller fish was over 50% that of the larger specimen, the former never gave up during a combat.

After agonistic interactions, we identified the winning fish because it always kept the dorsal fin unfolded while the loser fled and always kept its dorsal fin folded.

We categorized the fight intensity of the first aggressive interaction between fish using a qualitative scale, from higher to lower intensity: (1) frontal attack (the fish hits its opponent on the head, normally close to the eyes); (2) lateral display (both fish swam in circles around each other with the dorsal fins extended, shaking their bodies, and sometimes nipping each other on the flanks during several seconds (over 10 sec); (3) attack (the fish hits its opponent on any part of the body except on the head, normally on the flanks; this aggressive interaction is short, over 1 sec); and (4) chase (without body contact). This categorization was based

© Del documento, los autores. Digitalización realizada por ULPGC. Biblioteca Universitaria, 2009

on our experience from previous studies using this species [Castro and Caballero, 1998; Castro and Santiago, 1998].

The statistical analysis of data was conducted to find any relationship existing between the differences in sizes of combatant fish and the proportion of resident winners. The null hypothesis ($H_0$) was that larger fish, independent of their residence status, always wins. Results were evaluated using separated Fisher Exact Probability Tests [Siegel, 1986] as already carried out by Wazlavek and Figler [1989].

## RESULTS

The range in length of fish used during the trial was 3.4–5.7 cm ($\bar{x}$ = 4.53, SD = 0.63 cm). Of the 125 bouts between resident and intruder fish, no interactions between them were observed in 12 cases (no agonistic behaviour occurred within 10 min after initiation of the trial). The resident won in 110 of the 113 interactions involving a fight. There were 66 bouts where the resident was larger than the intruder (the size differences were higher than 5%), of which 3 produced no interaction and 63 were won by the resident fish. Thirty-one bouts were carried out between fish of similar size (the size differences were equal to or lower than 5%), of which 2 were without interaction and 29 were won by the residents. In the 28 bouts where the resident fish were smaller than intruders (the size differences were between 5% and 21%), 7 produced no interaction, 18 were won by the resident, and 3 were won by the intruder fish. All the interactions were always initiated by the resident fish.

The $H_0$ tested was accepted only when the residents were the larger fish because they won 100% of the combats. However, it was not accepted when the intruder fish were larger than the residents because they only won 14.3% of the combats. When both the intruder and resident fish were of similar size, the Ho tested was that the probability of either winning the fight would be equal (statistically not significant). However, in this case, the probability that the resident fish would win was statistically significant ($P < 0.05$). In fact the residents always won.

There was a significant correlation between fight intensity and size asymmetry (Pearson's correlation r = 0.2961; $P < 0.0001$) in favour of the resident fish. During agonistic interactions, the frontal attacks were more frequent when pairs were composed of a resident and a larger intruder (Table I). Lateral displays were less frequent in combats between pairs where the intruder was smaller than when they were larger or of similar size to the resident. In the same way, attacks to the flanks and chases were more frequent in pairs where the intruder was smaller.

TABLE I. Percentage of the Different Types of Agonistic Interactions Between Pairs of Juvenile White-Seabream in Relation to the Size of Contenders

| | Resident < intruder | Resident = intruder | Resident > intruder |
|---|---|---|---|
| Number of bouts | 28.0 | 31.0 | 66.0 |
| Frontal attack | 18.3 | 10.1 | 03.6 |
| Lateral display | 30.1 | 36.2 | 12.2 |
| Attack | 26.6 | 43.4 | 66.9 |
| Chase | 00.0 | 03.7 | 12.7 |
| No interaction | 25.0 | 06.5 | 04.5 |

© Del documento, los autores. Digitalización realizada por ULPGC. Biblioteca Universitaria, 2009

## DISCUSSION

Despite the scarce number of studies carried out on asymmetry due to resident status in marine fish, most studies of territoriality in animals have documented that winners in the competition for territories gain substantial foraging, survival, or other benefits that ought to translate into heightened reproductive success [Austad, 1982; Beaugrand and Beaugrand, 1991; Drickamer et al., 1996; Gabor and Jaeger, 1995; Gribbin and Thompson, 1991; Haley, 1994; Krebs, 1982; Roithmair, 1994; Tobias, 1997]. Given the value of territorial possession, it seems paradoxical that when a territory holder is challenged by a rival, the owner almost always wins the contest [Alcock, 1993; Englund and Otto, 1991; Gribbin and Thompson, 1991]. Although body size is often an indicator of the asymmetry in fighting ability or resource holding potential of an individual [Maynard-Smith and Parker, 1976], when body size differences between interacting juveniles of white-seabream are under 20%, these appeared to have weaker effects than asymmetry due to residence status.

The consistency with which territory holders are able to repel competitors has generated a number of alternative explanations [Krebs and Davies, 1993; see introduction]. The quality of the limiting resource should be one of the most important factors in assessing the benefits of owning a territory [Gabor and Jaeger, 1995], and owners value the resource more than intruders [Krebs, 1982; Krebs and Davies, 1993].

Compared with small individuals, large fish were expected to be better competitors [Bronstein, 1984; Enquist et al., 1987; Huntingford et al., 1990; Turner and Huntingford, 1986] and to perform more frequent aggressive behaviour and less retreat behaviour. However, the combative nature of juvenile white-seabream may depend more on assessment of the value of the territory (i.e., since the owner will have information about features such as food sources and refuge [Archer, 1988]) than on factors associated with the individual's own body size. Maynard-Smith and Parker [1976] pointed out that in asymmetric contest, one individual (e.g., the territorial intruder) may have less information about the asymmetry and, thus, about cost and benefits involved in contesting the territory. The residents would possess advantages derived from their knowledge of the area [Archer, 1988].

In agreement with Turner and Huntingford [1986], Beeching [1992], and Turner [1994], the resident fish was more aggressive and persistent in attacks, and contests were more intense, when the size of the intruder was larger. As was observed in other fish species [Beeching, 1992; Morris et al., 1995], there was a significant correlation between fight intensity and size asymmetry in favour of the resident fish. The fight pattern depended on the size of the intruder. The small intruders were expelled with attacks to the flanks followed by short chases. However, when the intruders were of similar size to the residents, fights were longer and the most frequent combats were lateral displays. The intruders larger than the residents were attacked frontally and were hit on the head close to the eyes. Generally, these combats were the most violent and persistent. The time limitation imposed on the combats (10 min) possibly impeded the larger fish winning and expelling the smaller resident after a succession of aggressive interactions. Nevertheless, we can expect that in the wild the violent and brief aggressive interaction would cause the flight of the intruder after the first attack by the resident, allowing the latter to preserve its territory. Contrary to what was predicted by Parker's model [1974], our results seem

© Del documento, los autores. Digitalización realizada por ULPGC. Biblioteca Universitaria, 2009

to indicate that in some conflicts (e.g., against larger intruders), the resident fish will not assess their opponent's fighting ability before entering into a fight (undoubtedly, this strategy is very risky and may produce injury).

The behavioural patterns of juvenile white-seabream suggest that asymmetry in residency is an important factor governing the outcome of contest between individuals of this species. More aggression by residents indicates that they are capable of recognizing and defending an area as their own.

## ACKNOWLEDGMENTS

We thank Dr. Vicente Hernández, Mr. J.A. Santiago, and Mrs. A. Santana Ortega for their help in housing fish and collection of data.

## REFERENCES

Alcock J. 1993. Animal behavior: an evolutionary approach. 5th edition. Sunderland, MA: Sinauer Associates. Inc. Publishers. 625 p.

Archer J. 1988. The behavioural biology of aggression. Cambridge. MA: Cambridge University Press. 257 p.

Austad SN. 1982. First male sperm priority in the bowl and doily spider, *Frontinella pyramitela* (Walckenaer). Evolution 36:377–785.

Austad SN. 1983. A game theoretical interpretation of male combat in the bowl and doily spider (*Frontinella pyramitela*). Animal Behav 31:59–73.

Beaugrand JP. Beaugrand M. 1991. Prior residency and the stability of dominance relationships in pairs of green swordtail fish *Xiphophorus helleri* (Pisces. Poeciliidae). Behav Process 24: 169–175.

Beaugrand JP. Payette D. Goulet C. 1996. Conflict outcome in male green swordtail fish dyads (*Xiphophorus helleri*): interaction of body size, prior dominance/subordination experience, and prior residency. Behaviour 133:303–319.

Beeching SC. 1992. Visual assessment of relative size in a cichlid fish, the oscar, *Astronotus ocellatus*. Ethology 90:177–186.

Bronstein PM. 1984. Agonistic and reproductive interactions in *Betta splendens*. J Compar Psychol 98:421–431.

Castro JJ. Caballero C. 1998. Dominance structure in small groups of juvenile white-seabream (*Diplodus sargus cadenati* de la Paz. Bauchot & Daget 1974). Aggr Behav 24:197–204.

Castro JJ. Santiago JA. 1998. The influence of food distribution upon the aggressive behaviour of juvenile white-seabream (*Diplodus sargus cadenati* de la Paz. Bauchot & Daget 1974). Aggr Behav 24:379–384.

Drickamer LC. Vessey SH. Meikle D. 1996. Animal behaviour. 4th edition. Dubuque, IA: Wm. C. Brown Publishers. 447 p.

Edwards DD. Dimock RV Jr. 1991. Relative importance of size versus territorial residency in intraspecific aggression by symbiotic male water mites (Acari: Unionicolidae). Exp Appl Acarol 12:61–65.

Englund G. Otto C. 1991. Effects of ownership status, weight asymmetry, and case fit on the outcome of case contests in two populations of *Agrypnia pagetana* (Trichoptera: Phryganeidae) larvae. Behav Ecol Sociobiol 29:113–120.

Enquist M. Ljungberg T. Zandor A. 1987. Visual assessment of fighting ability in the cichlid fish *Nannacara anomala*. Animal Behav 35:1262–1263.

Evan DL. Shehadi-Moacdieh M. 1988. Body size and prior residency in staged encounters between female prawns, *Palaemon elegans* Rathke (Decapoda: Palaemonidae). Animal Behav 36:452–455.

Figler MH. Finkelstein JE. Twum M. Peeke HVS. 1995. Intruding male red swamp crayfish, *Procambarus clarkii*, immediately dominate members of established communities of smaller, mixed-sex conspecifics. Aggr Behav 21:225–236.

Gabor CR. Jaeger RG. 1995. Resource quality affects the agonistic behaviour of territorial salamanders. Animal Behav 49:71–79.

Gribbin SD. Thompson DJ. 1991. The effects of size and residency on territorial disputes and short-term mating success in the damselfly *Pyrrhosoma nymphula* (Sulzer) (Zygoptera: Coenagrionidae). Animal Behav 41:689–695.

Haley MP. 1994. Resource-holding power asymmetries, the prior residence effect, and reproductive payoffs in male northern elephant seal fights. Behav Ecol Sociobiol 34:427–434.

© Del documento, los autores. Digitalización realizada por ULPGC. Biblioteca Universitaria, 2009

Huntingford FA, Metcalfe NB, Thorpe SE, Graham WD, Adams CE. 1990. Social dominance and body size in Atlantic salmon parr, *Salmo solar* L. J Fish Biol 36:877–881.

Jennions MD, Backwell PRY. 1996. Residency and size affect fight duration and outcome in the fiddler crab *Uca annularis*. Biol J Linnean Society 57:293–306.

Krebs JR. 1982. Territorial defence in the great tit (*Parus major*): do residents always win? Behav Ecol Sociobiol 11:185–194.

Krebs JR, Davies NB. 1993. An introduction to behavioural ecology. 3rd edition. London: Blackwell Scientific Publications. 420 p.

Leimar O, Enquist M. 1984. Effects of asymmetries in owner-intruder conflicts. J Theor Biol 111:475–491.

Maynard-Smith J. 1974. The theory of games and the evolution of animal conflict. J Theor Biol 47:209–221.

Maynard-Smith J. 1976. Evolution and the theory of games. Am Sci 64:41–45.

Maynard-Smith J, Parker GA. 1976. The logic of asymmetric contests. Animal Behav 24:159–175.

Metcalfe NB, Taylor AC, Thorpe JE. 1995. Metabolic rate, social status and life-history strategies in Atlantic salmon. Animal Behav 49:431–436.

Morris MR, Gass L, Ryan MJ. 1995. Assessment and individual recognition of opponents in the pygmy swordtails *Xiphophorus nigrensis* and *X. multilineatus*. Behav Ecol Sociobiol 37:303–310.

Parker GA. 1974. Assessment strategy and the evolution of fighting behaviour. J Theor Biol 47:223–243.

Riechert SE. 1984. Games spiders play III: cues underlying context-associated changes in agonistic behaviour. Animal Behav 32:1–15.

Roithmair ME. 1994. Male territoriality and female mate selection in the dart-poison frog *Epipedobates trivittatus* (Dendrobatidae, Anura). Copeia 1994:107–115.

Pierotti R, Annett C. 1994. Patterns of aggression in gull: asymmetries and tactics in different social categories. Condor 96:590–599.

Siegel S. 1986. Estadística no paramétrica aplicada a las ciencias de la conducta. 2nd edition. México D.F.: Editorial Trillas. 344 p.

Sigurjònsdòttir H, Parker GA. 1981. Dungfly struggles: evidence for assessment strategy. Behav Ecol Sociobiol 8:219–230.

Smith EM, Pough FH. 1994. Intergeneric aggression among salamanders. J Herpetol 28:41–45.

Tobias J. 1997. Asymmetric territorial contests in the European robin: the role of settlement cost. Animal Behav 54:9–21.

Turner GF. 1994. The fighting tactics of male mouthbrooding cichlids: the effects of size and residency. Animal Behav 47:655–662.

Turner GF, Huntingford FA. 1986. A problem for game theory analysis: assessment and intention in male mouthbreeder contest. Animal Behav 34:961–970.

Wagner WE Jr. 1989. Fighting assessment and frequency alteration in Blanchard's cricket frog. Behav Ecol Sociobiol 25:429–436.

Wazlavek BE, Figler MH. 1989. Territorial prior residence, size asymmetry, and escalation of aggression in convict cichlids (*Cichlasaoma nigrofasciatum* Guenther). Aggr Behav 15:235–244.

Wiltenmuth EB. 1996. Agonistic and sensory behaviour of the salamander *Ensatina eschscholtzii* during asymmetrical contests. Animal Behav 52:841–850.

© Del documento, los autores. Digitalización realizada por ULPGC. Biblioteca Universitaria, 2008

ELSEVIER

Journal of Volcanology and Geothermal Research 94 (1999) 169–190

Journal of volcanology and geothermal research

www.elsevier.com/locate/jvolgeores

# Giant Quaternary landslides in the evolution of La Palma and El Hierro, Canary Islands

Juan Carlos Carracedo [a,*], Simon J. Day [b], Hervé Guillou [c], Francisco J. Pérez Torrado [d]

[a] Estación Volcanológica de Canarias, IPNA, CSIC, 38260 La Laguna, Tenerife, Canary Islands, Spain
[b] Benfield Greig Centre for Hazard Research, University College London, London, UK
[c] Laboratoire des Sciences du Climat et de l'Environnement, CNRS-CEA, Gif sur Yvette, France
[d] Dpto. de Fisica-Geologia, Universidad de Las Palmas, Gran Canaria, Canary Islands, Spain

Received 10 May 1999

**Abstract**

In the past, large morphological escarpments in the Canaries have been generally related to explosive and/or erosive processes. Recent onshore and offshore investigations drastically changed this interpretation, by providing evidence of the importance of giant lateral collapses in the evolution of the islands, especially in their earlier stages of growth. Giant landslide scars and deposits are readily observed both onshore and offshore in the younger, western Canaries, and seem to be a common feature of the development of the entire archipelago. At least one catastrophic collapse is apparent on La Palma: the Cumbre Nueva giant landslide, which occurred about 560 ka ago. This collapse removed some 200 $km^3$ of central-western La Palma, forming a large embayment. Three successive giant landslides and evidence of an aborted attempt at another are seen in the island of El Hierro. The combined volume of those collapses (estimated at about 400–500 $km^3$) considerably exceeds the present subaerial volume of the island (about 140 $km^3$). Giant landslides and erosion during the past million years have removed more than half of the total subaerial volume of La Palma and El Hierro. © 1999 Elsevier Science B.V. All rights reserved.

*Keywords:* Canary Islands; La Palma; El Hierro; gravitational collapses; Quaternary

## 1. Development of ideas concerning collapse structures in the Canary Islands

Steep escarpments, tens of kilometres long and up to a kilometre or more in height, that bound seaward-facing embayments, have been recognised as prominent features of the western Canary Islands since the time of the first geological investigations (Buch, 1825; Lyell, 1855). Erosive or explosive processes have consistently been favoured to explain the origin of these features (Hausen, 1961; Fúster et al., 1968). Bravo (1952; 1962) was the first to explain the Las Cañadas caldera and the Orotava and Güímar valleys in Tenerife partly as the result of gravitational landslides. The model proposed by Bravo is interesting inasmuch as it is a very early report (1952, 1962) relating gravitational block sliding and the generation of these large morphological escarp-

* Corresponding author. E-mail: jcarracedo@ipna.csic.es

0377-0273/99/$ - see front matter © 1999 Elsevier Science B.V. All rights reserved.
PII: S0377-0273(99)00102-X

© Del documento, los autores. Digitalización realizada por ULPGC. Biblioteca Universitaria, 2009

ments. He identified a polygenetic breccia in the subsoil of the Orotava valley that he related to great explosions that destroyed a previous volcano. This explosion breccia, changed into a plastic layer (fanglomerate) by alteration and water saturation, favoured landsliding of unstable masses of the overlying volcano, giving place gradually to the aforementioned features. This model, however, differs significantly from the generally accepted idea of giant landslides (as originally proposed with respect to the Hawaiian islands by Moore, 1964; see McGuire, 1996 for a review of the development of the giant landslide concept), as a single, fundamentally instantaneous event. In this type of model, breccias such as those in the Orotava valley are best interpreted as collapse scar fill (fanglomerate) deposits, and thus as a result of, rather than a cause of, the gravitational slide.

The important role of giant landslides, both in the Canary Islands and the Hawaiian Islands (Carracedo, 1999), has been recognised in recent years largely as the result of offshore surveys. In the case of the Canaries, Holcomb and Searle (1991) were the first to analyse GLORIA sonographs from around the island of El Hierro. They interpreted submarine features off the southwestern coast of the island as deposits of a giant landslide from the collapse of the southwest flank of the island, to produce the present El Julan embayment. These authors hypothesised that similar landslide deposits, with a similar origin, would be on the seafloor north and east of El Hierro (later confirmed by Masson and Watts in 1995, as discussed below), off the prominent El Golfo and Las Playas embayments, that would have a similar origin.

Since the pioneering work of Holcomb and Searle, increasing evidence relating giant landslides to straight-walled valleys, calderas and wide coastal embayments has been found onshore (Ancochea et al., 1994; Carracedo, 1994, 1996; Guillou et al., 1996; Carracedo et al., 1997a,b,c; Day et al., 1997; Stillman, 1999-this volume) and offshore (Weaver et al., 1992; Masson and Watts, 1995; Watts and Masson, 1995; Masson, 1996; Canals et al., 1997; Urgeles et al., 1997; Masson et al., 1998) in the archipelago.

The Canaries provide examples of a relationship between giant gravitational collapses and rift zones (Carracedo, 1994, 1996). Wide, arcuate landslide embayments systematically occur between two rifts, while the part of the volcano built along a third rift acts as a buttress (Tiñor, El Julan and El Golfo giant landslides in El Hierro; Las Cañadas caldera in Tenerife). If the rifts grow unevenly, such that one becomes more active than the others (as is presently the case with the Cumbre Vieja volcano, La Palma, as discussed below), collapse is most likely to occur on one flank of this rift.

Giant landslides, as well as the related rifts, are most easily identifiable in the juvenile stage (shield-building stage) of a volcano (Tenerife, La Palma and El Hierro). Erosion and late-stage volcanism remove and cover onshore information, while oceanic sedimentation blankets offshore evidence. Nonetheless, some evidence of old giant gravitational collapses has been identified in Gran Canaria (Schmincke et al., 1997) and Fuerteventura (Stillman, 1999-this volume).

Giant landslides play an important role in the geological evolution of the Canarian volcanoes. In contrast to most of the intraplate oceanic volcanoes, subsidence is not significant in the Canary Islands (Carracedo, 1999), where the islands remain emergent until completely removed by erosion. Giant collapses, most common when the island volcanoes are at their peak stage of development, play a major role in the mass-wasting of important volumes of these island volcanoes (Carracedo et al., 1998).

Eleven giant landslides have been identified in the islands of La Palma, El Hierro, Tenerife, Fuerteventura and Gran Canaria (Fig. 1) by means of onshore and offshore data (Navarro and Coello, 1989; Holcomb and Searle, 1991; Weaver et al., 1992; Ancochea et al., 1994; Carracedo, 1994, 1996; Masson and Watts, 1995; Watts and Masson, 1995; Guillou et al., 1996; Carracedo et al., 1997a,b,c; Day et al., 1997; Masson, 1996; Canals et al., 1997; Schmincke et al., 1997; Urgeles et al., 1997; Masson et al., 1998; Stillman, 1999-this volume)). However, other morphological features of similar characteristics may have a similar origin in these islands, and similar but less well-preserved landslide structures may have occurred in Fuerteventura and Lanzarote, as shown in Fig. 1.

In this paper we discuss onshore geological information of Quaternary gravitational landslides in the

© Del documento, los autores. Digitalización realizada por ULPGC. Biblioteca Universitaria, 2009

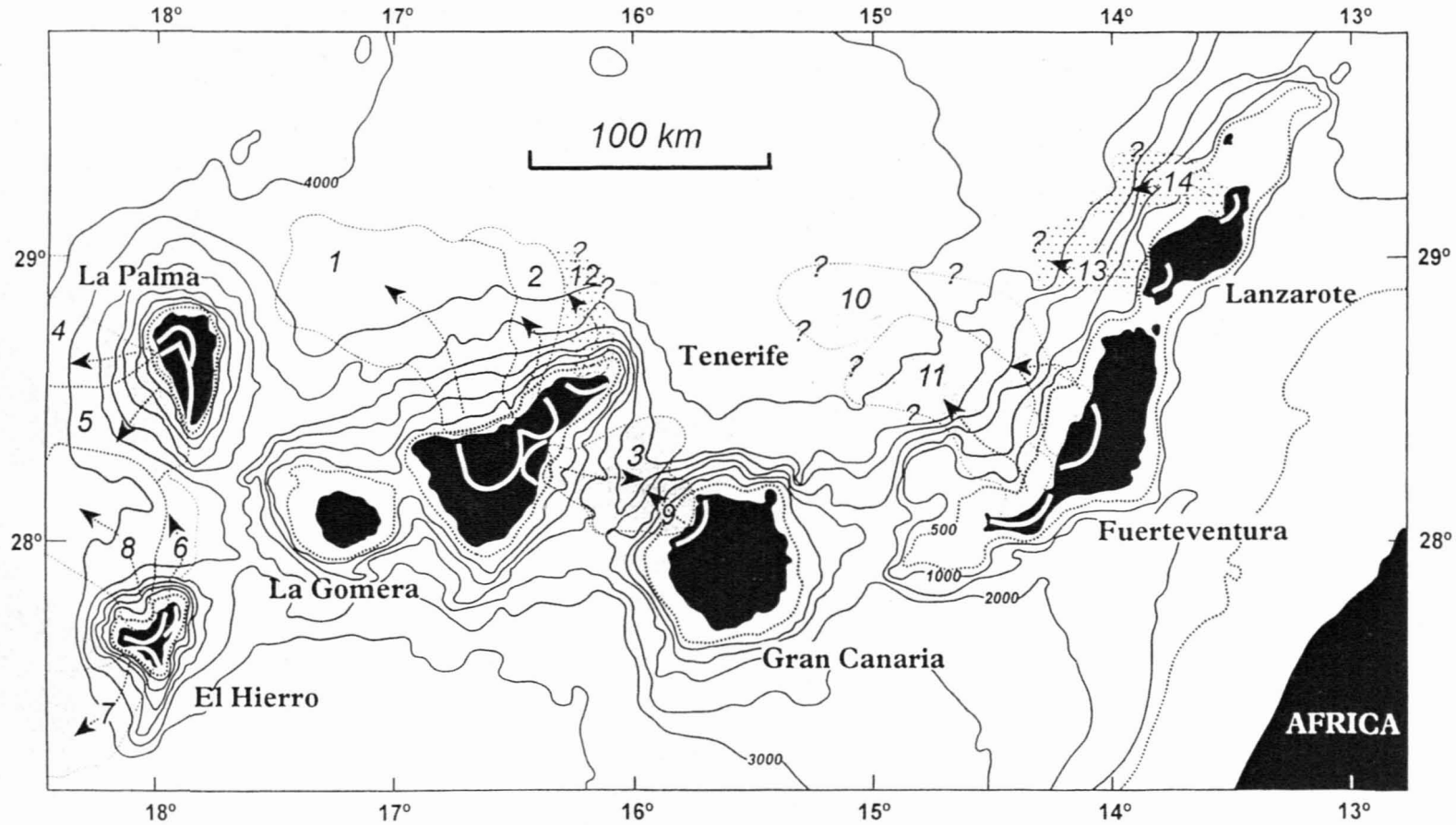


Fig. 1. Eleven giant lateral collapses have been identified onshore and offshore around the Canary Islands (references in the text). Other features in the islands of Tenerife and Lanzarote may be also related to gravitational collapses and are tentatively indicated in the figure (12 to 14).



© Del documento, los autores. Digitalización realizada por ULPGC. Biblioteca Universitaria, 2009

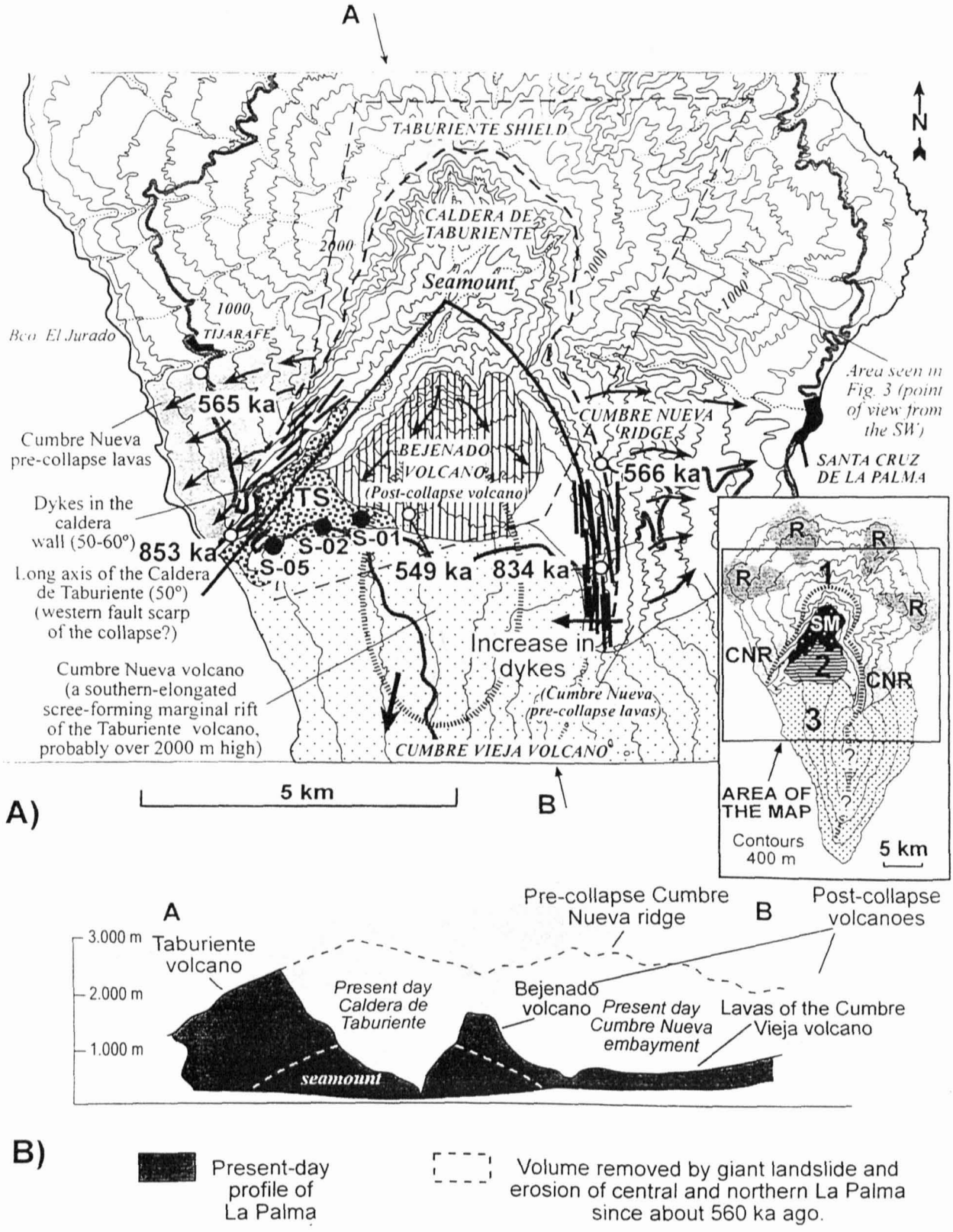


© Del documento, los autores. Digitalización realizada por ULPGC. Biblioteca Universitaria, 2009

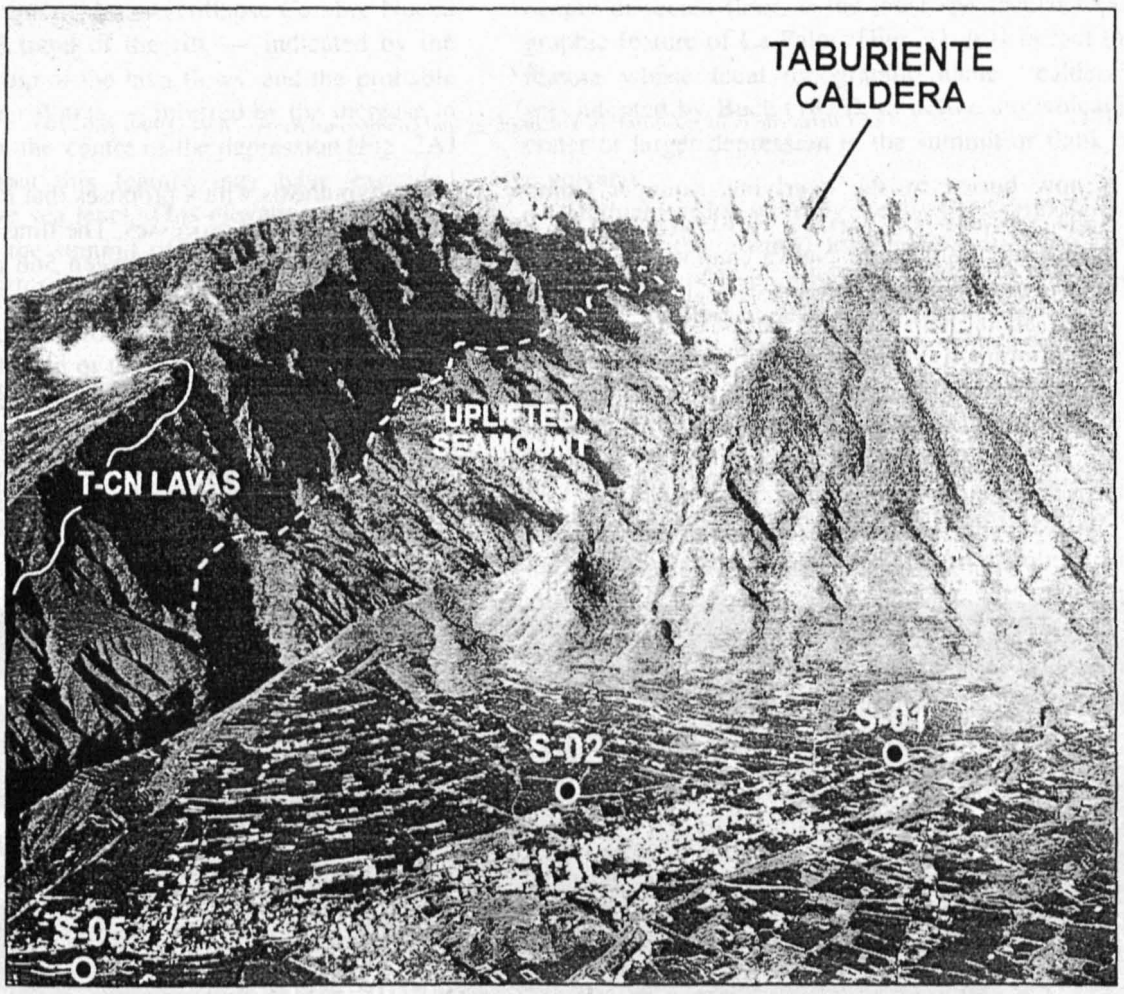


Fig. 3. Oblique aerial view of the Caldera de Taburiente, viewed from the southwest. S-01, S-02 and S-03 show the location of the boreholes discussed in the text.

western islands of La Palma and El Hierro, which play a main role in the evolution and shaping of these islands.

## 2. Quaternary collapse structures in La Palma

The island of La Palma is formed by an uplifted seamount (SM in the inset of Fig. 2A) and three consecutive subaerial volcanoes: the Taburiente, Bejenado and Cumbre Vieja volcanoes (1, 2 and 3, respectively, in the inset of A). The Taburiente volcano developed between about 1.7 and 0.5 Ma as a steep shield with five radial rift zones (R and CNR in the inset), the age and geometry of which are currently under study. The southern rift (the Cumbre Nueva ridge, CNR in the inset) enlarged the shield towards the south: the southern part of this rift zone

Fig. 2. (A) The occurrence of the Cumbre Nueva giant lateral collapse is tightly constrained by the ages of the top pre-collapse lavas and the post-collapse lavas of the Bejenado volcano. More discussion in the text. Inset: simplified geological map of La Palma. (B) Cross-section showing present-day N–S profile of the Taburiente volcano and the Cumbre Nueva ridge showing the volume removed by the Cumbre Nueva giant landslide and subsequent erosion.

© Del documento, los autores. Digitalización realizada por ULPGC. Biblioteca Universitaria, 2009

is now buried by the overlying, younger Cumbre Vieja volcano (Fig. 2A).[1] However, as with the other rifts, the Cumbre Nueva cannot be considered to be a different volcano since its development between about 850 and 500 ka is contemporaneous with continued, although slower, growth of the rest of the Taburiente volcano. Emission vents and lavas of the Cumbre Nueva and the other rifts are interbedded with lavas from vents located at the summit of the Taburiente volcano.

Most of the central part of the Cumbre Nueva rift is occupied by a 5-km-wide embayment, partially filled by the younger Bejenado and Cumbre Vieja volcanoes (Fig. 2A). The dip of the lava flows at the eastern and western flanks of the ridge and the increasing number of dykes towards the centre of this depression suggest that the Cumbre Nueva rift may have exceeded 2,000 m and was probably aligned in a N–S direction approximately coincident with the centre of the present embayment. Lavas at the flanks of the rift clearly flow from vents that were located in the present embayment (Fig. 2A).

Boreholes drilled in the embayment (S-01, S-02 and S-05 in Figs. 2A and 3) confirm the presence of a direct contact between Seamount series and Bejenado lavas at sea-level, without the presence of Cumbre Nueva volcanics inside the embayment. The surface outcrop in the vicinity of these boreholes is formed by a sequence consisting primarily of the lavas of the Bejenado volcano and the thick sedimentary sequence of El Time (TS in Fig. 2A), an alluvial fan post-dating the Bejenado volcano. These boreholes cross the Bejenado lavas and pyroclasts before passing down into a homogeneous unit of fragments of basalts, from fine gravel to large blocks, in a loose sandy matrix. The recovered clasts are all of unaltered subaerial basic lavas, without the distinctive metamorphosed pillow basalts and gabbros of the Seamount Series. The thickness of these sediments is about 100 m, determined in borehole S-02 that cuts into the pillow lavas of the uplifted Seamount Series.

The volume removed to form the present Cumbre Nueva embayment (Fig. 2B) presents a problem for any hypothesis which proposes that it was formed by normal erosional processes. The time available for its formation, constrained between 566 and 549 ka, the minimum age of the Cumbre Nueva ridge (the age of one of the topmost lava flows) and the Bejenado volcano, is insufficient for it to have been formed by erosion. Deposition of the sedimentary breccias of the embayment — filling sequence below the Bejenado lavas — must have taken place in a short period of time, as indicated by the aforementioned radiometric ages.

### 2.1. The Cumbre Nueva giant landslide

Ancochea et al. (1994) have inferred the presence of at least one old collapse structure buried within the Taburiente edifice. According to these authors, a SSW oriented "palaeocaldera" was formed by a gravitational landslide at the end of the final stages of building of the central Taburiente shield, some 1.2 Ma ago. These authors also relate the embayment in the area of Los Llanos (our Cumbre Nueva embayment) to a large lateral collapse. The above mentioned short time interval between the upper Cumbre Nueva lavas and the oldest rocks of the Bejenado volcano, the presence of sedimentary breccias in the contact Seamount series/Bejenado lavas and the absence of Cumbre Nueva lavas inside the embayment all strongly support an interpretation of this depression as having formed by a large lateral collapse (Carracedo et al., 1999).

The geometry and extent of the volume removed by the Cumbre Nueva lateral collapse can be deduced from field observations and the information obtained from the boreholes mentioned above. The eastern headwall of the mass movement was an arcuate scarp parallel to the present-day Cumbre Nueva escarpment, and is now partially concealed by the northern end of the Cumbre Vieja volcano. The displacement of the block towards the S–SW probably formed a linear detachment scarp at its northwestern boundary (Fig. 2A), possibly coinciding with the present axis of the Caldera de Taburiente, which may have been initiated by the collapse as discussed below.

The volume involved in the Cumbre Nueva collapse, estimated to exceed 200 km$^3$, is dependent

[1] The local naming of Cumbre Nueva (New Summit) to a feature older than the Cumbre Vieja (Old Summit) may be confusing to read.

© Del documento, los autores. Digitalización realizada por ULPGC. Biblioteca Universitaria, 2009

upon the location of the pre-collapse Cumbre Nueva rift. The N–S trend of the rift — indicated by the dykes — the dip of the lava flows, and the probable location of the rift axis — inferred by the increase in dykes towards the centre of the depression (Fig. 2A) — suggest that this feature may have exceeded 2,000 m above sea level. This elevation is less than the height of the summit of the Taburiente volcano of which it forms a part, estimated by the dip of the lava flows in about 3000 m (Fig. 2B).

### 2.2. Genesis of the Caldera de Taburiente

The Caldera de Taburiente, a 15-km-long and 6-km-wide depression, up to 1.5 km deep, with precipitous bounding cliffs on most sides and a deeply dissected floor, is the most spectacular topographic feature of La Palma (Fig. 3). It is in fact the feature whose local topographic name "caldera" was adopted by Buch (1825), to define any volcanic crater or larger depression in the summit or flank of a volcano.

Gradual erosion has consistently been proposed as the process that formed this caldera after the first interpretation of Lyell (1855). Ancochea et al. (1994) proposed that the caldera de Taburiente formed by a lateral collapse, distinct from that which produced the Cumbre Nueva collapse scar.

Our observations of age relationships in this part of La Palma provide important constraints on the origin of the Caldera de Taburiente (Carracedo et al., 1999). It deeply dissects the Taburiente and Beje-

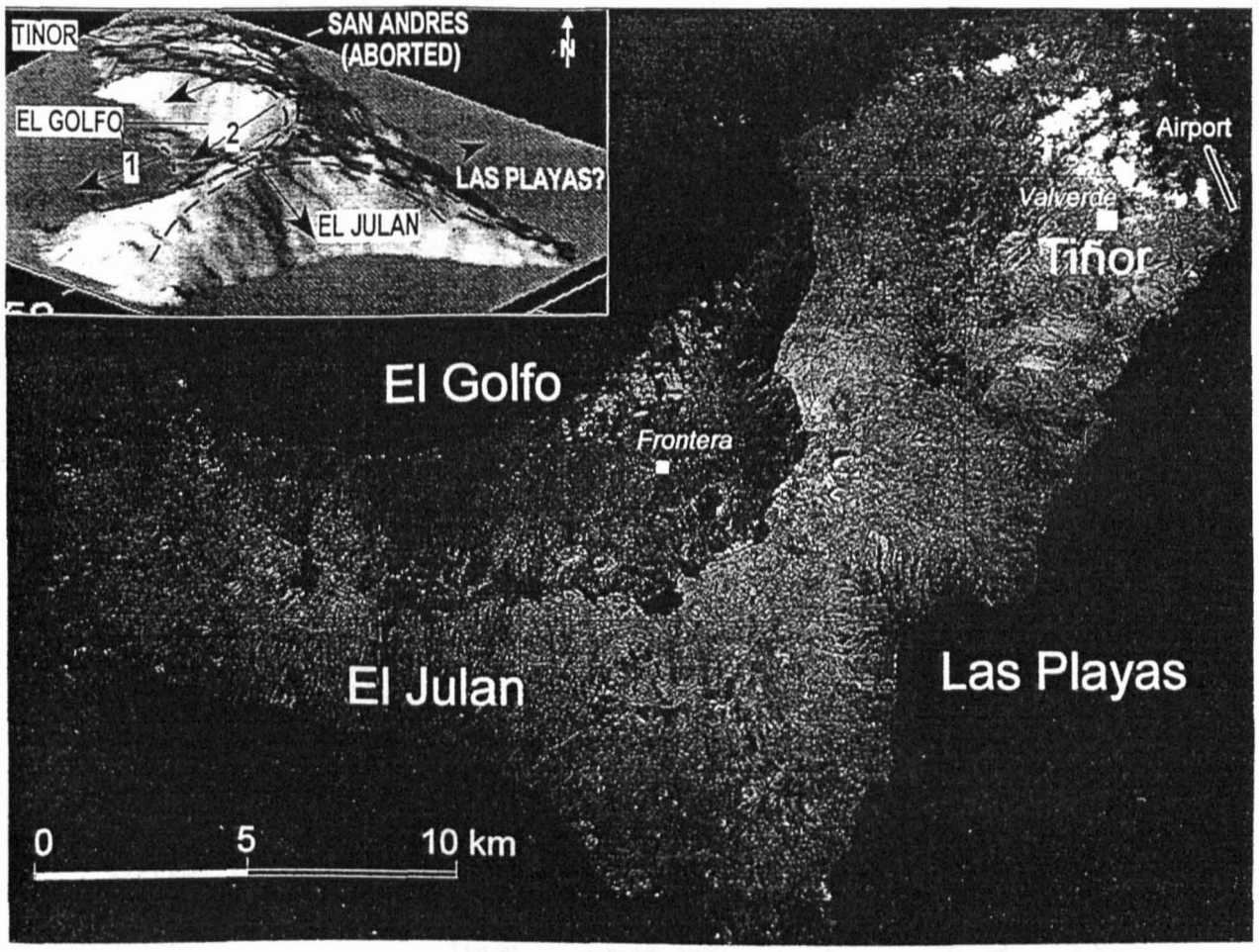


Fig. 4. Satellite view of El Hierro (Landsat mosaic assembled by the Spanish Geographic Institute). Inset: 3D image showing the different giant lateral collapses in the island.

© Del documento, los autores. Digitalización realizada por ULPGC. Biblioteca Universitaria, 2009

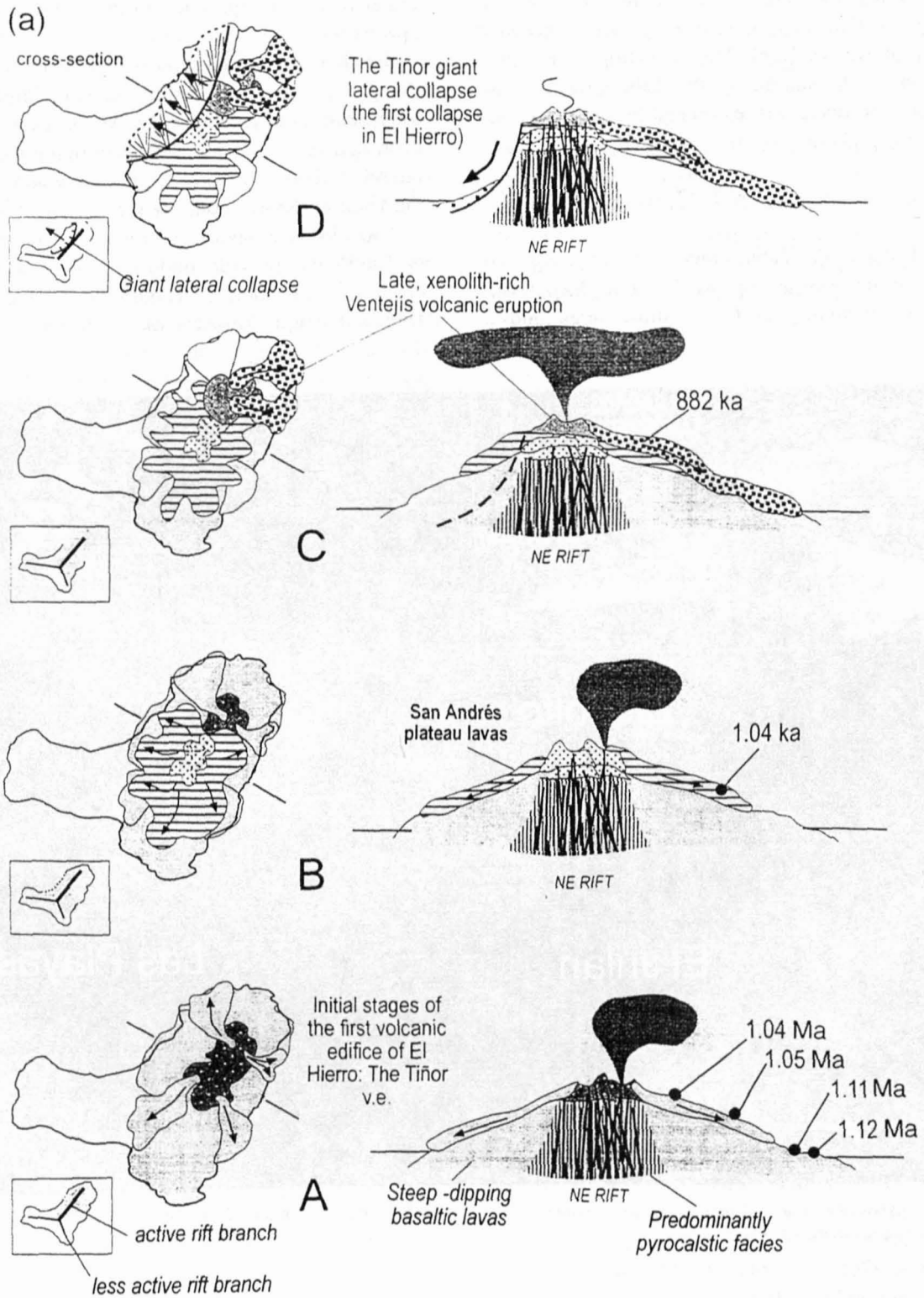


Fig. 5. (a) Reconstruction of the volcanic history of El Hierro, illustrating the development of the Tiñor volcano (A–C), the Tiñor giant collapse (D), the El Golfo volcano (E), the El Julan collapse (F) and the El Golfo collapse (G–H) (Carracedo et al., 1997b).

© Del documento, los autores. Digitalización realizada por ULPGC. Biblioteca Universitaria, 2009

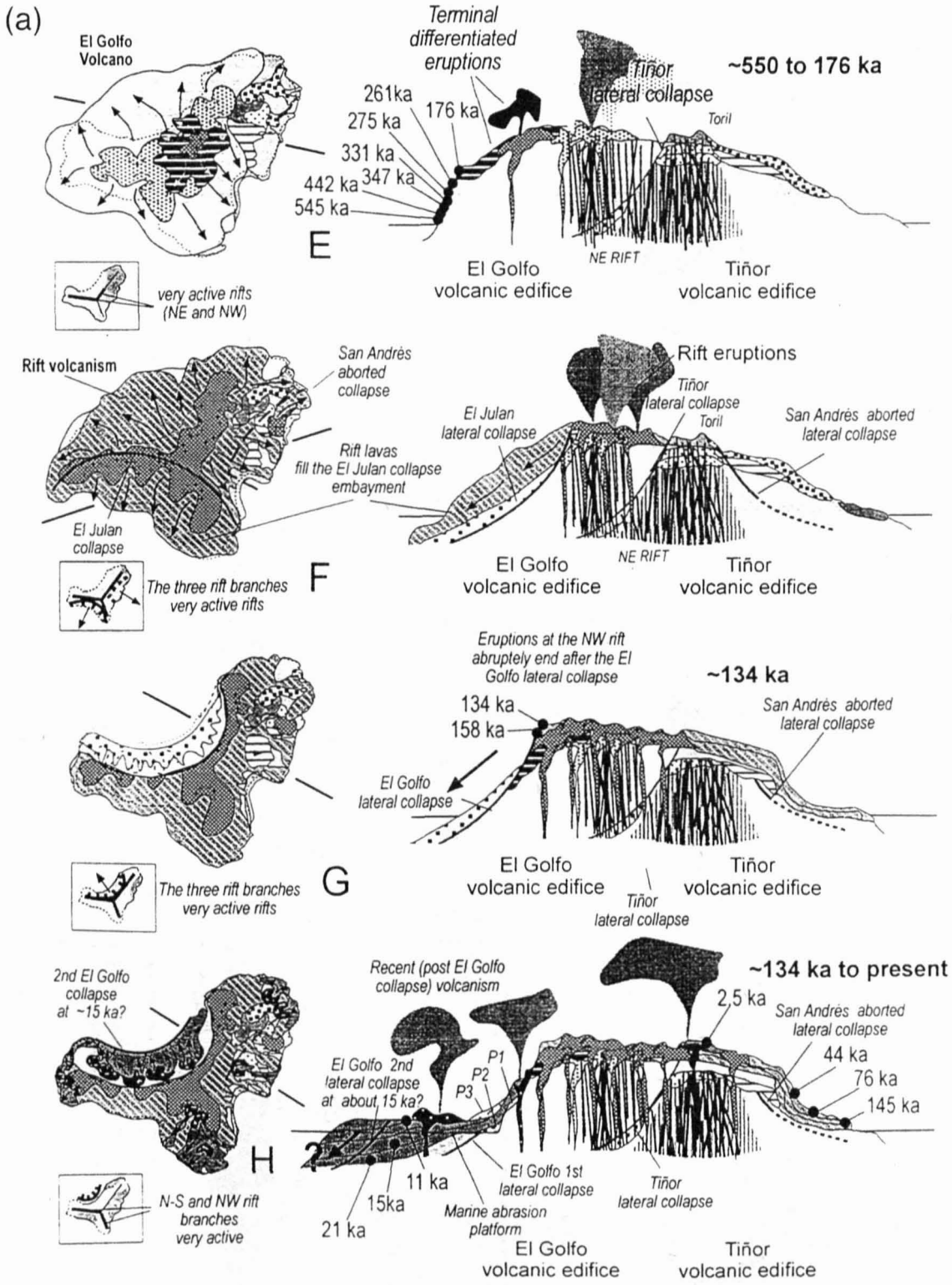


Fig. 5 (continued).

© Del documento, los autores. Digitalización realizada por ULPGC. Biblioteca Universitaria, 2009

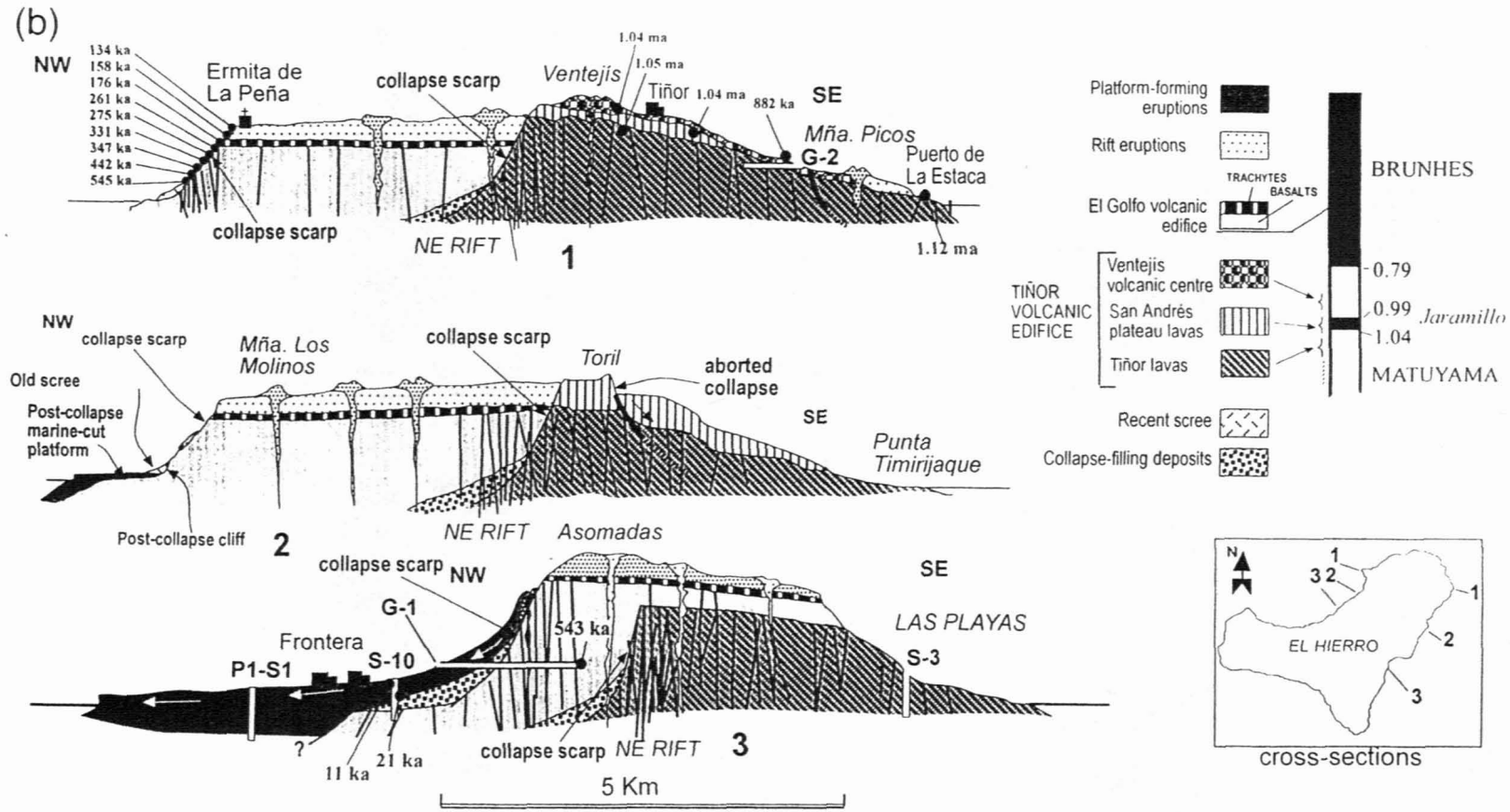


Fig. 5. (b) Different cross-sections (see lower inset map) illustrating the growth and collapse of the El Golfo volcano, which developed inside the embayment of the previous Tiñor collapse. Magnetic stratigraphy (upper inset) has been a crucial tool in the definition of these collapses (Guillou et al., 1996; Carracedo et al., 1997b).

© Del documento, los autores. Digitalización realizada por ULPGC. Biblioteca Universitaria, 2009

nado volcanoes, and must therefore post-date both, but runs in a NE–SW-trending direction parallel to, and approximately coincident with, the inferred position of the north-western sidewall of the Cumbre Nueva collapse structure. We therefore propose that the Caldera de Taburiente formed as a result of the trapping of a drainage system between the wall of the Cumbre Nueva collapse structure and the growing Bejenado volcano, in the period after the collapse. Thus trapped, and fed by drainage from the Bejenado volcano, this system eroded deeply and rapidly into both the older and younger volcanic sequences, and eventually into the underlying Seamount Series. With time the Caldera de Taburiente deepened, enlarged and extended outside the pre-existing lateral collapse structure, incising the sedimentary sequence (the El Time formation) at its mouth and beheading the less vigorous drainage system east of Pico Bejenado (Carracedo et al., 1997a,c,d). This interpretation has some similarity to the erosive model for the formation of the Caldera de Taburiente proposed by Lyell (1855) and many authors since (Hausen, 1961; Ancochea et al., 1994; Navarro and Coello, 1994). However, we emphasise the importance of the Cumbre Nueva collapse structure, particularly its north-western fault-like boundary, in controlling the position and development of the Caldera de Taburiente.

### 2.3. Instability of the Cumbre Vieja Volcano

Recent volcanic activity in La Palma has been concentrated in the south of the island. This activity has produced a large polygenetic volcano. This forms the Cumbre Vieja ridge, with a maximum height of 1950 m above sea level and extremely steep flanks (see inset in Fig. 2A), with average subaerial slope angles of 16° to 20° (Carracedo, 1994).

There is no central vent complex: instead, a long north–south trending ridge forms the summit of the volcano. This ridge is formed by the main concentration of largely monogenetic volcanic fissures and vents, which together define a dominant N–S volcanic rift zone. A number of historic eruptions (< 500 years) have occurred in the rift and in broadly E–W fissures on the west flank of the volcano (Carracedo et al., 1999).

An interesting possibility is that the Cumbre Vieja volcano has grown along the headwall scarp of the Cumbre Nueva collapse, which may have extended down to the southern edge of the island (see inset in Fig. 2A). The rift forms a wide arch, open towards the west, that may reflect the collapse scarp. This will explain the presence of the oldest lavas in the western cliffs of the volcano (Carracedo et al., 1997d), as the first lavas filling the collapse embayment.

### 2.4. Structural evolution of the Cumbre Vieja volcano: precursors of lateral collapse?

Although the bulk of volcanic activity in Cumbre Vieja volcano has been located on the N–S rift, a good part of the vents were disperse in the western and eastern margins of the volcano until about 7 or 8 ka (Carracedo et al., 1997d), defining diffuse NE and NW rift zones. Since then, eruptive vents focused at the summit of the rift, although some fissures opened on the western flank of the volcano. This change can be interpreted in terms of a reconfiguration of the underlying dyke swarms resulting from a redistribution of stresses within the volcano (Day et al., 1999-this volume).

During the most recent eruption to affect the summit region of volcano, that of June–August 1949, an array of west-facing normal faults ruptured the surface of the volcano on or about July 1st, at the peak of seismic activity associated with the eruption (Bonelli, 1950; Carracedo, 1994). These faults formed between the vents active in the eruption but they do not seem to be the surface expression of near-surface dykes connecting the vents. There is no evidence of fumarolic gas escape along the fault fissures and the faults consistently downthrow en echelon to the west rather than forming a graben.

It therefore appears that a weak detachment fault or zone of fracturing may already be present beneath the western flank of the Cumbre Vieja volcano, although there may be other, non-tectonic explanations (Kluegel et al., 1999-this volume). As already mentioned, it is possible that the Cumbre Nueva collapse extends to the south of the island and the western flank of the Cumbre Vieja volcano is filling the embayment. In that case, a sedimentary unit may

© Del documento, los autores. Digitalización realizada por ULPGC. Biblioteca Universitaria, 2009

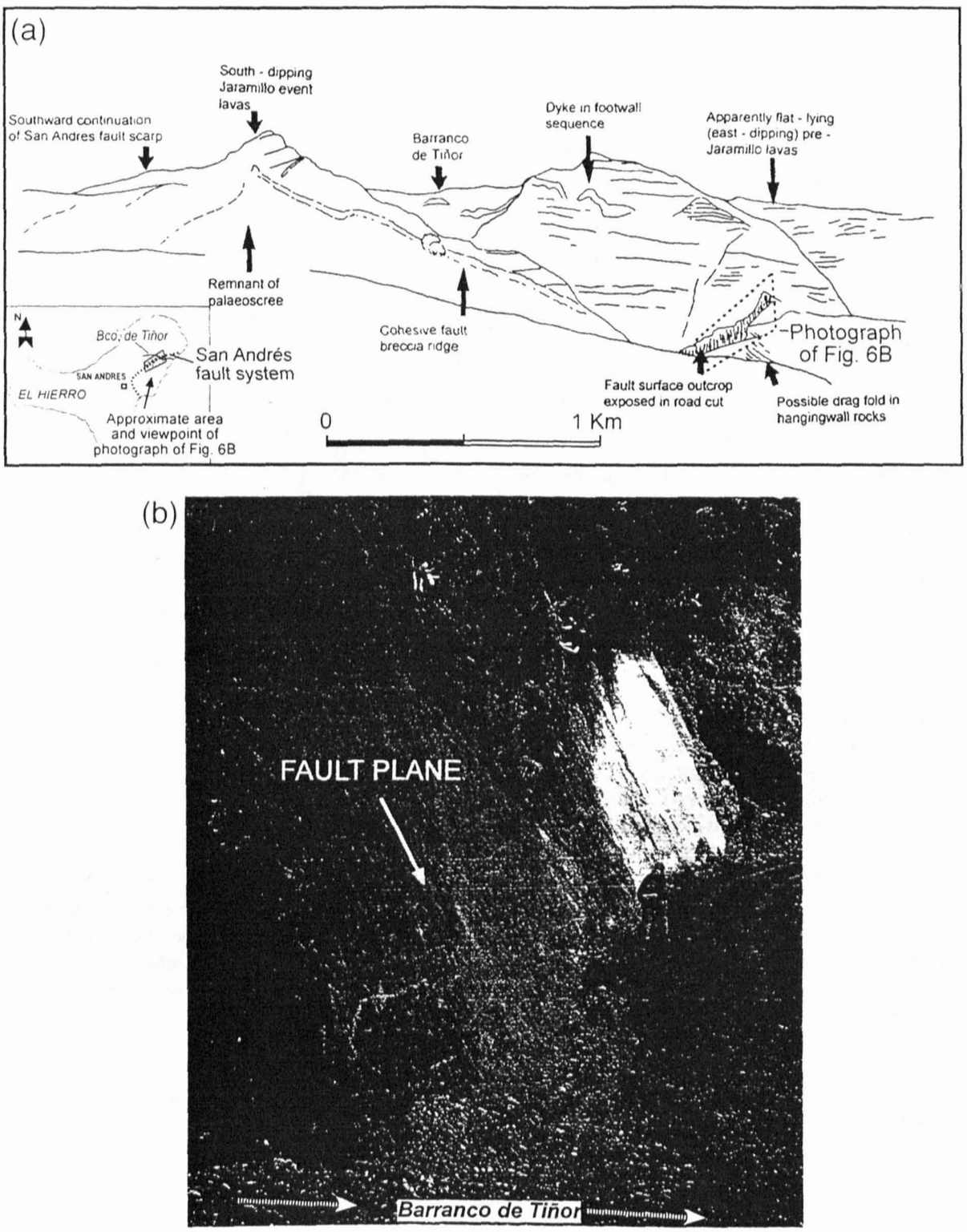


Fig. 6. (a) Sketch of the fault related to the San Andrés aborted giant lateral collapse, northeast of El Hierro. (b) Close-up picture of the San Andrés fault.

© Del documento, los autores. Digitalización realizada por ULPGC. Biblioteca Universitaria, 2009

be also present at the base of the Cumbre Vieja lavas, considerably increasing the instability of the volcano (Day et al., 1999-this volume).

However, the associated lack of seismicity in the present, inter-eruptive period indicates that the detachment, if present, is only activated by the intrusion of magma into the upper part of the volcano. A geodetic network covering the fault system at the crest of the Cumbre Vieja ridge recorded no ground deformation between 1994 and 1997 (Moss and McGuire, 1997). At present, therefore, the volcano need only be regarded as unstable, and perhaps liable to collapse, during eruptions.

## 3. Collapse structures in El Hierro

The island of El Hierro is a volcanic shield with the characteristic trilobate form whose origin lies in the presence of a well-developed, regular, three-armed rift system (Carracedo, 1994; Guillou et al., 1996). These rifts played a key role in the generation of giant gravitational collapses which removed important volumes of the island in several episodes throughout its geological history (Carracedo et al., 1997b).

Three giant lateral collapses can be recognised from the onshore geology of El Hierro: The Tiñor, El Julan and El Golfo (inset of Fig. 4). The San Andrés fault, in the NW flank of the island, may correspond to an aborted lateral collapse and the embayment of Las Playas, at the SE flank of the island may be a similar feature, although there is not onshore geological evidence to support this hypothesis.

### 3.1. The Tiñor giant landslide

The first subaerial volcanic activity in El Hierro formed a steep volcano — the Tiñor volcano — that developed between about 1.12 Ma and 882 ka (Guillou et al., 1996) at the eastern part of the island (Fig. 5a). This volcano was affected by a north-west directed giant collapse, the scar thus formed has since been largely buried by later volcanism.

The evidence for this giant collapse is shown in the cross-sections of Fig. 5b. The El Golfo volcano, overlying the Tiñor volcano and with ages consistently younger, is of normal (Brunhes) polarity, whereas the Tiñor volcano is predominantly of reverse (Matuyama) polarity (see inset in Fig. 5b). A gallery (horizontal tunnel to mine groundwater) excavated in the El Golfo embayment scarp crosses most of the El Golfo volcano (Fig. 5b-3) towards the lavas of the Tiñor volcano. At the end of the tunnel, the El Golfo lavas of 543 ka and normal (Brunhes) polarity are at the same level as gently east-dipping lavas more than 1.04 Ma old and of reverse polarity (Matuyama pre-Jaramillo). This disposition requires a major tectonic process, such as the giant collapse described above.

The Tiñor collapse probably followed the late explosive episodes of the volcano that took place about 882 ka ago (Fig. 5a, C and D). The north-west flank of the volcano, possibly more than half of its subaerial volume, volcano may have been removed. Subsequently, another volcanic edifice, the El Golfo volcano, completely filled the Tiñor collapse embayment (Fig. 5a, C and E).

### 3.2. The El Julan landslide

The SW flank of El Hierro forms a 16-km-wide embayment — El Julan — completely covered with lavas from vents located at the summit of the NW rift (see Fig. 4 and inset). Although there is no clear onshore evidence relating this feature to a lateral collapse, Holcomb and Searle (1991) identified this feature as a gravitational collapse from offshore GLORIA images, and considered it to be older than the Sahara debris flow. Masson (1996) bracketed the occurrence of this collapse between about 500 and 300 ka.

The lack of outcrops of the collapse scarp makes the dating of this event from onshore evidence difficult. Water galleries in the El Julan collapse embayment only cross a part of the embayment-filling lavas of the younger rift series volcanism, without reaching the post-collapse sediments or the collapse scarp. The El Julan collapse, which destroyed the SW flank of the El Golfo volcano, probably occurred when this volcano was well developed (Fig. 5a, F).

### 3.3. The San Andrés aborted collapse

The San Andrés fault, developed along the flank of the steep-sided NE rift of El Hierro (see inset in

© Del documento, los autores. Digitalización realizada por ULPGC. Biblioteca Universitaria, 2009

Figs. 4 and 6a), has been interpreted as an aborted giant collapse (Day et al., 1997). This fault is a relatively young feature, between 545 and about 261–176 ka old (Day et al., 1997).

According to Day et al. (1997), field evidence indicates only one major episode of movement on this fault, in contrast to the very large number of small (metre-sized) slip events on the active Hawaiian fault systems (Swanson et al., 1976; Clague and Denlinger, 1994). Although the fault has undergone little erosion, cataclasites which formed close to the palaeosurface are well-exposed (Fig. 6b). These cataclasites are amongst the first fault rocks to be described from volcano lateral collapse structures and include the only pseudotachylytes to have been identified in such structures to date (Day et al., 1997).

The well-developed topographic fault scarp associated with the San Andrés fault system led to the suggestion that it was an active incipient collapse structure and, therefore, a major natural hazard (Navarro and Soler, 1994). However, the age relationships of the faults to lavas and other volcanic rocks which have been dated recently (Guillou et al., 1996) lead to a different conclusion. The critical constraints upon the age of the San Andrés fault system are: (a) the occurrence of rift lavas which cross the fault without displacement, in barrancos incised into the fault scarp; (b) the faults in the

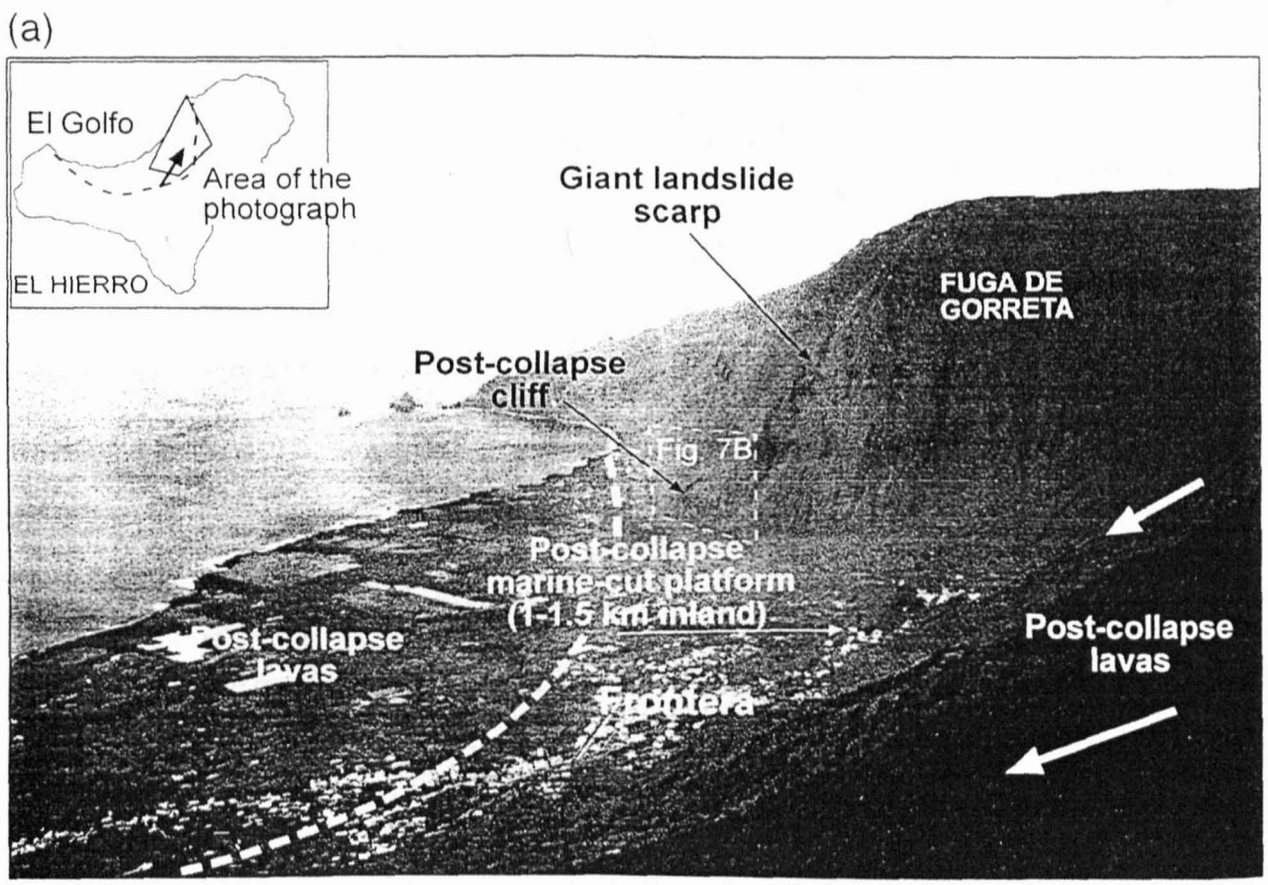


Fig. 7. (a) Panoramic of the eastern half of the El Golfo collapse scarp and embayment and the post-collapse lavas that partially filled the embayment. (b) Close-up view of the eastern collapse scarp. Two successive generations of cliffs and scree deposits can be observed. As discussed in the text, the age of these features are in conflict with the model of Masson (1996) that the El Golfo collapse is only about 15 ka old.

© Del documento, los autores. Digitalización realizada por ULPGC. Biblioteca Universitaria, 2009

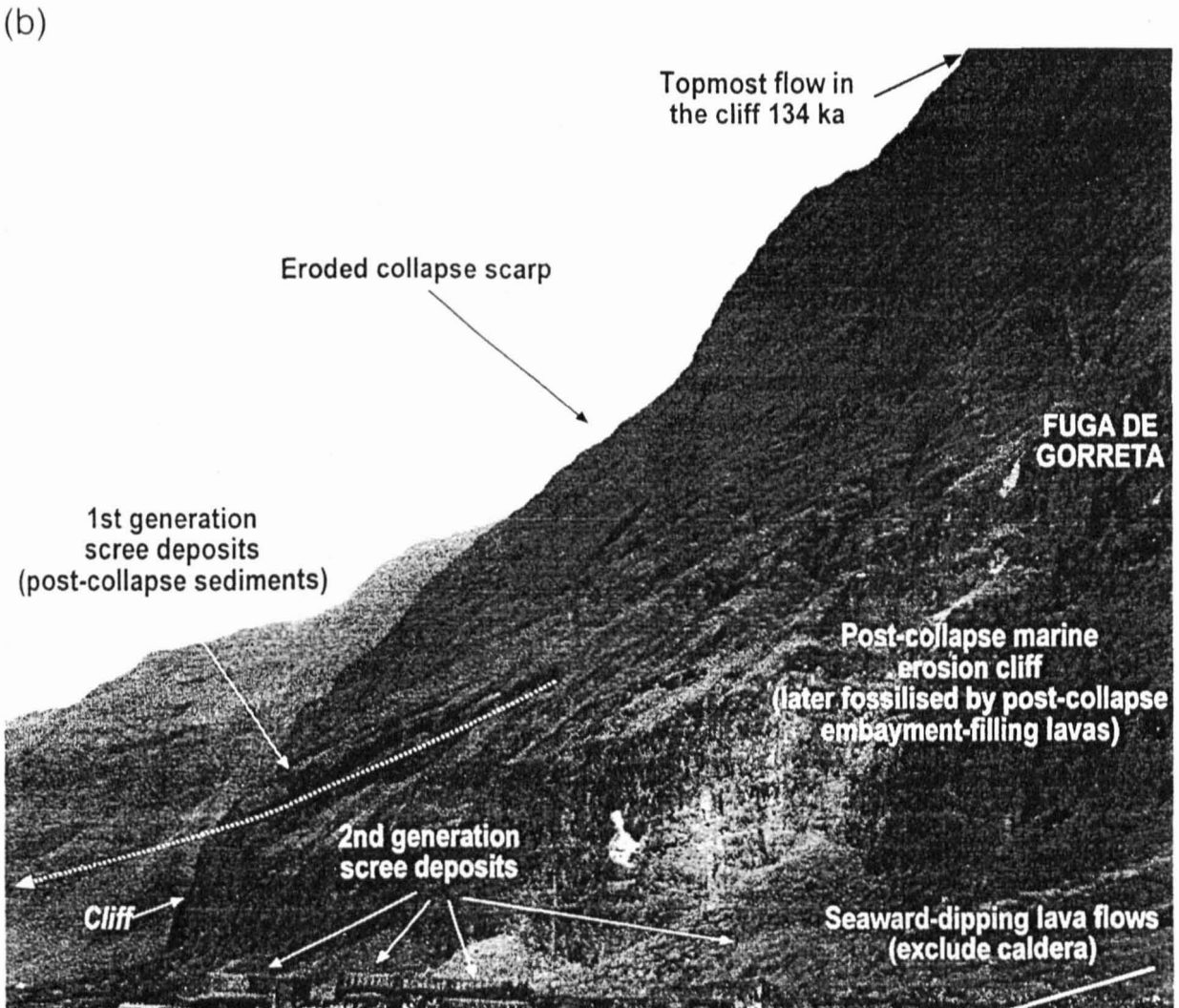


Fig. 7 (continued).

headwall of the Las Playas barranco are truncated by an erosion surface overlain by unfaulted basaltic to trachytic lavas of the upper El Golfo Formation, dated in 176–261 ka (Guillou et al., 1996).

These constraints indicate a minimum age for the San Andrés fault system of between approximately 150 and 250 ka.

In conclusion, this is an old and inactive structure, which is unlikely to be reactivated since after the aborted collapse, the El Golfo giant landslide occurred without reactivation of the San Andrés fault despite the intense seismic ground shaking that is likely to have accompanied this collapse.

### 3.4. The El Golfo collapse (or collapses?)

The El Golfo embayment is perhaps the most spectacular feature of El Hierro (Fig. 4 and inset). It is some 15 km across from Roques de Salmor to Arenas Blancas, extends some 10 km inland, and its

© Del documento, los autores. Digitalización realizada por ULPGC. Biblioteca Universitaria, 2009

headwall is in excess of 1.4 km high in places (Fig. 7a).

A volcano-tectonic mechanism ("block tectonics") was proposed for the generation of the El Golfo embayment as early as the 1960s, by Hausen (1964). Formation of the El Golfo embayment by catastrophic lateral collapse was first proposed by Holcomb and Searle (1991) on the basis of the discovery of a giant debris flow deposit offshore to the north. Conclusive offshore evidence identifying the El Golfo embayment as the most recent gravitational collapse in the Canaries has been recently obtained from the analysis of GLORIA and TOBI images (Masson, 1996; Canals et al., 1997; Urgeles et al., 1997; Masson et al., 1998).

The age of formation of El Golfo is still in debate. Masson (1996) proposed its formation in a single collapse that occurred between 13 and 17 ka. This author based this age on the correlation of the collapse debris avalanche deposits found offshore to the north with a turbidite (turbidite *b* of Weaver et al., 1992) in the Madeira abyssal plain that occurs at the boundary between pelagic sediments deposited in oxygen isotope stages 1 and 2. The inferred age of the collapse was thus proposed as between 9 and 15 or 10 and 17 ka according to the dating method, $^{14}C$ or U–Th, used to date the boundary between oxygen isotope stages 1 and 2 (Urgeles et al., 1997).

This offshore information strongly conflicts with onshore evidence for the age of the embayment. This

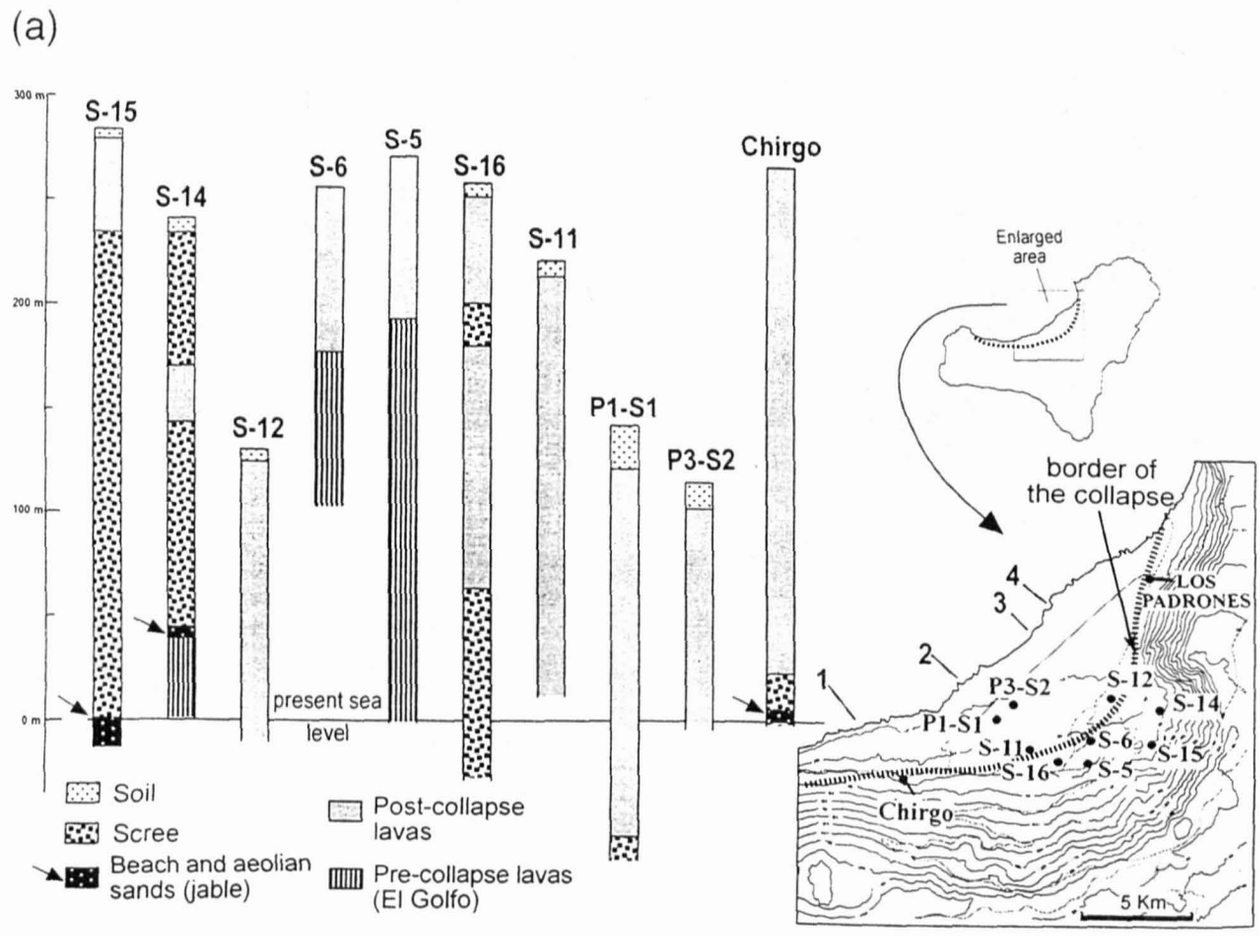


Fig. 8. (a) Boreholes drilled to investigate ground waters reveal the presence of a post-collapse marine abrasion platform, subsequently filled with lavas. Some of these boreholes cut into pre-collapse lavas, whereas other only cut post-collapse lavas filling the embayment, thus defining the boundary of the collapse scarp, buried under these lavas. (b) Cross-sections of the El Golfo embayment with information obtained from the boreholes.

© Del documento, los autores. Digitalización realizada por ULPGC. Biblioteca Universitaria, 2009

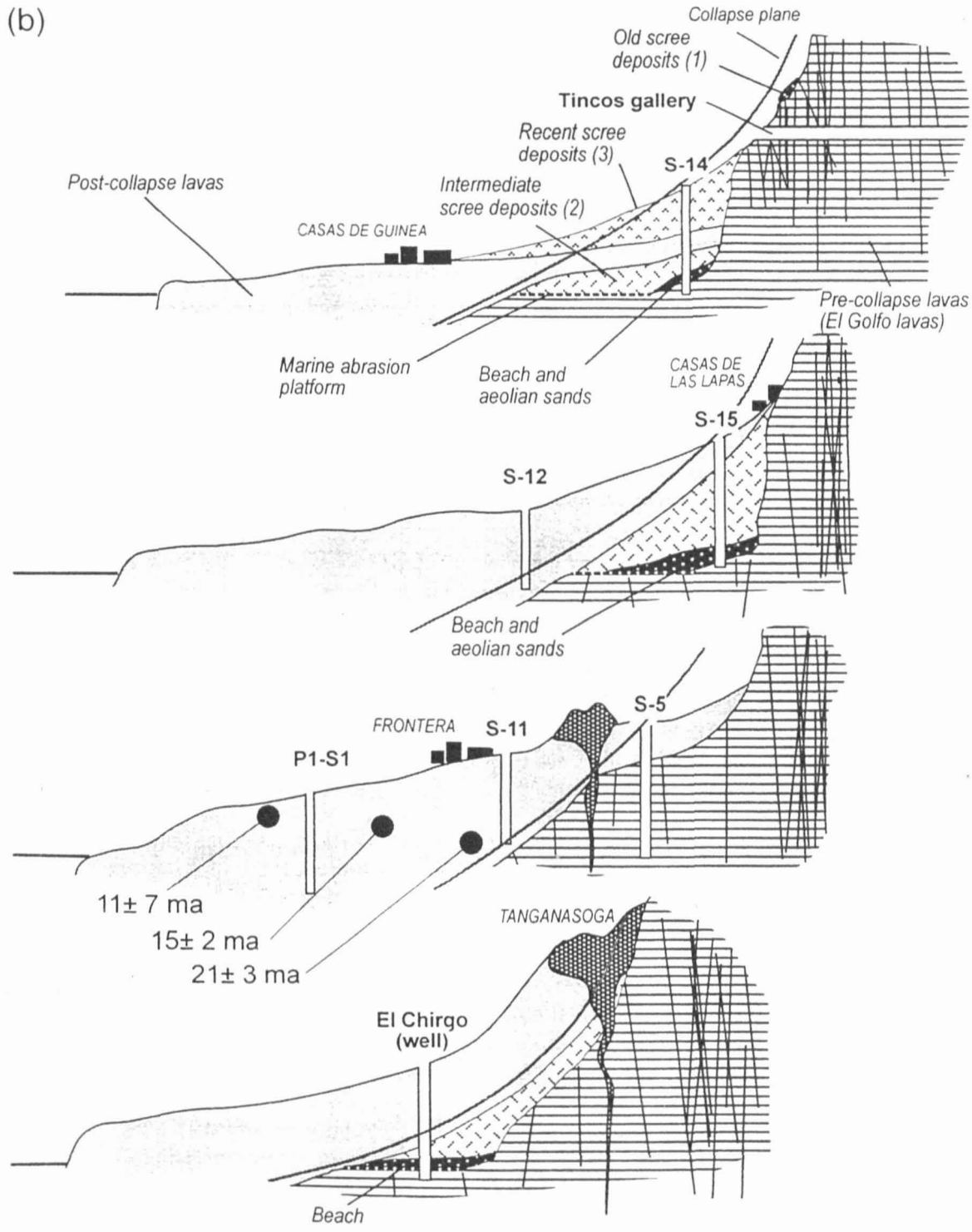


Fig. 8 (continued).

includes the morphology of the embayment headwall and the morphology of the marine abrasion platform beneath the lavas partially filling the embayment, which is identifiable through numerous boreholes

© Del documento, los autores. Digitalización realizada por ULPGC. Biblioteca Universitaria, 2009

(Fig. 8a and b) drilled for underground water exploration. Both features imply a long period of post-collapse erosion prior to the emplacement of the lavas that partially filled the collapse embayment. Another feature indicating a long period of post-collapse erosion is the presence of multiple generations of screes at the foot of the embayment cliffs and perched on the cliffs. Finally, the K–Ar ages of the uppermost lavas in the El Golfo cliffs and on those at the floor of the embayment show a difference of about 110 ka (see Figs. 7b and 8b).

Taken in isolation, these age constraints merely indicate that the embayment is younger than 134 ± 6 ka and older than 21 ± 3 ka, since the whole of the sequence in the present-day El Golfo cliff pre-dates the collapse and the lavas filling the embayment post-date the collapse. However, several of the boreholes drilled during the course of water exploration on the floor of the embayment (Fig. 8) revealed the presence of a broad, horizontal marine abrasion platform, up to 1.5 km wide, formed by pre-collapse lavas of El Golfo volcano, beneath the young lava sequence (Fig. 8). An abrasion platform inside the El Golfo embayment and post-dating El Golfo giant landslide has also been quoted by Bravo (1982). This author studied wells located inside the embayment and described horizontal beaches on a marine-cut platform under the post-collapse lavas and at about the present sea level and penetrating at least 1.100 m inside the embayment.

The Los Padrones water gallery recently excavated at the northern part of the embayment (inset in Fig. 8a) perforates 600 m in a 60-m-thick, horizontal lava flow, discordant to the embayment cliff and apparently resting in the abrasion platform (Guillou et al., 1996). The marine-cut plain is near present sea-level and extends from close to the back wall of the embayment to about 1 km from the present coastline (Fig. 7a). Sands, inferred to form a dune field, appear on top of this platform and beneath the lavas between 0 and 50 m a.p.s.l. Deposits of aeolian sands are at present being formed at the western end of El Golfo, in the Punta de Arenas Blancas. The abrasion platform cuts into El Golfo Series volcanic rocks and, east of Frontera, polymict breccias above and below El Golfo Series lavas. These breccias may represent elements of the El Golfo and Tiñor debris avalanches, respectively, or of extensive post-collapse scree breccias. The formation of this abrasion platform indicates a long period of post-collapse erosion whose duration can possibly be evaluated by consideration of Quaternary sea-level variations.

The lack of pillow basalts or hyaloclastites in the post-collapse, embayment-filling lavas, which are entirely subaerial, implies that there has been no recent uplift of El Hierro. Therefore, the abrasion platform must have formed when sea-level was close to or above its present level. The last time this was so was about 100–130 ka ago during the last interglacial. The subsequent fall in sea-level would have exposed the abrasion platform, consistent with the development of a subaerial aeolian dune field. This argument therefore implies that the El Golfo collapse took place at least 100–130 ka ago and was followed by a 70 ka long period of volcanic repose before eruptive activity resumed in the embayment.

A maximum age for the embayment is in principle provided by the 134 ± 6 ka age of the topmost lava in the cliff-forming sequence at Ermita de la Peña.

The west-facing cliff north of Fuga de Gorreta provides the best surface exposures of evidence for the marine abrasion platform found in the boreholes (Fig. 7). The lowest 50 m or so of the cliff are vertical and relatively fresh, whereas higher parts of the cliff are steeply inclined, more intensely weathered and vegetated. Furthermore, perched on this higher part of the cliff are the truncated remains of screes that predate the formation of the lower cliff. We infer that the latter is a coastal cliff, which formed at the back of the marine abrasion platform as marine erosion removed the earlier-formed screes (1st generation screes of Figs. 7b, 8b and 9) which had developed at an earlier stage of retreat of the collapse scar.

These lines of evidence therefore suggest that the subaerial embayment formed by a giant lateral collapse soon after the emplacement of the lavas at the top of the cliff sequence, at about 134 ka. The collapse therefore occurred at the end of a glacial low sea level stand period or during the subsequent rise in sea-level. The embayment thus formed was subsequently affected by marine erosion and the abrasion platform developed during the period of high sea-level stand in the last interglacial before the present one (oxygen isotope stage 5), that is to say

© Del documento, los autores. Digitalización realizada por ULPGC. Biblioteca Universitaria, 2009

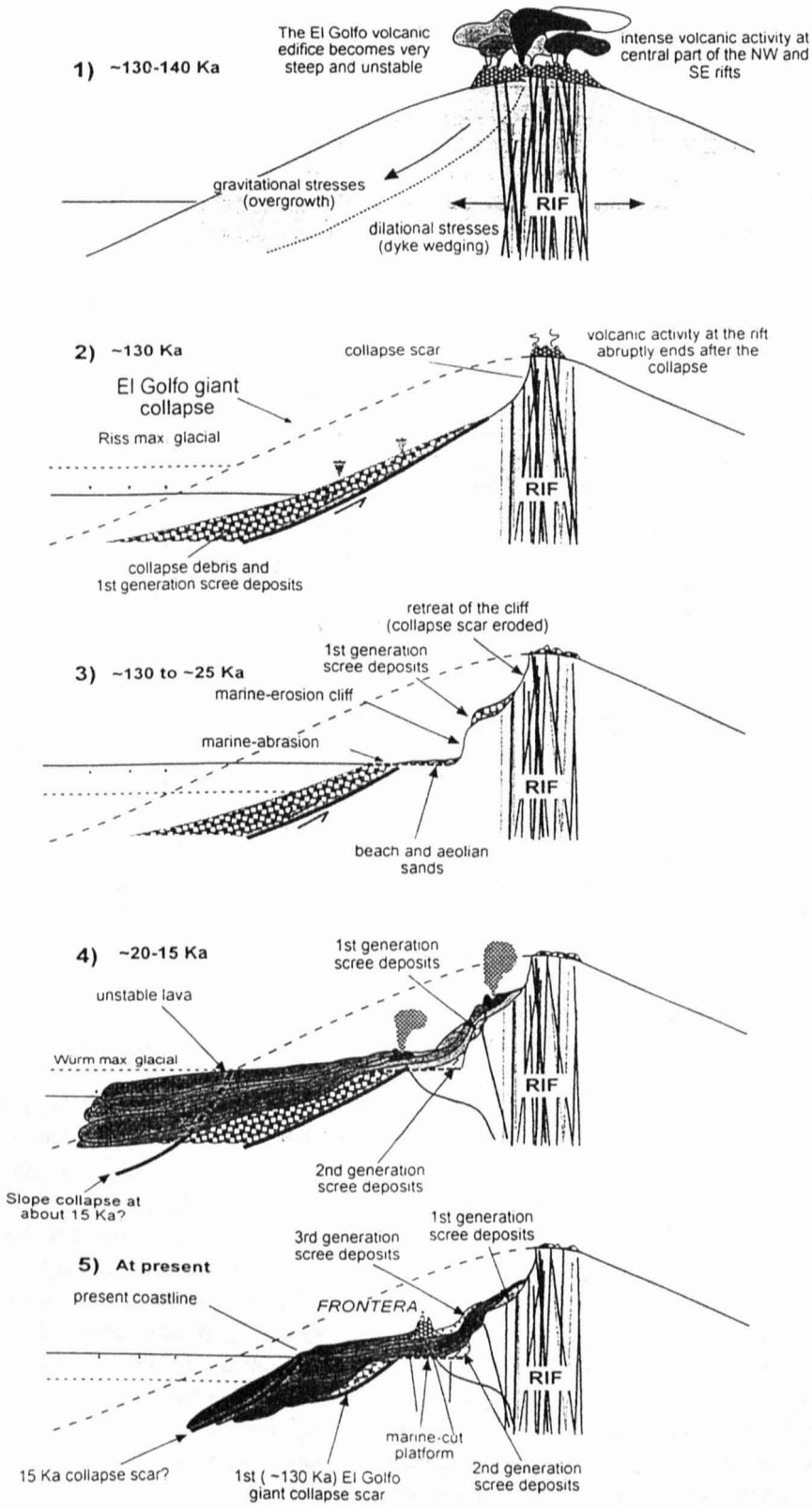


Fig. 9. Cartoon illustrating the El Golfo collapse as two separate events at about 130 ka and 20–15 ka. See text for further explanation.

© Del documento, los autores. Digitalización realizada por ULPGC. Biblioteca Universitaria, 2009

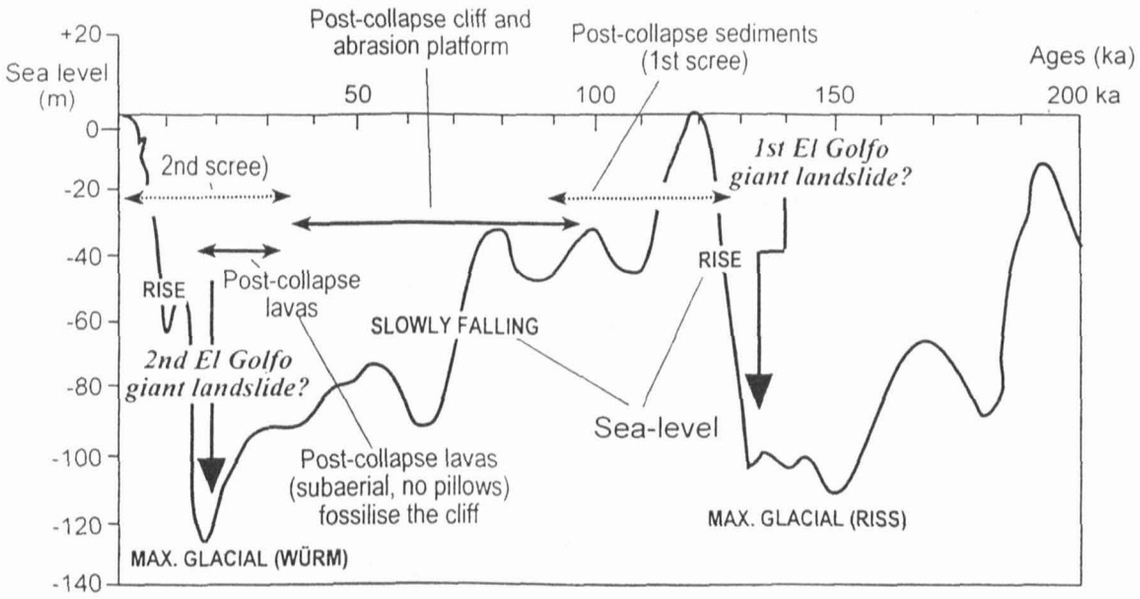


Fig. 10. The age constraints defined for the El Golfo collapses are consistent with both events occurring in periods of low sea-level stands (glacial maxima), the Riss and Wurm glaciations, respectively, as shown in the figure. Sea-level curve from Labeyrie et al. (1987).

before about 100 ka. This therefore provides a minimum age for the collapse.

A possible means of reconciling the contradictory onshore and offshore evidence is to postulate the occurrence of two lateral collapses: one largely subaerial and occurring about 130 ka ago, and the other affecting the seaward parts of the lava platform built up within the embayment, and also the submarine slope of the island down to considerable depths. This latter event, that may have taken place between 17 ka and 9 ka, would thus be the one that produced the megaturbidite *b*. This sequence of events is summarised in Fig. 9.

The age constraints are thus consistent with both collapse events occurring in periods of low sea level stands (glacial maxima) during the Riss and Wurm glaciations, respectively, and/or with the post-glacial rises in sea-level. This is consistent as well with the inference of Weaver et al. (1992) that megaturbidites in the Madeira abyssal plain occur at isotope stage boundaries coinciding with changing sea-level (Fig. 10).

The volume of subaerial material removed in the formation of the El Golfo embayment is at least 180 $km^3$, taking into consideration that the likely original height of the edifice may have exceeded 2000 m (Urgeles et al., 1997). In addition, the available bathymetry indicates that a similar volume has been removed below sea level (Masson, 1996).

## 4. Discussion and conclusions

Giant gravitational landslides are a common feature in the Canary Islands, as in the other intraplate hotspot-induced oceanic volcanoes in the world. They can be readily identified in the youngest, shield-stage islands of Tenerife, La Palma and El Hierro by means of onshore and offshore observations.

Giant landslides are a natural process that help restore gravitational stability to steep volcano slopes. In contrast to the Hawaiian islands and most of the oceanic volcanoes, subsidence is not comparatively significant in the Canaries. Consequently, these islands have an extended geological life of over 2 Ma, that ends by the joint action of catastrophic mass-wasting (in the earliest, most active shield stages) and erosion.

More than half of the total subaerial volume of the western islands (La Palma and El Hierro) has been removed by giant landslides and erosion in the past million years. The precise calculation of these

© Del documento, los autores. Digitalización realizada por ULPGC. Biblioteca Universitaria, 2009

volumes is difficult. A consequence of this is that the evaluation of the eruptive rates in the islands is also subject to significant uncertainty.

The island of El Hierro has been affected at least by three successive giant landslides and an old aborted gravitational flank collapse. The combined volume of those collapses (estimated at about 400–500 $km^3$) considerably exceeds the present subaerial volume of the island (about 140 $km^3$).

La Palma may have had two giant landslides, although the existence of the older one has not as yet been unambiguously verified. Both affect the northern, Plio-Quaternary Taburiente shield-volcano. The last one (the Cumbre Nueva giant landslide) took place at about 560 ka and involved a volume possibly exceeding 200 $km^3$. Since then, the Taburiente shield became extinct and eruptive activity concentrated in a predominant N–S-trending rift (the Cumbre Vieja volcano).

The Cumbre Vieja volcano is very steep and may be unstable (Day et al., 1999-this volume). Its western flank may rest on the Cumbre Nueva collapse scarp if this feature extends to the south end of the island, as suggested by the disposition of the summit of the volcano. A long (up to 3 km), arcuate zone of en echelon faults developed in the 1949 eruption at the summit of the Cumbre Vieja volcano (Bonelli, 1950; Carracedo, 1994). The possibility that these faults may indicate that the unstable block has already started to move is being monitored by seismic and geodetic techniques (Moss and McGuire, 1997).

A feature that may prove to be interesting is the apparently coupled development of La Palma and El Hierro during the Quaternary. Although still speculative, there seem to be periods of simultaneous rapid growth in both islands in an "on–off" sequence, apparently linked to the occurrence of catastrophic landslides (Carracedo et al., 1997e). Precise geochemical investigations, especially isotopic, are required to clarify whether both islands have a common magmatic source that can alternatively feed volcanoes in both islands following massive collapses.

## Acknowledgements

Constructive reviews by Wendell Duffield and another anonymous journal referee are gratefully acknowledged. Stimulating discussions with colleagues during the La Palma workshop in September 1997 greatly contributed to clarify ideas and are here acknowledged. This work has been supported by the Spanish DGICYT (PB92-0119), the French C.E.A. and C.N.R.S/I.N.S.U. (D.B.T.) and a NATO (CRG 940609) research project.

## References

Ancochea, E., Hernán, F., Cendrero, A., Cantagrel, J.M., Fœster, J.M., Ibarrola, E., Coello, J., 1994. Constructive and destructive episodes in the building of a young oceanic island, La Palma, Canary Islands, and genesis of the Caldera de Taburiente. J. Volcanol. Geotherm. Res. 60 (3–4), 243–262.

Bonelli, J.M., 1950. Contribución al estudio de la erupción del Volcán del Nambroque o San Juan (Isla de La Palma), 24 de Junio–4 de Agosto de 1949. Instituto Geográfico y Catastral, Madrid.

Bravo, T., 1952. Aportación al estudio geomorfológico y geológico de la costa de la fosa tectónica del valle de la Orotava. Bol. R. Soc. Esp. Hist. Nat., Tomo L, pp. 1–30.

Bravo, T., 1962. El circo de Las Cañadas y su dependencia. Bol. R. Soc. Esp. Hist. Nat. G 60, 93–108.

Bravo, T., 1982. Formaciones geológicas de la isla de El Hierro. Inst. Estudios Canarios, Aniversario, Aula Cultura, Cabildo Tenerife, Vol. 50, pp. 85–96.

Buch, von L.V., 1825. Physicalische Beschreibungen der Canarischen Inseln. Berlin, pp. 1–201.

Canals, M., Alibes, B., Urgeles, R., Alonso, B., 1997. Landsliding on the Canary Islands. The missing submarine sediment record. Internat. Workshop on Immature Oceanic Islands, La Palma, Sept., 1997, pp. 106–109.

Carracedo, J.C., 1994. The Canary Islands: an example of structural control on the growth of large oceanic-island volcanoes. J. Volcanol. Geotherm. Res. 60 (3–4), 225–241.

Carracedo, J.C., 1996. A simple model for the genesis of large gravitational landslide hazards in the Canary Islands. In: McGuire, Jones, Neuberg (Eds.), Volcano Instability on the Earth and Other Planets. Geological Society London Sp. Pub. 110, pp. 125–135.

Carracedo, J.C., 1999. Growth, structure, instability and collapse of Canarian volcanoes and comparisons with Hawaiian volcanoes. J. Volcanol. Geotherm. Res. 94, 1–19.

Carracedo, J.C., Day, S., Guillou, H., 1997. Late (Quaternary) shield-stage volcanism in La Palma and El Hierro, Canary Islands. Internat. Workshop on Immature Oceanic Islands, La Palma, Sept., 1997, pp. 63–65.

Carracedo, J.C., Day, S., Guillou, H., Pérez Torrado, J.F., 1997. El Hierro Geological Excursion Guidebook. Internat. Workshop on Immature Oceanic Islands, La Palma, Sept., 1997, pp. 1–43.

Carracedo, J.C., Day, S., Guillou, H., 1997. La Palma Geological

© Del documento, los autores. Digitalización realizada por ULPGC. Biblioteca Universitaria, 2009

Excursion Guidebook. Internat. Workshop on Immature Oceanic Islands, La Palma, Sept., 1997, pp. 1–84.

Carracedo, J.C., Day, S., Guillou, H., Gravestock, P., 1997. Colour geological map (1:33,000) of the Cumbre Vieja volcano. Internat. Workshop on Immature Oceanic Islands, La Palma, Sept., 1997.

Carracedo, J.C., Day, S., Guillou, H., Rodríguez Badiola, E., Canas, J.A., Pérez Torrado, F.J., 1997. Geochronological, structural and morphological constraints in the genesis and evolution of the Canary Islands. Internat. Workshop on Immature Oceanic Islands, La Palma, Sept., 1997, pp. 45–48.

Carracedo, J.C., Day, S., Guillou, H., Rodríguez Badiola, E., Canas, J.A., Pérez Torrado, F.J., 1998. Hotspot volcanism close to a passive continental margin: the Canary Islands. Geol. Mag. 135 (5), 591–604.

Carracedo, J.C., Day, S.J., Guillou, H., Gravestock, P., 1999. The later stages of the volcanic and structural evolution of La Palma, Canary islands: The Cumbre Nueva giant collapse and the Cumbre Vieja Volcano. Geol. Soc. Am. Bull. 111 (5), 755–768.

Clague, D.A., Denlinger, R.P., 1994. Role of olivine cumulates in destabilizing the flanks of Hawaiian volcanoes. Bull. Volcanol. 6 (6–7), 425–434.

Day, S.J., Carracedo, J.C., Guillou, H., 1997. Age and geometry of an aborted rift flank collapse: the San Andres fault system, El Hierro, Canary Islands. Geol. Mag. 134 (4), 523–537.

Day, S.J., Carracedo, J.C., Guillou, H., Gravestock, P., 1999. Recent structural evolution of the Cumbre Vieja volcano, La Palma, Canary Islands: volcanic rift zone reconfiguration as a precursor to volcanic flank instability? J. Volcanol. Geotherm. Res. 94, 135–167.

Fúster, J.M., Araña, V., Brandle, J.L., Navarro, M., Alonso, U., Aparicio, A., 1968. Geología y volcanología de las Islas Canarias: Tenerife. Instituto "Lucas Mallada", C.S.I.C., Madrid.

Guillou, H., Carracedo, J.C., Pérez Torrado, F., Rodríguez Badiola, E., 1996. K–Ar ages and magnetic stratigraphy of a hotspot-induced, fast grown oceanic island: El Hierro, Canary Islands. J. Volcanol. Geotherm. Res. 73, 141–155.

Hausen, H., 1961. Canarian calderas. Bull. Commis. Geol. Finlande 196, 1–47.

Hausen, H., 1964. Rasgos geológicos generales de la isla de El Hierro. Anuario de Estudios Atlánticos 10, 547–593.

Holcomb, R.T., Searle, R.C., 1991. Large landslides from oceanic volcanoes. Marine Geotechnology 10, 19–32.

Kluegel, A., Schmincke, H.U., White, J.D.L., Hoernle, K.A., 1999. Chronology and volcanology of the 1949 multi-vent rift-zone eruption on La Palma, Canary Islands. J. Volcanol. Geotherm. Res. 94, 267–282.

Labeyrie, L., Duplessy, J.C., Blanc, P.L., 1987. Variations in mode of formation and temperatures of oceanic deep water over the past 125,000 years. Nature 327, 477–482.

Lyell, C., 1855. A Manual of Elementary Geology II. London, pp. 1–498.

Masson, D.G., 1996. Catastrophic Collapse of the Volcanic Island of El Hierro 15 ka ago and the History of Landslides in the Canary Islands.

Masson, D.G., Watts, A., 1995. Slope failures and debris avalanches on the flanks of volcanic oceanic islands: the Canary Islands, off NW Africa. Landslide News 9, 21–24.

Masson, D.G., Canals, M., Alonso, B., Urgeles, R., Huhnerbach, V., 1998. The Canary debris flow: source area morphology and failure mechanisms. Sedimentology 45, 411–432.

McGuire, W.J., 1996. Volcano instability: review of contemporary themes. In: McGuire, Jones, Neuberg (Eds.), Volcano Instability on the Earth and other Planets. Geol. Soc. London Spec. Publ., 110, pp. 1–23.

Moore, J.G., 1964. Giant submarine landslides on the Hawaiian ridge. United States Geological Survey Professional Paper 501-D, pp. 95–98.

Moss, J., McGuire, W.J., 1997. Establishing baseline ground deformation studies on La Palma using GPS. Internat. Workshop on Immature Oceanic Islands, La Palma, Sept., 1997, pp. 126–128.

Navarro, J.M., Coello, J., 1989. Depressions originated by landslide processes in Tenerife. ESF Meeting on Canarian Volcanism, Lanzarote.

Navarro, J.M., Coello, J.J., 1994. Mapa Geológico de la Caldera de Taburiente. Pub. Organismo Autónomo De Parques Nacionales, Madrid.

Navarro, J.M., Soler, C., 1994. El agua en El Hierro. Resumen del Avance del Plan Hidrológico. Public. Cabildo de El Hierro and Consej. O.P. Gob. Canarias, pp. 1–59.

Schmincke, H.U., Sumita, M., Funck, T., 1997. Growth and destruction of Gran Canaria: evidence from land studies, bathymetry, offshore seismic studies and drilling during ODP Leg 157. Internat. Workshop on Immature Oceanic Islands, La Palma, Sept., 1997, pp. 11–12.

Stillman, C., 1999. Giant Miocene landslides and the evolution of Fuerteventura, Canary Islands. J. Volcanol. Geotherm. Res. 94, 89–104.

Swanson, D.A., Duffield, W.A., Fiske, R.S., 1976. Displacement of the south flank of Kilauea volcano: the result of forceful intrusion of magma into the rift zones. U.S. Geol. Surv. Prof. Pap. 963, 1–39.

Urgeles, R., Canals, M., Baraza, J., Alonso, B., Masson, D., 1997. The most recent megaslides on the Canary Islands: the El Golfo debris avalanche and the Canary debris flow north-west El Hierro island. J. Geophys. Res. 102, 20305–20323.

Watts, A., Masson, D., 1995. A giant landslide on the north flank of Tenerife, Canary Islands. J. Geophys. Res. 100, 24487–24498.

Weaver, P.P.E., Rothwell, R.G., Ebbing, J., Gunn, D.E., Hunter, P.M., 1992. Correlation, frequency of emplacement and source directions of megaturbidites on the Madeira Abyssal Plain. Mar. Geol. 109, 1–20.

© Del documento, los autores. Digitalización realizada por ULPGC. Biblioteca Universitaria, 2009

SCI. MAR., 63 (3-4): 317-325 SCIENTIA MARINA 1999

BIOLOGY AND FISHERY OF DOLPHINFISH AND RELATED SPECIES. *E. MASSUTÍ and B. MORALES-NIN (eds.)*

# Growth and reproduction of the dolphinfish (*Coryphaena equiselis* and *Coryphaena hippurus*) in the Canary Islands, Central-East Atlantic (preliminary results)*

J.J. CASTRO[1], J.A. SANTIAGO[1], V. HERNÁNDEZ-GARCÍA[1] and C. PLA[2]

[1]Departamento de Biología, Universidad de Las Palmas de Gran Canaria, Apdo. 550, Las Palmas de Gran Canaria, Canary Islands, Spain. E-mail: josejuan.castro@biologia.ulpgc.es
[2]Lab. Ictiologia Genètica, Universitat de Girona, Campus Montilivi, 17071 Girona, Spain.

SUMMARY: The size, growth and spawning characteristics of pompano dolphin (N=150) and common dolphinfish (N=36) caught off the Canary Islands between May and September 1995 and between July and September 1996 were examined. Fork length (FL) of pompano dolphin was in the range 28.3-62.8 cm. In 1995, the mean length increased significantly from June to September. However, in 1996, the mean length was significantly larger in July than in September. The overall length-weight relationship was $W=0.0287*FL^{2.774}$ (r=0.97), while these relationships by sex were as follows: $W=0.031*FL^{2.758}$ (r=0.98) and $W=0.0282*FL^{2.776}$ (r=0.97), for males and females respectively. Spawning takes place at the beginning of the Summer (June-July). All the individuals obtained showed developing gonads, but females showed a higher gonadosomatic index (GSI) than males. The highest GSI values were obtained in June ($\bar{x}$=3.10±1.73), and decreased progressively towards the end of the season (September), when the average of this index was $\bar{x}$= 1.86±0.87. Similarly, the condition index decreased significantly from June to September. The proportion of females was always significantly higher than males, except in July 1996 when it was 1:1. There was a high correspondence between growth rates determined by annuli scale interpretation and modal progression analysis. According to scale annuli interpretation, the individuals caught showed more than five age classes. However, there are doubts about age assignation from scales. Fork length of common dolphinfish was in the range of 76.5-103.0 cm. The length-weight relationships obtained for all the specimens caught was $W=0.00095FL^{3.527}$ (r=0.96), while these relationships by sex were as follows: $W=0.00398FL^{3.222}$ (r=0.94) and $W=0.01656FL^{2.973}$ (r=0.91), for males and females respectively. Spawning probably takes place at the beginning of the Summer. All the individuals obtained showed developing gonads, although the GSI of females were higher than males. The highest GSI values were obtained in June ($\bar{x}$=5.50±2.17). In the same way, the condition index decreased from May to June. The proportion of females was always slightly higher than males (1:1.4), but the ratio was not significantly different from 1:1.

*Key Words*: *Coryphaena equiselis*, *Coryphaena hippurus*, growth, reproduction, Canary Islands.

## INTRODUCTION

*Coryphaena* is the only genus in the Coryphaenidae family and is made up of two species, *Coryphaena hippurus* (Linnaeus, 1758) and *Coryphaeana equiselis* (Linnaeus, 1758). According to Collette (1981) and Palko *et al.* (1982), *C. equiselis* is differentiated from *C. hippurus* by the fact that the adult of the pompano dolphin has a body depth of over 25% the standard length, and that the tooth patch on the tongue of *C. hippurus* is smaller and oval in comparison with the broader and square

*Received October 28, 1997. Accepted October 8, 1998.



© Del documento, los autores. Digitalización realizada por ULPGC. Biblioteca Universitaria, 2009

tooth patch of the *C. equiselis*. There are also differences in the number of rays on the different fins of both species, although their ranges overlap. In view of these distinctive characteristics, it might seem that these two species would be easy to distinguish, however they are not. During the CORY programme financed by the Commission of the European Communities (D.G. XIV), we were only able to segregate them using a genetic marker (Morales-Nin *et al.*, 1995; Pla and Pujolar, 1999), because none of the morphological characteristicss allowed for quick and reliable recognition.

*Coryphaena hippurus* grows very quickly and its maximum longevity has been estimated at four years (Beardsley, 1967; Oxenford and Hunter, 1983; Uchiyama *et al.*, 1986). Morales-Nin *et al.* (1995) from otoliths, reported that fish of 55 cm of FL, caught off Majorca, were 176 days old, and from scales, found that specimens of *C. hippurus*, caught off the Canary Islands within a range of between 76 to 103 cm FL, were two and three years old. However, there is no data relating to the longevity of *C. equiselis* although, according to Palko *et al.* (1982), the life span is believed to be shorter than for that of *C. hippurus*. However, Morales-Nin *et al.* (1995) found that specimens of *C. equiselis*, within a range of between 32 to 52 cm FL, were spread over four year classes. This fact indicates that the pompano dolphin has a slower growth rate and greater life span than the common dolphinfish.

*Coryphaena hippurus* is a circumtropical oceanic pelagic species that is common in waters of the Atlantic, Pacific and Indian Oceans (Briggs, 1960; Beardsley, 1967; Rose and Hassler, 1968; Johnson, 1978), and is generally restricted by the 20°C isotherm (Gibbs and Collette, 1959). *C. equiselis* generally inhabits open waters, and less frequently occurs in coastal waters. There is little information with respect to its geographical distribution, but it is probably distributed in more tropical and subtropical waters than *C. hippurus* (Collette, 1981), but is generally not found in waters with surface temperatures lower than 24°C (Mather and Day, 1954). In the East Atlantic, common dolphinfish have been observed from the Gulf of Biscay to SouthAfrica (Shcherbachev, 1973), and are also frequent in the Mediterranean (Massutí and Morales-Nin, 1995). However, pompano dolphin have been observed from the Azores to Senegal (Palko *et al.*, 1982), although their range is not known to any degree of exactitude because sometimes they are confused with *C. hippurus*. They have also been reported in the Mediterranean sea (Shcherbachev, 1973), although they could possibly be confused with the juvenile of the common dolphinfish (Massutí *et al.* 1997). *C. hippurus* has occasionally been observed in coastal waters (Johnson, 1978) and during the Summer of 1995, we observed several common dolphinfish swimming into the port of Arguineguín (Gran Canaria), at only 2-4 m depth.

Dolphinfish are abundant in the waters of the Canary Islands, although the volume of commercial catches of these species is not large. There are three reasons which may explain these low catches. The first is cultural. In some islands, and especially among the fishermen, these species are known by the local name of "corpse eater" mainly as a result of their tendency to aggregate under floating objects (Fedoryako, 1988), including corpses. The second reason for low catches, relates to the absence of a large scale marketing and distribution network for these species beyond the insular markets. All catches of dolphinfishes are currently sold fresh to local restaurants or to the local market, whose capacity level is very limited. Thirdly, the seasonal presence of the skipjack tuna (*Katsuwonus pelamis*), coincides with that of the *Coryphaena* species in Canary waters, strongly depressing the potential catches of dolphinfish. This results from the fact that skipjack has a well structured marketing network and is exported to foreign markets (i.e. Japan) so that the coastal fishing fleet is exclusively devoted to fishing tuna. So, dolphinfish are only taken by tuna boats as by-catch.

The aim of the present paper is to report the first information on growth and reproduction of *Coryphaena equiselis* and *C. hippurus* in waters off the Canary Islands.

## MATERIAL AND METHODS

A total of 150 specimens of pompano dolphin and 36 specimens of common dolphinfish were obtained from commercial catches off Gran Canaria (Canary Islands) between May and September 1995 and between July and September 1996. Fish samples were caught by the artisanal tuna fleet using live bait. Examination of the samples was undertaken immediately after landing. Each fish was measured, to the nearest millimetre, for fork length (FL), standard length (SL), distance to the anal fin (AL), distance to the ventral fin (VL), distance to the pectoral fin (PL), distance to the dorsal fin (DL), cephalic



© Del documento, los autores. Digitalización realizada por ULPGC. Biblioteca Universitaria, 2009

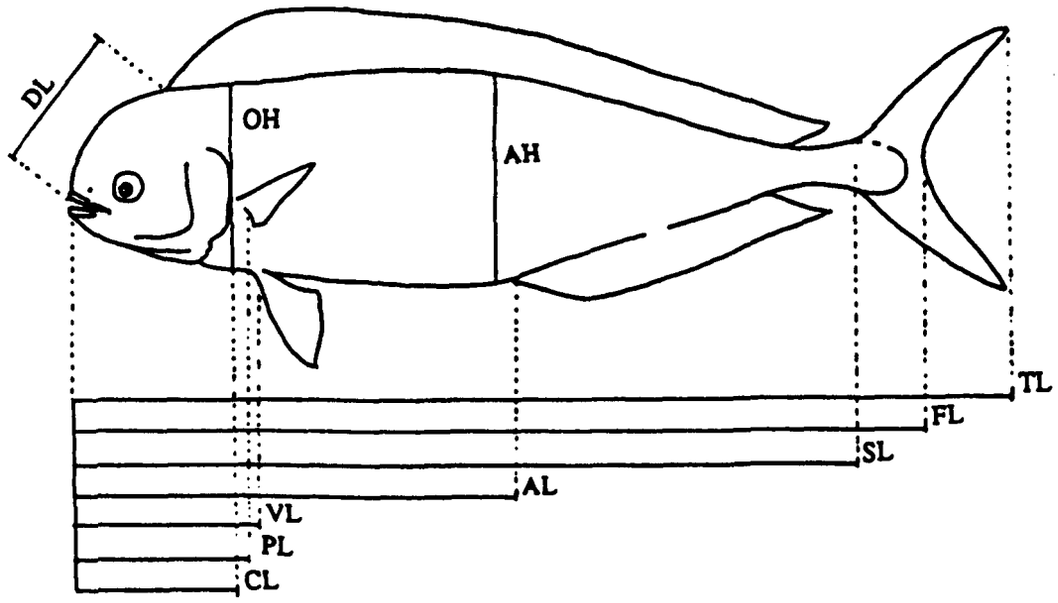


FIG. 1. – Morphometric measurements taken for *Coryphaena equiselis* and *Coryphaena hippurus*: Total length (TL); fork length (FL); standard length (SL); distance to the anal fin (AL), distance to the ventral fin (VL); distance to the pectoral fin (PL); distance to the dorsal fin (DL): cephalic length (CL); opercular height (OH); and anal height (AH).

length (CL), opercular height (OH) and anal height (AH) (Fig. 1). The total weight (W) and the eviscerated weight were also recorded to the nearest 0.1 g. The gonads and the liver were weighed to the nearest 0.01 g. The sex and stage of maturity of each specimen were ascertained from head morphology and by macroscopic observation of the gonads, following the classification proposed by Holden and Raitt (1975) (I, immature; II resting; III, ripe; IV, running ripe; V, spent). The gonadosomatic index (GSI) was calculated as GSI=100GW/W (Anderson and Gutreuter, 1983), and used to determine the spawning season.

All fish sampled were genetically analysed with protein electrophoresis technique using 11% starch gel. Tissue extraction, electrophoresis and procedures for visualizing proteins generally followed the methods outlined in Aebersold *et al.* (1987) with minor modifications (García-Marín *et al.*, 1991).

The length-weight relationship was established by linear regression, using logarithm values. The relative condition factor (Kn) was calculated as Kn=100W/TW, where TW is the estimated weight of fish of the same length, derived from the length-weight equation (Anderson and Gutreuter, 1983).

Morphometric relationships between FL, taken as an independent variable, and each of the remaining variables taken as dependent variables, were calculated in the following way: $Y_{ij}=a_i FL_j^{bi}$, where FL is the fork length of individual j, Y is the i variable of individual j and $a_i$ and $b_i$ are the parameters of the relationship between fork length and variable i. Calculations were carried out using logarithmic values.

Statistical analyses were carried out with CSS statistic software (StatSoft, Inc.).

Growth rates were determined by modal progression analysis of length frequency distributions obtained in 1995 and 1996. These were fitted at the 95% confidence level by the computer programme NORMSEP (Hasselblad, 1966) included in the FISAT software (Gayanilo *et al.* 1994).

## RESULTS

### Sample composition

Pompano dolphin sampled ranged in size from 28.3 to 62.8 cm FL, and weighed between 292 and 2810 g. The length of females ranged from 28.3 to 57.9 cm FL and the weight ranged from 292 to 2184 g. Males ranged from 29.2 to 62.8 cm FL and from 352 to 2810 g in weight. The length distributions in 1995 and 1996 were significantly different (ANOVA, F=21.85, P<0.0001; Table 1). The 1995 sample ranged from 32 to 52 cm FL and in 1996, from 28 to 63 cm FL (Fig. 2). In 1995, the mean length increased significantly from June to September (ANOVA, F=3.824, P=0.014). In 1996 the mean length was significantly larger in July than in September (ANOVA, F=49.838, P<0.001; Table 1).



© Del documento, los autores. Digitalización realizada por ULPGC. Biblioteca Universitaria, 2009

TABLE 1. – Number (N) of *Coryphaena equiselis* and *Coryphaena hippurus* measured each month during 1995 and 1996, mean fork length ($\bar{x}$), standard deviation (SD), and length range (MINimal and MAXimal fork length).

| | | 1995 | | | | | 1996 | | | |
|---|---|---|---|---|---|---|---|---|---|---|
| | | JUN | JUL | AUG | SEP | TOTAL | JUL | AUG | SEP | TOTAL |
| *Coryphaena equiselis* | N | 22 | 14 | 14 | 14 | 64 | 40 | - | 46 | 86 |
| | $\bar{x}$ | 41.9 | 37.6 | 41.6 | 43.1 | 41.1 | 40.7 | - | 34.0 | 37.1 |
| | SD | 05.3 | 04.6 | 04.3 | 03.2 | 04.9 | 05.5 | - | 03.1 | 05.5 |
| | MIN | 32.0 | 31.7 | 35.0 | 38.0 | 31.7 | 31.6 | - | 28.3 | 28.3 |
| | MAX | 52.2 | 47.7 | 49.5 | 49.5 | 52.2 | 62.8 | - | 41.6 | 62.8 |
| | | MAY | JUN | | TOTAL | | | | | |
| *Coryphaena hippurus* | N | 10.0 | 25.0 | | 35.0 | | | | | |
| | $\bar{x}$ | 88.3 | 86.1 | | 86.8 | | | | | |
| | SD | 10.3 | 07.3 | | 08.1 | | | | | |
| | MIN | 76.5 | 77.0 | | 76.5 | | | | | |
| | MAX | 103.0 | 99.5 | | 103.0 | | | | | |

Common dolphinfish measured ranged in size from 76.5-103.0 cm FL (Fig. 2), weighing between 3368 and 13718 g. The length of females ranged from 76.5 to 99.0 cm FL and weight from 3368 to 9800 g. Males ranged from 80.5 to 103.0 cm FL and from 5600 to 13718 g in weight. During 1995, 35 individuals were sampled, but in 1996 only one spent female (91.0 cm FL) was sampled. The mean length did not increase significantly from May to June (ANOVA, F=0.552, P=0.462). Females did not increase in length (ANOVA, F=0.727, P=0.405), but males did (ANOVA, F=9.280, P=0.0094; Table 1) during the same period.

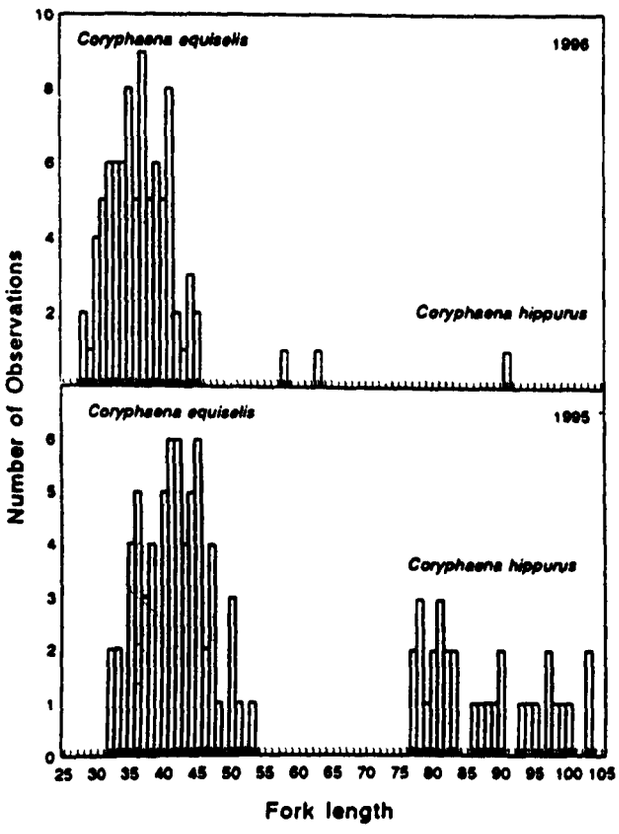


FIG. 2. – Length-frequency histograms for dolphinfishes caught in 1995 and 1996.

## Growth

For pompano dolphin, the modal progression analysis shows the existence of four ($\chi^2$ = 72.812, df=9, P<0.05) and five size classes ($\chi^2$=62.904, df=10, P<0.05) in 1995 and 1996 respectively (Table 2). There was a high correspondence between annuli scale interpretation and the modal progression analysis for the individuals caught in 1995 (Mann-Whitney U-test, U=14.0, Z=-0.57, P=0.57), and also for the individuals caught in 1996 (Kruskal-Wallis ANOVA, H=2.04, P=0.36) (Table 2).

For common dolphinfish, the modal progression analysis shows three age classes ($\chi^2$=99.334, P<0.05) (Table 2). There was also a high correspondence between modal length classes and the half year classes (Observed vs. expected $\chi^2$= 0.149, P<0.93).

## Relative growth

Length-weight relationships were calculated separately for females, males and all fish (Table 3).

For the pompano dolphin, analysis of variance showed no significant difference between the length (ANOVA, F=0.652, P=0.42) and weight distributions (ANOVA, F=1.226, P=0.269) of the two sexes. Analysis of covariance indicated no significant differences in the length-weight relationships between the two sexes (ANCOVA, F=1.229, P=0.27). The slopes of the length-weight regressions indicated



© Del documento, los autores. Digitalización realizada por ULPGC. Biblioteca Universitaria, 2009

TABLE 2. – Size-at-age data derived from scale annuli interpretation by Morales-Nin *et al.* (1995) and its correspondence with the size groups (mean length and standard deviation) obtained from the modal progression analysis of the size distribution of *Coryphaena equiselis* and *Coryphaena hippurus* caught in 1995 and 1996.

| | Age (years) | Size at age (Morales-Nin *et al.*, 1995) | Modal Progression Analysis 1995 | 1996 |
|---|---|---|---|---|
| *Coryphaena equiselis* | 1.0 | | | 27.5±0.3 |
| | 1.5 | 32.0 | 31.9±0.5 | 31.0±1.4 |
| | 2.0 | 37.1±3.3 | 35.0±0.6 | 35.0±2.1 |
| | 2.5 | 38.5±4.5 | 37.7±1.8 | 39.8±1.8 |
| | 3.0 | 41.2±4.7 | 42.6±2.4 | - |
| | 3.5 | 43.2±4.1 | - | - |
| | 4.0 | 46.3 | - | 45.0±0.5 |
| | 4.5 | 50.0 | 50.1±0.8 | - |
| | Plus | - | - | 58.0-63.0 |
| *Coryphaena hippurus* | 2.0 | 81.0±4.0 | 78.8±2.0 | |
| | 2.5 | 81.5±3.7 | - | |
| | 3.0 | 88.7±8.1 | 87.5±3.3 | |
| | 3.5 | 98.6±3.8 | 96.6±3.6 | |

TABLE 3. – Parameters of the allometric relationships of *Coryphaena equiselis* and *Coryphaena hippurus* (Interval at the 95% confidence level).

| | | Males | | | | Females | | | | All Fish | | | |
|---|---|---|---|---|---|---|---|---|---|---|---|---|---|
| | | a | b | R | Interval | a | b | R | Interval | a | b | R | Interval |
| *C. equiselis* | W | 0.03 | 2.76 | 0.98 | (2.59-2.92) | 0.03 | 2.78 | 0.97 | (2.63-2.90) | 0.03 | 2.77 | 0.97 | (2.67-2.88) |
| | SL | 0.99 | 0.98 | 0.99 | (0.95-1.00) | 1.05 | 0.97 | 0.98 | (0.93-1.00) | 1.03 | 0.97 | 0.99 | (0.95-1.00) |
| | DL | 0.33 | 0.80 | 0.84 | (0.65-0.94) | 0.44 | 0.73 | 0.85 | (0.63-0.83) | 0.40 | 0.75 | 0.84 | (0.66-0.82) |
| | AL | -0.11 | 0.89 | 0.98 | (0.84-0.95) | -0.69 | 0.89 | 0.87 | (0.78-0.99) | -0.08 | 0.88 | 0.89 | (0.80-0.95) |
| | VL | -0.45 | 0.89 | 0.95 | (0.81-0.97) | 0.36 | 0.85 | 0.94 | (0.77-0.90) | 0.39 | 0.86 | 0.94 | (0.81-0.91) |
| | PL | -0.55 | 0.94 | 0.96 | (0.86-1.01) | -0.55 | 0.94 | 0.95 | (0.88-1.00) | -0.55 | 0.94 | 0.96 | (0.89-0.98) |
| | CL | -0.49 | 0.87 | 0.96 | (0.81-0.94) | -0.46 | 0.86 | 0.95 | (0.80-0.91) | -0.48 | 0.87 | 0.96 | (0.82-0.91) |
| | OH | -0.84 | 1.15 | 0.89 | (1.04-1.26) | -0.89 | 1.14 | 0.89 | (1.06-1.26) | -0.92 | 1.16 | 0.85 | (1.08-1.24) |
| | AH | -0.68 | 1.04 | 0.85 | (0.89-1.19) | -0.69 | 1.04 | 0.89 | (0.94-1.14) | -0.73 | 1.07 | 0.87 | (0.98-1.16) |
| *C. hippurus* | W | 0.004 | 3.22 | 0.94 | (2.66-3.78) | 0.02 | 2.87 | 0.91 | (2.15-3.58) | 0.001 | 3.53 | 0.96 | (3.13-3.92) |
| | SL | -0.10 | 1.04 | 0.99 | (0.89-1.09) | -0.01 | 0.99 | 0.99 | (0.87-1.11) | 0.00 | 0.99 | 0.99 | (0.94-1.03) |
| | DL | -1.37 | 1.26 | 0.84 | (0.78-1.75) | -0.23 | 0.65 | 0.41 | (-0.43-1.73) | -1.77 | 1.46 | 0.90 | (1.03-1.88) |
| | AL | -0.38 | 1.04 | 0.98 | (0.76-1.32) | -0.26 | 0.99 | 0.87 | (0.78-1.20) | 0.03 | 0.84 | 0.95 | (0.70-0.97) |
| | VL | -0.18 | 0.75 | 0.85 | (0.36-1.14) | -1.34 | 1.35 | 0.83 | (0.67-2.03) | -0.65 | 0.99 | 0.89 | (0.74-1.24) |
| | PL | -0.21 | 0.77 | 0.86 | (0.52-1.01) | -0.60 | 0.96 | 0.95 | (0.38-1.53) | -0.87 | 1.10 | 0.94 | (0.87-1.32) |
| | CL | -0.48 | 0.88 | 0.76 | (0.65-1.10) | -0.80 | 1.04 | 0.76 | (0.64-1.43) | -0.73 | 1.00 | 0.97 | (0.86-1.13) |
| | OH | -1.18 | 1.28 | 0.81 | (0.72-1.83) | -0.72 | 1.01 | 0.57 | (0.40-1.61) | -2.01 | 1.69 | 0.93 | (1.34-2.03) |

negative allometric growth in both sexes. There were significant differences between the mean opercular height (ANOVA, F=10.318, P=0.002) and mean anal height (ANOVA, F=9.094, P=0.003) of the two sexes. The mean cephalic length was larger in males than in females, although not significant (ANOVA, F=1.901, P=0.17). Analysis of covariance only indicated significant differences in the relationships between the CL-FL (F=4.707, P=0.03), FL-AL (F=19.58, P<0.001), FL-OH (F=57.922, P<0.001) and FL-AH (F=14.015, P<0.001) of the two sexes. Negative allometric growth was found in the relationships between FL and all the other variables, except with AH which behaved isometrically, and with OH which showed a positive allometric growth (Table 3).

For the common dolphinfish, analysis of variance showed significant difference between the length (ANOVA, F=20.199, P<0.001) and weight distributions (ANOVA, F=30.84, P<0.001) of both sexes. The slopes of the length-weight regressions indicated positive allometric growth. Positive allometric growth was found in the relationships FL versus DL and OH. Isometric growth was found in FL versus SL, VL, PL and CL. Negative allometric growth was only found in the relationship FL versus AL (Table 3).

The relationships between the body height (OH and AH) and the body length (FL or SL) did not show a clear lower limit as proposed by Collette (1981) which could be used to differenciate *Coryphaena equiselis* from *C. hippurus* (Table 5).



© Del documento, los autores. Digitalización realizada por ULPGC. Biblioteca Universitaria, 2009

TABLE 4. – Mean values and range of variation of gonadosomatic index (GSI) and relative condition factor (Kn) per month, for females and males of *Coryphaena equiselis* and *Coryphaena hippurus*.

| | | Males | | | | | Females | | | | |
|---|---|---|---|---|---|---|---|---|---|---|---|
| | | N | GSI | | Kn | | N | GSI | | Kn | |
| | | | x̄ | range | x̄ | range | | x̄ | range | x̄ | range |
| *Coryphaena equiselis* | | | | | | | | | | | |
| 1995 | JUNE | 5 | 1.11±0.18 | 0.92-1.41 | 1.04±0.07 | 0.91-1.09 | 17 | 3.68±1.53 | 0.95-6.28 | 1.02±0.07 | 0.87-1.09 |
| | JULY | 6 | 1.10±0.32 | 0.83-1.68 | 0.99±0.05 | 0.94-1.07 | 8 | 3.10±1.70 | 0.93-6.07 | 0.94±0.08 | 0.82-1.14 |
| | AUGUST | 3 | 0.96±0.25 | 0.64-1.14 | 0.95±0.05 | 0.90-1.01 | 11 | 3.35±0.62 | 2.17-4.09 | 0.99±0.12 | 0.66-1.12 |
| | SEPTEMBER | 5 | 1.04±0.13 | 0.83-1.16 | 0.94±0.05 | 0.86-1.00 | 9 | 2.32±0.74 | 0.93-3.43 | 0.92±0.09 | 0.77-1.01 |
| | TOTAL | 19 | 1.05±0.23 | 0.64-1.68 | 0.98±0.07 | 0.86-1.09 | 45 | 3.22±1.32 | 0.93-6.28 | 0.97±0.10 | 0.66-1.14 |
| 1996 | JULY | 22 | 1.54±0.64 | 0.58-3.51 | 1.54±0.08 | 0.93-1.21 | 18 | 3.79±0.77 | 2.50-5.20 | 1.06±0.06 | 0.94-1.18 |
| | SEPTEMBER | 13 | 0.91±0.35 | 0.40-1.91 | 0.99±0.07 | 0.87-1.10 | 33 | 1.51±0.74 | 0.42-3.15 | 0.97±0.06 | 0.97-1.08 |
| | TOTAL | 35 | 1.29±0.62 | 0.40-3.51 | 1.04±0.08 | 0.87-1.21 | 51 | 2.32±1.33 | 0.42-5.20 | 1.00±0.07 | 0.79-1.18 |
| *Coryphaena hippurus* | | | | | | | | | | | |
| 1995 | MAY | 4 | 1.47±0.10 | 1.35-1.57 | 1.13±0.09 | 1.14-1.25 | 6 | 4.97±1.20 | 3.29-6.46 | 0.90±0.10 | 0.76-1.03 |
| | JUNE | 10 | 1.53±0.63 | 1.14-2.26 | 1.03±0.07 | 0.94-1.16 | 12 | 5.78±2.17 | 3.81-8.30 | 0.90±0.07 | 0.81-1.01 |
| | TOTAL | 14 | 1.49±0.37 | 1.14-2.26 | 1.06±0.08 | 0.94-1.25 | 18 | 4.81±2.23 | 3.21-8.30 | 0.90±0.08 | 0.77-1.03 |

Only the relationship between SL and AH showed an average similar to the 25% reported by Collette, but its range (22.4 to 29.9 %) did not allow us to use it as a valid and definitive criteria of identification.

## Sex ratio

Of the total number of pompano dolphin examined, 96 were females (45 in 1995 and 51 in 1996) and 54 were males (19 in 1995 and 35 in 1996). The overall ratio of males to females was 1:2 and the proportion of females was always significantly higher than males ($\chi^2$ observed vs. expected= 88.97; P< 0.001), except in July 1996 when it was 1:1. Females predominated (1:2) in size intervals lower than 45 cm FL, while in larger size intervals the proportion between males and females was 1:1.

Common dolphinfish sampled were 21 females (20 in 1995 and 1 in 1996) and 15 males (all sampled in 1995). The overall ratio of males to females was 1:1.4 and the proportion of females was always higher than males (1:1.5 in May and 1:1.3 in June). Females predominated in size intervals lower than 85 cm FL, while in size intervals larger than 90 cm the males predominated.

## Spawning period

During the sampling periods, ovaries and testes of both species were well developed with all the individuals in the stage III of the scale of Holden and Raitt (1975). We did not find any specimens in stages IV or V.

The monthly GSI values of females of pompano dolphin were usually higher than those of males (Table 4). In 1995, the highest values of the GSI in both sexes ocurred between June and July, with a peak in June for females and July for males. In 1996, the maximum GSI for both sexes was recorded in July. However, there were no samples in June and August of that year (Table 4). In 1995, the GSI decreased, from June to September in both sexes (Kruskal-Wallis ANOVA; H=7.39, P=0.06 in females and H=1.01, P=0.79 in males). The mean Kn showed a peak during July, while the lowest was observed in September for both sexes (Table 4). In 1996, Kn followed a similar pattern as in 1995

TABLE 5. – Mean ratio (%), standard deviation (SD) and range in the % ratios, between the fork length (FL) or standard length (SL) and the body height measured at the level of the operculus (OH) or at the anus (AH), in females and males of *Coryphaena equiselis*.

| | OH/FL | | | AH/FL | | | OH/SL | | | AH/SL | | |
|---|---|---|---|---|---|---|---|---|---|---|---|---|
| | % | SD | range | % | SD | range | % | SD | range | % | SD | range |
| Males | 22.8 | 1.30 | 19.6-25.7 | 24.3 | 1.48 | 21.9-28.0 | 24.4 | 1.47 | 21.0-28.2 | 25.9 | 1.72 | 23.1-29.9 |
| Females | 21.2 | 1.24 | 17.9-24.9 | 23.3 | 1.01 | 21.1-25.4 | 22.5 | 1.32 | 19.9-26.3 | 24.6 | 1.00 | 22.4-27.2 |
| Total Fish | 21.8 | 1.50 | 17.9-25.7 | 23.7 | 1.34 | 21.1-28.0 | 23.2 | 1.64 | 19.9-28.2 | 25.1 | 1.55 | 22.4-29.9 |



© Del documento, los autores. Digitalización realizada por ULPGC. Biblioteca Universitaria, 2009

(Table 4). In 1995, Kn decreased from June to September in both sexes but it was only significant in females (Kruskal-Wallis ANOVA; H= 9.90; P=0.02).

The monthly GSI values of females of common dolphinfish were usually higher than that of males (Table 4). The highest values of the GSI in both sexes ocurred in June. The GSI increased, although not significantly, from May to June in both sexes (Kruskal-Wallis ANOVA; H=0.24, P= 0.62 in females and H=0.50, P=0.48 in males). There were no significant variations in Kn values during both months (Table 4).

## DISCUSSION

Off the Canary Islands, captures of *Coryphaena hippurus* and *Coryphaena equiselis* are reported together as "dorados". The data series of dolphinfish species landed in the port of Mogán (Southwest of Gran Canaria) from 1981 onwards, is very irregular and shows an abundance peak catch in Summer and a slough in January-April. During 1995 and 1996, catches of *C. equiselis* were more frequent, especially from June to September. However, *C. hippurus* seems to be more abundant during May and June. Nevertheless, *Coryphaena* species are caught almost all the year round, although the majority of captures outside of the normal fishing season are reported by long-liner or sport fishing. On 15th June 1994, a fishing vessel reported a capture of over 3 tons, caught under a drifting object off the east coast of Gran Canaria. Daily captures of 1030 Kg and 760 Kg per boat were reported on 27th October and 19th November 1994 respectively, but in any case it was not recorded which species of dolphinfish was captured nor the length range. In 1994, the average catch per day per boat was 223.1 Kg, while in 1995 it decreased to 99.8 Kg. Catches in 1996 and 1997 were negligible. The low rates of capture between years are caused, among other factors, by the total lack of commercial network for these species beyond the insular markets, and the strong market for skipjack tuna, in the same season and fishing ground.

Pompano dolphin and common dolphinfish caught in the Canary Island waters reveal an unbalanced sex ratio in favour of females. However, in pompano dolphin in the size intervals of over 45 cm fork length, the sex ratio was 1:1, and in the case of common dolphinfish, in size intervals larger than 90 cm, the males predominated. This may be due to a different life-span for both sexes, with a higher mortality rate in females than in males when larger in size. However, unbalanced sex ratios in dioecious species is extremely rare, and it is probably safer to assume that the sex ratios observed were a consequence of sampling caused by differences in the behaviour (and hence in catchability) of males and females, and of fish of different sizes, as has been reported for common dolphinfish (Rose and Hassler, 1974; Gibbs and Collette, 1959; Beardsley, 1967). Differential growth rates for both sexes of common dolphinfish, with adult males larger than females of the same age (Kraul, 1999), also should be considered as another motive for unbalanced sex ratio according to the size class.

Adult males of the dolphinfish species develop a bony crest on the front of head (Collette, 1981). Shcherbachev (1973) noted that sexual dimorphism in the pompano dolphin is noted only at a length of more than 35 cm SL and at smaller sizes, males and females are externally indistinguishable, while male common dolphinfish start to develop the bony crest at approximately 40 cm FL (Beardsley, 1967). We did not find differences in the cephalic length between males and females of *C. equiselis* for the overall length range measured. However, the analysis of covariance indicates that there are significant differences in growth of the head with the body length of the two sexes. Both sexes also differ morphometrically in that males have a greater body depth than females.

While the slopes of the length-weight relationships of common dolphinfish were allometrically positive, these indicated a negative allometric growth in both sexes of pompano dolphin. That is to say, contrary to what occurs with the common dolphinfish, pompano dolphin increase more quickly in length than in weight during growth. Positive allometric growths were only found in the relationships between fork length and opercular height and anal height in both sexes of pompano dolphin. However, in common dolphinfish, the dorsal part of the body and body height of males show a positive allometric growth, the posterior region (opercular, pectoral and ventral lengths) grows isometrically, while the anal region shows negative allometric growth. This could be related to a progressive bend of the dorsal region of the body and the development of the bony crest on the front of the head in the adult males (Collette, 1981). Females did not show this positive allometric growth in the dorsal region. Positive allometric



© Del documento, los autores. Digitalización realizada por ULPGC. Biblioteca Universitaria, 2009

ratios were found in the relationships between fork length and height in both sexes.

Individuals caught of both species were normally adults. The modal progression analysis of the size distribution of pompano dolphin in 1995 shows four age classes. Morales-Nin *et al.* (1995), from scale annuli interpretation of 66 of these individuals, found four age classes which correspond to between 1.5 to 4.5 years old (Table 2). According to this, in 1996, four age classes were also recorded and another age class made up of two individuals of 58 and 63 cm. The high correspondence between modal length classes and the half year classes suggests that the population of pompano dolphin is made up of two cohorts each year, as a consequence of two separate and well-defined recruitment periods. On the other hand, the modal progression analysis of the size distribution of common dolphinfish caught in 1995 shows four size classes. Morales-Nin *et al.* (1995), from scale annuli interpretation of 17 of these individuals, found two age classes which correspond to between 2 to 3.5 years old.

Uchiyama *et al.* (1986) using age from daily increment on the sagitta otoliths, reported that *Coryphaena equiselis* appeared to grow as rapidly as *C. hippurus* during the first four months, then grew at a slower rate. Pompano dolphin also reached sexual maturity at about four months (Uchiyama *et al.*, 1986). Growth checks on scales due to spawning or migrations (Summerfelt and Hall, 1987) could bias annuli scale interpretation if validation has not previously been carried out.

Spawning of the pompano dolphin in the Canary Islands area takes place at the beginning of the Summer (June-July). All the individuals obtained showed ripening gonads, although the highest GSI values were obtained in June-July and decreased progressively towards the end of the season. The Kn decreased in the same way, indicating a weight loss toward the end of the season, probably due to spawning. Common dolphinfish spawn in surface waters. Their reproductive season is extensive with frequent multiple spawning (Johnson, 1978; Massutí, 1997). Due to the scarce number of fish sampled, it is difficult to specify the spawning season of the common dolphinfish off the Canary Islands. However, this probably takes place at the beginning of the Summer. The highest values of the GSI were obtained in June, coinciding with the lowest Kn values.

The results obtained during this study are regarded as preliminary due to the small number of individuals analysed. Large numbers of specimens are required in order to confirm the trends shown over the data reported in this paper.

## ACKNOWLEDGEMENTS.

We are grateful to Silvia Hildebrandt for her assistance in data collection. Thanks are also given to Dr. Beatriz Moralez-Nin, Dr. Enric Massutí and the two anonymous referees for their valuable suggestions. This research was financed by the Commission of the European Communities (Projects DG. XIV, 94/013 and 95/73).

## REFERENCES

Aebersold, P.B., G.A. Winans, D.J. Steel, G.B. Milner and F.M. Utter. – 1987. Manual for starch gel electrophoresis: a method for detection of gel variation. *NOAA. Tech. Rep.*, 61:1-19

Anderson, R.O. and S.J. Gutreuter. – 1983. Length, weight, and associated structural indices. In: L.A. Nielsen and D.L. Johnson (Eds.): *Fisheries Techniques*. American Fisheries Society, pp. 283-300. Bethesda, MD.

Beardsley, G.L. – 1967. Age, growth, and reproduction of the dolphin, *Coryphaena hippurus*, in the Straits of Florida. *Copeia*, 1967:441-451.

Briggs, J.C. – 1960. Fishes of worldwide (circumtropical) distribution. *Copeia*, 1960:171-180.

Collette, B.B. – 1981. Family Coryphaenidae. In: Fischer, W. G. Bianchi and W.B. Scott (eds): *FAO Species identification sheets for fishery purposes. Easter Central Atlantic: fishing areas 34, 47 (in part)*. Canada Funds-in-Trust. Ottawa, Department of Fisheries and Oceans Canada, by arrangement with the Food and Agriculture Organization of the United Nations.

Fedoryako, B.I. – 1988. Skopleniya ryb v otkrytom okeane u stationarnykh buev. *Okeanologiya Oceanology Mosc.*, 28(4): 667-669.

García-Marín, J.L., P.E. Jorde, N. Ryman, F.M. Utter and C. Pla. – 1987. Management implications of genetic differentiation between native and hatchery population of brown trout (*Salmo trutta*) in Spain. *Aquaculture*, 95: 235-249.

Gayanilo, F.C. Jr., P. Sparre and D. Pauly. – 1994. The FAO-ICLARM stock assessment tools (FISAT) user's guide. *FAO computerized Information Series*. Rome, FAO.

Gibbs, R.H. Jr. and B.B. Collette. – 1959. On the identification, distribution, and biology of the dolphins *Coryphaena hippurus* and *C. equiselis*. *Bull. Mar. Sci. Gulf. Caribb.*, 9: 117-152.

Holden, M.J. and D.F.S. Raitt. – 1975. Manual de ciencia pesquera. Parte 2. Métodos para investigar los recursos y su aplicación. *Doc. Téc. FAO Pesca*, 115, 211 pp.

Hasselblad, V. – 1966. Estimation of parameters for mixture of normal distributions. *Technometrics*, 8: 431-444.

Johnson, G.D. – 1978. Development of fishes of the Mid-Atlantic Bight. An atlas of eggs, larval, and juvenile stages. Vol. IV Carangidae through Ephippidae. *U.S. Dep. Inter., Fish Wildl. Serv., Biol. Serv. Prog.* FWS/OBS-78/12 ja. 1978: 123-128.

Kraul, S. – 1999. Seasonal abundance of the dolphinfish, *Coryphaena hippurus*, in Hawaii and the tropical Pacific Ocean. *Sci. Mar.*, 63(3-4): 261-266.

Massutí, E. – 1997. Biology of *Coryphaena hippurus* Linnaeus, 1758 (Pisces: Corypahenidae) in the Western Mediterranean. Ph. D. thesis, Univ. Illes Balears.

Massutí, E. and B. Morales-Nin. – 1995. Seasonality and reproduction of the dolphinfish (*Coryphaena hippurus*) in the Western Mediterranean. In: C. Bas, J.J. Castro and J.M. Lorenzo (eds.), *International Symposium on Middle-sized Pelagic Fish. Sci. Mar.*, 59(3-4): 357-364.

Massutí, E., B.B. Collette and P. Oliver. – 1997. Does the pompano



© Del documento, los autores. Digitalización realizada por ULPGC. Biblioteca Universitaria, 2009

dolphin, *Coryphaena equiselis* (Osteichthyes, Coryphaenidae), occur in the Mediterranean Sea? *Workshop on the biology and fishery of the dolphinfish and related species*. 20-23 October 1997. Palma de Mallorca (Spain).

Morales-Nin, B., P. Oliver, J.J. Castro, L. Cannizaro, A. Potoschi and C. Pla. – 1995. Biology and fishery of the dolphinfish in the western Mediterranean and Canary Islands Area. Final Draft Report. Commission of the European Communities. Directorate General for Fisheries (DG XIV). 94/031.

Oxenford, H.A. and W. Hunte. – 1983. Age and growth of dolphin, *Coryphaena hippurus*, as determined by growth rings in otoliths. *Fish. Bull.*, 84(4): 906-909.

Palko, B.J., G.L. Beardsley and W.J. Richards. – 1982. Synopsis of the biological data on the dolphinfishes, *Coryphaena hippurus* Linnaeus and *Coryphaena equiselis* Linnaeus. *FAO Fisheries Synopsis* No. 130.

Pla, C. and J.M. Pujolar. – 1999. Genetic homogeneity of dolphinfish (*Coryphaena hippurus*) in the western Mediterranean and the eastern Atlantic. *Sci. Mar.*, 63(3-4): 337-341.

Rose, C.D. and W.W. Hassler. 1968. Age and growth of the dolphin, *Coryphaena hippurus* (Linnaeus), in the North Carolina waters. *Trans. Am. Fish. Soc.*, 97: 271-276.

Rose, C.D. and W.W. Hassler. – 1974. Food habis and sex ratios of dolphin *Coryphaena hippurus* captured in the western Atlantic Ocean off Hatteras, North Carolina. *Trans. Am. Fish. Soc.*, 103: 94-100.

Shcherbachev, Yu.N. – 1973. The biology and distribution of the dolphins (Pisces, Coryphaenidae). (In Russ.) *Vopr. Ikhtiol.*, 13:219-230. (Trasl. in *J. Ichthyol.*, 13: 182-191).

Summerfelt, R.C. and G.E. Hall. – 1987. *Age and growth of fish*. Iowa State University Press/Ames. 544 pp.

Uchiyama, J.H., R.K. Burch and S.A.Jr. Kraul. – 1986. Growth of dolphins, *Coryphaena hippurus* and *C. equiselis*, in Hawaiian water as determined by daily increments on otoliths. *Fishery Bulletin*, 84(1): 186-191.



© Del documento, los autores. Digitalización realizada por ULPGC. Biblioteca Universitaria, 2009

SCI. MAR., 63 (3-4): 191-198 SCIENTIA MARINA 1999

BIOLOGY AND FISHERY OF DOLPHINFISH AND RELATED SPECIES. *E. MASSUTÍ and B. MORALES-NIN (eds.)*

# Fish associated with fish aggregation devices off the Canary Islands (Central-East Atlantic)*

J.J. CASTRO, J.A. SANTIAGO and V. HERNÁNDEZ-GARCÍA

Departamento de Biología, Universidad de Las Palmas de Gran Canaria, Apdo. 550, Las Palmas de Gran Canaria, Canary Islands, Spain. E-mail: josejuan.castro@biologia.ulpgc.es

SUMMARY: Sixteen fish aggregation devices (FADs) were deployed in 50 to 500 m deep of water in the Canary Islands. Species composition and abundance were determined by visual census carried out by divers on 55 occasions from April to October 1995 and from August 1996 to May 1997. A total of 15 species representing nine families of fish were observed. *Pseudocaranx dentex* (Bloch and Schneider, 1810), *Seriola* spp. and *Naucrates ductor* (Linnaeus, 1758) were the most abundant species. The number of species associated with FADs increased with immersion time, but fish biomass did not increase. The maximum number of fish species registered exactly under the FADs at any one time was five. The average estimated biomass was 9.47 Kg per FAD (SD= 25.2). However, when only baitfish were taken into account, the mean aggregated fish biomass was 3.20 Kg (SD= 4.32). The estimated biomass was higher when *Coryphaena* spp. was present, increasing to 53.9 Kg per FAD (SD=53.6). A significantly lower fish biomass and number of species was observed in FADs deployed in shallower waters (50-100 m depth).

*Key words*: FADs, Fish assemblages, floating structures, artisanal fisheries, Central-East Atlantic.

## INTRODUCTION

The tendency of fish to aggregate around floating objects has been known for some time (Mortensen, 1917; Uda, 1933; Kojima, 1956; Galea, 1961; Hunter, 1968). The first commercial fish aggregation devices (FADs) were deployed in the waters of the Philippines in the early 1970s (Kihara, 1981) to attract *Thunnus albacares* (Bonnaterre, 1788). Due to the success of FADs in aggregating fish, these have come to play an important role in the commercial, subsistence, and recreational fisheries of all the tropical and sub-tropical oceans of the world (Pollard and Matthews, 1985; Frusher, 1986; Wilkins and Goodwin, 1989; Biais and Taquet, 1990; Holland *et al.*, 1990; Buckley and Miller, 1994; Friedlander *et al.*, 1994; Higashi, 1994; Kitamado and Kataoka, 1996).

This fishing method has most specifically been used in large scale commercial tuna fisheries over the last three decades and has given a higher yield of fish (Greenblatt, 1979; Fonteneau, 1992). The method yields an average catch of 40 tonnes of tuna per fishing operation around flotsam in comparison with 20 tonnes for free schools (Fonteneau and Hallier, 1993). Sometimes up to 200 tonnes of tuna have been harvested in a single fishing operation (Sacchi, 1986).

The first studies designed to ascertain the mechanisms leading to aggregation under floating objects were carried out by Gooding and Magnuson (1967) and Hunter and Mitchell (1967). Subsequent to

Received January 20, 1998. Accepted January 21, 1999.



© Del documento, los autores. Digitalización realizada por ULPGC. Biblioteca Universitaria, 2009

these, there have been many more including those by Greenblatt (1979), Matsumoto *et al.* (1981), de Silva (1982), Myatt and Myatt (1982), Beets (1989), Buckley *et al.* (1989). Four methods have been used to study the fauna associated with flotsam: 1. direct observation (Rountree, 1989; 1990; Parin and Fedoryako, 1992); 2. use of fishing (Hunter and Mitchell, 1967; Massutí and Reñones, 1994); 3. combination of both (Wickham and Russell, 1974); 4. use of ultrasonic tags (Brill *et al.*, 1984. Holland *et al.*, 1990; Cayré, 1991; Cayré and Marsac, 1993).

Several hypotheses have been suggested to explain aggregation under floating objects (Kingsford, 1993). Amongst many other factors, the most appealing are: Fish congregate around flotsam looking for refuge from predators (Hunter and Mitchell, 1968; Feigebaum *et al.*, 1989). Fish may aggregate because more food is available under flotsam (Gooding and Magnuson, 1967). The disturbance produced by the flotsam in the uniformity of the ocean may be a reason for the attraction (Holland *et al.*, 1990; Hunter and Mitchell, 1967). However, it seems to be the consequence of many factors which influence fish behavior (Fonteneau, 1992; Hall, 1992; Kingsford, 1993).

Several fish species approach FADs looking for food, and feed on the invertebrate that grow on the FADs (i.e. hydrozoans, cirripedes, amphipods and crabs)(Kojima, 1967; Ida *et al.*, 1967; Rountree, 1990; Massutí and Reñones, 1994). It is thought that large predators like tunas, sharks and dolphin-fish, are attracted by the fish aggregated under the FADs (Wickham *et al.*, 1973, Arenas *et al.*, 1992). However, there are doubts that these species prey on the fish fauna associated with the FADs (Brock, 1985; Cort, 1990; Fonteneau, 1992; Massutí and Reñones, 1994). It is also possible that some species like dolphin-fish use FADs as spawning places, due to the fact that drifting objects indicate the presence of oceanic currents where eggs and larvae may drift more efficiently towards better nursery areas.

Studies carried out on the fish communities associated with FADs off the West coast of Africa are few, and deal mostly with the large scale tuna fisheries under flotsam (Wood, 1989; Fonteneau, 1992; Kwei and Bannerman, 1993). In the Canary Island waters, there is no traditional commercial fishing around flotsam, and there is only one previous study on the fish communities associated with artificial habitats (i.e. FADs and cinder blocks on the bottom) (Bortone *et al.*, 1994). In this paper, we describe the faunal composition and abundance of fishes associated with FADs anchored at the south of the island of Gran Canaria, using census data and information from commercial catches over two years. The aim of this paper is to study the fish community associated with FADs, and the variations in the number of species and biomass aggregated in relation to season, depth of anchoring and immersion time. Observation of the behaviour of the species associated with FADs was also recorded to provide further details on the fish community structure.

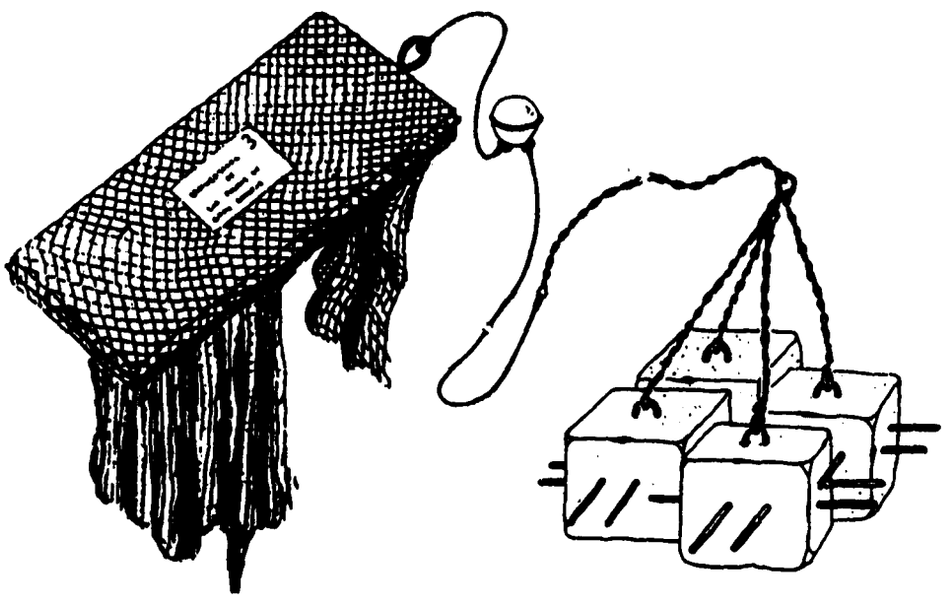

FIG. 1. – Fish Aggregation Devices and anchorages used during the study period. FAD was a mattress of foam (200x100x12.5 cm), covered with a black plastic film and a piece of net. The submerged volume was increased with fragments of old nets (about 1.5 m of longitude). The anchorage was composed of four 50 kg concrete blocks.



© Del documento, los autores. Digitalización realizada por ULPGC. Biblioteca Universitaria, 2009

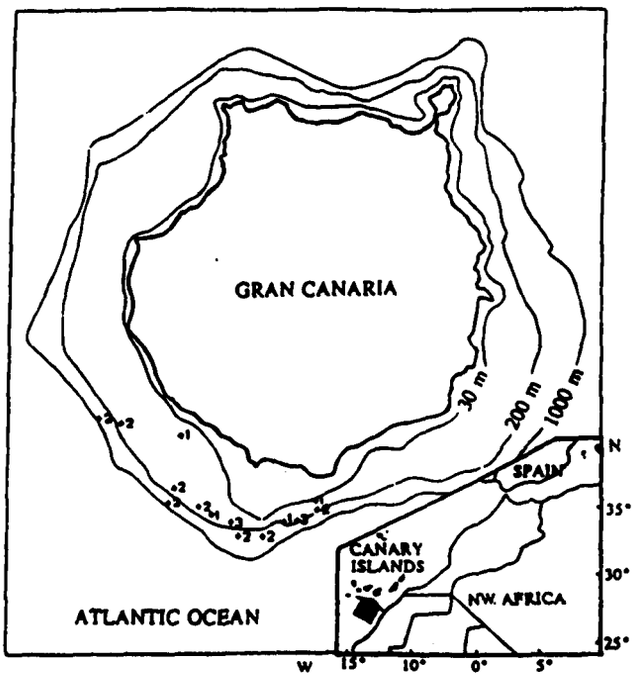


FIG. 2. – Location of the FADs deployed in waters off Gran Canaria (Canary Islands, Spain).

## MATERIALS AND METHODS

In 1995, 1996 and 1997, 16 Fish Aggregation Devices (FADs) were constructed (four in 1995, ten in 1996, and two in 1997) using blocks of foam of expanded polystyrene (200x100x12.5 cm). These blocks were covered with a black plastic film to protect the "foam" from the sun and damage caused by seagulls. Each unit was netted to hold the flotsam to the anchor. The submerged float volume was increased by adding fragments of old nets (about 1.5 m in length) hanging from the float (Fig. 1). No float unit surpassed 10 Kg in weight.

The anchorage of each FAD was composed of four concrete blocks, each weighing 50 Kg, held together with chains. The floats were tied to the anchorages using synthetic ropes about 20% longer than the depth of the area, to avoid sinking the FAD due to current or tidal drag. The FADs were deployed at depths between 50 and 500 m (Fig. 2). The cost of the FADs ranged between 200 and 370 US $, depending on the depth of the anchorage.

From April until October 1995 and August 1996 to May 1997, observations of fish associated with the FADs were carried out almost fortnightly. The number of visits to the FADs in 1995 and 1996-97 were 26 and 29 respectively. During each of these visits, two divers undertook a visual census of all the fish within the range of visibility from the FADs (visibility around the FADs ranged from 15 to 30 m). Divers recorded the number of fish of each species and their approximate size. The size (total length) recorded was transformed to weight, using the length-weight relationships of each species obtained from the literature (Isidro, 1990; García-Gómez, 1993; Gordo, 1996) and from our own non-published data. During observations, video recordings were also taken to verify the census and to provide records for use in subsequent studies of the behavior and spatial distribution of fish around the FADs.

We carried out a statistical analysis in order to test the following hypotheses: 1) Fish community change with the season of the year, as a consequence of the recruitment processes of the local fish fauna (sensus Rountree, 1990). 2) The depth of anchorage (50-100, 120-160 and >300 m) influences the fish community structure, so that we can expect to find fish biomass and the number of species associated to FADs increasing from shallow to deep waters. 3) The fish community is expected to increase the diversity of the species as immersion time and maturity increase (sensus Vinogradov, 1983).

We also logged the fish captures carried out 100 m around FADs by artisanal fleet based in nearby fishing ports. This fleet was composed of wooden vessels of 11-16 m length, using live-bait and trawling lines. Fishermen were provided with form sheets where they recorded the daily catches by FAD (all FADs were numbered to facilitate their location on a chart).

## RESULTS

### Composition by species

Nine families and 15 species of fish were observed under or near the FADs (Tables 1 and 2), eight of which had commercial value in the Canary Islands. *Katsuwonus pelamis* (Linnaeus, 1758) and *Thunnus alalunga* (Bonnaterre, 1788) were the most important species for the local market, followed by *Coryphaena* spp. (only after genetic analysis were we able to isolate *C. hippurus* Linnaeus, 1758 from *C. equiselis* Linnaeus, 1758, since visual census did not allow for segregation of both species), *Seriola* spp., and *Pseudocaranx dentex* (Bloch and Schneider, 1810). The most frequently observed family was Carangidae.



© Del documento, los autores. Digitalización realizada por ULPGC. Biblioteca Universitaria, 2009

TABLE 1. – Fish species associated with Fish Aggregation Devices in waters off Gran Canaria, recorded from diver visual counts from April 1995 to May 1997 (*fish species only recorded through fishing).

| Family | Species | Length range (cm) | Period 1 April-October 1995 | Period 2 Aug 1996 - May 1997 |
|---|---|---|---|---|
| Carangidae | *Trachurus* spp. | 5-35 | April-May | August-October and May |
| | *Naucrates ductor* | 5-30 | May-August | August-May |
| | *Seriola* spp. | 3-20 | June-October | August-February |
| | *Pseudocaranx dentex* | 2-20 | July-October | August-February and May |
| Coryphaenidae | *Coryphaena hippurus* | 70-100 | May-June | August-September and November |
| | *C. equiselis* | 50 | June-August | |
| Balistidae | *Balistes carolinensis* | 25-30 | July-August | October-November |
| Kyphosidae | *Kyphosus sectator* | 10-20 | April-October | December-February and May |
| Sphyraenidae | *Sphyraena viridensis* | 10 | June | |
| Sparidae | *Boops boops* | 5-10 | July | |
| Centrolophidae | *Schedophilus ovalis* | 10-50 | April | August-November and February-May |
| Scombridae | *Scomber japonicus** | 18-22 | | August |
| | *Katsuwonus pelamis** | 3-5 Kg | June-August | August-September |
| | *Thunnus alalunga** | 4-7 Kg | | August-September |
| Carcharhinidae | *Prionace glauca** | 120 Kg | | September |

TABLE 2. – Abundance of fish (in Kg) from visual counts along the studied period (Mean biomass taken, Standard Deviation, Maximal biomass recorded in one visit and Total biomass located beneath the FAD).

| SPECIES | Mean | SD | Max | Total |
|---|---|---|---|---|
| *Trachurus* spp. | 0.18 | 0.57 | 3.00 | 8.15 |
| *Naucrates ductor* | 1.40 | 3.28 | 13.02 | 61.79 |
| *Seriola* spp. | 0.11 | 0.22 | 1.00 | 5.01 |
| *Pseudocaranx dentex* | 0.93 | 2.43 | 10.00 | 41.13 |
| *Coryphaena* spp. | 6.69 | 25.35 | 150.00 | 294.20 |
| *Balistes carolinensis* | 0.08 | 0.27 | 1.40 | 3.50 |
| *Kyphosus sectator* | 0.05 | 0.10 | 0.35 | 2.15 |
| *Sphyraena viridensis* | $4 \times 10^{-4}$ | $3 \times 10^{-3}$ | 0.02 | 0.02 |
| *Boops boops* | $4 \times 10^{-3}$ | 0.03 | 0.20 | 0.20 |
| *Schedophilus ovalis* | 0.33 | 0.92 | 3.50 | 14.40 |

*Seriola* spp., *Trachurus picturatus* (Bowdich, 1825), *P. dentex*, *Kyphosus sectator* (Linnaeus, 1758), *Boops boops* (Linnaeus, 1758) and *Sphyraena viridensis* (Jordan and Evermann, 1896), were only represented by juveniles, while *Coryphaena* spp. and *Balistes carolinensis* (Gmelin, 1788), were only represented by adults. *Naucrates ductor* and *Schedophilus ovalis* (Cuvier and Valenciennes, 1833) were represented by adult and juvenile individuals. *Scomber japonicus* (Houttuyn, 1788), *K. pelamis*, *T. alalunga* and *Prionace glauca* (Linnaeus, 1758) were registered only through fishing in the vicinity of FADs.

*Seriola* spp., *N. ductor*, and *P. dentex* were the most frequently observed species under FADs (60, 56 and 47% of observations respectively). *Trachurus* spp., *S. ovalis*, and *K. sectator* were noted in 24, 25 and 30% of the observations respectively. *Coryphaena* spp. were found beneath the FADs in 11% of the observations, while *B. carolinensis*, *B. boops* and *S. viridensis* were rarely encountered (7, 2 and 2% respectively) around the FADs.

## Aggregated fish biomass

There were significant differences in the fish biomass under FADs by month (ANOVA, F=2.17, P=0.039), with the maximum aggregations in September (Fig. 3). Although the number of species underneath FADs increased significantly with the immersion time (ANOVA, F=2.90, P=0.023; Pearson's correlation r=0.4503, P<0.001, N=53; Fig. 4), the fish biomass aggregated did not (ANOVA, F=0.94, P=0.46). The average biomass found was 8.93 Kg (SD=23.6); however, when only baitfish (juvenile fish) were taken into account, the mean biomass aggregated was 3.38 Kg (SD=4.84), with a maximum of 23.37 Kg. The census where *Coryphaena* spp. was present offered a mean aggre-

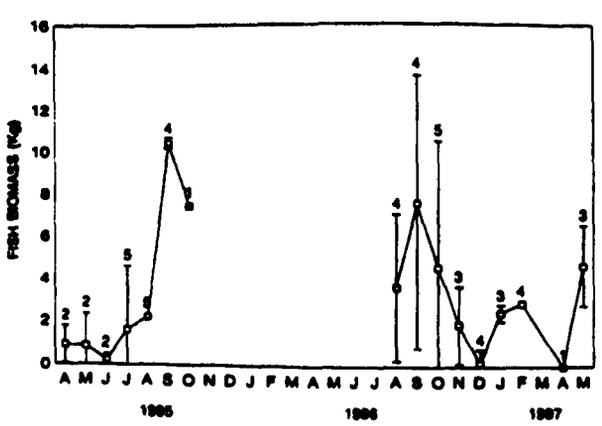


FIG. 3. – Changes in abundance in fish biomass over the study period (the figures on top of bars indicated the maximum number of species counted each month).



© Del documento, los autores. Digitalización realizada por ULPGC. Biblioteca Universitaria, 2009

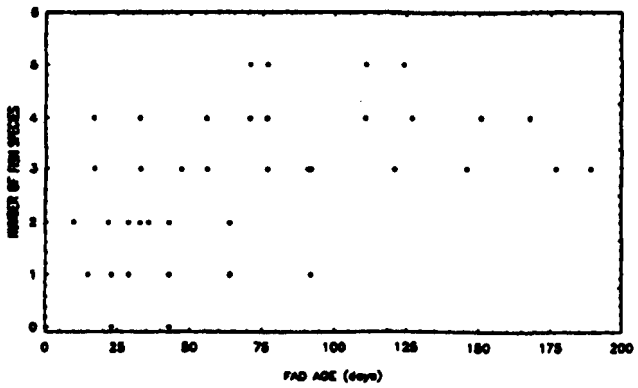


FIG. 4. – Variation in the number of fish species with the length of time that the devices were in place (Pearson's correlation r= 0.4503, P<0.001, N=53).

gated biomass of 53.9 Kg (SD=53.6), with a maximum of 150 Kg.

The FADs deployed in shallower waters gave an aggregated biomass which was significantly lower for baitfish than for those deployed in deeper areas (ANOVA, F=3.457, P=0.039; Pearson's correlation r=0.4417, P<0.001, N=53; Fig. 5). The largest number of species registered in any one census of a single FAD was five (mean=2.72; SD=1.31). However, we observed a significant difference in the number of species present as a function of the anchoring depth of the FADs (ANOVA, F=4.484, P=0.016). Generally, the FADs deployed on shallower waters gave a lower number of species aggregated.

## Fish behaviour around FADs

Depending on the size of the individuals, the schools of juvenile *P. dentex* and *Trachurus* spp. aggregated under the protection of fragments of net hanging from the flotsam (Fig. 1) or deeper, always close to the rope (the juveniles smaller than 5 cms. in length, of both species, frequently established

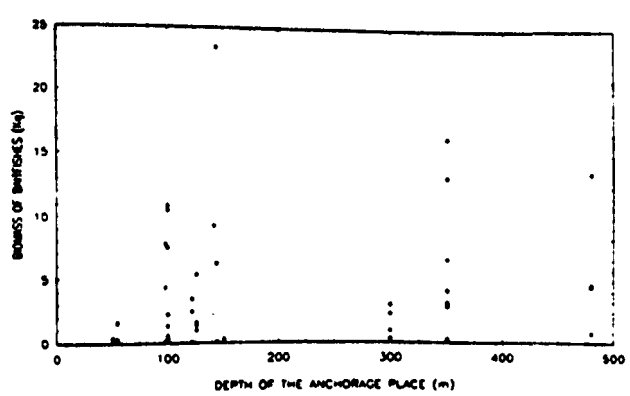


FIG. 5. – Variation of the baitfish biomass under FAD with the depth of anchorage (Pearson's correlation r=0.4417, P<0.001, N=53).

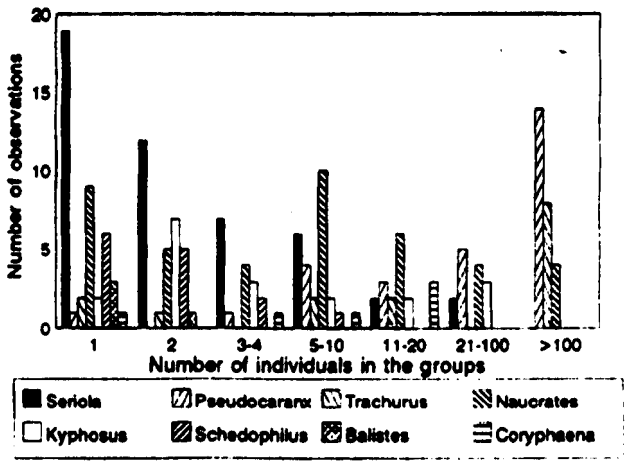


FIG. 6. – Number of observations of group size for each species counted by divers.

mixed schools). The juvenile *P. dentex* even aggregated around other fish such as *B. carolinensis*, when they were close to the FAD. These juveniles, when they reached a body length of between 15 and 20 cms, moved no further than 20 m from the FAD, aggregating around whatever object passed closeby, even the divers, and later returning to the proximity of the FAD when the object moved further than 20 m from the same. Frequently, these individuals swam to deep waters following the anchorage rope, out of the visible range of divers (over 30 m).

The juvenile of *Seriola* spp. and *Schedophilus ovalis* were solitary or constituted small loose groups of 2-5 individuals (Fig. 6). Those smaller than 10 cms. did not move away from the refuge of the submerged structure of the float. Juvenile of *K. sectator* less than 15 cm long took refuge between the hanging nets of the FAD, while larger specimens were observed up to 20 m away. Aggregated juveniles (5-10 cm) and adults (30-50 cm) of *S. ovalis* remained a few centimetres under the float.

A male and two females of *Coryphaena* spp were observed and video recorded during courting/spawning around a FAD. This species was normally observed, aggregated in small groups of under 15 individuals (Fig. 6).

## The fouling community

The fouling community of the FADs was composed of algae and invertebrates, especially Cirripedia and Hydrozoans. The most abundant invertebrate was *Lepas anatifera* (Linné) which began the colonization of the FADs two week after deployment and completed it after four months (colonizing



© Del documento, los autores. Digitalización realizada por ULPGC. Biblioteca Universitaria, 2009

the flotsam, nets and the rope). Between the hanging nets of the FAD, colonized by hydrozoans and algae, the amphipod *Caprella acutifrons* Latreille and the crab *Planes minutus* (Linnaeus) were frequently detected.

The most frequent algae were *Hiucksia mitchelliae* (Harvey) P.C. Silva, followed by *Polysiphonia myrioccoca* Montagne and its epiphyte *Audouinella microscopica* (Nägeli) Woelkerling.

**Fish captures around FADs**

Two hundred tons of tuna (*K. pelamis* and *T. alalunga*) were caught in the vicinity of one FAD between August and September 1996. These catches had a market value of US$ 323 thousand, thus the cost of this FAD represented only 0.13% of the obtained catch value. During the 1995 and 1996 fishing seasons (from June to October), commercial catches of *Katsuwonus pelamis* around FADs fluctuated between 200 and 7000 kg per fishing day and per FAD, whilst the average catch was approximately 1000 kg. The catches of *Coryphaena* spp. fluctuated between 10 and 400 kg per fishing day and per FAD, giving an average catch of 100 kg.

## DISCUSSION

During our observations, fish under or near the FADs were generally juveniles belonging to eight species and five families (although we registered nine families and 15 species of fish). *Seriola* spp., *Naucrates ductor* and *Pseudocaranx dentex* were the most common species.

In agreement with Rountree (1990), our observations indicated that seasonally regulated juvenile fish availability, as a consequence of the natural recruitment processes in the region, is apparently the most important factor determining FAD species composition and abundance. Most of the species registered around FADs in the Canary Islands spawn during Spring or at the beginning of Summer (i.e. carangids) (Fischer *et al.*, 1981), so recruitment to the area peaks at the end of the Summer.

However, there are other factors which also seem to have an effect. The abundance of the fauna under FADs was affected by the depth of the anchorage. But, contrary to what we initially expected, the FADs deployed in shallower waters showed a lower biomass and a reduced number of aggregated species. This result may be biased by the characteristics of the shelf of the island (very narrow and abrupt) where deeper anchorage areas are not far enough from the shore when compared with shallower ones. On the other hand, floats undergo a maturation process (Arenas *et al.*, 1992) and it is possible that since older FADs are more completely colonized by a fouling community (algae, hydrozoans and crustaceans, hence available food resources), they can support a higher aggregated biomass, and with increasing maturity, the diversity of species in the communities increases. Nevertheless, the age of FADs (immersion time) had no effect on the aggregated biomass, unlike the number of species aggregated,which increased proportionately in the way we expected.

As pointed out by Hunter and Mitchell (1968) and Feigebaum *et al.* (1989) juvenile fish probably congregate around flotsam looking for the shelter that FADs provide. In general, the fish observed around our FADs were distributed spatially in accordance with their body size, with the smaller individuals to the FAD, taking refuge between the hanging net and the same. It is also possible that fish found local high concentration of available food under flotsam (Gooding and Magnuson, 1967) or around the FADs. Most of the natural drifting devices (i.e. drift algae, limbs, etc) are carried away by currents which come from places where floats are frequently generated (i.e. a river mouth or coastal areas) and introduced into the pelagic environment (Hunter and Mitchell, 1967). It is usually assumed that currents carry away the phytoplankton production from the region of its formation into oligotrophic regions (Vinogradov, 1983). Concentrations of biotic structures are often intensified by oceanographic features, such as fronts (Kingsford, 1993). So, some pelagic fish species could associate drifting floats and the area around them with currents where larvae and juveniles will find suitable food availability during their early life stages. This could explain the observed courting/spawning behaviour of *Coryphaena* spp. around FADs. We have also found anomalous and significant higher biomass of zooplankton under several anchored FADs as compared to the surrounding area (ANOVA P=0.03; authors unpublished data) which could support the hyphothesis proposed by Gooding and Magnuson. This anomalous concentration of zooplankton may be due to eddies generated by the interaction of floats and ropes of anchorage with the current (in the same way as the current field around a boat in



© Del documento, los autores. Digitalización realizada por ULPGC. Biblioteca Universitaria, 2009

agreement with Lindquist and Pietrafesa (1989)). However, this is an issue which needs confirmation in further studies.

Most of the species observed by divers under the FADs in this study did not occur in sizes large enough to become attractive for fishing, except *Coryphaena* spp. and possibly *N. ductor*. However, FADs aggregate baitfish which are thought to attract other species of higher economic value into the general area (Rountree, 1990).

## ACKNOWLEDGEMENTS

We thank Prof. Angel Luque, Dr. Asunción Viera, Dr. May Gómez, Mr Manuel Velázquez, Mr Aritz Arrizabalaga and Mr Javier Pérez for assistance with data collection. Thanks are also given to the crew of the fishing vessel Juan Carlos, Port of Arguineguín. The research was supported by the Fishing Council of the Canary Islands Government. A special word of thanks goes to Dr. Carlos Bas and Mrs M. Dolores Ojeda.

## REFERENCES.

Arenas, P., M. Hall and M. García. - 1992. The association of tunas with floating objects and dolphins in the Eastern Pacific Ocean. VI. Association of fauna with floating objects in the EPO. In: *International workshop on fishing for tunas associated with floating objects*. (11-14 February 1992. La Jolla, California): 38 pp.

Beets, J. - 1989. Experimental evaluation of fish recruitment to combinations of fish aggregating devices and benthic artificial reefs. *Bull. Mar. Sci.*, 44(2): 973-983.

Biais, G. and M. Taquet. - 1990. Dispositifs de concentration de poissons a la Reunion. *Equinoxe*, 34:20-26

Bortone, S.A., J. Van-Tassell, A. Brito, J.M. Falcon, J. Mena and C.M Bundrick. - 1994. Enhancement of the nearshore fish assemblage in the Canary Islands with artificial habitats. *Bull. Mar. Sci.*, 55(2-3):602-608.

Brill, R.W., K.N. Holland and J.S. Ferguson. - 1984. Use of ultrasonic telemetry to determine the short-term movements and residence times of tunas around fish aggregating devices. In: *Proceedings of the Pacific Congress on Marine Technology, Honolulu, Hawaii*, April 24-27, 1984. Marine Technology Soc., Munou, HI USA. Hawaii Sect 1984. pp. MRM1/1-7.

Brock, R.E. - 1985. Preliminary study of the feeding habits of pelagic fish around Hawaiian fish aggregation devices or can fad enhance local fisheries productivity. *Bull. Mar. Sci.*, 37(1): 40-49.

Buckley, R.M., D.G. Itano and T.W. Buckley. - 1989. Fish aggregation device (FAD) enhacement of offshore fisheries in American Samoa. *Bull. Mar. Sci.*, 44(2): 942-949.

Buckley, T.W. and B.S. Miller. - 1994. Feeding habits of yellowfin tuna associated with fish aggregation devices in American Samoa. *Bull. Mar. Sci.*, 55(2-3): 445-459.

Cayré, P. - 1991. Behaviour of yellowfin tuna (*Thunnus albacares*) and skipjack tuna (*Katsuwonus pelamis*) around fish aggregating devices (FADs) in de Comoros Islands as determined by ultrasonic tagging. *Aquat. Living Resour.*, 4: 1-12.

Cayré, P. and F. Marsac. - 1993. Modelling the yellowfin tuna (*Thunnus albacares*) vertical distribution using sonic tagging results and local environmental parameters. *Aquat. Living Resour.*, 6(1): 1-14.

Cort, J.L. - 1990. Biología y pesca del atún rojo, *Thunnus thynnus* (L.), del mar Cantábrico. *Publ. Espc. Inst. Esp. Oceanogr.*, 4: 1-272.

de Silva, D.P. - 1982. Potential for increasing artisanal fisheries production from floating artificial habitats in the Caribean. *Proc. Gulf Carib. Fish. Inst.*, 34: 156-167.

Fischer, W., G. Bianchi and W.B. Scott (eds). - 1981. FAO species identification sheets for fishery purposes. Eastern Central Atlantic; fishing areas 34, 47 (in part). Canada Funds-in-Trust. Ottawa, Department of Fisheries and Oceans Canada, by arrangement with the food and Agriculture Organization of United Nations, vols. 1-7.

Feigebaum, D., A. Fridlander and M. Bushing. - 1989. Determination of the feasibility of fish attracting devices for enhancing fisheries in Puerto Rico. *Bull. Mar. Sci.*, 44(2): 950-959.

Fonteneau, A. - 1992. Pêche thoniere et objects flottants: Situation mondiale et perspectives. In: *Rapport de Synthèse sur Groupe de Travail IATTC "objects flottants et thons" presenté à la 12ème Semaine des Pêches dos Açores, mars 1992*: 31 pp.

Fonteneau, A. and J. Hallier. - 1993. La pesca del atun bajo objetos flotantes. *Mundo Científico*, 131(13): 76-77.

Friedlander, A., J. Beets and W. Tobias. - 1994. Effects of fish aggregating device design and location on fishing success in the U.S. Virgin Islands. *Bull. Mar. Sci.*, 55(2-3): 592-601.

Frusher, S.D. - 1986. Utilization of small-scale fish aggregation devices by Papua New Guinea's artisanal fishermen. In: Maclean, J.L., L.B. Dizon and L.V. Hosillos (eds). *Proceedings of the 1st Asian Fisheries Forum, Manila, Philippines*, 26-31 May 1986, pp. 371-374.

Galea, J.A. - 1961. The "Kannizzati" fishery. *Proceedings and Technical Papers of the General Fisheries Council for the Mediterranean*, 6:85-91.

García-Gómez, A. - 1993. Primeras experiencias de crecimiento de juveniles de seriola mediterránea (*Seriola dumerili* Risso, 1810) alimentadas con una dieta semihúmeda. *Bol. Inst. Esp. Oceanogr.*, 9(2): 347-360.

Gooding, R.M. and J.J. Magnuson. - 1967. Ecological significance of a drifting object to pelagic fishes. *Pac. Sci.*, 21:486-497.

Gordo, L.S. - 1996. On the age and grwth of bogue, *Boops boops* (L), from the Portuguese coast. *Fish. Manage. Ecol.*, 3(2): 157-164

Greenblatt, P.R. - 1979. Associations of tuna with flotsam in the Eastern tropical Pacific. *Fish. Bull.*, 77(1): 147-155.

Hall, M. - 1992. The association of tuna with floating objects and dolphins in the Eastern Pacific Ocean. VII. Some hypotheses on the mechanisms governing the associations of tunas with floating objects and dolphins. In: *International workshop on fishing for tunas associated with floating objects*. (11-14 February 1992. La Jolla, California): 6 pp.

Higashi, G.R. - 1994. Ten years of fish aggregating device (FAD) design development in Hawaii. *Bull. Mar. Sci.*, 55(2-3): 651-666.

Holland, K., R. Brill and R.K.C. Chang. - 1990. Horizontal and vertical movements of yellowfin and bigeye tuna associated with fish aggregating devices. *Fish. Bull.*, 88(3): 493-507.

Hunter, J.R. - 1968. Fishes beneath flotsam. *Sea Frontiers*, 14: 280-288.

Hunter, J.R. and C.T. Mitchell. - 1967. Field experiments on the attraction of fish to floating objects. *J. Cons. Perm. Int. Explor. Mer*, 31: 427-434.

Hunter, J. R. and C. T. Mitchell. - 1968. Association of fishes with flotsam in the offshore watters of Central America. *Fish. Bull.*, 66(1): 13-29.

Ida, H., Y. Hiyama and T. Kusaka. - 1967. Study on fishes gathering around floating seaweed-II. Behaviour and feeding habits. *Bull. Jap. Soc. Sci. Fish.*, 33(10): 472-478.

Isidro, H.A. - 1990. Age and growth of *Trachurus picturatus* (Bowdich, 1825) (Teleostei: Carangidae) from the Azores. *Archipelago Cienc. Nat. Life Earth Sci.*, 8: 45-54.

Kihara, Y. - 1981. Fishery based on the payao method in the Philippines. *Suisan Sekai*, 30: 78-84.

Kingsford, M.J. - 1993. Biotic and abiotic structure in the pelagic environment: importance to small fishes. *Bull. Mar. Sci.*, 53(2): 393-415.

Kitamado,T. and C. Kataoka. - 1996. A study for the realization of sustainable fisheries. A case of Payang fishery in the southern coast of west Jawa, Indonesia. *Bull. Fac. Fish. Nagasaki Univ.*, 77: 117-126



© Del documento, los autores. Digitalización realizada por ULPGC. Biblioteca Universitaria, 2009

Kojima, S. – 1956. Fishing for dolphins in the Western part of the Japan Sea - II. Why do the fish take shelter under floating materials?. *Bull. Jap. Soc. Sci. Fish.*, 21(10): 1049- 1052.

Kojima, S. – 1967. Studies on fishing conditions of the dolphin, *Coryphaena hippurus*, in the Western Regions of the Sea of Japan - XIII. "Tsukegi" as a source of food for dolphins. *Bull. Jap. Soc. Sci. Fish.*, 33(4): 320-324.

Kwei, E.A. and P. Bannerman. – 1993. The effect of the introduction of new devices (FAD) and bird radars in the baitboat fishery of tuna in Ghana. *Collect. Vol. Sci. Pap. ICCAT*, 40(2): 473-479. ICCAT SCRS/92/151.

Lindquist, D.G. and L.J. Pietrafesa. – 1989. Current vortices and fish aggregations: the current field and associated fishes around tugboat wreck in Onslow Bay, North Carolina. *Bull. Mar. Sci.*, 44: 533-544.

Matsumoto, W.M., T.K. Kazama and D.C. Aasted. – 1981. Anchored fish aggregation devices in hawaiian waters. *Mar. Fish. Rev.*, 43(9): 1-13.

Massutí, E. and O. Reñones. – 1994. Observaciones sobre la comunidad de peces pelágicos asociados a objetos flotantes en aguas oceánicas de Mallorca. *Bol. Inst. Esp. Oceanogr.*, 10(1):81-93.

Mortensen, T. – 1917. Observations on protective adaptation and habits, mainly in marine animals. In: *Papers from Dr. Th. Mortensen's Pacific Expedition 1914-1916*. Vidensk. *Medd. Dansk Naturhist. Forem.*, 69: 57-96.

Myatt, D.O. and E. Myatt. – 1982. Midwater fish attractors. In: *1982 Record game fish. The international game fish association*, pp. 57-71. Fort Lauderdale, Florida.

Parin, N.V. and B.I. Fedoryako. – 1992. Pelagic fish communities around floating objects in the open ocean. In: *Groupe de Travail IATTC "objects flottants et thons" presenté à la 12ème Semaine des Pêches dos Açores, mars 1992*: 5 pp.

Pollard, D.A. and J. Matthews. – 1985. Experience in the construction and siting of artificial reefs and fish aggregation devices in Australian waters, with notes on and a bibliography of Australian studies. *Bull. Mar. Sci.*, 37(1): 299-304.

Rountree, R.A. – 1989. Association of fishes with fish aggregation devices: effects of structure size on fish abundance. *Bull. Mar. Sci.*, 44(2): 960-972.

Rountree, R.A. – 1990. Community structure of fishes attracted to shallow waters fish aggregation devices off South Carolina, USA. *Env. Biol. Fish.*, 29: 241-262.

Sacchi, J. – 1986. Les dispositifs de concentration de poissons et le développement des pêches côtières. *Equinoxe*, 9: 14-22.

Uda, M. – 1933. Types of skipjack schools and their fishing qualities: the shoals of 'katuwo' and their angling. *Bull. Jap. Soc. Sci. Fish.* 2:107-111. (Transl. by W.G. Van Campen, 1952, *U.S. Fish Wilds. Ser. Spec. Sci. Rep. Fish.* 83: 68-78).

Vinogradov, M.E. – 1983. Open-ocean ecosystems. In: Kinne, O. (ed.), *Marine ecology. A comprehensive,integrated treatise on life in oceans and coastal waters* pp. 657-737. John Wiley and Sons. Chichester.

Wickham, D.A. and G.M. Russell. – 1974. An evaluation of midwater artificial structures for attracting coastal pelagic fishes. *Fish. Bull.*, 72(1): 181-191.

Wickham, D., J. Watson and L. Ogren. – 1973. The efficacy of midwater artificial structures for attracting sport fish. *Trans. Amer. Fish. Soc.*, 3: 563-673

Wilkins, R.M. and M.H. Goodwin. – 1989. Progress report on the evaluation of fish aggregating devices for the eastern Caribbean. In: Waugh, G.T. and M.H. Goodwin (eds), *Proceedings of the thirty ninth annual Gulf and Caribbean Fisheries Institute, Hamilton, Bermuda*, Nov. 1986. vol. 39: 405-407.

Wood, J. – 1989. Cape Verde. Consultancy for construction and deployment of fish aggregating device (FAD) in the Republic of Cape Verde (8 April-7 June 1989). Rome-Italy *FAO* 1989. 26 pp.



© Del documento, los autores. Digitalización realizada por ULPGC. Biblioteca Universitaria, 2009

INT. J. REMOTE SENSING, 1999, VOL. 20, no. 7, 1419–1433

# Seasonal and interannual pigment concentration in the Canary Islands region from CZCS data and comparison with observations from the ESTOC

R. DAVENPORT†¶, S. NEUER†, A. HERNÁNDEZ-GUERRA‡, M. J. RUEDA§, O. LLINAS§, G. FISCHER† and G. WEFER†

†Fachbereich Geowissenschaften, Universität Bremen, Klagenfurterstr., 28359 Bremen, Germany
‡Facultad de Ciencias del Mar, Universidad de Las Palmas de Gran Canaria, Apartado 550, 35080 Las Palmas, Spain
§Instituto Canario de Ciencias Marinas, Direccion General de Universidades e Investigacion Consejeria de Educacion, Cultura y Deportes, Apartado 56, 35200 Telde, Canary Islands, Spain

**Abstract.** We have compared historical data from the Nimbus-7 Coastal Zone Color Scanner (CZCS) with recent *in situ* measurements at the European Station for Time-Series in the Ocean, Canary Islands (ESTOC). CZCS data show an annual winter phytoplankton maximum in January but with a large interannual variation. In sediment traps moored at ESTOC we observed winter sedimentation peaks at 1000 m and 3000 m depth occurring about 1 month later. We also observed sedimentation peaks in other seasons which probably result from material advecting into the region. CZCS data suggest that one possible source is the Cape Ghir upwelling filament off the north-west African coast.

## 1. Introduction

The European Station for Time-Series in the Ocean, Canary Islands (ESTOC) is situated approximately 100 km north of the island of Gran Canaria in the Canary Islands region (coordinates 29°07′N, 15°27′E) (Llinas *et al.* 1994, Neuer and Rueda 1997b). A major purpose of the station is to investigate biogeochemical cycles in this region with the aim of providing insight into the processes controlling the flux of carbon and associated elements in the ocean on seasonal and interannual time scales. As part of these investigations sediment traps have been moored at ESTOC since December 1991 at 1000 m and 3000 m depths (Neuer *et al.* 1997a). Although ESTOC is almost 400 km from Cape Yubi, the nearest point on the north-west African coast, it was recognized from the outset that the station would probably be influenced by coastal upwelling effects (Wooster *et al.* 1976, Speth and Detlefsen 1982).

Several studies of the north-west African upwelling region using remote sensing data have been performed (Nykjaer 1988, Llinas *et al.* 1989, Van Camp *et al.* 1991, Nykjaer and Van Camp 1994). These investigations have concentrated on identifying the major characteristics of the entire upwelling region and in particular the relationship between shelf sea surface temperature (SST) and large-scale winds using the

¶e-mail: bob.davenport@ri.dasa.de

*International Journal of Remote Sensing*
ISSN 0143-1161 print/ISSN 1366-5901 online © 1999 Taylor & Francis Ltd
http://www.tandf.co.uk/JNLS/res.htm
http://www.taylorandfrancis.com/JNLS/res.htm

© Del documento, los autores. Digitalización realizada por ULPGC. Biblioteca Universitaria, 2009

Nimbus-7 Coastal Zone Color Scanner (CZCS), the Advanced Very High Resolution Radiometer (AVHRR) sensors of the National Oceanic and Atmospheric Administration (NOAA) satellite series and wind data from the European Centre for Medium-Range Weather Forecasts (ECMWF). These studies here also confirmed the existence of several coastal upwelling filaments and investigated the factors influencing such filament growth.

For the Canary Island region, CZCS data and AVHRR SST measurements have been used to identify characteristic pigment patterns and their relationship with *in situ* chlorophyll/temperature data. Hernández-Guerra *et al.* (1993) and Arístegui *et al.* (1994) identified two different phytoplankton pigment patterns in the ocean surrounding the islands: large upwelling filaments (up to 300 km long) extending from the African coast and lee filaments (up to 100 km) and cyclonic eddies (60–80 km in diameter) probably caused by the disruptive effect of the Canary Islands on the Canary current.

To gain some understanding of the long-term surface biological activity to be expected at the ESTOC position we first investigated the seasonal and interannual phytoplankton pigment concentration using historical data from the CZCS. Although CZCS observations cover the period 1979–1985, the pigment patterns are unlikely to be significantly different to recent *in situ* data. We compared the pigment concentration derived from CZCS data with ESTOC sediment trap observations and *in situ* chlorophyll measurements to determine if the historical data could aid in interpretation of recent *in situ* measurements. We then investigated the effects of coastal upwelling at ESTOC using CZCS data and in particular the role of filaments in transporting material into the Canary Islands region.

## 2. Regional setting

The Canary Islands are located in the north-east Atlantic Ocean between 100 km and 600 km off the north-west African coast. They lie on the path of the weak, south-westwards flowing Canary Current, which is an eastern branch of the North Atlantic subtropical gyre (Stramma 1984). The ESTOC station lies about 100 km north of the island of Gran Canaria; the water depth is 3500 m (figure 1).

The north-west African coastal upwelling is a major feature of the region. Upwelling of cold, nutrient-rich North Atlantic Central Water (NACW) originating from depths not exceeding 200–300 m (Mittelstaedt 1986) is confined to a relatively narrow 50–70 km coastal band. The upwelling intensity is in general correlated with the position of the Azores High which migrates northwards during spring and summer, reaching its most northerly position in July–August. North of 25° N the upwelling is most intense in summer and autumn (Wooster *et al.* 1976, Mittelstaedt 1991).

A characteristic feature of coastal upwelling is the regular development of filament structures at specific coastal positions such as Cape Ghir, Cape Yubi and Cape Bojador. These filaments may extend several hundred kilometres offshore. Nykjaer (1988), for example, reported that the Cape Ghir filament has a length scale of 100–300 km, a width of 10–50 km and remains stationary over several weeks. Filaments are visible in AVHRR SST images as cold tongues and meanders and in CZCS data as regions with enhanced pigment concentration compared with ambient levels often showing complex mesoscale eddy structures at the offshore end. The main factor promoting filament growth appears to be favourable high wind stress (Van Camp *et al.* 1991). Nevertheless other factors must be considered, as it has

© Del documento, los autores. Digitalización realizada por ULPGC. Biblioteca Universitaria, 2009

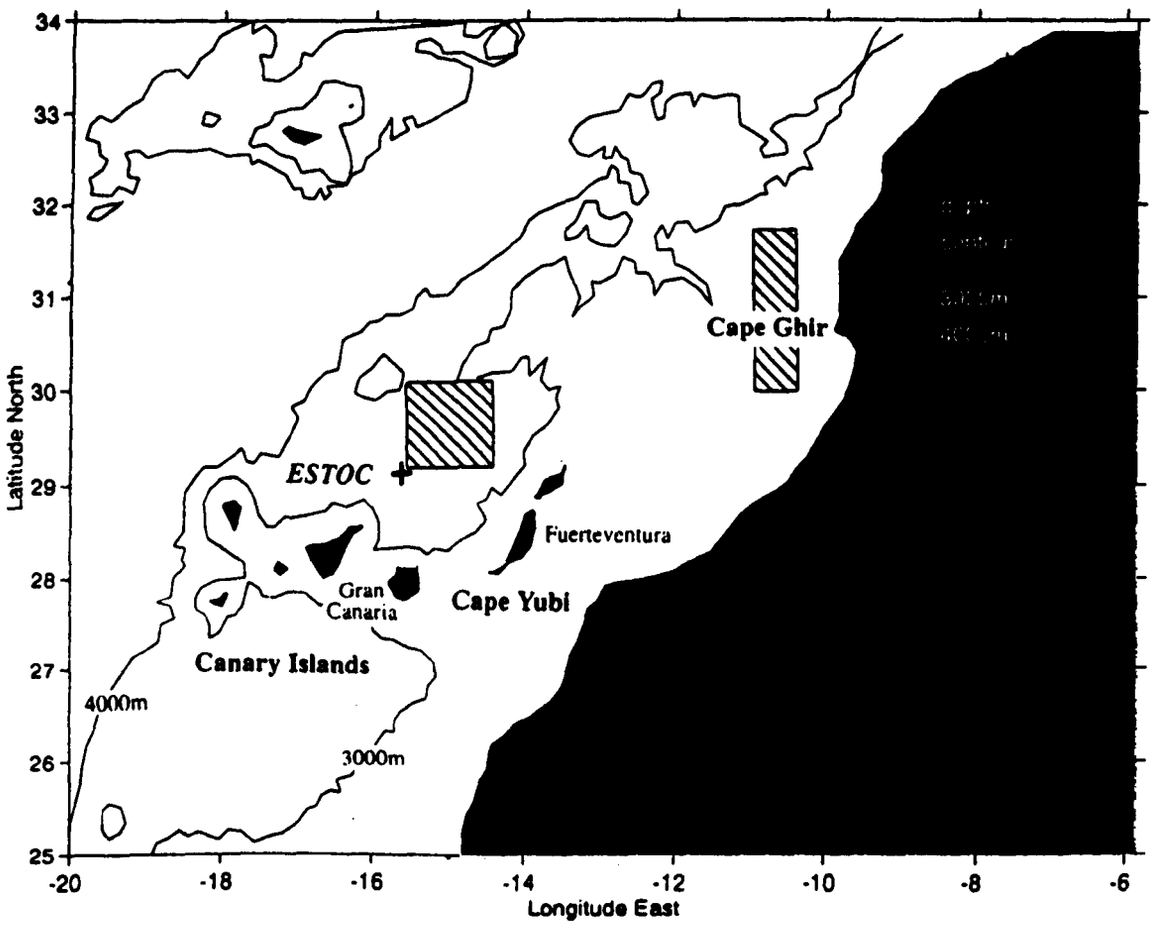


Figure 1. Location of the ESTOC in relation to the Canary Islands and the north-west African coast. The shaded square directly northeast of ESTOC is the source box for material sinking to the 1000 m trap. The shaded rectangle west of Cape Ghir is the area chosen to monitor the pigment concentration of the Cape Ghir filament.

been shown for Cape Ghir that there is a 3-month phase lag between the onset of the maximum Trade Winds in summer and the time of the most intense upwelling (Nykjaer and Van Camp 1994); irregularities in bottom topography may modulate coastal upwelling in this case. The Cape Yubi and Cape Bojador filaments can have an influence on the Canary Islands (Hernández-Guerra *et al.* 1993). In general though these effects are observed east and south of the islands as enhanced pigment features. There are no published data regarding possible effects of the Cape Ghir filament on the Canary Island region.

## 3. Data and methods

To compare phytoplankton pigment concentration derived from CZCS data at the ESTOC position with recent *in situ* measurements, we first identified a possible source region for material sinking to the traps. Deuser *et al.* (1990) argued that it is impossible to know the size and shape of a potential source region for material sinking to a deep-sea trap. Instead it is only possible to match sediment flux measurements at the trap with average pigment concentrations over a fixed surface area of crudely estimated size and arbitrary shape. Therefore, for this study, a square-shaped source region was chosen which has the advantage of simplifying the image processing.

© Del documento, los autores. Digitalización realizada por ULPGC. Biblioteca Universitaria, 2009

The size and position of the source box for particles sinking to the 1000 m trap was determined using the Canary Current speed and direction, the mean eddy kinetic energy over the sinking depth of the particles and a typical particle sinking rate (Deuser *et al.* 1990, Siegel *et al.* 1990). We ignored the 3000 m trap because this approach is not applicable to such depths given the complex vertical current structure and particle life cycle. Since the Canary Current geostrophic flow is south-westwards (Stramma 1984), it was assumed that the most likely source region was to the north-east of the ESTOC. In the region of the Canary Islands, moored observations show that the mean geostrophic current over one or more years at 200 m water depth can reach speeds up to 4–5 cm $s^{-1}$ (Siedler and Onken 1996). At ESTOC current speeds as measured by a continuously recording INFLUX current meter positioned 20 m below the 1000 m trap ranged from 3–15 cm $s^{-1}$ but were mostly below 10 cm $s^{-1}$. Since for this study we used monthly composite CZCS data, a range of 5–10 cm $s^{-1}$ was taken as most representative of the current speed. For the eddy kinetic energy we took a value of 10 $cm^2$ $s^{-1}$ for depths between 100 m and 2000 m (Dickson 1983). The rate at which particles sink is very much dependent on the nature of the particle (Siegel *et al.* 1990). Ultraplankton for example sink at <0.1–2 m $d^{-1}$ (Bienfang 1980), algal aggregates at 40–150 m $d^{-1}$ (Smetacek 1985) and mesozooplankton fecal pellets at 20–900 m $d^{-1}$ (Fowler and Small 1972). For the ESTOC 1000 m trap during peak fluxes in March 1992 and January and February–March 1993, carbonate contributed between 44 and 55% to the total flux (Fischer *et al.* 1996). Microscopic observations showed large numbers of coccolithoporids in the trap samples which dominated the carbonate flux in the late winter to early spring sedimentation. Because of their small size, coccolithophorids must be transported to the depths via aggregates (Honjo 1982) or in fecal pellets (Honjo 1978). Indeed at ESTOC mesozooplankton fecal pellets have been visually observed to be packed with coccoliths during periods of high particle flux and may constitute up to 26% of the total flux (Fischer *et al.* 1996). Hence for this study we assumed 100 m $d^{-1}$ as a reasonable value for the sinking rate of trap particles. It then follows that for a particle to sink to the 1000 m trap within 10 days, the maximum distance of the source region cannot exceed 100 km (Siegel *et al.* 1990). Therefore a source box 100 km × 100 km was chosen north-east of the ESTOC position (figure 1).

CZCS is a multispectral scanner using six channels at 443, 520, 550, 670, 700–800 nm and 10.5–12.5 $\mu$m of which the first four were selected to measure the upwelled radiance from the ocean surface. Extraction of valid chlorophyll data from the sensor-measured radiance is a complex process as the ocean upwelled radiance is usually less than 10% of the total signal; atmospheric corrections have to be made for both Rayleigh and aerosol scattering (Sturm 1981, Bricaud and Morel 1987, Gordon *et al.* 1988). For this study we analysed monthly composite images from CZCS data for the period 1979–1985 from the Ocean Colour European Archive Network (OCEAN) level-3 database for north-west Africa supplied by the Joint Research Centre, Ispra, Italy. Level-3 data provide final pigment concentration values (in mg $m^{-3}$) for each valid image pixel. The pixel size is about 1 × 1 $km^2$. The error in the absolute pigment concentration compared with *in situ* concentration measurements up to 1983 is a factor of two, i.e. for a measured pigment value of 0.5 mg $m^{-3}$ then the true value may be between 0.25 and 1.0 mg $m^{-3}$. For post-1983 data, when degradation in the CZCS 443 nm channel was more than 40%, the error in measured pigment concentration may be up to a factor of three (Sturm, personal communication). Non-valid pixels represented clouds or missing data. Monthly composite

© Del documento, los autores. Digitalización realizada por ULPGC. Biblioteca Universitaria, 2009

images rather than daily images were chosen as these are better suited to comparison with trap data which had a time resolution of 8–21 days. For each month the average pigment concentration was calculated using all valid pixels in the source box. The derived average pigment concentration was rejected if the source box contained less than 20% valid pixels.

We deployed cone-shaped multisample sediment traps (Kiel Aquatec) at 1000 m and 3000 m depth. These traps are similar in shape and aspect ratio to the Mark V traps described by Honjo and Doherty (1988). For this study we used the total particle flux observed in the traps measured in $mg\,m^{-2}\,d^{-1}$. The deployment data are shown in table 1.

*In situ* concentrations of chlorophyll-*a* were determined by sampling 2–3 l of sea water, filtering onto GF/C filters and freezing for laboratory analysis. The filters were later extracted in 90% acetone and chlorophyll-*a* concentration was measured spectrophotometrically.

We also investigated the seasonal activity of the Cape Ghir filament by performing a similar analysis of the CZCS data as for the ESTOC region, only this time the source box was $50 \times 200\,km^2$ with the centre point about 100 km off Cape Ghir (figure 1). Visual examination of the images derived from CZCS data showed that such a box will 'see' most of the filament activity associated with Cape Ghir. This source box is sufficiently far from the coast not to include turbid Case 2 waters for which there was no valid atmospheric correction.

## 4. Results

### 4.1. *Pigment concentration*

Figure 2 shows the average monthly phytoplankton pigment concentration for 1979–1985 for the source box north-east of the ESTOC. Data are missing for nine out of 84 months (all in May/June/July or August) due to cloud cover or the CZCS being non-operational. A prominent peak was observed annually in January and this is interpreted as the winter bloom signal. There were large interannual variations in this winter peak with a maximum value of $0.19\,mg\,m^{-3}$ observed for December 1979–February 1980 compared with a maximum of $0.05\,mg\,m^{-3}$ for December 1981–February 1982. For other seasons only one further peak event occurred in August/September 1980 with a maximum value of $0.06\,mg\,m^{-3}$. The lowest annual pigment concentration, at about $0.03\,mg\,m^{-3}$, was observed each year in summer. This value is the typical minimum pigment concentration observed in CZCS data for open ocean waters off north-west Africa.

Figure 3 shows the recent *in situ* chlorophyll concentration as measured at the ESTOC for 1994. Maximum chlorophyll concentrations between 0 and 25 m depth, reflecting the annual late winter/early spring bloom, probably occurred in February

Table 1. Sediment trap mooring periods at the ESTOC.

| Mooring no. | Period | Total deployment time (days) | Sampling interval (days) |
|---|---|---|---|
| CI 1 | 25 November 1991 to 25 September 1992 | 305 | 15 |
| CI 2 | 1 October 1992 to 9 April 1993 | 190 | 10 |
| CI 3 | 12 April 1993 to 7 June 1994 | 430 | 21 |
| CI 4 | 9 June 1994 to 2 September 1994 | 86 | 8 |

© Del documento, los autores. Digitalización realizada por ULPGC. Biblioteca Universitaria, 2009

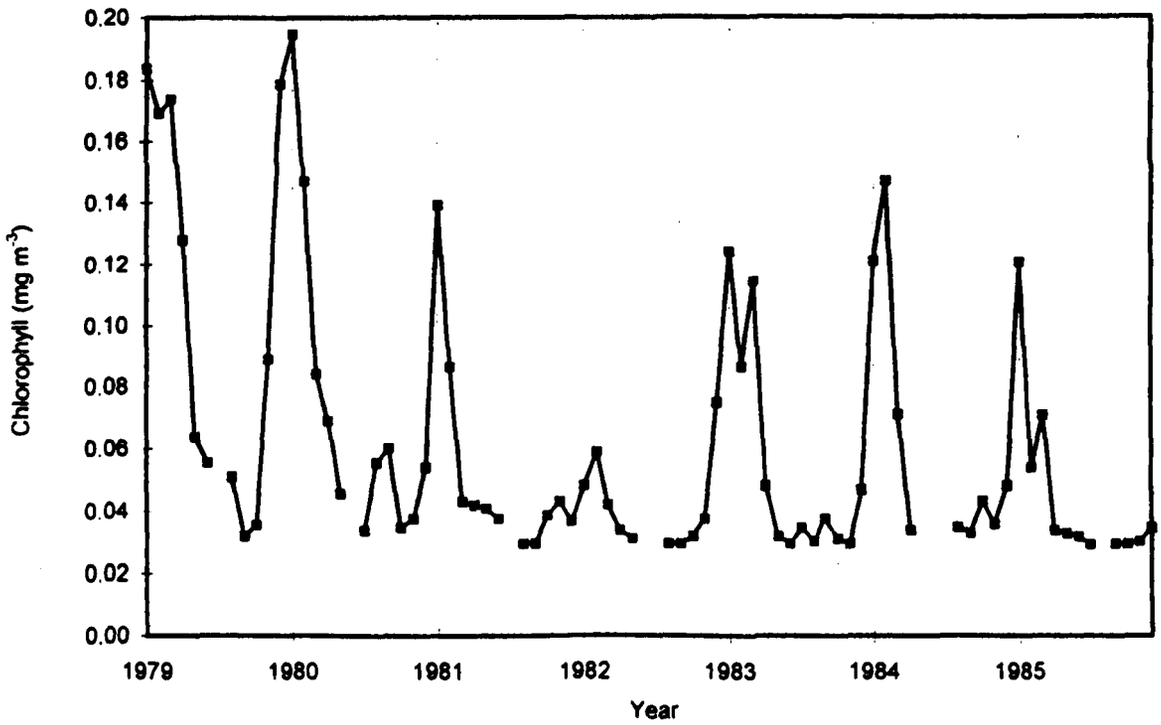


Figure 2. Average monthly phytoplankton pigment concentration for the ESTOC source box derived from CZCS data for the period 1979–1985. Note the pronounced but highly variable annual winter bloom peak in January (the first data point for each year) and the lack of peaks in other seasons (except for the low peak in August 1980).

(data interpolation) with a peak value between 0.25 and 0.3 mg m$^{-3}$. In spring/summer the chlorophyll maximum was observed to sink to 100 m depth and the near-surface concentration was 0.05 mg m$^{-3}$. In autumn the surface concentration increased to 0.15 mg m$^{-3}$.

4.2. *Sediment trap total particle fluxes*

Figure 4 shows the total particle flux measured in the 1000 m and 3000 m traps for the period December 1991–August 1994. A full dataset is only available for the 3000 m trap. For the 1000 m trap no data were available for the period August 1993 to May 1994.

At 3000 m the particle flux was observed to be highly seasonal with the highest flux recorded in late February–early March. This late winter peak showed large interannual variations, e.g. a flux of 118 mg m$^{-2}$ d$^{-1}$ in 1994 and 188 mg m$^{-2}$ d$^{-1}$ in 1992. During winter 1993 three distinct maxima were observed. Besides the late winter peak additional sedimentation events were observed in other seasons. For example, peaks were observed in July 1992, October 1992, May/June 1993 and July/August 1994. None of these events reach the flux levels seen in the winter peaks (Neuer *et al.* 1997a).

At 1000 m depth the late winter sedimentation event was also observed for 1992 and 1993 and the same three distinct peaks were seen in 1993. The flux for 1992 was only some 25% of that recorded in the deep trap, while in 1993 it was about 70%. Similar peaks to those observed in the 3000 m trap at other seasons were also observed at 1000 m but again with lower total flux levels (Neuer *et al.* 1997a).

© Del documento, los autores. Digitalización realizada por ULPGC. Biblioteca Universitaria, 2009

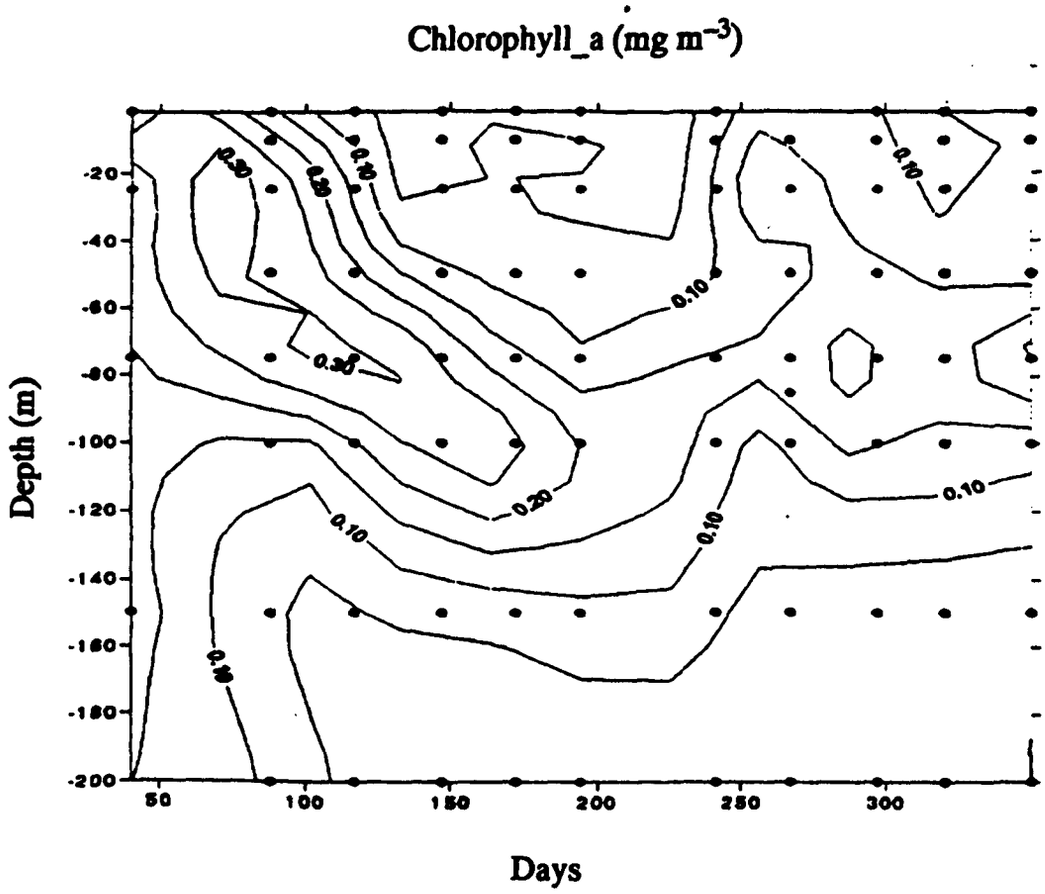


Figure 3. *In situ* chlorophyll concentration at the ESTOC for 1994. Note that the time axis starts at the beginning of February. The black dots are the measurement points. Full curves are interpolated chlorophyll concentrations.

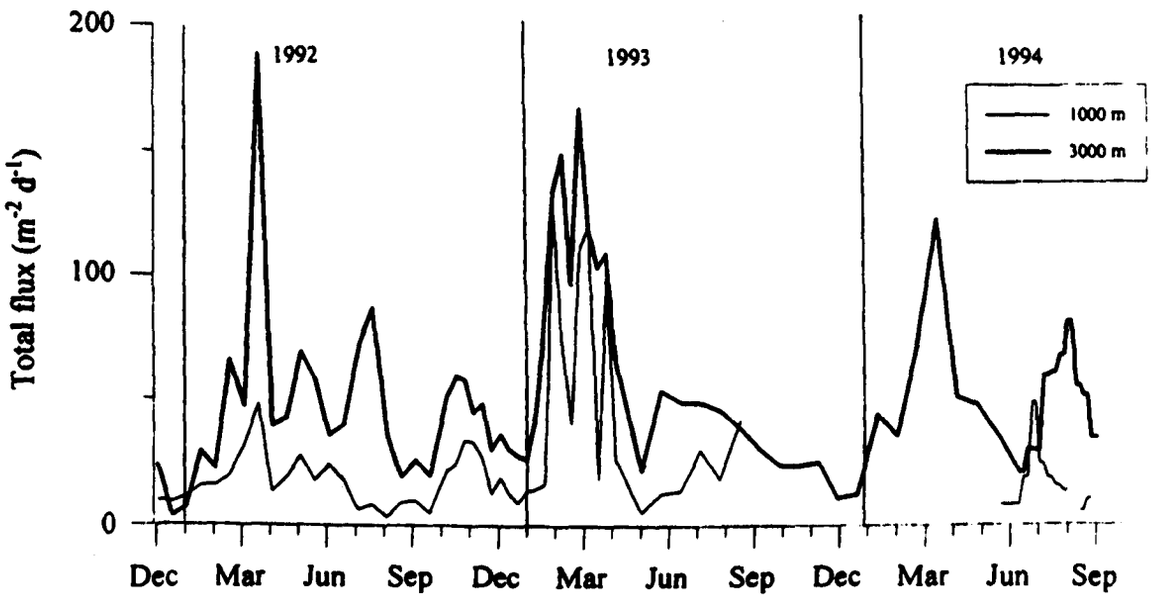


Figure 4. Total particle flux for the period December 1991–August 1994 observed in sediment traps moored at the ESTOC. Note the pronounced sedimentation event at 3000 m in February/March each year and the additional sedimentation events observed in other seasons. Also note that some of these events are also observed in the 1000 m trap, but always with lower total flux levels.

© Del documento, los autores. Digitalización realizada por ULPGC. Biblioteca Universitaria, 2009

### 4.3. *Cape Ghir filament—seasonal and interannual phytoplankton pigment concentration*

Figure 5 shows the monthly average phytoplankton pigment concentration from CZCS data for Cape Ghir over the period 1979–1985. As at the ESTOC location, an annual winter bloom was observed with peak values in January, but the peak values were much higher at Cape Ghir than at ESTOC. For example, a phytoplankton pigment concentration of 0.5 mg $m^{-3}$ was observed in January 1980 at Cape Ghir compared with 0.19 mg $m^{-3}$ at ESTOC. In other seasons additional peaks were clearly visible in most of the 7 years. One peak event was observed repeatedly in September/October for all years except 1979 where it appeared to be merged with the broad winter bloom. The other non-winter bloom peaks showed no obvious annual cycle. They were observed in April 1979, June 1979, August/September 1979, July 1980 and May 1984.

## 5. Discussion

### 5.1. *Comparison between phytoplankton pigment concentration derived from CZCS data and* in situ *ESTOC chlorophyll measurements*

In order to compare the CZCS data with the *in situ* chlorophyll data we restricted the latter to 0–25 m depth. This is assumed to be the maximum optical depth for an ocean colour sensor in oligotrophic waters.

The peak winter bloom occurs in January/February in the CZCS data and in February in the *in situ* ESTOC data, but the ESTOC interpolated peak concentration is somewhat higher at 0.25–0.3 mg $m^{-3}$ compared with the largest value of 0.19 mg $m^{-3}$ in January 1980 from CZCS data. In spring/summer the lowest concentration measured at ESTOC is about 0.5 mg $m^{-3}$ compared with 0.03 mg $m^{-3}$ for CZCS.

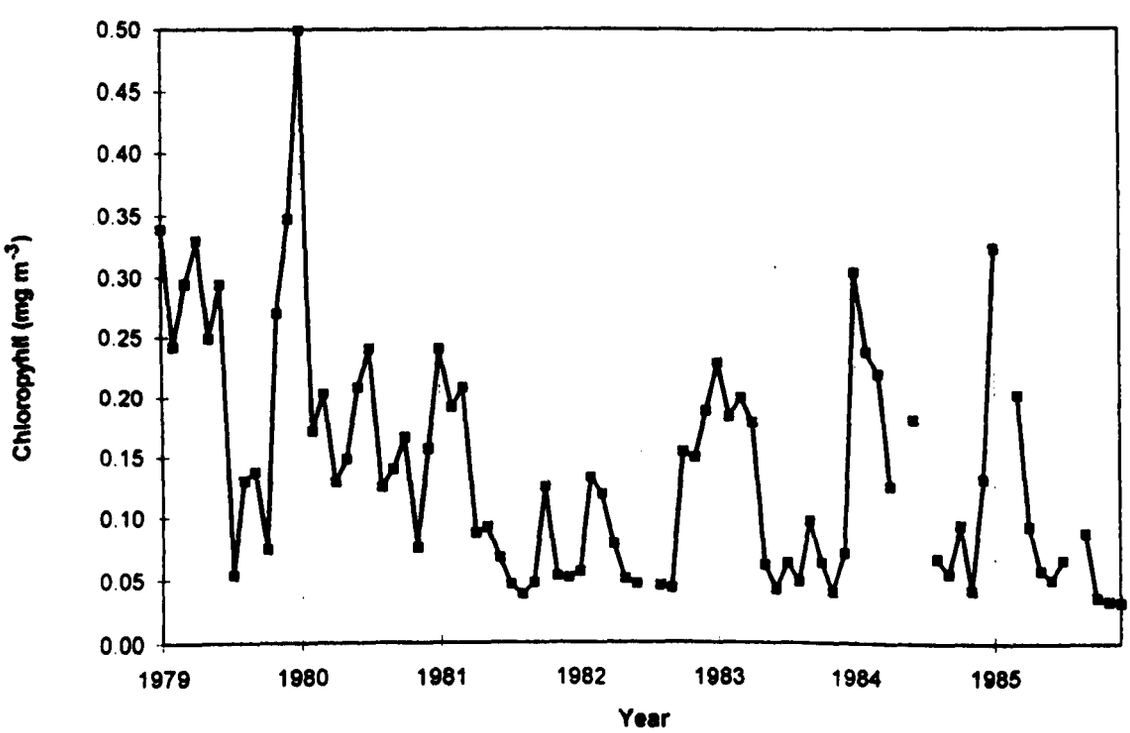


Figure 5. Average monthly phytoplankton pigment concentration in the Cape Ghir region derived from CZCS data for the period 1979–1985. The annual peak in September/October correlates with the onset of maximum upwelling for this region (Nykjaer and Van Camp 1994).

© Del documento, los autores. Digitalización realizada por ULPGC. Biblioteca Universitaria, 2009

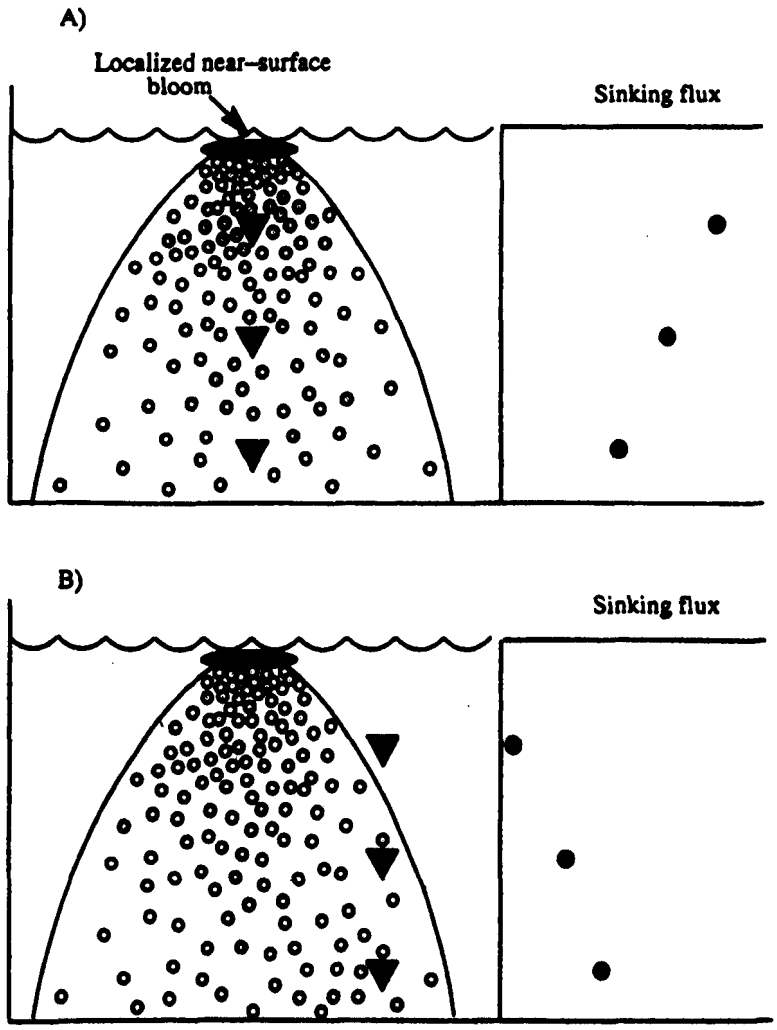


Figure 6. Schematic illustration of relationship between near-surface phytoplankton bloom and particle fluxes measured by a deep-sea sediment trap array. (*a*) Traps located directly below the bloom. (*b*) Traps located to the side of the bloom (redrawn from Siegel *et al.* (1990)).

The peak event of 0.06 mg $m^{-3}$ observed in August 1980 in the CZCS data may be the result of phytoplankton development in the mixed layer as seen at the ESTOC station in autumn 1994 when the surface chlorophyll concentration increased to 0.15 mg $m^{-3}$. Interpretation of CZCS data should be treated with caution though, given the errors in chlorophyll values derived from the OCEAN level-3 data. Nevertheless since the patterns of annual cycles are the same in both sets of data we conclude that the CZCS observed annual cycle is valid.

### 5.2. *Comparison between CZCS data and sediment trap observations: the winter bloom*

The peak winter bloom in January/February as observed in the historical CZCS data (figure 2) occurs about 1 month earlier than the peak particle flux observed in the sediment traps (figure 4). Given the complex biological and physical processes involved in the export of material from the euphotic zone to the deep ocean it is not obvious that a surface bloom will somehow result in a sedimentation event as recorded in the traps. However, we offer the suggestion that both events are strongly coupled. The 1-month time delay between a surface bloom and a peak sedimentation

© Del documento, los autores. Digitalización realizada por ULPGC. Biblioteca Universitaria, 2009

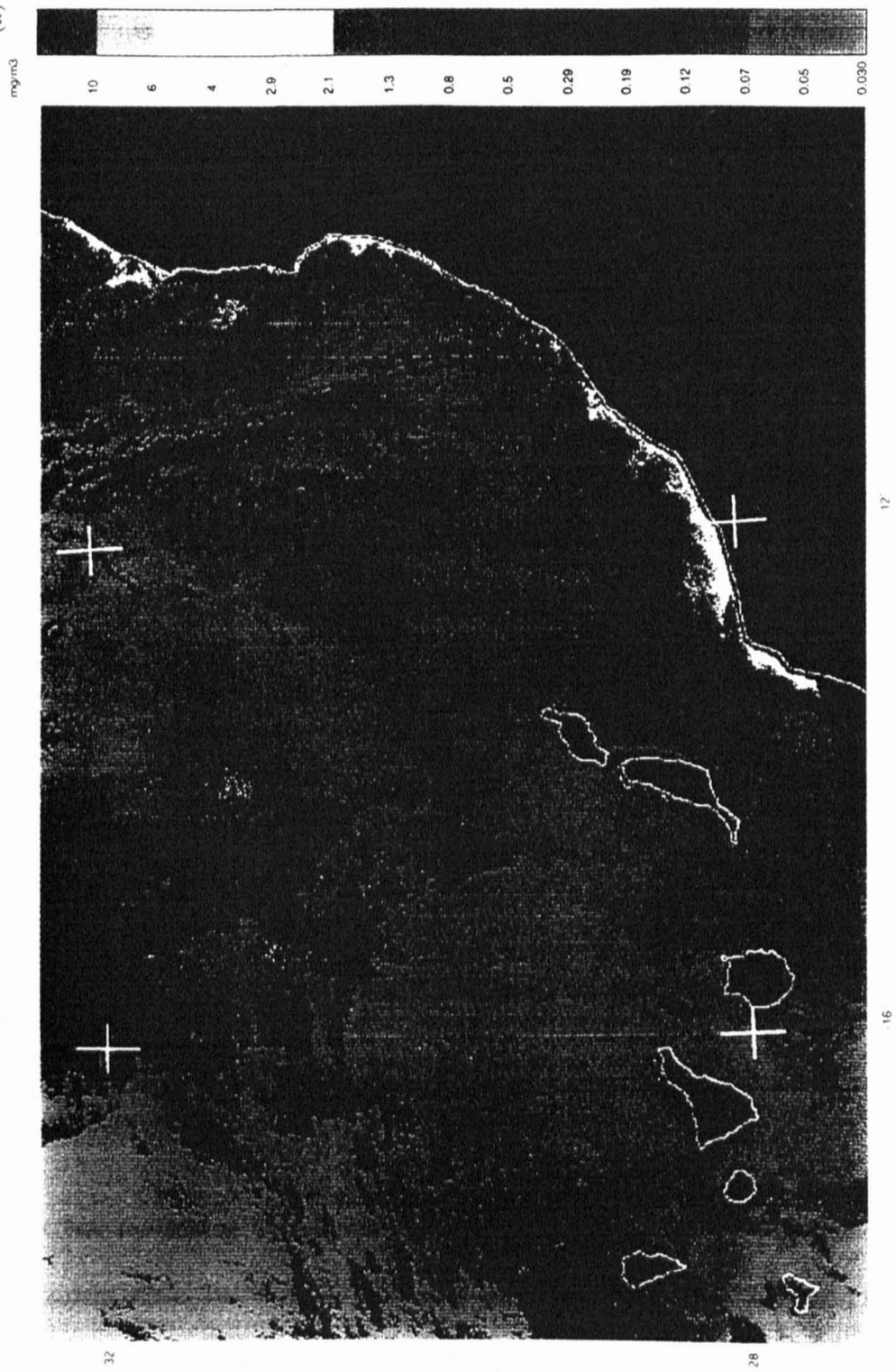


© Del documento, los autores. Digitalización realizada por ULPGC. Biblioteca Universitaria, 2009

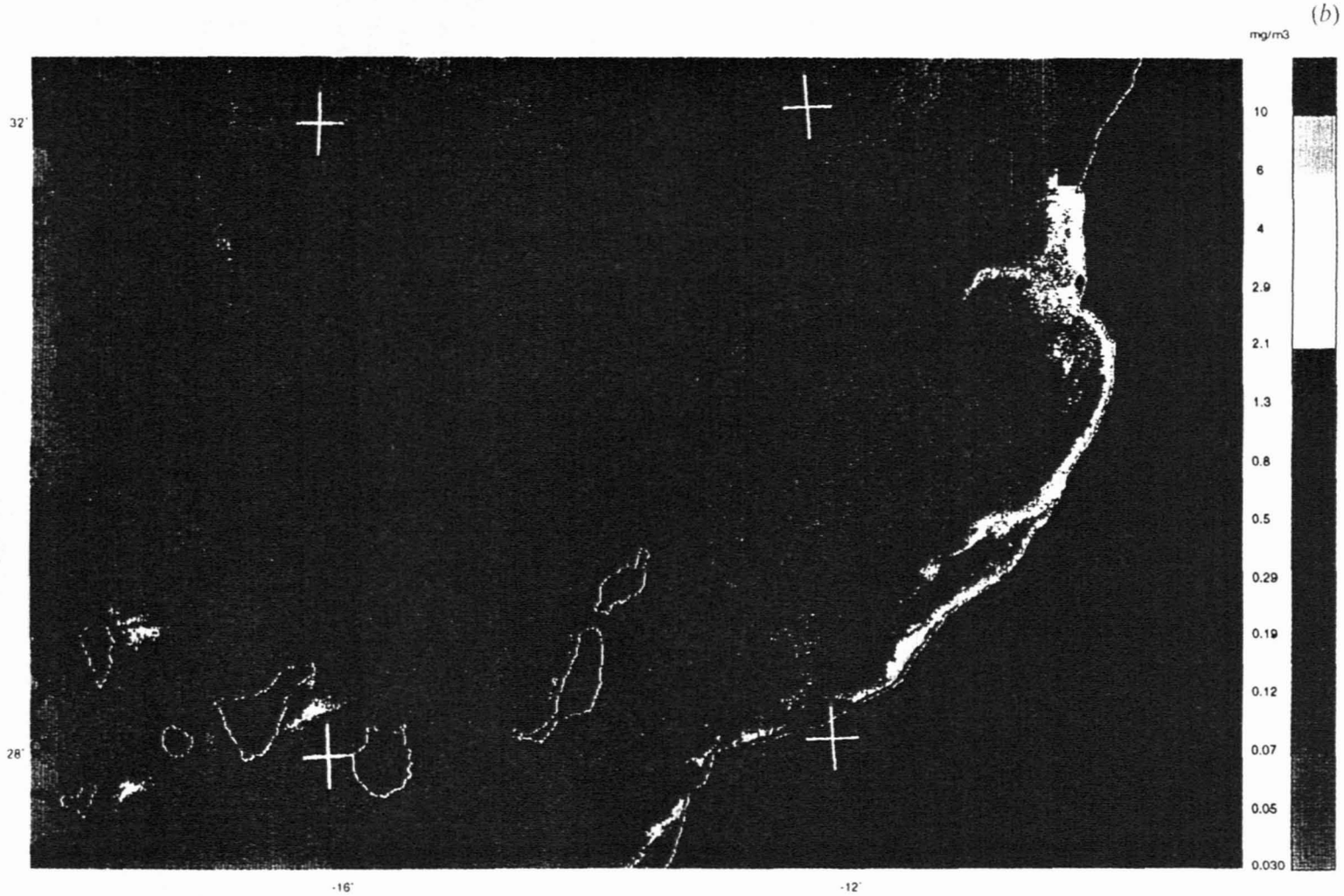


Figure 7. Phytoplankton pigment concentration from the Nimbus-7 CZCS for (*a*) 6 November 1981 and (*b*) 19 October 1980. Notice in (*a*) that the Cape Ghir filament has two parts: one filament stretches north-westwards nearly 200 km to Lanzarote and the other westwards to Fuerteventura then south-westwards towards Gran Canaria. Both filaments appear to be blocked by the Canary Islands westwards. Note also in (*b*) that the Cape Ghir filament stretches at least 300–400 km offshore and develops complex meanders that suggest the presence of mecoscale eddies (Nykjaer 1988).

© Del documento, los autores. Digitalización realizada por ULPGC. Biblioteca Universitaria, 2009

event rather than the 10 days assumed earlier for a typical trap particle probably represents the delay between a peak phytoplankton bloom and the onset of zooplankton grazing and subsequent fecal pellet production. Indeed these observations can also be compared with those of Deuser *et al.* (1990) who observed a 1.5-month phase lag between surface phytoplankton blooms and sedimentation events in a trap at 3200 m depth in the Sargasso Sea.

### 5.3. *Comparison between CZCS data and sediment trap observations: other seasonal peaks*

The absence of chlorophyll peaks outside of the winter bloom over 7 years of CZCS data (except for the single peak in August 1980) contrasts sharply with the peaks recorded in the traps over 3 years. Combining this fact with the observation that for concurrent peaks in both traps, the 3000 m fluxes are always higher than those in the 1000 m trap strongly suggests that these trap sedimentation events are not connected with surface blooms in the ESTOC region. We rejected the possibility of bottom sediment resuspension partly because the lower trap was moored 500 m above the ocean floor but, more convincingly, because the same events are seen in the upper trap which is 2500 m above the bottom.

We suggest instead that material is laterally advecting into the ESTOC region. Figure 6 (adapted from Siegel *et al.* 1990) shows conceptually how a trap not lying directly under a surface bloom but instead to one side may result in the observation of more material in the lower than in the upper traps. Although we believe this is a possible explanation for the trap results, the absence of peaks outside of the winter bloom in the CZCS data indicates that such material must be coming from surface events > 100 km distant. In determining the size of the source square we assumed a constant particle sinking rate and eddy kinetic energy. Siegel *et al.* (1990) point out though that the physical state of a particle may change considerably with depth through aggregation, break-up, consumption and transformation processes. The residence time in the deep ocean may therefore be significantly increased thus increasing the spatial averaging scale. In particular slowly sinking aggregates (1–35 m $d^{-1}$ (Asper 1987)) would have length scales of 100–500 km for a 1000 m trap (Siegel *et al.* 1990). Also, since we are considering a region influenced by the Canary Current, particles will be subject to higher eddy kinetic energy near the surface than the value assumed above and hence the spatial averaging scale will also be increased. It therefore seems plausible to investigate possible source regions for ESTOC trap material that are more than 100 km distant.

### 5.4. *Upwelling effects on the Canary Island region*

Three possible sources of upwelling in the Canary Island region can be considered: the Cape Yubi and Cape Ghir filaments on the African coast (Nykjaer 1988, Van Camp *et al.* 1991) and filaments resulting from upwelling off the north-west coast of Fuerteventura in the Canary Islands (Real *et al.* 1981, Molina and Laatzen 1989). The Cape Bojador filament is not considered because it is too far south and appears only to affect the region south of the Canary Islands (Hernández-Guerra *et al.* 1993).

We first consider the Cape Yubi filament. Figure 7(*a*) is an image derived from CZCS data for 6 November 1981 and shows a well developed Cape Yubi filament structure. It consists of two parts: one filament stretching almost 200 km north-westwards to the island of Lanzarote and a second stretching westwards to

© Del documento, los autores. Digitalización realizada por ULPGC. Biblioteca Universitaria, 2009

Fuerteventura and then turning south-west towards Gran Canaria. Both filaments appear to be blocked by the Canary Islands westwards. The southerly filament also appears to be impacted by the south-westwards flowing Canary Current. This conclusion is supported by other CZCS image analyses (e.g. Hernández-Guerra *et al.* 1993). It is therefore unlikely that this filament transports material to the ESTOC position north of the islands.

Filaments having higher than ambient pigment levels have been observed using CZCS data off the west coast of Fuerteventura in November 1983 (Hernández-Guerra *et al.* 1993). We have also observed higher pigment concentrations off the north-west coast of Fuerteventura for an image derived from CZCS data for 9 July 1980 (not presented here). Although such island filaments are never as extensive as those of Cape Ghir or Cape Yubi, they occur less than 200 km from the ESTOC. Fuerteventura filaments may therefore influence particle sedimentation in the ESTOC traps.

Figure 7(*b*) is a CZCS image from 19 October 1980 and shows a well developed Cape Ghir filament. High pigment concentration associated with this filament stretches at least 300–400 km westwards from Cape Ghir. The complex structure of the filament offshore may indicate the presence of mesoscale eddies as suggested by Nykjaer (1988). Although cloud cover makes it difficult to see how the filament develops further west there are suggestions in the cloud breaks of transport in a south-west direction towards the Canary Islands. The seasonal and interannual phytoplankton pigment concentrations over 7 years in the region of the Cape Ghir filament (figure 5) show peaks that follow an annual pattern as well as additional random events. Thus, as with the ESTOC data, the annual peak in January is interpreted as the winter bloom. The annual peak observed in September/October is probably a result of the onset of maximum upwelling in autumn as reported by Nykjaer and Van Camp (1984) for the Cape Ghir region. The random events may be the result of short periods of coastal upwelling. Because of the different time periods involved in CZCS data for Cape Ghir and ESTOC trap data we have not attempted to correlate the observed peak events in the two sets of data. Nevertheless we suggest that given the annual pattern of the Cape Ghir filament and its geographical location with respect to the ESTOC it should at least be considered a possible source of advected trap material in all seasons.

## 6. Conclusion

For a region north of the Canary Islands analysis of monthly composite images derived from CZCS data over the period 1979–1985 shows a prominent winter pigment concentration each year in January. This is interpreted as the winter bloom signal. In other seasons only one extra peak event in August 1980 was observed over the 7-year period. Comparison of CZCS data with *in situ* chlorophyll data from the ESTOC in 1994 positioned about 100 km north of Gran Canaria shows the same overall annual cycle.

Sediment traps deployed at 1000 m and 3000 m depths from December 1991–August 1994 also showed late winter sedimentation events but with a delay of about 1 month in February/March. We suggest that the peak fluxes of particulate matter result from the sedimentation of the winter bloom as observed in the historical CZCS data. In other seasons additional sedimentation events were observed although they were not as significant as the winter bloom signal. In addition, particle flux in the lower trap was higher than that in the shallow trap. By combining the trap

© Del documento, los autores. Digitalización realizada por ULPGC. Biblioteca Universitaria, 2009

observations with the lack of non-winter peaks in the CZCS data we conclude that material is advecting into the ESTOC region from distances >100 km. Analysis of images derived from CZCS data for the north-west African upwelling region has identified two possible sources of trap material: the Cape Ghir filament and blooms possibly associated with an upwelling off the west coast of Fuerteventura.

**Acknowledgments**

The CZCS data were supplied by the Joint Research Centre, Commission of the European Communities, Ispra, Italy. We would like to thank Vittorio Barale and David Larkin of the Joint Research Centre for providing us with OCEANcode for processing the CZCS data and patiently answering the many e-mails we generated while learning to use the software. We would also like to thank Leo Nykjaer for several helpful discussions regarding the north-west African upwelling region and Alexander Bachem who developed additional software for analysis of the CZCS data.

**References**

Arístegui, J., Sangrá, P., Hernández-León, S., Cantón, M., Hernández-Guerra, A., and Kerling, J. L., 1994, Island-induced eddies in the Canary Islands. *Deep-Sea Research*, **41**, 1509–1525.

Asper, V. L., 1987, Measuring the flux and sinking speeds of marine snow aggregates. *Deep-Sea Research*, **34**, 1–17.

Bienfang, P. K., 1980, Phytoplankton sinking rates in oligotrophic waters off Hawaii, USA. *Marine Biology*, **61**, 69–77.

Bricaud, A., and Morel, A., 1987, Atmospheric corrections and interpretation of marine radiances in CZCS imagery: use of a reflectance model. *Oceanologica Acta*, **7**, 33–50.

Deuser, W. G., Muller-Karger, F. E., Evans, R. H., Brown, O. B., Esaias, W. E., and Feldman, G. C., 1990, Surface-ocean color and deep-ocean carbon flux: how close a connection? *Deep-Sea Research*, **37**, 1331–1343.

Dickson, R. R., 1983, Global summaries and intercomparisons: flow statistics from long-term current meter moorings. In *Eddies in Marine Science*, edited by A. R. Robinson (New York: Springer-Verlag), pp. 278–353.

Fischer, G., Neuer, S., Wefer, G., and Krause, G., 1996, Short-term sedimentation pulses recorded with a fluorescence sensor and sediment traps at 900 m depth in the Canary Basin. *Limnology and Oceanography*, **41**, 1354–1359.

Fowler, S. W., and Small, L. F., 1972, Sinking rates of euphasiid fecal pellets. *Limnology and Oceanography*, **17**, 293–296.

Gordon, H. R., Brown, J. W., and Evans, R. H., 1988, Exact Rayleigh scattering calculations for use with the Nimbus-7 Coastal Zone Color Scanner. *Applied Optics*, **27**, 862–871.

Hernández-Guerra, A., Arístegui, J., Cánton, M., and Nykjaer, L., 1993, Phytoplankton pigment patterns in the Canary Islands area as determined using Coastal Zone Colour Scanner data. *International Journal of Remote Sensing*, **14**, 1431–1437.

Honjo, S., 1978, Sedimentation of materials in the Sargasso Sea at a 5367 m deep station. *Journal of Marine Research*, **36**, 469–492.

Honjo, S., 1982, Seasonality and interaction of biogenic and lithogenic particulate flux at the Panama basin. *Science*, **218**, 883–884.

Honjo, S., and Doherty, K. W., 1988, Large scale aperture time-series sediment traps; design, objectives, construction and application. *Deep-Sea Research*, **35**, 135–149.

Llinás, O., De Leon, A. R., Siedler, G., and Wefer, G., 1994, The ESTOC time series station started operation. *International WOCE Newsletter*, **17**, 20.

Llinás, O., Rueda, M. J., and Pérez-Martell, E., 1989, Aportación de la teledetección a la cuantificación de algunos fenómenos oceanograficos de interés en Canarias. *III Reunión cientifica del grupo de trabajo en teledetección, Madrid, 1989*, edited by C. Antón-Pacheco and J. L. Labrandero, pp. 327–336.

Mittelstaedt, E., 1986, Upwelling regions. In *Oceanography, Landolt–Börnstein New Series, Group V, vol. 3c*, edited by J. Sündermann (New York: Springer-Verlag), pp. 135–163.

© Del documento, los autores. Digitalización realizada por ULPGC. Biblioteca Universitaria, 2009

MITTELSTAEDT, E., 1991, The ocean boundary along the northwest African coast: circulation and oceanographic properties at the sea surface. *Progress in Oceanography*, **26**, 307–355.

MOLINA, R., and LAATZEN, F. L., 1989, Hidrografía en la región Canaria. Campaña Canarias I. *Boletín del Instituto Español de Oceanografía*, **5**, 71–86.

NEUER, S., RATMEYER, V., DAVENPORT, R., FISCHER, G., and WEFER, G., 1997a, Deep water particle flux in the Canary Island region: seasonal trends in relation to long-term satellite derived pigment data and lateral sources. *Deep-Sea Research*, **44**, 1451–1466.

NEUER, S., and RUEDA, M. J., 1997b, European Time Series Station in Operation North of Canary Islands. *US JGOFS News*, **8**, No. 2, 9 and 15.

NYKJAER, L., 1988, Remote sensing applied to the Northwest African upwelling area. PhD Thesis, University of Copenhagen, Denmark.

NYKJAER, L., and VAN CAMP, L., 1994, Seasonal and interannual variability of coastal upwelling along northwest Africa and Portugal from 1981 to 1991. *Journal of Geophysical Research*, **99**, 14197–14207.

REAL, F., DE ARMAS, J. D., and BRAUN, J. G., 1981, Distribución espacial de la clorofila a y del carbono orgánico particulado en aguas costeras superficiales de las Islas Canarias. *Boletin Instituto Español de Oceanografía*, **6**, 109–115.

SIEDLER, G., and ONKEN, R., 1996, Eastern recirculation. In *The Warm water sphere of the North Atlantic Ocean*, edited by W. Krauss (Berlin: Bornträger), pp. 339–364.

SIEGEL, D. A., GRANATA, T. C., MICHAELS, A. F., and DICKEY, T. D., 1990, Mesoscale eddy diffusion, particle sinking, and the interpretation of sediment trap data. *Journal of Geophysical Research*, **95**, 5305–5311.

SMETACEK, V. S., 1985, Role of sinking diatom life-history cycles: ecological, evolutionary and geological significance. *Marine Biology*, **84**, 239–251.

SPETH, P., and DETLEFSEN, H., 1982, Meteorological influences on upwelling off Northwest Africa. In *Rapports et Procès—Verbaux des Réunions, Conseil International pour l'Exploration de la Mer., Copenhagen, Denmark*, **180**, 29–35.

STRAMMA, L., 1984, Geostrophic transport in the warm water sphere of the eastern subtropical North Atlantic. *Journal of Marine Research*, **42**, 537–558.

STURM, B., 1981, The atmospheric correction of remotely sensed data and the quantitative determination of suspended matter in marine water surface layers. In *Remote Sensing in Meteorology, Oceanography and Hydrology*, edited by A. P. Cracknell (Chichester: Ellis Horwood), pp. 163–197.

VAN CAMP, L., NYKJAER, L., MITTELSTAEDT, E., and SCHLITTENHARDT, P., 1991, Upwelling and boundary circulation off Northwest Africa as depicted by infrared and visible satellite observations. *Progress in Oceanography*, **26**, 357–402.

WOOSTER, W., BAKUN, A., and MCLAIN, D. R., 1976, The seasonal upwelling cycle along the eastern boundary of the North Atlantic. *Journal of Marine Research*, **34**, 131–141.

© Del documento, los autores. Digitalización realizada por ULPGC. Biblioteca Universitaria, 2009

© Del documento, los autores. Digitalización realizada por ULPGC. Biblioteca Universitaria, 2009

# Application of cloud-point methodology to the determination of polychlorinated dibenzofurans in sea water by high-performance liquid chromatography

**A. Eiguren Fernández, Z. Sosa Ferrera and J. J. Santana Rodríguez***

*Department of Chemistry, Faculty of Marine Sciences, University of Las Palmas de G.C., 35017 Las Palmas de G.C., Spain*

*Received 3rd December 1998, Accepted 26th January 1999*

Polychlorinated dibenzofurans (PCDF) are organic compounds with very toxic effects for humans and the environment. As they are present in low concentrations, an extraction technique is necessary prior to their determination by high-performance liquid chromatography (HPLC). In this work, the methodology of cloud-point extraction, using two non-ionic surfactants oligoethylene glycol monoalkyl ether (Genapol X-080) and polyoxyethylene-10-cetyl ether (Brij 56), is applied to the extraction and preconcentration of PCDF in sea water samples prior to their determination by HPLC with fluorescence detection.

## Introduction

Interest in determining trace levels of contaminants in environmental samples has increased with the recognition that even trace levels of pollutants can pose risks for humans.

The polychlorinated dibenzofurans (PCDF) are considered one of the most hazardous pollutants of the environment.[1] It is known that isomers of PCDF having substituents at positions 2,3,7 and 8 are among the strongest synthetic poisons possessing carcinogenic and mutagenic effects.[2–4]

Various combustion processes represent major sources of these compounds in the environment. The PCDF formed are emitted to the atmosphere, and due to their hydrophobic and lipophilic properties they are dispersed onto land or into water and will adsorb strongly to organic material, both in the particulate and dissolved phases.

The analysis of PCDF is complicated due their extremely low levels of concentration in the samples. Tedious, costly and time consuming methods for extraction with an organic solvent or clean-up steps are required prior to the analysis of these compounds by gas or liquid chromatography.[5–7]

Micelles and other organized amphiphilic assembles are increasingly utilized in analytical methods.[8] Their unique microheterogeneous structures capable of selective interaction with different solute molecules, can strongly modify solubility, chemical equilibria, kinetics and the spectroscopic properties of analytes and reagents.

Separation procedures based on the peculiar properties of aqueous non-ionic and zwitterionic surfactant solutions have been also proposed as an alternative to the use of traditional organic solvents. Efficient preconcentrations of organic solutes have been obtained using the cloud-point phase separation phenomena.[9–13] The analytical potential of the cloud-point phenomenon mediated phase separations, cloud-point extraction (CPE), has been discussed by several authors.[12–17] The small volume of the surfactant-rich phase allows us to preconcentrate and extract the analytes in one step, prior to gas or liquid chromatographic analysis. Moreover, the surfactant-rich phase is compatible with the micellar and aqueous–organic mobile phase in liquid chromatography, which facilitates the application of this analytical method, with the obvious benefits.

In this work, we report the results of a study of the experimental parameters which affect the extraction efficiency and preconcentration factor of the CPE process of a series of PCDF previous to their determination by high-performance liquid chromatography (HPLC), using two non-ionic surfactants, oligoethylene glycol monoalkyl ether (Genapol X-080) and polyoxyethylene-10-cetyl ether (Brij 56). This CPE methodology has been applied to the analysis of a mixture of PCDF in sea water samples.

## Experimental

### Reagents

Stock solutions of $1.0 \times 10^{-4}$ M of PCDFs (AccuStandard, Inc., New Haven, CT, USA) were prepared by dissolving appropriate amounts of each PCDF in ethanol (Merck, Darmstadt, Germany).

Stock solutions of the surfactants, oligoethylene glycol monoalkyl ether (Genapol X-080) (Sigma, St. Louis, MO, USA), and polyoxyethylene-10-cetyl ether (Brij 56, Sigma) were prepared in deionized water.

HPLC-grade methanol and $KNO_3$ were obtained from Panreac Quimica, S.A. (Barcelona, Spain).

All solvents and analytes were filtered through a 0.45 μm nylon membrane filter, and ultra-high-quality water, obtained using a water purification system, was used throughout.

### Apparatus

The HPLC system consisted of a Waters pump (model 510) fitted with a Rheodyne injector valve (model 7725i) with a 20 μl sample loop and a Waters 474 scanning fluorescence detector. The system and the data management are controlled by Millennium software from Waters (Waters Cromatografia S.A., Barcelona, Spain)

The stationary-phase column was a Waters Nova-Pack $C_{18}$, 3.9 × 150 mm id, 4 μm particle diameter.

The maxima $\lambda_{ex}$ and $\lambda_{em}$ of each PCDF in the presence of surfactant were determined using a Perkin-Elmer Hispania, S.A. (Madrid, Spain) luminescence spectrophotometer, model LS-50. Excitation and emission slits of 5 nm were used.



© Del documento, los autores. Digitalización realizada por ULPGC. Biblioteca Universitaria, 2009

A thermostatted bath (model Tectron 200) and a centrifuge (model Mixtasel), from Selecta (Barcelona, Spain), were also used.

### Procedure

**Preconcentration.** The preconcentration step was carried out keeping aliquots of 10 ml, which contain the analytes and surfactant (2% w/v), in a thermostatically controlled bath for 15 min, at a temperature of 95 °C for both surfactants. After this time, the aliquots were centrifuged for 5 min (3500 rpm) to achieve the separation of the two phases. Previous to the centrifugation, the tube holder was heated for 15 min at a temperature close to 95 °C in an electric system.

**Liquid chromatography analysis with fluorescence detection.** The study of the chromatographic conditions established a methanol–water (85 + 15) mobile phase and 1 ml $min^{-1}$ flow rate as the most adequate conditions in order to obtain an efficient separation of the six PCDF.

As the extracted surfactant-rich phase is compatible with the mobile phase, 20 µl of the extracted volume was injected directly into the liquid chromatograph and the detection of the analytes was carried out by monitoring the relative intensity of fluorescence at the maxima $\lambda_{em}$ and $\lambda_{ex}$ of each PCDF under study. Two different ranges were studied: 3.4–27.2 µg $ml^{-1}$ and 168–3405 ng $ml^{-1}$.

The fluorescent conditions ( $\lambda_{em}$ and $\lambda_{ex}$ ) were previously determined using solutions containing a known concentration of each PCDF and a surfactant concentration above the critical micellar concentration ( Table 1).

**Determination of PCDF in sea water samples.** Prior to the analysis, sea water was passed successively through filters of different porosity (0.45 and 0.22 µm) and ultraviolet radiation to avoid the posible interference of marine microorganisms. Solutions of 10 ml containing 5 ml sea water and 2% (w/v) surfactant concentration were spiked with suitable amounts of PCDF and analysed according to the established CPE method.

## Results and discussion

The cloud-point temperature of these surfactants, necessary for the extraction step, was studied in a previous work.[12] In that study, the consolution curve of each surfactant was obtained when the temperature at which the turbidity appeared was represented against the concentration of surfactant in solution. The phase diagrams indicate a cloud-point temperature of 75–80 °C for Genapol X-080 and 85–90 °C for Brij 56. At the same time, the ratio between the concentration and volume of the added surfactant and the surfactant-rich phase volume obtained after the cloud-point process was studied for both surfactants. The results showed an increase in the extracted volume of surfactant-rich phase with the surfactant concentration in solution, but the volume of added surfactant had no influence on the volume of surfactant-rich phase.[12] A 2% (w/v) surfactant concentration and a volume of 4 ml were chosen for the study carried out in this work, obtaining in these conditions a preconcentration factor of 10.

**Table 1** Fluorescent characteristics of PCDF in 2% (w/v) aqueous solutions of Genapol X-080 and Brij 56

| No. | PCDF | Abbreviation | Genapol $\lambda_{ex}$/nm | Genapol $\lambda_{em}$/nm | Brij 56 $\lambda_{ex}$/nm | Brij 56 $\lambda_{em}$/nm |
|---|---|---|---|---|---|---|
| 1 | Dibenzofuran | DBF | 278 | 316 | 278 | 316 |
| 2 | 4-Chlorodibenzofuran | MonoCDF | 265 | 333 | 280 | 321 |
| 3 | 2,8-Dichlorodibenzofuran | DiCDF | 255 | 334 | 291 | 334 |
| 4 | 2,4,8-Trichlorodibenzofuran | TriCDF | 256 | 335 | 291 | 337 |
| 5 | 2,3,7,8-Tetrachlorodibenzofuran | TetraCDF | 258 | 335 | 302 | 337 |
| 6 | 1,2,3,4,8-Pentachlorodibenzofuran | PentaCDF | 258 | 335 | 294 | 344 |

### Optimization of the preconcentration factor

There are different factors that can alter the extraction process and it is very important to optimize them in order to obtain good recovery factors. Some of these variables are concentration and volume of added surfactant, pH, ionic strength, pressure, *etc.*[18,19] In the case of PCDF, some of the factors have no influence on the recovery percentages, thus pH is not important because these compounds do not present ionic forms; therefore, only the equilibration time, initial concentration of analyte in solution, ionic strength and surfactant concentration are the parameters which have been optimized.

**Effect of the equilibration time.** The recovery percentage, and because of this the efficiency of the cloud-point extraction process, depends on the time that the analytes have to interact with micelles and get into their core. For this reason, to optimise the extraction process, it is necessary to study the behavior of each surfactant when the equilibration time varies.

If we represent recovery percentages against equilibration time, two different behaviors can be observed: the behavior of the analytes with an even number of chlorine atoms and those with an odd number of chlorine atoms. This different behavior would be due to the structure of the molecules (different position of chlorine atoms) which generate different interactions between the analyte and the surfactant micelles, and therefore the solubilization effect would also be different.

For Genapol X-080, we observed that MonoPCDF presents a similar behavior to the PCDF with a even number of chlorine atoms. The recovery percentages of these analytes decrease with time, to 13 min, increasing to 15 min ( maximum recovery percentage) and going down again for longer times. In the case of PCDF with odd numbers of chlorine atoms, recovery percentages increase with time to 13 min, decreasing for 15 min and increasing for longer periods ( Fig. 1a).

When we used Brij 56, the recovery percentages decreased sharply for all the PCDF with time up to 13 min, but with longer periods two behaviors could be observed: for PCDF with even

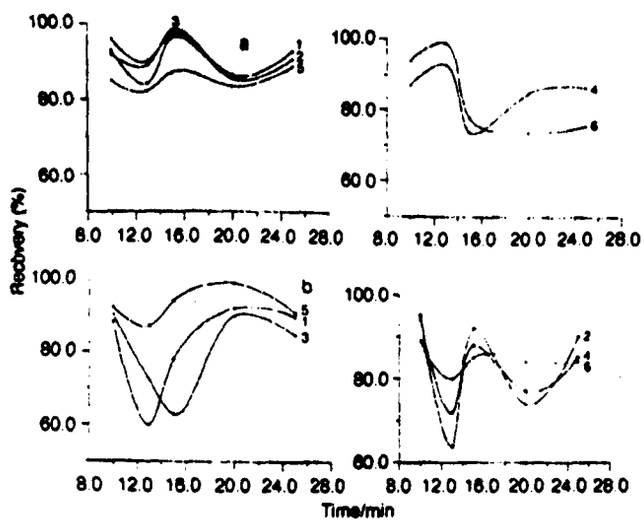


**Fig. 1** Influence of equilibration time on recovery percentages of PCDF using: (a) Genapol X-080, (b) Brij 56; (1) DBF; (2) MonoCDF; (3) DiCDF; (4) TriCDF; (5) TetraCDF; (6) PentaCDF.



© Del documento, los autores. Digitalización realizada por ULPGC. Biblioteca Universitaria, 2009

numbers of chlorine atoms, the recovery percentage, in all the range of concentration, increased up to 20 min, decreasing gradually over longer periods; the rest of the PCDF presented low recovery percentages for 20 min, increasing up to 25 min (Fig. 1b).

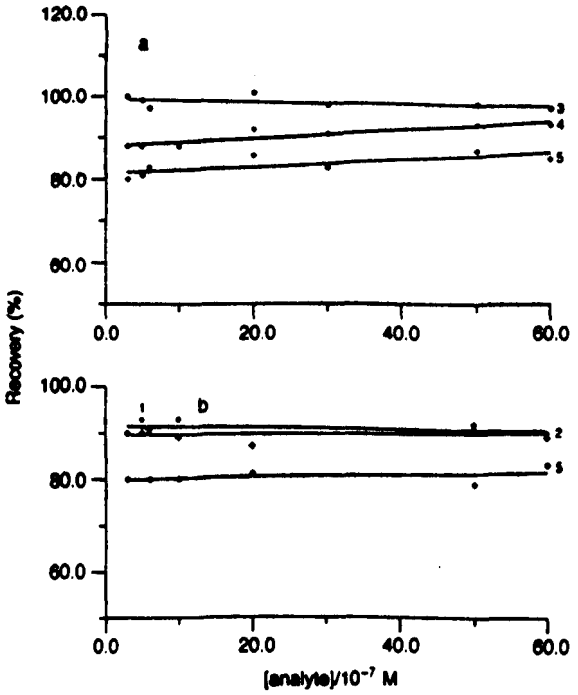


Fig. 2 Effect of the initial analyte concentration in solution on the recovery percentages: (a) Genapol X-080, (b) Brij 56; (1) DBF; (2) MonoCDF; (3) DiCDF; (4) TriCDF; (5) TetraCDF.

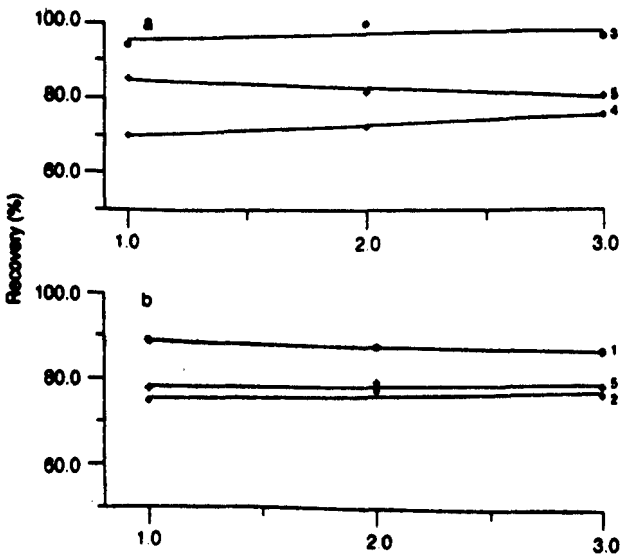


Fig. 3 Influence of added surfactant percentage (w/v) on the recovery percentages: (a) Genapol X-080, (b) Brij 56; (1) DBF; (2) MonoCDF; (3) DiCDF; (4) TriCDF; (5) TetraCDF.

An equilibration time of 15 min was chosen as adequate for all the analytes in solutions.

**Effect of the ionic strength.** The presence of salt in the solution can be important for the extraction process and in the extracted volume of surfactant-rich phase. The study of the influence of this parameter was carried out by adding different percentages of $KNO_3$ (1–10% w/v) to the solution. The results indicated that the addition of salts does not affect the extracted volume of surfactant-rich phase and as the recovery percentages obtained are similar we can conclude that the ionic strength does not have notable influence on the extraction process. But the addition of the inert salt increases the density of the bulk aqueous phase and facilitates the separation process of the two phases. These results are in accord with those obtained by other authors.[20]

**Effect of the analyte concentration.** The initial concentration of analyte is another factor that can affect the recovery percentages. To determine this effect, solutions containing different concentrations of PCDF were subjected to the CPE procedure. As the analyte concentration varied between 50.4–2043 ng $ml^{-1}$ the recovery percentages remained practically constant for all the analytes studied in both surfactants, so we can conclude that the initial concentration of PCDF in solution had no influence on the recovery percentages when we used Genapol X-080 and Brij 56 as extractants (Fig. 2).

**Effect of the added surfactant percentage.** When the influence of the added surfactant percentage (w/v) was studied, the results showed that this parameter had no influence on the recovery percentages for the analytes under study (Fig. 3).

## Cloud-point preconcentration and liquid chromatographic analysis

Another important step in this study is the optimization of the chromatographic conditions. Once the conditions of CPE were optimized to obtain good recovery percentages, it was necessary to optimize the conditions for the separation and determination of PCDF using HPLC with fluorescence detection.

When chromatography is used as a separation technique, it is necessary to obtain a good relationship between analysis time

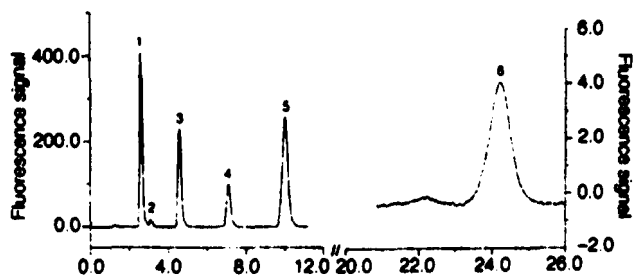


Fig. 4 Elution of a mixture of seven PCDF using 2% (w/v) Genapol X-080 as preconcentrant: (1) DBF; (2) MonoCDF; (3) DiCDF; (4) TriCDF; (5) TetraCDF; (6) PentaCDF. Concentration of each PCDF, 500 ng $ml^{-1}$; eluent, methanol–water (85 + 15); flow rate, 1 ml $min^{-1}$.

Table 2 Analytical parameters for the determination of PCDF with CPE

| Calibration range | Parameter | DBF | MonoCDF | DiCDF | TriCDF | TetraCDF | PentaCDF |
|---|---|---|---|---|---|---|---|
| 168–3405 ng $ml^{-1}$ | $a$ ($\times 10^{-6}$)[a] | 1.2 | 0.1 | 1.1 | 0.6 | 2.5 | 0.1 |
| | $b$ ($\times 10^{-5}$)[b] | 4.0 | 0.1 | 1.0 | 0.4 | 1.1 | 0.2 |
| 3.4–27.2 μg $ml^{-1}$ | $a$ ($\times 10^{-4}$)[a] | 12.2 | 0.6 | 10.3 | 58.0 | 23.6 | 0.7 |
| | $b$ ($\times 10^{-4}$)[b] | 14.8 | 1.5 | 13.9 | 36.6 | 1.1 | 0.7 |

[a] $a$ = Slope. [b] = Intercept.



© Del documento, los autores. Digitalización realizada por ULPGC. Biblioteca Universitaria, 2009

and analyte separation. An efficient separation of the six PCDF in study, in a relatively short period, was obtained when we used a methanol–water (85 + 15) mobile phase and a flow rate of 1 ml $min^{-1}$ (Fig. 4).

The study of the analytical characteristics of the determination of PCDF using Genapol X-080 and Brij-56 showed a similar behavior for both surfactants. The calibration curves were obtained by duplicate injection of the sample containing 2% (w/v) of surfactant and the corresponding PCDF concentration. Two different ranges were studied: 3.4–27.2 μg $ml^{-1}$ and 168–3405 ng $ml^{-1}$. A linear relationship between fluorescence signal and concentration of analyte was observed and high correlation coefficents were obtained for the different calibration curves (0.999–0.998). Table 2 lists the calibration characteristics of the method.

Once the methodology under study was optimized, the recovery percentages for each PCDF were determined. Different mixtures of PCDF were prepared in 10 ml of 2% (w/v) aqueous solutions of Genapol X-080 and Brij 56. After the CPE step, 20 μl of the extracted surfactant-rich phase were injected directly into the chromatographic system. The data obtained, listed in Table 3, show excellent recovery percentages for the different analytes studied in both surfactants.

The limits of detection[21] calculated for each PCDF in Genapol X-080 and Brij 56, using CPE methodology, are listed in Table 4, together with the relative standard deviation for six samples to which the complete procedure (cloud-point preconcentration and extraction and chromatographic separation) was applied for all the compounds studied in 2% (w/v) Genapol X-080 and Brij 56 solutions. The results obtained for both parameters were similar when Genapol X-080 and Brij 56 were used.

**Table 3** Recovery percentages obtained for each PCDF after CPE and chromatographic determination*

| | 168–3405 ng $ml^{-1}$ | | 3.45–27.2 μg $ml^{-1}$ | |
|---|---|---|---|---|
| PCDF | Genapol Recovery % | Brij 56 Recovery % | Genapol Recovery % | Brij 56 Recovery % |
| DBF | 100 | 96 | 96 | 92 |
| MonoCDF | 98 | 94 | 97 | 92 |
| DiCDF | 99 | 93 | 98 | 90 |
| TriCDF | 88 | 95 | 93 | 95 |
| TetraCDF | 98 | 92 | 88 | 99 |
| PentaCDF | 97 | 68 | 99 | 89 |

* Referred to the initial concentration of PCDF in solution.

## Analytical applications

The proposed method was applied to the determination of PCBF in sea water samples from different Spanish areas (Arinaga and Agaete, Canary Islands and Elantxobe, Vizcaya). Sea water samples were previously spiked with suitable amounts of each PCBF. The results indicate satisfactory recovery percentages. (Table 5).


## Acknowledgements

This work was supported by funds provided by D.G.I.C.Y.T. (Spain), research Project No. PB94-0431.


**Table 4** Relative standard deviation (in range 168–3405 ng $ml^{-1}$) and limits of detection for PCDF

| PCDF | DBF | MonoCDF | DiCDF | TriCDF | TetraCDF | PentaCDF |
|---|---|---|---|---|---|---|
| RSD ($n$ = 6) | 0.009 | 0.204 | 0.016 | 0.131 | 0.043 | 0.087 |
| LOD/ng $ml^{-1}$ | 0.5 | 17.6 | 13.3 | 4.9 | 0.7 | 27.5 |

**Table 5** Recovery percentages for PCDF in sea water samples

| | | Genapol | | | | | | Brij 56 | | | | | |
|---|---|---|---|---|---|---|---|---|---|---|---|---|---|
| Origin of sample | PCDF | Added*/ ng $ml^{-1}$ | Found*/ ng $ml^{-1}$ | Recovery (%) | Added*/ ng $ml^{-1}$ | Found*/ ng $ml^{-1}$ | Recovery (%) | Added*/ ng $ml^{-1}$ | Found*/ ng $ml^{-1}$ | Recovery (%) | Added*/ ng $ml^{-1}$ | Found*/ ng $ml^{-1}$ | Recovery (%) |
| Agaete | DBF | 84.0 | 83.2 | 99 | 840 | 789.6 | 94 | 84.0 | 77.3 | 92 | 840 | 789.6 | 94 |
| | MonoCDF | 101.2 | 91.1 | 90 | 1012 | 931.1 | 92 | 101.2 | 95.1 | 94 | 1012 | 991.7 | 98 |
| | DiCDF | 118.5 | 104.3 | 88 | 1185 | 1054.6 | 89 | 118.5 | 107.8 | 91 | 1185 | 1102.0 | 93 |
| | TriCDF | 135.7 | 127.6 | 94 | 1357 | 1302.7 | 96 | 135.7 | 119.4 | 88 | 1357 | 1262.0 | 93 |
| | TetraCDF | 153.0 | 142.3 | 93 | 1530 | 1468.8 | 96 | 153.0 | 137.7 | 90 | 1530 | 1514.7 | 99 |
| | PentaCDF | 170.2 | 163.4 | 96 | 1702 | 1615.0 | 95 | 170.2 | 115.7 | 68 | 1702 | 1565.8 | 92 |
| Aringa | DBF | 84.0 | 84.8 | 101 | 840 | 764.4 | 91 | 84.0 | 79.8 | 95 | 840 | 756.0 | 90 |
| | MonoCDF | 101.2 | 105.2 | 104 | 1012 | 921.0 | 91 | 101.2 | 93.1 | 92 | 1012 | 961.4 | 95 |
| | DiCDF | 118.5 | 117.3 | 99 | 1185 | 1149.4 | 97 | 118.5 | 107.8 | 91 | 1185 | 1208.7 | 102 |
| | TriCDF | 135.7 | 133.0 | 98 | 1357 | 1262.0 | 93 | 135.7 | 123.5 | 91 | 1357 | 1411.3 | 104 |
| | TetraCDF | 153.0 | 148.4 | 97 | 1530 | 1591.2 | 104 | 153.0 | 146.9 | 96 | 1530 | 1407.6 | 92 |
| | PentaCDF | 170.2 | 161.7 | 95 | 1702 | 148.9 | 91 | 170.2 | 127.6 | 75 | 1702 | 1582.9 | 93 |
| Elentrobe | DBF | 84.0 | 87.3 | 104 | 840 | 806.4 | 96 | 84.0 | 83.2 | 99 | 840 | 756.0 | 90 |
| | MonoCDF | 101.2 | 89.0 | 88 | 1012 | 971.5 | 96 | 101.2 | 99.2 | 98 | 1012 | 961.4 | 95 |
| | DiCDF | 118.5 | 111.4 | 94 | 1185 | 1161.3 | 98 | 118.5 | 106.6 | 90 | 1185 | 1196.8 | 101 |
| | TriCDF | 135.7 | 124.8 | 92 | 1357 | 1357.0 | 100 | 135.7 | 119.4 | 88 | 1357 | 1411.3 | 104 |
| | TetraCDF | 153.0 | 145.3 | 95 | 1530 | 1606.5 | 105 | 153.0 | 139.2 | 91 | 1530 | 1560.6 | 102 |
| | PentaCDF | 170.2 | 161.7 | 95 | 1702 | 1719.0 | 101 | 170.2 | 119.1 | 70 | 1702 | 1688.0 | 98 |

* Referred to the initial concentration of PCDF in solution.



© Del documento, los autores. Digitalización realizada por ULPGC. Biblioteca Universitaria, 2009

## References


1 C. Rappe, *Pure Appl. Chem.*, 1996, **68**(9), 1781.
2 C. L. Fletcher and W. A. McKay, *Chemosphere*, 1993, **26**, 1041.
3 D. Broman, C. Näf, C. Rolff and Y. Zebühr, *Environ. Sci. Technol.*, 1991, **25**, 1850.
4 R. E. Clement, *Anal. Chem.*, 1991, **63**, 1130.
5 B. Larsen and S. Facchetti, *Fresenius' J. Anal. Chem.*, 1994, **348**, 159.
6 M. Oehme, A. Bartonova and J. Knutzen, *Environ. Sci. Technol.*, 1990, **24**, 1836.
7 E. Maier, B. Griepink and U. Fortuniti, *Fresenius' J. Anal. Chem.*, 1994, **348**, 23.
8 E. Pramauro, *Ann. Chim. (Rome)*, 1990, **80**, 101.
9 R. G. Laughrin, in *Advances in Liquid Crystals*, ed. G. H. Brown, Academic Press, New York, 1978, vol. 3, pp. 41, 76, 106.
10 H. Watanabe, in *Solution Behavior of Surfactants*, Plenum Press, New York, 1982, pp. 1305–1313.
11 W. L. Hinze and E. Pramauro, *Crit. Rev. Anal. Chem.*, 1993, **24**, 113.
12 A. Eiguren Fernández, Z. Sosa Ferrera and J. J. Santana Rodríguez, *Quim. Anal.*, 1997, **16**, (2), 283.
13 A. Eiguren Fernández, Z. Sosa Ferrera and J. J. Santana Rodríguez, *Anal. Chim. Acta*, 1998, **358**, 145.
14 W. L. Hinze, *Ann. Chim. (Rome)*, 1987, **77**, 167.
15 N. D. Gullickson, J. F. Scamehorn and J. H. Harwell, in *Surfactant-Based Separation Processes*, eds. J. F. Scamehorn and J. H. Harwell, Marcel Dekker, New York, 1989, pp. 139–151.
16 H. Hoshino, T. Saitoh, H. Taketoni, T. Yotsuyanagi, H. Watanabe and K. Tachikawa, *Anal. Chim. Acta*, 1983, **147**, 339.
17 T. Saitoh and W. L. Hinze, *Talanta*, 1995, **42**(1), 119.
18 R. P. Frankewich and W. Hinze, *Anal. Chem.*, 1994, **66**, 944.
19 S. P. Moulik, *Curr. Sci.*, 1996, **71**(5), 368.
20 E. Minati and D. Zanette, *Colloids Surf. A*, 1996, **113**, 237.
21 S. Lindsay, in *High Performance Liquid Chromatography*, Wiley, New York, 1992, pp. 71, 72.


*Paper 8/09457H*

© Del documento, los autores. Digitalización realizada por ULPGC. Biblioteca Universitaria, 2009

© Del documento, los autores. Digitalización realizada por ULPGC. Biblioteca Universitaria, 2009

# Application of cloud-point methodology to the determination of polychlorinated dibenzofurans in sea water by high-performance liquid chromatography

**A. Elguren Fernández, Z. Sosa Ferrera and J. J. Santana Rodríguez***

*Department of Chemistry, Faculty of Marine Sciences, University of Las Palmas de G.C., 35017 Las Palmas de G.C., Spain*

*Received 3rd December 1998, Accepted 26th January 1999*

Polychlorinated dibenzofurans (PCDF) are organic compounds with very toxic effects for humans and the environment. As they are present in low concentrations, an extraction technique is necessary prior to their determination by high-performance liquid chromatography (HPLC). In this work, the methodology of cloud-point extraction, using two non-ionic surfactants oligoethylene glycol monoalkyl ether (Genapol X-080) and polyoxyethylene-10-cetyl ether (Brij 56), is applied to the extraction and preconcentration of PCDF in sea water samples prior to their determination by HPLC with fluorescence detection.

## Introduction

Interest in determining trace levels of contaminants in environmental samples has increased with the recognition that even trace levels of pollutants can pose risks for humans.

The polychlorinated dibenzofurans (PCDF) are considered one of the most hazardous pollutants of the environment.[1] It is known that isomers of PCDF having substituents at positions 2,3,7 and 8 are among the strongest synthetic poisons possessing carcinogenic and mutagenic effects.[2–4]

Various combustion processes represent major sources of these compounds in the environment. The PCDF formed are emitted to the atmosphere, and due to their hydrophobic and lipophilic properties they are dispersed onto land or into water and will adsorb strongly to organic material, both in the particulate and dissolved phases.

The analysis of PCDF is complicated due their extremely low levels of concentration in the samples. Tedious, costly and time consuming methods for extraction with an organic solvent or clean-up steps are required prior to the analysis of these compounds by gas or liquid chromatography.[5–7]

Micelles and other organized amphiphilic assembles are increasingly utilized in analytical methods.[8] Their unique microheterogeneous structures capable of selective interaction with different solute molecules, can strongly modify solubility, chemical equilibria, kinetics and the spectroscopic properties of analytes and reagents.

Separation procedures based on the peculiar properties of aqueous non-ionic and zwitterionic surfactant solutions have been also proposed as an alternative to the use of traditional organic solvents. Efficient preconcentrations of organic solutes have been obtained using the cloud-point phase separation phenomena.[9–13] The analytical potential of the cloud-point phenomenon mediated phase separations, cloud-point extraction (CPE), has been discussed by several authors.[12–17] The small volume of the surfactant-rich phase allows us to preconcentrate and extract the analytes in one step, prior to gas or liquid chromatographic analysis. Moreover, the surfactant-rich phase is compatible with the micellar and aqueous–organic mobile phase in liquid chromatography, which facilitates the application of this analytical method, with the obvious benefits.

In this work, we report the results of a study of the experimental parameters which affect the extraction efficiency and preconcentration factor of the CPE process of a series of PCDF previous to their determination by high-performance liquid chromatography (HPLC), using two non-ionic surfactants, oligoethylene glycol monoalkyl ether (Genapol X-080) and polyoxyethylene-10-cetyl ether (Brij 56). This CPE methodology has been applied to the analysis of a mixture of PCDF in sea water samples.

## Experimental

### Reagents

Stock solutions of $1.0 \times 10^{-4}$ M of PCDFs (AccuStandard, Inc., New Haven, CT, USA) were prepared by dissolving appropriate amounts of each PCDF in ethanol (Merck, Darmstadt, Germany).

Stock solutions of the surfactants, oligoethylene glycol monoalkyl ether (Genapol X-080) (Sigma, St. Louis, MO, USA), and polyoxyethylene-10-cetyl ether (Brij 56, Sigma) were prepared in deionized water.

HPLC-grade methanol and $KNO_3$ were obtained from Panreac Quimica, S.A. (Barcelona, Spain).

All solvents and analytes were filtered through a 0.45 μm nylon membrane filter, and ultra-high-quality water, obtained using a water purification system, was used throughout.

### Apparatus

The HPLC system consisted of a Waters pump (model 510) fitted with a Rheodyne injector valve (model 7725i) with a 20 μl sample loop and a Waters 474 scanning fluorescence detector. The system and the data management are controlled by Millennium software from Waters (Waters Cromatografia S.A., Barcelona, Spain)

The stationary-phase column was a Waters Nova-Pack $C_{18}$, 3.9 ×150 mm id, 4 μm particle diameter.

The maxima $\lambda_{ex}$ and $\lambda_{em}$ of each PCDF in the presence of surfactant were determined using a Perkin-Elmer Hispania, S.A. (Madrid, Spain) luminescence spectrophotometer, model LS-50. Excitation and emission slits of 5 nm were used.



© Del documento, los autores. Digitalización realizada por ULPGC. Biblioteca Universitaria, 2009

A thermostatted bath (model Tectron 200) and a centrifuge (model Mixtasel), from Selecta (Barcelona, Spain), were also used.

### Procedure

**Preconcentration.** The preconcentration step was carried out keeping aliquots of 10 ml, which contain the analytes and surfactant (2% w/v), in a thermostatically controlled bath for 15 min, at a temperature of 95 °C for both surfactants. After this time, the aliquots were centrifuged for 5 min (3500 rpm) to achieve the separation of the two phases. Previous to the centrifugation, the tube holder was heated for 15 min at a temperature close to 95 °C in an electric system.

**Liquid chromatography analysis with fluorescence detection.** The study of the chromatographic conditions established a methanol–water (85 + 15) mobile phase and 1 ml $min^{-1}$ flow rate as the most adequate conditions in order to obtain an efficient separation of the six PCDF.

As the extracted surfactant-rich phase is compatible with the mobile phase, 20 µl of the extracted volume was injected directly into the liquid chromatograph and the detection of the analytes was carried out by monitoring the relative intensity of fluorescence at the maxima $\lambda_{em}$ and $\lambda_{ex}$ of each PCDF under study. Two different ranges were studied: 3.4–27.2 µg $ml^{-1}$ and 168–3405 ng $ml^{-1}$.

The fluorescent conditions ( $\lambda_{em}$ and $\lambda_{ex}$ ) were previously determined using solutions containing a known concentration of each PCDF and a surfactant concentration above the critical micellar concentration ( Table 1).

**Determination of PCDF in sea water samples.** Prior to the analysis, sea water was passed successively through filters of different porosity (0.45 and 0.22 µm) and ultraviolet radiation to avoid the posible interference of marine microorganisms. Solutions of 10 ml containing 5 ml sea water and 2% (w/v) surfactant concentration were spiked with suitable amounts of PCDF and analysed according to the established CPE method.

## Results and discussion

The cloud-point temperature of these surfactants, necessary for the extraction step, was studied in a previous work.[12] In that study, the consolution curve of each surfactant was obtained when the temperature at which the turbidity appeared was represented against the concentration of surfactant in solution. The phase diagrams indicate a cloud-point temperature of 75–80 °C for Genapol X-080 and 85–90 °C for Brij 56. At the same time, the ratio between the concentration and volume of the added surfactant and the surfactant-rich phase volume obtained after the cloud-point process was studied for both surfactants.The results showed an increase in the extracted volume of surfactant-rich phase with the surfactant concentration in solution, but the volume of added surfactant had no influence on the volume of surfactant-rich phase.[12] A 2% (w/v) surfactant concentration and a volume of 4 ml were chosen for the study carried out in this work, obtaining in these conditions a preconcentration factor of 10.

**Table 1** Fluorescent characteristics of PCDF in 2% (w/v) aqueous solutions of Genapol X-080 and Brij 56

| No. | PCDF | Abbreviation | Genapol $\lambda_{ex}$/nm | Genapol $\lambda_{em}$/nm | Brij 56 $\lambda_{ex}$/nm | Brij 56 $\lambda_{em}$/nm |
|---|---|---|---|---|---|---|
| 1 | Dibenzofuran | DBF | 278 | 316 | 278 | 316 |
| 2 | 4-Chlorodibenzofuran | MonoCDF | 265 | 333 | 280 | 321 |
| 3 | 2,8-Dichlorodibenzofuran | DiCDF | 255 | 334 | 291 | 334 |
| 4 | 2,4,8-Trichlorodibenzofuran | TriCDF | 256 | 335 | 291 | 337 |
| 5 | 2,3,7,8-Tetrachlorodibenzofuran | TetraCDF | 258 | 335 | 302 | 337 |
| 6 | 1,2,3,4,8-Pentachlorodibenzofuran | PentaCDF | 258 | 335 | 294 | 344 |

### Optimization of the preconcentration factor

There are different factors that can alter the extraction process and it is very important to optimize them in order to obtain good recovery factors. Some of these variables are concentration and volume of added surfactant, pH, ionic strength, pressure, *etc.*[18,19] In the case of PCDF, some of the factors have no influence on the recovery percentages, thus pH is not important because these compounds do not present ionic forms; therefore, only the equilibration time, initial concentration of analyte in solution, ionic strength and surfactant concentration are the parameters which have been optimized.

**Effect of the equilibration time.** The recovery percentage, and because of this the efficiency of the cloud-point extraction process, depends on the time that the analytes have to interact with micelles and get into their core. For this reason, to optimise the extraction process, it is necessary to study the behavior of each surfactant when the equilibration time varies.

If we represent recovery percentages against equilibration time, two different behaviors can be observed: the behavior of the analytes with an even number of chlorine atoms and those with an odd number of chlorine atoms. This different behavior would be due to the structure of the molecules (different position of chlorine atoms) which generate different interactions between the analyte and the surfactant micelles, and therefore the solubilization effect would also be different.

For Genapol X-080, we observed that MonoPCDF presents a similar behavior to the PCDF with a even number of chlorine atoms. The recovery percentages of these analytes decrease with time, to 13 min, increasing to 15 min ( maximum recovery percentage) and going down again for longer times. In the case of PCDF with odd numbers of chlorine atoms, recovery percentages increase with time to 13 min, decreasing for 15 min and increasing for longer periods ( Fig. 1a).

When we used Brij 56, the recovery percentages decreased sharply for all the PCDF with time up to 13 min, but with longer periods two behaviors could be observed: for PCDF with even

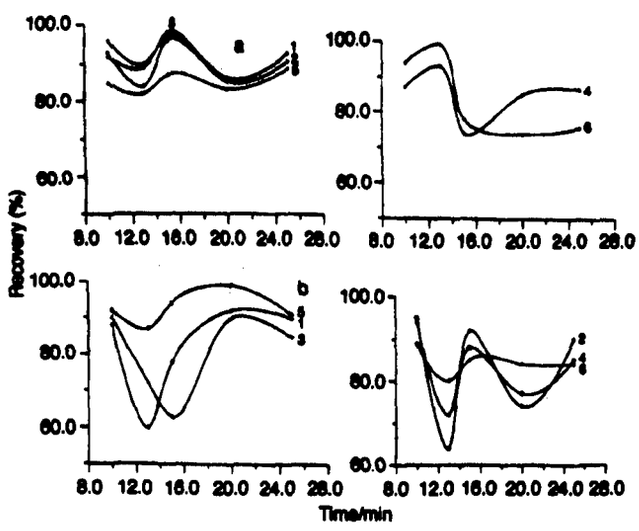


**Fig. 1** Influence of equilibration time on recovery percentages of PCDF using: (a) Genapol X-080, (b) Brij 56; (1) DBF; (2) MonoCDF; (3) DiCDF; (4) TriCDF; (5) TetraCDF; (6) PentaCDF.



© Del documento, los autores. Digitalización realizada por ULPGC. Biblioteca Universitaria, 2009

numbers of chlorine atoms, the recovery percentage, in all the range of concentration, increased up to 20 min, decreasing gradually over longer periods; the rest of the PCDF presented low recovery percentages for 20 min, increasing up to 25 min (Fig. 1b).

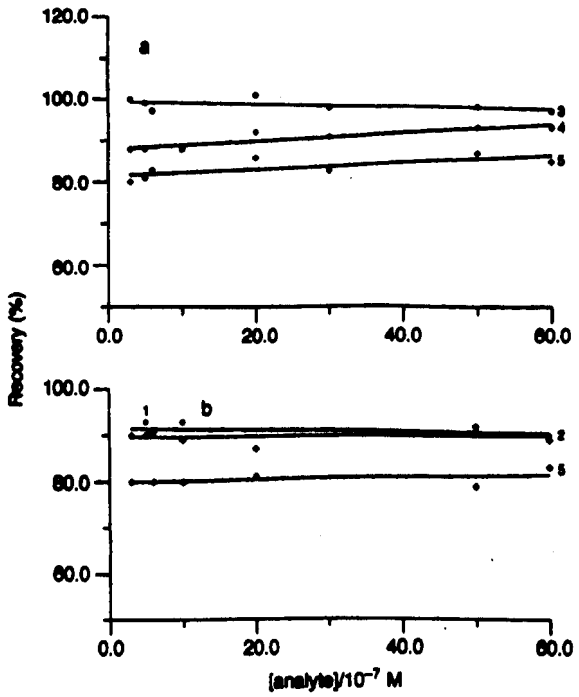


Fig. 2 Effect of the initial analyte concentration in solution on the recovery percentages: (a) Genapol X-080, (b) Brij 56; (1) DBF; (2) MonoCDF; (3) DiCDF; (4) TriCDF; (5) TetraCDF.

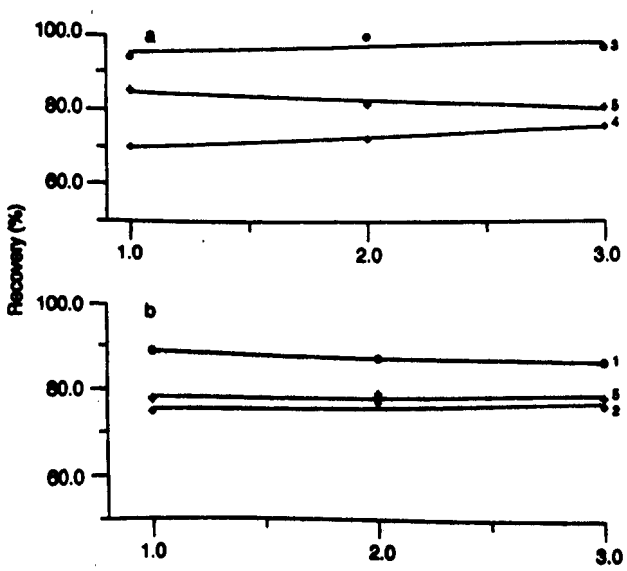


Fig. 3 Influence of added surfactant percentage (w/v) on the recovery percentages: (a) Genapol X-080, (b) Brij 56; (1) DBF; (2) MonoCDF; (3) DiCDF; (4) TriCDF; (5) TetraCDF.

An equilibration time of 15 min was chosen as adequate for all the analytes in solutions.

**Effect of the ionic strength.** The presence of salt in the solution can be important for the extraction process and in the extracted volume of surfactant-rich phase. The study of the influence of this parameter was carried out by adding different percentages of $KNO_3$ (1–10% w/v) to the solution. The results indicated that the addition of salts does not affect the extracted volume of surfactant-rich phase and as the recovery percentages obtained are similar we can conclude that the ionic strength does not have notable influence on the extraction process. But the addition of the inert salt increases the density of the bulk aqueous phase and facilitates the separation process of the two phases. These results are in accord with those obtained by other authors.[20]

**Effect of the analyte concentration.** The initial concentration of analyte is another factor that can affect the recovery percentages. To determine this effect, solutions containing different concentrations of PCDF were subjected to the CPE procedure. As the analyte concentration varied between 50.4–2043 ng $ml^{-1}$ the recovery percentages remained practically constant for all the analytes studied in both surfactants, so we can conclude that the initial concentration of PCDF in solution had no influence on the recovery percentages when we used Genapol X-080 and Brij 56 as extractants (Fig. 2).

**Effect of the added surfactant percentage.** When the influence of the added surfactant percentage (w/v) was studied, the results showed that this parameter had no influence on the recovery percentages for the analytes under study (Fig. 3).

## Cloud-point preconcentration and liquid chromatographic analysis

Another important step in this study is the optimization of the chromatographic conditions. Once the conditions of CPE were optimized to obtain good recovery percentages, it was necessary to optimize the conditions for the separation and determination of PCDF using HPLC with fluorescence detection.

When chromatography is used as a separation technique, it is necessary to obtain a good relationship between analysis time

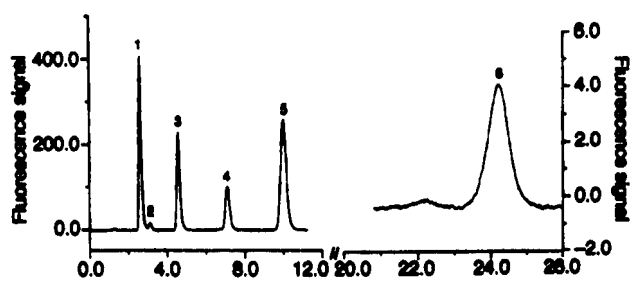


Fig. 4 Elution of a mixture of seven PCDF using 2% (w/v) Genapol X-080 as preconcentrant: (1) DBF; (2) MonoCDF; (3) DiCDF; (4) TriCDF; (5) TetraCDF; (6) PentaCDF. Concentration of each PCDF, 500 ng $ml^{-1}$; eluent, methanol–water (85 + 15); flow rate, 1 ml $min^{-1}$.

Table 2 Analytical parameters for the determination of PCDF with CPE

| Calibration range | Parameter | DBF | MonoCDF | DiCDF | TriCDF | TetraCDF | PentaCDF |
|---|---|---|---|---|---|---|---|
| 168–3405 ng $ml^{-1}$ | $a$ ($\times 10^{-6}$)[a] | 1.2 | 0.1 | 1.1 | 0.6 | 2.5 | 0.1 |
| | $b$ ($\times 10^{-5}$)[b] | 4.0 | 0.1 | 1.0 | 0.4 | 1.1 | 0.2 |
| 3.4–27.2 μg $ml^{-1}$ | $a$ ($\times 10^{-4}$)[a] | 12.2 | 0.6 | 10.3 | 58.0 | 23.6 | 0.7 |
| | $b$ ($\times 10^{-4}$)[b] | 14.8 | 1.5 | 13.9 | 36.6 | 1.1 | 0.7 |

[a] $a$ = Slope. [b] $b$ = Intercept.



© Del documento, los autores. Digitalización realizada por ULPGC. Biblioteca Universitaria, 2009

and analyte separation. An efficient separation of the six PCDF in study, in a relatively short period, was obtained when we used a methanol–water (85 + 15) mobile phase and a flow rate of 1 ml $min^{-1}$ (Fig. 4).

The study of the analytical characteristics of the determination of PCDF using Genapol X-080 and Brij-56 showed a similar behavior for both surfactants. The calibration curves were obtained by duplicate injection of the sample containing 2% (w/v) of surfactant and the corresponding PCDF concentration. Two different ranges were studied: 3.4–27.2 μg $ml^{-1}$ and 168–3405 ng $ml^{-1}$. A linear relationship between fluorescence signal and concentration of analyte was observed and high correlation coefficents were obtained for the different calibration curves (0.999–0.998). Table 2 lists the calibration characteristics of the method.

Once the methodology under study was optimized, the recovery percentages for each PCDF were determined. Different mixtures of PCDF were prepared in 10 ml of 2% (w/v) aqueous solutions of Genapol X-080 and Brij 56. After the CPE step, 20 μl of the extracted surfactant-rich phase were injected directly into the chromatographic system. The data obtained, listed in Table 3, show excellent recovery percentages for the different analytes studied in both surfactants.

The limits of detection[21] calculated for each PCDF in Genapol X-080 and Brij 56, using CPE methodology, are listed in Table 4, together with the relative standard deviation for six samples to which the complete procedure (cloud-point preconcentration and extraction and chromatographic separation) was applied for all the compounds studied in 2% (w/v) Genapol X-080 and Brij 56 solutions. The results obtained for both parameters were similar when Genapol X-080 and Brij 56 were used.

**Table 3** Recovery percentages obtained for each PCDF after CPE and chromatographic determination*

| | 168–3405 ng $ml^{-1}$ | | 3.45–27.2 μg $ml^{-1}$ | |
|---|---|---|---|---|
| PCDF | Genapol Recovery % | Brij 56 Recovery % | Genapol Recovery % | Brij 56 Recovery % |
| DBF | 100 | 96 | 96 | 92 |
| MonoCDF | 98 | 94 | 97 | 92 |
| DiCDF | 99 | 93 | 98 | 90 |
| TriCDF | 88 | 95 | 93 | 95 |
| TetraCDF | 98 | 92 | 88 | 99 |
| PentaCDF | 97 | 68 | 99 | 89 |

* Referred to the initial concentration of PCDF in solution.

## Analytical applications

The proposed method was applied to the determination of PCBF in sea water samples from different Spanish areas (Arinaga and Agaete, Canary Islands and Elantxobe, Vizcaya). Sea water samples were previously spiked with suitable amounts of each PCBF. The results indicate satisfactory recovery percentages. (Table 5).


## Acknowledgements

This work was supported by funds provided by D.G.I.C.Y.T. (Spain), research Project No. PB94-0431.


**Table 4** Relative standard deviation (in range 168–3405 ng $ml^{-1}$) and limits of detection for PCDF

| PCDF | DBF | MonoCDF | DiCDF | TriCDF | TetraCDF | PentaCDF |
|---|---|---|---|---|---|---|
| RSD ($n$ = 6) | 0.009 | 0.204 | 0.016 | 0.131 | 0.043 | 0.087 |
| LOD/ng $ml^{-1}$ | 0.5 | 17.6 | 13.3 | 4.9 | 0.7 | 27.5 |

**Table 5** Recovery percentages for PCDF in sea water samples

| | | Genapol | | | | | | Brij 56 | | | | | |
|---|---|---|---|---|---|---|---|---|---|---|---|---|---|
| Origin of sample | PCDF | Added*/ ng $ml^{-1}$ | Found*/ ng $ml^{-1}$ | Recovery (%) | Added*/ ng $ml^{-1}$ | Found*/ ng $ml^{-1}$ | Recovery (%) | Added*/ ng $ml^{-1}$ | Found*/ ng $ml^{-1}$ | Recovery (%) | Added*/ ng $ml^{-1}$ | Found*/ ng $ml^{-1}$ | Recovery (%) |
| Agaete | DBF | 84.0 | 83.2 | 99 | 840 | 789.6 | 94 | 84.0 | 77.3 | 92 | 840 | 789.6 | 94 |
| | MonoCDF | 101.2 | 91.1 | 90 | 1012 | 931.1 | 92 | 101.2 | 95.1 | 94 | 1012 | 991.7 | 98 |
| | DiCDF | 118.5 | 104.3 | 88 | 1185 | 1054.6 | 89 | 118.5 | 107.8 | 91 | 1185 | 1102.0 | 93 |
| | TriCDF | 135.7 | 127.6 | 94 | 1357 | 1302.7 | 96 | 135.7 | 119.4 | 88 | 1357 | 1262.0 | 93 |
| | TetraCDF | 153.0 | 142.3 | 93 | 1530 | 1468.8 | 96 | 153.0 | 137.7 | 90 | 1530 | 1514.7 | 99 |
| | PentaCDF | 170.2 | 163.4 | 96 | 1702 | 1615.0 | 95 | 170.2 | 115.7 | 68 | 1702 | 1565.8 | 92 |
| Aringa | DBF | 84.0 | 84.8 | 101 | 840 | 764.4 | 91 | 84.0 | 79.8 | 95 | 840 | 756.0 | 90 |
| | MonoCDF | 101.2 | 105.2 | 104 | 1012 | 921.0 | 91 | 101.2 | 93.1 | 92 | 1012 | 961.4 | 95 |
| | DiCDF | 118.5 | 117.3 | 99 | 1185 | 1149.4 | 97 | 118.5 | 107.8 | 91 | 1185 | 1208.7 | 102 |
| | TriCDF | 135.7 | 133.0 | 98 | 1357 | 1262.0 | 93 | 135.7 | 123.5 | 91 | 1357 | 1411.3 | 104 |
| | TetraCDF | 153.0 | 148.4 | 97 | 1530 | 1591.2 | 104 | 153.0 | 146.9 | 96 | 1530 | 1407.6 | 92 |
| | PentaCDF | 170.2 | 161.7 | 95 | 1702 | 148.9 | 91 | 170.2 | 127.6 | 75 | 1702 | 1582.9 | 93 |
| Elentrobe | DBF | 84.0 | 87.3 | 104 | 840 | 806.4 | 96 | 84.0 | 83.2 | 99 | 840 | 756.0 | 90 |
| | MonoCDF | 101.2 | 89.0 | 88 | 1012 | 971.5 | 96 | 101.2 | 99.2 | 98 | 1012 | 961.4 | 95 |
| | DiCDF | 118.5 | 111.4 | 94 | 1185 | 1161.3 | 98 | 118.5 | 106.6 | 90 | 1185 | 1196.8 | 101 |
| | TriCDF | 135.7 | 124.8 | 92 | 1357 | 1357.0 | 100 | 135.7 | 119.4 | 88 | 1357 | 1411.3 | 104 |
| | TetraCDF | 153.0 | 145.3 | 95 | 1530 | 1606.5 | 105 | 153.0 | 139.2 | 91 | 1530 | 1560.6 | 102 |
| | PentaCDF | 170.2 | 161.7 | 95 | 1702 | 1719.0 | 101 | 170.2 | 119.1 | 70 | 1702 | 1688.0 | 98 |

* Referred to the initial concentration of PCDF in solution.



© Del documento, los autores. Digitalización realizada por ULPGC. Biblioteca Universitaria, 2009

## References


1 C. Rappe, *Pure Appl. Chem.*, 1996, **68**(9), 1781.
2 C. L. Fletcher and W. A. McKay, *Chemosphere*, 1993, **26**, 1041.
3 D. Broman, C. Näf, C. Rolff and Y. Zebühr, *Environ. Sci. Technol.*, 1991, **25**, 1850.
4 R. E. Clement, *Anal. Chem.*, 1991, **63**, 1130.
5 B. Larsen and S. Facchetti, *Fresenius' J. Anal. Chem.*, 1994, **348**, 159.
6 M. Oehme, A. Bartonova and J. Knutzen, *Environ. Sci. Technol.*, 1990, **24**, 1836.
7 E. Maier, B. Griepink and U. Fortuniti, *Fresenius' J. Anal. Chem.*, 1994, **348**, 23.
8 E. Pramauro, *Ann. Chim. (Rome)*, 1990, **80**, 101.
9 R. G. Laughrin, in *Advances in Liquid Crystals*, ed. G. H. Brown, Academic Press, New York, 1978, vol. 3, pp. 41, 76, 106.
10 H. Watanabe, in *Solution Behavior of Surfactants*, Plenum Press, New York, 1982, pp. 1305–1313.
11 W. L. Hinze and E. Pramauro, *Crit. Rev. Anal. Chem.*, 1993, **24**, 113.
12 A. Eiguren Fernández, Z. Sosa Ferrera and J. J. Santana Rodríguez, *Quim. Anal.*, 1997, **16**, (2), 283.
13 A. Eiguren Fernández, Z. Sosa Ferrera and J. J. Santana Rodríguez, *Anal. Chim. Acta*, 1998, **358**, 145.
14 W. L. Hinze, *Ann. Chim. (Rome)*, 1987, **77**, 167.
15 N. D. Gullickson, J. F. Scamehorn and J. H. Harwell, in *Surfactant-Based Separation Processes*, eds. J. F. Schamehorn and J. H. Harwell, Marcel Dekker, New York, 1989, pp. 139–151.
16 H. Hoshino, T. Saitoh, H. Taketoni, T. Yotsuyanagi, H. Watanabe and K. Tachikawa, *Anal. Chim. Acta*, 1983, **147**, 339.
17 T. Saitoh and W. L. Hinze, *Talanta*, 1995, **42**(1), 119.
18 R. P. Frankewich and W. Hinze, *Anal. Chem.*, 1994, **66**, 944.
19 S. P. Moulik, *Curr. Sci.*, 1996, **71**(5), 368.
20 E. Minati and D. Zanette, *Colloids Surf. A*, 1996, **113**, 237.
21 S. Lindsay, in *High Performance Liquid Chromatography*, Wiley, New York, 1992, pp. 71, 72.


*Paper 8/09457H*

© Del documento, los autores. Digitalización realizada por ULPGC. Biblioteca Universitaria, 2009

© Del documento, los autores. Digitalización realizada por ULPGC. Biblioteca Universitaria, 2009

ELSEVIER

Journal of Biotechnology 70 (1999) 227–229

JOURNAL OF Biotechnology

# Sporulation and sterilization method for axenic culture of *Gelidium canariensis*

P. Garcia-Jimenez *, F.D. Marian, M. Rodrigo, R.R. Robaina

*Department of Biology, Faculty of Marine Sciences, University of Las Palmas G.C., Box 550, Las Palmas, Gran Canaria, Spain*

Received 21 October 1998; received in revised form 3 December 1998; accepted 22 December 1998

**Abstract**

A sporulation and sterilization procedure was used to establish axenic cultures of sporelings of *Gelidium canariensis*. Sporangial branchlets excised from the thallus were rinsed in distilled water twice and in 1% sodium hypochlorite (2 min). The branchlets were cultivated overnight in multiwell plates with 0.3 ml of autoclaved seawater to promote spore liberation in 90% of the cultivated branchlets. The branchlets were transferred to an antibiotic solution made of ampicillin, penicillin, rifampicin, nystatin (0.2 mg $ml^{-1}$ each) and 0.1 g $ml^{-1}$ of $GeO_2$ in liquid PES for 45 days, during which clusters of spores (85–100 spores) were observed on the surface of the branchlet. After 55 days, they became axenic sporelings with the prostrate and erect system characteristic of *Gelidium canariensis*. © 1999 Elsevier Science B.V. All rights reserved.

*Keywords:* Axenic culture; *Gelidium canariensis*; Rhodophyta; Sporelings

## 1. Introduction

Heterotrophic culture may provide a cost-effective large-scale alternative method for cultivation of algae that utilize organic carbon sources (Chen, 1996). Axenic heterotrophic cell and tissue cultures from macroalgae can be established from precultured axenic carposporelings. For example, axenic heterotrophic cultures of the carragenophytic macroalga *Grateloupia doryphora*, which produces secondary metabolites, sulfated polysaccharides and lipids, were successfully initiated from axenic spores (Garcia-Jimenez et al., 1996, 1998; Rodrigo and Robaina, 1997).

Axenic cultures of *Gelidium*, another important genus of macroalgae, producing over 50% of the agar and agarose world market (Armisen and Galatas, 1987), have not been established yet, although laboratory and field cultures of its spores have already been reported (Rodriguez, 1996, and Refs. therein; Rojas et al., 1996). Here, a sporulation and sterilization method for producing axenic sporelings of *Gelidium canariensis* is described.

* Corresponding author.

*E-mail address:* pilar.garcia@biologia.ulpgc.es (P. Garcia-Jimenez)

0168-1656/99/$ - see front matter © 1999 Elsevier Science B.V. All rights reserved.
PII: S0168-1656(99)00077-2

© Del documento, los autores. Digitalización realizada por ULPGC. Biblioteca Universitaria, 2009

## 2. Materials and methods

Sporangial branchlets were excised from epiphyte-free thalli of *G. canariensis* collected at the North coast of Gran Canaria. Some branchlets were directly used to test the effect of the antibiotics according to the one-step antibiotic method (Saga and Sakai, 1982). As a result, we obtained an effective and non-inhibitory antibiotic solution mixture made of (final concentration in the culture medium): ampicillin (0.2 mg $ml^{-1}$), penicillin (0.2 mg $ml^{-1}$), rifampicin (0.2 mg $ml^{-1}$) nystatin (0.2 mg $ml^{-1}$) and germanium dioxide (0.1 g $ml^{-1}$).

To establish axenic cultures of sporelings we proceeded as follows: the branchlet was treated with 1% sodium hypochlorite for 2 min and then incubated overnight in 0.3 ml of sterilised seawater in multiwell plates. The seawater evaporated partially (between 30 and 50%), thus promoting a hydric stress for sporulation. The sporulation and sterilization procedure went on by transferring the branchlets to petri dishes with 20 ml of PES (Provasoli-enriched seawater; Provasoli, 1968) medium and the antibiotic solution described above. Controls of axenity were performed in bacteriological Marine Agar (Difco) to check the presence of surface contaminants, namely bacteria, fungi and other heterotrophic organisms. Thus, bacterial and fungal growth was not observed. Algal endophytes or epiphytes normally associated to *Gelidium* thalli were not recorded in the branchlets or sporelings.

Fig. 1. Part of a sporangial branchlet (b) of *G. canariensis* discharging tetraspores (small arrow). In detail, higher magnification of sporelings. Scale bar = 0.2 mm.

## 3. Results and discussion

Sporulation was mainly observed when preceded by hydric stress. Ninety percent of all cultivated branchlets cultivated under hydric stress released spores, while in controls without hydric stress, only 40–50% of branchlets sporulated. The hydric stress overnight and rehydration of the branchlet in the medium with antibiotics seemed to push the spores out. The benefits of a hydric stress for sporulation have previously been reported in other algae (Edding et al., 1987). Clusters of axenic spores, attached to the branchlet in a mucous layer, were formed within 30–45 days after reculture (ca 85–100 spores per cluster. One or two clusters per branchlet (Fig. 1)).

The development of the spores of *G. canariensis* was similar to that described in other Gelidiales (Macler and West, 1987; Fredriksen and Rueness, 1989). The first divisions were observed 3 or 4 days after, when the spores settled in the culture dishes and formed new cells (germ tube), that developed a pigmented cell which originated an erect axis. Within 55 days, the latter became an incipient prostrate system with small buds along the axis (Fig. 2).

In conclusion, the sporulation induced by hydric stress and sterilization with an appropriate mixture of antibiotics made it possible to establish axenic cultures from spores of the agarophytic red seaweed *Gelidium canariensis*. It remains to investigate whether the spores will grow in media supplemented with organic carbon sources.

## Acknowledgements

This work was financially supported by the Canarian Government grant PI1998/079.

© Del documento, los autores. Digitalización realizada por ULPGC. Biblioteca Universitaria, 2009

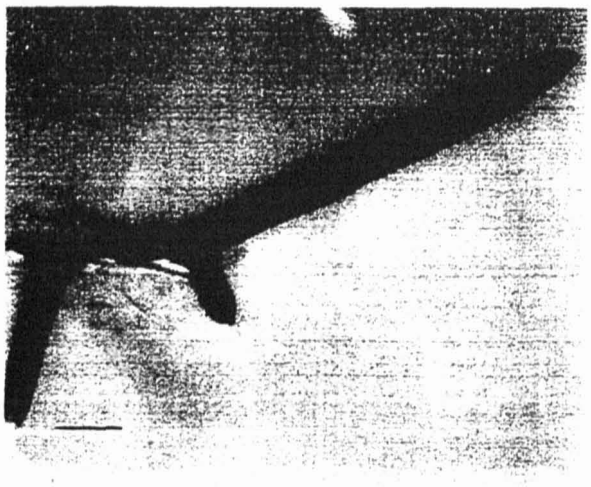

Fig. 2. Germinated and axenic sporelings showing elongation of a bud (b) after 45 days in Petri dish culture. Scale bar = 0.2 mm.

## References


Armisen, R., Galatas, F., 1987. Production, properties and uses of agar. In: McHugh, D.J. (Ed.), Production and Utilization of Products from Commercial Seaweed. FAO Fish Technical Papers. FAO, pp. 228–240.

Chen, F., 1996. High cell density culture of microalgae in heterotrophic growth. Trends Biotechnol. 14, 421–426.

Edding, M., León, C., Ambler, R., 1987. Growth of *Gracilaria* sp. in the laboratory. Hydrobiologia 151/152, 375–379.

Fredriksen, S., Rueness, J., 1989. Culture studies of *Gelidium latifolium* (Grev.) Born. et Thur. (Rhodophyta) from Norway. Growth and nitrogen storage in response to varying photon flux density, temperature and nitrogen availability. Bot. Mar. 32, 539–546.

Garcia-Jimenez, P., Robaina, R.R., Luque, A., Tsekos, I., 1996. Glycerol-activated cellular and biosynthetic activity during growth and morphogenesis of carpospore seedlings of *Grateloupia doryphora* (Cryptonemiales, Rhodophyta). Phycologia 35, 261–269.

Garcia-Jimenez, P., Rodrigo, M., Robaina, R.R., 1998. Influence of plant growth regulators, polyamines and glycerol interaction on growth and morphogenesis of carposporelings of *Grateloupia* cultured in vitro. J. Appl. Phycol. 10, 95–100.

Macler, B.A., West, J.A., 1987. Life history and physiology of the red alga *Gelidium coulteri*, in unialgal culture. Aquaculture 61, 281–293.

Provasoli, L., 1968. Media and prospects for the cultivation of marine algae. In: Watanabe, A., Hattori, A. (Eds.), Cultures and Collection of Algae. Japanese Society of Plant Physiologists, Tokyo, pp. 63–67.

Rodrigo, M., Robaina, R.R., 1997. Stress tolerance of photosynthesis in sporellings of the red alga *Grateloupia doryphora* compared to that of Stage III thalli. Mar. Biol. 128, 689–694.

Rodriguez, D., 1996. Vegetative propagation by fragmentation of *Gelidium sclerophyllum* (Gelidiales, Rhodophyta). Hydrobiologia 326/327, 361–365.

Rojas, H.R., León, N.M., Rojas, O.R., 1996. Practical and descriptive techniques for *Gelidium rex* (Gelidiales, Rhodophyta) culture. Hydrobiologia 326/327, 367–370.

Saga, N., Sakai, Y., 1982. A new method for pure culture of macroscopic algae, the one step selection method. Jpn. J. Phycol. 30, 40–43.


© Del documento, los autores. Digitalización realizada por ULPGC. Biblioteca Universitaria, 2009

ELSEVIER

Aquaculture 179 (1999) 489–497

Aquaculture

# Rearing techniques for red porgy (*Pagrus pagrus*) during larval development

C.M. Hernández-Cruz [a,*], M. Salhi [b], M. Bessonart [c], M.S. Izquierdo [a], M.M. González [b], H. Fernández-Palacios [b]

[a] *Universidad de Las Palmas de Gran Canaria, Facultad de Ciencias del Mar, Tafira Baja, 35017 Las Palmas de Gran Canaria, Canary Islands, Spain*

[b] *Instituto Canario de Ciencias Marinas, Gobierno de Canarias, Apdo. 56, 35200 Telde, Las Palmas, Canary Islands, Spain*

[c] *Instituto de Biología, Facultad de Ciencias, Universidad de la República, Iguá 4225, 11400 Montevideo, Uruguay*

**Abstract**

Red porgy can be considered as a potential candidate to diversify aquaculture production of sparids, due both to the importance of red porgy fisheries and market within Europe, and to its phylogenetic closeness to gilthead seabream. Spontaneously spawned eggs were obtained from a broodstock of wild individuals captured in Canarian waters. Different rearing trials were conducted to study the success of: (a) different egg stocking densities (100, 150 and 200 eggs/l); (b) first feeding with rotifers enriched with different products (Powersh-fish oil, freeze-dried shark eggs and Selco supplemented with *Nannochloropsis* sp); and (c) supply of rotifers to larval cultures at different concentrations (5, 7 and 10 rotifers/ml). In all cases, larval feeding lasted for 14 days. Larval length was measured at the time of mouth opening, at day 10 of life, and at the end of the experiments. Larval survival was estimated at the end of each experiment by counting all the remaining live larvae. Total lipid and fatty acid composition of rotifers and larvae were analyzed and discussed in relation to larval growth and survival. In this study, egg densities between 100 and 150 eggs/l and the use of rotifers enriched with Powersh-W, containing a high level of 22:6$n-3$, at concentrations of 5–7 rotifers/ml produced the best larval growth and survival. © 1999 Elsevier Science B.V. All rights reserved.

*Keywords: Pagrus pagrus* larvae; Egg density; Rotifer concentration; Enrichment diets; Lipid composition

* Corresponding author. Tel.: +34-07-928-132900; Fax: +34-07-928-132908; E-mail: carmenh@iccm.rcanaria.es

0044-8486/99/$ - see front matter © 1999 Elsevier Science B.V. All rights reserved.
PII: S0044-8486(99)00182-9

© Del documento, los autores. Digitalización realizada por ULPGC. Biblioteca Universitaria, 2009

## 1. Introduction

European aquaculture is restricted to the production of few marine fish species (Atlantic salmon, seabream, European seabass and turbot), diversification is one of today's greatest challenges for further aquaculture development. This interest in diversification focuses on only a few species, most of them belonging to the family Sparidae which plays an important role in world production (New, 1991).

The potential of sparids as a new species for aquaculture relies in the high degree of development achieved with some species of this family such as red or gilthead seabreams, and in particular of those new species with close biological characteristics. In the past, there have been several studies on new culture techniques to promote the diversification of aquaculture of these species (Hussain et al., 1981; Girin, 1982; Cejas et al., 1993a,b; Riera et al., 1993; Fernández-Palacios et al., 1994; Méndez et al., 1995; Tulli and Tibaldi, 1995).

Red porgy is a sparid with very good prospects for aquaculture due to its high commercial value in the Mediterranean and South Atlantic areas of Spain. However, studies carried out on this species in captivity are scarce, and primarily directed to reproduction, behavior in culture tanks and spawning (Fernández-Palacios et al., 1983; Kentouri et al., 1992), and embryonic and larvae development (Hernández-Cruz et al., 1990; Méndez et al., 1995). Consequently, the culture of the red porgy is still in an experimental phase.

Among the many parameters affecting larval culture success which could differ between red porgy and gilthead seabream, initial larval density, rotifer concentration in the culture tanks and type of enrichment were selected in the present study.

## 2. Materials and methods

Larval culture was conducted in cylindrical tanks filled with 100 l of seawater (36 g/l salinity) and kept under natural photoperiod (approximately 12 h light) and thermoperiod conditions. Central and continuous aeration was also provided.

The larval culture tanks were seeded with eggs from spontaneous spawnings obtained from a broodstock (*Pagrus pagrus*) of wild individuals captured in Canarian waters. All tanks were kept under a flow-through rearing system without feeding during the first three days after hatching, with a water flow of 0.5 l/min. Food was added from the 3rd to the 17th day post-hatch. During the feeding period the water flow was closed, except for a water exchange (21.6 l/h for 24 h) in the middle of the experiment to maintain good water quality.

Food was added on a daily basis. In all treatments, green water containing 3/4 *Nannochloropsis* sp and 1/4 *Isochrysis galbana* was supplied to achieve a concentration of $3 \times 10^5$ cells/ml and $0.3 \times 10^5$ cells/ml, respectively, in the culture tanks.

Three types of experiments were conducted: (A) the effect of different egg density (100, 150 and 200 eggs/l). Larvae were fed rotifers enriched with a commercial emulsion prepared with 1 g of Powersh-W (Oriental Yeast, Tokyo, Japan) and 100 ml

© Del documento, los autores. Digitalización realizada por ULPGC. Biblioteca Universitaria, 2009

water emulsion was added to 10 l of rotifer culture at a concentration of 150 rotifers/ml plus *Nannochloropsis* sp, during 18 h. The physical–chemical conditions during this experiment were: water temperature 19.18 ± 1.0°C; pH 8.00 ± 0.1; dissolved oxygen 6.92 mg/l; nitrates 3.80 μmole/l.

(B) The effect of type of rotifer enrichment during first feeding. The enrichments used were: (1) PFO: Powersh-W fish oil (Oriental Yeast, Tokyo, Japan) with the same conditions as the previous experiment. (2) SE: freeze-dried shark eggs (Oriental Yeast, Tokyo, Japan): 0.8 g/10 l of rotifer culture at a concentration of 150 rotifers/l) and *Nannochloropsis* sp, during 18 h. (3) S: Selco (Inve Animal Health, Gent, Belgium): 0.3 g Selco/10 l for each 10 l rotifer culture at a concentration of 200 rotifers/ml) and *Nannochloropsis* sp, during 18 h. The physical–chemical conditions during this experiment were: water temperature 17.9 ± 1.01°C; pH 7.90 ± 0.1; dissolved oxygen 7.46 mg/l; nitrates 1.21 μmole/l.

(C) The effect of supplying rotifers to larval cultures at different concentrations (5, 7 and 10 rotifers/ml). Rotifers were enriched in the same way as experiment (A). The physical–chemical conditions during this experiment were: water temperature 19.12 ± 1.0°C; pH 7.93 ± 0.1; dissolved oxygen 5.92 mg/l; nitrates 1.16 μmole/l.

Total lengths of 3-, 10- and 17-day old larvae were recorded to compare growth among the different treatments (30 larvae were measured per replicate). Larval survival was determined by individually counting the remaining live larvae at the end of the study. All treatments were tested in triplicate.

Rotifers and larvae from trial B where analyzed for total, polar and neutral lipid content and fatty acid composition. Lipids were extracted with a chloroform:methanol (2:1) mixture as described by Folch et al. (1957) and neutral and polar fractions were separated by adsorption chromatography on silica cartridges (Sep-pak, Waters, Milford, MA) as described by Juaneda and Rocquelin (1985). Fatty acid methyl esters were obtained by transesterification with 1% sulfuric acid in methanol (Christie, 1982), and separated, identified and quantified by gas chromatography. GLC conditions were the same as described by Izquierdo et al. (1990).

The statistical analysis was conducted using an ANOVA and Tukey test for multiple comparison of means (Sokal and Rohlf, 1981).

## 3. Results

Hatching rates were always close to 100% (98.61–99.35) and larval survival at day 3 was high (71–79%). In the first experiment, the highest egg concentration at seeding in the rearing tanks (200 eggs/l) significantly reduced larval growth from the beginning of the experiment (Table 1). Thus, larval total lengths at day 10 and 17 were significantly ($P < 0.01$) lower when 200 eggs/l were seeded instead of 100 or 150 eggs/l. There was no difference ($P > 0.05$) in larval survival, although the highest value was obtained with 100 eggs/l and the lowest with 200 eggs/l (Table 1).

Regarding the effect of enrichment products, the best growth (final total length) was found in larvae fed with rotifers enriched with Powersh-W followed by larvae fed with rotifers enriched with shark eggs (although not significantly different was larvae from

© Del documento, los autores. Digitalización realizada por ULPGC. Biblioteca Universitaria, 2009

Table 1
Growth and survival of 10- and 17-day old larvae obtained from eggs stocked at different densities. Total length of 3-day old larvae = 3.78 ± 0.14 mm. Mean within the same column followed by the same letter are not significantly different $P < 0.05$

| Egg density (eggs/l) | Total length (mm); mean ± sd, $n = 90$ | | Survival (%); mean ± sd, $n = 3$ |
|---|---|---|---|
| | 10-day old | 17-day old | 17-day old |
| 100 | 4.34 ± 0.27 a | 5.45 ± 0.50 a | 15.83 ± 19.64 |
| 150 | 4.38 ± 0.25 a | 5.46 ± 0.39 a | 4.52 ± 0.07 |
| 200 | 4.20 ± 0.22 b | 4.96 ± 0.57 b | 3.31 ± 0.03 |

the previous treatment at day 17). The lowest growth and survival ($P < 0.01$) were obtained in larvae fed with rotifers enriched with Selco (Table 2).

Total lipid content in rotifers enriched with Powersh-W was slightly higher than in those enriched with shark eggs and Selco (Table 3), mainly due to an increase in the percentage of neutral lipid. Rotifers enriched with Powersh-W had a higher $n-3$ HUFA, DHA (22:6$n-3$) and EPA (20:5$n-3$) content in their total lipid than those enriched with shark eggs and Selco. Both of the latter rotifers were similar in their total $n-3$ HUFA content, although the DHA/EPA ratio of S rotifers was lower than that of SE rotifers; the DHA/EPA ratio found in PFO was similar to that of SE rotifers (Table 3).

Total lipid content of larvae fed the different enriched rotifers was lower than that found in the initial larvae, mainly due to a reduction in the percentage of neutral lipid (Table 4). At the end of the experiment, larvae fed any of the enriched rotifers (PFO, SE, S) showed a marked reduction in the $n-3$ HUFA content in total lipid, due to a strong reduction in the DHA content, and in spite of the increase in EPA, relative to the initial levels. Although the $n-3$ HUFA content in the total lipid was similar among the larvae fed with the enriched rotifers, the larvae fed with Selco rotifers showed a higher amount of EPA and a third of the DHA level than the other two treatments (Table 4). Regarding neutral lipid composition, larvae fed with rotifers were characterized by a general increase in EPA and a decrease in DHA levels in comparison to initial values and, accordingly, with lower DHA/EPA ratios. DHA, $n-3$ HUFA content, and DHA/EPA ratio of larvae fed with PFO rotifers were higher than in the other larvae

Table 2
Total length and survival of 10- and 17-day old larvae fed rotifers enriched with the different treatments. Total length of 3-day old larvae = 3.78 ± 0.13 mm. Mean within the same column followed by the same letter are not significantly different $P < 0.01$

| Enrichment treatment | Total length (mm); mean ± sd, $n = 90$ | | Survival (%); mean ± sd, $n = 3$ |
|---|---|---|---|
| | 10-day old | 17-day old | 17-day old |
| PFO | 4.32 ± 0.27 a | 5.30 ± 0.50 a | 17.70 ± 2.16 |
| SE | 4.21 ± 0.26 b | 5.24 ± 0.56 a | 10.54 ± 11.71 |
| S | 4.11 ± 0.25 c | 4.58 ± 0.34 b | 8.82 ± 4.51 |

© Del documento, los autores. Digitalización realizada por ULPGC. Biblioteca Universitaria, 2009

Table 3
Lipid (% dry weight) and selected fatty acid composition (% total fatty acids) of total lipids of rotifers enriched with the different treatments

| Lipid composition | PFO | SE | S |
|---|---|---|---|
| Total lipid | 24.28 | 22.07 | 22.71 |
| Neutral lipid | 16.79 | 13.79 | 14.50 |
| Polar lipid | 7.49 | 8.28 | 8.21 |
| $n-3$ HUFA | 27.24 | 17.48 | 16.42 |
| 20:5$n-3$ | 11.07 | 5.79 | 9.51 |
| 22:6$n-3$ | 13.21 | 7.82 | 3.89 |
| DHA/EPA | 1.19 | 1.35 | 0.41 |

including the initial one (except for the DHA/EPA ratio which was higher in the initial larvae), followed by those fed with SE rotifers (Table 4). In the polar lipids, DHA and $n-3$ HUFA content of fed larvae were lower than in the initial larvae, whereas EPA showed a trend to increase. Among treatments, larvae fed with Selco rotifers showed the highest $n-3$ HUFA and EPA levels, and lower DHA content. Larvae fed with shark eggs rotifers had the highest DHA proportion in polar lipids of larvae.

Table 4
Lipid (% dry weight) and selected fatty acid composition (% total fatty acids) of 3- (initial) and 17-day old red porgy larvae fed with Powersh-W fish oil (PFO), shark eggs (SE) and Selco (S)-enriched rotifers

| Lipid composition | Initial | Treatment | | |
|---|---|---|---|---|
| | | PFO | SE | S |
| Total lipid (TL) | 31.96 | 21.35 | 19.98 | 24.61 |
| Neutral lipid (NL) | 18.13 | 8.07 | 7.84 | 8.92 |
| Polar lipid (PL) | 13.83 | 13.28 | 12.14 | 15.69 |
| *Fatty acids in TL* | | | | |
| $n-3$ HUFA | 33.20 | 26.74 | 26.59 | 26.54 |
| 20:5$n-3$ | 4.51 | 7.18 | 7.44 | 10.65 |
| 22:6$n-3$ | 26.90 | 15.46 | 14.42 | 5.69 |
| DHA/EPA | 5.97 | 2.15 | 1.94 | 0.90 |
| *Fatty acids in NL* | | | | |
| $n-3$ HUFA | 21.01 | 29.69 | 20.37 | 15.94 |
| 20:5$n-3$ | 3.38 | 8.30 | 7.02 | 7.48 |
| 22:6$n-3$ | 15.90 | 16.94 | 9.13 | 4.20 |
| DHA/EPA | 4.70 | 2.04 | 1.30 | 0.56 |
| *Fatty acids in PL* | | | | |
| $n-3$ HUFA | 49.18 | 25.00 | 30.61 | 32.58 |
| 20:5$n-3$ | 5.98 | 6.51 | 7.71 | 12.45 |
| 22:6$n-3$ | 41.38 | 14.60 | 17.84 | 12.71 |
| DHA/EPA | 6.91 | 2.24 | 2.31 | 1.02 |

© Del documento, los autores. Digitalización realizada por ULPGC. Biblioteca Universitaria, 2009

Table 5
Growth and survival of 10- and 17-day old larvae fed at different rotifer concentration. Total length of 3-day old larvae = 3.79 ± 0.23 mm. Mean within the same column followed by the same letter are not significantly different $P < 0.05$

| Concentration (rotifers/ml) | Total length (mm); mean ± sd, $n = 90$ | | Survival (%); mean ± sd, $n = 3$ |
|---|---|---|---|
| | 10-day old | 17-day old | 17-day old |
| 5 | 4.27 ± 0.27 | 5.28 ± 0.63 | 9.32 ± 12.54 |
| 7 | 4.29 ± 0.23 | 5.25 ± 0.52 | 13.90 ± 16.07 |
| 10 | 4.24 ± 0.28 | 5.31 ± 0.41 | 4.89 ± 11.65 |

With respect to rotifer concentration, there were no significant differences in larval growth and survival among treatments (Table 5).

## 4. Discussion

In all experiments the rates of hatching and larval survival at first feeding were high, indicating the quality of eggs obtained from the experimental broodstock was good (Fernández-Palacios et al., 1995).

In the first trial the low larval growth and survival obtained when 200 eggs/l were seeded may be associated with several factors such as higher competition for prey, deterioration in water quality, reduction in prey availability, or chronic stress caused by overcrowding. As egg density was increased over 150 eggs/l, survival was reduced to a third of that obtained with a density of 100 eggs/l. These results agree well with the egg stocking density used in sparids larviculture (100 egg/l or less) (Tandler and Helps, 1985; Foscarini, 1988; Tandler et al., 1989; Kentouri et al., 1995).

The poor larval growth performance obtained with Selco-enriched rotifers seems to be related either to the low DHA (0.78% d.w.) content or to the low DHA/EPA ratio (0.41) in the rotifers, rather than to the total $n-3$ HUFA (3.28% d.w.) content, since shark egg-enriched rotifers, with the same $n-3$ HUFA (3.39% d.w.) level but a higher DHA (1.51% d.w.) and DHA/EPA (1.35) gave better results. DHA is known to have a higher efficiency as essential fatty acid than EPA (Watanabe et al., 1983), the former being particularly accumulated in the olfactory nerve, retina and central neural system (Sargent et al., 1993; Mourente and Tocher, 1992). But, besides a minimum dietary requirement for DHA, its relative proportion with EPA in larval diets and body tissues seems to be related with better larval performance, as competitive interactions between both fatty acids are present at different levels in fatty acid metabolism (Izquierdo et al., 1999). Thus, a reduction in the DHA/EPA ratio from 1 (DHA and $n-3$ HUFA 1.1 and 2.5% d.w., respectively) to 0.65 (DHA 1.1 and $n-3$ HUFA 1.1 and 3% d.w., respectively) in microdiets for gilthead seabream larvae, displaced the DHA from larval phosphatidyl choline (PC), increased the EPA content in phosphatidyl ethanolamine (PE) and reduced larval growth (Bessonart, 1997; Izquierdo et al., 1999). Higher DHA/EPA ratios in wild copepods fed to Atlantic halibut have also been associated with higher DHA/EPA ratios in eye PC and PE and normally pigmented fish (McEvoy

© Del documento, los autores. Digitalización realizada por ULPGC. Biblioteca Universitaria, 2009

et al., 1998). In the present experiment, larvae fed with Selco-enriched rotifers showed lower DHA content in larval neutral and polar lipid together with high EPA content in polar lipids. This observation has been associated with a reduction in growth in other sparids (Izquierdo, 1996; Izquierdo et al., 1989; Rodríguez, 1994; Bessonart, 1997).

On the other hand, after 7 days feeding, larvae fed with Powersh-W-enriched rotifers showed better growth than those fed with shark egg-enriched rotifers, suggesting a higher DHA need during the first days of larval life, as seen in a parallel study on patterns of lost and conservation of fatty acids in fed and starved larval red porgy (Bessonart et al., 1998). In fact, the high DHA/EPA ratio found in total lipid of the 3-day old larvae (5.97/1) compared to that observed in *Sparus aurata* larvae (2.0/1 by Rodríguez et al. (1993) and 1.4/1 to 3.2/1 by Hernández-Cruz (1993)) supports this argument. Accordingly, several authors have demonstrated the importance of DHA as a structural component of developing organs and tissues (Arnaiz et al., 1993; Coo et al., 1993), and consequently in the larval growth and development of marine fish (Watanabe et al., 1989; Mourente and Tocher, 1992; Mourente et al., 1993; Koven et al., 1993; Izquierdo, 1996). In addition, inadequate dietary DHA may have a negative effect on the visual capacity of the fish in its predation ability and subsequently in its growth (Mourente and Tocher, 1992).

On the other hand, growth and survival of larvae was not affected by the concentrations of rotifers employed. Similar results have been obtained for several species, such as gilthead seabream, 10–15 rot/ml (Tandler and Sherman, 1981), red seabream, 3–5 rot/ml (Foscarini, 1988), and dentex, 7–9 rot/ml (Glamuzina et al., 1989).

## Acknowledgements

We acknowledge Dr. Toshio Takeuchi from Tokyo University of Fisheries, who kindly provided some of the enrichment media. This study has been financed by the CICYT (project AGF94-0882-C03-01) for 1994-1997 and the Vice Ministry of Fisheries of the Canarian Government in the frame of the National Plans of Marine Culture.

## References

Arnaiz, R., Coo, A., Coroobado Oñate, F., Rua, N., Amoedo, F., 1993. Una hipótesis nutricional de la mortalidad asociada al periodo crítico. Órganos y desarrollo larvario de rodaballo (*Scophthalmus maximus*) y dorada (*Sparus aurata*). Necesidades de DHA. In: Cerviño, A., Landín, A., Coo, A., Guerra, A., Torre, M. (Eds.), Actas. IV Congreso Nacional de Acuicultura, Villagarcía de Arosa, Spain, pp. 73–78.

Bessonart, M., 1997. Effecto de las relaciones EPA/DHA y EPA/AA en el cultivo larvario de la dorada (*Sparus aurata* L.). PhD Thesis, Universidad de Las Palmas de Gran Canaria, Spain, 181 pp.

Bessonart, M., Salhi, M., Hernández-Cruz, C.M., Izquierdo, M.S., Fernández-Palacios, H., 1998. Fatty acid composition of eggs and fed and starved larvae of red porgy (*Pagrus pagrus* L.). In: G.I.A. Grupo de Investigación en Acuicultura (Eds.), Recent Advances in Finfish and Crustacean Nutrition. Abstracts VIII International Symposium on Nutrition and Feeding of Fish, 1–4 June, Las Palmas de G.C., Spain, pp. 206.

Cejas, J., Jerez, S., Santamaría, F.J., Samper, M., 1993. Estudios preliminares de la reproducción y cultivo larvario de la breca (*Pagellus erythrinus*) en cautividad. In: Cerviño, A., Landín, A., Coo, A., Guerra, A., Torre, M. (Eds.), Actas. IV Congreso Nacional de Acuicultura, Villagarcía de Arosa, Spain, pp. 61–65.

Cejas, J., Samper, M., Jerez, S., Forés, R., Villamandos, J., 1993. Perspectivas de cultivo de breca (*Pagellus*

© Del documento, los autores. Digitalización realizada por ULPGC. Biblioteca Universitaria, 2009

*erythrinus*) y sargo (*Diplodus sargus*); primeros resultados de crecimiento comparado con la dorada (*Sparus aurata*). In: Cerviño, A., Landín, A., Coo, A., Guerra, A., Torre, M. (Eds.), Actas. IV Congreso Nacional de Acuicultura, Villagarcía de Arosa, Spain, pp. 127–132.

Christie, W.W., 1982. Lipid Analysis. Pergamon, Oxford, England, 207 pp.

Coo, A., Moscoso, E., Arnaiz, R., Corcobado Oñate, F., Rua, N., Varela, J.A., López, M., 1993. Estudio histológico, de crecimiento, mortalidad y desarrollo del aparato digestivo, branquial e hígado, en larvas de rodaballo, sometidas a ayuno y diferentes niveles de deficiencias en HUFAs w3. In: Cerviño, A., Landín, A., Coo, A., Guerra, A., Torre, M. (Eds.), Actas. IV Congreso Nacional de Acuicultura, Villagarcía de Arosa, Spain, pp. 79–84.

Fernández-Palacios, H., Moreno, E., Falcón, J.C., Fernández-Palacios, J.E., Hernández-Cruz, C.M., De la Portilla, Y., Ramírez, R., Sacristán, D., Vergara, J.M., O'Shanahan, L., Medina, A., Santana, C., 1983. Plan para el establecimiento de los cultivos marinos en aguas de archipiélago canario. In: Consejería de Agricultura y Pesca, Gobierno de Canarias (Eds.). Santa Cruz de Tenerife, Spain, 294 pp.

Fernández-Palacios, H., Montero, D., Socorro, J., Izquierdo, M.S., Vergara, J.M., 1994. First studies on spawning, embryonic and larvae development of *Dentex dentex* (Rafinesque, 1810) (Osteichthyes) under controlled conditions. Aquaculture 122, 63–73.

Fernández-Palacios, H., Izquierdo, M.S., Robaina, L., Salhi, M., Vergara, J.M., 1995. Effect of $n-3$ HUFA level in broodstock diets on egg quality of gilthead sea bream (*Sparus aurata* L.). Aquaculture 132, 325–337.

Folch, J., Lees, M., Sloane Stanley, G.H., 1957. A simple method for the isolation and purification of total lipids from animal tissues. J. Biol. Chem. 226, 497–509.

Foscarini, R., 1988. A review: intensive farming procedure for red sea bream (*Pagrus major*) in Japan. Aquaculture 72, 193–240.

Girin, M., 1982. The Sparidae: a warmwater finfish family with world-wide mariculture potential. In: Stickney, R.R., Meyers, S.P. (Eds.), Proceedings of the Warmwater Fish Culture Workshop, Louisiana State University, Baton Rouge, Vol. 3, pp. 3–14.

Glamuzina, B., Juc-Dujakovic, J., Katavic, I., 1989. Preliminary studies on reproduction and larval rearing of common dentex, *Dentex dentex* (Linnaeus 1758). Aquaculture 77, 75–84.

Hernández-Cruz, C.M., 1993. Mejora de las técnicas de cultivo larvario de dorada (*Sparus aurata* L., 1758). PhD Thesis. Universidad de la Laguna, Spain, 149 pp.

Hernández-Cruz, C.M., Fernández-Palacios, H., Fernández-Palacios, J.E., 1990. Estudio preliminar del desarrollo embrionario y larvario del bocinegro, *Pagrus pagrus* (Piscis: Sparidae), en cultivo. Vieraea 19, 215–224.

Hussain, N., Akatsu, S., El-Zahr, C., 1981. Spawning, egg and early larval development, and growth of *Acanthopagrus cuvieri* (Sparidae). Aquaculture 22, 125–136.

Izquierdo, M.S., 1996. Essential fatty acid requirements of cultured marine fish larvae. Aquacult. Nutr. 2, 183–191.

Izquierdo, M.S., Watanabe, T., Takeuchi, T., Arakawa, T., Kitajima, C., 1989. Requirement of larval red seabream *Pagrus major* for essential fatty acids. Nippon Suisan Gakkaishi 55, 859–867.

Izquierdo, M.S., Watanabe, T., Takeuchi, T., Arakawa, T., Kitajima, C., 1990. Optimal EFA levels in *Artemia* to meet the EFA requirements of red seabream (*Pagrus major*). In: Takeda, M., Watanabe, T. (Eds.), The Current Status of Fish Nutrition in Aquaculture. Tokyo University Fisheries, Tokyo, pp. 221–232.

Izquierdo, M.S., Socorro, J., Arantzamendi, L., Hernández-Cruz, C.M., 1999. The interaction between lipid nutrition, fatty acid metabolism and growth in marine fish. Fish Physiol. Biochem., in press.

Juaneda, P., Rocquelin, G., 1985. Rapid and convenient separation of phospholipids from rat heart using silica cartridges. Lipids 20, 40–41.

Kentouri, M., Koumoundourus, G., Divanach, P., Sterioti, A., 1992. The embryonic development of red porgy (*Pagrus pagrus*) and of common dentex (*Dentex dentex*) in Crete. C.I.E.S.M. XXXIIIe Congres-Assemple Pleniere Triest, 12–17 Oct. 1992.

Kentouri, M., Pavlides, M., Papandroulakis, N., Divanach, P., 1995. Culture of the red porgy, *Pagrus pagrus*, in Crete. Present knowledge, problems and perspectives. Cah. Options Méditerr. ISSN 16, 65–78.

Koven, W.M., Tandler, A., Sklan, D., Kissil, G.W.M., 1993. The association of eicosapentaenoic and docosahexaenoic acids in the phospholipidids of different age *Sparus aurata* larvae with growth. Aquaculture 116, 71–82.

© Del documento, los autores. Digitalización realizada por ULPGC. Biblioteca Universitaria, 2009

McEvoy, L.A., Naess, T., Bell, J.G., Lie, O., 1998. Lipid and fatty acid composition of normal and malpigmented Atlantic halibut (*Hippoglossus hippoglossus*) fed enriched *Artemia*: a comparison with fry fed wild copepods. Aquaculture 163, 237–250.

Méndez, E., Anastasiadis, P., Kentouri, M., Pavlidis, M., Divanach P., 1995. Preliminary data on spawning activity of five mediterranean teleost species kept in captivity, in Crete (Greece). In: Castelló, F., Calderer, A. (Eds.), Actas V Congreso Nacional de Acuicultura, San Carles de la Rápita, Spain, pp. 398–403.

Mourente, G., Tocher, D.R., 1992. Effects of weaning onto a pelleted diet on docosahexaenoic acid (22:6$n-3$) levels in brain of developing turbot (*Scophthalmus maximus* L.). Aquaculture 105, 363–377.

Mourente, G., Rodríguez, A., Tocher, D.R., Sargent, J.R., 1993. Effects of dietary docosahexaenoic acid (DHA; 22:6$n-3$) on lipid and fatty acid compositions and growth in gilthead seabream (*Sparus aurata* L.) larvae during first feeding. Aquaculture 112, 79–98.

New, M.B., 1991. Turn of the millennium aquaculture. Navigating troubled waters or riding the crest of the wave?. World Aquacult. 22 (3), 28–49.

Riera, F., Pastor, E., Grau, A.M., Pou, S., Grau, A., Massuti E., 1993. Experiencias en el cultivo del dentón (*Dentex dentex*). In: Cerviño, A., Landín, A., Coo, A., Guerra, A., Torre, M. (Eds.), Actas, IV Congreso Nacional de Acuicultura, Villagarcía de Arosa, Spain, pp. 143–148.

Rodríguez, C., 1994. Estudio de los requerimientos de ácidos grasos esenciales de la dorada europea (*Sparus aurata* L.) durante las dos primeras semanas de alimentación. PhD Thesis. Universidad de La Laguna, Spain, 284 pp.

Rodríguez, C., Pérez, J.A., Izquierdo, M.S., Mora, J., Lorenzo, A., Fernández-Palacios, H., 1993. Essential fatty acid requirements of larval gilthead sea bream, *Sparus aurata* (L.). Aquacult. Fish. Manage. 24, 295–304.

Sargent, J.R., Bell, M.V., Tocher, D.R., 1993. Docosaheaenoic acid and the development on brain and retina in marine fish. In: Drevon, C.A., Baksaas, I., Krokan, H.E. (Eds.), Omega-3 fatty acids: metabolism and biological effects. Birkhauser Verlag, Basel, Switzerland, pp. 139–149.

Sokal, R.R., Rohlf, J., 1981. Biometry. The Principles and Practice of Statistics in Biological Research, 2nd edn. Freeman, New York, 859 pp.

Tandler, A., Helps, S., 1985. The effect of photoperiod and water exchange rate on growth and survival of gilthead seabream (*Sparus aurata*, Linnaeus, Sparidae) from hatching to metamorphosis in mass rearing systems. Aquaculture 48, 71–82.

Tandler, A., Sherman, R., 1981. Food organism concentration, environmental temperature and survival of the gilthead seabream *Sparus aurata* Linnaeus, Sparidae). Spec. Publ. Eur. Maricult. Soc. 6, 237–248.

Tandler, A., Harel, M., Wilks, M., Levinson, A., Brickell, L., Christie, S., Avital, E., Barr, Y., 1989. Effect of environmental temperature on survival, growth and population structure in mass rearing of gilthead seabream, *Sparus aurata*. Aquaculture 78, 277–284.

Tulli, F., Tibaldi, E., 1995. Changes in fatty acid and amino acid composition of *Dentex dentex* during early development. In: Lavens, P., Jaspers, E., Roelants, I. (Eds.), Larvi 1995. European Aquaculture Society, Spec. Publ., 24, pp. 39–43.

Watanabe, T., Tamiya, T., Oka, A., Hirata, M., Kitajima, C., Fujita, S., 1983. Improvement of dietary value of live foods for fish larvae by feeding them $\omega 3$ highly unsaturated fatty acids and fat soluble vitamins. Bull. Jpn. Soc. Sci. Fish. 49, 471–479.

Watanabe, T., Izquierdo, M.S., Takeuchi, T., Satoh, S., Kitajima, C., 1989. Comparison between eicosapentaenoic and docosahexaenoic acids in terms of essential fatty acid efficacy in larval red seabream. Nippon Suisan Gakkaishi 55, 1635–1640.

© Del documento, los autores. Digitalización realizada por ULPGC. Biblioteca Universitaria, 2009

*Journal of Oceanography*, Vol. 55, pp. 471 to 482, 1999

# Large-Scale and Mesoscale Distribution of Plankton Biomass and Metabolic Activity in the Northeastern Central Atlantic

SANTIAGO HERNÁNDEZ-LEÓN[1], LUTZ POSTEL[2], JAVIER ARÍSTEGUI[1], MAY GÓMEZ[1], MARÍA FERNANDA MONTERO[1], SANTIAGO TORRES[1], CARLOS ALMEIDA[1], EUGEN KÜHNER[3], ULLRICH BRENNING[3] and EBERHARD HAGEN[2]

[1]*Facultad de Ciencias del Mar, Campus Universitario de Tafira, 35017 Las Palmas de Gran Canaria, Islas Canarias, Spain*
[2]*Institut für Ostseeforschung, Seestr. 15, D 18119, Warnemünde, Rostock, Germany*
[3]*Universität Rostock, Fachbereich Biologie, Rostock, Germany*

(Received 5 May 1998; in revised form 26 January 1999; accepted 27 January 1999)

**Plankton biomass and indices of metabolism and growth [electron transport system (ETS), glutamate dehydrogenase (GDH) and aspartate transcarbamylase (ATC) activities] were studied over a 2,800 km east-west section of the tropical North Atlantic Ocean (21°N) in <200, 200–500 and >500 μm size classes. On the large-scale, zooplankton (>200 μm) enzymatic activities increased westward in the study section, where large cyanobacteria chains (*Trichodesmium spp.*) were observed. Parallel to it, an increase in medium calanoids (1–2 mm length) was observed towards the western part of the transect, whereas small calanoids (<1 mm) were dominant throughout the boundary area of the subtropical gyre. Microplankton ETS and mesoplankton ETS and ATC activities seemed to match the wave length of low frequency waves. Our results suggest that such waves are related to the observed enhancement of metabolic activity of micro- and mesoplankton. The large-scale and mesoscale variability observed give evidence of the inadequacy of assuming a steady-state picture of the euphotic zone of tropical and subtropical waters.**

Keywords:
- Plankton,
- biomass,
- metabolism,
- northeast Central Atlantic.

## 1. Introduction

Subtropical gyres are considered to be among the most stable areas of the ocean. The thermal and saline structures of the water column do not undergo drastic seasonal changes. Generally, low variations are observed in the values of both chlorophyll and zooplankton biomass. In contrast, high fluctuations are found in temperate and equatorial areas, where seasonality and large-scale divergences cause variations in the thermal structure (e.g., Voituriez and Herbland, 1977; Kaiser and Postel, 1979). The relationship between the productivity of a system and the vertical structure of the water column has been widely studied during the last decades. Extensive work has been carried out related to the presence of subsurface chlorophyll maxima (see Longhurst and Harrison, 1989), the importance of new and regenerated production (Platt *et al.*, 1992), the role of zooplankton in controlling the vertical structure of phytoplankton populations (Roman *et al.*, 1986) and zooplankton vertical migrations as a mediating process in the vertical transport of organic and inorganic material in the ocean (Longhurst *et al.*, 1990). However, most of these studies were done in single locations and the results extrapolated to large regions of the ocean (see Longhurst and Harrison, 1989 for review).

Recent work on the effect of mesoscale and large-scale physical variability on phytoplankton in subtropical waters, has shown that these areas are not as homogeneous as believed. Venrick (1990) suggested that long period waves (e.g., Rossby waves) were probably responsible of the mesoscale variability of phytoplankton in the Central Pacific. However, this author stated that the agreement between spatial scales of chlorophyll and dynamic topography could result from vertical displacement of the chlorophyll profile without a change in absolute concentration, or alternatively, the redistribution of chlorophyll in the water column, or the effect of phytoplankton growth. Patterns of biological variability in relation to these mesoscale physical instabilities in tropical and subtropical areas still remain relatively unknown.

Here we report the results of a transect of 2,800 km, perpendicular to the African coast at 21°N (Fig. 1) which was sampled every 60 nautical miles in order to study the variability of both micro- and mesoplankton biomass and metabolic activity distributions caused by large-scale and mesoscale physical processes. Measurements of stock pa-



Copyright © The Oceanographic Society of Japan.

© Del documento, los autores. Digitalización realizada por ULPGC. Biblioteca Universitaria, 2009

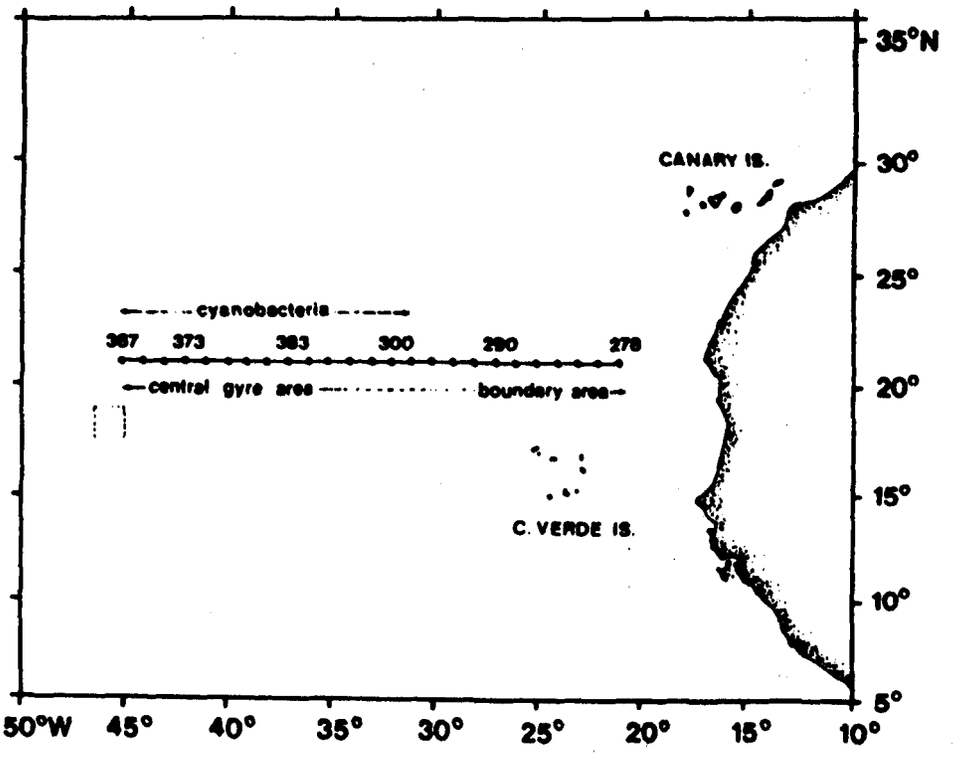


Fig. 1. Location of oceanographic sampling stations in the north Central Atlantic. The research cruise was conducted in September 1989 and biological sampling was carried out every 60 miles. Indicated boundary and central gyre conditions are based on temperature and salinity data. Presence of cyanobacteria chains is also indicated, as observed from plankton net catches. The squared area south of station 367 correspond to the area where stations 318, 346 and 362 of Table 1 were sampled.

rameters such as plant pigment concentrations could not be used to detect biological consequences of physical instabilities because of the uncertainties mentioned by Venrick (*op. cit.*) as well as the effect of grazing on a day-night basis (Le Bouteiller and Herbland, 1982). Moreover, very low values of chlorophyll and primary production are commonly observed in those areas (e.g., Gieskes and Kraay, 1986; Venrick, 1990). The lack of a phytoplankton-specific productivity method and the effect of grazing hinder the observation of the physical instability effects on the autotrophic communities of warm waters. The rates of processes related to the transfer of energy between the different trophic levels is high in warm oceanic waters, and the energy flow must be rapidly channeled to the so-called microbial loop and zooplankton. Therefore, indices of metabolism and growth can lead to the ultimate result of an increase in phytoplankton specific production. Enzymatic methods were used as indices to study the variability in plankton metabolism and growth. The electron transport system (ETS), glutamate dehydrogenase (GDH) and aspartate transcarbamylase (ATC) activities were used respectively as indices of respiration (Packard, 1969, 1971; King and Packard, 1975; Owens and King, 1975 and others), ammonium excretion (Bidigare and King, 1981; Bidigare *et al.*, 1982; King, 1984; King *et al.*, 1987) and growth (Bergeron and Buestel, 1979; Alayse-Danet, 1980; Bergeron, 1982) or moulting (Hernández-León *et al.*, 1995). Other approaches would not be useful in this case because classical procedures could not produce enough data to get a sufficient resolution in space. Nowadays, there is some agreement that this methodology produces rather good estimations when the enzyme is not limited by intracellular substrates (Hernández-León and Gómez, 1996; Packard *et al.*, 1996; Hernández-León and Torres, 1997). A clear underestimation of metabolic activity is achieved when the cell is substrate limited. Therefore, our estimations should be considered as a lower limit on metabolic activity.

## 2. Material and Methods

The transect was carried out on board the R/V "A.v. Humboldt" during August–September, 1989 (Fig. 1). Stations 278 to 308 were sampled from August 30th to September 5th and stations 367 to 383 from September 14th to 17th. Measurements of temperature and salinity were made by means of a CTD probe mounted in a rosette with Niskin-type bottles (3 L) from which samples for salinity, nutrients and primary production were obtained. Nutrients (nitrate, phosphate and silicate) were analysed using the procedures described in Strickland and Parsons (1972), although only phosphate concentrations are shown in the figures.



© Del documento, los autores. Digitalización realizada por ULPGC. Biblioteca Universitaria, 2009

Community production and respiration were measured by the oxygen method. Water samples were prefiltered through a 200 μm mesh, poured into acid-cleaned plastic carboys and mixed well before using for productivity experiments. Problems related to the formation of air bubbles inside the bottles restricted the sampling to the mixed layer. Six to eight clear and dark acid-cleaned borosilicate bottles (c.a. 125 ml) were incubated for 8 to 12 hours from dawn to dusk. We used on-deck incubators cooled with surface water, screened to simulate the "in situ" light conditions. Dissolved oxygen was measured with the Winkler technique following the recomendations of Carrit and Carpenter (1966), Bryan *et al.* (1976) and Grasshoff *et al.* (1983). The final end point of the titration process was controlled by means of an automated precise oxygen titration system similar to that described by Williams and Jenkinson (1982). Corrections for "in situ" temperature and salinity at the time of fixing the samples were taken into consideration. The precision achieved in the replicates was in the order of CV < 0.1%. Only experiments where differences between the initial dark and clear bottles were statistically significant at the 95% confidence limits were considered. $^{14}C$-uptake determinations were obtained after incubating two clear and one dark 125 ml bottles, at saturating light levels, in an artificial-light incubator for three hours. At the end of the experiment, samples were filtered, dried, fumed over concentrated HCl and stored for later analysis in the laboratory.

For microplankton ETS activity determinations, about five liters of seawater were sampled with acid-cleaned Niskin bottles (5 L) at standard depths ranging from surface to 100 m. Only samples for the determination of respiration/ETS (R/ETS) ratio in microplankton were obtained from the rosette sampler. Filtration was done immediately onto glass fiber filters (Whatman GF/F), after prefiltering the samples through 200 μm. The plankton-coated filters were then immediately frozen in liquid nitrogen until assayed in the laboratory. ETS activity was measured using the procedure of Kenner and Ahmed (1975). Samples were incubated at 18°C, but all the activities were corrected to "in situ" temperature using the Arrhenius equation and an activation energy of 15 kcal·mol$^{-1}$ (Packard *et al.*, 1975).

Zooplankton were caught by means of a WP-2 double net (UNESCO, 1968), equipped with a 200 μm mesh size net in the 0–25, 25–75 and 75–200 m layers. Seawater volume filtered was measured with a previously-calibrated TSK-like flowmeter in one of the two nets. Biomass was determined as protein content (Lowry *et al.*, 1951) using bovine serum albumine (BSA) as the standard. Samples were fractionated on board for the 200–500 μm and >500 μm size classes. $N_2$ fixating cyanobacteria were found in the plankton net catches over long distances in our transect (Fig. 1). We were unable to quantify the biomass and production of these organisms, mainly due to methodological problems. We opted to avoid these organisms from our micro- and mesoplankton samples. These large cyanobacteria chains could interfere with our measurements of biomass and metabolic indices, hindering the response of plankton to the presence of such organisms. Therefore, care was taken in order to clean the samples as much as possible from *Trichodesmium spp.* in the fractionation process. Samples

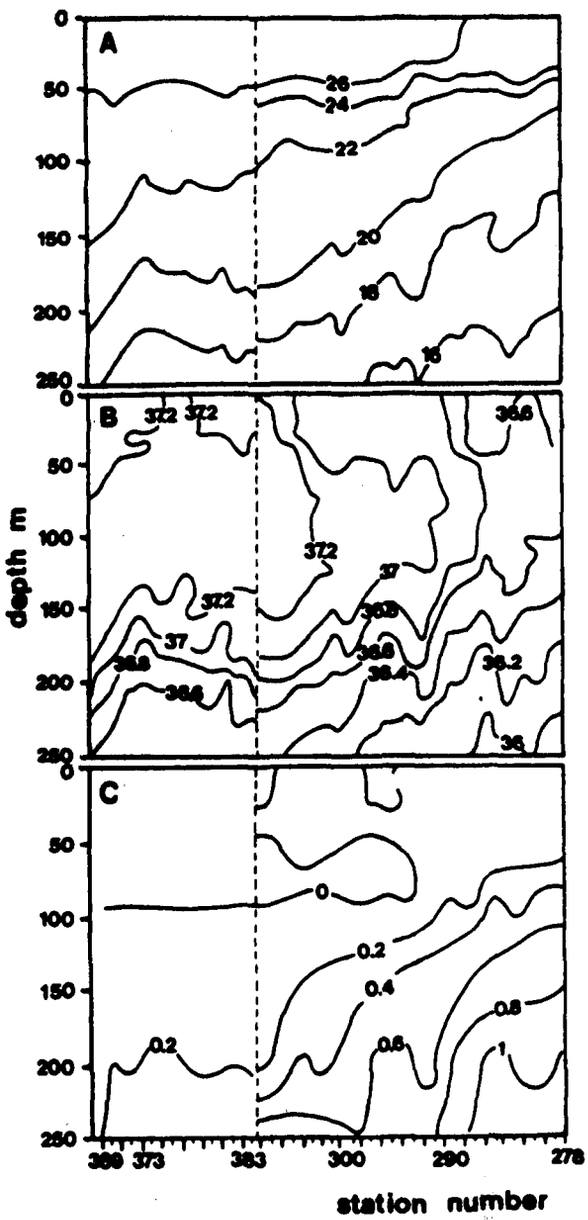


Fig. 2. Temperature (°C), salinity (PSU) and phosphate (μmol·dm$^{-3}$) profiles. The vertical line in the profiles represents a break of 12 days between the two sampling periods of the transect (see text). Observe the differences in temperature, salinity and phosphate between the east and west sides of the section. Changes in salinity and phosphate distribution were used to distinguish between boundary and central gyre conditions.



© Del documento, los autores. Digitalización realizada por ULPGC. Biblioteca Universitaria, 2009

of the >500 μm size fraction were easily cleaned of cyanobacteria while a slightly higher water pressure was applied to the 200–500 μm samples until those organisms visually disappeared. Samples were preserved in liquid nitrogen until analysis in the laboratory. Electron transport system (ETS), glutamate dehydrogenase (GDH) and aspartate transcarbamylase (ATC) activities were also measured from the same samples we used for the protein content determination. We utilized the procedures given by Kenner and Ahmed (1975) for the determination of ETS activity. Details of the assay are provided in Hernández-León (1988) and Hernández-León and Gómez (1996). GDH activity was measured by the method proposed by Bidigare *et al.* (1982) with the difference that total volume in the cuvette of the spectrophotometer was 3.0 ml (Hernández-León and Torres, 1997). ATC activity was measured using the procedure given by Bergeron and Alayse-Danet (1981). Details of the procedure are given in Hernández-León *et al.* (1995).

The zooplankton taxonomic composition was determined to the species level by binocular microscope analysis, although only data grouped by sizes are presented for the purposes of the paper.

## 3. Results

### *3.1 Large-scale distribution*

#### *3.1.1 Hydrological structure*

Sampling took place (August–September) when the surface waters are warmer in relation to the annual cycle and the north Trade Winds are still blowing with persistence. An apparently stable thermal structure was observed in the upper 100 m, with a seasonal thermocline at 50–75 m depth. Temperature and salinity increased in the surface layer from east to west whereas phosphate concentration declined slightly (Fig. 2). Surface layer thickness increased to the west while the lowest salinity values was observed in the eastern part of the transect. These indicated two areas representative of boundary and central gyre conditions. Nutrient values increased not only in the eastern part but also with depth due to the presence of South Atlantic Central Water.

#### *3.1.2 Microplankton*

Gross production ranged from 0.01 to 0.05 μmol $O_2 \cdot l^{-1} \cdot h^{-1}$. These values were of the same magnitude as those obtained by the $^{14}C$ method at the same depths and

Table 1. Gross production, community respiration, net community production and $^{14}C$ uptake measurements in microplankton (<200 μm). All rates are expressed as $\mu moles \cdot dm^{-3} \cdot h^{-1}$. Sampling depths are given in meters. PQ is the apparent photosynthetic quotient ($O_2/^{14}C$) and R/ETS is the respiration/electron transport system activity ratio. "n.d." stand for no data available.

| Station | Depth | Gross prod. | Resp. | Net prod. | PP ($^{14}C$) | PQ | R/ETS |
|---|---|---|---|---|---|---|---|
| 290 | 25 | 0.02 | 0.11 | -0.09 | 0.03 | 0.7 | 0.82 |
| 300 | 40 | 0.01 | 0.16 | -0.15 | n.d. | — | 1.22 |
| 383 | 1 | 0.01 | 0.12 | -0.11 | n.d. | — | 1.24 |
| 310 | 25 | 0.02 | 0.24 | -0.22 | 0.02 | 1.0 | n.d. |
| 318 | 25 | 0.03 | 0.18 | -0.15 | 0.02 | 1.5 | n.d. |
| 346 | 25 | 0.02 | 0.14 | -0.12 | 0.02 | 1.0 | 1.29 |
| 362 | 25 | 0.05 | 0.28 | -0.23 | 0.05 | 1.0 | n.d. |
| Average | | 0.03 | 0.16 | -0.13 | 0.03 | 1.04 | 1.14 |
| (±SD) | | (0.02) | (0.08) | (0.08) | (0.01) | (0.29) | (0.22) |

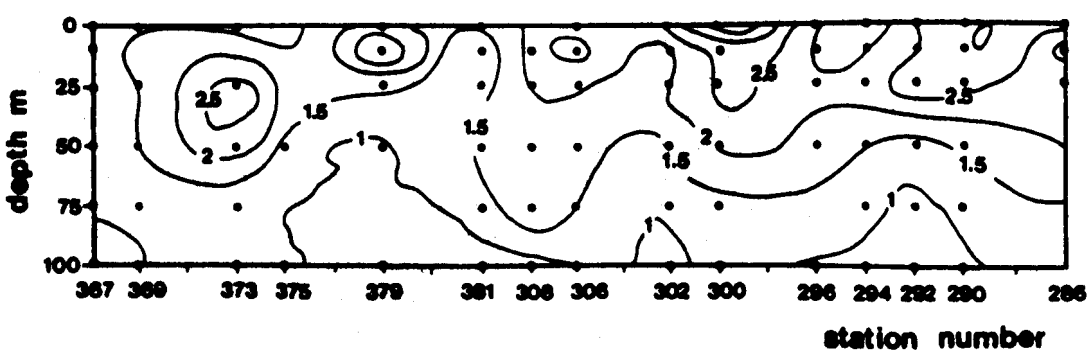


Fig. 3. Microplankton ETS activity profiles (in μl $O_2 \cdot dm^{-3} \cdot h^{-1}$) showing the enhanced activity in the upper 50 m.



© Del documento, los autores. Digitalización realizada por ULPGC. Biblioteca Universitaria, 2009

stations (Table 1). Respiration rates varied from 0.11 to 0.28 $\mu$mol $O_2 \cdot l^{-1} \cdot h^{-1}$. Net production was always negative indicating that oxygen consumption of microplankton was higher than its production at those depths. ETS activity showed higher values in the upper 50 m layer (Fig. 3), the R/ETS ratio varying between 0.82 and 1.28 (Table 1).

*3.1.3 Mesozooplankton*

In order to suppress daily variability, biomass values were converted according to the night/day (N/D) ratios obtained for both size fractions (Table 2). Using a significance test according to the Student distribution, we observed no significant differences in the N/D ratio of zooplankton ETS activities for the two size classes studied at the different depth levels. This agreed with the ETS activity results obtained for the same ratio in the Canary Island waters (Hernández-León, 1991). No differences were also observed for GDH activities, except for the >500 $\mu$m size class in the upper 25 m ($p < 0.01$). Significant differences were observed, however, between day and night ATC activity values in the upper 25 m ($p < 0.05$) and in the average value for the 200–500 $\mu$m fraction ($p < 0.05$). Therefore, these values were converted according to the N/D ratio.

Average values of biomass were always higher in the upper layer (0–25 m) in both size fractions (Table 2). Biomass by night was higher in the large size fraction, while it decreased in the 200–500 $\mu$m size class. ETS and GDH activities did not show any difference between day and night. However, ATC activity showed an increase during night in the surface layer (Table 2). Biomass and ATC activity data were recalculated using the N/D ratios of Table 2 in order to suppress the daily variability (Fig. 4). The integrated biomass down to a depth of 200 m reflected the pattern of transition between the eastern boundary and central gyre area by a reduction towards the west in the amount of biomass in both size classes (Fig. 4C). A minimum was observed in the 0–25 m layer for the larger size fraction in the central part of the transect, with a slight westward increase in biomass (Fig. 4B). Calanoid copepods were grouped into three different size classes. The abundance of small calanoids (<1 mm) diminished from east to west in the surface layer (Fig. 5A). This feature was observed from the surface to a depth of 75 m, but not for the 75–200 m layer. Large calanoids (>2 mm) were present in very low densities showing no defined patterns in their distribution along the transect. Cyclopoid abundance gradually increased westward at the surface layer, as expected from observed boundary and central gyre conditions (not shown).

Average values of specific ETS activity in the 200–500

Table 2. Average values (±SD) and night to day (N/D) ratios of protein biomass ($mg \cdot m^{-3}$), specific activities of ETS ($\mu l$ $O_2 \cdot mg$ $prot^{-1} \cdot h^{-1}$), GDH ($\mu$mol $NH_4 \cdot mg$ $prot^{-1} \cdot h^{-1}$) and ATC (nmol carbamyl-aspartate·mg $prot^{-1} \cdot min^{-1}$) for the two size fractions.

| Depth (m) | 200–500 $\mu$m | | | >500 $\mu$m | | |
|---|---|---|---|---|---|---|
| | Day | Night | N/D | Day | Night | N/D |
| *Biomass* | | | | | | |
| 0–25 | 1.38 ± 1.21 | 1.20 ± 0.68 | 0.87 | 1.20 ± 0.56 | 2.43 ± 0.49 | 2.03 |
| 25–75 | 0.78 ± 1.01 | 0.62 ± 0.24 | 0.79 | 0.72 ± 0.31 | 1.44 ± 0.52 | 2.00 |
| 75–200 | 0.23 ± 0.10 | 0.14 ± 0.10 | 0.61 | 0.48 ± 0.25 | 0.64 ± 0.25 | 1.33 |
| Average | 0.80 ± 1.01 | 0.65 ± 0.60 | 0.81 | 0.80 ± 0.49 | 1.50 ± 0.86 | 1.88 |
| *Specific ETS* | | | | | | |
| 0–25 | 79.86 ± 28.47 | 81.71 ± 18.35 | 1.02 | 64.47 ± 47.87 | 59.44 ± 17.42 | 0.92 |
| 25–75 | 57.56 ± 27.88 | 61.45 ± 34.16 | 1.07 | 49.81 ± 21.71 | 55.86 ± 20.17 | 1.12 |
| 75–200 | 45.22 ± 39.53 | 48.93 ± 21.27 | 1.08 | 32.16 ± 14.42 | 30.17 ± 7.49 | 0.94 |
| Average | 60.98 ± 34.78 | 64.03 ± 28.03 | 1.05 | 48.82 ± 33.29 | 48.67 ± 20.37 | 1.00 |
| *Specific GDH* | | | | | | |
| 0–25 | 1.17 ± 0.82 | 0.83 ± 0.45 | 0.71 | 0.47 ± 0.23 | 0.94 ± 0.33 | 2.00 |
| 25–75 | 1.04 ± 0.50 | 1.25 ± 0.57 | 1.20 | 1.51 ± 0.99 | 1.25 ± 0.28 | 0.83 |
| 75–200 | 1.18 ± 0.40 | 1.54 ± 1.03 | 1.31 | 1.03 ± 0.35 | 1.06 ± 0.39 | 1.03 |
| Average | 1.13 ± 0.58 | 1.19 ± 0.74 | 1.05 | 1.00 ± 0.77 | 1.06 ± 0.34 | 1.06 |
| *Specific ATC* | | | | | | |
| 0–25 | 0.63 ± 0.86 | 3.19 ± 3.02 | 5.06 | 1.03 ± 1.54 | 2.60 ± 2.06 | 2.52 |
| 25–75 | 0.76 ± 1.51 | 1.33 ± 1.28 | 1.75 | 1.11 ± 1.21 | 0.66 ± 0.63 | 0.59 |
| 75–200 | 1.74 ± 1.13 | 2.10 ± 1.51 | 1.21 | 1.22 ± 1.10 | 1.29 ± 1.23 | 1.06 |
| Average | 1.00 ± 1.26 | 2.13 ± 2.04 | 2.13 | 1.12 ± 1.29 | 1.40 ± 1.55 | 1.25 |



© Del documento, los autores. Digitalización realizada por ULPGC. Biblioteca Universitaria, 2009

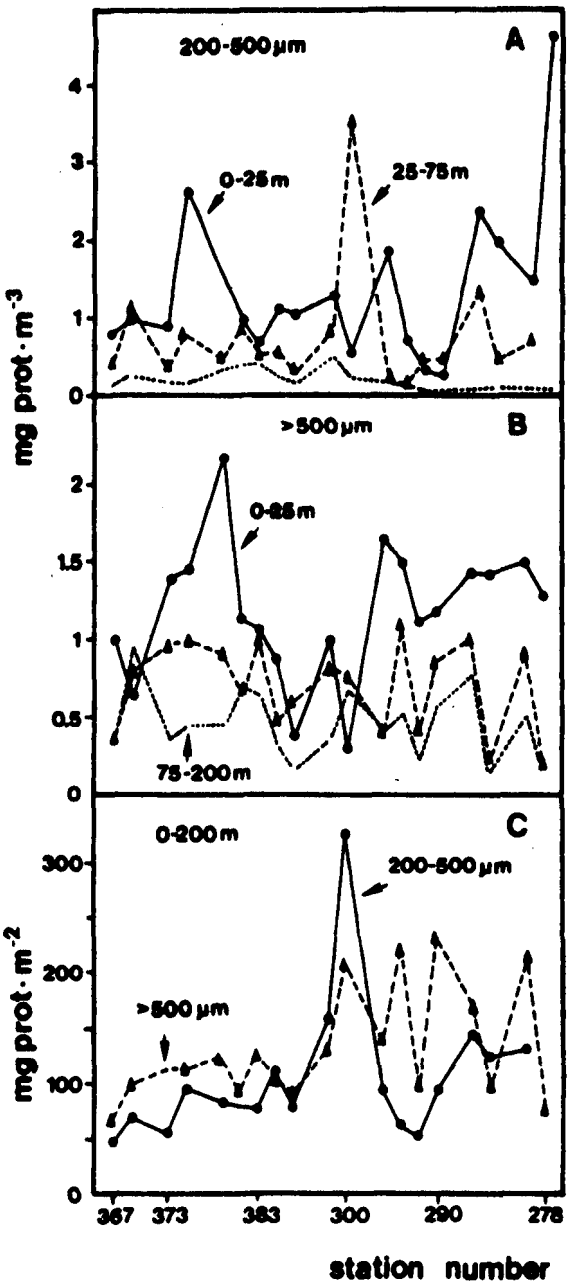


Fig. 4. Zooplankton biomass as protein in size fractionated samples for the (A) 200–500, (B) >500 µm size classes and (C) total biomass integrated in 0–200 m.

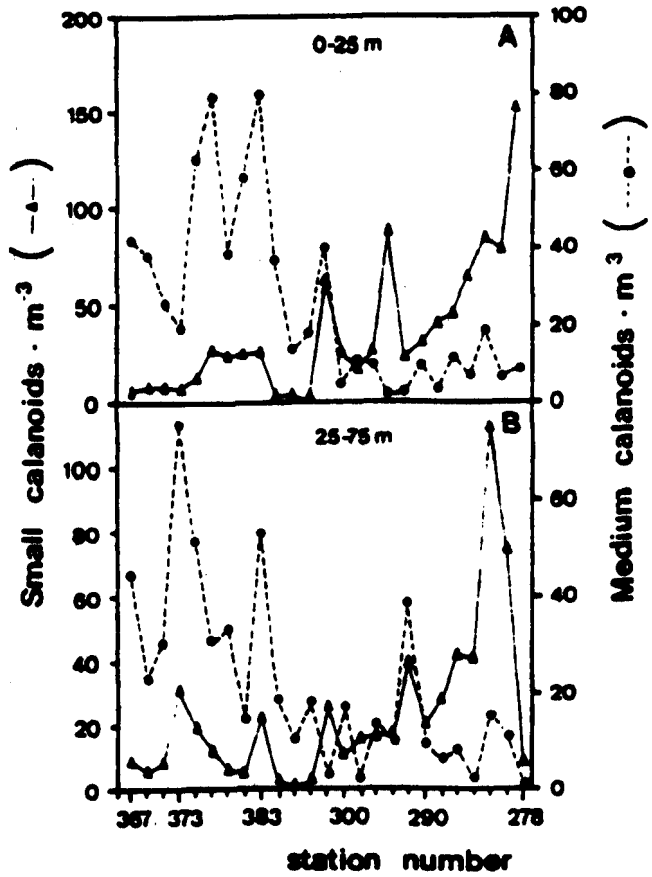


Fig. 5. Copepod density (A) at the surface (0–25 m) and (B) at the seasonal thermocline (25–75 m) layers. The two sizes considered were <1 mm (solid line) and 1–2 mm (dashed line), representing small and medium size calanoid copepods. The increase in medium size calanoids was not observed at the deeper layer (75–200 m).

and >500 µm fractions, as well as GDH and ATC activities in 200–500 µm, showed an increasing trend westward from the middle of the section (Fig. 6). This trend coincided with the increases in the number of medium size calanoids and the presence of *Trichodesmium spp.*

Respiration and ammonia excretion rates were calculated from ETS and GDH activities using the respiration/ETS (0.34) and ammonia/GDH (0.77) ratios experimentally obtained during the cruise (Table 3). Respiration rates by day represented 5.9% of primary production while by night this percentage increased to 8.9. This 50% increase by night was due to the large size fraction which showed nightly values of more than 100% higher. The ammonia excretion rate was 3.4% of primary production by day while by night it was 6.9%. Once again the increase in biomass by night due to vertical migration produced the important increase in community metabolic rates.

### 3.2 *Mesoscale distribution*

#### 3.2.1 *Hydrological structure*

Hagen (1992), in a preliminary analysis of our transect, found a wave-like zonal pattern which was consistent with the westward dispersion of Rossby waves radiating from the coastal region. In a more detailed study of the same transect, Hagen (in prep.) found an average zonal wave length of 727 km. The residuals of the thickness of the layer between the 15 and 18°C isotherms in dbars (Fig. 7A) analysed by Hagen (1992; in prep.) indicate potential energy anomalies in this



© Del documento, los autores. Digitalización realizada por ULPGC. Biblioteca Universitaria, 2009

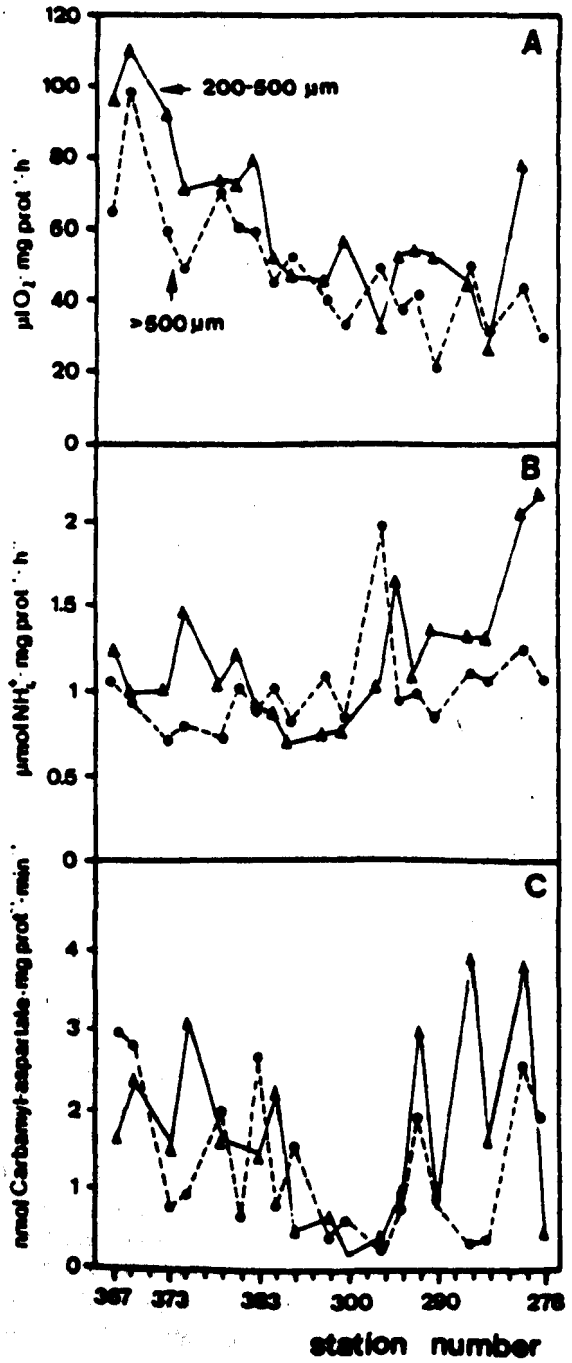


Fig. 6. Average specific ETS, GDH and ATC activities (A, B and C respectively) for the 200–500 µm (solid line) and >500 µm (dashed line) size classes. ATC activity has been corrected for differences between day and night values (see text).

intermediate layer. That excludes processes such as wind mixing and convection, which are surface-driven. The variations in the distance between isotherms reflect the presence of a Rossby wave-like phenomenon (Hagen, 1992). The zonal wave length was found to be determined in the range between 620–830 km.

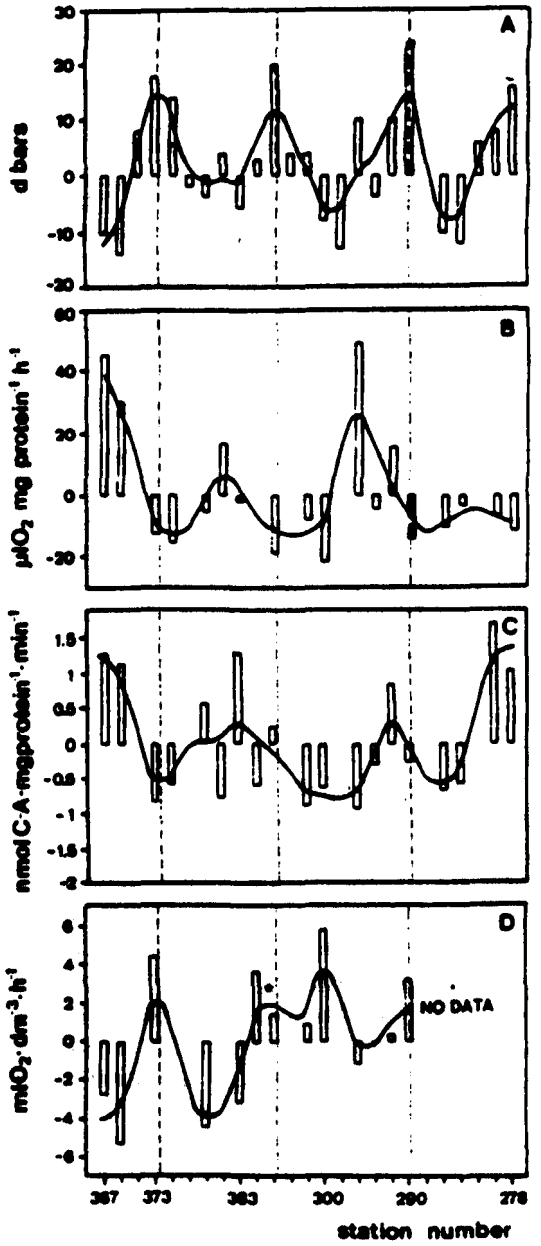


Fig. 7. Comparison of the deviations of (A) the distance between the 15 and 18°C isothermes (from Hagen, 1992) after substracting the large-scale zonal gradient, (B) mesoplankton specific ETS activity in the >500 µm at the seasonal thermocline level, (C) average specific ATC activity in mesoplankton >500 µm and (D) ETS activity (on a unit-volume basis) in microplankton at the seasonal thermocline level. Samples were taken at depths of 25, 50 and 75 m. Cyanobacteria chains were excluded because samples were drained using a 200 µm mesh net. ETS activity in (D) has been calculated after substracting the increasing eastward trend in activity. ATC activity in (C) has been corrected for differences between day and night values. The superimposed line in A, B, C and D is the smoothed representation of data (histograms). C–A in (C) stand for carbamyl-aspartate. Note that ETS activity in micro- and mesoplankton presents clear peaks in the central gyre area.



© Del documento, los autores. Digitalización realizada por ULPGC. Biblioteca Universitaria, 2009

Table 3. Average values (±SD) of respiration and ammonia excretion calculated from ETS and GDH activities and using the respiration /ETS (0.34) and ammonia/GDH (0.77) ratios obtained experimentaly during the cruise. Percentages of respiration and of the contribution of regenerated nitrogen by mesozooplankton in relation to primary production (oxygen method) are also given. An average value of 30 nmol $O_2 \cdot dm^{-3} \cdot h^{-1}$ and O/C and N/C ratios of 2.66 and 0.16 were used. %PP stand for the percentage of primary production respired or regenerated by mesozooplankton.

| | ETS $\mu l\ O_2 \cdot m^{-3} \cdot h^{-1}$ | Respiration nmol $O_2 \cdot dm^{-3} \cdot h^{-1}$ | %PP | GDH $\mu mol\ NH_4 \cdot dm^{-3} \cdot h^{-1}$ | Excretion nmol $NH_4 \cdot dm^{-3} \cdot h^{-1}$ | %PP |
|---|---|---|---|---|---|---|
| 200–500 μm | | | | | | |
| Day | 63.18 ± 37.48 | 0.96 ± 0.57 | 3.2 | 0.85 ± 0.55 | 65.95 ± 42.62 | 1.83 |
| Night | 65.37 ± 29.39 | 0.99 ± 0.45 | 3.3 | 0.84 ± 0.52 | 65.41 ± 40.38 | 1.81 |
| >500 μm | | | | | | |
| Day | 54.09 ± 40.51 | 0.82 ± 0.61 | 2.7 | 0.76 ± 0.35 | 58.59 ± 26.74 | 1.62 |
| Night | 110.99 ± 36.19 | 1.68 ± 0.55 | 5.6 | 2.38 ± 0.82 | 184.14 ± 63.47 | 5.10 |

### 3.2.2 *Micro- and mesoplankton*

Zooplankton biomass showed a high variability in the two size classes studied as well as at the different depth levels (Fig. 4). The very low values observed did not allow us to recognize any pattern of distribution at the mesoscale. However, specific ETS activity in the >500 μm size class at the thermocline level showed a succession of mesoscale peaks (Fig. 7B). This plot was obtained by substracting the westward increase in activity. This trend was also found in the 200–500 μm fraction within the central gyre area (not shown). Additionally, this effect was also observed in the average specific ATC activity in the >500 μm size fraction (Fig. 7C). Microplankton ETS activity at the seasonal thermocline level (Fig. 7D) showed an inverse pattern to the one observed for zooplankton ETS and ATC activities. Since microplankton ETS activity is given in a unit-volume basis, which is highly related to biomass, it is suggested that zooplankton might control the microplankton community (<200 μm).

## 4. Discussion

Our results show that microplankton respiration clearly exceed gross primary production. These results agree with Duarte and Agustí (1998) conclusions that unproductive aquatic ecosystems support a disproportionately higher rate respiration than that of productive ecosystems, tending to be heterotrophic and acting as a carbon dioxide source. In our case, microplankton respiration rates were even slightly higher than those reported by other authors for oligotrophic waters (e.g., Williams, 1984). A simple explanation for these differences may account for the fact that, during most of our sampling, the surface waters were dominated by colonies of *Trichodesmium spp.* (see material and methods) which are known to exhibit, jointly with the associated bacteria, high respiration rates (Kana, 1992; Carpenter *et al.*, 1993). Respiration/ETS ratios were also higher than those obtained in experiments with phytoplankton cultures (0.15 in Kenner and Ahmed, 1975) or in natural samples were phytoplankton predominated (about 0.3 in Packard and Williams, 1981). However, they agree with rates reported for active growing populations of bacteria (Christensen and Packard, 1979), or from natural communities in other oligotrophic areas like the Mediterranean Sea or the Canary Island waters (Arístegui and Montero, 1995).

Zooplankton activity increased in the western part of the zonal section. The magnitude of metabolic processes was as high or higher in the central subtropical gyre than in the boundary area of the ocean. Figure 6 shows increased activity westward of the transect, where *Trichodesmium spp.* were observed. The contamination of the small size fraction (200–500 μm) with cyanobacteria could be a possible cause of the increased activity westward. Although we visually tested the samples, cells could remain in the 200 μm filters after the washing procedure. However, this possibility is unlikely as the fact that both size fractions displayed the same pattern of activity along the transect (Fig. 6A). Therefore, it is suggested that the presence of cyanobacteria could promote an increased zooplankton activity in the central gyre area, as well as the increase in medium-sized calanoid copepods (Fig. 5). In this respect, small calanoids were expected to be found mostly in central gyre conditions, due to the presumably predominance of small phytoplankton cells in oligotrophic waters. However, medium size copepods were more abundant westward. The relationship between the increase in zooplankton activity and the presence of *Trichodesmium spp.* is unknown, although it has been observed that some mesozooplanktonic organisms feed directly on *Trichodesmium spp.* (Carpenter, 1983), or on associated organisms. However, we were unable to measure biomass and production of the cyanobacteria chains. Therefore, it was not possible to assess the contribution of this new production on the increase of zooplankton metabolism in the central gyre area. The coupling between both processes remains unknown although one possibility to



© Del documento, los autores. Digitalización realizada por ULPGC. Biblioteca Universitaria, 2009

explain those increases in activity and the presence of medium sized calanoids would be related to the growth increment of other organisms associated with *Trichodesmium* such as protista.

Our observations at the mesoscale level suggest that the presence of a low frequency phenomena could influence the biomass and metabolism of planktonic organisms. Baroclinic Rossby waves have been observed to play a major role in the mesoscale variation of thermocline displacement and sea level height in the central north Pacific (see Van Woert and Price, 1993, and references therein). These waves are of long wavelength and low period and are generated due to temporal variations in the wind stress curl (White and Saur, 1981) and sea level height (White and Saur, 1983) along the eastern boundary (Van Woert and Price, 1993). Recent models suggest that these waves are expected to be produced annually in the central north Atlantic (Hermann and Krauss, 1989). Hagen (1992) observed a zonal wave pattern related to a Rossby wave-like phenomena which could be forced in the east with wave-lengths between 620 and 830 km. Using a zonally-averaged value for the internal Rossby radius of 48 km from the belt placed between 20° and 40°W and 20° and 25°N (Emery *et al.*, 1984) together with the range of zonal wave lengths estimated, we obtained a period range which includes a semiannual cycle. If we accept the notion that our observations result from a resonant oceanic response, then we may speculate about semiannual forcing. We know from the literature that in our area under consideration the half-year period is also a very energy rich cycle due to the meridional displacement of the northeast Trade Winds.

In the present work, the low frequency phenomena observed seemed to influence the hydrographic environment of micro- and mesoplankton along the extended zonal section. The peaks in zooplankton ETS activity at the level of the seasonal thermocline coincided with the reduction in distance between isotherms considered by Hagen (1992) (Fig. 7). This was also true for the index of growth. The processes involved in the increase in biological activity are thought to be quite complex. They could be related to the mesoscale eddy-like structures produced by the wave associated pressure instability and the lag normally observed in biological systems among the different trophic levels, as well as among the different responses of physiological rates (Checkley *et al.*, 1992) or enzymatic activities. In fact, we observed a slight mismatch of ETS and ATC peaks in relation to Rossby wave-like phenomena observed (Fig. 7). This uncoupling between the hydrological and biological data as well as the low number of stations at the mesoscale level meant that we could not attach any statistical significance to the apparent correlations. Moreover, Siedler and Finke (1993) measured temperature from an array of five moorings at 28°N to the west of the Canary archipelago. They found a superposition of two first-order baroclinic waves with annual and semi-annual periods and a baroclinic wave with a 90-day period. This complexity in the physical environment must produce difficult to explain variability in the associated biological measurements. Nevertheless, our observations suggest that Rossby wave-like phenomena and mesoscale associated eddies, could enhance and/or promote increased productivity in those areas due to positive vertical displacements in the wave crests. Eddy diffusivity at the crests of these subsurface waves may inject nutrients into the euphotic zone, or perhaps, the physical shallowing of nutrient-rich subsurface water enable motile phytoplankton to access nutrients. Whatever the mechanism is, they must be taken into account when time series studies in tropical or subtropical oceanic areas are undertaken. In trying to explain biological variability, such a pattern of biological instability can produce background noise in the data. This could produce serious problems when interpreting trends in time.

Diel variability showed an unexpected low N/D ratio in the 200–500 $\mu$m zooplankton fraction (Table 2). Differences between night and day hauls may be caused by methodological bias. Animals could more easily avoid the net during daylight hauls. However, if this were the case, the N/D ratio should be higher than unity. Another potential factor affecting this ratio might be the existence of an inverse migration, but the N/D ratio is lower than unity in the three layers sampled (Table 2). That is to say that these smaller organisms would have to migrate below 200 m from the upper most layers, which is something unexpected in these small organisms (200–500 $\mu$m). The important increase in biomass at night in the upper layers due to organisms >500 $\mu$m could produce an impact on the amount of prey animals in this size range. Our observation of an inverse relationship between the specific ETS in zooplankton and microplankton enzymatic activity (on a unit-volume basis) at the mesoscale (Fig. 7) also supports the previous observation about the control exerted by the large zooplankton on the smallest size fractions. There is evidence in the literature of such a diel impact on phytoplankton standing crop in equatorial waters. Le Bouteiller and Herbland (1982) found that the amount of chlorophyll *a* in the upper layers was always lower during the night. Lampitt *et al.* (1993) also found a strong diel variability of marine snow. They suggested that mid-water biota and their migratory behaviour were responsible for such a variability. In these warm environments, grazing and carnivorous activity could have important consequences on a daily basis as the >500 $\mu$m organisms could control the abundance of this small metazooplankton community (see also Hernández-León, 1998).

Daily impact of mesozooplankton on primary production could be assessed from our measurements of enzymatic activities. Hernández-León and Gómez (1996) found that values of R/ETS of 0.5 are rather conservative because of the influence of cell substrate limitation in the variability



© Del documento, los autores. Digitalización realizada por ULPGC. Biblioteca Universitaria, 2009

of the R/ETS relationship. This is an inherent problem to enzymatic measurements as also stated by Packard *et al.* (1996) and Hernández-León and Torres (1997). Our experimentally obtained R/ETS ratio of 0.34 also seems conservative. Therefore, our metabolic calculations should be considered as a base line for the area considered.

A rough estimate of ingestion can be obtained by assuming that about two-thirds of the ingested food is assimilated, and one half of the assimilated food is metabolized and the other half is used for growth and reproduction. This estimate indicates that mesozooplankton potentially consume (assuming herbivorous feeding) 46% of primary production, ingestion being 33% higher by night than by day. This estimate agrees with the values calculated by Lenz *et al.* (1993) who found that potential grazing could account for half of the daily primary production in subtropical waters of the Atlantic Ocean. Therefore, mesozooplankton are processing an important amount of the energy which enter daily and then circulates into the pelagic ecosystem. This impact is even higher during the night because of the presence in the epipelagic zone of diel vertical migrators. This increase in ingestion at night could also explain, at least in part, the low N/D ratio of the small size fraction.

In summary, the main finding of this study is the inadequacy of assuming an steady-state picture in tropical and subtropical environments. The estimation of biological productivity in stations selected at random along the transect gave a low variability in the values of gross and net production (Table 1). However, our much finer sampling of plankton biomass and indices of metabolism detected important differences at the large-scale and mesoscale. Low frequency phenomena could be an important mechanism in thermocline variability (Van Woert and Price, 1993), and associated mesoscale eddies may enhance primary production in oligotrophic waters. Although further research is required in order to elucidate the importance of the large-scale and mesoscale variability observed, the changes in plankton activity associated with the long period waves and the presence of $N_2$ fixing organisms observed in the present work suggest that a better estimation in the biological calculation of new and export production of tropical and subtropical waters in relation to these features is needed.

**Acknowledgements**

The authors would like to thank two anonymous referees for their comments on the manuscript and constructive criticism. We are also grateful to C. Fraga for drawing the figures and to the crew and scientists of the R.V. "A.v. Humboldt". This work was partly supported by the "Comisión Interministerial de Ciencia y Tecnología" (CICYT PB88-0436) of the Spanish Government and the Autonomic Government of the Canary Islands (GAC 22/01.06.88).

**References**

Alayse-Danet, A. M. (1980): Aspatate transcarbamylase in *Artemia* during early stages of development. In *The Brine Shrimp Artemia*, ed. by G. Persoone, P. Soorgeloos, O. Roels and E. Jaspers, Universal Press, Wetteren, Belgium, Vol. 2, 259–275.

Arístegui, J. and M. F. Montero (1995): The relationship between community respiration and ETS activity in the ocean. *J. Plankton Res.*, **17**, 1563–1571.

Bergeron, J. P. (1982): L'aspartate transcarbamylase, indice de croissance des organismes marins: perspectives et limites. In *Actualités de Biochimie marine: indices biochimiques et milieux marins*, Publ. CNEXO, Actes Colloq., **14**, 177–192.

Bergeron, J. P. and A. M. Alayse-Danet (1981): Aspartate transcarbamylase de la coquille Saint-Jaques *Pecten maximus* L. (Mollusque Lamellibranche): Methode de dosage et variations de L'activite dans le monteau et la gonade. *J. Exp. Mar. Biol. Ecol.*, **50**, 99–117.

Bergeron, J. P. and D. Buestel (1979): L'Aspartate transcarbamylase, indice de l'activité sexuelle de la coquille Saint-Jaques (*Pecten maximus* L.). Premier resultats, p. 301–308. In *Cyclic Phenomena in Marine Plants and Animals*, ed. by E. Naylor and R. G. Hartnoll, Pergamon Press, N.Y.

Bidigare, R. R. and F. D. King (1981): The measurement of glutamate dehydrogenase activity in *Praunus flexousus* and its role in the regulation of ammonium excretion. *Comp. Biochem. Physiol.*, **70B**, 409–413.

Bidigare, R. R., F. D. King and D. C. Biggs (1982): Glutamate dehidrogenase (GDH) and respiratory electron transport system (ETS) activities in Gulf of Mexico zooplankton. *J. Plankton Res.*, **4**, 895–911.

Bryan, J. R., J. P. Riley and P. J. L. Williams (1976): A winkler procedure for making precise measurements of oxygen concentration for productivity and related studies. *J. Exp. Mar. Biol. Ecol.*, **21**, 191–197.

Carpenter, E. J. (1983): Physiology and ecology of marine planktonic Oscillatoria (*Trichodesmium*). *Mar. Biol. Lett.*, **4**, 69–85.

Carpenter, E. J., J. M. O'Neil, R. Dawson, D. G. Capone, P. J. A. Siddiqui, T. Roenneberg and B. Bergman (1993): The tropical diazotrophic phytoplankter *Trichodesmium*: biological characteristics of two common species. *Mar. Ecol. Progr. Ser.*, **95**, 295–304.

Carrit, D. E. and J. H. Carperter (1966): Comparison and evaluation of currently employed modifications of the Winkler method for determining dissolved oxygen in seawater. A NASCO Report. *J. Mar. Res.*, **24**, 286–318.

Checkley, D. M., M. J. Dagg and S. Uye (1992): Feeding, excretion and egg production by individuals and populations of the marine, planktonic copepods, *Acartia spp.* and *Centropages furcatus*. *J. Plankton Res.*, **14**, 71–96.

Christensen, J. P. and T. T. Packard (1979): Respiratory electron transport activities in phytoplankton and bacteria: Comparison of methods. *Limnol. Oceanogr.*, **24**, 576–583.

Duarte, C. M. and S. Agustí (1998): The $CO_2$ balance of unproductive aquatic ecosystems. *Science*, **281**, 234–236.

Emery, W. J., W. G. Lee and L. Magaard (1984): Geographic and



© Del documento, los autores. Digitalización realizada por ULPGC. Biblioteca Universitaria, 2009

seasonal distributions of Brunt-Väisälä Frequency and Rossby Radii in the North Pacific and North Atlantic. *J. Phys. Oceanogr.*, **14**, 294–317.

Gieskes, W. W. and G. W. Kraay (1986): Floristic and physiological differences between the shallow and the deep nanophytoplankton community in the euphotic zone of the open tropical Atlantic revealed by HPLC analysis of pigments. *Mar. Biol.*, **91**, 567–576.

Grasshoff, P., M. Ehrhardt and K. Kremling (1983): Methods of seawater analysis. Verlag Chemie, *FRG*, **419**, 61–72.

Hagen, E. (1992): On the zonal structures of the 15°C–18°C layer thickness in the central eastern North Atlantic. *Beitr. Meereeskunde*, **63**, 131–135.

Hermann, P. and W. Krauss (1989): Generation and propagation of annual Rossby waves in the North Atlantic. *J. Phys. Oceanogr.*, **19**, 727–744.

Hernández-León, S. (1988): Gradients of mesozooplankton biomass and ETS activity in the wind-shear area as evidence of an island mass effect in the Canary Island waters. *J. Plankton Res.*, **10**, 1141–1154.

Hernández-León, S. (1991): Accumulation of mesozooplankton in a wake area as a causative mechanism of the "Island-Mass effect". *Mar. Biol.*, **109**, 141–147.

Hernández-León, S. (1998): Annual cycle of epiplanktonic copepods in Canary Island waters. *Fish. Oceanogr.*, **7**, 252–257.

Hernández-León, S. and M. Gómez (1996): Factors affecting the Respiration/ETS ratio in marine zooplankton. *J. Plankton Res.*, **18**, 239–255.

Hernández-León, S. and S. Torres (1997): The relationship between ammonia excretion and GDH activity in marine zooplankton. *J. Plankton Res.*, **19**, 587–601.

Hernández-León, S., C. Almeida and I. Montero (1995): The use of aspartate transcarbamylase activity to estimate growth rates in zooplankton. *ICES J. Mar. Sci.*, **52**, 377–383.

Kaiser, W. and L. Postel (1979): Importance of the vertical nutrient flux for biological production in the equatorial undercurrent region at 30°W. *Mar. Biol.*, **55**, 23–27.

Kana, T. M. (1992): Oxygen cycling in cyanobacteria with special reference to oxygen protection in *Trichodesmium spp.* p. 29–41. In *Marine Pelagic Cyanobacteria: Trichodesmium and Other Diazotrophs*, ed. by E. J. Carpenter, D. G. Capone and J. G. Rueter, Kluwer Academic Publishers.

Kenner, R. A. and S. I. Ahmed (1975): Measurements of electron transport activities in marine phytoplankton. *Mar. Biol.*, **33**, 119–127.

King, F. D. (1984): The vertical distribution of zooplankton glutamate dehydrogenase in relation to chlorophyll in the vicinity of the Nantucket Shoals. *Mar. Biol.*, **79**, 249–256.

King, F. D. and T. T. Packard (1975): Respiration and the respiratory electron transport system in marine zooplankton. *Limnol. Oceanogr.*, **20**, 849–854.

King, F. D., T. L. Cucci and D. W. Townsend (1987): Microzooplankton and macrozooplankton glutamate dehydrogenase as indices of the relative contribution of these fractions to ammonium regeneration in the Gulf of Maine. *J. Plankton Res.*, **9**, 277–289.

Lampitt, R. S., W. R. Hillier and P. G. Challenor (1993): Seasonal and diel variation in the open ocean concentration of marine snow aggregates. *Nature*, **362**, 737–739.

Le Bouteiller, A. and A. Herbland (1982): Diel variation of chlorophyll *a* as evidenced from a 13-day station in the equatorial Atlantic Ocean. *Oceanol. Acta*, **5**, 433–441.

Lenz, J., A. Morales and J. Gunkel (1993): Mesozooplankton standing stock during the North Atlantic spring bloom study 1989 and its potential grazing pressure on phytoplankton: a comparison between low, medium and high latitudes. *Deep-Sea Res. II*, **40**, 559–572.

Longhurst, A. R. and W. G. Harrison (1989): The biological pump: Profiles of plankton production and consumption in the upper ocean. *Progr. Oceanogr.*, **22**, 47–123.

Longhurst, A. R., A. W. Bedo, W. G. Harrison, E. J. H. Head and D. D. Sameoto (1990): Vertical flux of respiratory carbon by oceanic diel migrant biota. *Deep-Sea Res.*, **37**, 685–694.

Lowry, P. H., N. J. Rosenbrough, A. L. Farr and R. J. Randall (1951): Protein measurement with a Folin Phenol reagent. *J. Biol. Chem.*, **193**, 265–275.

Owens, T. G. and F. D. King (1975): The measurement of respiratory electron transport system activity in marine zooplankton. *Mar. Biol.*, **30**, 27–36.

Packard, T. T. (1969): The estimation of the oxygen utilization rate in seawater from the activity of the respiratory electron transport system in plankton. Ph.D. Thesis, Univ. Washington, Seattle, 115 pp.

Packard, T. T. (1971): The measurement of respiratory electron transport activity in marine phytoplankton. *J. Mar. Res.*, **29**, 235–244.

Packard, T. T. and P. J. L. Williams (1981): Rates of respiratory oxygen consumption and electron transport in surface waters from the Northwest Atlantic. *Oceanol. Acta*, **4**, 351–358.

Packard, T. T., A. H. Devol and F. D. King (1975): The effect of temperature on the respiratory electron transport system in marine plankton. *Deep-Sea Res.*, **22**, 237–249.

Packard, T. T., E. Berdalet, D. Blasco, S. O. Roy, L. St-Amand, B. Lagcé, K. Lee and J.-P. Gagné (1996): Oxygen consumption in the marine bacterium *Pseudomonas nautica* predicted from ETS activity and bisubstrate enzyme kinetics. *J. Plankton Res.*, **18**, 1819–1835.

Platt, T., P. Jauhari and S. Sathyendranath (1992): The importance and measurement of new production. p. 273–284. In *Primary Productivity and Biogeochemical Cycles in the Sea*, ed. by P. G. Falkowski and A. W. Woodhead, Plenum Press, New York.

Roman, M. R., C. S. Yentsch, A. L. Gauzens and D. A. Phinney (1986): Grazer control of the fine-scale distribution of phytoplankton in warm-core gulf stream rings. *J. Mar. Res.*, **44**, 795–813.

Siedler, G. and M. Finke (1993): Long-period transport changes in the Eastern North Atlantic and their simulation by propagating waves. *J. Geophys. Res.*, **98**, 2393–2406.

Strickland, J. D. H. and T. R. Parsons (1972): A practical handbook of seawater analysis. *Fish. Res. Bd. Canada*, Bull., 167 pp.

UNESCO (1968): *Zooplankton sampling*. Monogr. Oceanographic Methods, **2**, 174 pp.

Van Woert, M. L. and J. M. Price (1993): Geosat and advanced very high resolucion radiometer observations of Oceanic planetary waves adjacent to the Hawaiian Islands. *J. Geophys. Res.*, **98**, 14619–14631.

Venrick, E. L. (1990): Mesoscale patterns of chlorophyll *a* in the



© Del documento, los autores. Digitalización realizada por ULPGC. Biblioteca Universitaria, 2009

central north Pacific. *Deep-Sea Res.*, 37, 1017–1031.

Voituriez, B. and A. Herbland (1977): Étude de la production pelagique de la zone équatoriale de l'Atlantique a 4°W. I. Relation entre la structure hydrologique et la production primaire. *Cah. O.R.S.T.O.M. sér. Oceanogr.*, 15, 313–331.

White, W. and J. F. T. Saur (1981): A source of annual baroclinic waves in the eastern subtropical North Pacific. *J. Phys. Oceanogr.*, 11, 1452–1462.

White, W. and J. F. T. Saur (1983): Sources of interannual baroclinic waves in the eastern subtropical North Pacific. *J. Phys. Oceanogr.*, 13, 531–544.

Williams, P. J. LeB. (1984): A review of measurements of respiration of marine plankton populations. p. 357–389. In *Heterotrophic Activity in the Sea*, ed. by J. E. Hobbie and P. J. LeB. Williams, Plenum Press, New York.

Williams, P. J. LeB. and N. W. Jenkinson (1982): A transportable microprocessor-controlled precise winkler titration suitable for field station and shipboard use. *Limnol. Oceanogr.*, 27, 576–584.



© Del documento, los autores. Digitalización realizada por ULPGC. Biblioteca Universitaria, 2009

Polar Biol (1999) 21: 214–219 © Springer-Verlag 1999

ORIGINAL PAPER

S. Hernández-León · S. Torres · M. Gómez · I. Montero
C. Almeida

# Biomass and metabolism of zooplankton in the Bransfield Strait (Antarctic Peninsula) during austral spring

Accepted: 5 September 1998

**Abstract** Zooplankton biomass (as dry weight), respiration and ammonia excretion were studied in three different size classes (200–500, 500–1000 and > 1000 μm) in the Bransfield Strait during December 1991. Average mesozooplankton biomass was 86.45 ± 56.74 mg · dry weight · $m^{-2}$, which is in the lower range of the values cited in the literature for polar waters. Higher biomass was observed in the Weddell water. The small size fraction accounted for about 50% of total biomass while the largest one represented 35%. Rather high metabolic rates were found, irrespective of whether the organisms were incubated in the presence of food. No significant differences were observed in mass specific respiration and ammonia excretion rates between different temperatures of incubation (0.2–2.3°C) and between the size classes studied. Because of the very low biomass values observed, the metabolic requirements of mesozooplankton during December represented a small fraction of the primary production.

## Introduction

The role of zooplankton in the energy flow of the Antarctic ecosystem is at present poorly quantified. This is partly because attention has been paid exclusively to krill in pioneering works (e.g., the BIOMASS project), but also because of the high variability found in the values of zooplankton biomass. Moreover, the wide size spectrum of organisms controlling primary production in these waters is an added complication in understanding the pelagic ecosystem of the Southern Ocean ecosystem.

Zooplankton metabolism gives a baseline of the fraction of the autotrophic production circulating through this community. Knowledge of metabolism should aid in an evaluation of the importance of these animals on the fate of primary production in Antarctic waters. However, metabolic studies on zooplankton in the Southern Ocean are scarce, especially in copepods (Conover and Huntley 1991). Most studies have been done on feeding, mainly in euphausiids, because of their importance in the economy of these waters and because they are very efficient grazers and have an important impact on the occurrence of phytoplankton patches (Price et al. 1988; Granéli et al. 1993; Lancelot et al. 1993). However, zooplankton other than euphausiids have not been the subject of intensive biomass and metabolic research. Copepods could account for 50–90% of zooplanktonic numbers in Antarctic waters (Conover and Huntley 1991, and references therein) and they are of smaller size and are, therefore, better contributors to the energy flow in these cold waters (Boysen-Ennen et al. 1991). Moreover, they have a more widespread distribution than micronektonic forms like krill, which are more patchy (Godlewska 1993; Miller et al. 1993; Siegel and Kalinowski 1994).

During December 1991, biomass, respiration and ammonia excretion rates were measured in different size classes of zooplankton. In order to estimate the metabolic role of the most common and uniformly widespread planktonic animals of Antarctic waters, we estimated biomass and performed different experiments using three zooplankton size fractions (200–500, 500–1000 and > 1000 μm). Our objective was also to obtain a better understanding of zooplankton distribution in relation to the complex water mass distribution of the Bransfield Strait, as well as the study of the role of mesoplankton in the energy flow of these waters in relation to primary production.

S. Hernández-León (✉)
Facultad de Ciencias del Mar, Universidad de Las Palmas de Gran Canaria, Campus Universitario de Tafira,
35017 Las Palmas,
Canary Islands
e-mail: santiago.hernandez-leon@biologia.ulpgc.es,
Fax: +34-28-454490

© Del documento, los autores. Digitalización realizada por ULPGC. Biblioteca Universitaria, 2009

## Materials and methods

Zooplankton samples were obtained between 9 December 1991 and 2 January 1992 in the Bransfield Strait (Antarctic Peninsula). Vertical hauls (0–200 m or 5–10 m from the bottom at the shallower stations) were made using a 200-µm mesh size WP-2 net (UNESCO 1968). A 100-µm-mesh net was tried but a large amount of phytoplankton cells were collected in the 100- to 200-µm size fraction. These cells interfered in our biomass determinations, and therefore we opted to use the 200-µm-mesh net. Samples were size fractionated in the 200–500, 500–1000 and > 1000-µm size classes, the 200- to 500-µm fraction being washed out of phytoplankton by allowing the sample to be in a water stream over the mesh. Large zooplankton (very large krill, amphipods, large chaetognaths and salps) appeared occasionally in our samples and were excluded from the large size fraction because the WP-2 net does not sample those organisms effectively in vertical hauls. The patchy distribution of large zooplankton gave no confidence to samples obtained using this procedure. Organisms were frozen in liquid nitrogen (−196°C) and biomass was measured in the laboratory as dry weight using the procedure described by Lovegrove (1966). Samples were dried for 24 h and later weighed on a microbalance.

Organisms used for physiological experiments were collected in slow vertical hauls with the WP-2 net (200 µm). After the haul, the samples were gently size fractionated in the 200- to 500-, 500- to 1000- and > 1000-µm size classes in a bucket containing filtered seawater (FSW). After the sieving process the organisms of each size fraction were placed in large buckets containing FSW. No species selection was made in the two smaller size fractions and non-sedimented organisms were slowly siphoned into the incubation bottles. In the large size class, we sorted out the copepod *Calanoides acutus* and the Antarctic krill *Euphausia superba*. Organisms used for experiments were placed into 500-ml bell-jars and incubated at temperatures between 0.2 and 2.3°C (±0.1°C) in dim light. Stocking densities were 3.6–19.36 mg dry weight for the 200–500-µm size class, 1.39–3.76 for the 500- to 1000-µm size class, 2.99–13.96 for *C. acutus* (corresponding to 6–30 individuals) and 40.74–76.73 mg dry weight for *E. superba* (5–6 individuals). After 16–27 h, depending on animal density on the incubation bottles, the organisms were removed and immediately frozen in liquid nitrogen. Two different experiments were carried out at 0.2°C with the large copepods; a first set was performed using filtered seawater (Whatman GF/F) while a second set was carried out at different food levels from 0.04 to 4.29 µg Chl a · $l^{-1}$. The differences in oxygen and ammonia concentrations between the control bottles (without animals) and the bottles containing the experimental organisms were assumed to be the zooplankton respiration and ammonia excretion, respectively. Oxygen consumption by microplankton was measured using control bottles in order to account for microplankton respiration during incubations. The oxygen consumed by microplankton was added to the oxygen values of both experimental and control bottles. No correction was made for feeding inside the experimental bottles. In those experiments, we did not measure the ammonia uptake, and therefore no corrections were made for this consumption by phytoplankton.

Dissolved oxygen concentration was measured according to the method described by Bryan et al. (1976) using a photometric endpoint detector and a digital microburette capable of dispensing 0.1 µl sodium thiosulfate. Ammonia release was measured according to the hypochlorite-phenol method described by Parsons et al. (1984).

## Results

Hydrographic data collected during the cruise (Aristegui and Montero 1995; Rojas et al., in press) showed the presence of Weddell water (cold and salty) entering from the eastern area, parallel to the Antarctic Peninsula. This water mass turned clockwise and produced a sharp front with the Bellingshausen water (warm and fresh) flowing from the Bellingshausen Sea and the Gerlache Strait. This pattern of water mass distribution in the Bransfield Strait seems to be characteristic of the area (Grelowski and Tokarczyk 1985; Niiler et al. 1991; Garcia et al. 1994). Subsurface temperature (10 m depth) ranged from more than 1°C in the southwestern zone to less than −0.5°C in the eastern area of the Bransfield Strait, near the Antarctic Peninsula. At 5-, 10- and 50-m depths the isohalines of 34.2 and 34.3 psu defined the frontal area (see Fig. 1) between both water masses (Aristegui and Montero 1995; Rojas et al. in press). Chlorophyll *a* data showed a high variability (40–150 mg · $m^{-2}$) and values were always higher in the Weddell water (Aristegui and Montero 1995).

Significative higher biomasses were found in the Weddell (115.0 ± 63.5 mg · dry weight · $m^{-2}$) compared to the Bellingshausen waters (60.4 ± 27.4 mg · dry weight · $m^{-2}$, Fig. 1). Very low biomass values were found for all size classes studied (Fig. 2). The relative importance of each size fraction to total biomass showed that about 50% of the biomass was due to organisms between 200 and 500 µm, while the largest organisms represented about 35% (Table 1).

Our lowest respiration rates obtained (Table 2) agree with previous estimations on Antarctic copepods (Ikeda and Hing Fay 1981; Ikeda and Mitchell 1982; Drits et al. 1993). Although few experiments were made on copepods of the 200- to 500- and 500- to 1000-µm size classes,

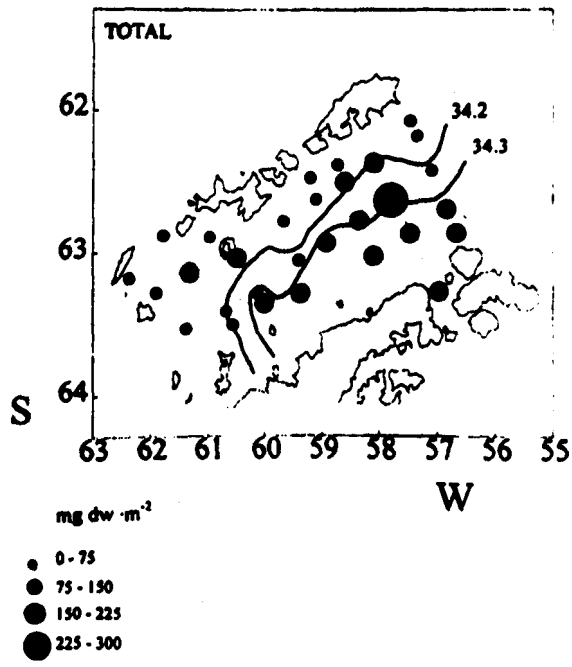


**Fig. 1** Total biomass (mg dry weight · $m^{-2}$) of non-krill mesozooplankton in the Bransfield Strait. The frontal zone between the Bellingshausen and Weddell waters is defined by the isohalines of 34.2 and 34.3 psu

© Del documento, los autores. Digitalización realizada por ULPGC. Biblioteca Universitaria, 2009

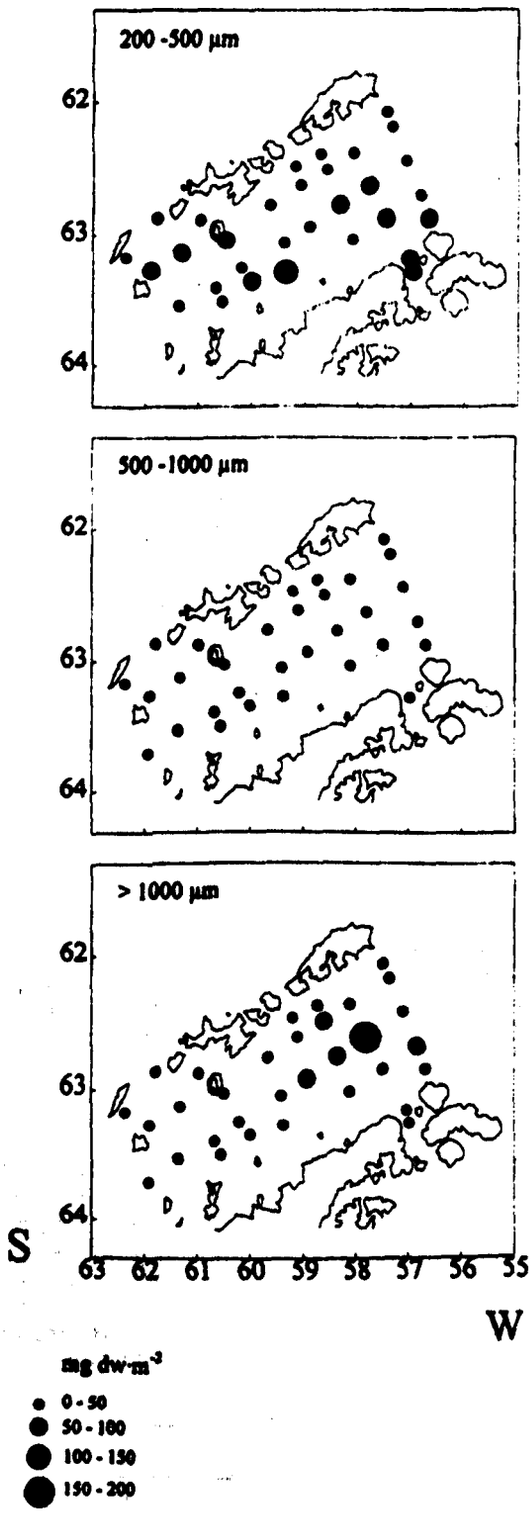


**Fig. 2** Zooplankton biomass (mg dry weight · $m^{-2}$) in the (A) 200- to 500-µm, (B) 500- to 1000-µm, and (C) > 1000-µm size fractions in the Bransfield Strait (Antarctic Peninsula)

our results showed no significant differences in mass specific respiration and ammonia excretion rates between the three size classes considered. Also, no significant differences (ANOVA test) were found in respiration

**Table 1** Zooplankton biomass (as dry weight, *dw*) in the Bransfield Strait during December 1991 in three different size fractions. The percentage of each size class in relation to the total biomass is also given. Very large organisms were excluded from the > 1000-µm size fraction (see text for explanation)

| Size fraction (µm) | Biomass ± SD (mg dw $m^{-2}$) | Percentage | *n* |
|---|---|---|---|
| 200–500 | 44.37 ± 29.85 | 51.01 | 38 |
| 500–1000 | 11.41 ± 9.60 | 13.28 | 38 |
| > 1000 | 30.51 ± 34.32 | 35.71 | 39 |
| Total | 86.45 ± 56.74 | - | 37 |

and excretion rates of organisms incubated at different temperatures (Fig. 3). Quite high values (and high standard deviations) were observed at 0.2°C while we did not observe any increase of metabolic rates at the higher temperatures (Fig. 3). Large copepods (> 1000 µm) were also incubated in the presence of food. No statistical differences (ANOVA test) were observed between the food and non-food treatments for both respiration and excretion rates.

## Discussion

Zooplankton biomass in the Bransfield Strait during December 1991 was very low and at the lower range of previous estimations of mesoplankton for Antarctic (Boysen-Ennen et al. 1991), as well as for Arctic, waters (Hirche et al. 1994). This result could be the effect of removing the very large macroplankton from the samples (see Materials and methods), which could produce a unique set of data. However, there is a considerable difference with the values of 0.8–3.6 g dw · $m^{-2}$ reported by Boysen-Ennen et al. (1991) for mesoplankton < 14.5 mm and those of Ward et al. (1995), who found values as high as 13 g dw · $m^{-2}$, northwest of South Georgia, also excluding krill. However, Robins et al. (1995) observed low values of biomass (0.02–0.21 gC · $m^{-2}$) in the Bellingshausen Sea during November/December. In the present study, about half of the biomass measured in the Bransfield Strait was observed in the smaller size fraction. This small fraction was mainly composed of large numbers of cyclopoid copepods and copepodite stages of calanoid copepods. From our results, it seems that biomass distribution agreed with the general pattern of water masses in the Bransfield Strait, with higher biomasses appearing in relation to the Weddell waters. This distribution is consistent with the observation of Aristegui and Montero (1995) of higher chlorophyll values in the Weddell water and a higher activity of the electron transport system (ETS) of microplankton in the frontal zone betweeen the Bellingshausen and Weddell waters during the same cruise.

However, the spatial heterogeneity observed in the literature for the zooplankton biomass around the

© Del documento, los autores. Digitalización realizada por ULPGC. Biblioteca Universitaria, 2009

Antarctic Peninsula seems to be a general feature for this area of the ocean (Schnack-Schiel and Mujica 1994). Foxton (1956) observed that zooplankton biomass increased towards the Polar Front and Jazdzewski et al. (1982) also observed about 2–3 times higher biomass in the Antarctic zone north of the South Shetland Islands than in the continental zone in the Bransfield Strait. A possible explanation for the very low biomass sometimes observed near the continent would be the inverse relationship between krill and non-krill zooplankton found by Hosie (1994). This author explained this phenomenon as the consequence of exclusion by krill and/or that krill dominate areas unsuitable for mesozooplankton species. However, it is known that euphausiids are able to predate on copepods (Price et al. 1988; Atkinson and Snÿder 1997) and that there is a positive election for animal food in the presence of both zooplankton and phytoplankton (Granéli et al. 1993). Atkinson and Snÿder (1997) reported a potentially high predation impact of krill on copepods at South Georgia, observing that copepod numbers were low within krill swarms and dispersed krill tended to be located within aggregations of copepods. High values of krill biomass have also been reported for the northern area of the Antarctic Peninsula (Everson and Miller 1994; Siegel and Kalinowski 1994). Therefore, predation by krill could be another possible explanation for the low biomass found in this study and for the heterogeneity normally observed in these waters. This would imply that mesozooplankton organisms are not food limited and therefore their growth and reproduction are not inhibited.

Respiration rates showed average values higher than the ones previously observed in the literature (around 1 µl $O_2 \cdot mg^{-1}$ dw $\cdot$ $day^{-1}$). Rather high values were obtained in our experiments whether or not copepods were incubated in the presence of food (Fig. 3). Because incubation time varied in our experiments between 16 and 27 h (see Materials and methods), and it is known that metabolic rates are higher at the beginning of incubation, decreasing to standard rates during starvation, the high variability observed could be related to variable incubation time. This possibility cannot be ruled out. However, no significative difference was found between respiratory rates in food and non-food treatments. Another explanation for the high variability in respiration rates observed could be derived from the fact that animals can achieve standard and routine metabolism

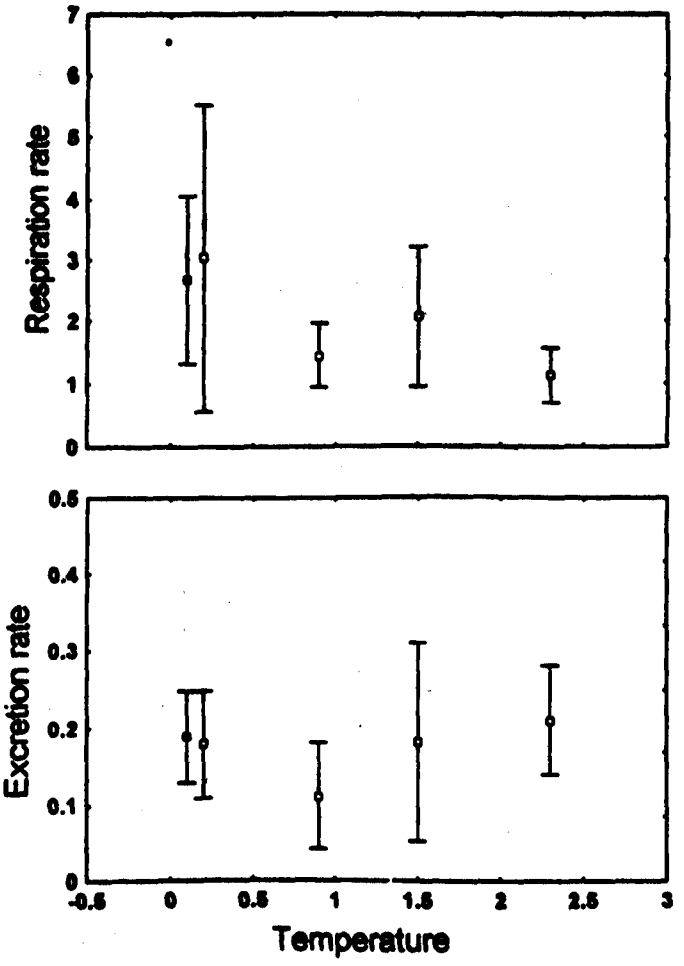


**Fig. 3** A Mass specific respiration (µl $O_2 \cdot mg^{-1}$ dw $\cdot$ $h^{-1}$), and B excretion rates (µg N $\cdot$ $mg^{-1}$ dw $\cdot$ $h^{-1}$) of *Calanoides acutus* in relation to temperature. *Bars* indicate standard deviation. *Unfilled symbols* indicate experiments performed in filtered seawater and *filled symbols* experiments carried out in the presence of phytoplankton

**Table 2** Respiration and ammonia excretion rates (± standard deviation) of zooplankton of different size classes in the Bransfield Strait during December 1991. Experiments with organisms > 1000 µm were performed in the absence (*FSW*) and presence (*Fed*) of food. The O/N ratio was calculated taking the nitrogen excretion in terms of ammonia release

| Size fraction (µm) | Respiration rates (µl $O_2 \cdot mg^{-1}$ dw $\cdot$ $h^{-1}$) | Excretion rates (µg N $\cdot$ $mg^{-1}$ dw $\cdot$ $h^{-1}$) | O/N |
|---|---|---|---|
| 200–500 | 1.01 ± 0.48 ($n$ = 4) | 0.07 ± 0.05 ($n$ = 5) | 31 ± 16 ($n$ = 4) |
| 500–1000 | 2.10 ± 1.61 ($n$ = 3) | 0.08 ± 0.06 ($n$ = 3) | 35 ± 8 ($n$ = 3) |
| > 1000 FSW | 1.95 ± 1.40 ($n$ = 12) | 0.16 ± 0.08 ($n$ = 13) | 20 ± 17 ($n$ = 12) |
| > 1000 Fed | 2.57 ± 1.48 ($n$ = 8) | 0.18 ± 0.06 ($n$ = 7) | 18 ± 14 ($n$ = 7) |
| *Euphausia superba* | 0.36 ± 0.11 ($n$ = 6) | 0.06 ± 0.01 ($n$ = 6) | 8 ± 3 ($n$ = 6) |

© Del documento, los autores. Digitalización realizada por ULPGC. Biblioteca Universitaria, 2009

(sensu Brett 1964) during the course of experiments. A three to fourfold increase in metabolic rates could be related to locomotory and feeding activities, as well as to the so-called specific dynamic action, which represents the metabolic cost of protein synthesis (Kiørboe et al. 1985; Brown and Cameron 1991). However, our respiration and excretion rate experiments were performed within a temperature range of less that 2.5°C. The narrow range of experimental temperature could explain the lack of relationship between temperature and physiological rates. However, the ammonia excretion rates observed are higher than the values previously reported in the literature. Values given by Ikeda and Hing Fay (1981) were obtained after maintaining copepods for 2–6 weeks after collection. Values reported by Huntley and Nordhausen (1995) of 0.02 $\mu g\ N \cdot mg^{-1}\ dw \cdot h^{-1}$ were obtained in winter in a contrasting situation to the onset of the bloom in these waters.

Our average respiration rates converted to carbon units, assuming a protein-based metabolism (see Conover and Huntley 1991), indicate that respiration accounted for less than 1% of primary production during the cruise (average value of 333 $mgC \cdot m^{-2} \cdot day^{-1}$; Basterretxea and Aristegui, 1998). Assuming a constant N/C ratio of 0.16 for the assimilation of primary producers (Goldman and McCarthy 1978), our higher estimate of ammonia excretion by mesozooplankton indicates that this community could account for less than 0.5% of the $^{14}C$ primary production. A rough estimate of ingestion, assuming that about two-thirds of the ingested food is assimilated and one-half of the assimilated food is metabolized and the other half is used for growth and reproduction, indicates that potential grazing (assuming herbivorous feeding) was 2.4% of primary production. This value agrees with the ones reported by Atkinson and Shreeve (1995) who observed that the control exerted on primary production by mesozooplankton is a low number (normally much less than 8%). However, our measurements, as well as those of Atkinson and Shreeve (1995), did not consider the impact of *Euphausia superba*. The biomass of euphausiids for the Southern Ocean has been estimated to be in the range of 1–2 g dry weight $\cdot m^{-2}$ (Siegel 1986, in Boysen-Ennen et al. 1991). Taking into account the upper range of biomass (2 g dry weight $\cdot m^{-2}$) and our measurements of respiration for krill (Table 2), we found that their metabolic requirements accounted for 2.7% of the available primary production. Calculating potential grazing by krill as above, we deduced that those organisms consume only 8.1% of primary production assuming herbivorous feeding. Recently, Pakhomov and Perissinotto (1996) found that *Euphausia crystallorophias* also ingest a small fraction of primary production (0.02–1.12%) but the presence of dense swarms may result in the local removal of levels of daily primary production as high as 13.6–96.5%. Although control of primary production by krill could be occasionally high, our results (based on an upper limit calculation) show that an important amount of the measured $^{14}C$ primary production is not generally consumed by meso- and macrozooplankton.

These results support the finding of Aristegui et al. (1996) who observed that up to 50% of gross primary production is respired by microplankton. Therefore, phytoplankton sinking (Bodungen et al. 1986) and their respiratory losses may account for a large portion of the fate of primary production. It cannot be ruled out that krill, non-krill and krill swarm scenarios may produce quite important differences in the flux of energy and this fact must be considered in future studies and models of the Southern Ocean ecosystem. However, from our estimates of potential grazing pressure, the high chlorophyll values (see Aristegui and Montero 1995), and taking into account the omnivorous feeding behaviour of copepods, it seems that mesozooplankton is not food limited, at least during the course of our sampling. However, food limitation is not only a function of quantity but also of quality (Kleppel 1993; Jónasdóttir et al. 1995; McKinnon 1996). Therefore, food quality and predation could be important factors explaining the low abundances of copepods in these waters. Diatoms were observed to be abundant while protozoa are also an abundant component of microplankton in polar waters (see Stoecker and Capuzzo 1990), and these food components are considered of standard quality for mesozooplankton. Krill are able to predate on copepods (Price et al. 1988; Atkinson and Snÿder 1997), they select mesozooplankton (Granéli et al. 1993) and they are abundant around the Antarctic Peninsula (Everson and Miller 1994; Siegel and Kalinowski 1994). Therefore, it is suggested that krill could produce a top-down effect that could explain the low values of mesozooplankton biomass sometimes found around the Antarctic Peninsula. Further research is needed to elucidate this effect of krill in the structure of mesozooplankton communities of Antarctic waters.

**Acknowledgements** This work was supported by the "Comisión Interministerial de Ciencia y Tecnologia – Programa Antártico Español" (project "Oceanografía del Estrecho de Bransfield, 1991"). Helpful comments on the manuscript made by three anonymous referees were greatly appreciated.

## References

Aristegui J, Montero MF (1995) Plankton community respiration in Bransfield Strait (Antarctic Ocean) during austral spring. J Plankton Res 17:27–39

Aristegui J, Montero MF, Ballesteros S, Basterretxea G, Lenning K van (1996) Planktonic primary production and microbial respiration measured by $^{14}C$ assimilation and dissolved oxygen changes in coastal waters of the Antarctic Peninsula during austral summer: implications for carbon flux studies. Mar Ecol Prog Ser 132:191–201

Atkinson A, Shreeve RS (1995) Response of the copepod community to a spring bloom in the Bellingshausen Sea. Deep Sea Res 42:1291–1311

Atkinson A, Snÿder R (1997) Krill-copepod interactions at South Georgia, Antarctica. I. Omnivory by *Euphausia superba*. Mar Ecol Prog Ser 160:63–76

© Del documento, los autores. Digitalización realizada por ULPGC. Biblioteca Universitaria, 2009

Basterretxea G, Aristegui J (1998) Phytoplankton biomass and production during late austral spring (1991) and summer (1993) in the Bransfield Strait. Polar Biol (in press)
Bodungen B, Smetacek VS, Tilzer MM, Zeitzschel B (1986) Primary production and sedimentation during spring in the Antarctic Peninsula region. Deep Sea Res 33:177–194
Boysen-Ennen E, Hagen W, Hubold G, Piatkowski U (1991) Zooplankton biomass in the ice-covered Weddell Sea, Antarctica. Mar Biol 111:227–235
Brett JR (1964) The respiratory metabolism and swimming performance of young sockeye salmon. J Fish Res Board Can Symp 21:1183–1226
Brown CR, Cameron JN (1991) The relationship between specific dynamic action (SDA) and protein synthesis rates in the channel catfish. Physiol Zool 64:298–309
Bryan JR, Riley JP, Williams PJL (1976) A Winkler procedure for making precise measurements of oxygen concentration for productivity and related studies. J Exp Mar Biol Ecol 21:191–197
Conover RJ, Huntley M (1991) Copepods in ice-covered seas. Distribution, adaptations to seasonally limited food, metabolism, growth pattern and life cycle strategies in polar seas. J Mar Systems 2:1–41
Drits AV, Pasternak AF, Kosobokova KN (1993) Feeding, metabolism and body composition of the Antarctic copepod *Calanus propinquus* Brady with special reference to its life cycle. Polar Biol 13:13–21
Everson I, Miller DGM (1994) Krill mesoscale distribution and abundance: results and implications of research during the BIOMASS programme. In: El-Sayed SZ (ed) Southern Ocean ecology. The biomass perspective. Cambridge University Press, London, pp 129–143
Foxton P (1956) The distribution of the standing crop of zooplankton in the Southern Ocean. Discovery Rep 28:191–236
Garcia MA, Lopez O, Sospedra J, Espino M, Gracia V, Morrison G, Rojas P, Figa J, Puigdefabregas J, Arcilla AS (1994) Mesoscale variability in the Bransfield Strait region (Antarctica) during austral summer. Ann Geophys 12:887–902
Godlewska M (1993) Acoustic observations of krill (*Euphausia superba*) at the ice edge (between Elephant I. and South Orkney I. Dec. 1988/Jan.1989). Polar Biol 13:507–514
Goldman JC, McCarthy JJ (1978) Steady state growth and ammonium uptake of a fast growing marine diatom. Limnol Oceanogr 23:695–703
Granéli E, Granéli W, Mozzan Rabbani M, Daugbjerg N, Fransz G, Cuzin-Roudy J, Alder VA (1993). The influence of copepod and krill grazing on the species composition of phytoplankton communities from the Scotia-Weddell Sea. Polar Biol 13:201–213
Grelowski A, Tokarczyk R (1985) Hydrological condition in the region of Bransfield Strait and southern part of Drake pasage in the period from December 10, 1983 and January 8, 1984 (BIOMASS-SIBEX). Pol Polar Res 6:31–41
Hirche J, Hagen W, Mumm N, Richter C (1994) The northeast water polynya, Greenland Sea. III Meso- and macrozooplankton distribution and production of dominant herbivorous copepods during spring. Polar Biol 14:491–503
Hosie GW (1994) The macrozooplankton communities in the Prydz Bay region, Antarctica. In: El-Sayed SZ (ed) Southern Ocean ecology. The biomass perspective. Cambridge University Press, London, pp 98–123
Huntley ME, Nordhausen W (1995) Ammonium cycling by Antarctic zooplankton in winter. Mar Biol 121:457–467
Ikeda T, Hing Fay E (1981) Metabolic activity of zooplankton from the Antarctic Ocean. Aust J Mar Freshwater Res 32:291–930
Ikeda T, Mitchell AW (1982) Oxygen uptake, ammonia excretion and phosphate excretion by krill and other Antarctic zooplankton in relation to their body size and chemical composition. Mar Biol 71:283–298
Jazdzewski K, Kittel W, Lotocki K (1982) Zooplankton studies in the Southern Drake Passage and in the Bransfield Strait during the austral summer (BIOMASS-FIBEX, February–March 1981). Pol Polar Res 3:203–242
Jónasdóttir SH, Fields D, Pantoja S (1995) Copepod egg production in Long Island Sound, USA, as a function of chemical composition of seston. Mar Ecol Prog Ser 119:87–98
Kiørboe T, Møhlemberg F, Hamburger K (1985) Bioenergetics of the planktonic copepod *Acartia tonsa*: relation between feeding, egg production and respiration, and composition of specific dynamic action. Mar Ecol Prog Ser 26:85–97
Kleppel GS (1993) On the diets of calanoid copepods. Mar Ecol Prog Ser 99:183–195
Lancelot C, Mathot S, Veth C, Baar H de (1993) Factors controlling phytoplankton ice-edge blooms in the marginal ice-zone of the northwestern Weddell Sea during sea ice retreat 1988: field observations and mathematical modelling. Polar Biol 13:377–387
Lovegrove T (1966) The determination of the dry weight of plankton and the effect of various factors on the values obtained. In: Barnes H (ed) Some contemporary studies in marine science. Allen & Unwin, London, pp 429–467
McKinnon AD (1996) Growth and development in the subtropical copepod *Acrocalanus gibber*. Limnol Oceanogr 41:1438–1447
Miller DGM, Barange M, Klindt H, Murray AWA, Hampton I, Siegel V (1993) Antarctic krill aggregation characteristics from acoustic observations in the Southwest Atlantic Ocean. Mar Biol 117:171–183
Niiler PP, Amos A, Hu JH (1991) Water masses and 200 m. relative geostrophic circulation in the western Bransfield Strait region. Deep Sea Res 38:943–959
Pakhomov EA, Perissinotto R (1996) Antarctic neritic krill *Euphausia crystallorophias*: spatio-temporal distribution, growth and grazing rates. Deep Sea Res 43:59–87
Parsons TR, Maita Y, Lalli CM (1984) A manual of chemical and biological methods for seawater analysis. Pergamon Press, Oxford
Price HJ, Boyd KR, Boyd CM (1988) Omnivorous feeding behavior of the Antarctic krill *Euphausia superba*. Mar Biol 97:67–77
Robins DB, Harris RP, Bedo AW, Fernandez E, Fileman TW, Harbour DS, Head RN (1995) The relationship between suspended particulate material, phytoplankton and zooplankton during the retreat of the marginal ice zone in the Bellingshausen Sea. Deep Sea Res 42:1137–1158
Rojas P, Lopez O, Garcia M, Aristegui J, Torres S, Hernández-León S, Bastarrechea G, Amengual B, Escamez J, Morales B (1996) Hidrografía del Estrecho de Bransfield durante el verano Austral 91/92. Proc. V Spanish Symposium on Antarctic Studies. Comision Interministerial de Ciencia Technologia, Madrid, pp 403–411
Schnack-Schiel SB, Mujica A (1994) The zooplankton of the Antarctic Peninsula region. In: El-Sayed SZ (ed) Southern Ocean ecology. The biomass perspective. Cambridge University Press, London, pp 79–92
Siegel V (1986) Structure and composition of the Antarctic krill stock in the Bransfield Strait (Antarctic Peninsula) during the Second International BIOMASS Experiment (SIBEX). Arch Fischereiweiss 37:51–72
Siegel V, Kalinowski J (1994) Krill demography and small-scale processes: a review. In: El-Sayed SZ (ed) Southern Ocean ecology. The biomass perspective. Cambridge University Press, London, pp 145–163
Stoecker DK, Capuzzo JM (1990) Predation on protozoa: its importance to zooplankton. J Plankton Res 12:891–908
UNESCO (1968) Zooplankton sampling. Monogr Oceanogr Methodol 2
Ward P, Atkinson A, Murray AWA, Wood AG, Williams R, Poulet SA (1995) The summer zooplankton community at South Georgia: biomass, vertical migration and grazing. Polar Biol 15:195–208

© Del documento, los autores. Digitalización realizada por ULPGC. Biblioteca Universitaria, 2009

Grasas y Aceites
Vol. 50. Fasc. 6 (1999), 469-471



# Effect of glycerol on the lipids in the red alga *Gratelupia doryphora*

By A.P. Ivanova [1], R.R. Robaina [2], J. Martín [2] and K.L. Stefanov [3*]

[1] Institute of Plant Physiology, Bulgarian Academy of Sciences, Sofía 1113, Bulgaria.
[2] Dpto. Biología, Universidad de Las Palmas de G.C., Box 550, Las Palmas, G.C., Canary Islands, Spain.
[3] Institute of Organic Chemistry with Centre of Phytochemistry, Bulgarian Academy of Sciences, «Acad. G. Bonchev» Str., Bl. 9, Sofía 1113, Bulgaria.

**RESUMEN**

**Efecto del glicerol sobre los lípidos de la alga roja *Gratelupia doryphora*.**

Se cultivó alga roja *Gratelupia doryphora* en agua de mar enriquecida con Provasoli y en glicerol. La incubación en agua de mar condujo a un aumento en el porcentaje de los ácidos grasos poliinsaturados, mientras que el glicerol incrementó el contenido de lípidos totales. Por tanto, si la alga está siendo producida como un cultivo heterotrófico, es posible aumentar la biomasa de la misma así como el contenido de ácidos grasos biológicamente activos.

*PALABRAS-CLAVE: Alga roja - Glicerol (efecto del) - Gratelupia doryphora - Lípido.*

**SUMMARY**

**Effect of glycerol on the lipids in the red alga *Gratelupia doryphora*.**

The red alga *Gratelupia doryphora* was cultivated in Provasoli enricher (plain) seawater and in a glycerol media. The incubation in seawater leads to an increase in the percentage of polyunsaturated acids, while the glycerol increase the total lipid content. If the alga is being grown as a heterotrophic culture, it is possible to increase the alga biomass as well as the content of biologically-active fatty acids.

*KEY-WORDS: Glycerol (effect of) - Gratelupia doryphora - Lipid - Red alga.*

## 1. INTRODUCTION

The need for sea food and drugs is due to the increasing human population and to the biological potential of marine products. A reasonable way of meeting this deficiency is trough cultivation and production of valuable marine algae for food and pharmaceutical industry. As stated by Cheng (1996), heterotrophic culture may provide an alternative method of cultivation for some algae that utilise organic carbon substances.

Recently we have reported that glycerol stimulates vegetative growth and shoot emission with effects on morphogenesis and oxygen uptake and evolution. Furthermore, there are evidences of an intense accumulation of lipid and polisaccharidic substances when glycerol is added to the cultures (Robaina *et al.*, 1990a, b; Robaina *et al.*, 1995; García-Jiménez *et al.*, 1996, 1998).

The aim of the present work was to study the changes in the main lipid classes and their fatty acid (FA) profiles in *G. doryphora* when glycerol was used in the culture medium.

## 2. EXPERIMENTAL

Thalli of *Gratelupia doryphora* (voucher specimen deposited in the herbarium of the Jardin Canario, Gran Canaria, Canary Islands, Spain as sheet 129) were collected from the upper intertidal pools in the rocky littoral of San Cristóbal (Gran Canaria, Canary Islands). They were immediately transferred to the laboratory. Disc fragments of 3 mm diameter were excised within 2 h. The fragments were disinfected and tested for sterility as previously described (Robaina *et al.*, 1990 a, b). Explants were then cultivated in 100 ml Pyrex flasks with 50 ml of autoclaved seawater (20-25 explants per flask). The glycerol media was prepared with plain seawater diluted with distilled water (70:30 v/v) and 0.3 M glycerol. Seawater dilution is necessary to avoid osmotic stress due to the addition of glycerol. The osmolality of both culture media was 1.0 osmol $kg^{-1}$ as checked out with an osmometer (Robaina *et al.*, 1990 b). All culture media were supplemented with nutrients formulations and vitamins of the Provasoli enriched seawater medium (PES, Provasoli 1968).

© Del documento, los autores. Digitalización realizada por ULPGC. Biblioteca Universitaria, 2009

Cultures were placed in an orbital shaker for 5 days. They were subjected to 16 h light - 8 h dark photoperiod at 19 ± 2 °C and irradiance of 30 mmol photon $m^{-2}$ $s^{-1}$. Two grams (fresh weight) of thalli was also used to perform analysis as a control of the contents in natural samples (non cultivated). They were epiphyte-free thalli cleaned further with brushes to avoid the contamination with organism associated with the thallus.

The total lipids were extracted according to Bligh and Dyer (1959). The main lipid classes: triacylglycerols (TAG), monogalactosyl diacylglycerols (MGDG), digalactosyl diacylglycerols (DGDG) and phospholipids (PL) were separated by preparative thin-layer chromatography (Silica gel G, *Merck*, layer thickness 0.5 mm). The lipid spots were vizualized under UV-light after spraying with fluorescent indicator, scrapped off into small glass containers with teflon screw caps. After addition of internal standard (heptadecanoic acid) all lipid classes were transesterified with 15 % acetyl chloride in methanol. The analysis of the obtained fatty acid methyl esters (FAME) was carried out by flame-ionization detector - gas-liquid chromatography (FID-GLC) on a glass capillary column (30 m, 0.2 mm i.d. coated with SILAR 10 C). The column temperature was increased from 165 °C to 220 °C (2 deg $min^{-1}$) with nitrogen as a carrier gas at a flow rate 14 mL $s^{-1}$. The amount of each lipid class was determined on the basis of the FAME weight using converting factors as follows: 1.0 for TAG; 1.4 for MGDG and PL and 1.8 for DGDG (Elenkov *et al.*, 1993).

## 3. RESULTS AND DISCUSSION

Table I represents the effect of culture with plain seawater or glycerol media on the amounts of the main lipid classes in *G. doryphora* compared to natural samples. The plain seawater in the culture medium leads to a decrease of the amount of the total lipids and especially of the PL. The PL are substantial components of the cell membranes and their decrease may leads to changes in the membrane fluidity. There is a slight increase of the MGDG.

However the addition of glycerol in the culture medium leads to substantial increase of the total lipids and glycolipids. The amount of PL leaves constant.

The cultivation of the algae in plain seawater leads to substantial changes in the FA-profiles of the alga (Table II). The amount of the 20:5 acid increase almost twice, and 16:0 acid decrease. These changes are more expressed in the TAG and PL. As a result the FA-profiles of plain seawater-incubated algae are similar to those from a sample of *Grateloupia turuturu* Yam. from Japan Sea (Khotimchenko and Vaskovsky, 1990). In contrary, the incubation with a glycerol media has not significant effect on the FA-composition of the alga.

It is evident that changes in the culture medium lead to changes of the lipid content of the alga. If this alga being grown in heterotrophic cultures, it is possible to increase the algal biomass as well as to exploit the increase in biologically-active fatty acids. It remains to investigate whether the alteration of the nutrient or other paramethers of culture conditions (Falkowsky, 1988) could drive to even better yield in some lipid fractions.

Table I

**Effect of glycerol and PROVASOLI on the main lipid classes in *G. doryphora***

| Culture medium and lipid classes | mg $g^{-1}$ DW | % of total |
|---|---|---|
| **Control (collected in the nature)** | | |
| TAG | 8.7 ± 0.7 | 35.9 |
| MGDG | 3.4 ± 0.3 | 14.1 |
| DGDG | 4.2 ± 0.3 | 17.5 |
| PL | 7.8 ± 0.6 | 32.5 |
| Total | 24.1 ± 1.9 | 100.0 |
| **Plain seawater** | | |
| TAG | 7.3 ± 0.6 | 40.7 |
| MGDG | 5.5 ± 0.4 | 30.5 |
| DGDG | 2.4 ± 0.2 | 13.5 |
| PL | 2.8 ± 0.2 | 15.3 |
| Total | 18.0 ± 1.4 | 100.0 |
| **Glycerol media** | | |
| TAG | 11.5 ± 0 9 | 38.1 |
| MGDG | 5.5 ± 0 4 | 18.2 |
| DGDG | 6.0 ± 0.4 | 19.9 |
| PL | 7.2 ± 0 6 | 23.8 |
| Total | 30.2 ± 2 3 | 100.0 |

© Del documento, los autores. Digitalización realizada por ULPGC. Biblioteca Universitaria, 2009

Table II
Effect of glycerol and PROVASOLI on the fatty acid composition of *G. doryphora*

| Culture medium and lipid classes | Fatty acids (% on total FAME) | | | | | | | | |
|---|---|---|---|---|---|---|---|---|---|
| | 14:0 | 16:0 | 16:1 | 18:0 | 18:1 | 18:2 | 18:3 | 20:4 | 20:5 |
| **Control (collected in the nature)** | | | | | | | | | |
| TAG | 5.7 | 43.4 | 2.1 | 15.1 | 3.4 | 0.9 | 1.7 | 14.1 | 13.5 |
| MGDG | 11.3 | 53.2 | 2.4 | 1.8 | 0.9 | — | — | 14.0 | 16.1 |
| DGDG | 1.2 | 63.0 | 1.3 | 0.7 | — | — | — | 17.0 | 16.2 |
| PL | 7.3 | 60.9 | 2.2 | 1.1 | 2.3 | — | — | 12.8 | 13.2 |
| Total | 6.2 | 53.8 | 2.0 | 6.1 | 1.7 | 0.3 | 0.6 | 14.2 | 14.2 |
| **Plain seawater** | | | | | | | | | |
| TAG | 4.3 | 28.0 | 1.7 | 13.1 | 5.0 | 0.4 | 1.8 | 14.0 | 31.4 |
| MGDG | 11.4 | 45.8 | — | 5.0 | — | 3.8 | — | 20.0 | 13.7 |
| DGDG | 14.5 | 29.5 | 3.8 | 2.2 | — | — | — | 14.9 | 32.5 |
| PL | 12.5 | 40.0 | — | — | — | 4.2 | — | 13.7 | 25.6 |
| Total | 9.1 | 35.5 | 1.2 | 7.1 | 2.0 | 2.0 | 0.7 | 15.9 | 25.3 |
| **Glycerol media** | | | | | | | | | |
| TAG | 6.6 | 48.8 | 1.3 | 13.2 | 4.1 | — | 0.8 | 12.4 | 12.6 |
| MGDG | 7.3 | 54.1 | 0.6 | 8.4 | — | — | 0.9 | 12.7 | 15.2 |
| DGDG | 6.1 | 51.0 | 2.0 | 5.5 | — | — | 0.3 | 14.6 | 18.5 |
| PL | 8.3 | 48.2 | 5.3 | 1.6 | — | 4.2 | 5.3 | 10.7 | 15.3 |
| Total | 7.0 | 50.1 | 2.3 | 8.0 | 1.6 | 1.0 | 1.8 | 12.5 | 14.9 |

## ACKNOWLEDGEMENT

The authors are grateful to the National Foundation of Scientific research of Bulgaria for the partial financial support under contract X-617.

## REFERENCES

Bligh, E.G. and Dyer, W.J. (1959).—«A rapid method of total lipid extraction and purification».—Can. J. Biochem. Physiol. 37, 911-917.

Chen, F. (1996).—«High cell density culture of microalgae in heterotrophic growth».—Trends in Biotechnology 14, 421-426.

Elenkov, J.I., Ivanova, A.P., Stefanov, K.L., Seisova, K.A. and Popov, S.S. (1993).—«A quantitative determination of lipid classes in higher plants and algae by a gas-chromatographic procedure».—Bulg. Chem. Commun. 26, 98-103.

Falkowsky, P.G. 1988.—«Potential strategies for regulating the flux of carbon into specific chemical classes in microalgae».—In Polysaccharides from microalgae: a new agroindustry (Ramus J. & Jones M.C. eds.) Proc. US.- Israel Workshop. Beaufort. North Carolina, USA, pp. 83-91.

García-Jiménez, P., Robaina, R.R., Luque, A and Tsekos, I. (1996).—«Glycerol activated celular division and biosynthetic actitvity during growth and morphogenesis of carpospore-seedling of *Grateloupia doryphora*».—Phycologia 35, 261-269.

García-Jiménez, P., Rodrigo, M. and Robaina, R.R. (1998).—«Glycerol, polyamines and growth regulators interaction on growth and development of sporelings in vitro».—Journal of Applied Psychology (in Press).

Khotimchenko, S.V. and Vaskovsky, V.E. (1990).—«Distibution of $C_{20}$ polyenoic fatty acids in red macrophytic algae».—Botánica Marina 33, 525-528.

Provasoli, L. (1968).—«Media and prospects for the cultivation of marine algae».—In: Watenebe, A., Hattori, A. (eds.). Cultures and collections of algae. Jap. Soc. of Plant Physiology, Hakone, pp. 63-75.

Robaina, R.R., Brito, I., García-Jiménez, P. and Luque, A. (1995).—«Light control of the respiration of exogenous glycerol in the red macroalga *Grateloupia doryphora*».—European Journal Psychology 30, 81-86.

Robaina, R.R., García-Reina, G. and Luque, A. (1990a).—«The effect of the physical characteristics of the culture medium on the development of red seaweeds in tissue culture».—Hydrobiología, 204, 137-142.

Robaina, R.R., García-Jiménez, P. and Luque, A. (1990b).—«Morphogenetic effect of glycerol on tissue cultures of the red seaweed *Grateloupia doryphora*».—J. Appl. Psychol. 2, 137-143.

Recibido: Noviembre 1998
Aceptado: Abril 1999

© Del documento, los autores. Digitalización realizada por ULPGC. Biblioteca Universitaria, 2009

# Biology of a deep benthopelagic fish, roudi escolar *Promethichthys prometheus* (Gempylidae), off the Canary Islands

**José M. Lorenzo**
**José G. Pajuelo**
Departamento de Biología (Universidad de Las Palmas de Gran Canaria)
Edificio de Ciencias Básicas, Campus Universitario de Tafira
35017 Las Palmas, Spain
E-mail address (for J. M. Lorenzo): josemaria.lorenzo@biologia.ulpgc.es

**Abstract**—The roudi escolar *Promethichthys prometheus* is common in deep hook-and-line and longline catches of a small-scale fishery along the slope off the Canary Islands. Population structure, reproduction, growth, and mortality of the species were studied from sampling undertaken from August 1992 to July 1995. Range of length of fish in the catches was between 36 and 80 cm TL, with a main distribution between 56 and 66 cm. The overall ratio of males to females was 1:1.74. Females predominated in all sizes. The sex ratio varied throughout the period of study; the lowest discrepancy between males and females, however, was during the reproductive period. A vertical space partitioning among sexes was observed, with males predominating from 600 to 800 m depth, females from 300 to 500 m. The reproductive period of the species was from April to September, with a peak in spawning in June–July. The size at first maturity was 47.41 cm. The parameters of the length-weight relationship for all fish were $a$=0.004521 and $b$=2.98932. Age readings of otoliths indicated that the exploited population consisted of nine age groups (III–XI years). The von Bertalanffy growth parameters for all individuals were $L_\infty$=93.61 cm, $k$=0.18/years, and $t_0$=−1.54 years. The rates of mortality for all fish were $Z$=0.49/years, $M$=0.35/years, and $F$=0.14/years. The length at first capture for the whole population was 51.57 cm.

Manuscript accepted 23 April 1998.
Fish. Bull 97:92–99 (1999).

The family Gempylidae consists of 16 genera and 23 species. Only seven species are found off the Canary Islands, one of which is the roudi escolar *Promethichthys prometheus* (Cuvier, 1832), the only species recognized to date in the genus *Promethichthys* (Nakamura and Parin, 1993).

The roudi escolar is a benthopelagic marine fish that has a worldwide distribution in tropical and warm temperate waters. This species generally inhabits waters between 100 and 800 m in depth over seamounts and continental and insular slopes. It migrates upward at night, probably forming schools (Nakamura, 1981; Parin, 1986; Nakamura and Parin, 1993).

Published information on *P. prometheus* is very scarce. The majority of studies describe its morphological characteristics, geographical and depth distribution, and ecology (Nakamura, 1981; Parin, 1986; Nishikawa, 1987; Nakamura and Parin, 1993). Only Lorenzo and Pajuelo (1995) have studied some biological aspects of the species. These authors carried out a preliminary study on the sex ratio, reproduction, and age and growth of roudi escolar off the Canary Islands (central-east Atlantic) on the basis of a small number of specimens during one life cycle. This paper is an extension of their work, analyzing, in addition to all those aspects, population structure and mortality.

The roudi escolar is common in the catches of the deep hook-and-line and longline small-scale fishery over the slope off the Canary Islands. In this area, this species is captured year round without significant seasonal differences in landings.

## Materials and methods

Between August 1992 and July 1995, the TL (cm) of 1879 specimens of roudi escolar was measured monthly from commercial catches of the small-scale fleet. Fish were caught with baited hook-and-lines and longlines at depths of 285–870 m around the islands of the Canary archipelago (Fig. 1).

A subsample was taken by a random stratified method from each sample for biological examination. In total, 776 individuals were analyzed. For each fish, the TW (0.1 g) and the weight of the gonads (0.01 g) were measured, and sex and stage of maturation were ascertained macroscopically. The latter was classified as follows: I = immature; II = resting; III = ripe; IV = ripe and running; V = spent. Sagittal otoliths of the fish were extracted, cleaned, and stored dry. The length-frequency distribution of individuals in catches was calculated. Data were pooled for 1992–95.

© Del documento, los autores. Digitalización realizada por ULPGC. Biblioteca Universitaria, 2009

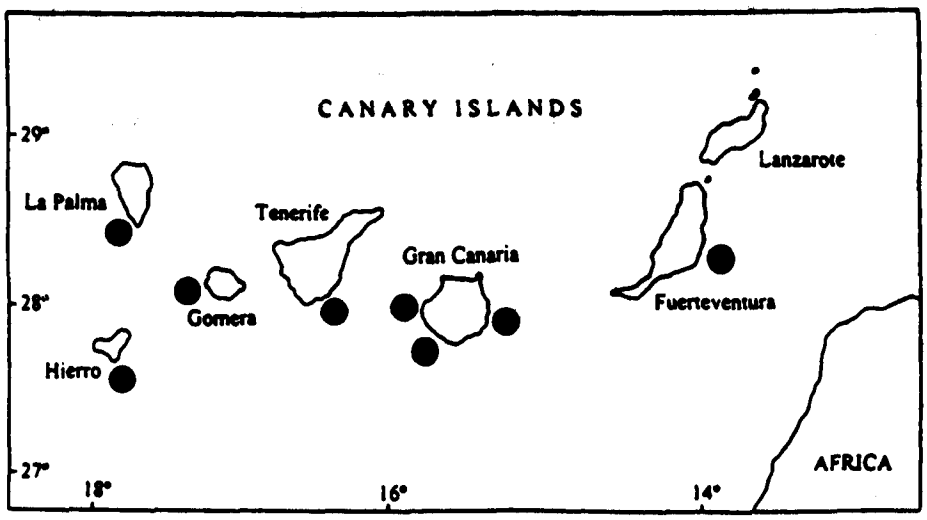


**Figure 1**
Location of sampling areas (●) in the Canary Islands.

The sex ratios (males:females) for the whole sample, for different size classes, for quarters of a year, and for depth strata were calculated. The reproductive season was determined on the basis of monthly variations of the gonadosomatic index (GSI) according to Anderson and Gutreuter (1983). The length at sexual maturity (length at which fifty percent of the specimens became mature) was estimated by means of a logistic function that was fitted to the proportion of the mature individuals (stages III, IV, and V) by using a nonlinear regression (Saila et al., 1988).

The ratio of total length to total weight was calculated over the whole period for males and females separately, as well as for the population as a whole, by applying a linear regression (Ricker, 1973). Age was determined by interpreting growth rings on the otoliths; whole otoliths were placed in a watch glass with a blackened bottom and containing glycerin and examined under a compound microscope with reflected light. Counts for each specimen were performed at least twice and only coincident readings were accepted. An index of average percent error (APE) developed by Beamish and Fournier (1981) was used to compare the precision of age determinations. Ageing was validated indirectly by examination of monthly changes in appearance of the margins of the otoliths (Morales-Nin, 1987). The date 1 July was considered as birthdate to assign the individual ages to age groups. The von Bertalanffy growth curve was fitted to data of the resulting age-length key by means of the Marquardt's algorithm for nonlinear least squares parameter estimation (Saila et al., 1988).

Length-frequency data were converted to age frequencies by using the estimated von Bertalanffy growth parameters (Pauly, 1983, 1984). The rate of total mortality ($Z$) was calculated from the length converted catch curve by using ELEFAN program (Gayanilo et al., 1988). The rate of natural mortality ($M$) was determined from the equation of Pauly (1980). Following estimation of $Z$ and $M$, the rate of fishing mortality ($F$) was calculated by substraction. The length at first capture was estimated from the selection ogive generated from the length converted catch curve (Pauly, 1984).

## Results

The size-frequency distribution showed a length range of 36 to 80 cm TL in the catches, with a main distribution between 56 and 66 cm (Fig. 2).

Of the 776 fish examined, 282 (36.3%) were male, 491 (63.3%) female. The sex of the remaining 3 (0.4%) individuals could not be identified macroscopically because they were immature and had very thin, translucent gonads. The overall ratio of males to females was 1:1.74 and $\chi^2$ analysis revealed this to be significantly different from a 1:1 ratio (Table 1). Females predominated in all size intervals. Sex ratios for males and females grouped into 5-cm length classes had significant departures from the 1:1 ratio for all size intervals (Table 1). The ratio of males to females varied throughout the period of study, but there were no significant differences from the 1:1 ratio during the spring and summer months (Table 2). There was a relationship between the sex of roudi escolar and depth; males predominated at 600 to 800 m depths, females at 300 to 500 m (Table 3).

The GSI showed higher values for females than for males (Fig. 3). The same temporal variation pat-

© Del documento, los autores. Digitalización realizada por ULPGC. Biblioteca Universitaria, 2009

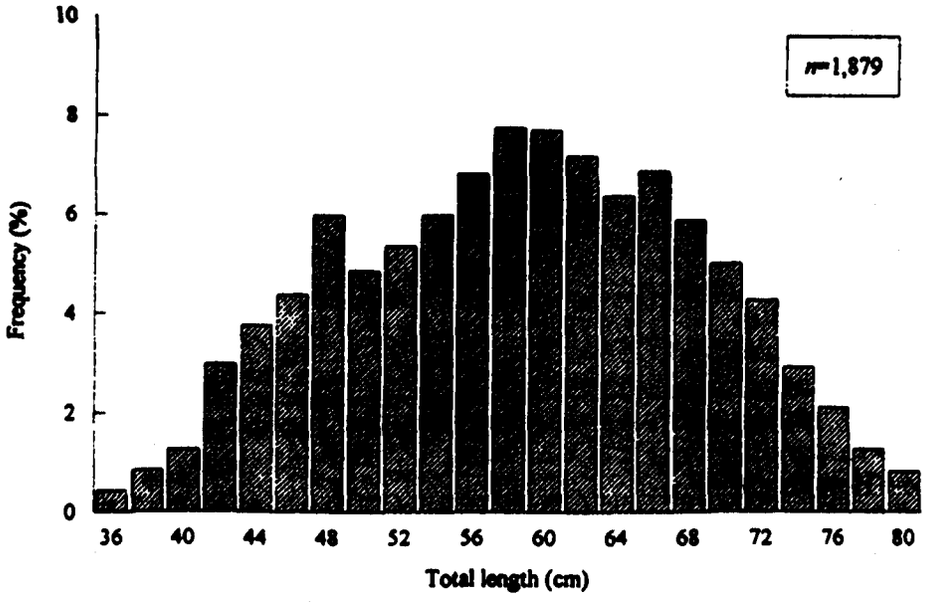


**Figure 2**

Length-frequency distribution for *P. prometheus* caught off the Canary Islands (August 1992–July 1995).

**Table 1**

Number of males and females of *P. prometheus* caught off the Canary Islands by 5-cm size class and sex ratio tested by chi-square analysis. *=$\chi^2 > \chi_t^2{}_{1,0.05}$=3.84.

| Length (cm) | Males | Females | Sex ratio | $\chi^2$ |
|---|---|---|---|---|
| 35.1–40.0 | 5 | 14 | 1:2.80 | 4.26* |
| 40.1–45.0 | 21 | 40 | 1:1.90 | 5.91* |
| 45.1–50.0 | 29 | 52 | 1:1.79 | 6.53* |
| 50.1–55.0 | 45 | 71 | 1:1.57 | 5.82* |
| 55.1–60.0 | 60 | 94 | 1.1.56 | 7.50* |
| 60.1–65.0 | 48 | 84 | 1:1.75 | 9.80* |
| 65.1–70.0 | 36 | 62 | 1:1.72 | 6.89* |
| 70.1–75.0 | 26 | 48 | 1:1.76 | 6.54* |
| 75.1–80.0 | 12 | 26 | 1:2.16 | 5.15* |
| Total | 282 | 491 | 1:1.74 | 56.50* |

**Table 2**

Number of males and females of *P. prometheus* caught off the Canary Islands by quarter and sex ratio tested by chi-square analysis. *= $\chi^2 > \chi_t^2{}_{1,0.05}$=3.84.

| Quarter | Males | Females | Sex ratio | $\chi^2$ |
|---|---|---|---|---|
| 3/92 | 16 | 23 | 1:1.44 | 1.25 |
| 4/92 | 13 | 35 | 1:2.69 | 10.08* |
| 1/93 | 13 | 37 | 1:2.85 | 11.52* |
| 2/93 | 24 | 37 | 1:1.54 | 2.77 |
| 3/93 | 24 | 34 | 1:1.42 | 1.72 |
| 4/93 | 14 | 38 | 1:2.71 | 11.07* |
| 1/94 | 29 | 51 | 1:1.75 | 6.05* |
| 2/94 | 36 | 49 | 1:1.36 | 1.98 |
| 3/94 | 39 | 50 | 1:1.28 | 1.35 |
| 4/94 | 24 | 44 | 1:1.83 | 5.88* |
| 1/95 | 31 | 59 | 1:1.90 | 8.71* |
| 2/95 | 19 | 34 | 1:1.79 | 4.24* |

tern was recorded for both sexes. Highest values occurred between April and September, peaking during June–July. From October to March the values were low.

No significant difference in length at sexual maturity was found between males and females ($t$-test, $t$=1.31<$t_{0.05,385}$=1.65). The length at which fifty percent of the fish became mature was 47.41 cm TL (Fig. 4).

Males were found to be between 38 and 80 cm TL, females between 36 and 80 cm. The length range of immature individuals was from 36 to 38 cm. The parameters of the total length to total weight relationship for males and females separately, and for the population as a whole, are given in Table 4. No significant difference in the allometric coefficient was found between males and females ($t$-test, $t$= 1.53<$t_{0.05,771}$=1.65). Isometric growth was observed in both sexes and for the whole population (Table 4).

Of the otoliths examined, 670 (86.4%) were readable and used for the study of age and growth. The

© Del documento, los autores. Digitalización realizada por ULPGC. Biblioteca Universitaria, 2009

APE value was only 3.4%. A false hyaline ring interrupting the normal growth pattern of the otolith was identified within the fourth annual opaque zone and in all subsequent opaque zones. Marginal zone analysis showed that one annulus was formed per year (Fig. 5). The percentage of otoliths with opaque edge was high in the months from April to September, and between June and August in particular.

Fish aged 3 to 11 years were present in the samples (Table 5). Growth parameters determined for males, females, and the entire population are shown in Table 6. No significant differences in the growth parameters were found between sexes (Hotelling's $T^2$-test, $T^2=5.29<T_0^2{}_{0.05,3,666}=7.88$).

The length converted catch curve is shown in Figure 6. The rates of total mortality, natural mortality, and fishing mortality were $Z=0.49$/year, $M=0.35$/year, and $F=0.14$/ year, respectively. The size at first capture was 51.57 cm TL.

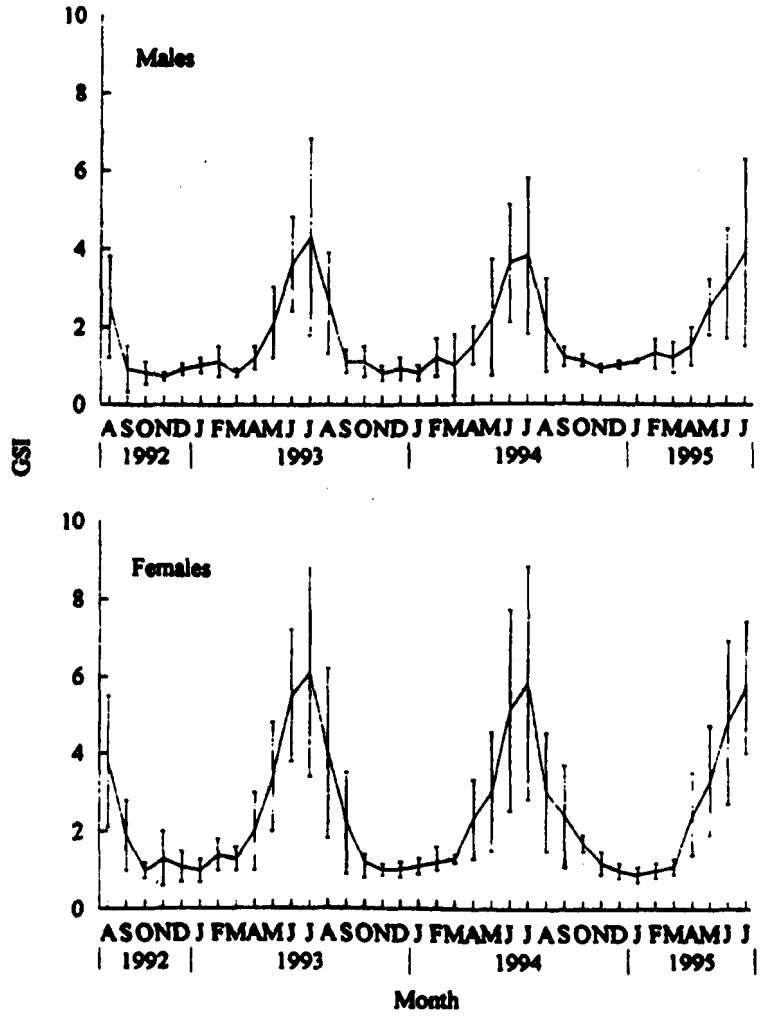


**Figure 3**

Monthly evolution of the gonadosomatic index (GSI) for males and females of *P. prometheus* caught off the Canary Islands (August 1992–July 1995).

## Discussion

*Promethichthys prometheus* is distributed along the slope to a depth of 800 m (Nakamura and Parin, 1993). In waters off the Canary Islands, greatest concentrations of this species are found between 400 and 700 m depth. Below this depth, the species is replaced by other trichiuroid fish present in the area, e.g. the black scabbardfish, *Aphanopus carbo* Lowe, 1839 (Uiblein et al., 1996).

The roudi escolar off the Canary archipelago is a gonochoristic species with no evidence of sexual dimorphism. The sex ratio is clearly unbalanced in favor of females. This fact could be explained by the differences between sexes in the spatial distribution. The lowest discrepancy between sexes observed during the reproductive season seems to confirm this conclusion. Because of the space partitioning between sexes and because females are fished more than males, this species could be classed as vulnerable to unrestrained fishing. Therefore, fishing for roudi escolar is an activity that has the potential to threaten its target population compared with fishing for more reliable and robust stocks (Csirke, 1988). This fishery will require a prudent exploitation strategy to reduce the potential risk of a collapse.

The roudi escolar has a definite reproductive period (extending from April to September, with a peak in spawning activity in June–July) which agrees with information reported by Parin (1986) and Nakamura and Parin (1993). These authors pointed out that the

**Table 3**

Number of males and females of *P. prometheus* caught off the Canary Islands by depth stratum and sex ratio tested by chi-square analysis. $*=\chi^2>\chi_t^2{}_{1,0.05}=3.84$.

| Depth (m) | Males | Females | Sex ratio | $\chi^2$ |
|---|---|---|---|---|
| 201–300 | 4 | 26 | 1:6.50 | 16.13* |
| 301–400 | 21 | 136 | 1:6.47 | 84.23* |
| 401–500 | 35 | 187 | 1:5.34 | 104.07* |
| 501–600 | 28 | 39 | 1:1.39 | 1.81 |
| 601–700 | 76 | 48 | 1.0.63 | 6.32* |
| 701–800 | 85 | 41 | 1:0.48 | 17.12* |
| 801–900 | 32 | 12 | 1.0.37 | 9.09* |

© Del documento, los autores. Digitalización realizada por ULPGC. Biblioteca Universitaria, 2009

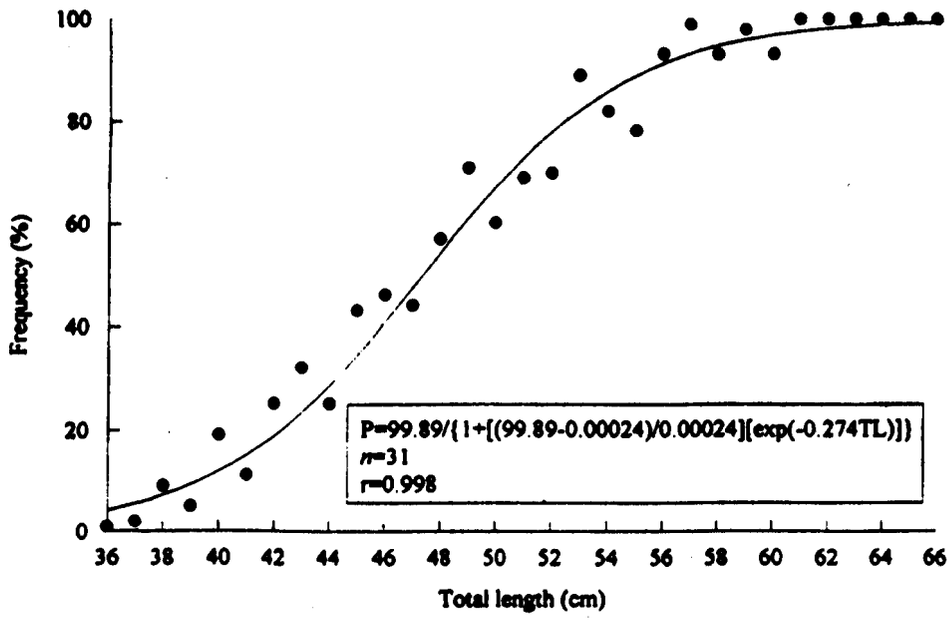


**Figure 4**

Sexual maturity ogive for *P. prometheus* caught off the Canary Islands (August 1992–July 1995).

spawning of this species occurs from August to September in the Atlantic off Madeira. Nishikawa (1987) found the highest concentration of gempylid larvae at the end of the summer months in the Pacific waters of Japan. In the Canary archipelago, the spawning of roudi escolar seems to be related to water temperatures, occurring when these reach greatest values. Possible significance of seasonal temperature variation to maturation and spawning in other bony fish species off the Canary Islands has been discussed by Lorenzo and Pajuelo (1996) and Pajuelo and Lorenzo (1995, 1996). Reproduction in roudi escolar does not involve horizontal migrations because during the spawning season the specimens are observed in the same areas where they are fished all year round. The lowest discrepancy in the number of males and females observed during the spawning period suggests an aggregation for breeding. Males and females were found aggregated mainly at depths of 450–650 m during this period.

Length at sexual maturity does not differ between males and females, corresponds approximately to 48 cm TL. In the age-length relationship, this size corresponds to 4-year-old specimens. The size at which fifty percent of the fish become mature is less than the length at first capture and the majority of the total catch is longer than this length, indicating a good exploitation pattern from the biological point of view. Furthermore, a low value of fishing mortality rate was obtained.

**Table 4**

Parameters of the length-weight relationship for males, females and all fish of *P. prometheus* caught off the Canary Islands and the possibility of isometry tested by Student's *t*-test. * = $t > t_{0.05,n>250} = 1.65$.

| | *a* | *b* | SE(b) | $r^2$ | *n* | *t*-test |
|---|---|---|---|---|---|---|
| Males | 0.004128 | 2.95321 | 0.03721 | 0.959 | 282 | 1.25 |
| Females | 0.004987 | 2.96214 | 0.03140 | 0.981 | 491 | 1.20 |
| All fish | 0.004521 | 2.98932 | 0.02341 | 0.992 | 776 | 0.45 |

The alternate pattern of opaque with translucent zones was easily distinguishable on the otoliths of the roudi escolar. These zones are deposited owing to alternating periods of rapid and slow growth (Williams and Bedford, 1974). The opaque zone is formed when the water temperature is higher, and food is abundant, and the translucent is formed when temperature is lower and the species spawns. This finding demonstrated the validity of using otoliths for estimating the age and growth of roudi escolar. The false hyaline zones observed within the fourth opaque ring and in subsequent opaque rings are probably spawning bands, because this species spawns in the summer months, when the opaque zone is formed in the otoliths. Morales-Nin (1987) pointed out that when the spawning does not take place during the period of hyaline zone formation, a false ring, known

© Del documento, los autores. Digitalización realizada por ULPGC. Biblioteca Universitaria, 2009

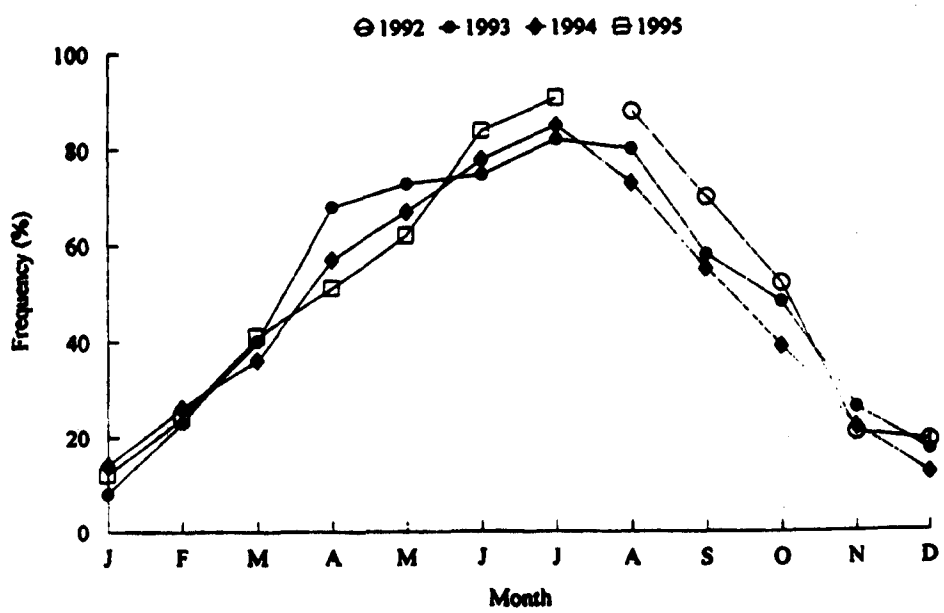


**Figure 5**

Monthly percentage of otoliths with opaque edge for *P. prometheus* caught off the Canary Islands (August 1992–July 1995).

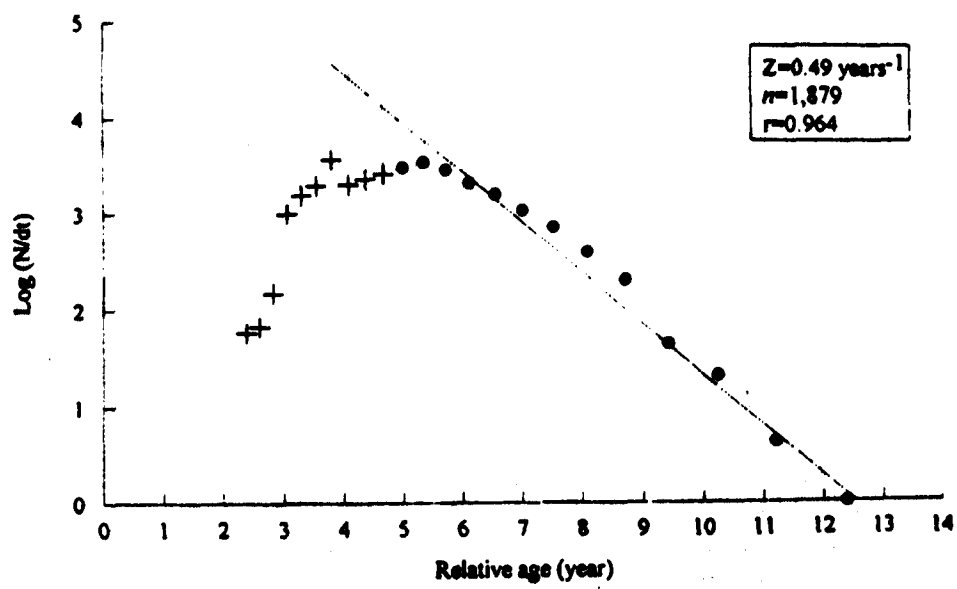


**Figure 6**

Length converted catch curve for *P. prometheus* caught off the Canary Islands (August 1992–July 1995). The initial data points (+) were not used in the regression.

s a spawning ring, may form within an opaque zone, ividing it into two.

The oldest age class observed was XI years, al- ıough this class, as well as age classes IX and X, 'ere poorly represented in the landings. As a whole, rowth of the roudi escolar is relatively fast and males and females grow at equal rates. The growth parameters obtained are reasonable because the theoretical maximal length value is greater than the size of the largest fish sampled and because the growth coefficient value indicates relatively rapid attainment of maximal size.

© Del documento, los autores. Digitalización realizada por ULPGC. Biblioteca Universitaria, 2009

**Table 5**

Age-length key for all fish of *P. prometheus* caught off the Canary Islands.

| Size (cm) | Age group (years) III | IV | V | VI | VII | VIII | IX | X | XI |
|---|---|---|---|---|---|---|---|---|---|
| 36 | 2 | | | | | | | | |
| 37 | 1 | | | | | | | | |
| 38 | 2 | | | | | | | | |
| 39 | 4 | | | | | | | | |
| 40 | 6 | | | | | | | | |
| 41 | 9 | | | | | | | | |
| 42 | 9 | 1 | | | | | | | |
| 43 | 7 | 3 | | | | | | | |
| 44 | 4 | 4 | | | | | | | |
| 45 | 3 | 8 | | | | | | | |
| 46 | 3 | 7 | | | | | | | |
| 47 | | 9 | | | | | | | |
| 48 | 2 | 13 | 1 | | | | | | |
| 49 | | 17 | 2 | | | | | | |
| 50 | | 14 | | | | | | | |
| 51 | | 7 | 4 | | | | | | |
| 52 | | 5 | 6 | | | | | | |
| 53 | | 4 | 8 | | | | | | |
| 54 | | 3 | 10 | 1 | | | | | |
| 55 | | | 16 | 3 | | | | | |
| 56 | | 2 | 22 | 3 | | | | | |
| 57 | | 1 | 19 | 6 | | | | | |
| 58 | | | 12 | 7 | | | | | |
| 59 | | | 8 | 11 | 2 | | | | |
| 60 | | | 4 | 17 | 2 | | | | |
| 61 | | | 2 | 28 | 3 | | | | |
| 62 | | | 3 | 21 | 6 | | | | |
| 63 | | | 1 | 11 | 8 | | | | |
| 64 | | | | 8 | 14 | 2 | | | |
| 65 | | | | 7 | 20 | 1 | | | |
| 66 | | | | 3 | 23 | 4 | | | |
| 67 | | | | 1 | 16 | 7 | | | |
| 68 | | | | 2 | 10 | 10 | 1 | | |
| 69 | | | | | 6 | 12 | 4 | | |
| 70 | | | | | 3 | 17 | 4 | | |
| 71 | | | | | 2 | 11 | 7 | 1 | |
| 72 | | | | | 1 | 6 | 9 | 2 | |
| 73 | | | | | | 5 | 9 | 2 | |
| 74 | | | | | | 1 | 7 | 3 | 1 |
| 75 | | | | | | 2 | 5 | 6 | 1 |
| 76 | | | | | | | 2 | 4 | 2 |
| 77 | | | | | | | 1 | 3 | 2 |
| 78 | | | | | | | | | 1 |
| 79 | | | | | | | | 1 | |
| 80 | | | | | | | | | 1 |
| *n* | 52 | 98 | 118 | 129 | 116 | 78 | 49 | 22 | 8 |
| *x* | 41.6 | 48.9 | 55.7 | 61.1 | 65.5 | 69.4 | 72.4 | 74.9 | 76.7 |
| SD | 2.4 | 2.8 | 2.6 | 2.6 | 2.4 | 2.2 | 2.0 | 1.8 | 1.7 |

**Table 6**

Parameters of the von Bertalanffy growth curve for males, females, and all fish of *P. prometheus* caught off the Canary Islands.

| | $L_\infty$ (cm) | $k$ (per year) | $t_0$ (years) | $r^2$ |
|---|---|---|---|---|
| Males | 91.93 | 0.18 | −1.66 | 0.964 |
| Females | 94.03 | 0.17 | −1.58 | 0.978 |
| All fish | 93.61 | 0.18 | −1.54 | 0.988 |

## Acknowledgments

We are grateful to all persons who participated in sampling. We thank C. Tascón and N. Hernández for help with improving our English. This study was partially financed by the Directorate General XIV (Fisheries) of the European Commission.

## Literature cited

**Anderson, R. O., and S. J. Gutreuter.**
1983. Length, weight, and associated structural indices. *In* L. A. Nielsen and D. L. Johnson (eds.), Fisheries techniques, p. 283–300. Am. Fish. Soc., Bethesda, MD.

**Beamish, R. J., and D. A. Fournier.**
1981. A method for comparing the precision of a set of age determination. Can. J. Fish. Aquat. Sci. 38:982–983.

**Csirke, J.**
1988. Small schoaling pelagic fish stock. *In* J. A. Gulland (ed.), Fish population dynamics: the implications for management (second edition), p. 271–302. John Wiley & Sons, Chichester.

**Gayanilo, F. C., Jr., M. Soriano, and D. Pauly.**
1988. A draft guide to the compleat ELEFAN. ICLARM Software 2, Contribution No. 435:1–65.

**Lorenzo, J. M., and J. G. Pajuelo.**
1995. Biological parameters of the roudi escolar *Promethichthys prometheus* (Pisces: Gempylidae) off the Canary Islands. Fish. Res. 24:65–71.
1996. Growth and reproductive biology of chub mackerel *Scomber japonicus* off the Canary Islands. S. Afr. J. Mar. Sci. 17:275–280.

**Morales-Nin, B.**
1987. Métodos de determinación de la edad en los osteictios en base a estructuras de crecimiento. Inf. Téc. Inst. Inv. Pesq. 143:1–30.

**Nakamura, I.**
1981. Gempylidae. *In* W. Fischer, G. Bianchi and W. B. Scott (eds.), FAO species identification sheets for fishery purposes. Vol II: Eastern central Atlantic; fishing areas 34, 47 (in part). FAO, Ottawa (unpaginated).

**Nakamura, I., and N. V. Parin.**
1993. FAO species catalogue. Vol. 15: Snake mackerels and cutlassfishes of the world (families Gempylidae and Trichiuridae): an annotated and illustrated catalogue of the snake mackerels, snoeks, escolars, gemfishes, sackfishes, domine, oilfish, cutlassfishes, scabbardfishes, hairtails, and frostfishes known to date. FAO Fish. Synop. 125:1–136.

**Nishikawa, Y.**
1987. Occurrence and distribution of gempylid larvae in the Pacific waters of Japan. Bull. Jpn Soc. Fish. Oceanogr. 51:1–8.

© Del documento, los autores. Digitalización realizada por ULPGC. Biblioteca Universitaria, 2009

**Pajuelo J. G., and J. M. Lorenzo.**
1995. Biological parameters reflecting the current state of the exploited pink dentex *Dentex gibbosus* (Pisces: Sparidae) population off the Canary Islands. S. Afr. J. Mar. Sci. 16:311–319.
1996. Life history of the red porgy *Pagrus pagrus* (Teleostei: Sparidae) off the Canary Islands, central-east Atlantic. Fish. Res. 28:163–177.

**Parin, N. V.**
1986. Gempylidae. *In* P. J. P. Whitehead, M. L. Bauchot, J. C. Hureau, J. Nielsen and E. Tortonese (eds.), Fishes of the north-eastern Atlantic and the Mediterranean, p. 967–973. UNESCO, Paris.

**Pauly, D.**
1980. On the interrelationships between natural mortality, growth parameters and mean environmental temperature in 175 fish stocks. J. Cons. Int. Explor. Mer 39: 175–192.
1983. Length-converted catch curves: a powerful tool for fisheries research in the tropics (part I). Fishbyte 1:9–13.
1984. Length-converted catch curves: a powerful tool for fisheries research in the tropics (part II). Fishbyte 2:17–19.

**Ricker, W. E.**
1973. Linear regression in fishery research. J. Fish. Res. Board Can. 30:409–434.

**Saila, S. B., C. W. Recksiek, and M. H. Prager.**
1988. Basic fishery science programs. Develop. Aquac. Fish. Sci. 18:1–230.

**Uiblein, F., F. Bordes, and R. Castillo.**
1996. Diversity, abundance and depth distribution of demersal deep-waters fishes off Lanzarote and Fuerteventura. Canary Islands. J. Fish Biol. 49:75–90.

**Williams, T., and B. Bedford.**
1974. The use of otoliths for age determination. *In* T. B. Bagenal (ed.), The ageing of fish, p. 114–123. Unwin Brothers, Surrey.

© Del documento, los autores. Digitalización realizada por ULPGC. Biblioteca Universitaria, 2009

# Variation of the tidal properties around Gran Canaria

**Antonio MARTINEZ [a], Esther PEREZ [a], Miguel BRUNO [b]**

[a] Facultad de Ciencias del Mar, Universidad de Las Palmas de Gran Canaria, Canary Islands, Spain
[b] Facultad de Ciencias del Mar, Universidad de Cádiz, Puerto Real, Spain

(Received 9 April 1997, revised 3 October 1997, accepted 17 October 1997)

**Abstract** – Analysis of water level and current meter series from different locations on the island shelf of Gran Canaria reveals strong variations in tidal properties. Semidiurnal sea level amplitudes agree with the results obtained from global tidal models for this region only on the northern coast of the island, while they decrease towards the southwest (10 cm difference for the $M_2$ constituent). Semidiurnal currents present maxima at the southeastern and northwestern extremities of the island (30–40 cm $s^{-1}$ for $M_2$) and minima in the north–northeast and southwest (3–6 cm $s^{-1}$ for $M_2$), showing simultaneous strong changes in the phase. Diurnal levels and currents display smaller variations than the semidiurnal band. The behaviour of semidiurnal constituents is studied with the help of analytical and numerical solutions, in which the incident wave is modelled by a barotropic $M_2$ Kelvin wave. The results show that the insular shelf could be a source of differences in level amplitudes around the island and could be also responsible for the enhancement of currents in the southeast and northwest. They also show that the variation of the current phases is due to the amplification of the standing character of the wave at the northeastern and southwestern parts of the shelf. © Elsevier, Paris / Ifremer / Cnrs / Ird

**tide / tidal current / island / numerical modelling / Canary Islands**

**Résumé – Variation des propriétés de la marée dans les eaux de la Grande Canarie.** L'analyse de séries chronologiques du niveau de la mer et de la courantométrie, en plusieurs points du plateau continental de la Grande Canarie, révèle de grandes variations dans les propriétés de la marée. Les amplitudes des variations semi-diurnes du niveau de la mer sont en accord avec le modèle global de marée au nord de l'île, mais elles diminuent au sud-ouest (de 10 cm pour la composante $M_2$). Le courant semi-diurne présente un maximum au sud-est et au nord-ouest de l'île (de 30 à 40 cm $s^{-1}$ pour $M_2$) et un minimum au nord-nord-est et au sud-ouest (de 3 à 6 cm $s^{-1}$ pour $M_2$) avec, simultanément, une forte variation de phase. Les variations de période diurne des niveaux et des courants sont plus faibles que celles de période semi-diurne. Les composantes semi-diurnes sont étudiées par des méthodes analytiques et numériques, en considérant que l'onde incidente est une onde barotrope de Kelvin. Les résultats indiquent que le plateau continental est probablement à l'origine des différences observées dans les variations du niveau de la mer autour de l'île et dans le renforcement des courants au sud-est et au nord-ouest. Ils montrent également que la variation de phase du courant est due à l'amplification du caractère stationnaire de l'onde sur le plateau continental, au nord-est et au sud-ouest de l'île. © Elsevier, Paris / Ifremer / Cnrs / Ird

**marée / courant de marée / île / modélisation numérique / Îles Canaries**

## 1. INTRODUCTION

Gran Canaria (28° 10' N, 15° 25' W) is part of the Canary Archipelago located in the northern part of the Eastern Central Atlantic (*figure 1*). The island is characterized by a circular form approximately 45 km in diameter. It presents a narrow shelf that rises sharply from 2000–3000 m depth and is not connected with the neighbouring islands by any common shelf.

Tides in this area are dominated by the semidiurnal constituents. Tidal maps obtained by the application of



© Del documento, los autores. Digitalización realizada por ULPGC. Biblioteca Universitaria, 2009

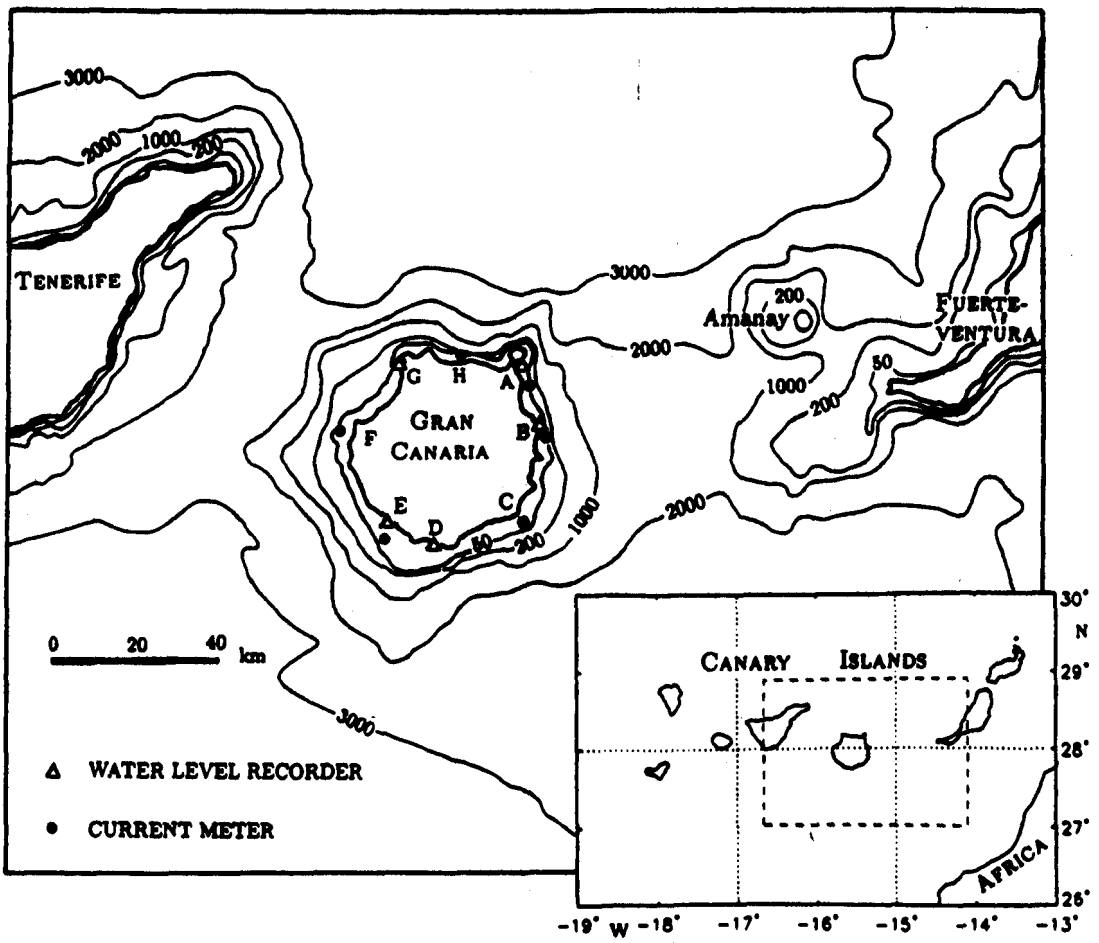


**Figure 1.** Location map for the Gran Canaria Island showing the positions of the instruments and the bottom bathymetry. Depths in metres.

hydrodynamical equations over the global ocean [21, 24] and maps obtained from a large number of recent models based on Geosat [5] and Topex/Poseidon [2] altimetry data, show that these waves propagate approximately northwards along the African shelf and that the amplitudes increase towards the coast. Analysis of current time series between 21° and 26° N across the slope of the African shelf [15] has shown mooring-averaged semidiurnal currents consistent with a progressive Kelvin wave model. Additionally, Dick and Siedler [7] and Siedler and Paul [25] have studied the semidiurnal tidal currents in the Iberian and Canary basins. Their most relevant findings for the oceanic waters that surround the Canary Islands are that: (a) the tidal currents are dominated by the barotropic mode; (b) the semidiurnal currents oscillate along a direction parallel to the continental slope off northwest Africa; (c) the amplitude of the principal semidiurnal constituent ($M_2$) is around 3–4 cm $s^{-1}$; and (d) the semidiurnal constituents are progressive waves. These results seem to corroborate the conclusion of Huthnance and Baines [15] ascribing the behaviour of semidiurnal tides in this zone to Kelvin waves.

A good understanding of the interaction between tidal waves and oceanic islands is important in order to determine which island data are representative of the deep ocean and consequently which ones are useful in mapping ocean tides. This problem has been recognised by the scientific community [20]. Authors such as Kagan and Kivman [16, 17] have studied the representativeness of island tidal measurements, estimating the diffraction disturbances produced in the tidal field without taking into account the effects of the island shelves. In the present work, sea level measurements are analysed in order to study the amplitude and phase variations of the tidal constituents on the shelf that surrounds Gran Canaria. The study is extended to include the variations of diurnal and semidiurnal currents. This comple-



© Del documento, los autores. Digitalización realizada por ULPGC. Biblioteca Universitaria, 2009

ments a further aim of gaining a quantitative understanding of the implications of island tidal currents for biological applications. To explain qualitatively the variations of the tidal properties around the island, the results of a Kelvin wave-forced numerical experiment are presented. The use of these ideal waves allows us to obtain an analytical solution for the diffraction at cylindrical islands and compare it with the numerical results.

The work is organised as follows: the data used and the details of the analysis are described in section 2. The results of the level and current data analysis are given in section 3. In section 4 an approximation for the diffraction of Kelvin waves at cylindrical islands is presented. The numerical experiments are described in section 5. In section 6 the results of the models and the comparison with the observations are discussed. In section 7 a brief summary of the study is presented.

## 2. MEASUREMENTS AND METHODS OF ANALYSIS

The analysis of tidal oscillations was made with measurements from the island shelf. Station positions around the island, indicated by the letters A to H, and bottom topography are shown in *figure 1*. Part of the data used are from various experiments realised between 1986 and 1990 on the east coast of the island [27]. In the present study, previous data have been completed with measurements of sea level at stations D and G and measurements of currents at stations F and H. *Table 1* abridges the locations, dates, record lengths and depths of the instruments. Aanderaa RCM7 current meters were used with recording intervals of between 15 and 30 min. All current meters were deployed between the 40 m and 50 m depth contours and at depths of between 15 and 40 m. The longest record is from the 6.5-month time series of current meter $C_A$-1. With the exception of station H, where only 12 days of data are available, the series have durations of between 1 and 4 months. The sea level measurements were taken with a *WLR5* Aanderaa level recorder. Also in this case, the longest series were collected at station A for 17.5 months, while the other data cover between 1 and 2 months.

The amplitudes and Greenwich phases of the principal tidal constituents for the sea level and the currents were firstly calculated by means of a least square fit harmonic analysis [9, 10]. This method cannot separate constituents with very similar frequencies when the record length is short. Within the above constituents, there are two pairs of considerable amplitude that cannot be extracted when the series are shorter than six months: the $K_1$-$P_1$ and $S_2$-$K_2$ pairs. These constituents have been inferred using the values obtained from the analysis of the longest series ($WLR_A$).

The amplitudes and phases obtained from the sea level series at station A were also used to calculate tidal level series for the same observation periods at all other stations. A cross-spectral analysis between computed tidal level series and the observed series was applied, assuming a constant admittance across each tidal band. The last condition is equivalent to assuming that the ratios of amplitudes and differences of phases between the differ-

**Table I.** Locations, dates, record lengths and data for water level recorders (*WLR*) and current meters (*C*). Subindices correspond to the positions marked in *figure 1*.

| Instrument | Latitude-Longitude | Date deployed | Days | Water depth (m) | Instrument depth (m) |
|---|---|---|---|---|---|
| $WLR_A$ | 28°07.5'N-15°24.8'N | 03.02.89 | 536 | 15 | 15 |
| $WLR_B$ | 27°59.2'N-15°22.0'N | 14.05.86 | 50 | 15 | 15 |
| $WLR_D$ | 27°45.4'N-15°37.5'N | 12.07.94 | 72 | 2 | 2 |
| $WLR_E$ | 27°07.5'N-15°24.8'N | 22.01.88 | 38 | 5 | 5 |
| $WLR_G$ | 28°08.6'N-15°42.0'N | 10.08.95 | 74 | 7 | 7 |
| $C_A$-1 | 28°05.YN-15°23.5'N | 18.12-89 | 201 | 50 | 15 |
| $C_A$-2 | 28°05.5'N-15°235'N | 18.12.89 | 124 | 50 | 30 |
| $C_B$- 1 | 27°59.0'N-15°21.0'N | 23.06.87 | 29 | 50 | 20 |
| $C_B$-2 | 27°59.0'N-15°21.0'N | 23.06.87 | 29 | 50 | 40 |
| $C_C$ | 27°47.5'N-15°25.5'N | 27.11.90 | 46 | 40 | 20 |
| $C_E$ | 27°45.0'N-15°44.2'N | 26.01.88 | 46 | 40 | 20 |
| $C_F$ | 27°59.9'N-15°50.9'N | 03.11.94 | 58 | 45 | 20 |
| $C_H$ | 28°10.0'N-15°33.4'N | 19.06.95 | 12 | 40 | 20 |



© Del documento, los autores. Digitalización realizada por ULPGC. Biblioteca Universitaria, 2009

ent constituents of each tidal band are the same as those calculated from the longest sea level record (station A). The admittances and phase lags thus obtained have been used to estimate the harmonic constituents for the stations where no 1-year record was available. This method [12, 13] allows the separation of constituents of very close frequencies when these constituents are known in the area. The current analysis is analogous to that of the sea level but for both eastern and northern components of the currents, and is expressed in terms of the ellipse parameters: semi-major (M) and semi-minor (m, negative when the rotation is clockwise) axes, orientation (θ) defined with respect to the east and increasing anticlockwise, and Greenwich phase lag (G) defined using the northern semi-major axis as reference. Some of the ellipses are oriented roughly east–west, which induce a 180° uncertainty on the phase. In this case, and in order to be consistent with the literature, a slightly lower than 180° has been replaced by θ–180° and the associated G by G + 180°.

In the study area the inertial frequency falls into the diurnal band (f = 0.0394 c/h). Some of the current records show important contributions of near-inertial oscillations (*figure 2*). This additional contribution affects the diurnal tidal harmonic constants calculated with least square fit analysis, especially the small constituents whose frequencies are between that of $O_1$ and $K_1$. The harmonic analysis done through admittances is particularly useful for the present study because it allows us to estimate those contributions of only tidal origin.

The temporal series were smoothed previously by means of low-pass filters type $A_nA_nA_{n+1}$ [11], where the operators An represent successive moving averages of $n$ observations. The response function of these filters is:

$$F(\sigma) = \frac{\sin^2(n\pi\sigma\Delta t)\sin[(n+1)\pi\sigma\Delta t]}{(n+1)n^2\sin^3(\pi\sigma\Delta t)} \qquad (1)$$

which allows the cut-off frequency to be calculated. In the present study the values of $n$ have been chosen according to $n = \Delta t^{-1}$ (t in hours), eliminating the frequencies equal and higher than one hour. The use of these filters produces some loss of amplitude in the tidal constituents that has been calculated and recovered by means of function (1).

## 3. ANALYSIS RESULTS

The results obtained for the sea level principal tidal constituents are presented in *table II*. The phases show that

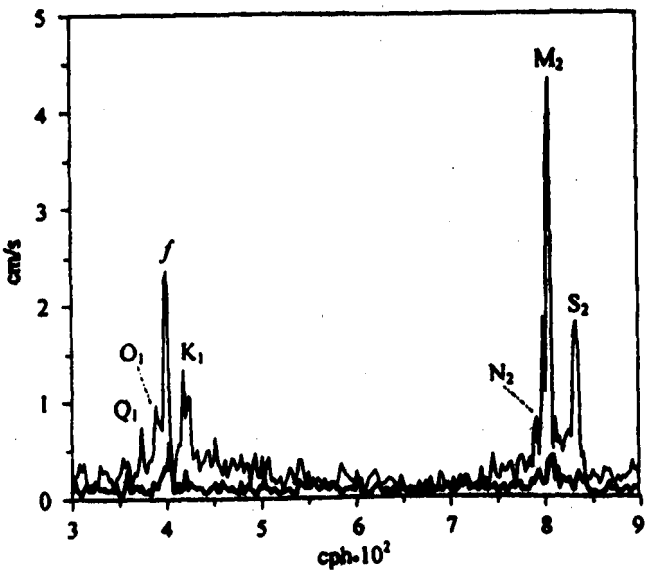


**Figure 2.** Amplitude spectra (FFT) of the currents parallel (thin line) and normal (thicker line) to the coast in station A. The following peaks are indicated: $M_2$, $S_2$, $N_2$ (semidiurnal constituents), $K_1$, $O_1$ (diurnal constituents), and $f$ (inertial frequency).

the progress of the diurnal and semidiurnal waves is approximately from south to north. The higher phase difference for the semidiurnal band is almost 2.7° between stations A and D, and 5° for the diurnal band between stations A and E. Likewise, the amplitudes of semidiurnal constituents are in accordance with the values shown by the tidal charts of the region (75–76 cm for $M_2$) only at the northern part of the island (stations A and G). For the remaining stations (B, D, and E), the amplitudes decrease gradually southwestwards (64 cm for $M_2$ at station E). The amplitudes of the diurnal constituents have similar values at every station, with a slight tendency to increase towards the southwest.

The results of the current analysis for the principal diurnal ($K_1$) and semidiurnal ($M_2$) constituents are presented in *table III*, which shows that the currents oscillate principally along the direction parallel to the island coast. In addition, the reader can see the differences displayed by the semidiurnal current amplitudes around the island. At the north–northeastern (H, A, and B) and southwestern (E) stations, the semi-major axes are relatively small, while at the southeastern and western stations (C and F) they are considerably larger, by about one order of magnitude. The semi-major axis of the dominant constituent $M_2$ increases from 2–3 cm $s^{-1}$ at the southwestern and northern extremities of the island, to 40 cm $s^{-1}$ in the southeastern (station C) and 28 cm $s^{-1}$ in the west



© Del documento, los autores. Digitalización realizada por ULPGC. Biblioteca Universitaria, 2009

**Table II.** Amplitudes (A) and phases (G) with respect to GMT of the principal constituents of the sea level at different sites around Gran Canaria. Results obtained from a least square fit are indicated in parentheses and the results obtained through admittances are presented without parenthesis.

| Cons. | $WLR_A$ | | $WLR_B$ | | $WLR_D$ | | $WLR_E$ | | $WLR_G$ | |
|---|---|---|---|---|---|---|---|---|---|---|
| | A | G | A | G | A | G | A | G | A | G |
| $O_1$ | (4.9) | (292.4) | 4.7 | 292.1 | 5.0 | 288.0 | 5.6 | 287.1 | 5.0 | 290.3 |
| | | | (4.6) | (295.1) | (4.4) | (288.7) | (5.0) | (287.0) | (5.0) | (290.6) |
| $K_1$ | (6.2) | (40.3) | 6.0 | 39.0 | 6.4 | 35.9 | 7.1 | 34.9 | 6.3 | 38.2 |
| | | | (6.3) | (38.8) | (6.8) | (37.2) | (6.3) | (38.1) | (6.7) | (40.2) |
| $N_2$ | (15.5) | (14.0) | 15.0 | 13.4 | 13.8 | 11.4 | 13.1 | 12.0 | 15.5 | 15.0 |
| | | | (15.2) | (11.0) | (11.9) | (13.6) | (17.2) | (15.7) | (13.8) | (104) |
| $M_2$ | (75.7) | (27.0) | 73.3 | 26.4 | 67.6 | 24.4 | 64.3 | 25.0 | 76.2 | 28.0 |
| | | | (73.7 | (26.0) | (67.6) | (24.6) | (63.9) | (24.9) | (75.6) | (28.9) |
| $S_2$ | (28.6) | (49.6) | 27.7 | 49.0 | 24.5 | 47.0 | 47.00 | 24.3 | 28.8 | 50.46 |
| | | | (27.0) | (53.5) | (24.9) | (43.5) | (43.5) | (26.8) | (28.5) | (47.3) |
| $K_2$ | (8.6) | (48.7) | 8.4 | 48.1 | 7.7 | 46.1 | 7.4 | 46.7 | 8.7 | 49.7 |
| | | | (8.1) | (52.7) | (7.5) | (42.6) | (8:1) | (46.0) | (8.6) | (46.4) |

(station F). However, the semi-major axes of the diurnal constituents are similar at every station (between 1.4 and 2.4 cm $s^{-1}$ for the principal diurnal constituent $K_2$), maxima being observed at stations C and F.

Current phases also show an important variation around the island. In order to study the origin of the variation, the tidal constituents have been decomposed into progressive and standing waves by inter-comparison of the current phases with the phases of the surface elevation, a method frequently used to characterize the tides [23, 7]. In the case of progressive waves, currents and surface elevation should be in phase, while in the case of standing waves they will have a 90° phase shift. The procedure consists of choosing the time of local high water as the origin time, so that the sea level displacement due to a component of frequency has the form $A \cos \sigma t$. Hence the current velocity V can be written as:

$$V(t) = W_E \cos(\sigma t - G'_E) + iW_E \cos(\sigma t G'_N) \quad (2)$$
$$(Wp_E + iWp_N) \cos \sigma t + (Ws_E + iWs_N) \sin \sigma t$$

**Table III.** Semi-major ($M$) and semi-minor (m) axes in cm $s^{-1}$, orientation with respect to the east ($\theta$) and phase with respect to GMT (G) of the principal diurnal ($K_1$) and semidiurnal ($M_2$) ellipses. The results obtained from a least square fit are indicated within parentheses and the results obtained through admittances are presented without parentheses.

| Current meter | $K_1$ | | | | $M_2$ | | | |
|---|---|---|---|---|---|---|---|---|
| | M | m | θ | G | M | m | θ | G |
| $C_A$-1 | 1.4 | -0.1 | 72.9 | 7.6 | 5.9 | -0.3 | 74.0 | 279.0 |
| | (2.1) | (-0.1) | (75.5) | (13.1) | (6.2) | (-0.4) | (73.7) | (274.0) |
| $C_A$-2 | 1.4 | -0.1 | 79.6 | 353.0 | 6.1 | -0.2 | 81.5 | 284.0 |
| | (20) | (0.2) | (77.2) | (2.4) | (6.3) | (-0.2) | (81.7) | (277.6) |
| $C_B$-2 | 1.5 | 0.0 | 80.6 | 53.7 | 9.3 | 2.9 | 53.5 | 282.8 |
| | (1.6) | (0.2) | (88.0) | (41.0) | (8.6) | (2.6) | (54.8) | (280.0) |
| $C_B$-2 | 1.2 | 0.1 | 72.8 | 40.5 | 9.4 | 2.0 | 45.2 | 283.5 |
| | (1.7) | (0.4) | (74.8) | (45.0) | (9.5) | (1.4) | (43.2) | (283.1) |
| $C_C$ | 2.4 | -0.3 | 36.9 | 32.8 | 41.4 | 1.8 | 30.2 | 13.8 |
| | (3.0) | (-0.2) | (33.3) | (38.5) | (42.0) | (1.0) | (29.5) | (14.6) |
| $C_E$ | 2.0 | -0.1 | 137.1 | 34.2 | 2.8 | 0.1 | 141.5 | 122.3 |
| | (3.3) | (-0.1) | (137.2) | (64.1) | (2.9) | (0.1) | (140.3) | (127.6) |
| $C_F$ | 2.4 | 0.1 | 76.8 | 95.2 | 27.9 | 4.3 | 62.9 | 326.9 |
| | (2.7) | (0.1) | (77.3) | (126.2) | (27.9) | (4.2) | (62.8) | (326.9) |
| $C_H$ | 1.4 | -0.1 | 4.2 | 70.3 | 2.7 | -0.2 | 179.7 | 139.5 |



© Del documento, los autores. Digitalización realizada por ULPGC. Biblioteca Universitaria, 2009

where ($W_E$, $W_N$) are the east–west and north–south observed amplitudes of the currents ($G^1_E$, $G^1_N$) the phase lags, ($Wp_E$, $Wp_N$) the progressive components, and ($Ws_E$, $Ws_N$) the standing wave components. The amplitudes of progressive $Wp = (Wp_E^2 + Wp_N^2)^{1/2}$ and of standing $Ws = (Ws_E^2 + Ws_N^2)^{1/2}$ waves computed in this way for the $K_1$ and $M_2$ constituents are presented in *table IV*. The standing wave for the $M_2$ constituent is the dominant one at the southwestern and north–northwestern stations (A, B, E, and H). The progressive wave enlarges at station F and dominates at station C. The variation of the ratio $Ws/(Wp + Ws)$ for $K_1$ is smaller than that of $M_2$, however, they show a similar pattern: the ratio presents two maxima at stations A and F.

## 4. BASIC EQUATIONS AND ANALYTICAL APPROXIMATION FOR KELVIN WAVE DIFFRACTION

The vertically-integrated equations of momentum and conservation of mass in a Cartesian coordinate system (neglecting horizontal viscosity terms) has the form:

$$\frac{\partial u}{\partial t} + u\frac{\partial u}{\partial x} + v\frac{\partial u}{\partial y} - fv = -g\frac{\partial \eta}{\partial x} - k\frac{u\sqrt{u^2+v^2}}{h+\eta} \tag{3}$$

$$\frac{\partial v}{\partial t} + u\frac{\partial v}{\partial x} + v\frac{\partial v}{\partial y} + fu = -g\frac{\partial \eta}{\partial y} - k\frac{v\sqrt{u^2+v^2}}{h+\eta} \tag{4}$$

$$\frac{\partial \eta}{\partial t} = -\frac{\partial[u(h+\eta)]}{\partial x} - \frac{\partial[v(h+\eta)]}{\partial y} \tag{5}$$

where $\eta$ is the surface elevation, $u$ and $v$ are the depth averaged horizontal velocity components, $g$ is the acceleration due to gravity, $h$ is the depth, and $k$ is the bottom friction coefficient.

With the objective of obtaining an analytical solution, cylindrical coordinates have been used ($r$, $\theta$ stand for the radial and angular directions, respectively) with the island contour represented by a circular cylinder of radius $r_a$. The inviscid linearized version of the equations (3)–(5) for harmonic motion, $\eta = Z(r, \theta)\exp(i\sigma t)$ in a uniformly-rotating plane ocean lead to the Helmholtz equation [18]: $(\nabla^2 + k^2)Z = 0$ where $k^2 = (\sigma^2 - f^2)(gh)^{-1}$. The $r$ and $\theta$ components of the currents are, respectively, $v_r = V_r\exp(i\sigma t)$ and $v_\theta = V_\theta\exp(i\sigma t)$ where:

$$V_r = \frac{g}{\sigma^2 - f^2}\left[i\sigma\frac{\partial Z}{\partial r} + \frac{f}{r}\frac{\partial Z}{\partial \theta}\right];$$
$$V_\theta = \frac{ig}{\sigma^2 - f^2}\left[if\frac{\partial Z}{\partial r} + \frac{\sigma}{r}\frac{\partial Z}{\partial \theta}\right] \tag{6}$$

Proudman [22] and later Larsen [19] studied the diffraction of Sverdrup waves of tidal frequencies at islands, showing that the interaction between tidal waves and islands leads to the appearance of scattered waves. The complete solution of the Helmholtz equation for the scattered wave is:

$$Z_s = \sum_{n=-\infty}^{\infty} B_n H_n^{(1)}(kr)\exp(-in\theta) \tag{7}$$

where $Z_s \to 0$ when $r \to \infty$.

$H_n^{(1)}$ are Hankel functions, and $B_n$ are constants. Since the radius of the island is small compared to the wavelength, the form of the scattered wave is dominated by the $n = \pm 1$ modes with $H_1^{(1)} \approx -iY_1$, $Y$ denoting a Neuman function.

**Table IV.** Amplitudes in cm $s^{-1}$ of the standing (Ws) and progressive (Wp) components of $K_1$ and $M_2$.

| Current meter | $K_1$ | | | $M_2$ | | |
|---|---|---|---|---|---|---|
| | *Wp* | *Ws* | *Ws/(Wp + Ws)* | *Wp* | *Ws* | *Ws/(Wp + Ws)* |
| $C_A$-1 | 1.18 | 0.76 | 0.39 | 1.80 | 5.42 | 0.75 |
| $C_A$-2 | 1.19 | 1.29 | 0.52 | 1.31 | 5.69 | 0.81 |
| $C_B$-2 | 1.46 | 0.35 | 0.19 | 3.50 | 8.70 | 0.71 |
| $C_B$-2 | 1.19 | 0.05 | 0.04 | 5.07 | 7.94 | 0.61 |
| $C_C$ | 2.34 | 0.42 | 0.15 | 38.84 | 9.29 | 0.19 |
| $C_E$ | 1.90 | 0.25 | 0.12 | 0.28 | 2.65 | 0.90 |
| $C_F$ | 1.35 | 1.92 | 0.59 | 16.00 | 22.00 | 0.58 |
| $C_H$ | 1.24 | 0.69 | 0.36 | 1.00 | 2.39 | 0.71 |



© Del documento, los autores. Digitalización realizada por ULPGC. Biblioteca Universitaria, 2009

The observations made in the open ocean near the Canary Islands, described in section 1, indicate that the semidiurnal constituents in this area are similar to Kelvin waves. Therefore, in order to study qualitatively the fundamental mechanisms that determine the behaviour of the tide at the insular shelf, the principal semidiurnal wave $M_2$ away from the island will be, from now on, approximated by a Kelvin wave. The diffraction of the Kelvin wave ($Z_k$) travelling in the positive $x$ direction, in cylindrical coordinates (using $x = r\cos\theta$ and $y = r\sin\theta$), can be approximated by:

$$Z = Z_k + Z_s \approx A\exp[-r(ik_0\cos\theta + \sin\theta)] + Y_1(kr)(C\sin\theta + D\cos\theta) \quad (8)$$

where $C = i(B_1 - B_{-1})$ and $D = (B_1 + B_{-1})$, $k_0 = \sigma(gh)^{-1/2}$ is the Kelvin wave number, and $m_0 = f(gh)^{-1/2}$ is the inverse of the Rossby radius of deformation.

At the island boundary $k_0 r_a << 1$ and $m_0 r_a << 1$, which imply $kr_a << 1$ and $Y_1(kr_a) \approx -2i/\pi kr_a$ [1]. Then the solution can be approximated by the following linear functions along the radial direction: $Z_k \approx A[1 - r_a(ik_0\cos\theta + m_0\sin\theta)]$ and $Z_s \approx -i2(C\sin\theta + D\cos\theta)/\pi kr_a$. The coefficients are then readily evaluated applying the boundary condition of null velocity normal to the coast:

$$C = i\frac{\pi}{2}Akr_a^2 m_0 \; ; \; D = \frac{\pi}{2}Akr_a^2 k_0 \quad (9)$$

We have calculated the function Z at the local latitude for a water depth $h$ = 3000 m and for an island of 23 km radius, which is approximately that of Gran Canaria. *Figure 3a* shows the resulting contours of amplitude and phase lag. The scattered wave produces a diminution of the amplitude on the right side of the island and an enlargement at the left, looking in the direction of the wave propagation. This effect compensates approximately the variation in amplitude of the incident Kelvin wave, producing almost constant amplitudes around the cylinder.

The tidal currents can be calculated with equation (6). They are a somewhat complicated function of the cylindrical coordinates, but the tidal ellipses were found to have negligible semi-minor axes around the island. *Figure 3b* shows the results for the current amplitudes. They change around the cylinder so that the minimum amplitudes are located at the front and back of the island while the maximum amplitudes are found at both sides (looking at the cylinder in the wave direction).

## 5. DESCRIPTION OF THE NUMERICAL EXPERIMENTS

Several numerical experiments were performed considering the incoming $M_2$ tide as a Kelvin wave. The equations (3)–(5) were integrated numerically with an explicit finite dif-

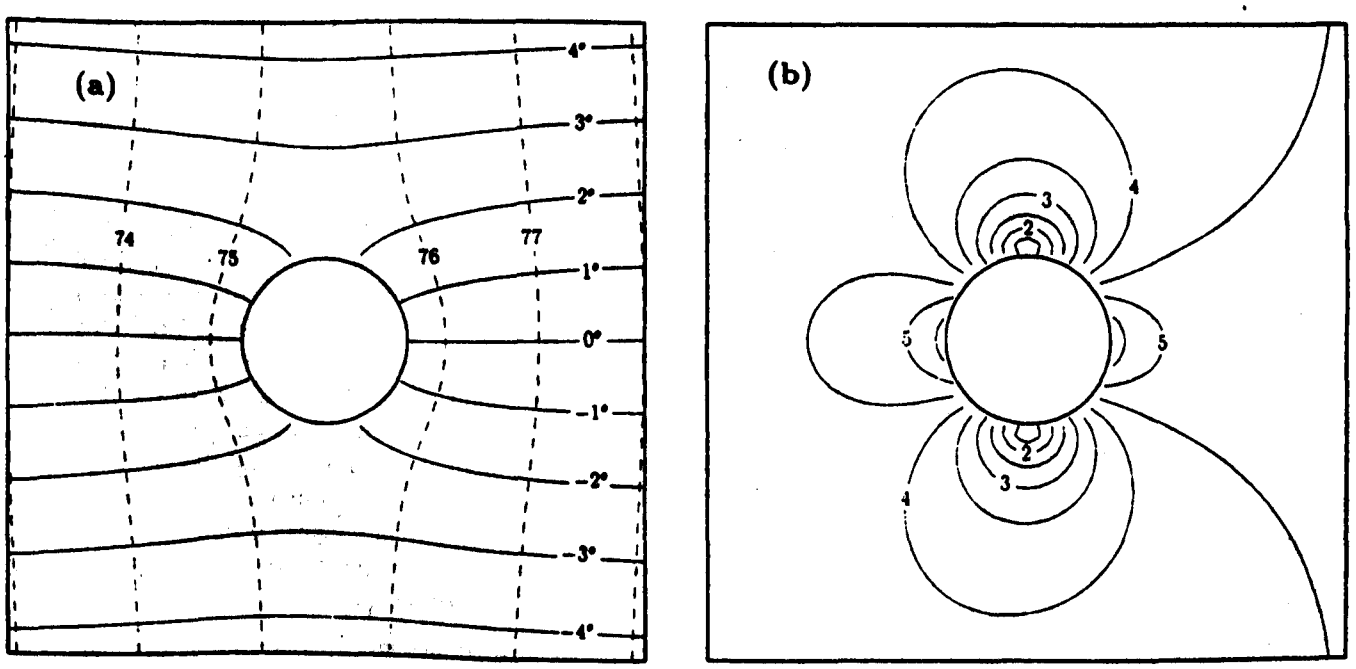


**Figure 3.** Analytical result for the diffraction of a Kelvin wave (progressing towards the top) due to a circular cylinder of radius 23 km. (a): vertical displacement ($\eta$). Continuous lines: phases. Dashed lines: amplitudes in cm. (b): current amplitudes in cm $s^{-1}$.



© Del documento, los autores. Digitalización realizada por ULPGC. Biblioteca Universitaria, 2009

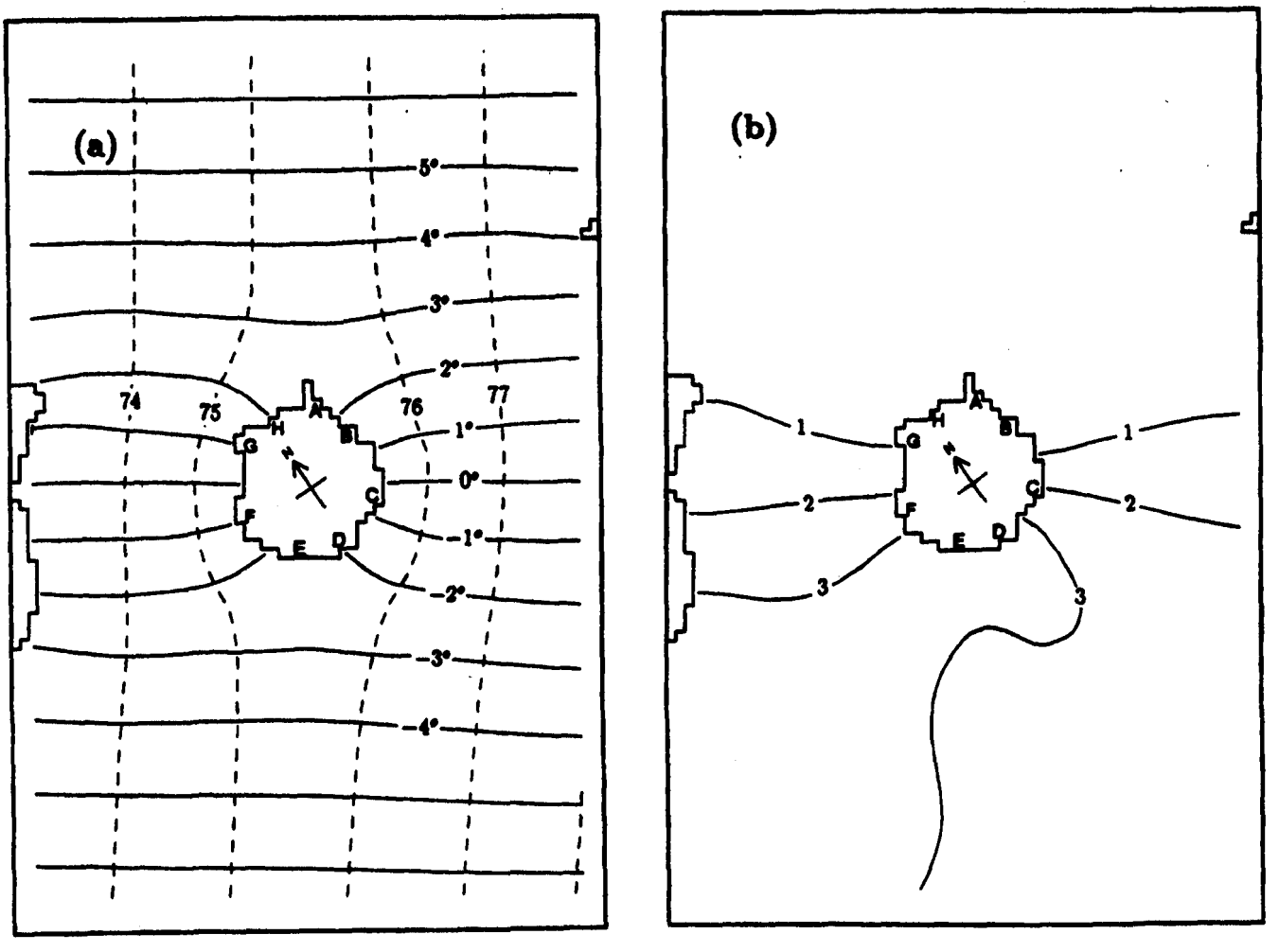


**Figure 4.** Numerical results for the case of Gran Canaria Island with uniform depth. (a): result for $\eta$. Continuous lines: phases. Dashed lines: Amplitudes (cm). (b): Percentage of standing wave ($[Wp/(Wp + Ws)] \times 100$).

ferences scheme (leapfrog type) on a rectangular Arakawa-C grid, already used in a previous study [14]. A 2625 by 2625 m grid resolution was used with the longitudinal axis oriented along 34° with respect to the north, which is approximately the direction of current oscillations observed in the open ocean [25]. A maximum water depth of 3000 m and a time step of $\Delta t = 3.2$ s were given to satisfy the Courant-Friederichs-Lewy (CFL) stability requirement [6].

The southeastern and northwestern boundaries of the model were assumed to be solid walls. Zero normal velocity was imposed at land boundaries and at the two solid walls of the channel. The model had an open boundary condition at its northeastern and southwestern extremes. At the ingoing boundary (southwest) the surface elevation produced by the Kelvin wave was specified, and along the outgoing boundary (northeast) the Sommerfeld condition was used to make it transparent to the Kelvin waves [3]. This channel model is the usual approximation to study any effect produced by a sudden change in topography over a Kelvin wave [8, 26]. This condition ensures that the only possible mode at a certain distance from the island is the Kelvin wave. In the this case, the reflection of the scattered waves on the solid walls affects the numerical solution around the island if the walls are not sufficiently separated. The procedure adopted to minimize this effect consists of progressively widening the channel to the point where the differences between successive experiments are negligible.

Two cases have been studied to separate the factors that determine the behaviour of the semidiurnal tide at the island shelf: (a) Gran Canaria with uniform depth of 3000 m; and (b) Gran Canaria with real bathymetry to a



© Del documento, los autores. Digitalización realizada por ULPGC. Biblioteca Universitaria, 2009

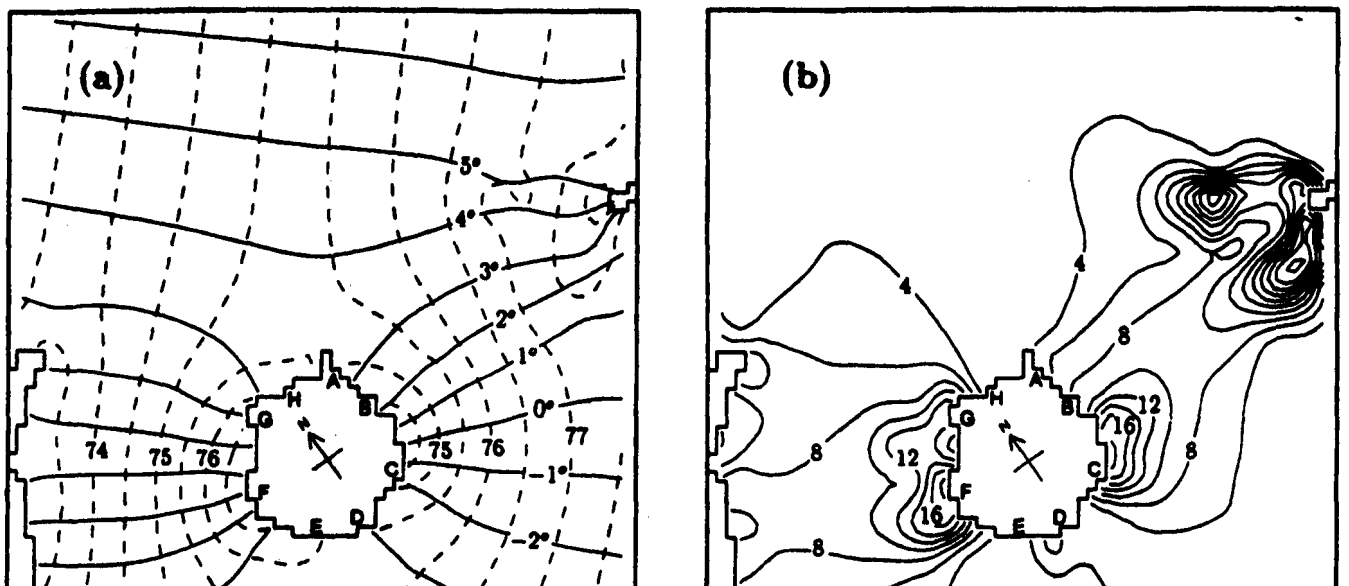


**Figure 5.** Numerical results for the case of Gran Canaria Island with real bathymetry. (a): amplitudes in cm (dashed lines) and phases (continuous lines) for $\eta$. (b): semi-major axis in cm $s^{-1}$.

maximum depth of 3000 m. The grid chosen was different for each case such that the presence of the channel walls had a minimum effect in the results around the island. In case (a), a 525 km length by 181 km wide grid, which fits the region between the neighbouring islands of Tenerife and Fuerteventura, was used. For case (b), it was necessary to increase the dimension to 929 by 469 km, considering a uniform depth of 3000 m remote from the region of study.

The tidal motion was generated from an initial state of rest ($\eta = u = v = 0$). This condition generates errors that disappear after a transitory time period [4]. Since the time-periodic solution has a cycle of 12.4206 h, the effect of starting errors can be evaluated by comparing the water level and velocities computed at a given instant with those computed 12.4206 h earlier. After a 20-day simulation, the time at which the periodic solution was found to be stable, the model was run continuously for five additional days. Time series, including hourly values of elevation and velocity components were extracted at each active computational point. The results were then subjected to an harmonic (least square) tidal analysis to evaluate the amplitudes and phase lags.

Additional experiments were performed to ascertain the importance of the nonlinear terms present in the equations (3)–(5). The equations were first solved without those terms, later retaining the bottom friction terms, and finally also including the convective terms. The results showed that the quadratic friction terms barely modify the solution. The convective terms created overtides and residual currents on the insular shelf. The residual currents were seen to be highly affected by the discretization of the coastal grid, indicating that it is necessary to use very good grid resolution around the island to solve it correctly. Nevertheless, the convective terms only produce very slight differences on the principal wave ($M_2$) whose behaviour is analysed in the next section.



© Del documento, los autores. Digitalización realizada por ULPGC. Biblioteca Universitaria, 2009

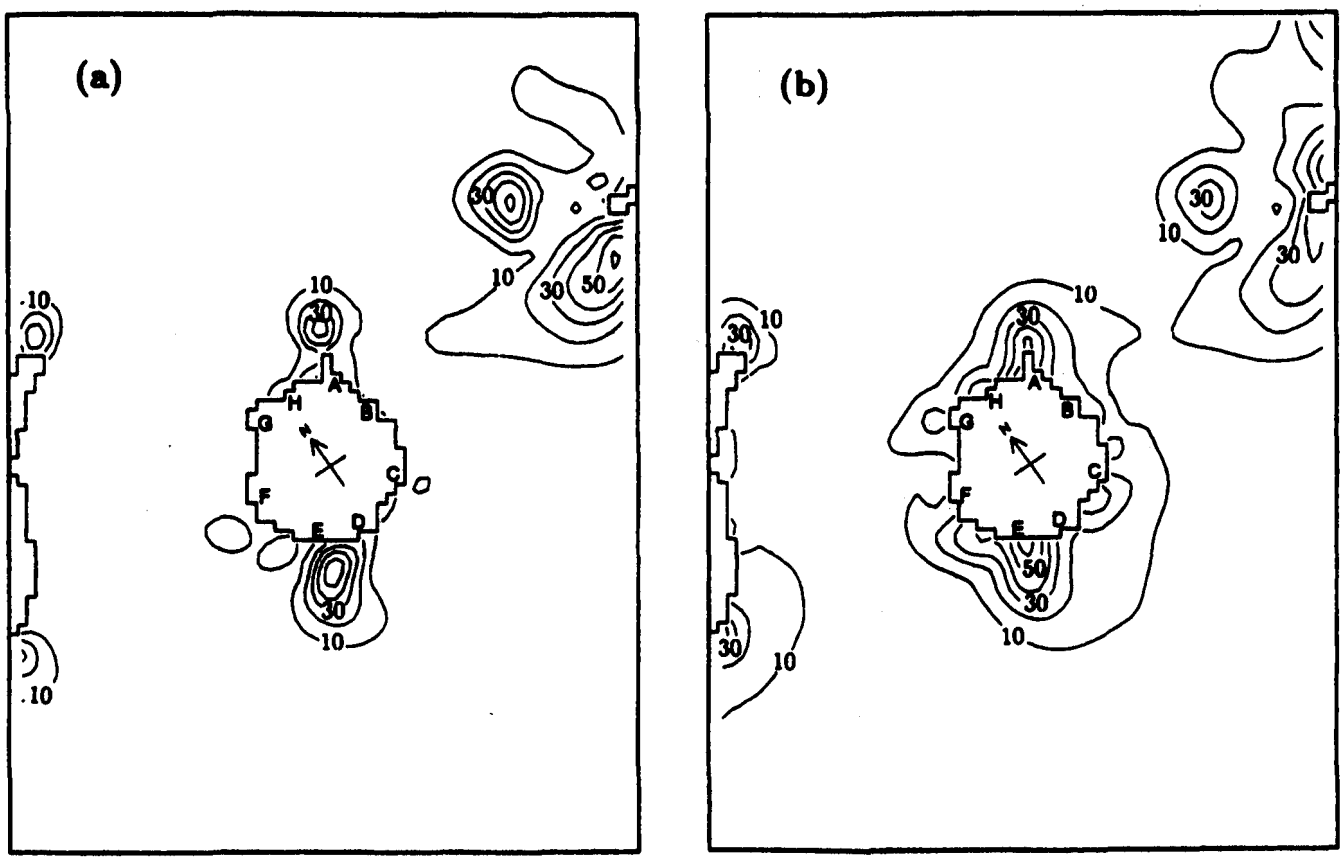


**Figure 6.** Numerical results for the case of Gran Canaria island with real bathymetry. (a): ellipticity ($m/M$). (b): percentage of standing wave.

## 6. NUMERICAL RESULTS AND COMPARISON WITH OBSERVATIONS

*Figure 4a* shows the water level amplitude and phase results of the numerical experiment for the case of uniform depth. The amplitudes of the Kelvin wave at the ingoing boundary were chosen such that the values around the island were about 75.5 cm. The result is similar to that obtained for a perfect cylinder, although with some deformation due to the precise geometry of the island. The current results also show a similar pattern to that of the analytical solution (not shown). The currents around the island are oriented parallel to the local direction of the coast. The maximum values were obtained at the southeast and northwest. *Figure 4b* shows that the standing wave ratio $Ws/(Ws + Wp)$ is very small (maximum 3 %) for the present case.

The result of the experiment with real bathymetry is depicted in *figures 5, 6*. The amplitude and phase results of $\eta$ are presented in *figure 5a*, which shows that the perturbation of the incident Kelvin wave is more important than that from the case of uniform depth. It decreases rapidly away from each island, indicating that variations of the tidal properties around the Gran Canaria Island are less affected by the presence of the neighbouring islands. The presence of the insular shelf produces a 2° variation of the phase between the northeastern and the southwestern island sides, larger than in the case of plane depth. While in the case of uniform depth the amplitudes around the island were constant, in the case being discussed here the bathymetry produces a change in the amplitudes. A minimum of 74 cm is found northeast of the island and a maximum of 77 cm is located southwest.

The result of the level data analysis (*table II*) shows a strong variation of the semidiurnal amplitude between the northeastern and the southwestern parts of Gran Canaria. The amplitudes to the north coincide with the expected values for the ocean tides in this part of the Atlantic, indicating that the phenomenon consists of a diminution of the amplitudes at the southwest of the island (stations E and D). The model results shown in *figure 5a* can explain the smaller amplitudes observed at station B with respect



© Del documento, los autores. Digitalización realizada por ULPGC. Biblioteca Universitaria, 2009

to station A. However, these results do not agree with the amplitude diminution at the southwest. The fact that the shelf is wider and shallower in the southwest may indicate that the measured lower amplitudes are due to local small-scale effects. Therefore, it would be necessary to use a numerical model with a grid of very fine resolution around the island and with more realistic boundary conditions in order to investigate this feature.

*Figure 5b* shows the variation of the semi-major axes around the island. The maximum axes are located in the southeast and northwest, but their magnitudes are considerably higher than those obtained for the case of uniform depth due to the enhancement effect of the shallow waters. This result qualitatively explains the variations observed in section 3. The shallow waters also produce important tidal currents south of Fuerteventura and at the Amanay Seamount.

The change in depth yields the appearance of semi-minor axes and the model gives the highest eccentricities (m/M) south of Fuerteventura and over the Amanay Sèamount (*figure 6a*). The major eccentricities around Gran Canaria are found over the insular slope where the wave goes through the bathymetry (northeast and southwest of the island). The percentage of the wave which is explained by the standing wave is presented in *figure 6b*. The figure illustrates a pattern that reflects the existence of two maxima close to 60 %, located in the coastal regions where the wave arrives and leaves, and of two minima at both sides (southeast and northwest). This result reproduces approximately the current phase variations observed at the insular shelf. The combined *figures 6a* and *6b* indicate that near the coast the shallow water amplifies the currents when they flow parallel to the coast. In the northeastern and southwestern parts of the island, this takes place a quarter of a wave period before and after the high water occurrence moment, while in the northwest and southeast the maximum currents occur at the same time as the high waters. Furthermore, the numerical results suggest analogous behaviour at Tenerife and Fuerteventura.

## 7. CONCLUSIONS

The first objective of this study was to provide, through the analysis of field data, a quantitative description of the tidal elevations and currents around Gran Canaria. The results show the following characteristics:

(a) The progression of tidal level constituents is approximately from south to north, confirming the indications given by the tidal charts for the area. Semidiurnal amplitudes and phases at the stations located north and northeast of the island coincide with the expected values from such charts (75–76 cm for $M_2$). However, the amplitudes suffer an important diminution at the southern and southwestern stations. This effect is not produced in the case of diurnal constituents which are less disrupted by the island.

(b) The semi diurnal semi-major axes are smaller in those regions where the waves arrive and leave, northeast and southwest, but considerably larger in the lateral regions (southeast and northwest). Furthermore, in the former regions the semidiurnal constituents have a near-standing character while in the latter ones they resemble progressive waves.

The analytical approximation obtained for the diffraction of a Kelvin wave at a cylinder and the numerical solution for the case of Gran Canaria with uniform depth show that the distortions of the semidiurnal waves (amplitudes and phases) are small, with the amplitudes being constant around the island. The result obtained in the case of real bathymetry does not explain the observed amplitude diminution southwest of the island. Probably, this is because the model grid does not have sufficient resolution to solve this local effect. However, the resolution is sufficient to reveal that the island shelf is responsible for the amplitude variation around the island. This result, together with the observed variation of semidiurnal amplitudes around the island, highlights the necessity of taking into account the insular shelves in the estimation of representativeness of island tidal measurements.

The numerical results for currents reproduce the variations of the semidiurnal current properties observed at the insular shelf. They show the amplification of the currents at the southeast and northwest of the island produced by the enhancement effect of shallower waters around the island. They also show that the standing and progressive characters observed around the island are due to the presence of the shelf, which increases the eccentricity of the current ellipses near the slope and amplifies the standing character at the southwestern and northeastern parts of the shelf.

## Acknowledgements

The authors wish to thank Gabriel Godin for useful discussions. This work was supported by Fundación Universitaria de Las Palmas and Astilleros Canarios S.A., and by the Spanish Government (CICYT) through grant AMB95-0731.



© Del documento, los autores. Digitalización realizada por ULPGC. Biblioteca Universitaria, 2009

## REFERENCES


[1] Abramowitz M., Stegun A., Handbook of mathematical functions, Dover Publications, Inc., 1965, 1046 p.

[2] Andersen O.B., Woodworth P.L., Flather R.A., Intercomparison of recent ocean tide models, J. Geophys. Res. 100 (1995) 25,261–25,282.

[3] Bills P, Noye J., An investigation of open boundary condition for tidal models of shallow seas, in: J. Noye (Ed.), Numerical modelling: applications to marine systems, Elsevier, North-Holland, 1987, 295 p.

[4] Bode L., Sobey R.J., Initial transients in Long Wave Computations, J. Hydr. Engineer, ASCE 110 (2) (1984) 237–255.

[5] Cartwright D.E., Ray R.D., Oceanic tides from Geosat altimetry, J. Geophys. Res. 95 (1991) 3069–3090.

[6] Courant R., Friedrichs K., Lewy H., Über die partiellen Differenzengleichungen der mathemathischen Physik, Math. Annalen 100 (1928) 32–74.

[7] Dick G., Siedler G., Barotropic tides in the northeast Atlantic inferred from moored current meter data, Dtsch. Hydrogr. Z. 38 (1985) 7–22.

[8] Falconer R.A., Wolanski E., Mardapitta-Hadjipandeli L., Modeling tidal circulation in an island's wake. J. Water., Port, Coast. and Ocean Engineer, ASCE 112 (2) (1986) 234–254.

[9] Foreman M.G.G., Manual for tidal heights analysis and prediction, Pacific Marine Science Report 77–10, Inst. of Ocean Sciences, Patricia Bay (1977).

[10] Foreman M.G.G., Manual for tidal currents analysis and prediction, Pacific Marine Science Report 786, Inst. of Ocean Sciences, Patricia Bay (1978).

[11] Godin G., The analysis of tides, University of Toronto Press, 1972, 264 p.

[12] Godin G., The use of the admittance function for the reduction and interpretation of tidal records, Marine Environmental Data service, MS Report (1976) 91p.

[13] Godin G., The analysis of tides and currents, in: Parker B.B. (Ed.), Tidal Hydrodynamics, J. Wiley, 1991, 675–709.

[14] Godin G., Martínez A., On the possibility of Kelvin-type motion in actual seas, Cont. Shelf Res. 14 (1994) 707–721.

[15] Huthnance J.M., Baines P.G., Tidal currents in the northwest African upwelling region, Deep-Sea Res. 20 (1982) 285–306.

[16] Kagan B.A., Kivman G.A., Modelling of global ocean tides with allowance for island effects, Dtsch. Hydrogr. Z. 1 (1993) 1–13.

[17] Kagan B.A., Kivman G.A., A necessary condition for the representativeness of island tidal measurements, J. Geophys. Res. 100 (1995) 11,047–11,051.

[18] Lamb H., Hydrodynamics, Cambridge Univ. Press (1932) 738 p.

[19] Larsen J.C., Cotidal charts for the Pacific Ocean near Hawaii using f-plane solutions, J. Phys. Oceanogr. 7 (1977) 100–109.

[20] Le Provost C., On the use of sea level gauge data for satellite altimetry validation: A review, Oceanol. Acta 15 (1992) 431–440.

[21] Le Provost C., Genco M.L., Lyard F., Vincent P., Canceil P., Spectroscopy of the world ocean tides from a finite element hydrodynamic model, J. Geophys. Res. 99 (1994) 24777–24797.

[22] Proudman J., Diffraction of tidal waves on flat rotating sheets of water, Proc. Lond. Math. Soc. 15 (1914) 89–102.

[23] Pugh D.T., Vassie J.M., Tide and surge propagation off-shore in the Dowsing region on the North Sea, Dtsch. Hydrogr. Z., 29 (1976) 361–372.

[24] Schwiderski E.W., On charting global ocean tides, Rev. Geophys. 18 (1980) 243–268.

[25] Siedler G., Paul U., Barotropic and baroclinic tidal currents in the eastern basins of the north Atlantic, J. Geophys. Res. 96 (1991) 22259–22271.

[26] Tee K.T., Dynamics of a two-dimensional topographic rectification process, J. Phys. Oceanogr. 4 (1994) 443–465.

[27] Tejedor B., Fenómenos dinámicos de interacción atmósfera-oceano, Ph.D Thesis, Univ. Las Palmas de Gran Canaria (1991) 289 p.




© Del documento, los autores. Digitalización realizada por ULPGC. Biblioteca Universitaria, 2009

# THE COMMUNITY STRUCTURE OF PHYTOPLANKTON AS INDICATOR OF COASTAL WATER QUALITY IN THE TOURIST AREA

By MEDINA, L., P. GARCIA-JIMINEZ, A. LUQUE AND R. ROBAINA *

With 6 figures

*ABSTRACT.* An annual evaluation (June 1994-July 1995) of the water quality from Punta de Tenefé to Punta de Taozo (Gran Canaria, Canary Islands) was done, as a part of an environmental assessment program in tourist coast. The ecological parameters to evaluate were chosen as representative of the human pressure exerted on the coast (crowded beaches, direct wastewater falls or emissaries, marinas) and were: qualitative and quantitative analysis of phytoplankton community structures, biomass and nutrients. The aim was to characterize the conflictive points as regard to seasonality, climatology and oceanographic conditions.

The phytoplankton (biomass and species) negatively correlated to nutrient species, particularly to silicate which decree as increased diatoms. Maximum biomass was observed by March when *Rhizosolenia stolteforthii, R. setigera, Chaetoceros decipiens y Ch. debilis* proliferated. Cosmopolitan species such as *Nitzchia closterium, N. seriata, Navicula sp., Fragilaria* sp., *Licmophora* sp among others were always present.

In spite of being scarce compared to diatoms; Dinoflagellate representatives *Protoperidinium sp., Ceratium sp.* and *C. furca* increased by summer. *Gonyaulax* sp., indicator-species of chemical and physical alterations, was observed in samples from stations located near underwater emissary exits.

*RESUMO.* Uma avaliação anual (Junho de 1994 a Julho de 1995) da qualidade da água do mar foi realizada entre a "Punta de Tenefé" e a "Punta de Taozo" (Gran Canária, Ilhas Canárias), como parte de um programa de estudos ambientais sobre a costa turística.Os parâmetros ecológicos avaliados foram escolhidos conforme sua representatividade em relação à pressão humana exercida sobre a costa (praias abarrotadas, descarga de efluentes, emissários, marinas). São eles: análise qualitativa e quantitativa da estructura da comunidade fitoplanctônica, biomassa e nutrientes. O objetivo era caracterizar zonas de conflito, relacionadas à sazonalidade, climatologia e condições oceanográficas.

* Coastal Ecology Group, Dpto. de Biología. Universidad de Las Palmas de Gran Canaria. 35015, Las Palmas, Spain

**Bol. Mus. Mun. Funchal, 50(288): 91-106, 1998** ISSN 0870-3876

© Del documento, los autores. Digitalización realizada por ULPGC. Biblioteca Universitaria, 2009

BIBLIOTECA GENERAL

O fitoplancton (biomassa e espécies) apresentou-se negativamente correlacionado aos tipos de nutrientes, particularmente ao silicato, o qual decresce com um incremento de diatomáceas. As maiores biomassas foram observadas em março quando *Rhizosolenia stolteforthii*, *R. setigera*, *Chaetoceros decipiens* y *Ch. debilis* proliferaram. Espécies cosmopolitas *Nitzchia closterium*, *N. seriata*, *Navicula sp.*, *Fragilaria sp.*, *Lichmophora sp.*, entre outras, estavam sempre presentes.

A pesar de serem escassas quando comparadas com diatomáceas, as espécies de dinoflagelados, representados por *Protoperidinium* sp., *Ceratium* sp., e *C. furca*, aumentaram no verão. *Gonyaulax sp.*, uma espécie indicadora de alterações quimimcas e físicas, foi observada em amostras de estações localizadas próximas ao emissário submarino existente.

## INTRODUCTION

Phytoplankton is the group of floating single-cell organisms which carry out photosynthesis in water. The principal taxa of planktonic producers in many of the world's oceans are diatoms, dinoflagellates, coccolithophores, silicoflagellates and blue-green bacteria (VALIELA, 1995). In ocean waters, average quantities of 20 to 200 cells per milliliter are found and although they may belong to several taxonomical groups, almost 95% of them can be classed as dinoflagellates, while the diatoms being the most represented group in coastal waters (MARGALEF, 1982;1992).

Numerous studies exist dedicated to the study of primary production or biomass indicated by the concentration of photosynthetic pigments, both in the waters of the Canary Islands and in the waters of the West Coast of the Africa (BRAUN, 1980; BRAUN & REAL, 1986; DE LEÓN & BRAUN, 1973; FERNÁNDEZ DE PUELLES & BRAUN, 1989; MINAS et al., 1982; REAL et al., 1982). However, papers dedicated to the study of the composition or identification of the species which make up the phytoplanktonic community in the coastal areas of the Canary Islands are scarce (CORRAL & GENICIO, 1970; BRAUN et al., 1985; OJEDA, 1985).

The aim of this study is to found seasonal variations as well as possible effects of emission of residual waters and the massive utilization of the beaches taking into account the different climatological and oceanographic conditions. Besides the data will be used to evaluate the environmental situation of the coast in the surface waters of the South of the island of Gran Canaria (tourist area).

## MATERIAL AND METHOD

Six points were chosen for sampling after the inspection of the centers of contamination previously detected in the southeast-southwest zone of Gran Canaria, which goes from the Punta de Tenefé to the Punta de Taozo (Fig. 1).

© Del documento, los autores. Digitalización realizada por ULPGC. Biblioteca Universitaria, 2009

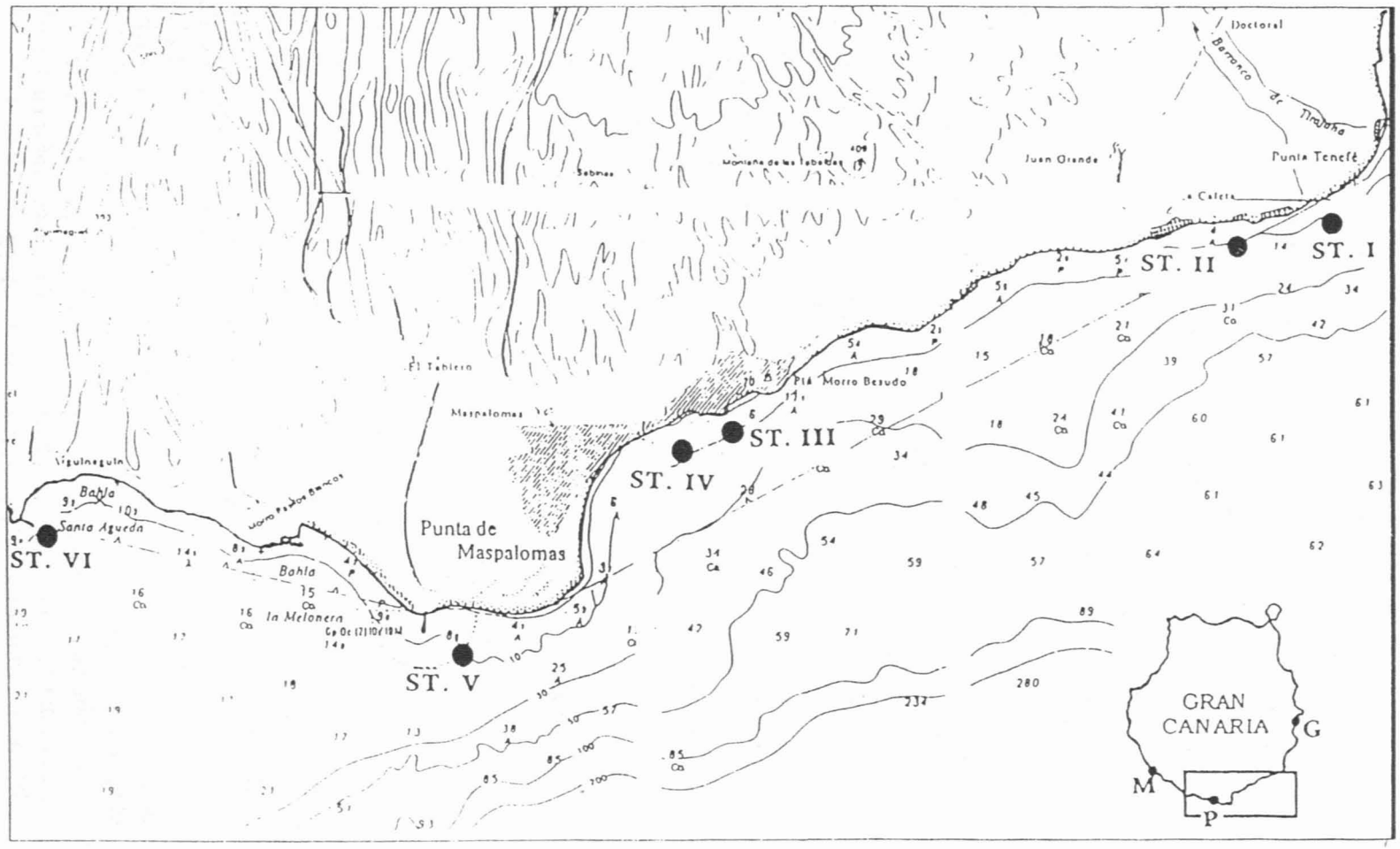


Fig. 1 - Area and localization the sampling points.

© Del documento, los autores. Digitalización realizada por ULPGC. Biblioteca Universitaria, 2009

The sampling was carried out periodically from June 1994 to July 1995, trying to evaluate the seasonal distribution of contaminants in the coastal area. The samples of sea water are collected using Niskin oceanographic bottles of a 5 l capacity, equipped with an inverted, protected thermometer.

The method used for the pigmentary content was that described by JEFFREY & HUMPHREY (1975) which allows the determination of the concentrations of chlorophyllic pigments (chlorophyll *a*, *b* and *c*) and non-chlorophyllic pigments (carotenes).

At the same time, the quantity of the products of the degradation of the chlorophyll was estimated, that is to say the concentration of phaeo-pigments (phaeoforbide and phaeophytin), using the method described by LORENZEN (1967) as an indicator of the state of the algal population.

For the taxonomical and quantitative study of the phytoplankton in terms of number of cells and volume of the samples of sea water, the methodology described by Utermöhl (1931) was used. The information obtained from the different species was subjected to an canonical principal components analysis (CPCA) represented by a correlation matrix.

The analysis of nutrient content (nitrates, nitrites, phosphates and silicates) are made according to the methodology described by GRASSHOFF et al., (1983).

In each sampling point measures of wind velocity and direction were taken, also the meteorological parameters provided by the National Meteorological Institute from its stations situated in Gando (27°55'45"N 15°23'20"W), Pasito Blanco (27°44'48"N, 15°37'00"W) and Mogán (27°47'00"N, 15°43'00"W) which cover the period from January 1994 to August or September 1995, according to the parameter, and therefore for the whole period of study in question.

## RESULTS

### Meteorology

* Dry air temperature

The dry air temperature shows its minimum values in the months from January to March and the maximum values in the period from July to November as happens in the station at Pasito Blanco. The temperatures are higher in the months of 1995, reaching up to 2.7°C in monthly average thermal increase for the common period between both years of the study (Fig. 2a and 2b).

The minimum monthly values for dry air temperature, between 14.17°C (±1.67) and 15.48°C, were recorded at 07.00 and the maximum, from 24.97°C (±1.54) to 26.36°C at 13.00 depending on the meteorological station during the entire period of study (January'94 / August'95).

The thermal difference between the average monthly values of the measurements recorded at 07.00 and 13.00 is no higher than 3°C in the station at Pasito Blanco, reaching 5.5°C in the stations at Gando and Puerto de Mogán.

© Del documento, los autores. Digitalización realizada por ULPGC. Biblioteca Universitaria, 2009

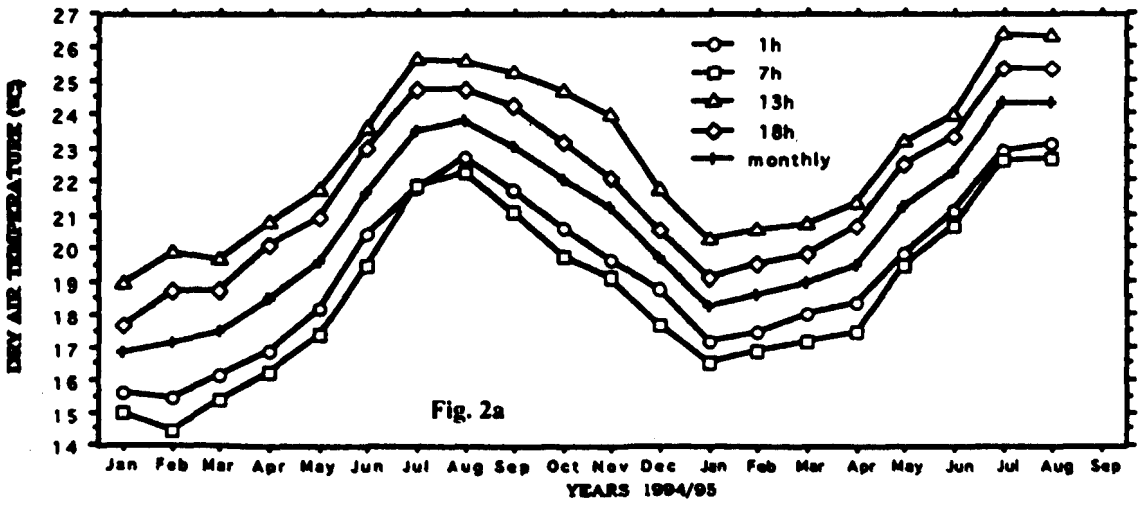


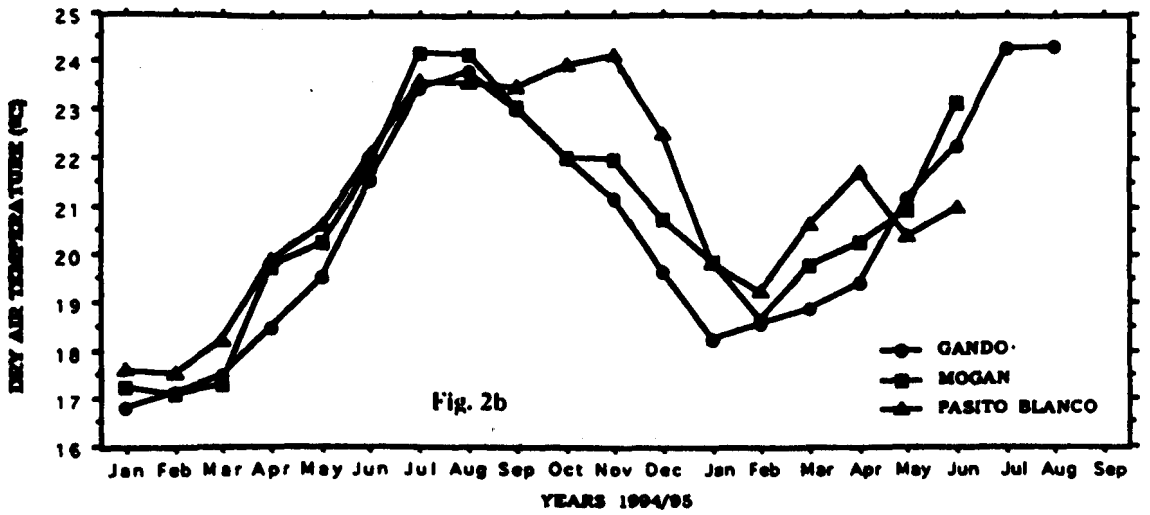


Fig. 2a - Dry air temperature (ºC ) at the meteorological station at east of Gran Canaria (Gando).
Fig. 2b - Dry air temperature (ºC) at the meteorological stations situated at east (Gando), south (Pasito Blanco) and southwest (Mogán) of Gran Canaria.

* Wind intensity

The parameter of wind intensity shows two types of monthly distributions according to the localization of the meteorological stations, one corresponding to the station at Gando situated in the east of the island with minimums in the winter months and maximums in the summer period while the opposite happens in the stations at Pasito Blanco and Mogán situated to the south and southwest of Gran Canaria, respectively (Fig. 3a).

© Del documento, los autores. Digitalización realizada por ULPGC. Biblioteca Universitaria, 2009

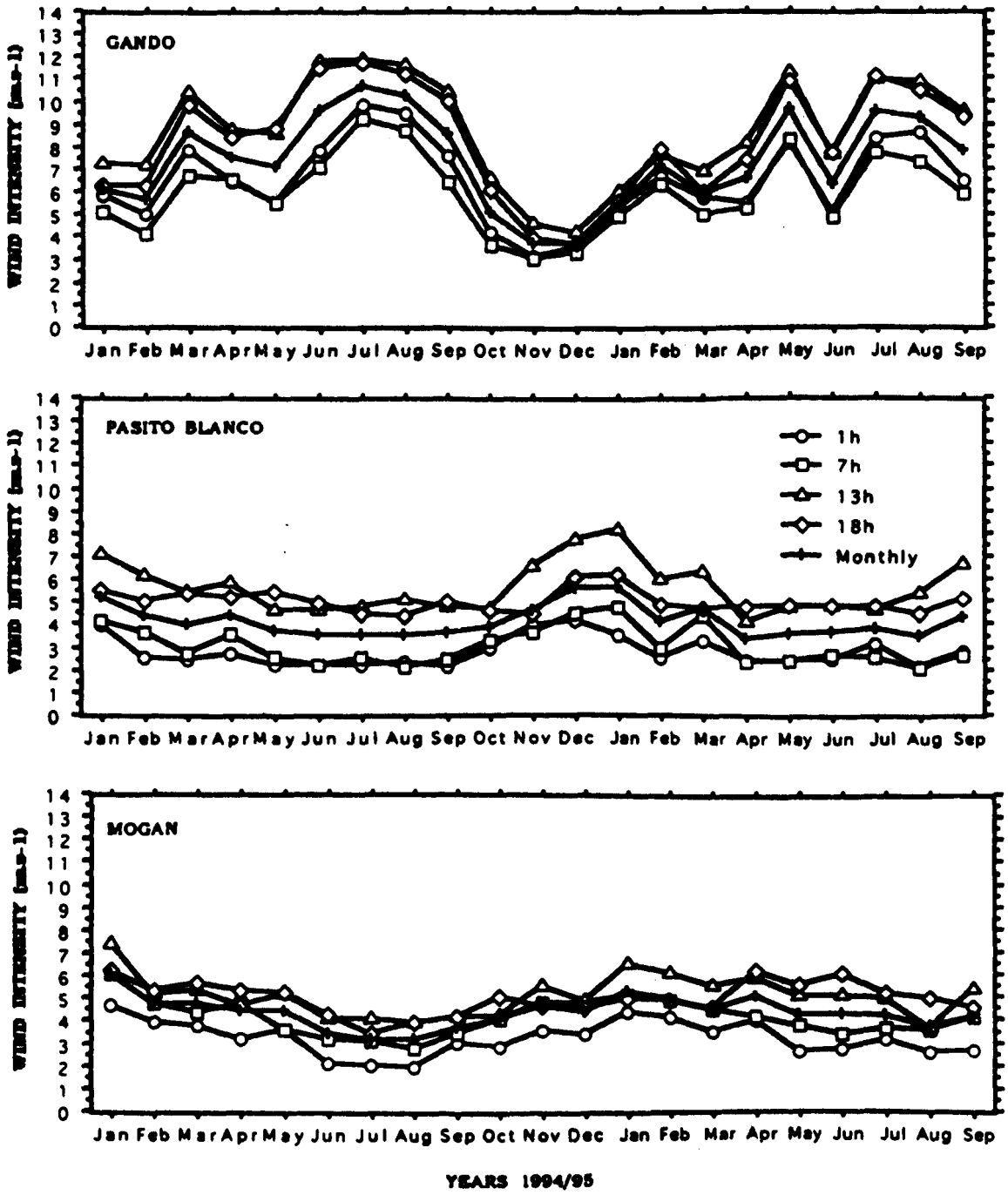


Fig. 3a - Wind intensity ($m.s^{-1}$) in the meteorological stations situated at east (Gando), south (Pasito Blanco) and southwest (Mogán) of Gran Canaria.

© Del documento, los autores. Digitalización realizada por ULPGC. Biblioteca Universitaria, 2009

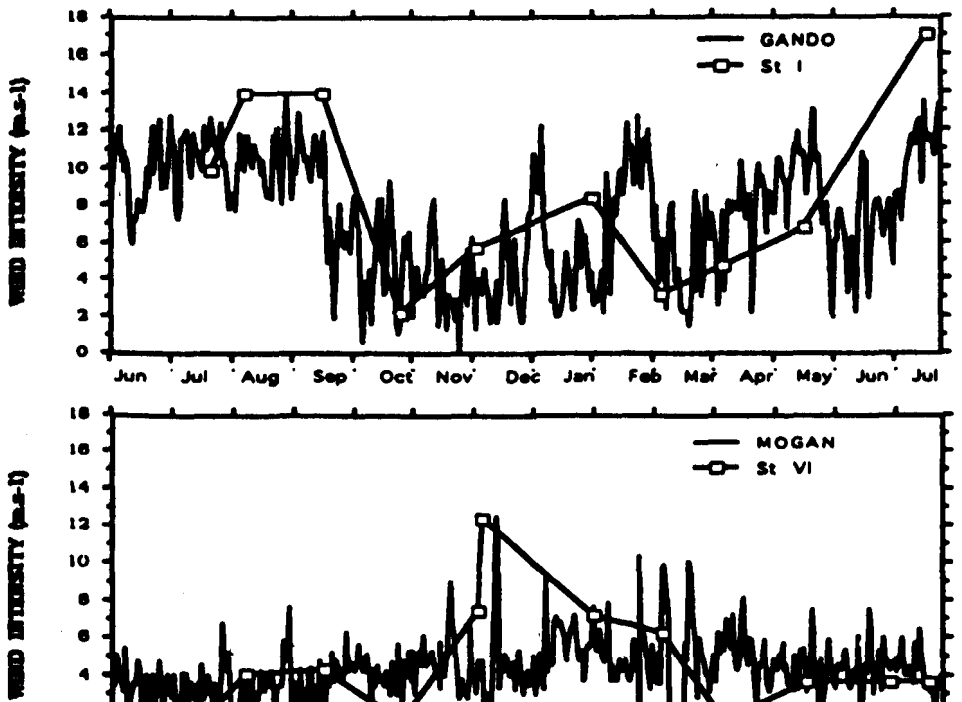


Fig. 3b - Wind intensity (m.s$^{-1}$) in the meteorological stations and oceanography stations ("in situ").

The hourly wind measurements taken at different hourly intervals show a similar distribution in the course of the months in the station at Gando where we can emphasize two periods: the night time with minimums and the day time when the highest wind speeds are recorded. This distribution is not so clear in the station at Mogán where the winds are more constant throughout the day, although of lesser intensity.

As regards the measurements recorded in the stations "in situ", we have an average wind intensity of only 2.17 m.s$^{-1}$ ($\pm$0.70) for the whole area in the month of October. The monthly distribution of wind intensity is going to correspond to the situation of the sampling stations (Fig. 3b), exposed to or sheltered from the dominant winds, and in this way we find that it is in the month of October when there is the transition with the two types of monthly variation described.

Taking into account the localization of the stations, we find that the maximum wind intensities are recorded in August (13.38 m.s$^{-1}$ $\pm$1.33) - September (12.99 m.s$^{-1}$ $\pm$0.65) for the whole group of stations (St. I, II, III and IV) situated in the southeast, emphasizing the 16.98 m.s$^{-1}$ measured in station I in the month of July. In contrast, for station VI situated in the southwest of the area, the greatest intensity of wind speed is recorded in December.

© Del documento, los autores. Digitalización realizada por ULPGC. Biblioteca Universitaria, 2009

* Seawater temperature

The surface temperature of seawater measured in the months during the sampling oscillates between the 18.1°C recorded in March to the 23.8°C recorded in October (Fig. 4). There is practically no spatial variation in the temperature of the seawater in the area under study. The greatest range of variation is of 1°C which is obtained in October, the month with the highest seawater temperature of 23.3°C (±0.3), and it corresponds to the thermal difference between the measurements from station I, located in the northeast, and the station situated to the southwest of the area. In the same way as happens with the air temperature, an increase in the temperature of seawater is observed (0.5-1.4°C) in the month of July, a fact which we can check by comparing the records from 1994 and 1995 in station I. As regards the distribution of the temperature with depth we find that the thermal slope is not superior to 0.6°C between the surface and the measurement taken at 15m., which was obtained in October.

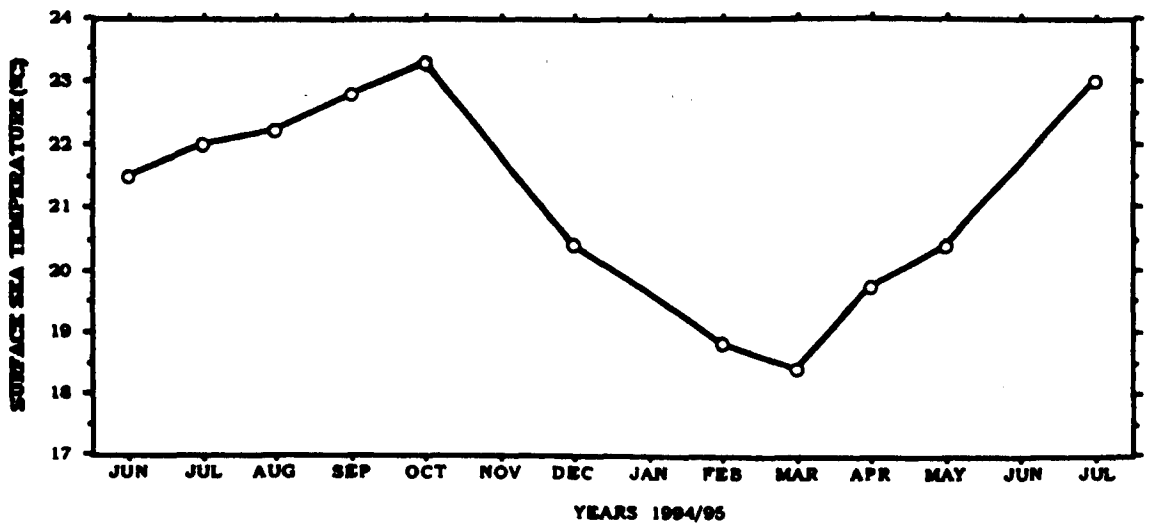


Fig. 4 - Sea surface temperature (°C) in the area.

Phytoplanktonic Biomass

* Concentration of pigments

In general, the concentrations of chlorophyll *a* are higher in the two stations used in the study situated in the southeast (St I and II). At the said stations, a high biomass is obtained (0.66 mg Chl *a* .m$^{-3}$) in July which hides the spring bloom (0.30 mg Chl *a* .m$^{-3}$) observed in the month of March as well as in the remaining seasons (0.11-0.24 mg Chl *a* .m$^{-3}$), Fig. 5a.

© Del documento, los autores. Digitalización realizada por ULPGC. Biblioteca Universitaria, 2009

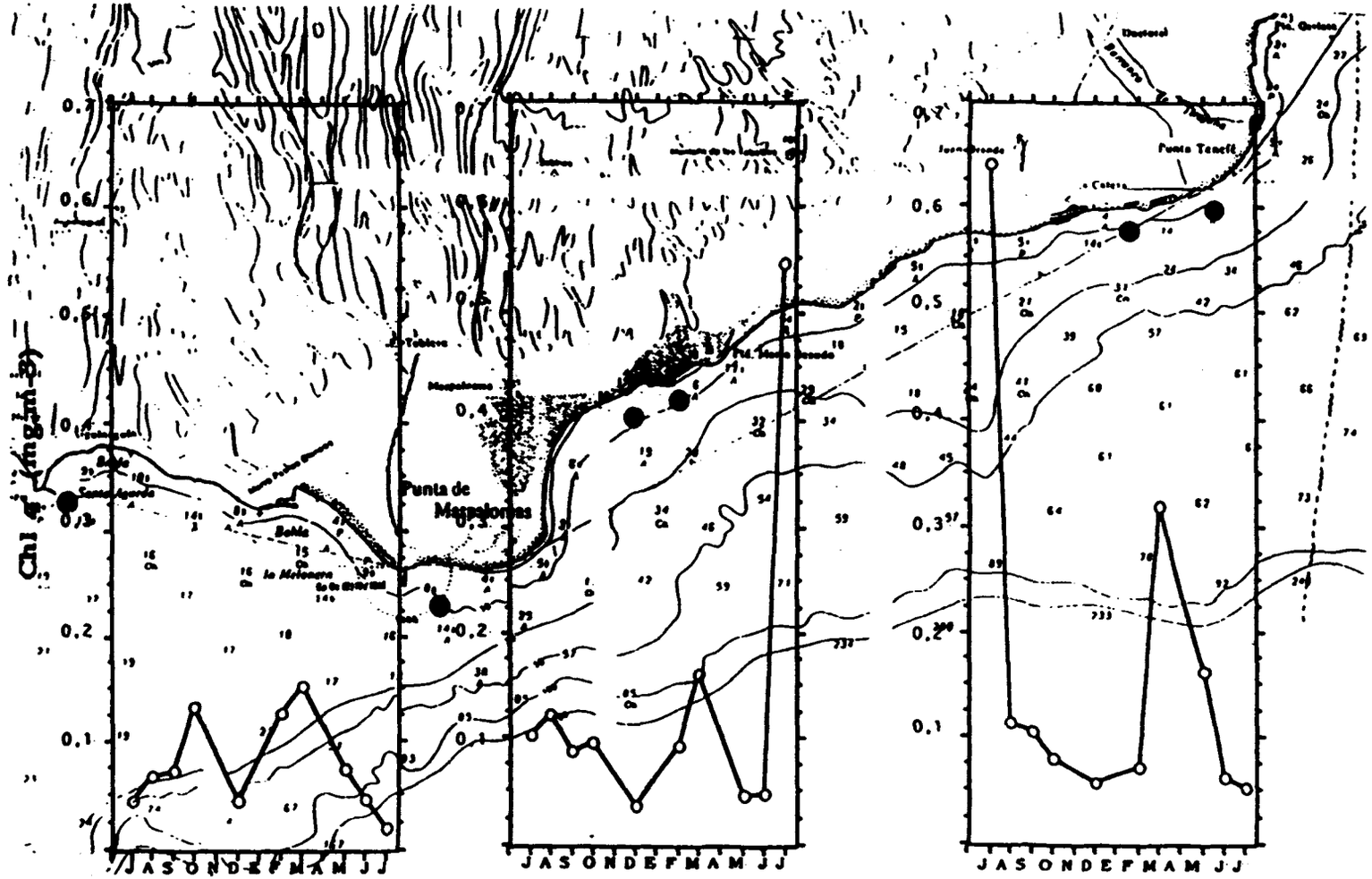


Fig. 5a - Phytoplankton biomass (mg Chl *a* .m$^{-3}$) in the stations sampling.

© Del documento, los autores. Digitalización realizada por ULPGC. Biblioteca Universitaria, 2009

© Del documento, los autores. Digitalización realizada por ULPGC. Biblioteca Universitaria, 2009



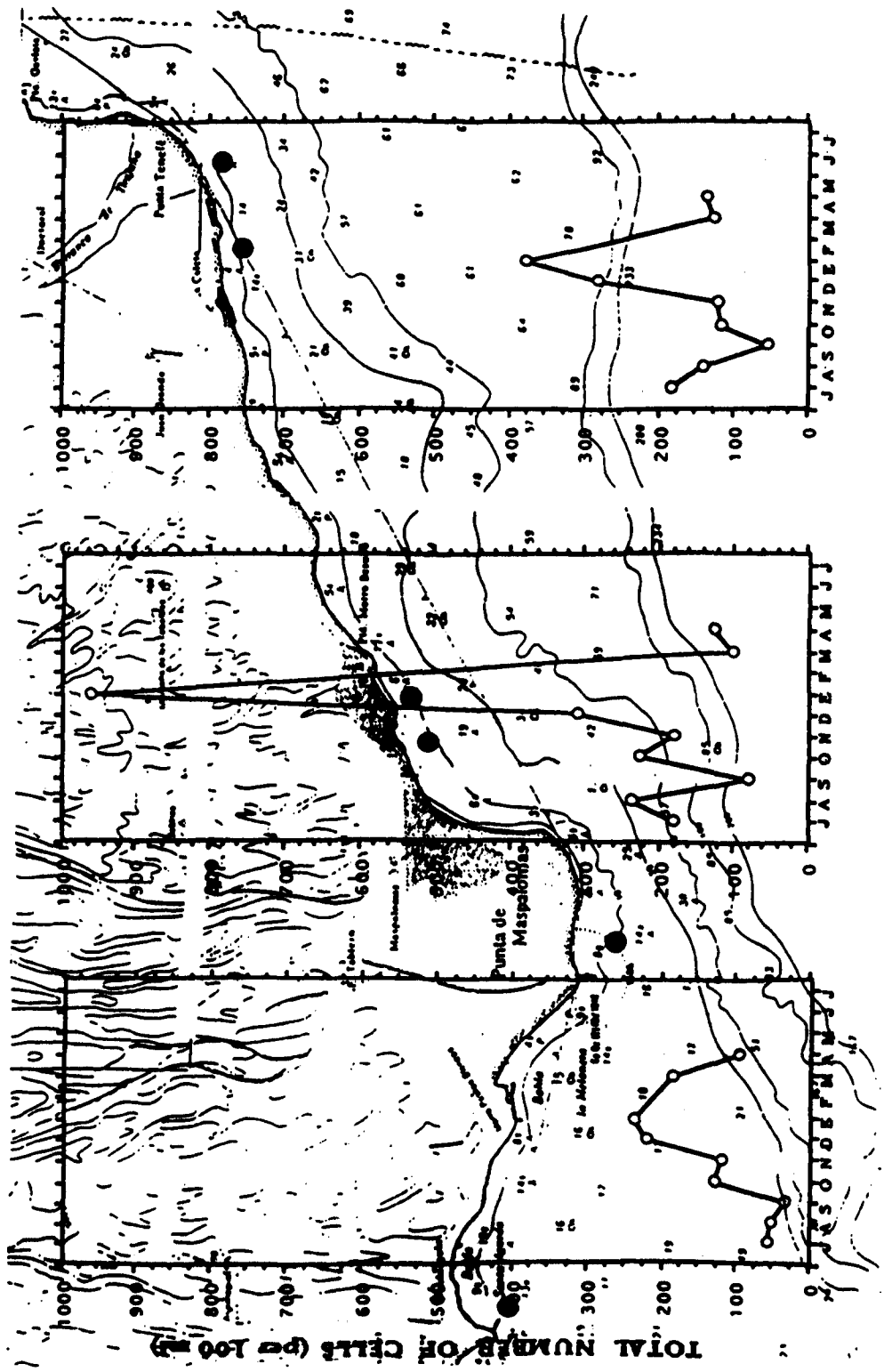


Fig. 5b - Phytoplankton biomass (cells/100ml) in the stations sampling.

In general, there is a correspondence between the biomass estimated as pigment concentration and that obtained from a cellular count, with a high concentration of chlorophyll obtained in station I in the month of July 1994.

* Counting and systematic identification

The values for total population density are low, no higher than 12 cells.ml$^{-1}$, and these values correspond to those quoted by MARGALEF (1983) for oligotrophic marine areas.

The maximum population density is obtained in the month of March, made up of Diatoms (principally *Rhizosolenia stolterforthii, R. setigera, Chaetoceros decipiens* and *Ch. debilis*) while in the summer period it consists of Dinoflagellates (*Protoperidinium sp.*, *Ceratium furca* and *Ceratium* sp.), Fig. 5b. By station, the recount of the number of cells present has a high value in station III, highlighting the presence of the dinoflagellates *Gonyaulax* sp. in the summer months. With the exception of this fact, the distribution, according to the different seasons, essentially obeyed the same pattern, and did not show qualitative differences and/or dominance of species. During the entire period of study, other species also appear, such as *Nitzchia closterium, N. seriata, Navicula sp., Fragilaria sp.*, and *Licmophora* sp.

The analysis of the principal components allowed a relationship to be established between the number of individuals present - taxonomical groups and seasonality (Fig. 6a) - and localization of the sampling points, (Fig. 6b) giving rise to a distribution influenced by the seasonal analysis of the groups of species.

Since the data obtained was abundant, the detailed analysis of the population was carried out taking into account the presence of the species in a high number of samples, its abundance and the degree of reliability in its identification. Parallel to this, the species were classified according to their taxonomy into dinoflagellates, pennate diatoms and centric diatoms. Within this last group, at the same time, the families Rhizosoleniaceae and Chaetoceraceae were considered.

The analysis of principal components according to the localization of the sampling points indicates that the composition of the samples presents geographical variations between stations III, II and the rest. This latter group incorporates those stations which show smaller differences between them (Fig. 6b).

The distribution corresponding to the seasonal variability indicates, at the same time, that the specific composition of the sample presents differential associations in October, February and the remaining months (Fig. 6a).

Therefore, these seasons and months were selected, together with station I and the month of March as respective representatives of the others with a greater degree of association (Fig.6b).

© Del documento, los autores. Digitalización realizada por ULPGC. Biblioteca Universitaria, 2009

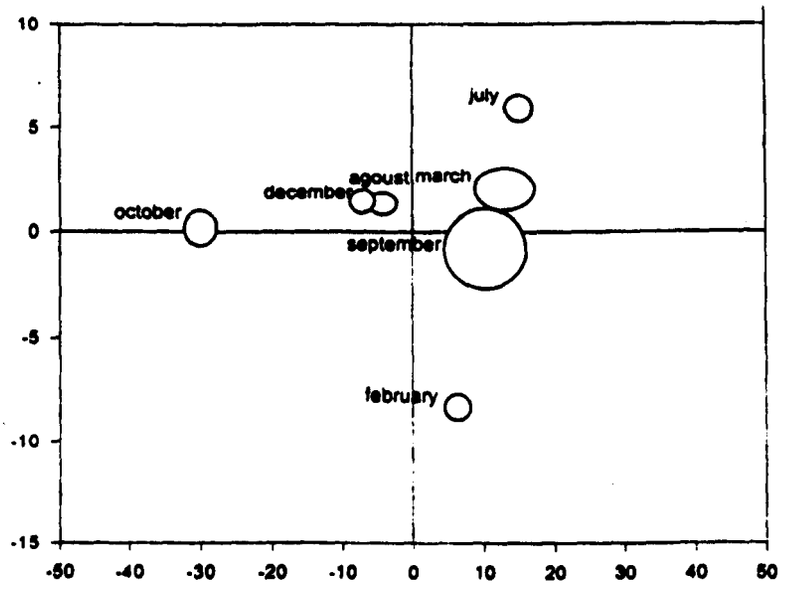


Fig. 6a - Monthly distribution by the taxonomical groups (five) and the sampling points.

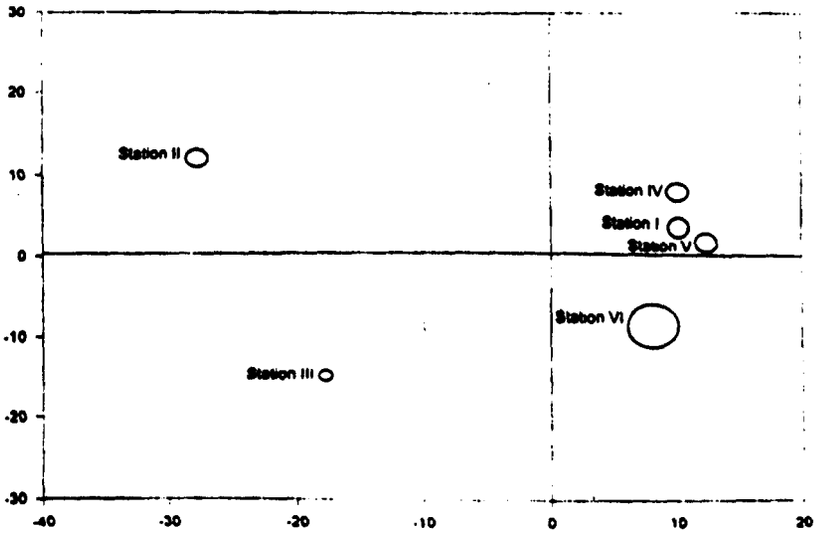


Fig. 6b - Distribution of the sampling points as function of the five taxonomical groups and the month.

## DISCUSSION

The daily difference of dry temperature, that is to say between the maximum and minimum recorded both in Gando and in Mogán, is a degree higher than the range obtained by TEJEDOR (1991). The monthly distribution of the wind intensity for 1994 in the station at Gando corresponds to that given by MEDINA (1995) for the same station in the period

© Del documento, los autores. Digitalización realizada por ULPGC. Biblioteca Universitaria, 2009

from 1985/89. The annual average of the wind intensity in 1994/95 and the hourly intensities in Gando are in accordance with the results of the study by TEJEDOR (1991) for a period of thirty years and with the annual average obtained for 1976/85 by PÉREZ-MARTELL (1988) and for 1985/89 obtained by MEDINA (1995) in this same station.

The pattern of monthly distribution of wind intensity in the stations situated in the south of the island, Pasito Blanco and Mogán, corresponds to that described by MEDINA (1995) for the station of Mogán. For the station at Gando the predominant directions are north (22.8-41.5%) and north-northeast (19.1-59.3%) throughout an annual cycle (TEJEDOR, 1991; PÉREZ-MARTELL, 1988). In the station at Mogán the northerly direction is less frequent than that of southeasterly, southerly and westerly (PÉREZ-MARTELL et al., in press), which is due to the leeward situation of the station which is protected by the mountains from the action of the trade winds.

The recorded measurements of surface temperature of seawater and thus its monthly distribution can be placed within those given for the area by MEDINA (1995) with minimums in February/April and maximums at the end of August/October depending on the area and year of the study.

For the area of the Canary Islands, we have found an average concentration of Chl *a* of around 0.1 $mg.m^{-3}$, except during spring bloom which can reach up to 1 $mg.m^{-3}$ (BRAUN et al., 1982).

The high content of nutrients which is found in February descends rapidly in March corresponding to an elevated biomass. The fluctuation in quantity of the nutritive elements is due to selective absorption by organisms (TAIT, 1987), and in all the stations we can find a direct relation between low concentrations of silicates and a high percentage of diatoms.

The total concentration of phytoplankton (n° of cells/100 ml) showed temporal variability, in the same way as the concentration of chlorophyll (mg Chl *a*. m-3). The biomass expressed in number of individuals corresponds to that expressed in the concentration of chlorophyll *a*., with the exception of the month of July.

These divergent values obtained on measuring the biomass (recount of cells vs. concentration of pigment extracted) could be explained by the heterogeneity in the distribution of the phytoplankton (ESTRADA, 1982). In this sense, in station II, the different entries of biomass could be due to the fact that a high number of non-identified cells were counted, but they were hidden by the maximum of phytoplanktonic population present in March.

The concentration of the populations of phytoplankton, in canarian waters, is situated between 13-65 $cells.ml^{-1}$, with a predominance of diatoms throughout the whole annual cycle (BRAUN & REAL, 1984; BORDES et al., 1992). However, an increasing number of individuals belonging to the dinoflagellates are found in the summer months, but without succession taking place between both taxonomical groups (OJEDA, 1985).

Throughout our sampling period, it is possible to observe this distribution, with

© Del documento, los autores. Digitalización realizada por ULPGC. Biblioteca Universitaria, 2009

higher concentrations, however, in the area of station III. This is characterized by the presence of dinoflagellates of the type *Ceratium sp.*, and *Protoperidium* sp., as well as a notable abundance of *Gonyaulax* sp.

These variations are so small to speak about phytoplankton blooms but enough to develop monitoring programs to control the wastwater discharges and the deputation processes.

## REFERENCES

BORDES, F. et al.:

1992. Cartografía y evaluación de recursos pesqueros de la plataforma y talud de Gran Canaria (Islas Canarias). Informe, Consejería de Pesca y Transportes del Gobierno Autónomo e Instituto Canario de Ciencias Marinas del Exc. Cabildo Insular de G. C..

BRAUN, J.G.:

1980. Estudios de producción en aguas de las Islas Canarias. I. Hidrografía, nutrientes y producción primaria. *Bol. Inst. Esp. Oceanogr.*, 285, pp: 140-154.

BRAUN, J.G. & F. REAL:

1984. Estudios de producción en la bahía de Antequera: una comparación con aguas oceánicas. *Bol. Inst. Esp. Oceanogr.* 1(2), pp: 134-140.

1986. Distribución vertical de la clorofila en aguas de las Islas Canarias. *Bol. Inst. Esp. Oceanogr.* 3(2), pp: 97-106.

BRAUN, J.G., F. REAL & J.D. DE ARMAS:

1982. Production studies in Canary Island waters. *Rapp. P.-v. Réun. Cons. Explo. Mer*, 180, pp: 219-220.

BRAUN, J.G., I. ORZAIZ, J.D. de ARMAS & F. REAL:

1985. Productividad y biomasa del ultraplancton, nanoplancton y fitoplancton de red en aguas de las Islas Canarias. *Bol. Inst. Esp. Oceanogr.* 2(1), pp: 192-204.

CORRAL, J. & M.F. GENICIO:

1970. Nota sobre el plancton de la costa noroccidental africana. *Bol. Inst. Esp. Oceanogr.*, nº 140.

DE LEON, A.R. & J.G. BRAUN:

1973. Ciclo anual de la producción primaria y su relación con los nutrientes en aguas canarias. *Bol. Inst. Esp. Oceanogr.*, n. 167, pp: 1-25.

© Del documento, los autores. Digitalización realizada por ULPGC. Biblioteca Universitaria, 2008

ESTRADA, M.:

1982. Ciclo anual del fitoplancton en la zona costera frente a la Punta Endata (Golfo de Vizcaya). *Inv. Pesq.* 46(3): 469-491.

FERNANDEZ DE PUELLES, M. & J.G. BRAUN:

1989. Dinámica de las comunidades planctónicas en una zona del Atlántico Subtropical (Isla de Tenerife). *Bol. Inst. Esp. Oceanogr.*, 5(2), pp: 87-100.

GRASSHOFF, K., M. EHRHART & K. KREMLING:

1983. *Methods of Seawaters Analysis*. Second, revised and extended edition. 419pp.

JEFFREY, S.W. & G.F. HUMPHREY:

1975. New spertrophotometric equations for determining chlorophylls *a, b, c1* and *c2* in higher plants, algae and natural phytoplankton. *Biochem. Physiol. Pflanzen.*, 167. pp: 191-194.

LORENZEN, C.J.:

1967. Determination of chlorophyll and phaeopigments: spectrophotometric equations. *Limnol. Oceanogr.*, 12, pp: 343-346.

MARGALEF, R.:

1982. *Ecología* . Omega S.A., 951pp.

1992. *Teoría de los ecosistemas ecológicos*. Planeta S.A.. 255pp..

MEDINA, L.:

1995. *Análisis multidisciplinar del ecosistema costero insular, balance energético, capa de mezcla y modelo biológico*. Tesis Doctoral. Universidad de Las Palmas G.C.. 316pp.

MINAS, H.J., L.A. CODISPOTI & R.C. DUGDALE:

1982. Nutrients and primary production off Northwest Africa. *Rapp. P.-v. Réun. Cons. Int. Explor. Mer*, 180, pp: 148-183.

OJEDA, A.:

1985. Especies fitoplanctónicas identificadas en aguas litorales de las Islas Canarias Orientales. Simp. Int. Afl. O Afr., *Inst. Inv. Pesq.*, Barcelona, v. I, pp: 403 - 415.

PEREZ-MARTELL, E.:

1988. *Interacción vientos-corrientes en profundidades reducidas. Un modelo para la costa Este de Gran Canaria*. Tesis Doctoral. Universidad Politécnica de Canarias. 271 pp..

© Del documento, los autores. Digitalización realizada por ULPGC. Biblioteca Universitaria, 2009

PEREZ-MARTELL, E., M.J. RUEDA & O. LLINAS:

IN PRESS. A study of the distribution of winds in the Canary Islands. Its application in surface marine dynamics. *Bol. Inst. Esp. Oceanogr.*

REAL, F., J.D. de ARMAS & J.G. BRAUN:

1981. Distribución espacial de la clorofila *a* y del carbono orgánico particulado en aguas costeras superficiales de las Islas Canarias. *Bol. Inst. Esp. Oceanogr.* Tomo VI, nº 292, pp: 109-115.

TAIT, R.V.:

1987. *Elementos de Ecología Marina.* Ed. Acribia, S.A. 446 pp.

TEJEDOR, B.:

1991. *Contribución al estudio de los fenómenos dinámicos de interacción atmósfera-océano en la costa oriental de Gran Canaria.* Tesis Doctoral, Univ. de Las Palmas G.C..

UTERMÖHL, H.:

1931. Neue wege in derquantitativen erfassung des planktons (mit besonderer berücksichtigung des ultraplanktons). *Verh. Int. Ver. Theor. Angew. Limnol.* 5(2), pp: 567-596.

VALIELA, I.:

1995. *Marine Ecological Processes.* 2nd Ed. Springer-Verlang, New York. 686pp.

Date received: 06-04-98.

© Del documento, los autores. Digitalización realizada por ULPGC. Biblioteca Universitaria, 2009

*Journal of Applied Phycology* 11: 15–19, 1999.
© 1999 *Kluwer Academic Publishers. Printed in Belgium.*



# Oleic acid is the main fatty acid related with carotenogenesis in *Dunaliella salina*

H. Mendoza[1]*, A. Martel[1], M. Jiménez del Río[2] & G. García Reina[1]
[1]*Instituto de Algología Aplicada, Universidad de Las Palmas de G. C., Muelle de Taliarte s/n, 35214 – Telde, Canary Islands, Spain*
[2]*Instituto Tecnológico de Canarias, Cebrian 3, 35003 Las Palmas de Gran Canaria, Canary Islands, Spain*

(*Author for correspondence; fax +34 928 132830)

Received 1 April 1998; revised 30 November 1998; accepted 30 November 1998

*Key words:* carotene, *Dunaliella salina*, fatty acid, irradiance, nitrogen starvation, oleic acid (18:1)

## Abstract

The variation of the fatty acid profile and the carotene content of *Dunaliella salina* in response to irradiance (80, 128, 640, 1000, 1500 $\mu$mol photon $m^{-2}$ $s^{-1}$) and nitrogen starvation were analysed. The highest fatty acid content per cell and the least polyunsaturated fatty acid percentage were exhibited under 1500 $\mu$mol photon $m^{-2}$ $s^{-1}$. Furthermore, the oleic acid (18:1) content maintained a positive and significant correlation with the carotene content per cell and with the irradiance. The composition of the carotene globules in *Dunaliella salina* may be the main determinant of this correlation.

## Introduction

The halotolerant green microalga *Dunaliella salina* has received much attention as an ideal organism for algal biotechnology and specifically for its $\beta$-carotene production (Borowitzka et al., 1984). This microalga has the unique ability to accumulate large amounts of carotene when exposed to stress conditions such as high irradiance, high salt concentration and nutrient deficiency (Semenenko & Abdullaev, 1980; Ben-Amotz et al., 1982). $\beta$-carotene is accumulated within oily globules in the inter-thylakoid spaces of the chloroplast and it is composed mainly of the two stero-isomers 9-*cis* and all-*trans* $\beta$-carotene (Ben-Amotz et al., 1982). Irradiance and growth stress (Ben-Amotz & Avron, 1983) affect the $\beta$-carotene content and the ratio of the 9-cis to all-trans isomers. Accumulation of $\beta$-carotene represents a possible strategy of defence against damage from high irradiance under growth limiting conditions (Ben-Amotz et al., 1989; Gómez-Pinchetti et al., 1992).

Different microalgae exposed to stress growth conditions (i.e. high irradiance and nitrogen starvation) accumulate intra- or extra-plastidic lipid bodies composed of triglycerides and carotenoids (Kivic & Vesk, 1972; Roessler, 1990; Vechtel et al., 1992). The aim of the present work was to characterise the variation in the fatty acid profile and the $\beta$-carotene content in a local strain of *Dunaliella salina* Teodoresco (IAA401) grown under nitrogen starvation and different irradiances.

## Materials and methods

### *Algae and growth conditions*

Cells of *Dunaliella salina* IAA401 (Microalgae Culture Collection, Institute of Applied Algology, ULPGC, Spain) originally isolated from salt works in the north of Gran Canaria island (Gómez-Pinchetti et al., 1992), were grown in the medium described by Jiménez-Río et al. (1993) containing 1M NaCl. Cultures were bubbled with 3% $CO_2$ in air, at 30 °C and continuous light (200 $\mu$mol photon $m^{-2}$ $s^{-1}$) provided by 20W low consumption lamps (Mazda, Eureka).

© Del documento, los autores. Digitalización realizada por ULPGC. Biblioteca Universitaria, 2009

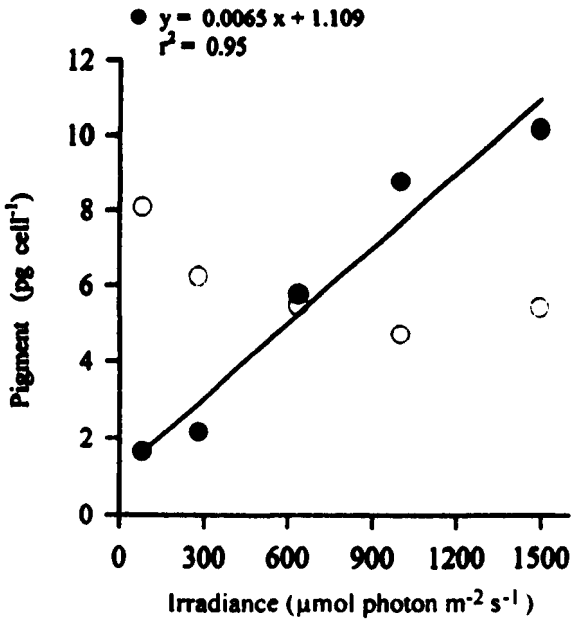


*Figure 1.* Relationship between carotene (●) and chlorophyll (○) contents of *D. salina* IAA 401 with irradiance.

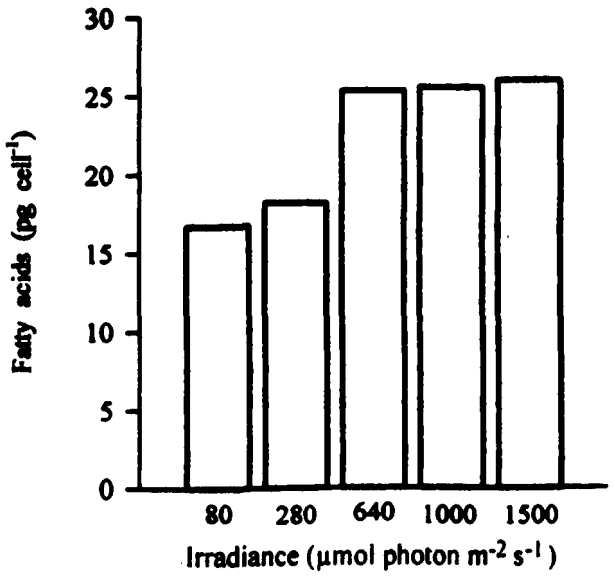


*Figure 2.* Effect of irradiance on total fatty acid content per cell in *D. salina* (IAA 401).

Cells were harvested at the exponential growth phase by centrifugation (5 min, 5000 × g, 5 °C), washed three times with 50mM Tris buffer containing 1M NaCl, and resuspended in fresh medium but without nitrogen, to a final density of $1.6 \times 10^5$ cells $mL^{-1}$. Experimental cells were then cultured under five different irradiances: 80, 280, 640, 1000, 1500 $\mu$mol photon $m^{-2}$ $s^{-1}$. Samples were collected at the stationary growth phase (5 min, 5000 × g, 5 °C) for the measurement of total carotene content and fatty acid composition. Three replicates were used in all experimental conditions.

*Cell growth and pigment analysis*

Cell numbers were estimated with a haemocytometer. Chlorophyll and total carotene were extracted from algal pellets with cold methanol and assayed according to Wellburn (1994).

*Fatty acid analysis*

Total lipid extract was transesterified with methanol saturated with HCl for 90 min, at 80 °C. The fatty acids methyl esters (FAME) were separated with diethylether and purified from lipophilic substances by thin-layer chromatography 10 × 10 cm plates, coated with silica gel type g (Sigma Co.). The running solution was hexane-diethylether (10:1 v/v) and the standard used was transmethylated sunflower oil (Petkov et al., 1990). After addition of pentadecanoic acid (15:0) as internal standard, FAME were dissolved with hexane.

FAME samples were analysed using a gas chromatograph (Shimadzu, GC-15A) with a FID detector, and a polar Supelcowax 10 (Supelco) fused-silica column (30 m × 0.32 mm id.). The FID was operated at 200 °C and the column oven temperature was 195 °C. Component peaks were integrated by a Cr5A integrator (Shimatzu) and identified by comparison of relative retention times of known standards (Sigma Co.).

*Statistical analysis*

Statistically significant differences were established by ANOVA. Non-significant statistical differences are reported as apparent differences. Correlations were tested by regression analysis.

## Results

A positive correlation ($r^2 = 0.95$) was found between irradiance and carotene content per cell (Figure 1). Cells grown at 1500 $\mu$mol photon $m^{-2}$ $s^{-1}$ had the highest carotene content, approximately 6 times higher than cells at 80 $\mu$mol photon $m^{-2}$ $s^{-1}$. The chlorophyll content per cell was not significantly correlated ($r^2 = 0.55$) with irradiance although the content was lower in cultures grown under high radiation (Figure 1).

© Del documento, los autores. Digitalización realizada por ULPGC. Biblioteca Universitaria, 2009

*Table 1.* Effect of irradiance on fatty acid composition of *Dunaliella salina*. (Data as percentage of total fatty acids ± sd; n = 3)

| Fatty acids | Irradiance ($\mu$mol photon $m^{-2}$ $s^{-1}$) | | | | |
|---|---|---|---|---|---|
| | 80 | 280 | 640 | 1000 | 1500 |
| 14:0 | trace | trace | trace | trace | trace |
| 16:0 | 5.45 ± 1.20 | 7.79 ± 0.63 | 11.35 ± 2.57 | 9.34 ± 0.85 | 24.78 ± 6.63 |
| 16:1 | 3.13 ± 0.09 | 2.00 ± 0.46 | 2.17 ± 0.02 | 2.89 ± 0.19 | 2.93 ± 0.06 |
| 16:2 | 3.64 ± 0.27 | 3.13 ± 0.81 | 2.11 ± 0.04 | 3.23 ± 0.10 | 2.45 ± 0.05 |
| 16:3 | 2.41 ± 0.07 | 2.09 ± 0.78 | 1.92 ± 0.05 | 3.56 ± 0.25 | 2.91 ± 0.08 |
| 16:4 | 35.05 ± 6.57 | 25.43 ± 0.97 | 16.31 ± 4.41 | 28.05 ± 5.12 | 21.22 ± 4.50 |
| 18:1 | 0.55 ± 0.03 | 1.76 ± 0.47 | 4.25 ± 0.21 | 5.12 ± 0.76 | 6.22 ± 1.49 |
| 18:2$\omega$6 | 10.99 ± 2.10 | 10.14 ± 2.37 | 16.17 ± 2.65 | 15.36 ± 1.68 | 14.39 ± 0.25 |
| 18:3$\omega$6 | 1.50 ± 0.12 | 1.36 ± 0.06 | 1.10 ± 0.08 | 0.87 ± 0.08 | 0.55 ± 0 |
| 18:3$\omega$3 | 36.87 ± 2.83 | 45.80 ± 6.26 | 44.33 ± 6.42 | 30.84 ± 6.24 | 24.17 ± 2.02 |
| 18:3$\omega$4 | trace | trace | trace | trace | trace |
| Sat.+monounsat. | 9.18 | 11.55 | 17.77 | 17.35 | 33.93 |
| Polyunsat. | 90.46 | 87.95 | 81.94 | 81.91 | 65.69 |
| Total (pg $cell^{-1}$) | 16.68 ± 0.05 | 18.1 ± 4.50 | 25.32 ± 4.73 | 25.55 ± 2.00 | 26.06 ± 0.86 |

The fatty acid content increased with increasing irradiance (Figure 2). Table 1 summarises the variation in the fatty acid profile under different culture conditions. High irradiance tended to increase the content of 16:0 and 18:1, and to decrease the content of 16:2, 16:4, 18:3$\omega$6 and 18:3$\omega$3. The percentage of unsaturated fatty acids decreased with an increase in irradiance (Table 1), while the ratio 16:0/16:4 (Figure 3) increased.

A significant correlation ($p < 0.05$), both in absolute and relative values, was found between oleic acid (18:1) and carotene content per cell (Figure 4).

## Discussion

The strong correlation between irradiance and carotene content per cell and the lack of variation in chlorophyll content (Figure 1) could be attributed to the important photoprotective role of carotene in *D. salina* (IAA401). This result contrasts with other *Dunaliella* species that are unable to accumulate large amounts of carotene under high irradiance (Berner et al., 1989). An increase in fatty acid content under stress (high irradiance or nitrogen starvation) conditions has been described in *Nannochloropsis* (Sukenik et al., 1989) and *D. salina* (Cho & Thompson, 1986). In our cultures the increase in fatty acids (saturated and monounsaturated) under carotenogenic conditions (Table 1, Figure 2) can be partially attributed to the increase in carotene globules (as they are composed of 14% triacylglycerols and diacylglycerols, Fried et al., 1982). This increase in fatty acids might play an important role in the structural stability of carotene globules and thus also in the effectiveness of the photoprotective role of carotene. Katz et al. (1995) has described the importance of the structural stability of the carotene globules on its photoprotective role.

The increase in the 16:0/16:4 ratio observed in *D. salina* during adaptation to high irradiances could be related to the change in the balance between storage and photosynthetic related fatty acid during the adaptation to environmental conditions. These results are in accordance with those reported by Goes et al. (1994), who demonstrated the association between 16:0/16:4 ratio with the photosynthetic status in the green alga *Tetraselmis* sp. The increase in this ratio and the observed decrease of the polyunsaturated fatty acid content (Table 1) in response to high irradiance in *D. salina* are less marked than in other species of *Dunaliella* (Thompson et al., 1990), which might be a consequence of the photoprotective role of $\beta$-carotene.

Oleic acid (18:1) has been described as an important reserve fatty acid, mainly associated with phosphatidylethanolamine, triacylglycerols and diacylglycerols in *Dunaliella* (Fried et al., 1982; Al-Hasan, 1987); the concentration in the cell increases under

© Del documento, los autores. Digitalización realizada por ULPGC. Biblioteca Universitaria, 2009

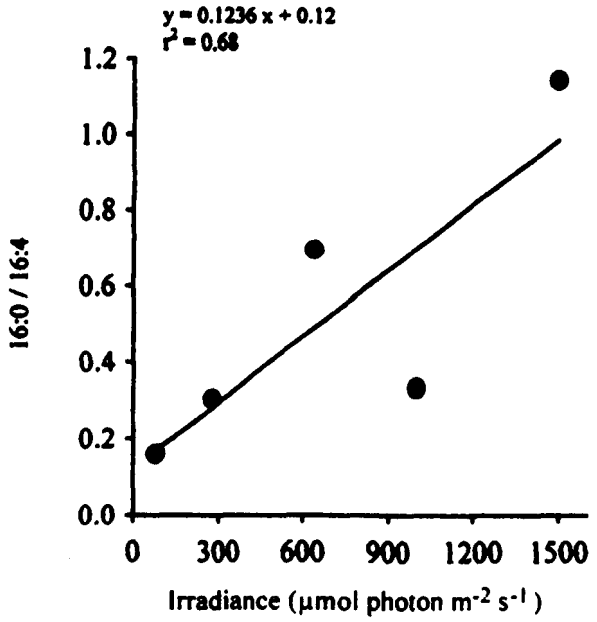


*Figure 3.* Relationship between 16:0/16:4 ratio of *D. salina* (IAA 401) and irradiance.

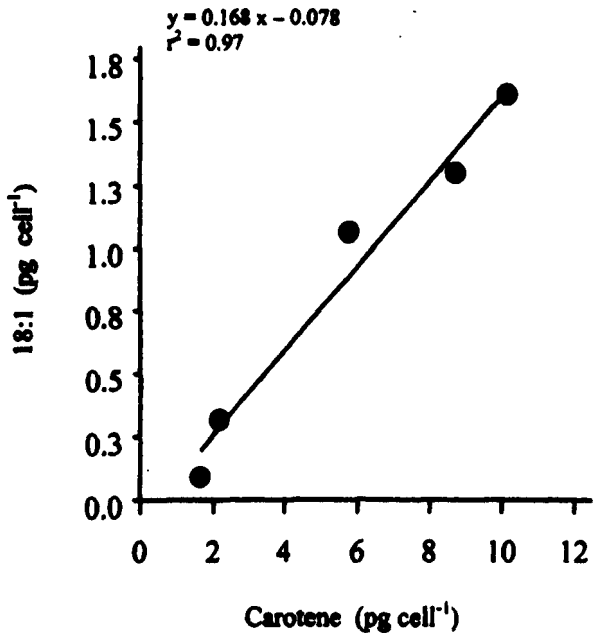


*Figure 4.* Relationship between oleic acid content and the carotene content per cell.

stress conditions (Mendoza et al., 1996). However, this is the first report describing the direct relation between stress, oleic acid and caroteneogenesis in *D. salina* (Figure 4). 18:1 may constitute the main fatty acid present in the $\beta$-carotene globules, which could explain the strong correlation between the oleic acid and the $\beta$-carotene contents during the adaptation to stress conditions.

The results suggest that the variations in fatty acid content and the carotenogenesis in *D. salina* could be closely related processes. This may be a consequence of the photoprotective role of carotene that determines the fatty acid profile in response to stress conditions, and to a direct relationship between oleic acid and carotenogenesis. Although there seems to be a clear correlation between carotene accumulation and oleic acid concentration, further investigations are needed to prove that the two processes are independent.

## Acknowledgements

We thank Dr G. Petkov for helping to set up the fatty acid determination method in our Institute and Mrs Paula Moreno Díez for technical assistance and help. This research was partially supported by CICYT/SPAIN (Project AMB-96-0962).

## References

Al-Hasan RH, Ghannoum MA, Sallal A-K, Abu-Eteen KH, Radwan SS (1987) Correlative changes of growth, pigmentation and lipid composition of *Dunaliella salina* in response to halostress. J. gen. Microbiol. 133: 2607–2617.

Ben-Amotz A, Avron M (1983) On the factors which determine massive $\beta$-carotene accumulation in the halotolerant alga *Dunaliella bardawil*. Plant Physiol. 72: 593–597.

Ben-Amotz A, Katz A, Avron M (1982) Accumulation of carotene in halotolerant algae: purification and characterisation of $\beta$-carotene globules from *Dunaliella salina* (Chlorophyceae). J. Phycol. 18: 529–537.

Ben-Amotz A, Shaish A, Mordhay A (1989) Mode of action of the massively accumulated $\beta$-carotene of *Dunaliella bardawil* in protecting the alga against damage by excess irradiation. Plant Physiol. 91: 1040–1043.

Berner T, Dubinsky A, Wyman K, Falkowski PG (1989) Photoadaptation and the 'package' effect in *Dunaliella tertiolecta* (Chlorophyceae). J. Phycol. 25: 70–78.

Borowitzka LJ, Borowitzka MA, Moulton TP (1984) The mass culture of *Dunaliella salina* for fine chemicals: From laboratory to pilot plant. Hydrobiologia 116/117: 115–125.

Cho SH, Thompson GA (1986) Properties of a fatty acid hydrolase preferentially attacking monogalactosyldiacylglycerols in *Dunaliella salina* chloroplasts. Biochim. Biophys. Acta 878: 353–359.

Fried A, Tietz A, Ben-Amotz A, Eichenberger W (1982) Lipid composition of the halotolerant alga. *Dunaliella bardawil*. Biochim. Biophys. Acta 713: 419–426.

Goes JI, Handa N, Taguchi S, Hama T (1994) Effect of UV-B radiation on the fatty acid composition of the marine phytoplankter *Tetraselmis* sp.: relationship to cellular pigments. Mar. Ecol. Progr. Ser. 114: 259–274.

© Del documento, los autores. Digitalización realizada por ULPGC. Biblioteca Universitaria, 2009

Gómez-Pinchetti JL, Ramazanov ZM, Fontes AG, García Reina G (1992) Photosynthetic characteristics of *Dunaliella salina* (Chlorophyceae, Dunaliella) in relation to β-carotene content. J. Appl. Phycol. 4: 11–15.

Jiménez del Río M, Ramazanov ZM, García-Reina G (1994) Dark induction of nitrate reductase in the halophilic alga *Dunaliella salina*. Planta 192: 40–45.

Katz A, Jiménez C, Pick U (1995) Isolation and characterisation of a protein associated with carotene globules in the alga *Dunaliella bardawil*. Plant Physiol. 108: 1657–1664.

Kivic PA, Vesk M (1972) Structure and function in the euglenoid eyespot apparatus: the fine structure, and response to environmental changes. Planta 105: 1–14.

Mendoza H, Jiménez del Río M, García Reina G, Ramazanov ZM (1996) Low temperature induced β-carotene and fatty acid synthesis, and ultrastructural reorganization of the chloroplast in *Dunaliella salina*. Eur. J. Phycol. 31: 329–331.

Petkov GD, Klyachko-Gruvich GD, Furnadjieva ST, Pronina NA, Ramazanov ZM (1990) Genotypic differences and phenotypic changes of lipid and fatty acid composition in strains of *Dunaliella salina*. Sov. Plant Physiol. 3: 268–272.

Roessler PG (1990) Environmental control of glycerolipid metabolism in microalgae: commercial implications and future research directions. J. Phycol. 26: 393–399.

Semenenko VE, Abdullaev AA (1980) Parametric control of β-carotene biosynthesis in *Dunaliella salina* cells under conditions of intensive cultivation. Sov. Plant. Physiol. 27: 22–30.

Sukenik A, Carmeli Y, Berner T (1989) Regulation of fatty acid composition by irradiance level in the eustigmatophyte *Nannochloropsis* sp. J. Phycol. 24: 445–452.

Thompson PA, Harrison PJ, Whyte JN (1990) Influence of irradiance on the fatty acid composition of phytoplankton. J. Phycol. 26: 278–288.

Vechel B, Eichenberger W, Ruppel HG (1992) Lipid bodies in *Eremosphaera viridis* De Bary (Chlorophyceae). Plant Cell Physiol. 33: 41–48.

Wellburn AR (1994) The spectral determination of chlorophylls a and b, as well as total carotenoids, using various solvents with spectrophotometers of different resolution. J. Plant Physiol. 144: 307–313.

© Del documento, los autores. Digitalización realizada por ULPGC. Biblioteca Universitaria, 2009

ELSEVIER

Aquaculture 171 (1999) 269–278

Aquaculture

# Effect of vitamin E and C dietary supplementation on some immune parameters of gilthead seabream (*Sparus aurata*) juveniles subjected to crowding stress

D. Montero [a,*], M. Marrero [b], M.S. Izquierdo [c], L. Robaina [c], J.M. Vergara [c], L. Tort [d]

[a] *Instituto Canario de Ciencias Marinas, Gobierno de Canarias, PO Box 56, 35200, Telde, Las Palmas, Canary Islands, Spain*

[b] *Alevines y Doradas (ADSA), Castillo del Romeral, San Bartolome de Tirajana, Las Palmas, Canary Islands, Spain*

[c] *Departamento de Biología, Universidad de Las Palmas de Gran Canaria, Campus Universitario de Tafira, 35017, Las Palmas de Gran Canaria, Canary Islands, Spain*

[d] *Departamento de Biología Celular y Fisiología, Facultad de Ciencias, Universidad Autónoma de Barcelona, 08193, Cerdanyola, Barcelona, Spain*

Accepted 2 September 1998

**Abstract**

High stocking density is an aquaculture-related situation which causes crowding stress in fish and potentially affecting the immune system. Protection against disease can be induced through immunostimulation, enhancing defence mechanisms. Vitamins C and E are among the most important nutrients influencing the immune system, although the effect of these vitamins in the amelioration of stress in fish has not been studied in detail. An experiment was carried out to study the effect dietary supplementation of vitamin C or vitamin E on the immune system of fish under a crowding stress situation in a commercial farm. A commercial diet for this species was supplemented with vitamin C or vitamin E and these diets were assayed at high stocking density (over 40 kg $m^{-3}$) and the results were compared with those from fish fed the commercial diet and held at farm conditions (20 kg $m^{-3}$). Some biological and immunological parameters were studied

* Corresponding author. Tel.: +34-928-132-900; Fax: +34-928-132-908; E-mail: dmontero@iccm.rcanaria.es

0044-8486/99/$ - see front matter © 1999 Elsevier Science B.V. All rights reserved.
PII: S0044-8486(98)00387-1

© Del documento, los autores. Digitalización realizada por ULPGC. Biblioteca Universitaria, 2009

at the end of the experimental period. Fish held at high stocking density showed lower final weight than fish held at lower stocking density. These also showed higher plasma cortisol levels (over 6 ng cortisol $ml^{-1}$ plasma for all the diets assayed) than those fish held at lower density (1.13 ng cortisol $ml^{-1}$ plasma). High stocking density produced higher serum lysozyme activity values in fish fed the commercial diet compared with those fish held at lower density (67.49 and 36.84 units $ml^{-1}$, respectively). This effect was not observed in fish held at high stocking density but fed vitamin C and vitamin E supplemented diets (lysozyme activity: 21.97 and 19.71 units $ml^{-1}$, respectively). High stocking density also appeared to decrease serum alternative complement activity. In those fish fed the vitamin E supplemented diet, levels were similar to fish held at low stocking density, suggesting the role of this vitamin in this defense mechanism. © 1999 Elsevier Science B.V. All rights reserved.

*Keywords:* Vitamin E; Vitamin C; Stress; Immunity; *Sparus aurata*

## 1. Introduction

Crowding has been reported to be an aquaculture-related chronic stressor which reduces fish growth (Pickering and Stewart, 1984) and affects the immune system in several species such as Atlantic salmon (Mazur and Iwama, 1993), common carp (Yin et al., 1995) or gilthead seabream (Tort et al., 1996). Changes in the immune system are very important for fish production, since its impairment leads to disease outbreaks or death (Maule et al., 1989).

The use of immunostimulants can induce protection against diseases, enhancing activities in the nonspecific defence mechanism (Anderson, 1992). Nutrition has an influence on health and immune responses of fish as reviewed by some authors (Landolt, 1989; Blazer, 1992; Lall and Olivier, 1993). Vitamins are among the most important nutrients that influence the immune system. For example, ascorbic acid deficiency increases disease susceptibility in different species, such as rainbow trout (Blazer, 1982), channel catfish (Li and Lovell, 1985) and Atlantic salmon (Hardie et al., 1991) and affects the immune system. Several effects of vitamin C deficiency have been reported, such as reduction of antibody production and complement activity in Atlantic salmon (Hardie et al., 1991) or reduction of macrophage function in channel catfish (Li and Lovell, 1985) and rainbow trout (Blazer, 1982; Verlhac et al., 1993). Supplementation of vitamin C enhances antibody production against *Edwarsiella ictaluri* in channel catfish (Li and Lovell, 1985) and against *Vibrio anguillarum* in rainbow trout (Navarre and Halver, 1989) and also enhances phagocytic activity and serum lysozyme levels in turbot (Roberts et al., 1995). Vitamin C is also a vitamin that has been suggested as having a positive role in the amelioration of stress (Fletcher, 1997).

Vitamin E is another nutrient related with immune system function which acts as an antioxidant in biological membranes. Vitamin E deficiency reduces lymphocyte T and B function in rainbow trout sensitized against *Yersinia ruckeri* (Blazer and Wolke, 1984), peritoneal macrophage function in rainbow trout (Blazer, 1982) and in channel catfish (Wise et al., 1993a,b) and serum complement function and the ability of serum to opsonize bacteria in Atlantic salmon (Hardie et al., 1990) and the activity of alternative

© Del documento, los autores. Digitalización realizada por ULPGC. Biblioteca Universitaria, 2009

complement pathway in gilthead seabream (Montero et al., 1998). Vitamin E supplementation seems to enhance antibody production against *Y. ruckeri* in rainbow trout (Ndoye et al., 1990) and phagocytic activity in turbot (Pulsford et al., 1995). However vitamin E supplementation did not affect humoral antibody responses in Atlantic salmon (Lall et al., 1988; Hardie et al., 1990) and had no significant influence on immunostimulation and resistance to bacterial kidney disease (*Renibacterium salmoninarum*) in chinook salmon (Leith and Kaattari, 1989).

Only a few studies have reported on the relationship between stress and dietary nutritent and even less have focused on marine fish (Thompson et al., 1993; Montero et al., 1998). The aim of this work was to investigate the effect of vitamin C or E supplementation on stress resistance of gilthead seabream juveniles reared at high stocking density. Among the wide number of immune responses that could be monitored after stress, the present study has focused on haemolytic and agglutinating activity of fish serum. The haemolytic activity is mainly based on the alternative complement pathway (ACP) that is a very important non-specific defense mechanism in fish which has been shown to occur at much higher levels than in mammals (Sunyer and Tort, 1995). Natural haemoagglutinins also play an important role as non-specific defence mechanism in fish. Finally, total plasma immunoglobulins and plasma lysozyme activity were also measured.

As a reference parameter of stress response, plasma cortisol was measured as the significant indicator. Cortisol is the main corticosteroid in fish (Idler and Truscott, 1972) and plasma levels are widely used as both general and endocrine indicators of stress in fish (Pickering and Pottinger, 1989).

## 2. Material and methods

### 2.1. Experimental procedures

The experiment presented in this study was carried out at the seabream farm ADSA (Alevines y Doradas, San Bartolome de Tirajana, Canary Islands, Spain).

Four thousand and five hundred gilthead seabream (*Sparus aurata*) (12.1 g mean weight) from a production tank with density of 4 kg/m$^3$ (production tank) were distributed among 9 fibreglass tanks (500 fish per tank, with an initial density of 12 kg/m$^3$). Each tank contained 500 l seawater, and was provided with natural light cycle (close to 12 h/12 h) and oxygen injection reaching up 200% saturation in all the tanks. Oxygen was measured and readjusted daily every 2 h. Water temperature, pH and ammonia levels were measured daily and flux rate was the same as the production tank.

### 2.2. Diets

Fish were fed 3 types of diet: Diet 1 was a commercial diet for this species (Control diet) (Mistral-21, EWOS, Dueñas, Palencia, Spain) whereas in diets 2 and 3 the control

© Del documento, los autores. Digitalización realizada por ULPGC. Biblioteca Universitaria, 2009

diet was supplemented with either 250 mg of ascorbyl phosphate or 250 mg of alpha-tocopheryl acetate per kg of diet, respectively. To prepare the vitamin supplemented diets, the control diet was milled by a feed producer, the vitamins added and the diets repelletized in a pellet mill (California Pellet Mills, CPM/ Europe, Amsterdan, Holland) using a 3 mm die. Each diet was assayed in triplicate.

Fish were fed four times per day at a feeding rate of 2.5% body weight per day for 9 weeks. Fish in the production tank were fed the commercial diet. Body weight was determined at the beginning and at the end of the experiment.

### 2.3. Blood collection and sample preparation

At the end of the experiment, blood samples were taken from fish for plasma cortisol, total immunoglobulins haemagglutination, alternative complement pathway (ACP) and lysozyme activities. Fish were individually captured from each tank, 10 fish being captured per tank in less than 8 min. Thus, fish handling time was less than 1 min per fish. As a result, the total capture time avoided capture stress effects on analyzed parameters (Pickering et al., 1982). No anaesthetic was used. Blood was obtained by caudal sinus puncture with 1 ml plastic syringe. An aliquot of blood was used for haematological and plasma determination and a second aliquot for serum analysis. Sampled fish were not reused.

The first aliquot of blood was divided into two portions. One portion was transferred to an Eppendorf tube coated with lithium heparin as anticoagulant for plasma determinations. The plasma was obtained by centrifugation at 3000 rpm for 10 min. Plasma was then separated and stored at −80°C. The second aliquot of blood was transferred to an Eppendorf tube without anticoagulant and allowed to clot at 4°C for 2 h. Serum was separated by centrifugation at 3000 rpm for 10 min, and stored at −80°C for serum complement activity determination.

### 2.4. Plasma analysis

Plasma cortisol level was determined by radioimmunoassay using the trypsin–antitrypsin method as previously described for gilthead seabream (Molinero and González, 1995). Total plasma immunoglobulin (Ig) concentration was measured as described by Anderson and Siwicki (1994) and validated for Sparid species (Rotllant et al., 1997).

### 2.5. Serum analysis

The haemolytic assay for alternative complement pathway (ACP) activity was performed as described by Sunyer and Tort (1995) for gilthead sea bream. Haemagglutination assays were performed using micro V-plates as described by Tort et al. (1996) and lysozyme activity assays were performed by a turbidimetric method of enzymatic activity as described by Anderson and Siwicki (1994), using egg-white lysozyme as a

© Del documento, los autores. Digitalización realizada por ULPGC. Biblioteca Universitaria, 2009

standard. The results were expressed in activity units. All analysis were conducted by triplicate.

### 2.6. Statistical analysis

Means and standard deviations (S.D.) were calculated for each parameter measured. All data were statistically treated using one-way ANOVA. Tukey's test for comparison of means from triplicates was applied (Sokal and Rolf, 1979).

## 3. Results

Total ammonia, measured at the beginning of the experiment, was approximately 0.4 mg/l for all the tanks whereas at the end of the experimental period, values were higher in the experimental tanks than in the production tank (4 and 2 mg/l, respectively). Temperature ranged from 20.9 to 22.6°C and pH ranged from 6.9 to 7.2 during the experimental period.

All fish held at high stocking density showed lower final body weight when compared with those held at low stocking density without significant difference in survival among the different experimental groups (Table 1). In addition, high stocking density produced significantly ($P < 0.05$) higher plasma cortisol levels in all experimental groups when compared to the low stocking density group (Table 2). No significant differences were found between fish held at different densities in agglutination activity or total plasma Ig (Table 2). No significant differences were neither found in these parameters among fish fed different supplemented diets.

High stocking density produced an elevation of lysozyme activity ($P < 0.05$) when compared with low stocking density group, but supplementation with either vitamin reduced this effect (Table 2). High stocking density also produced a significant ($P < 0.05$) reduction in the alternative complement pathway activity (ACP) in fish fed either the control or the vitamin C supplemented diets. On the contrary, fish fed the vitamin E supplemented diet showed the same ACP as those from the production tank (Table 2).

Table 1
Biological parameters measured during the experimental period (mean ± S.D.)[1]

| | Production tank | Diet | | |
|---|---|---|---|---|
| | | Control | Vit C | Vit E |
| Initial weight (g)[2] | 12.1 ± 5.2 | 12.1 ± 2.9 | 12.1 ± 4.2 | 12.1 ± 3.2 |
| Final weight (g)[2] | 65.23 ± 16.08[a] | 52.15 ± 8.18[b] | 56.04 ± 8.66[b] | 50.69 ± 9.55[b] |
| Initial density (kg $m^{-3}$) | 4 | 12 | 12 | 12 |
| Final density (kg $m^{-3}$) | 20[a] | 42.41 ± 0.67[b] | 44.74 ± 0.89[b] | 47.01 ± 1.2[b] |
| Survival (%) | 97.3[a] | 94.8 ± 1.6[b] | 94.8 ± 1.2[b] | 96.1 ± 0.6[b] |

[1] Values with different letter within a line are significantly different ($P < 0.05$).
[2] $n = 500 \times 3$, except for production tank were $n = 1000$.

© Del documento, los autores. Digitalización realizada por ULPGC. Biblioteca Universitaria, 2009

Table 2
Plasma and serum parameters measured during the experimental period (mean ± S.D.)[1]

| | Production tank | Diet | | |
|---|---|---|---|---|
| | | Control | Vit C | Vit E |
| Plasma cortisol (ng/ml) | 1.13 ± 0.92[a] | 7.65 ± 2.69[b] | 6.04 ± 1.24[b] | 7.98 ± 1.67[b] |
| Agglutination (titer) | 7.5 ± 0.21 | 7.2 ± 0.11 | 6.9 ± 0.25 | 7.7 ± 0.17 |
| Total Ig (mg/ml) | 22.17 ± 1.63 | 21.69 ± 1.58 | 24.42 ± 0.88 | 22.12 ± 0.99 |
| Serum lysozyme (units/ml) | 36.84 ± 0.21[a] | 67.49 ± 9.62[b] | 21.97 ± 3.91[a] | 19.71 ± 1.21[a] |
| ACP (ACH50 units/ml) | 135.1 ± 5.4[a] | 94.7 ± 8.7[b] | 95.9 ± 7.5[b] | 134.3 ± 6.6[a] |

[1] Values with different letter within a line are significantly different ($P < 0.05$).
$n = 10 \times 3$, except for production tank, were $n = 20$.

No significant differences were found among triplicates from each treatment for the different parameters analyzed.

## 4. Discussion

Crowding is considered a common aquaculture-related stressor and produces a wide variety of effects on fish such as reduced growth and reduced health and feed conversion ratios (Wedemeyer, 1997). Two factors can affect fish physiology under crowding conditions. The carrying capacity of the water to provide oxygen and to dilute metabolic wastes can act as a stressor. Also, the requirement for adequate space limits fish health. The rate of oxygen consumption and ammonia excretion are the factors that limit carrying capacity of the water (Colt and Orwicz, 1991). In the present study, oxygen was not a limiting factor as oxygen levels where maintained at 200% of saturation during the experimental period. However, ammonia levels were higher for the high stocking density groups compared with that at the low density condition at the end of the experimental period and could have acted as a limiting factor of fish loading. Chronic toxic concentrations of ammonia produces alterations in the feed conversion rate and growth (Smart, 1981). In the present experiment, fish held at the high density showed two fold higher values of ionized ammonia in the water. Hence it is possible that both factors, ammonia in the water and the effect of inadequate space in the tank were acting as limiting factors. Suppression of growth at high density when compared with fish held at low density is considered to be an effect of chronic stress (Pickering, 1990, 1993; Pankhurst and Van Der Kraak, 1997).

Plasma cortisol concentration is also a good indicator of stress (Barton and Iwama, 1991). Often, plasma cortisol levels rise at the beginning of a chronic stress situation such as high stocking density and decrease to initial values in a few days (Pickering and Stewart, 1984; Tort et al., 1996), showing adaptation of the fish to the new situation. However, in the present study, fish held at high stocking density showed higher plasma cortisol concentration when compared with fish held at low density, suggesting that the fish were not capable of adapting to this condition. High stocking density induced a moderate stress as other studies on this species have found post-stress plasma cortisol

© Del documento, los autores. Digitalización realizada por ULPGC. Biblioteca Universitaria, 2009

values of up to 25 ng/ml of plasma (Montero et al., 1998) or 80 ng/ml of plasma (Sunyer et al., 1995). This moderate stress was not diminished by the vitamin supplementation. The addition of vitamin C may prevent the conversion of unsaturated fatty acids into cholesterol esters which are important components of cortisol as hypothesized by Kibatchi (1967). However, recent studies report some evidence that post-stress concentration of plasma cortisol are independent of the vitamin C levels in diet (Dabrowska et al., 1991; Thompson et al., 1993). The addition of vitamin E has been shown to decrease plasma corticosteroids in rats (Watson and Petro, 1982) and calves (Mudron et al., 1996). Gilthead seabream fed a diet containing low levels of vitamin E (18.5 mg/kg diet) had higher plasma cortisol levels after stress when compared with fish fed a vitamin E supplemented diet (167.5 mg/kg diet) (Montero et al., 1998).

Elevation of plasma cortisol has been shown to produce immunosuppression in fish (Pickering and Pottinger, 1985; Maule et al., 1989), resulting in an increase of susceptibility to diseases (Barton and Iwama, 1991). Conversely, the addition of vitamins C or E in fish diets has been shown to enhance disease resistance in several species (reviewed by Blazer, 1992 and by Lall and Olivier, 1993). The results of the present study suggest that moderate elevation of plasma cortisol did not affect some of the immune parameters studied such as total plasma immunoglobulins and agglutinating activity.

Moderate stress affects lysozyme activity, causing either an increase (Möck and Peters, 1990; Roed et al., 1993; Rotllant et al., 1997) or a decrease (Möck and Peters, 1990; Yin et al., 1995). In the present study, serum lysozyme activity was elevated high stocking density except in fish fed the vitamin supplemented diets. This elevation of lysozyme activity could be due to moderate stress and supplementation of vitamins in the diet could be ameliorating the effect of the stress response in this particular factor.

High stocking density produced lower ACP activity except in fish fed the vitamin E supplemented diet. Elevation of plasma cortisol seems to produce depletion of serum haemolytic activity in some fish species (Sunyer et al., 1995; Tort et al., 1996). Complement activity seems to be related to dietary vitamin C levels in some species such as channel catfish (Li and Lovell, 1985), Atlantic salmon (Hardie et al., 1991; Waagbo et al., 1993) and rainbow trout (Verlhac et al., 1993), although the effect of dietary vitamin C on the complement system remains controversial (Yano et al., 1988; Lall, 1989). Vitamin E deficiencies appears to affect complement activation, producing a depletion of serum haemolytic activity in Atlantic salmon (Hardie et al., 1990) and on ACP activation in gilthead seabream (Montero et al., 1998). In the present study, fish fed the vitamin E supplemented diet and held at high stocking density showed the same ACP activity as fish from the production tank. This result suggest that vitamin E supplementation does not enhance ACP activity in gilthead seabream but supplementation of vitamin E in diet seems to protect the complement system against stress-related reduction of activity. Supplementation of vitamin E does not enhance complement activity in other species such as Atlantic salmon (Hardie et al., 1990). Supplementation of dietary vitamin C did not have the same protective effect on ACP. It is not clear if vitamin C has an effect on modulating the complement system of gilthead seabream as described for similar species such as red seabream (Yano et al., 1988) or if vitamin C influences the activity of the complement system by stimulating the synthesis of the first

© Del documento, los autores. Digitalización realizada por ULPGC. Biblioteca Universitaria, 2009

component in the classical pathway (Hardie et al., 1991) and has no effect on the alternative pathway. Further experiments are required to study the effect of vitamin C on complement system of gilthead seabream.

In conclusion, vitamin supplementation seemed to act on the stress response of gilthead seabream juveniles by preventing a stress-related immunosuppression. Vitamin E seemed to have more protective role against stress than vitamin C under these experimental conditions but further experiments are required to determine the role of both vitamins on the immune system of fish.

## References

Anderson, D.P., 1992. Immunostimulants, adjuvants, and vaccine carriers in fish: application to aquaculture. Annu. Rev. Fish Dis. 2, 281–307.

Anderson, D.P., Siwicki, A.K., 1994. Simplified assays for measuring non-specific defence mechanisms in fish. Am. Fish. Soc. Fish Health Section, Special Publ., Seattle, WA.

Barton, B.A., Iwama, G.K., 1991. Physiological changes in fish from stress in aquaculture with emphasis on the response and effects of corticosteroids. Annu. Rev. Fish Dis. 1, 3–26.

Blazer, V.S., 1982. The effect of marginal deficiencies of ascorbic acid and α-tocopherol on the natural resistance and immune response of rainbow trout (*Salmo gairdneri*). PhD dissertation. Univ. of Rhode Island, USA.

Blazer, V.S., 1992. Nutrition and disease resistance in fish. Annu. Rev. Fish. Dis. 2, 309–323.

Blazer, V.S., Wolke, R.E., 1984. The effects of α-tocopherol on the immune responses and non-specific resistance factors of rainbow trout (*Salmo gairdneri* Richardson). Aquaculture 37, 1–9.

Colt, J., Orwicz, K., 1991. Modeling production capacity in aquatic culture systems under freshwater conditions. Aquac. Enginee. 10, 1–29.

Dabrowska, H., Dabrowski, K., Meyer-Burgdorff, K., Hanke, W., Gunther, K.D., 1991. The effect of large doses of vitamin C and magnesium on stress responses in common carp *Cyprinus carpio*. Comp. Biochem. Physiol. 99A, 681–685.

Fletcher, T.C., 1997. Dietary effects on stress and health. In: Iwama, G.K. Pickering, A.D., Sumpter, J.P., Schreck, C.B. (Eds.), Fish Stress and Health in Aquaculture. Cambridge Univ. Press, Cambridge, pp. 223–246.

Hardie, L.J., Fletcher, T.C., Secombes, C.J., 1990. The effect of vitamin E on the immune responses of the Atlantic salmon (*Salmo salar* L.). Aquaculture 87, 1–13.

Hardie, L.J., Fletcher, T.C., Secombes, C.J., 1991. The effect of dietary vitamin C on the immune responses of the Atlantic salmon (*Salmo salar* L.). Aquaculture 95, 201–214.

Idler, D.R., Truscott, B., 1972. Corticosteroids in fish. In: Idler, D.R. (Ed.) Steroids in Non-Mammalian Vertebrates. London Academic press, pp. 127–252.

Kibatchi, A.E., 1967. Ascorbic acid in steroidogenesis. Nature 215, 1385–1386.

Lall, S.P., 1989. Disease control through nutrition. In: Proceedings of the Aquaculture International Congress and Exposition, B.C. Pavillion, Vancouver, Canada, pp. 607–612.

Lall, S.P., Olivier, G., 1993. Role of micronutrients in immune response and disease resistance in fish. In: INRA (Ed.), Fish Nutrition in Practice (Les Colloques, No. 61), pp. 101–118.

Lall, S.P., Olivier, G.O., Hines, J.A., Ferguson, H.F., 1988. The role of vitamin E in nutrition and immune response of Atlantic salmon (*Salmo salar*). Aquac. Can. Bull. 88 (1), 76–78.

Landolt, M., 1989. The relationship between diet and the immune response of fish. Aquaculture 79, 193–206.

Leith, D., Kaattari, S., 1989. Effects of vitamin nutrition on the immune response of hatchery-reared salmonids. Final report. U.S. Department of Energy, Bonneville Power Administration, Div. of Fish and Wildlife, Portland, OR, USA.

Li, Y., Lovell, R.T., 1985. Elevated levels of dietary ascorbic acid increase immune responses in channel catfish. J. Nutr. 115, 123–131.

© Del documento, los autores. Digitalización realizada por ULPGC. Biblioteca Universitaria, 2009

Maule, A.G., Tripp, R.A., Kaattari, S.L., Schreck, C.B., 1989. Stress alters the immune function and disease resistance in chinook salmon *Oncorhynchus tshawytscha*. J. Endocrinol. 120, 135–142.

Mazur, C.F., Iwama, G.K., 1993. Handling and crowding stress reduces number of plaque-forming cells in Atlantic salmon. J. Aquat. Anim. Health 5, 98–101.

Möck, A., Peters, G., 1990. Lysozyme activity in rainbow trout, *Oncorhynchus mykiss* (Walbaum), stressed by handling, transport and water pollution. J. Fish Biol. 37, 873–885.

Molinero, A., González, J., 1995. Comparative effects of MS-222 and 2-phenoxyethanol on gilthead sea bream (*Sparus aurata* L.) during confinement. Comp. Biochem. Physiol. 111, 405–414.

Montero, D., Tort, L., Izquierdo, M.S., Robaina, L., Vergara, J.M., 1998. Depletion of serum alternative complement pathway activity in gilthead seabream caused by α-tocopherol and $n-3$ HUFA dietary deficiencies. Fish Physiol. Biochem. 18, 399–407.

Mudron, P., Kovac, G., Bartko, P., Choma, J., Zezula, I., 1996. Effect of vitamin E on the cortisol and lactate levels and the acid base equilibrium of calves subjected to transport stress. Veterinary Medicine 41, 71–76.

Navarre, O., Halver, J.E., 1989. Disease resistance and humoral antibody production in rainbow trout fed high levels of vitamin C. Aquaculture 79, 207–221.

Ndoye, A., Ghanmi, Z., Koenig, J., Deshaux, P., 1990. Vitamin E et immunité: effets dela vitamine E sur la production d'anticorps anto *Yersinia ruckeri* chez la truite arc-en-ciel (*Salmo gairdneri*). Ichtyophysiol. Acta 13, 17–23.

Pankhurst, N.W., Van Der Kraak, G., 1997. Effects of stress on reproduction and growth of fish. In: Iwama, G.K., Pickering, A.D., Sumpter, J.P., Schreck, C.B. (Eds.), Fish Stress and Health in Aquaculture. Cambridge Univ. Press, Cambridge, pp. 73–93.

Pickering, A.D., 1990. Stress and the suppression of somatic growth in teleost fish. In: Epple, A., Scanes, C.G., Stetson, M.H. (Eds.), Progress in Comparative Endocrinology. Prog. Clin. Biol. Res., 342, pp. 473–479.

Pickering, A.D., 1993. Growth and stress in fish production. Aquaculture 111, 51–63.

Pickering, A.D., Pottinger, T.G., 1985. Cortisol can increase the susceptibility of brown trout, *Salmo trutta* L., to disease without reducing the white blood cell count. J. Fish Biol. 27, 611–619.

Pickering, A.D., Pottinger, T.G., 1989. Stress responses and disease resistance in salmonid fish: effects of chronic elevation of plasma cortisol. Fish Physiol. Biochem. 7, 253–258.

Pickering, A.D., Stewart, A., 1984. Acclimation of the interrenal tissue of the brown trout, *Salmo trutta* L., to chronic crowding stress. J. Fish Biol. 24, 731–740.

Pickering, A.D., Pottinger, T.G., Christie, P., 1982. Recovery of the brown trout, *Salmo trutta L.*, from acute handling stress: a time-course study. J. Fish Biol. 20, 229–244.

Pulsford, A.L., Crampe, M., Langston, A., Glynn, P.J., 1995. Modulatory effects of disease, stress, copper, TBT and vitamin E on the immune system of flatfish. Fish and Shellfish Immunol. 5, 631–643.

Roberts, M.L., Davies, S.J., Pulsford, A.L., 1995. The influence of ascorbic acid (vitamin C) on non-specific immunity in the turbot (*Scophthalmus maximus* L.). Fish and Shellfish Immunology 5, 27–38.

Roed, K.H., Larsen, H.J., Linder, R.D., Refstie, T., 1993. Genetic variation in lysozyme activity in rainbow trout (*Oncorhynchus mykiss*). Aquaculture 109, 237–244.

Rotllant, J., Pavlidis, M., Kentouri, M., Abad, M.A., Tort, L., 1997. Non-specific immune responses in the red porgy *Pagrus pagrus* after crowding stress. Aquaculture 156, 279–290.

Smart, G.R., 1981. Aspects of water quality producing stress in intensive fish culture. In: Pickering, A.D. (Ed.), Stress and Fish. Pergamon, London, pp. 277–293.

Sokal, R.R., Rolf, J., 1979. Biometría. Blume, Madrid.

Sunyer, J.O., Tort, L., 1995. Natural hemolytic and bactericidal activities of sea bream *Sparus aurata* serum effected by the alternative complement pathway. Vet. Immunol. Immunopathol. 45, 333–345.

Sunyer, J.O., Gómez, E., Navarro, V., Quesada, J., Tort, L., 1995. Physiological responses and depression of humoral components of the immune system in gilthead seabream (*Sparus aurata*) following daily acute stress. Can. J. Fish. Aquat. Sci. 52, 2339–2346.

Thompson, I., White, A., Fletcher, T.C., Houlihan, D.F., Secombes, C.J., 1993. The effect of stress on the immune response of Atlantic salmon (*Salmo salar* L.) fed diets containing different amounts of vitamin C. Aquaculture 114, 1–18.

Tort, L., Sunyer, J.O., Gómez, E., Molinero, A., 1996. Crowding stress induces changes in serum haemolytic

© Del documento, los autores. Digitalización realizada por ULPGC. Biblioteca Universitaria, 2009

and agglutinating activity in gilthead seabream *Sparus aurata*. Vet. Immunol. Immunopathol. 51 (1–2), 179–188.

Verlhac, V., N'doye, A., Gabaudan, J., Troutaud, D., Deschaux, P., 1993. Vitamin nutrition and fish immunity: influence of antioxidant vitamins (C and E) on immune responses of rainbow trout. In: INRA (Ed.), Fish Nutrition in Practice (Les Colloques, No. 61), pp. 167–177.

Waagbo, R., Glette, J., Raa-Nilsen, E., Sandnes, K., 1993. Dietary vitamin C, immunity and disease resistance in Atlantic salmon (*Salmo salar*). Fish Physiol. Biochem. 12 (1), 61–73.

Watson, R.R., Petro, T.M., 1982. Cellular immune responses, corticosteroid levels, and resistance to *Listeria monocytogenes* and murine leukemia in mice fed a high vitamin E diet. Ann. NY Acad. Sci., 205–208.

Wedemeyer, G.A., 1997. Effects of rearing conditions on the health and physiologycal quality of fish in intensive culture. In: Iwama, G.K., Pickering, A.D., Sumpter, J.P., Schreck, C.B. (Eds.), Fish Stress and Health in Aquaculture. Cambridge University Press, Cambridge, pp. 35–71.

Wise, D.J., Tomasso, J.R., Schwedler, T.E., Blazer, V.S., Gatlin III, D.M., 1993a. Effect of vitamin E on the immune response of channel catfish to *Edwardsiella ictaluri*. J. Aquat. Anim. Health 5, 183–188.

Wise, D.J., Tomasso, J.R., Gatlin, D.M. III, Bai, S.C., Blazer, V.S., 1993b. Effects of dietary selenium and vitamin E on red blood cell peroxidation, glutathione peroxidase activity, and macrophage superoxide anion production in channel catfish. J. Aquat. Anim. Health 5, 177–182.

Yano, T., Nakao, M., Furuichi, M., Yone, Y., 1988. Effects of dietary choline, pantothenic acid and vitamin C on the serum complement activity of red sea bream. Bull. Jpn. Soc. Sci. Fish. 54, 141–144.

Yin, Z., Lam, T.J., Sin, Y.M., 1995. The effects of crowding stress on the non-specific immune response in fancy carp (*Cyprinus carpio* L.). Fish and Shellfish Immunol. 5, 519–529.

© Del documento, los autores. Digitalización realizada por ULPGC. Biblioteca Universitaria, 2009

*Fish Physiology and Biochemistry* 20: 53–60, 1999.
© 1999 *Kluwer Academic Publishers. Printed in the Netherlands.*


# High stocking density produces crowding stress altering some physiological and biochemical parameters in gilthead seabream, *Sparus aurata*, juveniles

D. Montero[1], M. S. Izquierdo[2], L. Tort[3], L. Robaina[2] and J. M. Vergara[2]
[1]*Instituto Canario de Ciencias Marinas; Gobierno de Canarias. P.O. Box 56, 35200, Telde, Las Palmas. Canary Islands, Spain;* [2]*Departamento de Biología, Universidad de Las Palmas de Gran Canaria. Campus Universitario de Tafira. 35017. Las Palmas de Gran Canaria. Canary Islands. Spain;* [3]*Departamento de Biología Celular y Fisiología. Facultad de Ciencias. Universidad Autónoma de Barcelona. 08193. Cerdanyola, Barcelona, Spain; (Tel: +34-928-132-900; Fax: +34-928-132-908; E-mail: dmontero@iccm.rcanaria.es)*

Accepted: May 15, 1998

*Key words:* alternative complement, cortisol

## Abstract

High stocking density has been shown to produce a wide variety of effects on cultured fish populations, such as alterations in behavior and poor feed utilization, resulting in mortality and poor growth. High stocking density has also been reported to produce chronic stress and mobilization of energy sources in fish. There are few studies focusing on the effect of high stocking density on one of the most important marine fish species for Mediterranean aquaculture, gilthead seabream (*Sparus aurata*). Consequently, this study investigates the effect of high stocking density on juveniles of this species, focusing on effects of stocking density on growth, biochemical composition, immune status and hematology.

The results of this study showed that high stocking density produced a chronic stress situation. Plasma cortisol levels increased up to 16.25 ng $ml^{-1}$ in fish held at high stocking; this value was 4 fold that of fish held at low stocking; density (3.91 ng $ml^{-1}$ ). As a consequenceof this stressful situation, there was both haemoconcentration and a decrease in alternative complement pathway (ACP), an important component of the immune system of fish (from 167.23 U $ml^{-1}$ down to 146.37 U $ml^{-1}$). Haematocrit, haemoglobin concentration and red blood cell count were significantly higher in fish held at high stocking density (43.87%, 10.76 $9dl^{-1}$ and $3.36 \times 10^6$ $mm^{-3}$, respectively) compared with those fish held at low stocking density (37.21%, 9.32 $g/dlg^{-1}$ and $2.82 \times 10^6$ $mm^{-3}$, respectively).

In addition, high stocking density produced a decrease in hepatosomatic index (from 2.26 down to 2.04) and altered liver fatty acid composition. Oleic acid (18: 1n-9) decreased in liver total lipids of fish held at high stocking density and arachidonic acid (20: 4-n6) and n-3 high unsaturated fatty acids (n-3 HUFA) were reduced in liver polar lipids of those fish. These alterations reflect the effect of stocking density on lipid metabolism to help meet the increased energy demand.

## Introduction

The apparent efficiency of aquaculture systems can be maximized by increasing the rearing densities. However, poor growth and increased incidence of disease have often been observed in fish reared at high density, although it is not clear if these problems are directly related to high rearing density or due to the poor water quality often associated with such densities (Meade et al. 1985).

Much research effort has been focused on evaluating the effects of rearing density on variables such as fish growth (Holm et al. 1990; Björnsson 1994), fish survival (Sodeberg and Meade 1987), food intake

© Del documento, los autores. Digitalización realizada por ULPGC. Biblioteca Universitaria, 2009

(Jorgensen et al. 1993) and hormonal related changes (Leatherland and Cho 1985; Kebus et al. 1992). Recently, some authors have studied the effect of rearing densities on alteration of fish behaviour (Alanärä and Brännäs 1996), metabolism (Vijayan et al. 1990) and immunology due to the stress response often associated with high stocking density (Yin et al. 1995; Tort et al. 1996).

High stocking density has been shown to affect some metabolic pathways, such as those related to lipid metabolism. Vijayan et al. (1990) reported a mobilization of triglycerides in brook charr (*Salvelinus fontinalis*) to help meet the increased energy demand associated with high rearing density, suggesting an enhancement of gluconeogenic capacity from glycerol. Leatherland and Cho (1987) reported an effect of the rearing density on hepatosomatic index (HSI) and on plasma free fatty acid concentrations.

High stocking density has also been considered as an aquaculture-related chronic stressor (Vijayan and Leatherland 1988; Barton and Iwama 1991; Wedemeyer 1997) producing a chronic elevation of plasma cortisol (Barton 1988; Pickering and Pottinger 1989), the main corticosteroid in fish (Idler and Truscott 1972). Plasma cortisol level is widely used as a general indicator of stressful situations in vertebrates and particularly in fish (Pickering and Pottinger 1989).

An elevation of plasma cortisol induces a wide variety of secondary physiological responses (Barton and Iwama 1991), including a decrease in immune response (Maule et al.1989; Pickering and Pottinger 1989). Fish, like other vertebrates, respond to infectious pathogens in specific and non-specific ways. However, it has been suggested that the non-specific defences are the most important resistance mechanisms in fish (Anderson 1990). Increased amounts of corticosteroid released during stress affect the non-specific immune system, producing alterations in some processes such as phagocytic activity (Angelidis et al. 1987), lysozyme activity (Yin et al. 1995), or serum haemolytic and agglutinating activity (Tort et al. 1996).

Very little is known about the effect of high stocking density on gilthead seabream (Tort et al. 1996) one of the most important marine teleosts in Mediterranean intensive culture. This study was designed to investigate the effects of high stocking density on growth and non-specific immunological parameters in gilthead sea bream juveniles, and to determine the effects on biochemical and fatty acid composition of liver and muscle. Some haematological parameters were also included, as there are few data available in the literature for this species under these culture conditions.

## Materials and methods

### *Experimental procedures*

The experiment was carried out at the Instituto Canario de Ciencias Marinas of the Autonomous Government of Canary Islands, with gilthead seabream (*Sparus aurata*) juveniles. Four hundred and fifty gilthead seabream (22 g mean weight) supplied by a local farm (ADSA, San Bartolome de Tirajana, Canary Islands, Spain), were distributed among six circular fiberglass tanks. Each tank was filled with 250 l of sea water and was provided with water supply at a rate of 4.0 l $min^{-1}$. Dissolved oxygen ranged between 6.2 and 10.5 mg $l^{-1}$ along the experimental period. Water temperature ranged between 19.02 and 22.45 °C during the experimental period, whereas natural light illuminated the tanks at a light cycle close to 12hL/12hD. Three hundred and sixty fish were randomly stocked in 3 of these tanks at 120 fish per tank (initial and final densities 10.56 and 40.8 kg $m^3$ respectively), and 90 fish were randomly distributed in the other 3 tanks, 30 fish per tank at low stocking densities (initial and final densities 2.64 and 10.04 kg $m^3$ respectively).

Fish were fed twice daily with a sardine meal based pelleted diet at a feeding rate of 2.5% fish body weight per day, 6 days a week for 15 weeks. Body weight was measured at the beginning and at the end of the experiment in all the fish. At the end of the experiment, blood samples were taken for determination of haematological parameters, and plasma and serum were collected. Liver and a portion of muscle from six fish from each tank were taken to determine biochemical and fatty acid composition.

### *Biochemical analysis of liver*

Liver moisture and lipid content, as well as its fatty acid composition were determined. Lipids were extracted as described by Folch et al. (1957). The lipid class composition of liver lipids was obtained by TLC separation in chromarods, and flame ionization detector (FID) identification in a Iatroscan (Iatron Lab inc., Tokio). Polar lipids were separated using silica cartridges as described by Juaneda and Rocquelin (1985). Fatty acids were obtained by transmethylation as described by Christie (1982) and identified using

© Del documento, los autores. Digitalización realizada por ULPGC. Biblioteca Universitaria, 2009

gas chromatography under the conditions previously described (Izquierdo et al. 1990).

*Blood collection and sample preparation*

Fish were individually captured from each tank (10 fish were capture from each tank in less than 8 min). No anaesthetic was used. Fish handling time was less than 1 min per fish and total capture time was less than 8 min to avoid capture stress effects on analyzed parameters (Pickering et al. 1982). Blood was obtained by caudal sinus puncture; an aliquot of blood was used for haematological and plasma determination and a second aliquot for serum analysis. The first aliquot of blood was divided in two portions. One portion was transferred to an Eppendorf tube coated with lithium heparin as anticoagulant for cell counting and haemoglobin and haematocrit determinations. The remaining blood was used for plasma determinations. The plasma was obtained by centrifugation at 3000 rpm for 10 min. Plasma was then separated and stored at −80 °C. The second aliquot of blood was transferred to an Eppendorf tube without anticoagulant and allowed to clot at 4 °C for 2 h. Serum was separated by centrifugation at 3000 rpm for 10 min, and stored at −80 °C for serum complement activity determination.

*Haematology and plasma analysis*

Haematocrit (Ht) was determined by microcentrifugation of whole blood (3000 rpm, 10 min), haemoglobin (Hb) and the red blood cell (RBC) number was obtained using a haematological counter Sysmex 800. Fifty $\mu$l of blood were fixed in 2.5% glutaraldehyde, buffered with 1 mM Tris, and diluted in Cortland saline. This suspension was used for counting the lymphocyte and neutrophil number in a Neubauer hemocytometer. Mean cellular haemoglobin (MCH), mean cellular volume (MCV) and mean cellular haemoglobin concentration (MCHC) were calculated from haematological parameters as described by Klontz (1994). Plasma cortisol level was determined by radioimmunoassay using the trypsin-antitrypsin method as described for gilthead seabream (Molinero and González 1995). Total plasma protein and plasma glucose was determined using a commercially available kit (Boehringer-Mannheim S.A., Barcelona, Spain).

*Serum analysis*

The haemolytic assay was performed in Eppendorff tubes as described by Sunyer and Tort (1995) for gilthead sea bream. The following buffers were used: gelatin veronal buffer, GVB, isotonic veronal buffered saline, pH 7.3, containing 0.1% gelatin, EDTA-GVB, as GVB but containing 20 mM ethylenediaminetetraacetic acid, (EDTA) and Mg-EGTA-GVB, which is GVB with 10 mM $mg^{++}$ and 10 mM ethyleneglycol-bis (B-aminoethyl ether)-*N,N,N'*- tetraacetic acid (EGTA). Rabbit red blood cells (RaRBC) were used for alternative complement pathway (ACP) determination. Blood was withdrawn from the ear artery of a rabbit and placed into heparinized tubes. RaRBCs were washed four times in GVB and resuspended in GVB to a concentration of $2.5 \times 10^8$ cells per ml (Sunyer and Tort 1994).

ACP was determined using 25 $\mu$l of RaRBC suspension added to 100 $\mu$l of serially diluted serum in mg-EGTA-GVB buffer. Samples were incubated at room temperature (22 °C) for 100 min with regular shaking. The reaction was stopped by adding 1 ml of cold EDTA-GVB. Samples were then centrifuged and the extent of hemolysis was estimated by measuring the optical density of the supernatant at 414 nm using an spectrophotometer (Shimadzu Corporation, Kyoto, Japan). The ACH50 units were defined as the concentration of serum giving 50% haemolysis of RaRBC. All analysis were conducted in triplicate.

Haemagglutination assays were performed using micro V-plates as described by Tort et al. (1996). Serial dilutions of each serum sample were made in 25 $\mu$l of EDTA-GVB and 25 $\mu$l of $2.5 \times 10^8$ cells per ml RaRBC suspension were added to each well. After 1 h at room temperature, macroscopic aglutination was recorded, and results are given as $\log_2$ of the final serum dilution giving agglutination.

*Statistical analysis*

Means and standard deviations (SD) were calculated for each parameter measured. All triplicates were statistically treated using ANOVA. Student's *t*-test was used to test differences between fish held at high stocking density and low stocking density (Sokal and Rolf 1979).

© Del documento, los autores. Digitalización realizada por ULPGC. Biblioteca Universitaria, 2009

*Table 1.* Biological parameters, liver biochemical composition and liver lipid class of the fish held at different stocking densities

| | Low density | High density |
|---|---|---|
| Final weight (g) | 82.64 ± 12.06+ | 85.00 ± 11.62++ |
| Hepatosomatic index+++ | 2.26 ± 0.31 | 2.04 ± 0.38* |
| Liver lipid (% d.w.)+++ | 32.07 ± 3.89 | 28.10 ± 1.45 |
| Liver moisture+++ | 64.39 ± 1.50 | 64.84 ± 0.62 |
| Liver lipid class (area%) | | |
| Cholesterol +++ | 3.46 ± 0.37 | 3.17 ± 0.32 |
| Triacylglycerides +++ | 63.63 ± 6.32 | 66.27 ± 7.37 |
| Cholesterol ester+++ | 1.40 ± 0.31 | 1.63 ± 0.21* |
| Polar lipids+++ | 18.33 ± 4.93 | 22.08 ± 5.08 |

+ $n = 90$; ++ $n = 360$; +++ $n = 18$; * $P < 0.05$.

*Table 2.* Some fatty acids of liver total lipids of fish held at different stocking densities (area%)+

| | Low density | High density |
|---|---|---|
| 18:0 | 10.72 ± 2.15 | 12.15 ± 3.63 |
| 18:1n-9 | 35.31 ± 1.89 | 29.05 ± 5.31* |
| 20:4n-6 | 0.64 ± 0.10 | 0.18 ± 0.02* |
| Saturated | 38.20 ± 3.25 | 45.02 ± 10.10 |
| Monoenoics | 45.71 ± 2.17 | 39.67 ± 6.82 |
| n-3 | 9.38 ± 0.85 | 9.53 ± 2.02 |
| n-6 | 1.52 ± 0.12 | 1.47 ± 0.25 |
| n-9 | 37.95 ± 1.84 | 32.60 ± 5.76 |
| n-3 HUFA | 8.85 ± 0.82 | 8.92 ± 1.85 |

+ $n = 18$; * $P < 0.05$.

## Results

Fish held at different stocking densities showed no differences in food intake during the experimental period. There were no significant differences in final weight between groups (Table 1). However, high stocking density produced a significant decrease in liver weight and hepatosomatic index. Table 1 also shows a slight reduction, although not significant, of liver lipid content when stocking density was increased.

Cholesterol ester content of liver was significantly greater in fish reared at high density (Table 1), but no significant differences were found in cholesterol, triacylglycerides or polar lipid content between the two experimental groups.

Tables 2 and 3 show the fatty acid composition of total lipids and polar lipids of the liver of fish held at different stocking densities. There were significant differences between groups in total lipid fatty acid:

*Table 3.* Some fatty acids of liver polar lipids of fish held at different stocking densities (area%)+

| | Low density | High density |
|---|---|---|
| 18:0 | 10.28 ± 0.65 | 8.09 ± 0.29* |
| 18:1n-9 | 10.72 ± 0.29 | 14.29 ± 0.35* |
| 20:4n-6 | 2.56 ± 0.36 | 1.85 ± 0.04* |
| Saturated | 35.02 ± 0.21 | 31.79 ± 0.31* |
| Monoenoics | 14.97 ± 0.31 | 19.81 ± 0.39* |
| n-3 | 40.96 ± 0.16 | 39.03 ± 0.20* |
| n-6 | 3.53 ± 0.33 | 3.68 ± 0.05 |
| n-9 | 11.74 ± 0.31 | 14.89 ± 0.35* |
| n-3 HUFA | 40.96 ± 0.16 | 38.37 ± 0.20* |

+ $n = 18$; * $P < 0.05$.

arachidonic acid (20: 4n-6) and oleic acid (18: 1n-9) were lower in fish held at high stocking density. In addition, there were significant differences in some fatty acids in polar lipids (Table 3). There was a decrease in saturated fatty acids, mainly due to a decline in 18:0, in liver polar lipids of the fish held at high stocking density and there was an increase in both monoenoic and n-9 fatty acids in the high density group, mainly due to the increased quantities of oleic acid. On the other hand, there was a decrease in both n-3 and n-3 HUFA values in the fish on high density mainly due to a decrease in docosahexaenoic acid (DHA: 22:6n-3). Although there were no differences in n-6 fatty acids, there was a decrease of arachidonic acid in liver polar lipids of fish held at high stocking density.

Haematological parameters measured in the blood of fish held at different stocking densities are shown in Table 4. There were increases in haematocrit, haemoglobin content and RBC count in fish held at high stocking density, but no significant differences between groups in circulating lymphocytes or neutrophils. There were no significant differences in MCHC, MCV or MCH for the two experimental groups.

Table 5 shows values of different parameters measured in plasma and serum of fish held at different stocking densities. There was a significant increase in total plasma cortisol, glucose, and protein concentrations in fish held at high stocking density relative to those at low density. There was a significant decrease in serum haemolytic activity due to alternative complement pathway, measured as ACH50, but there were no significant difference on haemagglutination activity.

© Del documento, los autores. Digitalización realizada por ULPGC. Biblioteca Universitaria, 2009

*Table 4.* Haematological parameters of fish held at different stocking densitites+

| | Low density | High density |
|---|---|---|
| Ht (%) | 37.21 ± 6.35 | 43.87 ± 4.90* |
| Hb (g $dl^{-1}$) | 9.32 ± 1.98 | 10.76 ± 1.34* |
| RBC ($\times 10^6$ $mm^{-3}$) | 2.82 ± 0.54 | 3.36 ± 0.59* |
| Circulating lymphocytes ($\times 10^3$ $mm^{-3}$) | 21.69 ± 8.09 | 21.96 ± 5.73 |
| Lymphocytes/RBC | 0.80 ± 0.32 | 0.67 ± 0.19 |
| Circulating neutrophils ($\times 10^2$ $mm^{-3}$) | 5.26 ± 2.48 | 5.20 ± 3.95 |
| MCHC (g $dl^{-1}$) | 24.75 ± 2.40 | 24.73 ± 3.91 |
| MHC (pg) | 33.10 ± 3.75 | 32.54 ± 4.00 |
| MCV $nm^3$ | 135.05 ± 22.02 | 134.65 ± 26.16 |

+ $n = 30$

*Table 5.* Plasma and serum parameters of fish held at low and high stocking density+

| | Low density | High density |
|---|---|---|
| Plasma cortisol (ng $ml^{-1}$) | 3.91 ± 3.52 | 16.25 ± 23.62* |
| Plasma glucose (mg $ml^{-1}$) | 39.38 ± 5.97 | 44.24 ± 3.78* |
| Plasma proteins (g $ml^{-1}$) | 3.70 ± 0.65 | 4.22 ± 0.41* |
| ACH50 (U $ml^{-1}$) | 167.23 ± 21.67 | 146.37 ± 9.44* |
| Haemagglutination | 12.00 ± 1.35 | 11.36 ± 1.03 |

+ $n = 30$; * $P < 0.05$.

## Discussion

High stocking density has been reported to cause decreased growth in salmonids (Vijayan and Leatherland 1988) due to different factors such as decreased food consumption and social interactions (Wedemeyer 1997) or decreased water quality (Pickering and Stewart 1984). Moreover, high stocking density produces both hormonal and metabolic alterations (Leatherland and Cho 1985; Schreck et al. 1985) including a reduction in thyroid hormone activity (Vijayan and Leatherland 1988). This latter study shows a growth reduction in brook charr held at high stocking density related to changes in food consumption. However, Kebus et al. (1992) demonstrated that negative effects of rearing density on rainbow trout growth could be attributed, at least in part, to water quality deterioration caused by high loading rates. In the present study, neither food intake nor water quality were affected by stocking density and social behaviour alterations were not observed.

Suppression of growth is often considered to be a good indicator of chronic stress (Pickering 1990; Pankhurst and Van der Kraak 1997). It should be noted that the fish may have not been stressed in the present study. Fish may have to reach a critical size before density becomes stressful. Thus, it is possible that the effects of stocking density stressors on growth have not yet been seen. However, high stocking density produced a reduction in both liver weight and HSI. The reduction of HSI by high stocking density has been described for rainbow trout (Leatherland and Cho 1985) and for brook charr (Vijayan et al. 1990). This reduction seems to be related to a higher hepatic lipid utilization, associated with an increased lipid mobilization. In the present study, fish held at high stocking density showed a significantly higher level of liver cholesterol esters, suggesting an enhanced lipid mobilization. This reduction in hepatic lipid content could also be associated with a decrease in the activity of enzymes related to lipid synthesis, such as glucose-6-phosphate dehydrogenase, and to an increase in the activity of enzymes associated with lipid oxidation, such as hydroxyacyl-CoA-dehydrogenase (Vijayan et al. 1990).

In addition, high stocking density affected the fatty acid composition of the liver. There was a reduction in oleic acid in liver total lipid. This fatty acid is considered one of the most important lipid energy sources in situations that impose a high energy demand such

© Del documento, los autores. Digitalización realizada por ULPGC. Biblioteca Universitaria, 2009

as larval development (Izquierdo 1996) or starvation (Greene and Selivonchick 1987). On the other hand, the reduction of arachidonic acid together with the decline of 18:0 and n-3 HUFA within the polar lipids suggests a selective utilization of phosphatidilinositol under these culture conditions, as both fatty acids are main components of this lipid class (Lie 1993).

Another important effect of high stocking density was haemoconcentration, affecting haematocrit, haemoglobin, RBC count and total plasma proteins. This effect has been described as a strategy for increasing oxygen carrying capacity of blood during periods of high energy demand. In contrast, the control fish showed normal haematological parameters for this species (Montero et al. 1995, 1996). This effect was not due to the action of other stressors, as there was no erythrocyte swelling, indicated by no decline in MCHC, a feature normally associated with hypoxia (Soivio and Nikinmaa 1981). Polycytemia, as a cellular response to oxygen demand, has been observed under situations of stress (Wedemeyer and McLeay 1981), increased $\beta$-oxidation (Waagbo et al. 1995) and high stocking densities (Srivastava and Sahai 1987).

In general, plasma cortisol levels rise at the beginning of high stocking density condition and decrease to initial values in a few days (Pickering and Stewart 1984; Tort et al. 1996), showing adaptation of the fish to the new situation. Plasma cortisol level is widely used as an indicator of stress conditions (Barton and Iwama 1991). This effect has been described for different species, including coho salmon (Patino et al. 1986) and Arctic charr (*Salvelinus alpinus*) (Jorgensen et al. 1993). Vijayan et al. (1990) found high plasma cortisol values in brown trout held at high stocking density when compared with those held at low stocking density, but these values, although twice that of control, were not significantly different. However, in the present study, fish held at high stocking density showed significantly higher levels of plasma cortisol than those held at low density, suggesting the incapacity of these fish to reach adaptation under these conditions. A similar elevation of plasma cortisol with high rearing density has been described for Atlantic salmon, *Salmo salar* (Mazur and Iwama 1993).

In addition, high stocking density also produced an elevation of plasma glucose. It has been shown that plasma cortisol affects carbohydrate metabolism (Vijayan and Leatherland 1988; Vijayan et al. 1993) and high plasma cortisol levels can activate gluconeogenesis (Sheridan 1986; Barton and Iwama 1991) stimulating glucose production. This effect remains controversial (Andersen et al. 1991) as it is not clear whether plasma cortisol enhances plasma glucose levels either through gluconeogenesis or indirectly by modulating ephinephrine and insulin action on carbohydrate metabolism.

High plasma cortisol levels produce an immunosuppresive effect in fish (Pickering and Pottinger 1985; Maule et al. 1989; Barton and Iwama 1991) reducing circulating lymphocytes (Pickering 1984; Ellsaesser and Clem 1987) and increasing the susceptibility of fish to disease (Pickering and Duston 1983; Houghton and Matthews 1990). In the present study, although some immune parameters such as agglutinating activity or circulating neutrophil number were not affected in the fish held at high stocking density, other immune parameters were decreased at this level of stocking. Haemolytic activity due to alternative complement pathway was decreased in fish held at high stocking density. This effect has been reported to be a consequence of an elevation of plasma cortisol for species such as rainbow trout (Iida et al. 1989), carp (Yin et al. 1995) or gilthead sea bream (Sunyer et al. 1995; Tort et al. 1996), although the mechanism by which cortisol affects activation of complement remains unclear. As noted above, high plasma cortisol levels have been reported to affect lymphocyte population, inducing lymphocytopenia (Pickering et al. 1982; Pickering 1984; Pottinger et al. 1994) and affecting some functions of these cells (Grimm 1985; Mazur and Iwama 1993). In the present study, there was a slight reduction in the ratio of circulating lymphocytes/RBC in the fish held at high stocking density, an effect that may have arisen due to elevated plasma cortisol levels.

In conclusion, the results of the present study show that gilthead seabream held at high stocking density appear to be experiencing chronic stress, as indicated by the significant elevation in plasma cortisol. This crowding stress affected some physiological functions such as lipid distribution and immune activity. The fish showed no signs of disease but displayed symptoms of immunosuppression. Further experiments are required to study whether high stocking density affects the ability of fish to resist additional stressors, thus being more susceptible to stress and diseases..

**Acknowledgements**

The authors thank Dr T. Pottinger from the Institute of Freshwater Ecology in Windemere (U.K.), who kindly read the manuscript and gave valuable suggestions.

© Del documento, los autores. Digitalización realizada por ULPGC. Biblioteca Universitaria, 2009

## References


Alanärä, A. and Brännäs, E. 1996. Dominance-feeding behaviour in Artic charr and rainbow trout: the effect of stocking density. J. Fish Biol. 48: 242–254.

Andersen, D.E., Reid, S.D., Moon, T.W. and Perry, S.F. 1991. Metabolic effects associated with chronically elevated cortisol in rainbow trout *Oncorhynchus mykiss*). Can. J. Fish. Aquat. Sci. 48: 1811–1817.

Anderson, D.P. 1990. Immunological indicators: effects of environmental stress on immune protection and disease outbreaks. Am. Fish. Soc. Symp. 8: 38–50.

Angelidis, P., Baudin-Laurencin, F. and Youinou, P.. 1987. Stress in rainbow trout, *Salmo gairdneri*: effects upon phagocyte chemiluminiscence, circulating leucocytes and susceptibility to *Aeromonas salmonicida*. J. Fish Biol. (Suppl. A) 31: 113–122.

Barton, B.A. 1988. Endocrine and metabolic responses of fish to stress. Int. Assoc. Aquat. Anim. Med. Proc. 19: 41–55.

Barton., B.A. and Iwama, G.K. 1991. Physiological changes in fish from stress in aquaculture with emphasis on the response and effects of corticosteroids. Ann. Rev. Fish Dis. 1: 3–26.

Björnsson, B. 1994. Effects of stocking density on growth rate of halibut (*Hippoglossus hippoglossus* L.) reared in large circular tanks for three years. Aquaculture 123: 259–270.

Christie, W.W. 1982. Lipid analysis. Pergamon Press, Oxford.

Ellsaesser, C.F. and Clem, L.W. 1987. Cortisol-induced hematologic and immunologic changes in channel catfish (*Ictalurus punctatus*). Comp. Biochem. Physiol..87A: 405–408.

Folch, J., Lees, M. and Sloane-Stanley, G.H. 1957. A simple method for the isolation and purification of total lipids from animal tissues. J. Biol. Biochem. 226: 497–509.

Greene, D.H.S. and Selivonchick, D.P. 1987. Lipid metabolism in fish. Prog. Lipid. Res. 26: 53–85.

Grimm, A.S. 1985. Suppression by cortisol of the mitogen-induced proliferation of periferal blood leucocytes from plaice, *Pleuronectes platessa* L. *In* Fish Immunology. Pp 263–271. Edited by M.J. Manning and M.F. Tatner. Academic Press, London.

Holm, J.C., Refstie, T. and Bo, S. 1990. The effect of fish density and feeding regimes on individual growth rate and mortality in rainbow trout (*Oncorhynchus mykiss*). Aquaculture 89: 225–232.

Houghton, G. and Matthews, R.A. 1990. Immunosuppression in juvenile carp, *Cyprinus carpio* L.: The effects of the corticosteroid triamcinolone acetonide and hydrocortisone 21-hemisuccinate (cortisol) on acquired immunity and the humoral antibody response to *Ichthyophthirius multifiliis* Fouquet. J. Fish Dis. 13: 269–280.

Idler, D.R. and Truscott, B. 1972. Corticosteroids in fish.*In* Steroids in Non-mammalian Vertebrates. Pp. 127–252. Edited by D.R. Idler. Academic Press, London.

Iida, T., Takahashi, K. and Wakabayashi, H. 1989. Decrease in the bactericidal activity of normal serum during the spawning period of rainbow trout. Nippon Suisan Gakkaishi 55: 463–465.

Izquierdo, M.S. 1996. Essential fatty acid requirements of marine fish larvae. Aquacult. Nutr. 2: 183–191

Izquierdo, M.S., Watanabe, T., Takeuchi, T., Arakawa, T. and Kitajima, C. 1990. Optimum EFA levels in *Artemia* to meet the EFA requirements of red sea bream (*Pagrus major*). *In* The Current Status of Fish Nutrition in Aquaculture. Pp. 221–232. Edited by M. Takeda and T. Watanabe. Tokyo Univ. Fisheries, Tokyo.

Jorgensen, E.H., Christiansen, J.S. and Jobling, M. 1993. Effects of stocking density on food intake, growth performance and oxygen consumption in Artic charr (*Salvelinus alpinus*). Aquaculture 110: 191–204.

Juaneda, P. and Rocquelin, G. 1985. Rapid and convenient separation of phospholipids and non-phosphorous lipids from rat using silica cartridges. Lipids 20: 40–41.

Kebus, M.J., Collins, M.T., Brownfield, M.S., Amundson, C.H., Kayes, T.B. and Malison, J.A. 1992. Effects of rearing density on the stress response and growth of rainbow trout. J. Aquat. Anim. Health 4: 1–6.

Klontz, G.W. 1994. Fish hematology. *In* Techniques in Fish Immunology. Vol III. Pp. 121–131. Edited by J.S.Stolen, T.C. Fletcher, A.F. Rowley, J.T. Zelikoff, S.L. Kaattari and S.A. Smith. SOS Publications, Fair Haven.

Leatherland, J.F. and Cho, C.Y. 1985. Effect of rearing density on thyroid and interrenal gland activity and plasma and hepatic metabolite levels in rainbow trout, *Salmo gairdneri* Richardson. J. Fish Biol. 27: 583–592.

Lie, O. 1993. Changes in the fatty acid composition of neutral lipids and glycerophospholipids in developing cod eggs. *In* Physiological and Biochemical Aspects of Fish Development. Pp. 330–337. Edited by B.T. Walther and H.J. Fyhn. University of Bergen , Norway.

Maule, A.G., Tripp, R.A., Kaattari, S.L. and Schreck, C.B. 1989. Stress alters the immune function and disease resistance in chinook salmon *Oncorhynchus tshawytscha*. J. Endocrinol. 120: 135–142.

Mazur, C.F. and Iwama, C.K. 1993. Handling and crowding stress reduces number of plaque-forming cells in Atlantic salmon. J. Aquat. Anim. Health 5: 98–101.

Meade , J.W., Ramsey, J.F. and Williams, J.C. 1985. Effects of cumulative loading level, as fish weight per unit of flow, on water quality and growth of lake trout. J. World Maricult. Soc. 16: 40–51.

Molinero, A. and González, J. 1995. Comparative effects of MS-222 and 2-phenoxyethanol on gilthead sea bream (*Sparus aurata* L.) during confinement. Comp. Biochem. Physiol. 111: 405–414.

Montero, D., Tort, L., Izquierdo, M.S., Socorro, J., Robaina, L., Vergara, J.M. and Fernández-Palacios, H. 1995. Hematological recovery in *Sparus aurata* after bleeding. A time course study. Rev. Esp. Fis. 51: 219–226.

Montero, D., Tort, L., Izquierdo, M.S., Socorro, J., Robaina, L., Vergara, J.M. and Fernández-Palacios, H.1996. Effect of $\alpha$-tocopherol and n-3 HUFA deficient diets on blood cells, selected immune parameters and proximate body composition of gilthead seabream (*Sparus aurata*). In Modulators of Immune Response. The Evolutionary Trail. Pp. 251–266. Edited by J.S. Stolen, T.C. Fletcher, C.J. Bayne, C.J. Secombes, J.L. Zelikoff, L. Twerdok and D.P. Anderson. SOS Publications, Fair Haven.

Pankhurst, N.W. and Van Der Kraak, G. 1997. Effects of stress on reproduction and growth of fish. *In* Fish Stress and Health in Aquaculture Pp. 73–93. Edited by G.K. Iwama, A.D. Pickering, J.P. Sumpter and C.B. Schreck. Cambridge University Press, Cambridge.

Patino, R., Schreck, C.B., Blanks, J.L. and Zaugg, W.S. 1986. Effects of rearing conditions on the developmental physiology of smolting coho salmon. Trans. Am. Fish. Soc. 115: 828–837.

Pickering, A.D. 1984. Cortisol-induced lymphocytopenia in brown trout, *Salmo trutta* L. Gen. Comp. Endocrinol. 53: 252–259.

Pickering, A.D. 1990. Stress and the Suppression of Somatic Growth in Teleost Fish. Progress in Comparative Endocrinology. Wiley-Liss.

Pickering, A.D. and Duston, J. 1983. Administration of cortisol to brown trout, *Salmo trutta* L., and its effects on the susceptibility to *Saprolegnia* infection and furunculosis. J. Fish Biol. 23: 163–175.


© Del documento, los autores. Digitalización realizada por ULPGC. Biblioteca Universitaria, 2009

Pickering, A.D. and Pottinger, T.G. 1985. Cortisol can increase the susceptibility of brown trout, *Salmo trutta* L., to disease without reducing the white blood cell count. J. Fish Biol. 27: 611–619.

Pickering, A.D. and Pottinger, T.G. 1989. Stress responses and disease resistance in salmonid fish: effects of chronic elevation of plasma cortisol. Fish Physiol. Biochem. 7: 253–258.

Pickering, A.D. and Stewart, A. 1984. Acclimation of the interrenal tissue of the brown trout, *Salmo trutta* L., to chronic crowding stress. J. Fish Biol. 24: 731–740.

Pickering, A.D., Pottinger, T.G. and Christie, P. 1982. Recovery of the brown trout, *Salmo trutta* L., from acute handling stress: a time-course study. J. Fish Biol. 20: 229–244.

Pottinger, T.G., Moran, T.A. and Morgan, J.A.W. 1994. Primary and secondary indices of stress in the progeny of rainbow trout (*Oncorhynchus mykiss*) selected for high and low responsiveness to stress. J. Fish Biol. 44: 149–163.

Schreck, C.B., Patino, R., Pring, C.K., Winton, J.R. and Holway, J.E. 1985. Effects of rearing density on indices of smoltification and perfomance of coho salmon, *Oncorhynchus kitsutch*. Aquaculture 45:345–358.

Sheridan, M.A. 1986. Effects of thyroxin, cortisol, growth hormone, and prolactin on lipid metabolism of coho salmon, *Oncorhynchus kisutch*. Gen. Comp. Endocrinol. 81: 473–783.

Sodeberg, R.W. and Meade, J.W. 1987. Effects of rearing density on growth, survival, and fin condition af Atlantic salmon. Progr. Fish-Cult. 49: 280–283.

Soivio, A. and Nikinmaa, M. 1981. The swelling of erythrocytes in relation to the oxygen affinity of the blood of the rainbow trout, *Salmo gairdneri* Richardson. *In* Stress and Fish. pp. 103–119. Edited by A.D. Pickering. Academic Press. London.

Sokal, R.R. and Rolf, J. 1979. Biometría. Blume. Madrid.

Srivastava, S. and Sahai, I. 1987. Effects of loading density on carbohydrate metabolism and hematology in the Indian freshwater catfish, *Heteropneustes fossilis*. Aquaculture 66: 275–286.

Sunyer, J.O. and Tort, L. 1994. The complement system of the teleost fish *Sparus aurata*. Ann. N.Y. Acad. Sci. 712: 371–373.

Sunyer, J.O. and Tort, L. 1995. Natural hemolytic and bactericidal activities of sea bream *Sparus aurata* serum are effected by the alternative complement pathway. Vet. Immunol. Immunopath. 45: 333–345.

Sunyer, J.O., Gómez, E., Navarro, V., Quesada, J. and Tort, L. 1995. Physiological responses and depression of humoral components of the immune system in gilthead seabream (*Sparus aurata*) following daily acute stress. Can. J. Fish. Aquat. Sci. 52: 2339–2346.

Tort, L., Sunyer, J.O., Gómez, E. and Molinero, A. 1996. Crowding stress induced changes in serum haemolytic and agglutinating activity in the gilthead sea bream *Sparus aurata*. Vet. Immunol. Immunopath. 51: 179–188.

Vijayan, M.M. and Leatherland, J.F. 1988. Effect of stocking density on the growth and stress-response in brook charr, *Salvelinus fontinalis*. Aquaculture 75: 159–170.

Vijayan, M.M., Ballantyne, J.S. and Leatherland, J.F. 1990. High stocking density alters the energy metabolism of brook charr, *Salvelinus fontinalis*. Aquaculture 88: 371–381.

Vijayan, M.M., Foster, G.D. and Moon, T.W. 1993. Effects of cortisol on hepatic carbohydrate metabolism and responsiveness to hormones in the sea raven, *Hemitripterus americanus*. Fish Physiol. Biochem. 12: 327–335.

Waagbo, R., Hemre, G.I., Holm, J.C. and Lie, O. 1995. Tissue fatty acid composition, haematology and immunity in adult cod, *Gadus morhua* L., fed three dietary lipid sources. J. Fish Dis. 18: 615–622.

Wedemeyer, G.A. 1997. Effects of rearing conditions on the health and physiological quality of fish in intensive culture. In Fish Stress and Health in Aquaculture Pp. 35–71. Edited by G.K. Iwama, A.D. Pickering, J.P. Sumpter, and C.B. Schreck. Cambridge University Press, Cambridge.

Wedemeyer G.A. and McLeay, D.J. 1981. Methods for determining the tolerance of fishes to environmental stressors. In Stress and Fish Pp. 247–275. Edited by A.D. Pickering. Academic Press. London.

Yin, Z., Lam, T.J. and Sin, Y.M. 1995. The effects of crowding stress on the non-specific immune response in fancy carp (*Cyprinus carpio* L.). Fish Shellfish Immunol. 5: 519–529.

© Del documento, los autores. Digitalización realizada por ULPGC. Biblioteca Universitaria, 2009

INT. J. REMOTE SENSING, 1999, VOL. 20, no. 7, 1405–1418

# Seasonal variability of recurrent phytoplankton pigment patterns in the Canary Islands area

M. M. PACHECO† and A. HERNÁNDEZ-GUERRA

Departamento Física, Facultad Ciencias del Mar, Canary Islands, Universidad de Las Palmas de Gran Canaria, Spain

**Abstract.** Seasonal variability of recurrent phytoplankton pigment patterns in the Canary Islands area has been determined using historical data from Nimbus-7 Coastal Zone Color Scanner data. The main patterns associated with the islands are cyclonic and anticyclonic eddies downstream of the islands, apparently caused by their effect as a topographic obstacle to the flow of the Canary Current. These eddies are present during all seasons, suggesting that the speed of the Canary Current is always strong enough to develop eddies. The pattern associated with the influence of the coastal upwelling system off north-west Africa consists of upwelling filaments stretching from the African coast to the islands. They are fundamentally present during summer and early fall when strong Trade Winds blow over the area. Both patterns may contribute to the mesoscale activity south of the islands.

## 1. Introduction

The large-scale mean oceanic flow in the Canary Islands area (figure 1) is the Canary Current, which is the eastern boundary current of the North Atlantic subtropical gyre. The Canary Current is fed by the eastern branch of the Azores Current which turns southward east of Madeira Island (Stramma 1984, Stramma and Siedler 1988, Klein and Siedler 1989, Fiekas *et al.* 1992). The Canary Current flows southward along the African coast and turns south-westward around 20° N contributing to the North Equatorial Current. This is the large-scale behaviour of the eastern subtropical gyre which, of course, presents considerable time and space variability. According to Stramma and Siedler (1988), the seasonal variability consists of a southward shift of the Azores Current, a northward shift of the North Equatorial Current, and the approach of the Canary Current to the African coast during summer.

The Canary Current is predominantly normal to the zonal orientation of the Archipelago, which acts as a topographic obstacle. A well described result is the generation of eddies at the wake of an obstacle, which may contribute to mesoscale activity (Chopra 1973, Pattiaratchi *et al.* 1986, Boyer *et al.* 1987, Davies and Mofor 1990, Heywood *et al.* 1990). Hernández-Guerra *et al.* (1993) used Coastal Zone Color Scanner (CZCS) data to describe a 'lee filament' (defined as a narrow and

† e-mail: mercedes.pacheco@fisica.ulpgc.es

*International Journal of Remote Sensing*
ISSN 0143-1161 print/ISSN 1366-5901 online © 1999 Taylor & Francis Ltd
http://www.tandf.co.uk/JNLS/res.htm
http://www.taylorandfrancis.com/JNLS/res.htm

© Del documento, los autores. Digitalización realizada por ULPGC. Biblioteca Universitaria, 2009

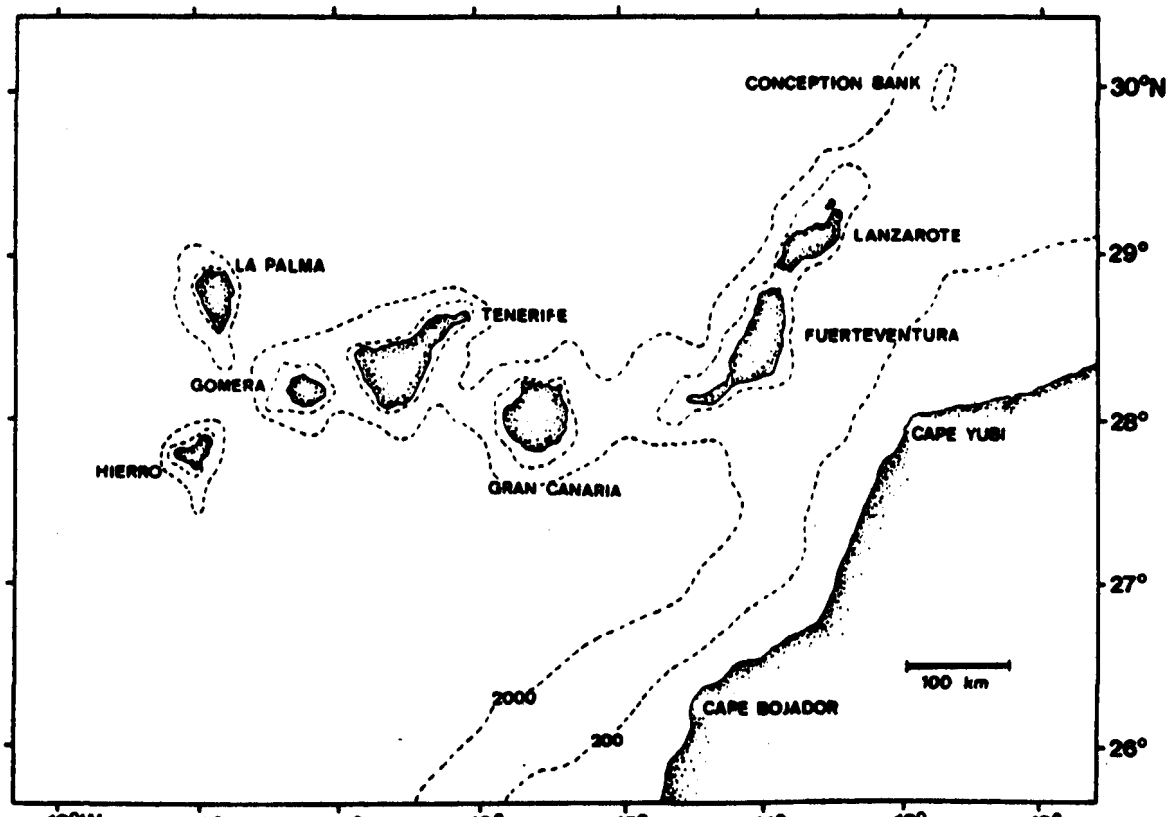


Figure 1. Area under study with selected bathymetry. The figure shows the large capes along the north-west African coast close to the Canary Islands.

elongated feature of pigment-rich waters appearing in the downstream side of the islands) that originated off the north-west coast of Gran Canaria. This lee filament ended as a large cyclonic eddy downstream the island. Arístegui *et al.* (1994) described the occurrence of cyclonic and anticyclonic eddies downstream of Gran Canaria using Airborne eXpendable BathyThermographs (AXBTs), Conductivity Temperature Depth (CTD) and Advanced Very High Resolution Radiometer (AVHRR) data. They observed that the two eddies extended from the surface to at least 400 m depth and suggested that eddies are sequentially detached from the island. The lee filament, ending as a cyclonic eddy, was also observed in several AVHRR images. Hernández-Guerra *et al.* (1993) described other phytoplankton pigment features associated with individual islands: a large filament stretching westward from an enrichment region on the west coast of Fuerteventura, which may be the biological response to an upwelling event, and enrichment centres in the northern position of all four western islands.

The large-scale mean atmospheric flow in the Canary Islands area is formed by the Trade Winds. The large-scale variation of the Trade Winds, which is coupled to the meridional shift of the Azores High, determines the strength and persistence of coastal upwelling along the African coast. During July/August the Azores high is at its northernmost position and the boundary of the Trade Winds is approximately between 32° N and 20° N. In fall, the Azores High begins to move southward until gaining its southernmost position in winter. Thus, coastal upwelling is strong in summer and early fall in the Canary Islands area (Wooster *et al.* 1976, Speth and Detlefsen 1982, Nykjaer and Van Camp 1994), with Cape Jubi and Cape Bojador apparently being the most intense coastal upwelling centres (Hughes and Barton

© Del documento, los autores. Digitalización realizada por ULPGC. Biblioteca Universitaria, 2009

1974, Molina and Laatzen 1986). The dynamics of coastal upwelling may cause mesoscale activity in the region and modify the structure of the Canary Current. Cold upwelling filaments stretch from the African coast to the islands, containing high phytoplankton pigment concentrations (Van Camp *et al.* 1991, Hernández-Guerra *et al.* 1993, Arístegui *et al.* 1997).

In this study we analyse the whole CZCS archive to determine the seasonal variability of recurrent phytoplankton pigment patterns in the Canary Islands region, which may contribute to the mesoscale activity in the region, and infer different physical mechanism to explain the patterns obtained.

## 2. Data and methods

The CZCS on board the Nimbus-7 satellite, launched on October 1978 and operative until 1986, was a multichannel radiometer scanning the oceans in six spectral bands. The first four were specifically designed to estimate the concentration of phytoplankton in the ocean. The fifth band was used to separate water from land and clouds and the sixth band operated in a thermal infrared window but these data were judged to be inaccurate.

The algorithm used for atmospheric correction of CZCS data has been described by Sturm (1981), Bricaud and Morel (1987) and Gordon *et al.* (1988). It takes into account the sensor sensivity loss, corrects for Rayleigh scattering in the atmosphere by a multiple scattering approach, and estimates pixel-by-pixel the phytoplankton pigment content in the upper layer of the ocean by comparing the sensor-derived radiances to an in-water bio-optical model (Bricaud and Morel 1987). This method is useful for Case 1 waters, such as those surrounding the Canary Islands. The estimates obtained for phytoplankton pigment concentrations are expected to be correct to within a factor of two as compared to *in situ* measurements of surface concentration. This is adequate for the purposes of this work, i.e. to visually appreciate the patterns in the Canary Islands area. Table 1 lists the number of CZCS images selected for this study from the complete CZCS archive of the Ocean Colour European Archive Network (OCEAN) Project. These were selected such that few images were contaminated by cloud cover and no saturation in Band 4 due to aerosols coming from the Sahara.

Table 1. Number of phytoplankton pigment concentration images selected for this study from the whole archive of CZCS scenes.

| | Winter | Spring | Summer | Fall | Total |
|---|---|---|---|---|---|
| 1978 | | | | 11 | 11 |
| 1979 | 15 | 8 | 7 | 6 | 36 |
| 1980 | 8 | 10 | 7 | 17 | 42 |
| 1981 | 9 | 11 | 14 | 19 | 53 |
| 1982 | 17 | 6 | 11 | 22 | 56 |
| 1983 | 2 | 11 | 14 | 9 | 36 |
| 1984 | 10 | 7 | 10 | 8 | 35 |
| 1985 | 8 | | | | 8 |
| Total | 69 | 53 | 63 | 92 | 277 |

© Del documento, los autores. Digitalización realizada por ULPGC. Biblioteca Universitaria, 2009

## 3. Results and discussion

Previous studies carried out on the Canary Islands area have illustrated the recurrent phytoplankton pigment patterns, but their seasonal variability has not been determined. The seasonal variability of recurrent patterns implies the existence of a seasonal variability of driving forces responsible for their generation. However, the fact that phytoplankton pigment content is not a stable property of the ocean must be considered. Thus, to gain a complete understanding of these patterns would require a considerable amount of additional data not available at this time.

Summer and early fall show similar behaviour and were considered together. We selected five images (figures 2–6) as representative of this period. These five images show the most recurrent oceanographic patterns present in the Canary Islands area: eddies downstream of several islands and upwelling filaments stretching from the African coast to the islands. Eddies are observed in one way or another during all seasons while upwelling filaments are fundamentally observed only in summer and early fall. The eddies are associated with Gran Canaria, Gomera and La Palma islands. Gran Canaria and Gomera islands are almost round obstacles whilst La Palma Island has a triangular shape, all of them interrupting the predominant flow of the Canary Current. These eddies are cyclonic except in Gran Canaria where it is possible to observe cyclonic and anticyclonic eddies, the latter showing deeper isotherms and nutrient isopleths in their centres. They show little change in surface phytoplankton pigment and temperature, these hence being hardly apparent in phytoplankton pigment and sea surface temperature (SST) images. The may be appreciated, however, through the indirect effects of their circulation on adjacent contrasting water masses. These are provided by the cold and high pigment

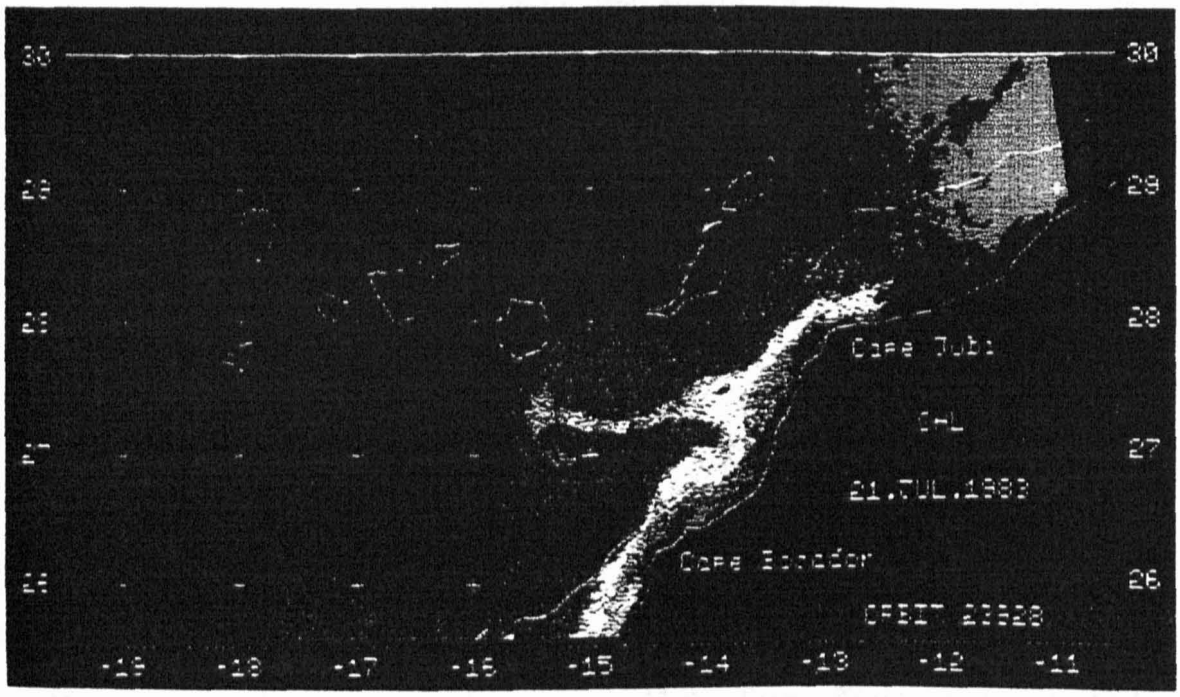


Figure 2. Processed phytoplankton pigment image of the Canary Islands area taken on 21 July 1983. Land, clouds and areas of dense haze, for which the atmospheric correction is not applicable, are represented in black and grey. The white crosses are one degree apart, both in latitude and in longitude. The two white curves along the African coast are the 0 and the 200 m isobath, the latter approximately coinciding with the edge of the shelf. CHL stands for phytoplankton pigment concentration image.

© Del documento, los autores. Digitalización realizada por ULPGC. Biblioteca Universitaria, 2009

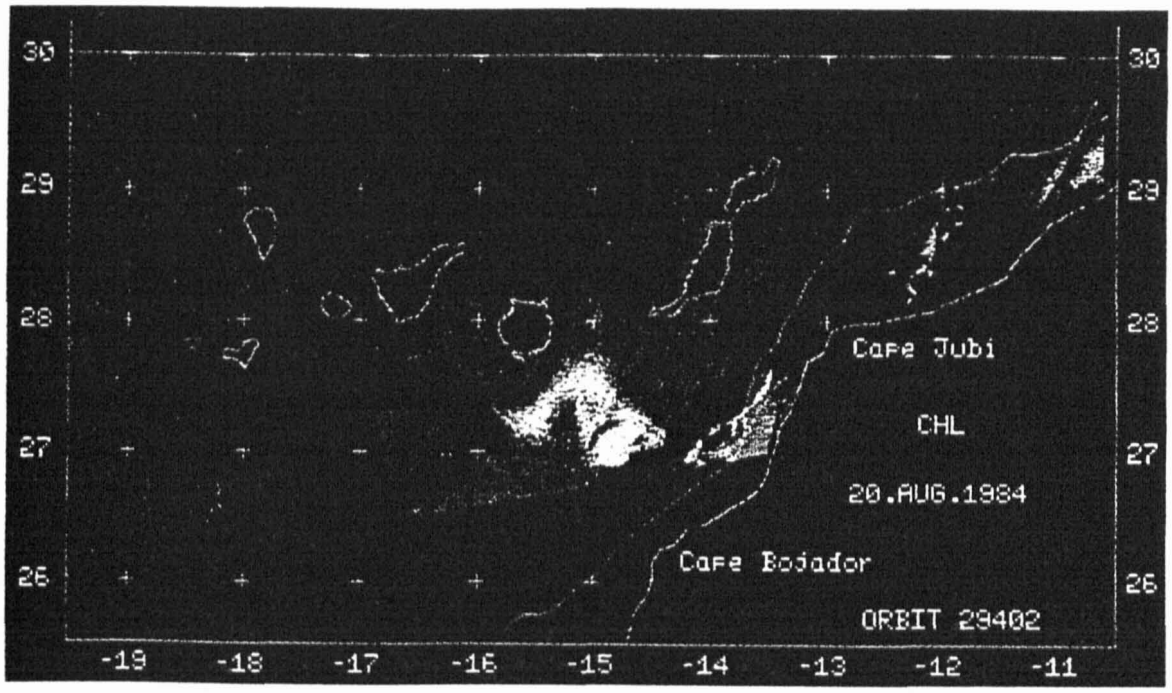


Figure 3. As figure 2, but on 20 August 1984.

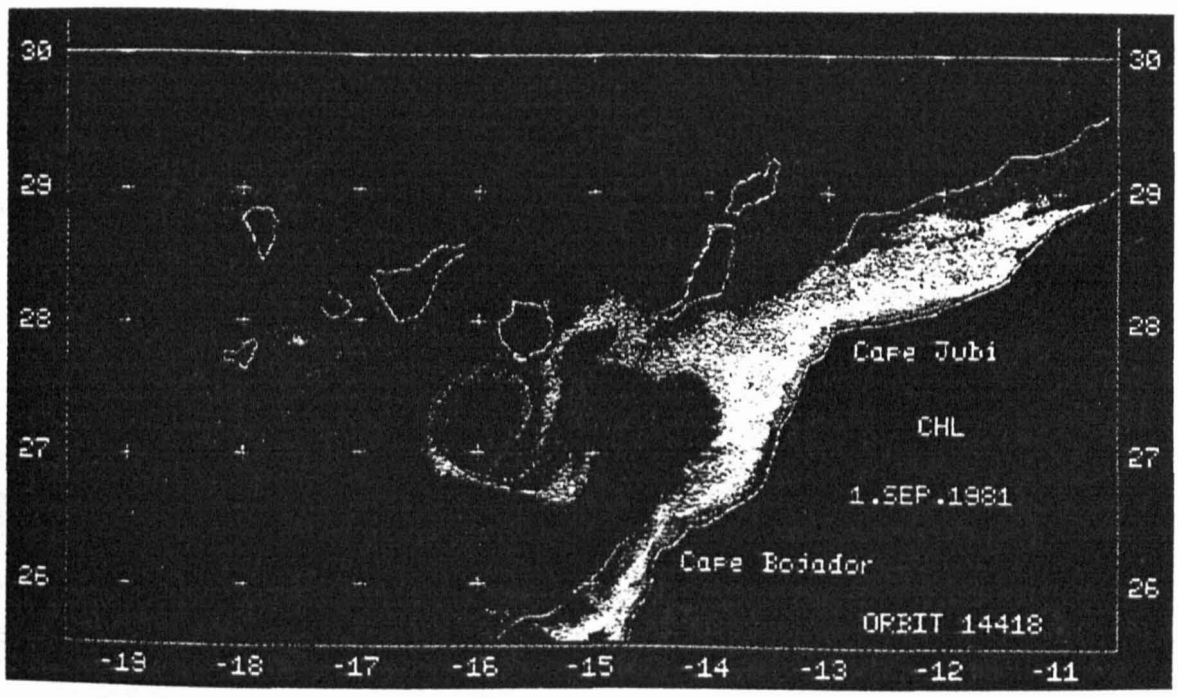


Figure 4. As figure 2, but on 1 September 1981.

concentration waters in upwelling filaments stretching from the African coast to the islands. Figure 4 clearly shows this: an upwelling filament stretching from the African coast to south of Gran Canaria and finishing as a large anticyclonic eddy. Every time an upwelling filament or its spreading approaches the south region of Gran Canaria, an anticyclonic eddy is observed. This implies that anticyclonic eddies associated with other islands may exist but are not observed in the phytoplankton pigment concentration images because no tracer is present close to these islands.

Several characteristics of the cyclonic eddies associated with Gran Canaria are

© Del documento, los autores. Digitalización realizada por ULPGC. Biblioteca Universitaria, 2009

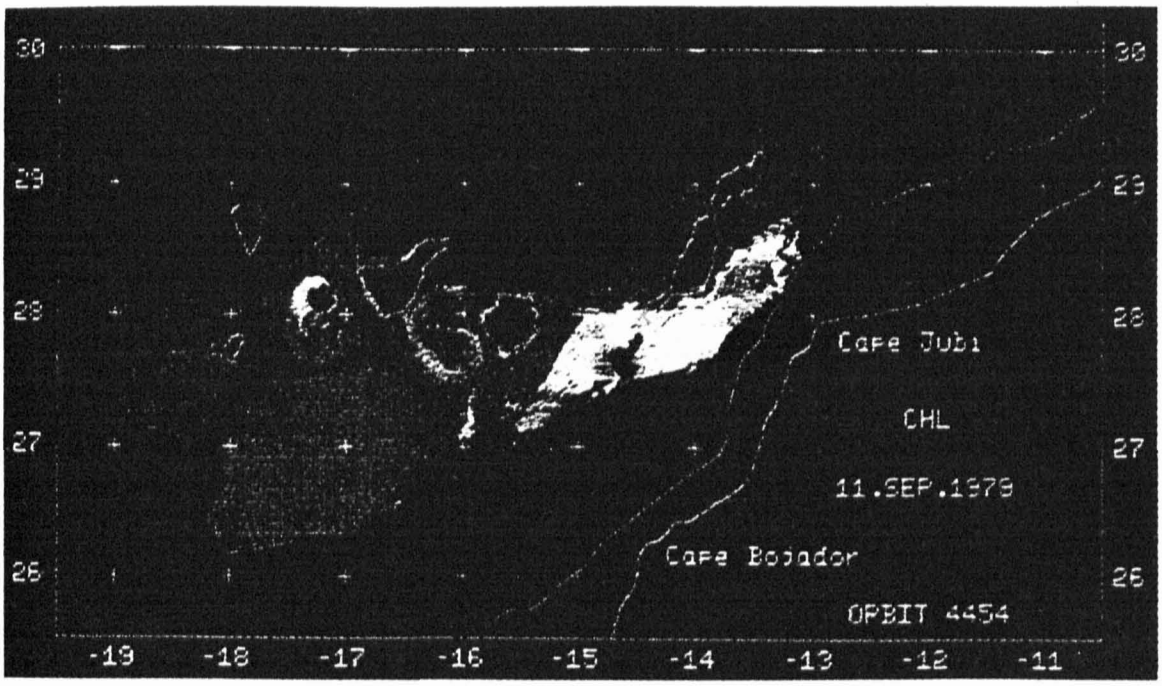


Figure 5. As figure 2, but on 11 September 1979.

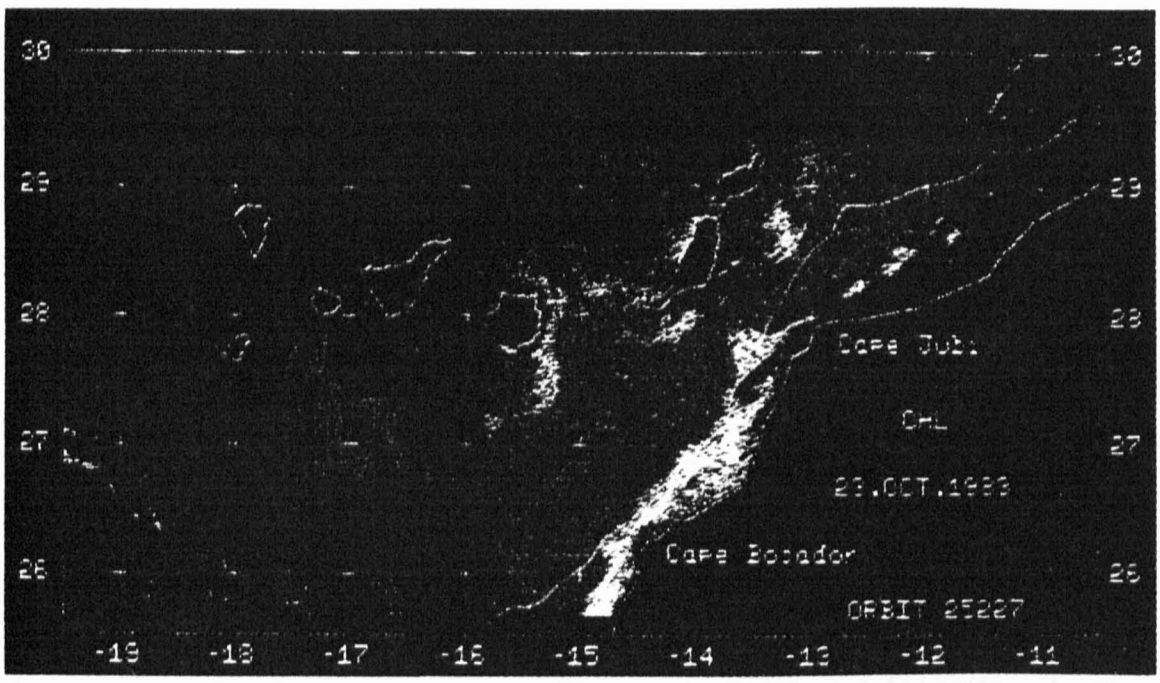


Figure 6. As figure 2, but on 23 October 1983.

to be noted in figures 2 to 6. (1) They are always attached to the north-west or west coast of Gran Canaria by a lee filament. (2) The horizontal length scale of the eddy is similar to the diameter of the island (54 km). (3) High phytoplankton pigment content is unambiguously apparent at the periphery of the eddy with lower values generally present at its core. This last characteristic is absent in figure 3, where a high phytoplankton pigment concentration is also found in the core of the eddy. We suggest that this is due to a different degree of development in this case: the distance between the eddy and the coast of Gran Canaria is maximum in this image.

The eddies range in shape from elliptical (as in figures 5 and 6) to circular (as in

© Del documento, los autores. Digitalización realizada por ULPGC. Biblioteca Universitaria, 2009

figures 3 and 4). We have plotted the eccentricity of the eddies, using the same approach as in Patzer (1969), i.e. $e=\sqrt{a^2-b^2}/a$, where $a$ and $b$ are the half major and half minor axis respectively, versus the distance of the centre of the eddy to the island (figure 7). This figure only shows the measurements for the anticyclonic eddy associated with Gran Canaria and the cyclonic eddy associated with Gomera. The cyclonic eddy associated with Gran Canaria was not considered because full eddies, such as those in figures 3 or 5, were not observed often enough for a statistical analysis. The cyclonic eddy was often observed as an open lee filament (e.g. figure 8) for which precise measurements of the major and minor axes could not be taken. Gran Canaria anticyclonic eddy (figure 7 (*b*)) exhibits an elliptical shape close to the island, presumably related to its early stages of development. Its eccentricity decreases

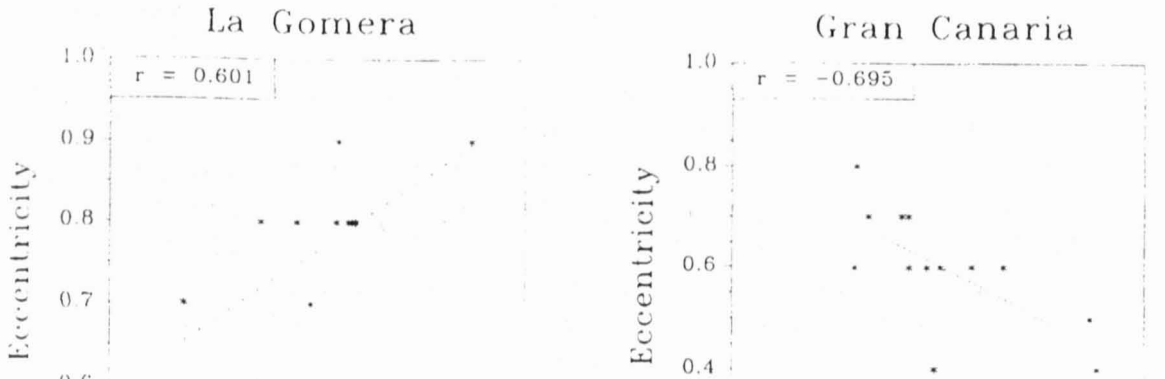


Figure 7. Observed eddy eccentricity versus distance of the eddy centre to the islands of (*a*) La Gomera and (*b*) Gran Canaria.

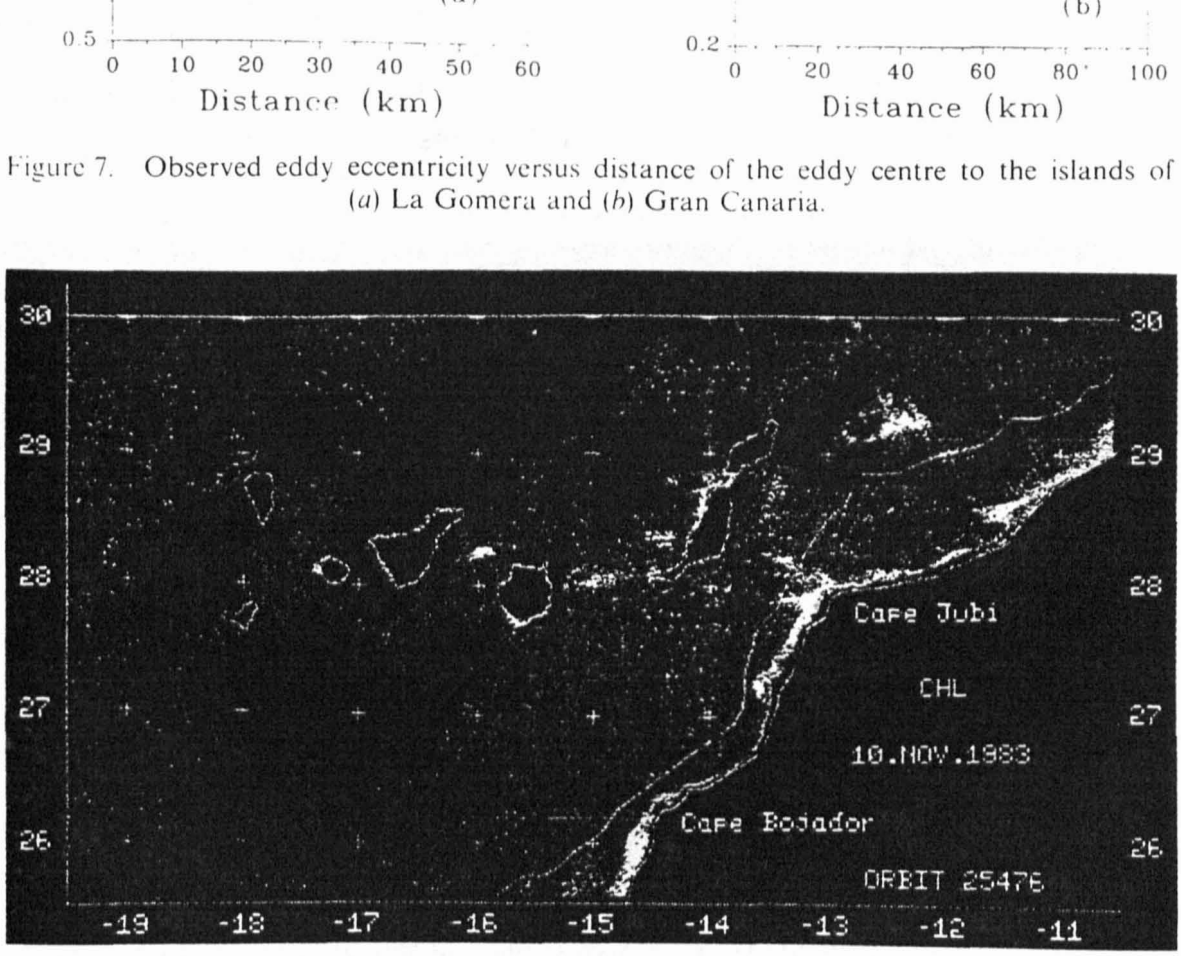


Figure 8. As figure 2, but on 10 November 1983.

© Del documento, los autores. Digitalización realizada por ULPGC. Biblioteca Universitaria, 2009

when the eddy moves further away from the island. This is similar to the laboratory experiments described in Boyer *et al.* (1984) and Chabert d'Hieres *et al.* (1989). On the other hand, the Gomera cyclonic eddy (figure 7 (*a*)) behaves in a completely inverse way that may be explained by the vicinity of El Hierro island which apparently disturbs the normal evolution of the eddy.

Results of laboratory and numerical studies on non-rotating flow past obstacles indicate that eddies are generated in the flanks and shed by the obstacle when the Reynolds number (*Re*) exceeds a critical value (Boyer 1970, Boyer and Davies 1982, Sangrá 1995). Since the Reynolds number is defined as $Re = U\ L/A_H$, where $U$ is the fluid velocity, $L$ is a typical horizontal dimension of the obstacle and $A_H$ is the horizontal eddy viscosity coefficient of the fluid, the condition for eddy development corresponds to its speed exceeding a critical value. Since eddies are apparently observed during all seasons, the speed of the Canary Current is always apparently strong enough to develop eddies.

Previous laboratory investigations of eddies shed by islands and capes have found that cyclonic and anticyclonic eddies are asymmetric for low Rossby numbers (*Ro*) in the sense that cyclonic eddies present small and sharply defined cores while anticyclonic eddies present large and diffuse cores (Boyer and Davies 1982, Boyer *et al.* 1984, Boyer and Tao 1987, Chabert d'Hieres *et al.* 1989). *Ro* is defined as $Ro = U/(f\ L)$, where $f = 2\Omega \sin \theta$ is the Coriolis parameter, $\Omega$ being the Earth's angular velocity and $\theta$ the latitude. In our case, if we consider $U = 0.3\ \mathrm{m\ s^{-1}}$ (possibly a maximum value of the typical geostrophic speed of the Canary Current), $\Omega = 7.3 \times 10^{-5}\ \mathrm{s^{-1}}$, $\theta = 28°$ (the Canary Islands' latitude) and $L = 54$ km (the diameter of Gran Canaria), we obtain $Ro = 0.08 \ll 1$. Examining figures 2 to 6, we can note that both cyclonic and anticyclonic eddies are symmetric, apparently contrary to previous laboratory investigations. As suggested by Sangrá (1995), this may be caused by both bottom and surface Ekman pumping of similar order, with secundary circulation inside the eddies leading to a symmetrical shape.

From a biological point of view, the importance of knowing the space and time variability of cyclonic eddies lies in their effect on water quality and the distributions of nutrient and marine fauna (Emery 1972, Hogg *et al.* 1978, Genin *et al.* 1986, Falkowski *et al.* 1991, Arístegui *et al.* 1997). Figure 6 clearly shows a westward filament stretching from the west coast of Fuerteventura. This filament stretches from an enrichment region and generally appears at the same time as the upwelling filaments in the continental upwelling system, suggesting that the same driving forces produce both features. A wind blowing alongshore produces a net transport of surface water 90° right to the wind direction, which is replaced by subsurface water. Molina and Laatzen (1989) observed upwelled water off the west coast of Fuerteventura.

Regarding the occurrence of upwelling filaments in the Canary Islands area, they are clearly related to seasonal variability of upwelled water off north-west Africa. Thus, one can expect to observe them during summer and early fall (figures 2 to 6). However, this does not mean that they will not be observed in other seasons: events of strong upwelling favourable winds blowing over the area may cause upwelled water and the occurrence of upwelling filaments. For example, Arístegui *et al.* (1997) reported an upwelling filament approximately 200 km long during March associated with a strong wind event blowing over the area. Upwelling filaments have been extensively studied, principally in the California Current System (reported in special issues such as volumes 92 and 96 of the *Journal of Geophysical Research*). Upwelling

© Del documento, los autores. Digitalización realizada por ULPGC. Biblioteca Universitaria, 2009

filaments are separated from the surrounding waters by significant fronts and are clearly visible through phytoplankton pigment concentration and SST images.

The upwelling filaments stretch off Cape Jubi and Cape Bojador and sometimes in a position in between. This means that the spatial distribution of the filaments appears in most cases to be closely related to the coastal topography and bathymetry of the African coast. Coastal dynamic processes associated with capes, such as separation of the alongshore coastal current and induced wind stress variations, may lead to strong offshore flow and upwelling filaments. Another filament production mechanism may be the existence of a permanent cyclonic eddy situated in the trough between Gran Canaria and the African coast.

During middle fall (figure 8), no upwelling filaments are apparent. In this image, a very narrow band of high phytoplankton pigment concentration is observed along the African coast although high phytoplankton pigment content still remains in the waters surrounding the Canary Islands. The lee filament associated with Gran Canaria is clearly seen. It skirts the eastern coast of Tenerife and the cyclonic eddy.

During winter (figures 9 and 10) a high phytoplankton pigment content is present over the whole area. This is a season of surface mixing due to winter convection and thus, phytoplankton pigment content is expected to be higher in winter than in other seasons in which the water column is less affected (De León and Braun 1973). This apparently corresponds to a phytoplankton bloom which is not as high as the North Atlantic bloom. This is confirmed by measurements of chlorophyll concentration collected during one year on a monthly basis at the European Station for Time Series in the Ocean, Canary Islands (ESTOC) located approximately 1° north of Gran Canaria (Davenport *et al.* 1998) and by previous chlorophyll measurements collected around the islands (De León and Braun 1973, Arístegui *et al.* 1989). Surface data indicated that the chlorophyll concentration is 5–6 times higher in winter than the rest of the year, with a secondary maximum in October. This secondary maximum is apparently due to spreading of upwelling filaments from south of the Canary Islands, as seen in figure 6.

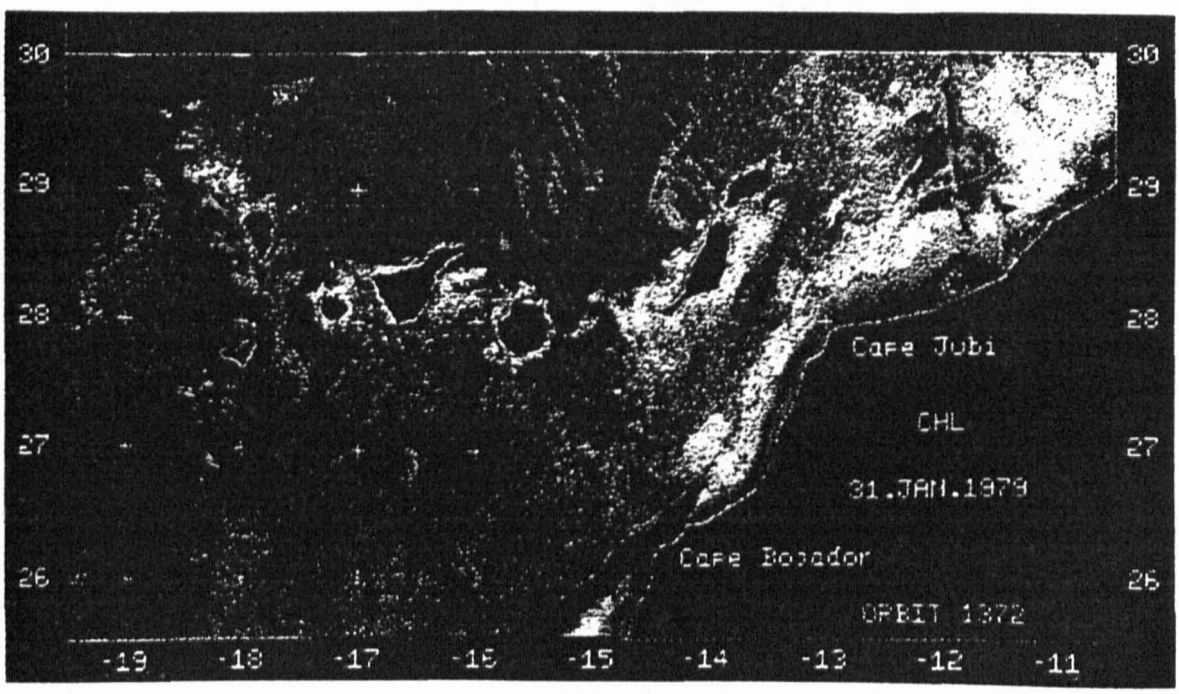


Figure 9. As figure 2, but on 31 January 1979.

© Del documento, los autores. Digitalización realizada por ULPGC. Biblioteca Universitaria, 2009

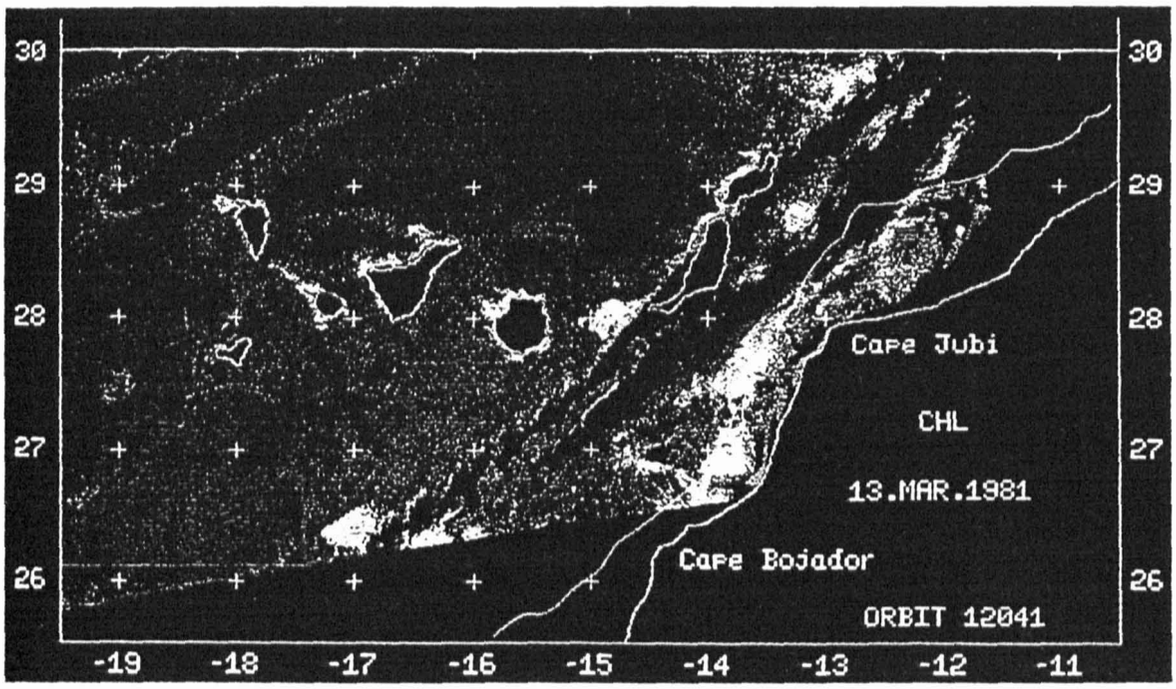


Figure 10. As figure 2, but on 13 March 1981.

During winter the high phytoplankton pigment content apparently masks the features associated with the islands, but these may be observed using density-enhancement techniques as shown in figure 11. The cyclonic and anticyclonic eddies associated with Gran Canaria are clearly seen, as well as the cyclonic eddy associated with La Palma. In early spring (figure 12) the pigment concentration is diminished but still remains around the coasts of the islands. In this and the next spring image (figure 13), the characteristic features of the islands can also be observed.

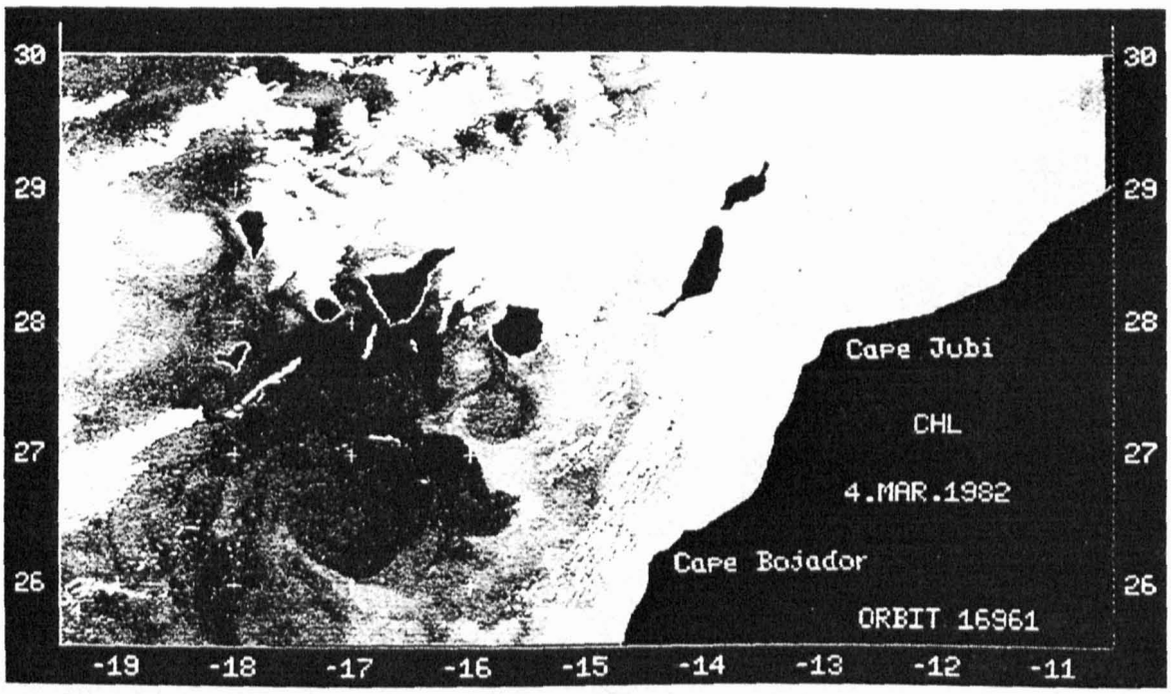


Figure 11. Image on 4 March 1982. This image is presented in grey levels using density-enhancement techniques in order to visualize the characteristic phytoplankton pigment patterns of the islands more clearly.

© Del documento, los autores. Digitalización realizada por ULPGC. Biblioteca Universitaria, 2009

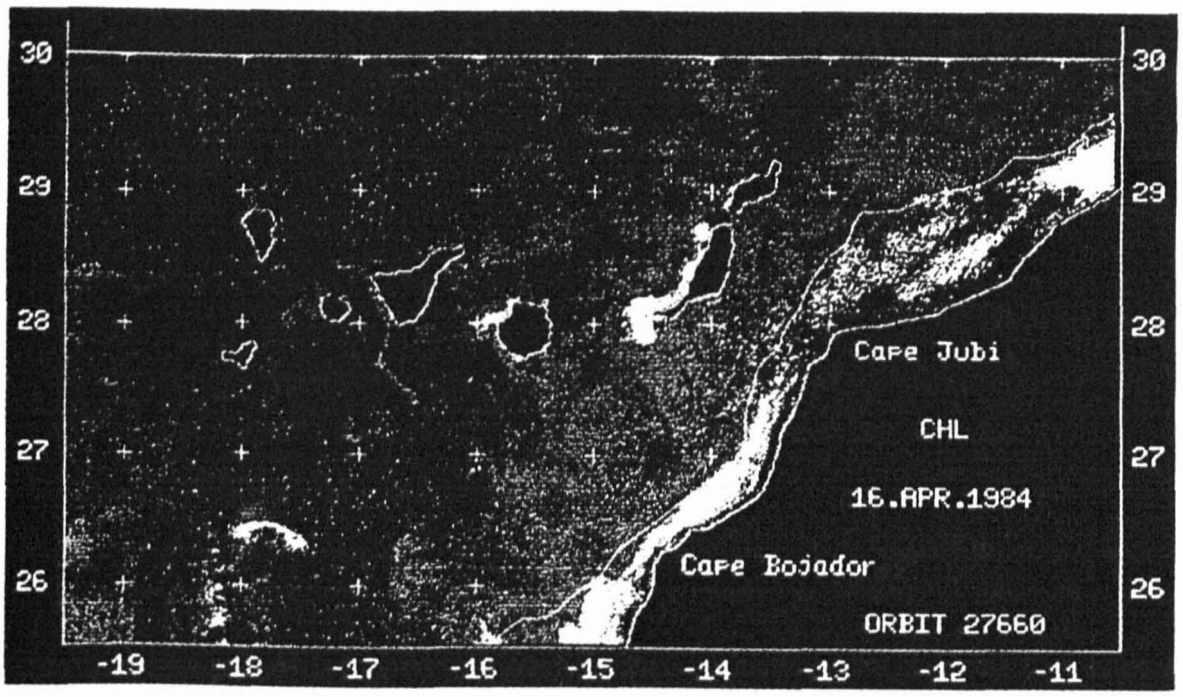


Figure 12. As figure 2, but on 16 April 1984.

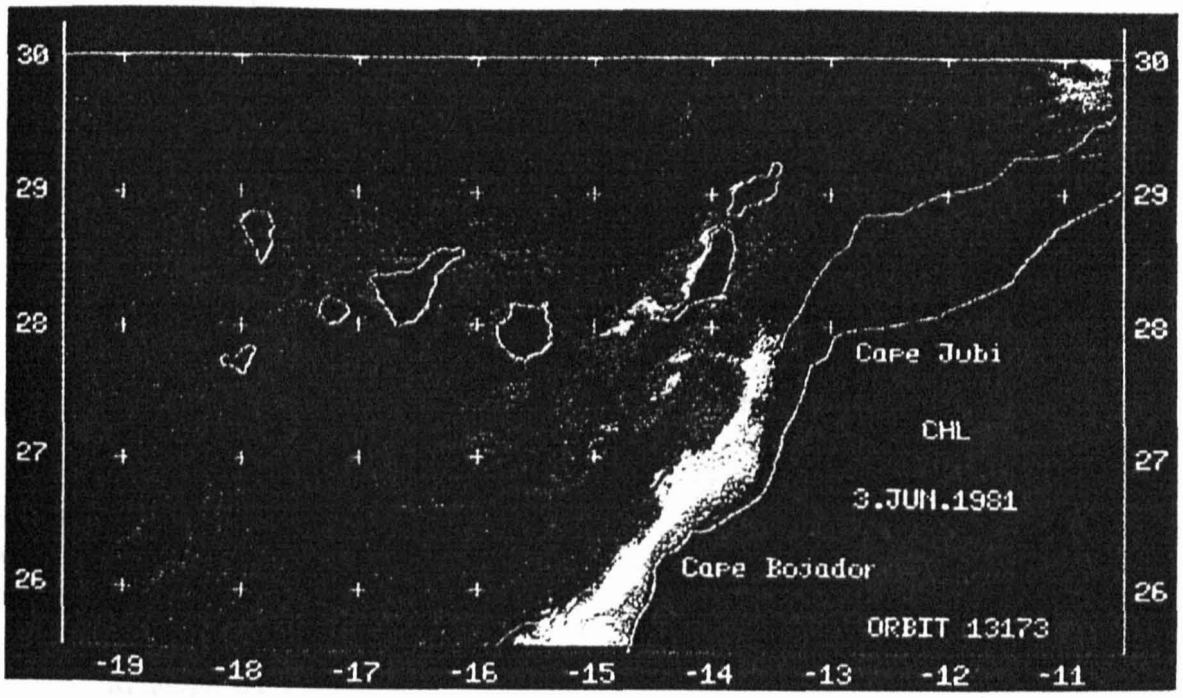


Figure 13. As figure 2, but on 3 June 1981.

## 4. Conclusions

We have analysed the whole archive of CZCS data to determine the seasonal variability of recurrent phytoplankton pigment patterns in the region of the Canary Islands and to infer the physical mechanisms which explain these patterns.

The two main phytoplankton pigment patterns in the Canary Islands area, associated with individual islands and with the north-west African coastal upwelling system, show different seasonal behaviour. Cyclonic and anticyclonic eddies are the main features associated with the islands, being present downstream of the islands

© Del documento, los autores. Digitalización realizada por ULPGC. Biblioteca Universitaria, 2009

in all seasons. This suggests that the speed of the Canary Current is always strong enough to develop *streets* of eddies. The cyclonic eddy associated with Gran Canaria is always attached to the north-west or west coast of the island by a lee filament, its horizontal length scale being similar to the diameter of the island, and a high phytoplankton pigment content is present either at its periphery or its core. Anticyclonic eddies are visible only by the indirect effects of their circulation on adjacent contrasting water masses provided by the upwelling filaments which stretch from the African coast to the islands. Cyclonic and anticyclonic eddies show sharply defined cores and have clearly defined spatial extents.

Another main feature associated with the islands is a westward filament stretching from a region of enrichment off the west coast of Fuerteventura. This upwelling filament generally appears at the same time as the upwelling filaments off north-west Africa, suggesting that this feature is caused by strong winds blowing alongshore Fuerteventura.

Upwelling filaments stretching from the African coast into the islands characterize the pattern associated with the influence of the continental upwelling system over the ocean surrounding the islands. They are present in summer and early fall when strong Trade Winds blow over the area. Upwelling filaments fundamentally stretch off Cape Jubi, Cape Bojador and somewhere in between. Thus, the spatial distribution of the filaments appears in most cases to be closely related to the coastal topography, bathymetry of the African coast, and a permanent cyclonic eddy.

During winter, a high phytoplankton pigment concentration is present in the whole area, apparently due to a phytoplankton bloom. This high phytoplankton pigment content is reduced in early spring, but still remains visible around the coasts of the islands.

## Acknowledgments

This work is based on results obtained in the framework of the Ocean Colour European Archive Network (OCEAN) Project, which was established in 1990 as a co-operation between the Joint Research Centre (JRC) of the European Commission (EC), with the support of Directorate General XI of the EC and the European Space Agency (ESA).

We express our gratitude to our colleagues in the Marine Environment (ME) Unit of the Institute for Remote Sensing Applications (IRSA) at the JRC EC and in other organizations involved in the OCEAN Application Demonstration Programme (ADP) who contributed in one way or another to the successful development of the Project.

## References

ARÍSTEGUI, J., HERNÁNDEZ-LEÓN, S., GÓMEZ, M., MEDINA, L., OJEDA, A., and TORRES, S., 1989, Influence of the north trade winds on the biomass and production of neritic plankton around Gran Canaria island. *Scientia Marina*, **53**, 223–229.

ARÍSTEGUI, J., SANGRÁ, P., HERNÁNDEZ-LEÓN, S., CANTÓN, M., HERNÁNDEZ-GUERRA, A., and KERLING, J. L., 1994, Island-induced eddies in the Canary Islands. *Deep-Sea Research*, **41**, 1509–1525.

ARÍSTEGUI, J., TETT, P., HERNÁNDEZ-GUERRA, A., BASTERRETXEA, G., MONTERO, M. F., WILD, K., SANGRÁ, P., HERNÁNDEZ-LEÓN, S., CANTÓN, M., GARCÍA-BRAUN, J. A., PACHECO, M., and BARTON, E. D., 1997, The influence of island-generated eddies on chlorophyll distribution: a case study around Gran Canaria. *Deep-Sea Research*, **44**, 71–96.

© Del documento, los autores. Digitalización realizada por ULPGC. Biblioteca Universitaria, 2009

BOYER, D. L., 1970, Flow past a right circular cylinder in a rotating frame. *Journal of Basic Engineering*, **92**, 430–436.

BOYER, D. L., and DAVIES, P. A., 1982, Flow past a circular cylinder on a beta plane. *Philosophical Transactions of the Royal Society* A, **306**, 533–556.

BOYER, D. L., DAVIES, P. A., HOLLAND, W. R., BIOLLEY, F., and HOMJI, H., 1987, Stratified rotating flow over and around isolated three-dimensional topography. *Philosophical Transactions of the Royal Society* A, **322**, 213–241.

BOYER, D. L., KMETZ, M. L., SMATHERS, L., CHABERT D'HIERES, G., and DIDELLE, H., 1984, Rotating open channel flow past right circular cylinders. *Geophysical and Astrophysical Fluid Dynamics*, **30**, 271–304.

BOYER, D. L., and TAO, L., 1987, On the motion of linearly-stratified rotating fluids past capes. *Journal of Fluid Mechanics*, **180**, 429–449.

BRICAUD, A., and MOREL, A., 1987, Atmospheric corrections and interpretation of marine radiances in CZCS imagery: use of a reflectance model. *Oceanologica Acta*, **7**, 33–50.

CHABERT D'HIERES, G., DAVIES, P. A., and DIDELLE, H., 1989, A laboratory study of the lift forces on a moving solid obstacle. *Dynamics of Atmosphere and Oceans*, **13**, 47–75.

CHOPRA, K. P., 1973, Atmospheric and oceanic flow problems introduced by islands. *Advances in Geophysics*, **16**, 297–421.

DAVIES, P. A., and MOFOR, L. A., 1990, Observations of flow separation by an isolated island. *International Journal of Remote Sensing*, **11**, 767–782.

DE LEÓN, A. R., and BRAUN, J. G., 1973, Ciclo anual de la producción primaria y su relación con los nutrientes en aguas Canarias. *Boletín del Instituto Español de Oceanografía*, **167**, 1–24.

EMERY, A. R., 1972, Eddy formation from an oceanic island: ecological effects. *Caribbean Journal of Science*, **12**, 121–126.

FALKOWSKI, P. G., ZIEMMAN, D., KOLBER, Z., and BIENFANG, P. K., 1991, Role of eddy pumping in enhancing primary production in the ocean. *Nature*, **352**, 55–58.

FIEKAS, V., ELKEN, J., MÜLLER, T. J., AITSAM, A., and ZENK, W., 1992, A view of the Canary Basin thermocline circulation in winter. *Journal of Geophysical Research*, **97**, 12495–12510.

GENIN, A., DAYTON, P. K., LONSDALE, P. F., and SPIESS, F. N., 1986, Corals on seamount peaks provide evidence of current acceleration over deep sea topography. *Nature*, **332**, 59–61.

GORDON, H. R., BROWN, J. W., and EVANS, R. H., 1988, Exact Rayleigh scattering calculations for use with the Nimbus-7 Coastal Zone Color Scanner. *Applied Optics*, **27**, 862–871.

HERNÁNDEZ-GUERRA, A., ARÍSTEGUI, J., CANTÓN, M., and NYKJÆR, L., 1993, Phytoplankton pigment patterns in the Canary Islands area as determined using Coastal Zone Colour Scanner data. *International Journal of Remote Sensing*, **14**, 1431–1437.

HEYWOOD, K. J., BARTON, E. D., and SIMPSON, J. H., 1990, The effects of flow disturbance by an oceanic island. *Journal of Marine Research*, **48**, 55 73.

HOGG, N. G., KATZ, E. J., and SANDFORD, T. B., 1978, Eddies, islands and mixing. *Journal of Geophysical Research*, **83**, 2921–2938.

HUGHES, P., and BARTON, E. D., 1974, Stratification and water mass structure in the upwelling area off northwest Africa in April/May 1969. *Deep-Sea Research*, **21**, 611–628.

KLEIN, B., and SIEDLER, G., 1989, On the origin of the Azores Current. *Journal of Geophysical Research*, **94**, 6159–6168.

MOLINA, R., and LAATZEN, F. L., 1986, Hidrología en la región comprendida entre las Islas Canarias orientales, Marruecos y la Isla Madeira. Campaña 'Norcanarias I'. *Boletín Instituto Español de Oceanografía*, **3**, 1–16.

MOLINA, R., and LAATZEN, F. L., 1989, Hidrografía en la región Canaria. Campaña 'Canarias I'. *Boletín Instituto Español de Oceanografía*, **5**, 71–86.

NYKJAER, L., and VAN CAMP, L., 1994, Seasonal and interannual variability of coastal upwelling along northwest Africa and Portugal from 1981 to 1991. *Journal of Geophysical Research*, **99**, 14197–14207.

PATTIARATCHI, C., JAMES, A., and COLLINS, M., 1986, Island wakes and headland eddies: a comparison between remotely sensed data and laboratory experiments. *Journal of Geophysical Research*, **92**, 783–794.

PATZER, W. C., 1969, Eddies in Hawaiian waters, Report N HIG-69-8, Institute of Geophysics, University of Hawaii.

© Del documento, los autores. Digitalización realizada por ULPGC. Biblioteca Universitaria, 2009

SANGRÁ, P., 1995, Perturbación de un flujo geofísico por un obstáculo: aplicacin a la isla de Gran Canaria. PhD Thesis, Universidad de Las Palmas de Gran Canaria.

SPETH, P., and DETLEFSEN, H., 1982, Meteorological influences on upwelling off northwest Africa. In *The Canary Current: Studies of an Upwelling System, Rapports et Procs-Verbaux des Runions, Conseil International pour L'exploration de la Mer* volume 180, edited by G. Hempel, pp. 29–35.

STRAMMA, L., 1984, Geostrophic transport in the warm water sphere of the eastern subtropical North Atlantic. *Journal of Marine Research*, **42**, 537–558.

STRAMMA, L., and SIEDLER, G., 1988, Seasonal changes in the North Atlantic subtropical gyre. *Journal of Geophysical Research*, **93**, 8111–8118.

STURM, B., 1981, The atmospheric correction of remotely sensed data and the quantitative determination of suspended matter in marine water surface layers. In *Remote Sensing in Meteorology, Oceanography and Hydrology*, edited by A. P. Cracknell (Chichester: Ellis Horwood), pp. 163–197.

VAN CAMP, L., NYKJÆR, L., MITTELSTAEDT, E., and SCHLITTENHARDT, P., 1991, Upwelling and boundary circulation off northwest Africa as depicted by infrared and visible satellite observations. *Progress in Oceanography*, **26**, 357–402.

WOOSTER, W. S., BAKUN, A., and MCLAIN, D. R., 1976, The seasonal upwelling cycle along the eastern boundary of the North Atlantic. *Journal of Marine Research*, **34**, 131–141.

© Del documento, los autores. Digitalización realizada por ULPGC. Biblioteca Universitaria, 2009

PERGAMON

Deep-Sea Research I 46 (1999) 1969–1984

DEEP-SEA RESEARCH
PART I

# Mesoscale distribution of fish larvae in relation to an upwelling filament off Northwest Africa

J.M. Rodríguez[a,*], S. Hernández-León[b], E.D. Barton[c]

[a]*Instituto Español de Oceanografía, Centro Oceanográfico de Canarias, Ctra. de San Andrés s/n, 38120 Santa Cruz de Tenerife, Spain*

[b]*Universidad de Las Palmas de Gran Canaria, Facultad de Ciencias del Mar, Campus Universitario de Tafira, 35017 Las Palmas de Gran Canaria, Spain*

[c]*University of Wales, School of Ocean Sciences, Bangor, Wales, UK*

Received 16 March 1998; received in revised form 4 May 1999; accepted 4 May 1999

**Abstract**

Fish eggs and larvae were studied in relation to an upwelling filament off Northwest Africa, near the Canary Islands, during August 1993. The filament was entrained around a quasi-permanent cyclonic eddy of diameter 100 km. The sampled ichthyoplanktonic community was dominated by neritic larvae, 94.2% of which were captured in the oceanic area. Horizontal distributions of neritic and oceanic larvae were strongly influenced by the oceanographic features characteristic of the coastal margin. Neritic larvae were associated with upwelling and filament structures, while oceanic larvae were strongly excluded from these features. The results suggest that coastal upwelling and filaments are mechanisms of transport for neritic ichthyoplankton into oceanic waters, that sardine larvae are good tracers of offshore movements of upwelled waters, and that the cyclonic eddy functions as a larval nursery ground for neritic fish species. © 1999 Elsevier Science Ltd. All rights reserved.

## 1. Introduction

Filaments are extensions of coastally upwelled water that reach hundreds of kilometres offshore. They are associated with narrow, elongated currents arising on the continental shelf, which transport the upwelled water large distances away from the coast (Brink, 1983). These structures have been referred to as tongues, plumes or jets, but the term *upwelling filament* (Flament et al., 1985) best describes their shape and relationship with regions of coastal upwelling. They are frequently observed in

* Corresponding author. Fax: 0034-2-25-49-554.
*E-mail address:* josema@ieo.rcanaria.es (J.M. Rodriguez)

0967-0637/99/$ - see front matter © 1999 Elsevier Science Ltd. All rights reserved.
PII: S0967-0637(99)00036-9

© Del documento, los autores. Digitalización realizada por ULPGC. Biblioteca Universitaria, 2009

satellite images of the California Current system (Bernstein et al., 1977; Flament et al., 1985) and the coastal margin of other eastern boundary currents of the subtropical gyres, such as the Canary Current (Nykjær et al., 1988; Nykjær and Van Camp, 1989; Van Camp et al., 1991; Hagen et al., 1996) or the Benguela Current (Armstrong et al., 1987; Shillington et al., 1990). They represent one of the persistent and dominant components of the dynamics of these eastern boundary current regions (Chavez et al., 1991). Studies carried out in situ have revealed that filaments observed in satellite images are the superficial manifestation of hydrographic anomalies that may extend to depths greater than 100 m. They are associated with strong seaward flows with velocities of 18–80 cm/s (Strub et al., 1991), and they have clear signs of physico-chemical and biological identity (Jones et al., 1991). Most of these studies have been carried out in the California upwelling region (e.g. Traganza et al., 1980,1981; Kosro and Huyer, 1986). Filaments have also been studied in the Benguela upwlling (e.g. Shillington et al., 1990; Duncombe Rae et al., in press; Nelson et al. (1998) and in the Canaries upwelling region (e.g. Hagen et al., 1996). Barton et al. (1998) and Navarro-Pérez and Barton (1998) report a multi-disciplinary study of a filament south of the Canary Islands, of which the present work forms part.

Upwelling filaments are offshore transport mechanisms for nutrients and plankton (Nelson et al., 1998), and fish larvae are amongst the plankton components susceptible to being swept away by the upwelling filaments (Duncombe Rae et al., in press). This may have important implications for the dynamics of neritic fish populations, whose larvae may be displaced offshore, far from their natural habitat. Entrainment of larvae in filaments may, moreover, provide useful tracers for studies of waters over the continental margin. Nevertheless, in order to use the fish larvae as tracers in flow patterns, it must be remembered that, apart from horizontal advection (Bishai, 1960; Norcross and Shaw, 1984; John, 1985), other factors, such as the location and strategy of spawning (Parrish et al., 1981; Norcross and Shaw, 1984; John, 1985; Myers and Drinkwater, 1989; Kim and Bang, 1990), their vertical distribution in the water column (John, 1985; Frank et al., 1992; Olivar and Sabatés, 1997) and their migratory behaviour (Parrish et al., 1981; Myers and Drinkwater, 1989), are involved in their horizontal distribution. It is probably also necessary to take account of the larval abundance because predation and natural mortality have a greater relative effect on larval populations, which are sparsely distributed in the water column.

In this paper, we study the relationship between ichthyoplankton, coastal upwelling and an upwelling filament off Northwest Africa. We have paid particular attention to the two species that may be considered to be *typical* of this coastal upwelling: the European sardine, *Sardina pilchardus*, and the European anchovy, *Engraulis encrasicolus*. These are two neritic pelagic species, with pelagic spawning, and their larvae were the most numerous in our catches.

## 2. Methods

Ichthyoplankton distributions data were obtained during the first part of the "Canarias 9308" cruise, carried out between 9 and 16 August 1993 on board RV

© Del documento, los autores. Digitalización realizada por ULPGC. Biblioteca Universitaria, 2009

*Hespérides* near 27°N, just south of the Canary Islands. Stations were arranged in six transects at about 30 km separation parallel to the coast and practically perpendicular to the filament (Fig. 1a). In total, 47 stations were sampled for ichthyoplankton.

Hydrographic conditions were sampled at every station with a SeaBird CTD (Navarro-Pérez et al., 1994), and at 47 stations a WP-2 net, with an estimated filtering efficiency of 94% (UNESCO, 1968), was used to collect the ichthyoplankton. The hauls sampled the water column vertically from 200 m (or from 5 to 10 m above the sea floor in shallower waters) to the surface at each station. The samples were preserved in 5% buffered formalin. Once in the laboratory, samples were sorted, and both ichthyoplanktonic components (eggs and larvae) were counted. Larvae were identified to the lowest taxonomic level possible, and sardine and anchovy larvae were measured to 0.1 mm with the aid of a micrometer eyepiece. The larvae data were standardised to number/10 $m^2$ (Smith and Richardson, 1979).

To investigate if there was any relationship between the horizontal distributions of neritic larvae and the oceanographic features associated with the upwelling and filament, relationships between the abundance of these larvae and the temperature were analysed using linear correlation. Particular emphasis was placed on sardine, the most common neritic taxon. Data were transformed logarithmically beforehand to normalise them and to stabilise their variances (Ibanez and Seguin, 1972).

The larvae were grouped into three categories based on the habitat of the adults and the region in which they reproduce: "neritic", "oceanic" and "other" (Table 1).

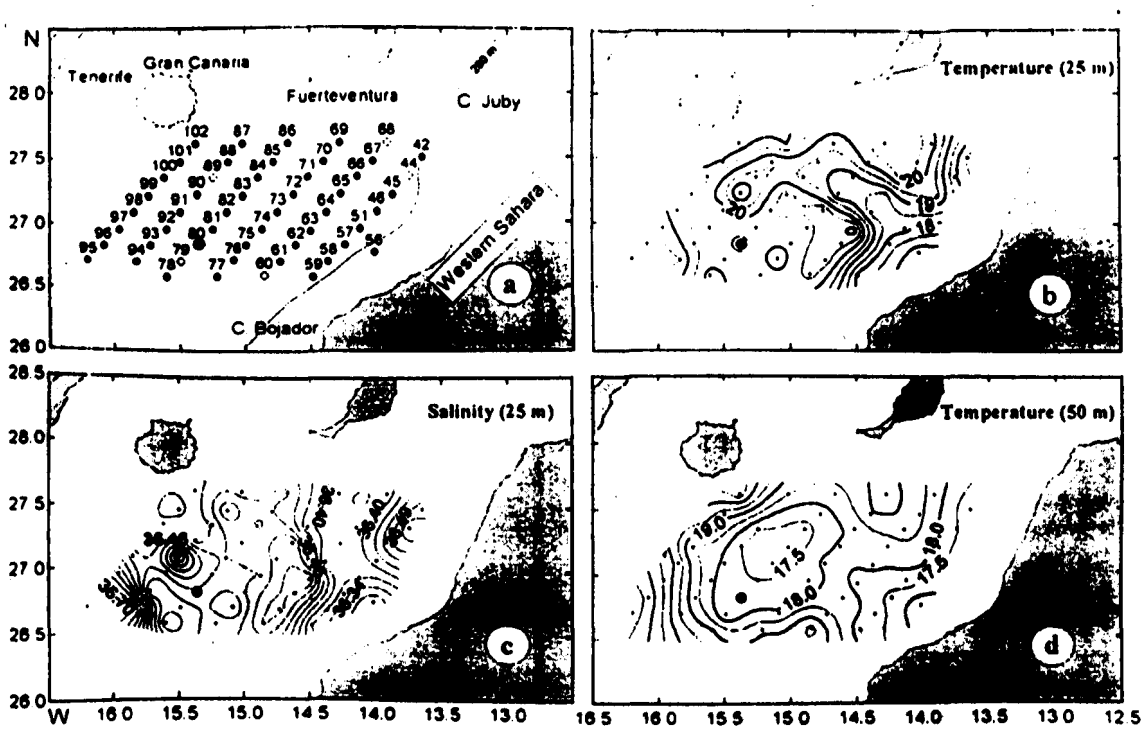


Fig. 1. (a) Study area in the northwest African upwelling region showing the sampling stations, (●) stations sampled for ichthyoplankton, and horizontal distribution of (b) temperature (°C) at 25 m depth, (c) salinity (standard units) at 25 m deph and (d) temperature (°C) at 50 m depth.

© Del documento, los autores. Digitalización realizada por ULPGC. Biblioteca Universitaria, 2009

Table 1
Taxonomic list of larvae caught, their origin (N neritic; O other; Oc Oceanic) and the percentage contribution of each species to the total numbers

| Species | Origin | % |
|---|---|---|
| Family Clupeidae | | |
| *Sardina pilchardus* (Walbaum, 1792) | N | 27.64 |
| *Sardinella aurita* Valenciennes, 1847 | N | 0.54 |
| *Sardinella maderensis* (Lowe, 1838) | N | 0.18 |
| Family Engraulidae | | |
| *Engraulis encrasicolus* (Linnaeus, 1758) | N | 7.50 |
| Family Gonostomatidae | | |
| *Cyclothone acclinidens* Garman, 1899 | | 0.09 |
| *Cyclothone alba*? Brauer, 1906 | Oc | 0.09 |
| *Cyclothone braueri* Jespersen and Tåning, 1926 | Oc | 4.25 |
| *Cyclothone microdon* Günther, 1878 | Oc | 0.09 |
| *Cyclothone pallida* Brauer, 1902 | Oc | 0.09 |
| *Cyclothone* spp | Oc | 0.18 |
| *Gonostoma atlanticum* Norman, 1930 | Oc | 0.18 |
| *Gonostoma denudatum* Rafinesque, 1810 | Oc | 0.09 |
| *Gonostoma elongatum* Günther, 1878 | Oc | 0.54 |
| *Gonostoma* sp d | Oc | 0.36 |
| Unidentified spp | Oc | 0.36 |
| Family Sternoptychidae | | |
| *Argyropelecus hemigymnus* Cocco, 1829 | Oc | 0.54 |
| *Argiropelecus* sp | Oc | 2.98 |
| *Maurolicus muelleri*? (Gmelin, 1788) | Oc | 0.09 |
| *Sternoptyx pseudoscura* Baird, 1791 | Oc | 0.27 |
| *Sternoptyx* spp | Oc | 0.27 |
| *Valenciennellus tripunctulatus* (Esmark, 1871) | Oc | 0.18 |
| Family Photichthydae | | |
| *Vinciguerria attenuata* (Cocco, 1838) | Oc | 0.09 |
| *Vinciguerria nimbaria* (Jordan and Williams, 1895) | Oc | 0.09 |
| *Vinciguerria poweriae* (Cocco, 1838) | Oc | 0.45 |
| *Vinciguerria* spp | Oc | 0.54 |
| Family Chauliodontidae | | |
| *Chauliodus sloani* Schneider, 1801 | Oc | 0.09 |
| Family Stomiidae | | |
| *Stomias boa boa* (Risso, 1810) | Oc | 0.18 |
| Family Melanostomiidae | | |
| Unidentified spp | Oc | 0.09 |
| Family Argentinidae | | |
| *Nansenia oblita* (Facciolá, 1887) | Oc | 0.09 |
| Family Myctophidae | | |
| *Benthosema suborbitale* (Gilbert, 1913) | Oc | 0.90 |
| *Ceratoscopelus maderensis* (Lowe, 1839) | Oc | 1.81 |
| *Ceratoscopelus warmingii* (Lütken, 1892) | Oc | 0.63 |
| *Diaphus holti* Tåning, 1918 | Oc | 0.54 |
| *Diaphus rafinesquii* (Cocco, 1838) | Oc | 0.27 |
| *Diaphus* sp | Oc | 0.09 |
| *Diaphus* sp 5 | Oc | 0.09 |
| *Diaphus* sp 15 | Oc | 0.63 |

© Del documento, los autores. Digitalización realizada por ULPGC. Biblioteca Universitaria, 2009

Table 1 (*continued*)

| Species | Origin | % |
|---|---|---|
| *Diaphus* spp | Oc | 1.54 |
| *Diogenichthys atlanticus* (Tåning, 1928) | Oc | 2.62 |
| *Hygophum benoiti* (Cocco, 1838) | Oc | 0.09 |
| *Hygophum hygomii* (Lütken, 1892) | Oc | 0.09 |
| *Hygophum reinhardtii* (Lütken, 1892) | Oc | 0.54 |
| *Lampanyctus pusillus* (Johnson, 1890) | Oc | 0.36 |
| *Lampanyctus* spp | Oc | 5.24 |
| *Lepidophanes gaussi* (Brauer, 1906) | Oc | 0.09 |
| *Lobianchia dofleini* (Zugmayer, 1911) | Oc | 0.63 |
| *Lobianchia gemellarii* (Cocco, 1838) | Oc | 0.18 |
| *Myctophum nitidulum* (Garman, 1899) | Oc | 0.09 |
| *Myctophum punctatum* (Rafinesque, 1810) | Oc | 0.45 |
| *Notolychnus valdiviae* (Brauer, 1904) | Oc | 2.80 |
| *Notoscopelus* sp | Oc | 0.09 |
| *Symbolophorus rufinus* (Tåning, 1928) | Oc | 0.05 |
| *Symbolophorus veranyi* (Moreau, 1888) | Oc | 0.63 |
| Unidentified spp | Oc | 1.26 |
| Family Scopelarchidae | | |
| *Benthalbella infans* (Zugmayer, 1911) | Oc | 0.36 |
| Family Paralepididae | | |
| *Lestidiops jayakari* (Boulenger, 1889) | Oc | 0.27 |
| *Paralepis atlantica atlantica* Krøyer, 1868 | Oc | 0.27 |
| *Sudis hialina* Rafinesque, 1810 | Oc | 0.09 |
| Unidentified spp | Oc | 0.09 |
| Family Muraenidae | | |
| Unidentified spp | N | 0.09 |
| Family Nettastomatidae | | |
| Unidentified spp | Oc | 0.09 |
| Family Scomberosocidae | | |
| *Scomberosox saurus saurus* (Walbaum, 1792) | Oc | 0.09 |
| Family Melamphaidae | | |
| *Melamphaes simus* Ebeling, 1962 | Oc | 0.09 |
| *Melamphaes* spp | Oc | 0.18 |
| Family Serranidae | | |
| *Anthia santhias* (Linnaeus, 1758) | N | 2.89 |
| *Serranus cabrilla* (Linnaeus, 1758) | N | 0.18 |
| Unidentified spp | N | 0.18 |
| Family Carangidae | | |
| Unidentified spp | N | 1.08 |
| Family Sparidae | | |
| *Pagellus acarne*? (Risso, 1826) | N | 0.54 |
| *Pagrus pagrus* (Linnaeus, 1758) | N | 0.36 |
| *Pagrus* spp | N | 0.81 |
| Unidentified spp | N | 1.45 |
| Family Labridae | | |
| Subfamily Corinae | | |
| *Coris julis* (Linnaeus, 1758) | N | 0.81 |
| *Xyrichthys novacula* (Linnaeus, 1758) | N | 0.18 |

(*continued on next page*)

© Del documento, los autores. Digitalización realizada por ULPGC. Biblioteca Universitaria, 2009

Table 1 (*continued*)

| Species | Origin | % |
|---|---|---|
| Subfamily Labrinae | | |
| *Labrus* sp | N | 0.09 |
| Unidentified spp | N | 0.09 |
| Family Trachinidae | | |
| *Trachinus draco* Linnaeus, 1758 | N | 0.18 |
| Family Gempylidae | | |
| *Diplospinus multistriatus* Maul, 1948 | Oc | 0.09 |
| Unidentified spp | Oc | 0.27 |
| Family Trichiuridae | | |
| *Lepidopus caudatus* (Eupharsen, 1788) | Oc | 0.18 |
| Unidentified spp | Oc | 0.09 |
| Family Scombridae | | |
| *Auxis* sp | Oc | 0.54 |
| Family Gobiidae | | |
| Unidentified spp | N | 4.97 |
| Family Callionymidae | | |
| *Callionymus reticulatus* Valenciennes, 1837 | N | 0.09 |
| Callionymus spp | N | 0.09 |
| Family Blenniidae | | |
| Unidentified spp | N | 0.09 |
| Family Sphyraenidae | | |
| *Sphyraena viridens* Cuvier. 1829 | N | 0.09 |
| Family Mugilidae | | |
| Unidentified spp | N | 0.09 |
| Family Scorpaenidae | | |
| *Scorpaena* sp | O | 0.18 |
| Unidentified spp | O | 0.81 |
| Family Bothidae | | |
| *Arnoglossus imperialis* Rafinesque, 1810 | N | 0.36 |
| *Arnoglossus thori* (Kyle, 19113) | N | 0.63 |
| *Arnoglossus* spp | N | 1.72 |
| *Bothus podas maderensis* Lowe, 1834 | N | 0.09 |
| Family Soleidae | | |
| *Microchirus ocellatus* Linnaeus, 1758 | N | 1.63 |
| Family Cynoglossidae | | |
| *Symphurus nigrescens* (Rafinesque, 1810) | N | 0.81 |

Neritic refers to the larvae of fish species whose adults normally inhabit and reproduce inside the limits of the neritic region (<200 m depth). Oceanic indicates the larvae of fish species which, in their adult stage, normally inhabit and reproduce in the oceanic region (>200 m depth). Other includes unidentified specimens and those identified only to the level of family, it includes both neritic and oceanic species. The species list of fish larvae was prepared following Whitehead et al. (1984).

© Del documento, los autores. Digitalización realizada por ULPGC. Bibliotecas Universitaria, 2009

## 3. Results

### 3.1. Hydrographic conditions

During the sampling period, an upwelling filament was present at approximately 27°N, with its origin situated on the continental shelf; it extended over 150 km towards the southeast of Gran Canaria Island (Canary Islands) and was associated with a cyclonic eddy 100 km in diameter (Barton et al., 1998; Navarro-Pérez and Barton, 1998). Strong offshore flow occurred on its northern edge, and it was bounded by strong temperature gradients to both north and south. The filament is a recurrent mesoscale feature in this area; in the present case it was observed in AVHRR imagery throughout August with relatively little change. The near-surface temperature map (Fig. 1b) shows the filament itself indicated by a plume of cooler (< 19°C) water, which extends from the African coast towards Gran Canaria and then curves cyclonically towards the south. The filament is less apparent in the near-surface salinity, which is more homogeneous (Fig. 1c). At deeper levels, e.g. 50 m, the temperature field reveals an oval-shaped, cold-core (< 17.5°C) cyclonic eddy centred south of the filament (Fig. 1d). The filament structure is clearly entrained around the cyclonic eddy, which is likely a quasi-permanent feature topographically trapped in the trough south of the sill between the Canary Islands and Africa (Barton et al., 1998; Navarro-Pérez and Barton, 1998).

### 3.2. Taxonomic composition of fish larvae

In total, 1107 fish larvae were caught. The neritic larvae dominated the fish larvae community and represented 56.1% of the catches, while 36.9% belonged to the oceanic group and 7% to the group other. Most of the neritic larvae (94.2%) were caught in the oceanic region, beyond what might be considered the boundary of their normal distribution, the 200 m isobath. In all, 76 species and 19 higher taxonomic categories pertaining to 33 fish families were identified (Table 1). The most numerous family was the Clupeidae (28.4% of total larvae catches). The most common species of fish larvae were *Sardina pilchardus*, 27.6%, and *Engraulis encrasicolus*, 7.5% (Table 1). The most diverse family, however, was the Myctophidae (Table 1). Nine of the families whose catch contributed over 1% pertained to the neritic group, while only four belonged to the oceanic group.

### 3.3. Horizontal distribution of fish eggs and larvae

The horizontal distribution of fish eggs was sparse: only 283 eggs were captured overall, most of them (65.4%) at station 56, the only station sampled within the neritic region.

Sardine eggs constituted 42.0% of the total number of eggs collected, and all of them were obtained at the only station sampled over the continental shelf. However, not a single anchovy egg was observed. Spatially, spawning of both species is restricted to the shelf area in the northwest Africa upwelling region (Furnestin and

© Del documento, los autores. Digitalización realizada por ULPGC. Biblioteca Universitaria, 2009

Furnestin, 1959; Blackburn and Nellen, 1976; FAO, 1980). Temporally, the NW African sardine spawns throughout the year, with the main period of reproduction in winter and minimal spawning in summer (Furnestin, 1950; Furnestin and Furnestin, 1959; Delgado and Fernández, 1985; Roy et al., 1989). In constrast, the anchovy in this area has its principal spawning period in summer (Furnestin and Furnestin, 1959).

On the basis of the physical oceanography, one would expect opposing tendencies in the distributions of the two types of larvae, neritic and oceanic, present in our sampling area. Abundances of neritic larvae are expected to diminish with distance offshore, while the opposite trend is expected for the oceanic larvae. As a result of this, the two types of larvae are considered separately.

Two areas were identified in the horizontal distribution of neritic larvae (Fig. 2a): a *coastal area* and an *oceanic area*. The *coastal area* included the two transects nearest to the African shelf, the external limit of which approximately coincided with the boundary of the upwelling; the *oceanic area* included the remaining transects. If we compare this distribution with those of temperature at 25 (Fig. 1b) or 50 m depth (Fig. 1d), we can see that it was strongly influenced by upwelling in the coastal area and by the filament in the oceanic area. Correlation analysis between larval abundance and near-surface temperatures ($r = -0.41$, $p = 0.005$, $n = 45$, where $n$ is the number of degrees of freedom) clearly showed that neritic larvae were associated with upwelling and filament structures. The negative correlation coefficient implies an inverse relationship among variables, i.e. the lower temperature of more recently upwelled coastal waters was related to a higher abundance of neritic larvae. The maximum abundance

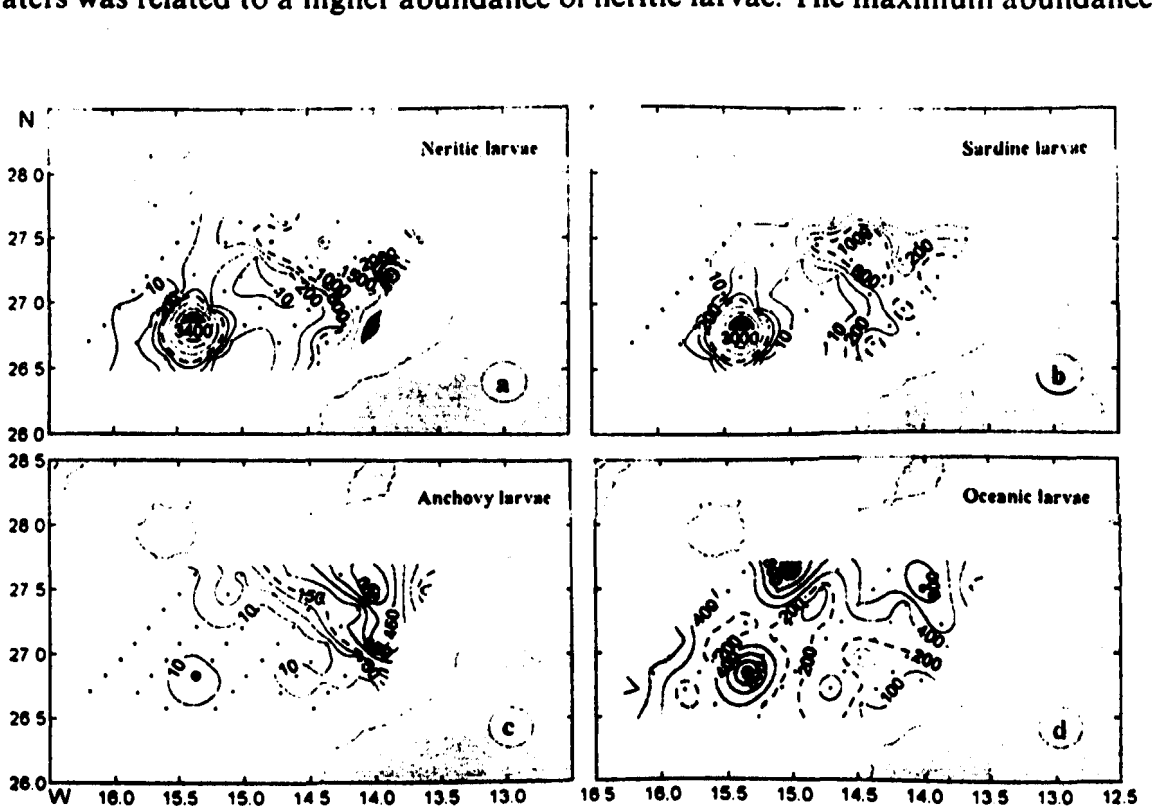


Fig. 2. Horizontal distribution of larvae (larvae/10 m$^2$) of (a) neritic group, (b) sardine, (c) anchovy and (d) oceanic species.

© Del documento, los autores. Digitalización realizada por ULPGC. Biblioteca Universitaria, 2009

(3787 larvae/10 $m^2$) for these larvae was recorded at station 80, located in the oceanic area.

The horizontal distribution of sardine larvae (Fig. 2b) was very similar to the one displayed for the entire group of neritic larvae and practically delineated the coastal upwelling and the filament. Similarly, the relation between sardine distribution and near-surface temperature was significant ($r = -0.60$, $p = < 0.001$, $n = 45$). The maximum value (3447 larvae/10 $m^2$) for the larval abundance of sardine was recorded at station 80, located on the outer edge of the cyclonic eddy (Fig. 1a). The mean length of the sardine larvae increased roughly with distance across the upwelling and along the filament (Fig. 3). The largest mean size was encountered at station 80, which temporally was furthest removed from the place of origin of these larvae. At this station sardine larvae ranged in length from 6.0 to 16.5 mm, with a mean of 10.6 mm for the 68 specimens measured (S.D. = 2.84).

The length $L$ of larvae, supposing a linear growth model, can be expressed as

$$L = L_{min} + rt + s,$$

where $L_{min}$ is the minimum size of newly hatched larvae, $r$ is the growth rate, $t$ is time elapsed since hatching, and $s$ is the shrinkage of specimens caused by the preservation technique (Theilacker, 1980). For sardine larvae, Russell (1976) reported a minimum size of $L_{min} = 3.3$ mm, identical to the smallest larvae in our samples. Blaxter and Hunter (1982) proposed growth rates for clupeoid larvae in the range 0.3–1 mm/d, so we assume an intermediate value of $r = 0.65$ mm/d. We ignore shrinkage as insignificant ($s = 0$). Substituting the above values into the equation suggests that larvae captured at station 80 would have an age between 4.2 and 20.3 d with a mean of 11.2 d.

Anchovy larvae were practically absent in the southern section of the sampling area, and their horizontal distribution showed a strong relationship with the filament, occurring principally to its north, i.e. to the offshore side of the current jet (Fig. 2c). The mean size of anchovy larvae was 10.1 mm (minimum 4 mm, maximum 19.2 mm, sample size 44 specimens; S.D. = 4.22). No significant variation in the size of these larvae was found with distance along the filament.

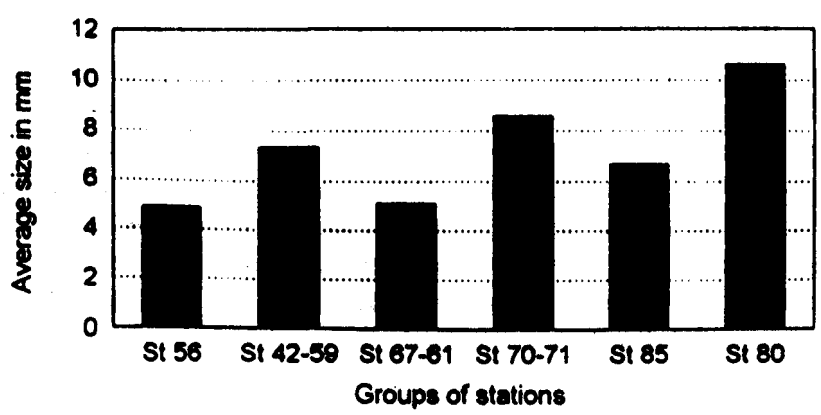


Fig. 3. Mean size of sardine larvae against distance across the upwelling and along the filament (indicative of elapsed time).

© Del documento, los autores. Digitalización realizada por ULPGC. Biblioteca Universitaria, 2009

For anchovy, a minimum size on hatching of 3–4 mm has been given by Russell (1976). We, therefore, assume $L_{min} = 3.5$ mm. Their growth rates estimated by Ré (1987) were in a range centred on $r = 0.41$ mm/d. For the mean size of larvae we sampled, the equation, ignoring shrinkage as previously, indicates a period of 16.1 d since hatching, 1.2 for the smallest and 38.3 for the largest. Regner (1985) found the period of embryonic development of these larvae was 2.7 d at a temperature of 17.14°C, close to the average surface layer (0–30 m) temperature over the shelf. The estimated times since spawning therefore range from 3.9 to 41.0 d with a mean estimate of 18.8 d.

Oceanic larvae decreased in abundance from the open sea towards the continental shelf (Fig. 2d). Their distribution pattern was also strongly influenced by the presence of the upwelling filament and the cyclonic eddy. In this case, the larvae were concentrated on the outer edge of the filament and eddy. The lowest and highest abundance values were registered in stations located approximately in the core and on the outer edge of the eddy, respectively.

## 4. Discussion

The results of the "Canarias 9308" cruise suggest a close relationship between ichthyoplankton distributions and oceanographic processes such as upwelling and the upwelling filament. This relationship was clearly demonstrated by horizontal distribution patterns and in the taxonomic composition of the larval assemblage.

### *4.1. Horizontal distribution of neritic larvae*

Neither the WP-2 sampling net used nor the vertical hauls carried out are ideal for precise quantitative sampling of fish larvae. The rigging of the net creates turbulence that can be detected by larvae, the most active of which may avoid capture (Smith and Richardson, 1979). The relatively slow towing speed and the small sample volume of the vertical haul-net render it most suitable for collecting eggs and early larval stages with minimal avoidance abilities (Heath, 1992). For these reasons, the larval abundance data may underestimate the true in situ values to some extent.

The horizontal distribution pattern of neritic larvae (Fig. 2a) was strongly related to the oceanographic conditions that prevailed during the sampling period. The coastal area represents typical coastal upwelling which results directly from the offshore displacement of near-surface water masses by Ekman transport. In the southern part of the area away from the influence of the filament, the neritic larvae transported offshore gradually decreased towards zero abundance near the offshore boundary of the upwelling. In the northern part, the upwelling, filament transported upwelled water beyond the limits of the upwelling itself, so that the neritic larvae were transported further offshore. The filament, entrained around the topographically trapped cyclonic eddy, trailed its load of fish larvae offshore. The maximum abundance for neritic larvae was found, as has already been seen, at station 80 located in the periphery of the eddy, the region of these cyclonic structures where fish larvae tend to

© Del documento, los autores. Digitalización realizada por ULPGC. Biblioteca Universitaria, 2009

concentrate (Lobel and Robinson, 1986,1988). The offshore transport of neritic larvae by the upwelling and filament is responsible for the predominance of these in the overall taxonomic composition of the sampled icthyoplanktonic community.

Our results indicate that the filament under study works as a mechanism transporting neritic fish larvae from the African coast offshore, similar to mechanisms suggested for zooplankton (Mackas et al., 1991) and established for phytoplankton (Jones et al., 1991; Strub et al., 1991) and ichthyoplankton (Duncombe Rae et al., in press) in other upwelling regions. With such transport, the larvae are displaced further offshore, outside the boundary of the upwelling itself, as defined by the upwelling front. Nevertheless, as Barton et al. (1998) suggest, a significant part of the offshore flow returns intact to the coastal zone by means of the cyclonic eddy around which the filament is entrained. This flow might represent a mechanism for the return of neritic larvae to the continental shelf (their place of origin), with an estimated recirculation time of about 7 d for a complete circuit of the system (Barton et al., 1998). The isolated maximum at station 80 may represent a parcel of upwelled water, containing high concentrations of neritic larvae, which has almost completed a circuit of the cyclonic eddy.

The relative high abundance of zooplankton in the waters of the filament and eddy in comparison to surrounding waters (Barton et al., 1998), the quasi-permanent nature of the eddy (Barton et al., 1998; Navarro-Pérez and Barton, 1998), the high concentration of neritic larvae found at station 80 on the southern edge of the cyclonic eddy, and the mean age of sardine larvae at that station and their increase in length (and age) along the filament support the idea (Bakun, 1998) that the filament and associated eddy constitute a favourable "fundamental triad" underlying the suitability of the region as a reproductive habitat (Bakun, 1996). In this way, the cyclonic eddy may provide a nursery ground for neritic fishes.

On the other hand, the filament might act as a one way transport mechanism for some neritic larvae from the African coast towards the Canary Islands. This may be supposed by taking into account the direction of the larval transport brought about by the filament (Fig. 2a) and the extent of this transport. As in this study (Figs. 1 and 2) the boundary of the filament has often been observed in close proximity to the southeast of Gran Canaria (Arístegui et al., 1994; Molina et al., 1996), presumably introducing with it the neritic larvae. These, which would conceivably reach the coasts of Gran Canaria (and clearly also Fuerteventura), might be displaced towards other islands by the cyclonic and anticyclonic eddies induced by the flow disturbance of the islands (Arístegui et al., 1994; Arístegui et al., 1997). Although this larval contribution may not be quantitatively important from the point of view of increasing the size of recruitment and, consequently, the size of neritic fish populations of the islands (a problem to be studied and evaluated), it may certainly serve to maintain the genetic flow, in this case unidirectional towards the Canary Islands. It could also have been used to colonise the islands by those fish species capable of occupying both types of habitat.

As for the species typical of this upwelling, the horizontal distribution of sardine larvae, the important presence of sardine eggs at the only neritic station sampled and the relatively low estimated age of the larvae suggest that the filament is transporting

© Del documento, los autores. Digitalización realizada por ULPGC. Biblioteca Universitaria, 2009

larvae spawned locally on the African shelf near the Canaries. This area was identified by Roy et al. (1989) as one of the main spawning areas for sardine.

Catches of anchovy larvae were practically limited to the northern side of the filament, i.e. to the offshore side of the current jet (Fig. 2c). This, the indicated age of the larvae and the total absence of eggs indicate that anchovy are spawning some significant distance to the north of the sampling region. Furnestin and Furnestin (1959) detected an important spawning area for this species north of Cape Juby. The eggs and larvae would be transported by the current, which, associated with the upwelling, flows southwards along the coast (Mittelstaedt, 1983) until it reaches the zone of influence of the filament. The eggs would have hatched along this route, and larvae would have been subject to offshore advection by Ekman transport and dispersion by lateral exchange across the upwelling front. On encountering the northern boundary of the filament they would be advected offshore on its oceanic side. From typical alongshore velocities of 20–50 cm/s (Mittelstaedt, 1983) and the elapsed time from spawning for the captured anchovy larvae, their spawning area would be situated at a mean distance of 172–430 miles north of the sampling area, compatible with an origin north of Cape Juby.

Both sardine and anchovy are pelagic species with pelagic spawning. Their larvae are found in the uppermost part of the water column and they seem to show little diurnal vertical migration (Russell, 1926,1928; John, 1982,1985; Palomera, 1991; Olivar and Sabatés, 1997). The horizontal distributions suggest that both, particularly sardine larvae, function as tracers of the flow regime in the NW African upwelling system, as was concluded by John (1986). The sardine is probably a more reliable tracer simply because of its greater abundance.

### 4.2. *Horizontal distribution of oceanic larvae*

The horizontal distribution of oceanic larvae was strongly influenced by upwelling and the presence of the filament, both of which represented an exclusion area for larvae concentrated at the northern limit of the filament and on the outer edge of the cyclonic eddy. The accumulation of larvae to the north of the filament may have been related: (a) to convergence at the thermal front that marked the northern boundary of the filament, as occurs with zooplankton (Le Fèvre, 1986) in other frontal zones, (b) to the jet associated with the filament, as occurs with phytoplankton (Strub et al., 1991) and zooplankton (Mackas et al., 1991) in the Californian upwelling region; or (c) to concentration of larvae in this area to exploit its greater richness a priori, a process suggested for other frontal zones (Kiørboe et al., 1988; Olivar, 1990; Sournia, 1994). The accumulation of fish larvae on the outer edges of the cyclonic eddy is, as has already been seen, a typical distribution presented by this planktonic component in the presence of an oceanographic structure of this type. It may be produced by the secondary circulation patterns inside the eddy (Patzert, 1969; Aristegui et al., 1994), by an increased food supply in relation to surrounding waters (Beckman et al., 1987; Lobel, 1989), and perhaps by the preference of the oceanic larvae for warmer water.

© Del documento, los autores. Digitalización realizada por ULPGC. Biblioteca Universitaria, 2009

## 5. Conclusions

Our results show: (i) that coastal upwelling and the presence of a quasi-permanent filament and cyclonic eddy play a major role in the horizontal distribution patterns of neritic larvae off NW Africa, while oceanic larvae are largely excluded from these structures, (ii) that neritic larvae transported offshore by the filament are likely to be entrained around the eddy, which may return many of the larvae to the nearshore region, not far from their place of origin, (iii) that a small number of larvae may be introduced into the waters close to the Canary Islands, so refreshing the island populations and (iv) that sardine larvae act as a strong tracer of the movement of upwelled waters in this region. Support is found for the hypothesis that the coastal upwelling, filament and eddy off Cabo Bojador and Juby constitute a "fundamental triad" (Bakun, 1998) that underpins the suitability of the region as a reproductive habitat for the neritic fish species.

## Acknowledgements

This work was supported by the MAST programme of the European Commission rough Project 0031 and the Instituto Español de Oceanografía. The extensive comments on the manuscript made by two anonymous referees were greatly appreciated.

## References

Aristegui, J., Sangrá, P., Hernández-León, S., Cantón, M., Hernández-Guerra, A., Kerling, J.L., 1994. Island-induced eddies in the Canary Islands. Deep-Sea Research I 41 (10), 1509–1525.

Aristegui, J., Tett, P., Hernández-Guerra, A., Basterretxea, G., Montero, M.F., Wild, K., Sangrá, P., Hernández-León, S., Cantón, M., Garcia-Braun, J.A., Pacheco, M., Barton, E.D., 1997. The influence of island-generated eddies on chlorophyll distribution: a study of mesoscale variation around Gran Canaria. Deep-Sea Research I 44 (1), 71–96.

Armstrong, D.A., Mitchell-Innes, B.A., Verheye-Dua, F., Waldron, H., Hutchings, L., 1987. Physical and biological features across an upwelling front in the southern Benguela. In: Payne, A.I.L., Gulland, J.A., Brink, K.H. (Eds.), The Benguela and Comparable Ecosystems. South African Journal of Marine Science 5, 171-190

Bakun, A., 1996. Patterns in the ocean: ocean processes and marine population dynamics. San Diego, California, University of California Sea Grant (in cooperation with Centro de Investigaciones Biológicas del Noroeste, La Paz, Baja California Sur, México), 323pp.

Bakun, A., 1998. Ocean Triads and Radical Interdecadal Stock Variability: Bane and Boon for Fishery Management Science. In: Pitcher, T.J., Hartand, P.J.B., Pauly, D. (eds.) Reinventing Fisheries Management. Chapman and Hall, London, pp. 331–358.

Barton, E.D., Aristegui, J., Tett, P., Garcia-Braun, J., Hernández-León, S., Nikjær, L., Almeida, C., Ballesteros, S., Basterretxea, G., Escánez, J., Garcia-Weill, L., Hernández-Guerra, A., López-Laatzen, F., Molina, R., Montero, M.F., Navarro-Pérez, E., Rodriguez, J.M., Vélez, H., Wild, K., 1998. The transition zone of the Canary Current upwelling region. Progress in Oceanography 41, 455–504.

Beckmann, W., Auras, A., Hemleben, Ch., 1987. Cyclonic cold-core eddy in the eastern North Atlantic. Marine Ecology Progress Series 39, 165–173.

Bernstein, R.L., Breaker, L., Whritner, R., 1977. California Current eddy formation: ship, air and satellite results. Science 195, 353–359.

© Del documento, los autores. Digitalización realizada por ULPGC. Biblioteca Universitaria, 2009

Bishai, H.M., 1960. The effect of waters current on the survival and distribution of fish larvae. Marine Biology 1041, 381–387.

Blackburn, M., Nellen, W., 1976. Distribution and ecology of pelagic fishes studied from eggs and larvae in an upwelling area off Spanish Sahara. Fishery Bulletin 74 (4), 885–896.

Blaxter, J.H.S., Hunter, J.R., 1982. The biology of the clupeoid fishes. In: Blaxter, J.H.S., Russell, F.S., Yonge, M. (Eds.) Advances in Marine Biology, Vol. 20. Academic Press, London, pp. 1–223.

Brink, K.H., 1983. The near surface dynamics of coastal upwelling. Progress in Oceanography 12, 223–257.

Chavez, F.P., Barber, R.T., Kosro, P.M., Huyer, A., Ramp, S.R., Stanton, T.P., Rojas de Mendiola, B., 1991. Horizontal transport and the distribution of nutrients in the coastal zone off northern California: effects on primary production, phytoplankton biomass and species composition. Journal of Geophysical Research 96 (C8), 14833–14848.

Delgado, A., Fernández, M.A.R., 1985. Datos sobre la biología de la sardina (Sardina pilchardus Walb., 1792) capturada por los cerqueros españoles en África Occidental de 1976 a 1982. In: Bas, C., Margalef, R., Rubies, P. (Eds.), Simposium Internacional del Afloramiento del Oeste Africano, Vol. II. Instituto de Investigaciones Pesqueras, Barcelona, pp. 935–956.

Duncombe Rae, C.M., Hutchings, L, Shannon, L.J., Boyd, A.J., Agenbag, J.J., Nelson, G., in press. Physical and biological observations during the decay phase of an upwelling filament off Cape West Coast. South African Journal of marine Science 21.

FAO, 1980. Rapport de la deuxième réunion du Groupe de Travail sur la sardine (Sardina pilchardus Walb.). COPACE/PACE Séries 79/15, 108pp.

Flament, P., Armi, L., Washburn, L., 1985. The evolving structure of an upwelling filament. Journal of Geophysical Research 90 (C6), 11765–11778.

Frank, K.T., Loder, J.W., Carscadden, J.E., Leggett, W.C., Taggart, Ch.T., 1992. Larval flatfish distributions and drift on the southern Grand Bank. Canadian Journal of Fisheries and Aquatic Sciences 49, 467–483.

Furnestin, J., 1950. Premières observations sur la biologie de la sardine marocaine. Rapports et Procès-vervaux des Réunions, Conseil International pour l'Exploration de la Mer, Rapport Atlantique, Vol. 126, pp. 57–61.

Furnestin, J., Furnestin, M.L., 1959. Reproduction de la sardine et de l'anchois des côtes atlantiques du Maroc (saisons et aires de ponte). Revue des Travaux de l' Institut des Pêches maritimes 23(1), 79–104.

Hagen, E., Zülicke, C., Feistel, R., 1996. Near-surface structures in the Cape Ghir filament off Morocco. Oceanologica Acta 19 (6), 577–598.

Heath, M.R., 1992. Field investigations of the early life stages of marine fish. In: Blaxter, J.H.S., Southward, A.J. (Eds.) Advances in Marine Biology, Vol. 28. Academic Press, London, pp. 1–174.

Ibanez, F., Seguin, G., 1972. Etude du cycle annuel du zooplancton d'Abidjan. Comparaison de plusieurs méthodes d'analyse multivariante: composantes principales, correspondances, coordonnées principales. Investigación Pesquera 36 (1), 81–108.

John, H.-Ch., 1982. Horizontal and vertical distribution of sardine and other fish larvae. Rapports et Procès-verbaux des Réunions, Conseil international pour l'Exploration de la Mer, Vol. 180, pp. 359–364.

John, H.-Ch., 1985. Horizontal and vertical distribution patterns of fish larvae off NW Africa in relation to the environment. In: Bas, C., Margalef, R., Rubies, P. (Eds.), Simposium Internacional del Afloramiento del Oeste Africano, Vol. I. Instituto de Investigaciones Pesqueras, Barcelona, pp. 489–512.

John, H.-Ch., 1986. On currents off north-west Africa as revealed by fish larvae distributions. UNESCO Technical Papers in Marine Biology 49, 149–155.

Jones, B.H., Mooers, C.N.K., Rienecker, M.M., Stanton, T., Washburn, L., 1991. Chemical and biological structure and transport of a cool filament associated with a jet-eddy system off northern California in July 1986 (OPTOMA21). Journal of Geophysical Research 96 (C12), 22207–22225.

Kim, S., Bang, B., 1990. Oceanic dispersion of larval fish and its implications for mortality estimates: case study of walleye pollock larvae in Shelikof Strait, Alaska. Fishery Bulletin 88 (2), 303–311.

Kiørboe, T., Munk, P., Richardson, K., Christensen, V., Paulsen, H., 1988. Plankton dynamics and larval herring growth, drift and survival in a frontal area. Marine Ecology Progress Series 44, 205–219.

Kosro, P.M., Huyer, A., 1986. CTD and velocity of seaward jets off Northern California, July 1981 and 1982. Journal of Geophysical Research 91 (C6), 7680–7690.

© Del documento, los autores. Digitalización realizada por ULPGC. Biblioteca Universitaria, 2009

Le Fèvre, J., 1986. Aspects of the biology of frontal systems. In: Blaxter, J.H.S., Russell, F.S., Yonge, M. (Eds.) Advances in Marine Biology, Vol. 23. Academic Press, London, pp. 163–299.

Lobel, P.S., 1989. Ocean current variability and the spawning season of Hawaiian reef fishes. Environmental Biology of Fishes 24 (3), 161–171.

Lobel, P.S., Robinson, A.R., 1986. Transport and entrapment of fish larvae by ocean mesoscale eddies and currents in Hawaiian waters. Deep-Sea Research 33 (4), 483–500.

Lobel, P.S., Robinson, A.R., 1988. Larval fishes and zooplankton in a cyclonic eddy in Hawaiian waters. Journal of Plankton Research 10 (6), 1209–1223.

Mackas, D.L., Washburn, L., Smith, S.L., 1991. Zooplankton community pattern associated with a California Current cold filament. Journal of Geophysical Research 96 (C8), 14781–14797.

Mittelstaedt, E., 1983. The upwelling area off Northwest Africa – A description of phenomena related to coastal upwelling. Progress in Oceanography 12, 307–331.

Molina, R., Cabanas, J.M., Laatzen, F., 1996. Corrientes e hidrografia en la región canaria. Campaña Canarias 9205. Boletin del Instituto Español de Oceanografia 12 (1), 43–51.

Myers, R.A., Drinkwater, K.F., 1989. Offshelf Ekman transport and larval fish survival in the northwest Atlantic. Biological Oceanography 6, 45–64.

Navarro-Pérez, E., Barton, E.D., 1998. The physical structure of an upwelling filament off the north-west African coast during August 1993. In: Pillar, S.C., Moloney, C.L., Payne, A.I.L., Shillington, F.A. (Eds), Benguela Dynamics: Impacts of Variability on Shelf-Sea Environments and their Living Resources. South African Journal of Marine Science 19, 61–74.

Navarro-Pérez, N., Velez-Muñoz, H.S., Wild, K.A., 1994. BIO Hesperides Cruise 9308 report: Hydrographic fields. Technical Report 0031-16, School of Ocean Sciences, Bangor, UK, 10pp + appendices.

Nelson, G., Boyd, A.J., Agenbag, J.J., Duncombe Rae, C.M., 1998. An upwelling filament north-west of Cape Town, South Africa. In: Pillar, S.C., Moloney, C.L., Payne, A.I.L., Shillington, F.A. (Eds), Benguela Dynamics: Impacts of Variability on Shelf-Sea Environments and their Living Resources. South African Journal of Marine Science 19, 75–88.

Norcross, B.L., Shaw, R.F., 1984. Oceanic and estuarine transport of fish eggs and larvae: a review. Transactions of the American Fisheries Society 113, 153–165.

Nykjær, L., Van Camp, L., 1989. Remote sensing of the Northwest African Upwelling Area. Analysis and interpretation of simultaneous pairs of GAC derived sea surface temperature and CZCS derived chlorophyll-like pigment concentration images. Unimar Sciences ApS 1, 74pp.

Nykjær, L., Van Camp, L., Schlittenhardt, P., 1988. The structure and variability of a filament in the Northwest African upwelling area as observed from AVHRR and CZCS images. Proceedings of IGARSS 88 Symposium, Edinburgh, Scotland, pp. 1097–1100

Olivar, M.P., 1990. Spatial patterns of ichthyoplankton in relation to hydrographic features in the Northern Benguela region. Marine Biology 106, 39–48.

Olivar, M.P., Sabatés, A., 1997. Vertical distribution of fish larvae in the north-west Mediterranean Sea in spring. Marine Biology 129, 289–300.

Palomera, I., 1991. Vertical distribution of eggs and larvae of Engraulis encrasicolus in stratified waters of the western Mediterranean. Marine Biology 111, 37–44.

Parrish, R.H., Nelson, C.S., Bakun, A., 1981. Transport mechanisms and reproductive success of fishes in the California Current. Biological Oceanography 1 (2), 175–203.

Patzert, W.C., 1969. Eddies in Hawaiian waters. Report No HIG-69-8, Institute of Geophysics, University Hawaii, 51pp., 71 Figs.

Ré, P., 1987. Ecology of the planktonic phase of the anchovy, Engraulis encrasicolus (Linnaeus, 1758), within Mira Estuary (Portugal). Investigaciones Pesqueras 51 (4), 581–598.

Regner, S., 1985. Ecology of the planktonic stages of the anchovy, Engraulis encrasicolus (Linnaeus, 1758), in the Central Adriatic. Acta Adriatica 26 (1), 5–113.

Roy, C., Cury, P., Fontana, A., Belvèze, H., 1989. Stratégies spatio-temporelles de la reproduction des clupéidés des zones d'upwelling d'Afrique de l'Ouest. Aquatic Living Resources 2, 21–29.

Russell, F.S., 1926. The vertical distribution of marine macroplankton. III. Diurnal observations on the pelagic young of teleostean fishes in the Plymouth Area. Journal of Marine Biology Association, United Kingdom 14 (2), 387–414.

© Del documento, los autores. Digitalización realizada por ULPGC. Biblioteca Universitaria, 2009

Russell, F.S., 1928. The vertical distribution of marine macroplankton. VIII. Further observations on the diurnal behaviour of the pelagic young of teleostean fishes in the Plymouth Area. Journal of Marine Biology Association, United Kingdom 15 (2), 829–850.

Russell, F.S., 1976. The Eggs and Planktonic Stages of Marine Fishes. Academic Press, London, pp. 524.

Shillington, F.A., Peterson, W.T., Hutchings, L., Probyn, T.A., Waldron, H.N., Agenbag, J.J., 1990. A cool upwelling filament off Namibia, southwest Africa: preliminary measurements of physical and biological features. Deep-Sea Research 37 (1), 1753–1772.

Smith, P.E., Richardson, S.L., 1979. Técnicas estandar para prospecciones de huevos y larvas de peces pelágicos. FAO Documentos Técnicos de Pesca 175, 107pp.

Sournia, A., 1994. Pelagic biogeography and fronts. Progress in Oceanography 34, 109–120.

Strub, P.T., Kosro, P.M., Huyer, A., 1991. The nature of the cold filaments in the California Current System. Journal of Geophysical Research 96 (C8), 14743–14768.

Theilacker, G.H., 1980. Changes in body measurements of larval northern anchovy, Engraulis mordax, and other fishes due to handling and preservation. Fishery Bulletin 78 (3), 685–692.

Traganza, E.D., Nestor, D.A., McDonald, A.K., 1980. Satellite observations of a nutrient upwelling off the coast of California. Journal of Geophysical Research 85 (C7), 4101–4106.

Traganza, E.D., Conrad, J.C., Breaker, L.C., 1981. Satellite observations of a cyclonic upwelling system and giant plume in the California current. In: Richards, F.A. (Ed.) Coastal Upwelling, Coastal and Estuarine Science, Vol. 1. American Geophysical Union, Washington, DC, pp. 228–241.

UNESCO, 1968. Zooplankton sampling. Monograph Oceanography Methods, no. 2, 147pp.

Van Camp, L., Nykjær, L., Mittelstaedt, E., Schlittenhardt, P., 1991. Upwelling and boundary circulation off Northwest Africa as depicted by infrared and visible satellite observations. Progress in Oceanography 26, 357–402.

Whitehead, P.J.P., Bauchot, M.L., Hureau, J.C., Nielsen, J., Tortonesse, E. (Eds.), 1984. Fishes of the North-eastern Atlantic and the Mediterranean. Vols. I–III. UNESCO, United Kingdom, pp. 1473.

© Del documento, los autores. Digitalización realizada por ULPGC. Biblioteca Universitaria, 2008

JOURNAL OF GEOPHYSICAL RESEARCH, VOL. 104, NO. C11, PAGES 25,891–25,912, NOVEMBER 15, 1999

# Diapycnal mixing in Gulf Stream meanders

A. Rodríguez-Santana, J. L. Pelegrí, P. Sangrà, and A. Marrero-Díaz
Departamento de Física, Facultad de Ciencias del Mar, Universidad de Las Palmas de Gran Canaria, Canary Islands, Spain

**Abstract.** We use historical data [*Bane et al.*, 1981], interpolated to isopycnic coordinates, to examine the possibility of significant diapycnal mixing within the upper thermocline layers of the Gulf Stream. The data consist of 28 air-dropped expendable bathythermograph (AXBT) sections in the northern Blake Plateau distributed in five different surveys done within 8 days. From the data we obtain a separation index between isopycnals $j = \rho\, \partial z/\partial \rho$, where $z$ is the depth of an isopycnal and $\rho$ is the density; the diapycnal shear $\partial v/\partial \rho$, where $v$ is the geostrophic velocity; and the gradient Richardson number $Ri$. Following *Pelegrí and Csanady* [1994], we postulate that the material derivative of the density, or density tendency $w_\rho = D\rho/Dt$, is the result of small-scale instabilities related to near-critical $Ri$ values. We present the distribution of these quantities ($j$, $\partial v/\partial \rho$, $Ri$, and $w_\rho$) and the diapycnal convergence/divergence ($\partial w_\rho/\partial \rho$) over isopycnals and on sections normal to the coast. The results show the passage of steep meanders being related to anomalously low $j$ values (strong density gradients) within the upper thermocline layers and the cyclonic filaments of the stream. The statically stable upper thermocline layers, however, are concurrent with large diapycnal shear and turn out to be dynamically unstable, characterized by low $Ri$ and high-density tendencies and diapycnal convergence/divergence. The errors involved in calculating the dependent variables from AXBT data are assessed using both an error propagation approach and a Monte Carlo error simulation. These errors, although significant, are not large enough to modify the observed patterns substantially.

## 1. Introduction

It is surprising that despite *Stommel's* [1965, p. 116] early proposal of localized intense diapycnal mixing within the upper thermocline layers of the Gulf Stream, until now there have been very few studies of this phenomenon. This is perhaps even more striking if we consider the structural similarities between the Gulf Stream and other oceanic and atmospheric jets, where shear-induced turbulence is substantial. Examples of these are the equatorial undercurrent [*Peters et al.*, 1988], the coastal upwelling jet [*Kundu and Beardsley*, 1991; *Pelegrí and Richman*, 1993, 1994], and the polar jet stream [*Keyser and Shapiro*, 1986].

One of the few studies on diapycnal mixing within the Gulf Stream is due to *Gregg and Sanford* [1980], who calculated gradient Richardson numbers $Ri$ within the Gulf Stream, using 50 m averaged temperature and velocity profiles. They obtained values as low as $Ri = 2$ and suggested that shear mixing was possible. However, because of the existence of step-like density structures and high Cox numbers, their conclusion was that this mechanism is probably not as important as double diffusion. Other studies concentrated on diapycnal mixing between shelf/slope waters and Gulf Stream waters [*Ruddick and Bennett*, 1985; *Lillibridge et al.*, 1990; *Churchill et al.*, 1993] and obtained estimates for $Ri$ near the north wall edge of the Gulf Stream that suggested the relatively little importance of shear mixing as compared with double diffusion.

Two relatively recent findings point at the need to revisit the possibility of shear-induced mixing within the upper thermocline layers of the Gulf Stream. The first one is the recognition that relatively little smoothing of the density and velocity data is very important for the calculations of $Ri$ in well-stratified regions. *Miller and Evans* [1985] and *Padman and Jones* [1985] have shown that the vertical density and velocity gradients are very sensitive to the chosen vertical scales and that smoothing over distances as small as 10 m causes a considerable increase in the estimates for $Ri$. The second one is our better understanding of two instability mechanisms that produce series of constant density steps as a result of the dependence of density flux with $Ri$. These are the Phillips-Posmentier mechanism [*Phillips*, 1972; *Posmentier*, 1977; *Ruddick et al.*, 1989; *Park et al.*, 1994] and a mechanism proposed by *Pelegrí and Sangrà* [1998] where shear-induced turbulence lasts during some characteristic finite time.

*Miller and Evans* [1985] and *Schmitt et al.* [1986] have studied the possibility of shear-induced mixing in cold-

Copyright 1999 by the American Geophysical Union.

Paper number 1999JC900219.
0148-0227/99/1999JC900219$09.00



© Del documento, los autores. Digitalización realizada por ULPGC. Biblioteca Universitaria, 2009

and warm-core rings formed by Gulf Stream meanders, respectively. *Schmitt et al.* [1986] used highly smoothed vertical shear (over 300 m) to calculate *Ri* and, even so, obtained values close to 1. They recognized that this smoothing leads to increased *Ri* values and suggested that shear-driven turbulence may be a strong mixing mechanism. *Miller and Evans* [1985] did a careful analysis on the effects of smoothing on *Ri* and found that smoothing over increasing vertical distances (ranging between 1 and 10 m) can cause *Ri* to go from subcritical to supercritical. They chose a smoothing interval of 2 m as a compromise between retaining high shear values and reducing contamination from small-scale turbulence. With this smoothing they then calculated mean *Ri* values over layers ~100 m thick, within a cold-dome Gulf Stream ring, and obtained values usually below 1 and often below 0.25. One corollary from the existence of low *Ri* values in Gulf Stream rings, which have their origin on meanders pinching off the Gulf Stream, is the possibility of similarly low values in steep meanders.

*Pelegrí and Csanady* [1991, 1994] obtained results indicating that diapycnal mixing is a likely phenomenon in the upper thermocline layers of the Gulf Stream. *Pelegrí and Csanady* [1991] examined water and nutrient balances for several isopycnals of the Gulf Stream to conclude that water is exchanged between the upper thermocline and surface layers. *Pelegrí and Csanady* [1994] observed good correspondence between regions of large diapycnal convergence and anomalies in both stratification and potential vorticity, as predicted from theoretical arguments. They defined an index of separation between isopycnals as $j = J\rho$, where $J = \partial z/\partial\rho$, $z$ is the depth of an isopycnal, and $\rho$ is its density, and postulated that diapycnal mixing is the consequence of anomalously low $j$ values (high stratification) produced during frontogenesis in some phase of the meanders.

More recently, *Pelegrí et al.* [1996] have discussed several pieces of evidence on the importance of diapycnal mixing. One significant evidence is the coincidence of large diapycnal mixing with nutrient anomalies taking place within the core of a nutrient stream. They propose that this exchange, repeated in time and space, is responsible for the overall diapycnal nutrient flux from the thermocline to the surface layers observed by *Pelegrí and Csanady* [1991] as well as for maintaining patchy productivity within the surface layers of the Gulf Stream. *Lohrenz et al.* [1993] have actually found episodic enhanced productivity downstream of meander crests and suggested that it may be caused by nutrient injection through shear-induced mixing.

*Iselin* [1950], *Rossby* [1951], and *Newton* [1959, 1961] early recognized the existence of structural and dynamic parallelisms between the Gulf Stream and the polar atmospheric jet stream. *Newton* [1978] pointed at similarities of convergence/divergence and vertical motions associated with meanders in both the Gulf Stream and the polar atmospheric jet, which have since been verified [*Bower*, 1989; *Bower and Rossby*, 1989]. Another similarity is the asymmetry between crests and troughs, with frontogenesis and increased (horizontal) cyclonic shear taking place between a crest and the subsequent trough [*Palmén and Newton*, 1969; *Newton*, 1978]. These and other analogies between the oceanic and atmospheric counterparts still require further research. Frontal zones of the polar jet stream, for example, are statically stable but experience vertical shearing instabilities (for a review, see *Keyser and Shapiro* [1986]), and it is plausible that this is also mirrored in the Gulf Stream.

In this paper we will analyze how and where diapycnal mixing may actually take place. Specifically, we will examine the hypothesis posed by *Pelegrí and Csanady* [1991, 1994] that diapycnal mixing is due to episodic high diapycnal shear and associated instability taking place during frontogenetical phases of Gulf Stream meanders. In section 2 we briefly review the procedure used to calculate *Ri* and the diapycnal convergence/divergence. In section 3 we present the data set and briefly discuss how it has been treated, leaving the details of a rather exhaustive error analysis for section 4. In section 5 we show the main results, and in section 6 we give the conclusions.

## 2. Diapycnal Convergence

To estimate the diapycnal convergence/divergence, we have essentially followed the procedure described by *Pelegrí and Csanady* [1994]. We now briefly review the main aspects of their formulation together with some differences in the parameterization of the vertical density diffusivity.

The mean density tendency $\tilde{w}_\rho$, or material change of density over a long timescale, is interpreted as the result of mixing taking place over shorter timescales. Decomposing the density and velocity fields into fast (prime) and slow (tilde) motions, $\rho = \tilde{\rho}+\rho'$, $u = \tilde{u}+u'$, etc., and taking the mean over the long timescale, we get

$$\begin{aligned}\tilde{w}_\rho &\equiv \frac{D\rho}{Dt} \equiv \frac{\partial\tilde{\rho}}{\partial t} + \tilde{u}\frac{\partial\tilde{\rho}}{\partial x} + \tilde{v}\frac{\partial\tilde{\rho}}{\partial y} + \tilde{w}\frac{\partial\tilde{\rho}}{\partial z} \\ &= -\nabla\cdot\tilde{\mathbf{F}} \simeq -\frac{\partial F_z}{\partial z}, \end{aligned} \tag{1}$$

where the Reynolds density flux vector is defined as $\tilde{\mathbf{F}} \equiv (\tilde{F}_x, \tilde{F}_y, \tilde{F}_z) \equiv (\overline{u'\rho'}, \overline{v'\rho'}, \overline{w'\rho'})$, and we have assumed incompressibility. The approximation used in (1) corresponds to the case of vertical flux convergence/divergence much larger than horizontal flux convergence/divergence, and it will be quantified later in this section.

The vertical component of the Reynolds density flux is parameterized as proportional to the vertical density gradient:

$$F_z = -K_v\frac{\partial\tilde{\rho}}{\partial z} = -\frac{K}{\tilde{J}}, \tag{2}$$

where $K_v$ is the vertical density eddy diffusivity and $\tilde{J} = \partial\tilde{z}/\partial\tilde{\rho}$, with $\tilde{z} = z(x, y, \rho = \tilde{\rho})$. Substitution into (1) leads to (hereafter, we will always refer to the long-time mean quantities, so we drop tildes)

© Del documento, los autores. Digitalización realizada por ULPGC. Biblioteca Universitaria, 2009

$$w_\rho \simeq \frac{1}{J}\frac{\partial(K_v/J)}{\partial\rho} = \frac{1}{J^2}\frac{\partial K_v}{\partial\rho} - \frac{K_v}{J^3}\frac{\partial J}{\partial\rho}. \quad (3)$$

Assuming that mixing is the result of shear-induced unstable geostrophic events, we can parameterize $K_v$ as a function of the gradient Richardson number $Ri$, approximated by

$$Ri = \frac{g\frac{\partial\rho}{\partial z}}{\rho\left(\frac{\partial v}{\partial z}\right)^2} = \frac{gJ}{\rho\left(\frac{\partial v}{\partial\rho}\right)^2} = \frac{f^2 j}{g\left(\frac{\partial z}{\partial x}\right)^2}, \quad (4)$$

where $g$ is the gravity acceleration, $f$ is the Coriolis parameter, $v$ is the along-stream geostrophic velocity, and $j = J\rho$ is the index of separation defined by *Pelegrí and Csanady* [1994]. The separation index could be interpreted as the distance over which the local density gradient would have to act to produce a total density change from zero to $\rho$. This quantity has the appeal that changes in $j$ are, together with changes in total vorticity, directly responsible for changes in potential vorticity [*Pelegrí and Csanady*, 1994, equation (33)].

In (4) we have approximated the vertical geostrophic shear by the vertical shear of the along-stream geostrophic velocity ($\partial v/\partial z$). The second equality is the appropriate expression in isopycnic coordinates, with $\partial v/\partial\rho$ being the diapycnal shear, while the last equality has made use of the thermal wind equation in isopycnic coordinates ($\rho f\,\partial v/\partial\rho = g\,\partial z/\partial x$). Note that the thermal wind equation allows for obtaining a geostrophic $Ri$ without needing a velocity reference level. In the absence of density inversions, $J$, $j$, and $Ri$ are negative numbers, but we will follow the usual convention of taking their absolute values.

In the above expression we actually calculate $Ri$ due to geostrophic shear in Gulf Stream meanders, in agreement with the hypothesis that subcritical regions are intermittently produced during frontogenetical phases of the meanders. These regions should be reflected by the spatial distribution of the above geostrophic $Ri$ and the associated mixing properties. Our geostrophic approach ignores the contribution to mixing by submesoscale features such as internal gravity waves or tides; these may be important but are not addressed here. Another difficulty with baroclinic tides is that they could produce significant cross-stream isopycnal displacements that would induce an error in our estimates of the geostrophic diapycnal shear (the importance of this error is assessed in section 4).

The choice of parameterization for $K_v = K_v(Ri)$ is a difficult issue. Since the early proposal by *Munk and Anderson* [1948] there have been numerous variations [e.g., *Pacanowski and Philander*, 1981; *Ueda et al.*, 1981; *Turner*, 1986; *Pelegrí and Csanady*, 1994] that follow Munk and Anderson's low inverse dependence with $Ri$. *Peters et al.* [1988] used simultaneous measurements of shear and microstructure in the equatorial undercurrent to obtain a two-regime $K_v(Ri)$ dependence, with a Munk and Anderson type function for high $Ri$ but with a quite different function for the $Ri < 0.4$ range. For these low $Ri$ values they obtained a nearly catastrophic dependence, $K_v \sim Ri^{-9}$, which is very appealing because it conforms to the theoretical condition of rapid mixing developing in subcritical conditions. Figure 1 shows the shape of the $K_v = K_v(Ri)$ dependence according to *Pacanowski and Philander* [1981], *Peters et al.* [1988], and *Pelegrí and Csanady* [1994]; in Figure 1 we have adapted a curve to *Peters et al.*'s [1988] measurements (dots) for the $Ri \geq 0.4$ region.

For our calculations we have chosen a two-regime parameterization for $K_v(Ri)$, with a *Munk and Anderson* [1948] type formulation for the high $Ri$ range and *Peters et al.* [1988] dependence for the low $Ri$ range:

$$K_v = \begin{cases} 1.1\times10^{-8}Ri^{-9.2} & Ri \leq 0.33 \\ 2.6\times10^{-3}(1+10Ri)^{-3/2} & Ri > 0.33. \end{cases} \quad (5)$$

The high $Ri$ range dependence has been chosen following *Pelegrí and Csanady* [1994], which conforms to the widely accepted $Ri^{-3/2}$ dependence for large $Ri$ [e.g., *Turner*, 1986]. This selection provides a relatively smooth transition between the low and high $Ri$ regimes taking place at $Ri = 0.33$. It may be justified as a compromise between the appealing high-order dependence for low $Ri$ values and *Peters et al.*'s [1988] recognition that their indirect method for flux determination may have significant uncertainties. In any case, as Figure 1 suggests, a change in parameterization would modify the absolute numbers of the mixing properties but not their spatial patterns.

We will now quantify the approximation in (1). Using the parameterization in (2) and a similar one for an arbitrary horizontal direction $x$, the approximation becomes

$$\left|\frac{\partial}{\partial z}\left(K_v\frac{\partial\rho}{\partial z}\right)\right| >> \left|\frac{\partial}{\partial x}\left(K_h\frac{\partial\rho}{\partial x}\right)\right|, \quad (6)$$

where $K_h$ is the horizontal density eddy diffusivity. Typical values of $K_h$ and $K_v$ in the upper permanent thermocline are 3 and $1.5\times10^{-5}$ m$^2$ s$^{-1}$, respectively [*Ledwell et al.*, 1993]. For a density change of 1 kg m$^{-3}$ the horizontal and vertical scales are $10^6$ and $10^3$ m, respectively. Substitution of these numbers into (6) shows that both terms are of the same order ($10^{-11}$ kg m$^{-3}$ s$^{-1}$), indicating that in the permanent thermocline the density tendency may indeed be controlled by both horizontal and vertical convergence/divergence.

The situation we are interested for Gulf Stream meanders is quite different from the previous one, essentially because of the existence of highly compressed regions that maintain a large diapycnal shear. Relation (4) above shows that under these conditions, $Ri$ may be subcritical; that is, these well-stratified layers may be dynamically unstable. A typical (vertically smoothed) value for the separation index in these layers is $j \simeq 10^5$ m (section 5), which corresponds to density and vertical scales of 0.1 kg m$^{-3}$ and 10 m, respectively. The value for $K_v$ in these regions corresponds to near-critical Richardson values (section 5), being $\sim4\times10^{-4}$ m$^2$ s$^{-1}$ (Figure 1). With these numbers a typical value for

© Del documento, los autores. Digitalización realizada por ULPGC. Biblioteca Universitaria, 2009

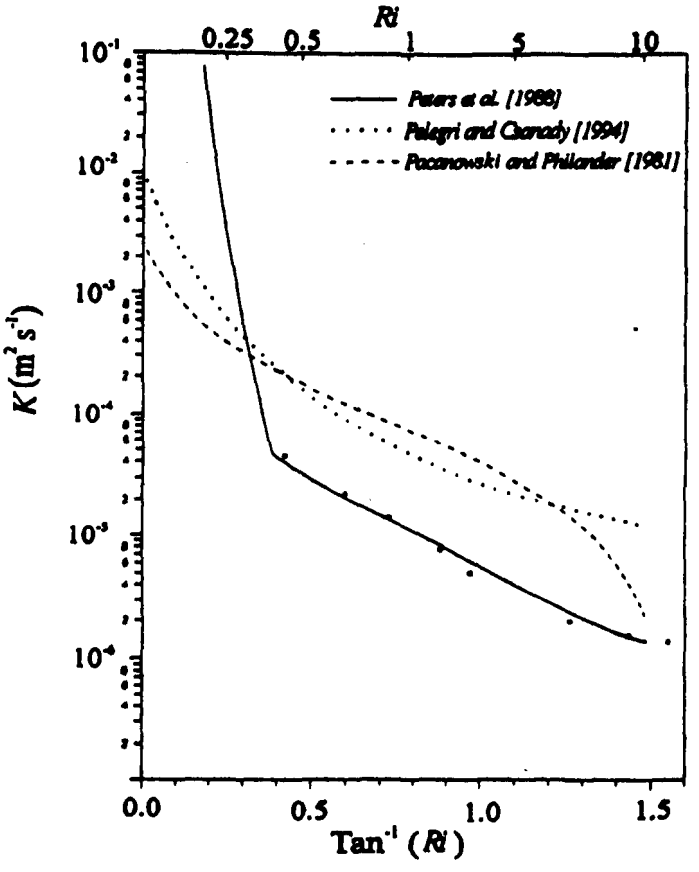


**Figure 1.** Vertical density eddy diffusivity $K$ as a function of the Richardson number $Ri$ according to parameterizations by *Pacanowski and Philander* [1981], *Peters et al.* [1988], and *Pelegrí and Csanady* [1994]. The parameterization used corresponds to the *Peters et al.* [1988] curve for $Ri \leq 0.33$ and to the *Pelegrí and Csanady* [1994] curve for $Ri > 0.33$.

$\partial F_z/\partial z$ is $4 \times 10^{-7}$ kg m$^{-3}$ s$^{-1}$ and much larger in subcritical regions because of the large inverse dependence $K_v \sim Ri^{-9}$.

The above number must now be compared with those associated with horizontal density convergence/divergence within the Gulf Stream. A first estimate may be obtained using *Ledwell et al.*'s [1993] values for $K_h$ (3 m$^2$ s$^{-1}$) and the horizontal density gradients associated with Gulf Stream meanders (changes of 0.6 kg m$^{-3}$ over some 20 km; see section 3), giving $\partial F_x/\partial x \simeq 4 \times 10^{-9}$ kg m$^{-3}$ s$^{-1}$. A similar estimate may be obtained using the mean horizontal density gradients (~0.8 kg m$^{-3}$ over 200 km) and a mean horizontal density diffusivity (250 m$^2$ s$^{-1}$) calculated from the overall distribution of scalar properties [*Bower et al.*, 1985; *Csanady and Hamilton*, 1988]. With these figures we get a typical value $\partial F_x/\partial x \simeq 5 \times 10^{-9}$ kg m$^{-3}$ s$^{-1}$. Both estimates for the horizontal density convergence/divergence agree, showing that the local horizontal diffusion can sustain the large-scale diffusion implied by the steady distribution of scalar properties within the Gulf Stream. These estimates, however, are 2 orders of magnitude smaller than the vertical density convergence/divergence, which verifies the approximation employed in (1).

Substitution of (5) into (3) allows us to calculate explicitly the density tendency $w_\rho$ and its diapycnal convergence $\partial w_\rho/\partial \rho$ over a grid with density-depth data. The intensity of the density tendency reveals the degree of mass (and tracers such as nutrients) exchange between adjacent isopycnal layers, while it is the diapycnal convergence that controls the separation between isopycnals. When diapycnal convergence is dominant, the mass conservation equation reduces to [*Pelegrí and Csanady*, 1994]

$$\frac{Dj}{Dt} \simeq -\frac{\partial w_\rho}{\partial \rho} j . \qquad (7)$$

This tells us that the separation between adjacent isopycnals will increase (decrease) with diapycnal convergence (divergence), i.e., with negative (positive) $\partial w_\rho/\partial \rho$ values (recall that $J$ is a negative quantity, although it is usual to show its absolute value).

## 3. Data Analysis

We have used a data set of sequential air-dropped expendable bathythermograph (AXBT) surveys over the Gulf Stream, provided to us by J. Bane from the University of North Carolina. It was obtained during February 1979 in the northern Blake Plateau (off the North and South Carolina coasts, north of Charleston Bump), where substantial meanders are observed to progress northward. These data have been previously used to study the generation, structure, dynamics, and energy characteristics of the meanders [*Bane et al.*, 1981; *Brooks and Bane*, 1981, 1983; *Hood and Bane*, 1983; *Chew et al.*, 1985; *Luther and Bane*, 1985].

An excellent attribute of this data set is the fast coverage (in a few hours) of a relatively large region down to almost 400 m, during five different flights done within 8 days (February 9, 11, 14, 15, and 17). The number of AXBT sections for each flight ranges between four and seven, for a total of 28 sections and over 250 stations. Although the sections taken during different flights are not exactly at the same location, they are close enough that we have decided to call them sections A, C, E, G, I, K, and M, from north to south (Figure 2).

Salinity $S$ is obtained from temperature $T$ by a recursive utilization of *Bryden*'s [1973] algorithm for potential temperature $\theta$ and *Armi and Bray*'s [1982] algorithm for the relationship between $S$ and $\theta$ in the northwestern Atlantic Ocean. Bryden's algorithm allows us to obtain a first estimate of $\theta$ from $T$ and pressure values, together with an initial choice of $S$. Armi and Bray's algorithm gives an estimate of $S$ from the first estimate of $\theta$. The procedure is repeated until convergence is obtained in both $\theta$ and $S$ values, and then the potential density ($\rho$) is calculated. (Hereafter, we will talk indistinctly about $\rho$ and sigma-theta defined as $\sigma_\theta \equiv \rho - 1000$, with $\rho$ in MKS units; furthermore, we will use the notation of $\sigma_\theta$ units with 1 $\sigma_\theta$ unit $\equiv$ 1 kg m$^{-3}$).

An important property for the upper thermocline waters of the Blake Plateau is the constancy of the $\theta$-$S$ relationship in both Sargasso Sea and Gulf Stream

© Del documento, los autores. Digitalización realizada por ULPGC. Biblioteca Universitaria, 2009

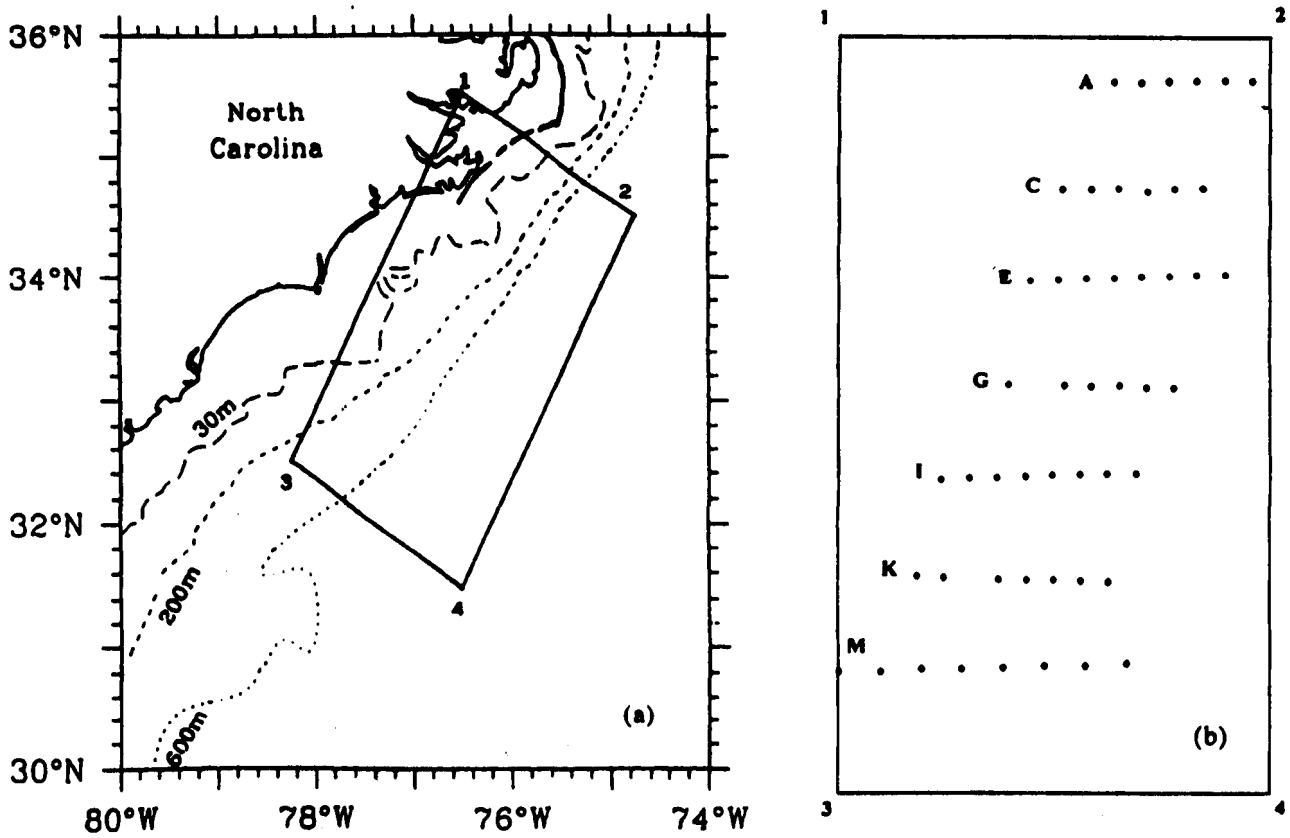


**Figure 2.** (a) Continental margin of the southeastern United States showing the region of this study. (b) Region after rotation and amplification in the cross-stream direction, with the approximate location of the air-dropped expendable bathythermograph (AXBT) sections.

waters [*Richards and Redfield*, 1955; *Atkinson*, 1983], which makes possible the utilization of *Armi and Bray's* [1983] algorithm. This is not so north of Cape Hatteras where there is substantial lateral mixing between the Gulf Stream and shelf and slope waters [*Fisher*, 1972; *Lillibridge et al.*, 1990; *Churchill et al.*, 1993: *Hitchcock et al.*, 1994]. Some variability in the $\theta$-$S$ relationship may appear in our area of study because of northward spreading of Antarctic Intermediate Water along the main axis of the Gulf Stream [*Atkinson*, 1983], but this occurs at depths larger (usually over 500 m) than the maximum depth in our data set. Another source of variability for our area comes from the possibility of thermohaline intrusions from coastal waters, which could cause errors in the estimation of potential density from Armi and Bray's algorithm; this will be examined in section 4.

The vertical resolution of the AXBTs is one data point every 4 m down to 200 m, beyond which it decreases to one point every 10 m. With this vertical resolution the number of data points within 0.1 $\sigma_\theta$ intervals ranges between 2 and more than 20. The potential density versus depth data have been interpolated at 0.01 $\sigma_\theta$ intervals, for the $26.2 \leq \sigma_\theta \leq 27.2$ range. The density range has been chosen because it is covered by the data in most stations; when this is not the case, however, we have interpolated only over the available data range. The selection of 0.01 $\sigma_\theta$ intervals has been made as a compromise between vertical resolution and accuracy. The interpolation procedure uses cubic splines subject to a smoothing tension factor; this procedure removes all depth inversions in the potential density, while at the same time it maintains the smoothing to a minimum in order not to increase excessively the *Ri* values [*Miller and Evans*, 1985].

A crucial aspect in our analysis will be the spatial interpolation of properties over isolevel/isopycnal surfaces or on cross-stream sections. This interpolation is obtained on a rectangular grid using standard kriging techniques [e.g., *Lancaster and Salkauskas*, 1986], which provide a value for the interpolation error. In order to improve the procedure of interpolation over the isolevel/isopycnal surfaces, however, we have chosen to rotate the original data set by 30°, such that the AXBT sections are in the direction of one grid axis. Figure 2b shows this rotated region which, for better visualization, is also amplified in the cross-stream direction. This region will be used in all our representations of quantities over isolevel (Figure 3) or isopycnal (Figures 4-9) surfaces.

## 4. Error Analysis

### 4.1. Sources of Error

In this Section we analize the potential errors in the AXBT data that may affect all other inferred quantities. There are several error sources, which may be grouped as follows.

© Del documento, los autores. Digitalización realizada por ULPGC. Biblioteca Universitaria, 2009

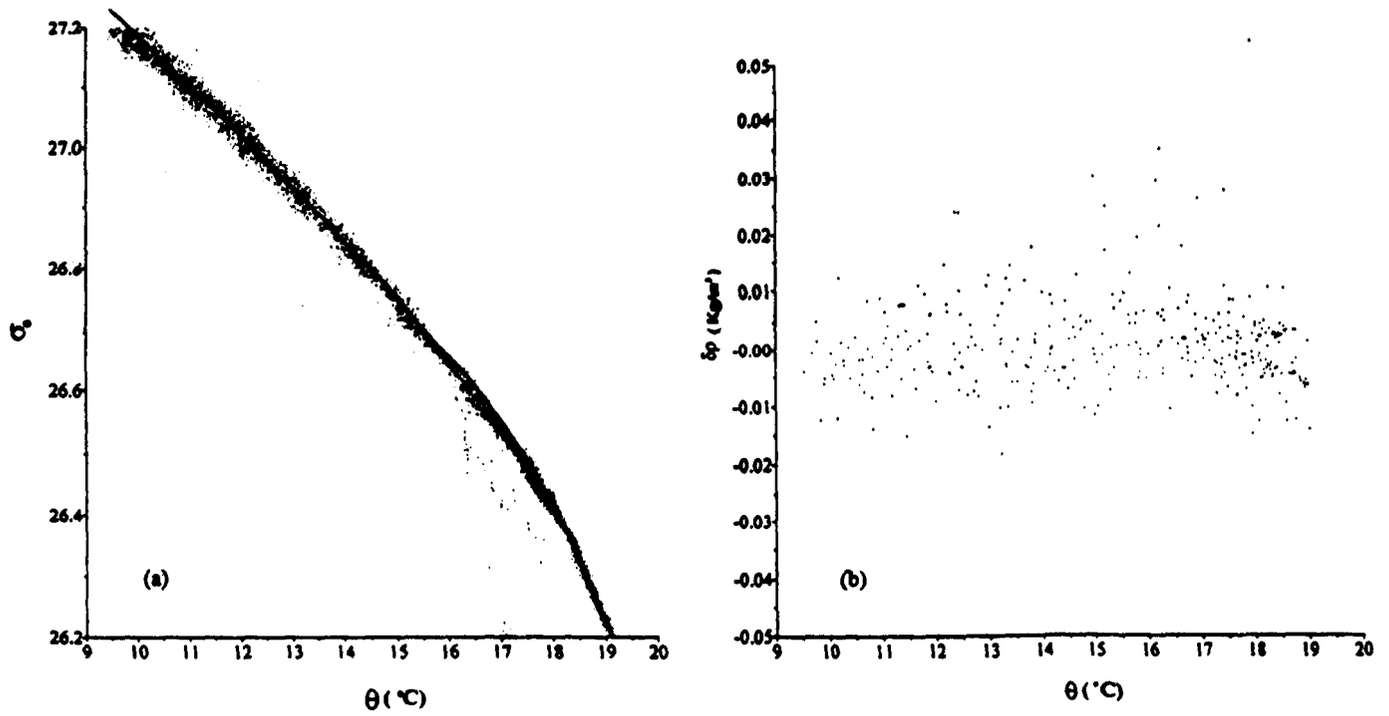


**Figure 3.** (a) The $\sigma_\theta$-$\theta$ diagram from 25 conductivity-temperature-depth (CTD) stations in our area of study (the three northernmost lines by *Atkinson* [1983]). The solid line corresponds to *Armi and Bray*'s [1982] empirical algorithm. (b) Individual density errors calculated for the same data set.

**4.1.1. Depth and temperature accuracy and resolution.** The AXBTs depth accuracy primarily depends on the probe's fall rate. The reported depth accuracy for AXBT probes varies from one manufacturer to another, typical values being ±2 and ±5%. The temperature accuracy specification is given in terms of frequency, which the unit transmits from the ocean surface to the aircraft. Several temperature accuracies are reported by different manufacturers, ranging between 0.05 and 0.56 °C. The depth and temperature resolution for AXBT probes are 0.1 m and 0.01°C, respectively.

The probes employed were manufactured by Hermes Electronics (J. Bane, personal communication, 1998). They were standard military qualified probes (as is the case with AXBTs manufactured by most companies), which conformed to a fall rate given by $z = 1.52t$, where $z$ is the depth (in meters) attained after an elapsed time $t$ (in seconds) in the water. Unfortunately, however, we have not found any published calibration work on this type of probes. There have been several studies on units manufactured by other companies [*Sessions et al.*, 1976; *Bane and Sessions*, 1984; *Boyd*, 1987; *Boyd and Linzell*, 1993], and although they conform to the same navy specifications, these are of sufficiently different design that we should not expect their calibration information to apply to the Hermes units. One possibility is to take both depth and temperature errors as corresponding to the largest accuracy reported values, i.e., ±5% the depth value and 0.56 °C. An accuracy value, however, supposedly provides a figure for the maximum error, providing a range that must be satisfied by all probes. Taking the accuracy value as the measured error hence will likely produce an overestimate of the standard error for the temperature and depth. Furthermore, the above studies have shown that typically, the fall rate for AXBT probes would perform better than the above specifications. For both reasons we choose the depth error as ±2% of the reported depth and the temperature error as 0.2 °C.

**4.1.2. Station position.** The station position was found with an inertial navigation system (INS) on the aircraft, which had a specified maximum drift rate of 4 km hr$^{-1}$ (J. Bane, personal communication, 1998). This means that the maximum error in absolute position is the drift rate times the elapsed time since takeoff, while the maximum error in relative position between two consecutive AXBTs (maximum relative error) is the drift rate times the time between AXBT deployments.

Each AXBT survey was done with the aircraft following cross-stream lines and then moving to the adjacent line. The time difference between consecutive AXBT deployments along a cross-stream line is typically ~2 min, so the maximum relative error is 130 m. This gives the maximum position error for our calculations of the cross-stream isopycnal slope and all the other quantities that depend on it (e.g., equation (4)).

The maximum time difference between stations in two adjacent lines is typically ~1 hour, so the maximum relative error in this case would be 4 km. The only role of this error, however, could be to modify the relative position of stations in adjacent lines that could affect the exact contouring of properties over isopycnal

© Del documento, los autores. Digitalización realizada por ULPGC. Biblioteca Universitaria, 2009

surfaces. Since 4 km is much less than the distance between adjacent lines (~50 km), we may conclude that this error will cause a rather insignificant alteration of the contour lines.

**4.1.3. Non-uniqueness of the $\theta$-$S$ relationship.** A unique $\theta$-$S$ relationship for our area of study would guarantee that given a $\theta$ value, we could obtain the $S$ and $\rho$ values. In our area of study, however, there may be some variability in the $\theta$-$S$ diagram, probably because of thermohaline intrusions, resulting in a nonunique $\theta$-$S$ relationship. This means that given a $\theta$ value, there will be some uncertainty on the $S$ value, leading to an error in the estimated $\rho$.

In order to assess the size of this error we have examined a conductivity-temperature-depth (CTD) data set, provided to us by L. Atkinson from Old Dominion University, corresponding to 25 stations done in September 1980 over our area of interest (these actually correspond to the three northernmost sections of *Atkinson* [1983], Figure 1). In Figure 3a we present the $\sigma_\theta$-$\theta$ diagram obtained with this data, plotted in the $26.2 \leq \sigma_\theta \leq 27.2$ range. In Figure 3a we have also plotted as a solid line the empirical curve obtained using *Armi and Bray*'s [1982] algorithm, which fits the data rather well. From Figure 3a we can also appreciate that there is some spreading in the $\sigma_\theta$-$\theta$ relationship, typically of ~0.05 $\sigma_\theta$ units and increasing toward the surface layers. This could perhaps be our first estimate for the density error, but the following discussion will show that it is actually an overestimate.

Let us call $\Delta\rho$ the density difference between data points (separated by a vertical distance $\Delta z$) as calculated from actual $S$ and $\theta$ data and $\Delta\hat{\rho}$ the density difference between the same data points as calculated from $\theta$ data and $S$ values inferred with *Armi and Bray*'s [1982] algorithm. These two quantities are related through $\delta\rho = |\Delta\hat{\rho} - \Delta\rho|$, $\delta\rho$ being the actual density error involved in our calculations. We may analyze the above unsmoothed CTD data, selecting a vertical distance $\Delta z = 10$ m, this being the order of both the vertical distance between our AXBT data points and the vertical size of finestructure in the Gulf Stream [*Gregg and Sanford*, 1980; *Pelegrí and Csanady*, 1994]. From the analysis we obtain that 55% of the data points have $\delta\rho$ below 0.01 $\sigma_\theta$ units and 85% have this error below 0.02 $\sigma_\theta$ units, the mean error being 0.011 $\sigma_\theta$ units. If we repeat the calculation with $\Delta z = 5$ m, we find similar numbers: 60% of the data points have $\delta\rho$ below 0.01 $\sigma_\theta$ units and 85% have this error below 0.02 $\sigma_\theta$ units, the mean error being 0.010 $\sigma_\theta$ units.

The above values are much smaller than those inferred from Figure 3a, but they still do not take into account the effects of vertical smoothing and relatively low vertical resolution of the analyzed AXBT data. In order to reproduce these effects we have repeated the above calculation for $\Delta z = 10$ m after having smoothed the CTD data with a running filter over 10 m. Figure 3b shows the results of this computation: in this case, 85% of the data points have an error below 0.01 $\sigma_\theta$ units, and 96% have an error below 0.02 $\sigma_\theta$ units, the mean error being 0.007 $\sigma_\theta$ units. The reason for these small $\delta\rho$ values is that the slope of the $\sigma_\theta(\theta)$ curve obtained from individual CTD casts is very similar to the slope of *Armi and Bray*'s [1982] empirical curve.

**4.1.4. Non-geostrophic displacements.** In a study near Cape Hatteras, *Johns et al.* [1989] have determined that the mean vertical isopycnal displacements due to internal tides range between ~2 m offshore and ~6 m near the Gulf Stream north wall. These small displacements are consistent with the small size of tidal current fluctuations in the northern Blake Plateau, which according to *Brooks and Bane* [1981], account for only ~10% of the variance in the along-stream velocity component. These results suggest that the fluctuations in the isopycnals' depth due to internal tides should be relatively small as compared with the isopycnal displacements between adjacent stations. The size of this error may be estimated as the fraction of the mean vertical displacement due to baroclinic tides divided by the mean depth difference of one isopycnal in two adjacent stations (in the cross-stream direction), i.e., $\delta z/\Delta z \simeq (5\ \text{m}/50\ \text{m}) = 0.1$. Note that this error will appear when calculating $\partial z/\partial x$ but not when computing $j$.

**4.1.5. Indirect errors.** The indirect errors are those related to the calculation of $\partial z/\partial x$ along surfaces that because of the above errors, are not truly isopycnals. Let us temporarily call the calculated potential density as $\hat{\rho}$, where the depth of a water particle is given by $z = z[x, y, \hat{\rho}(x, y, \rho, t), t]$. In this case the slope of the isopycnals and the slope of constant $\hat{\rho}$ surfaces are related through

$$\left.\frac{\partial z}{\partial x}\right|_\rho = \left.\frac{\partial z}{\partial x}\right|_{\hat{\rho}} + \left.\frac{\partial z}{\partial \hat{\rho}}\,\frac{d\hat{\rho}}{dx}\right|_\rho . \tag{8}$$

This shows that the error in the slope of an isopycnal must actually be increased with the second term in the right-hand side of (8).

## 4.2. Error Propagation

The maximum errors in the mixing properties may be estimated using a standard error propagation analysis [e.g., *Sánchez del Río*, 1989]. With this procedure we obtain the following expressions for the errors in the separation index ($\delta j$), the isopycnal slope ($\delta h$), and the Richardson number ($\delta Ri$):

$$\delta j = J\left(\delta\rho + \rho\frac{\delta z}{\Delta z} + \rho\frac{\delta\rho}{\Delta\rho}\right), \tag{9}$$

$$\delta h = h\left(\frac{\delta z}{\Delta z} + \frac{\delta x}{\Delta x}\right) + \delta h_a + \delta h_i , \tag{10}$$

$$\delta Ri = \frac{f^2}{gh^2}\delta j + \frac{2f^2 j}{gh^3}\delta h . \tag{11}$$

For convenience we have introduced here the slope of an isopycnal, $h \equiv \partial z/\partial x$, which is related to the diapycnal shear, $s \equiv \partial v/\partial \rho$, through the thermal wind equation, $\rho f s = gh$. In these expressions, $\Delta z$, $\Delta\rho$, and $\Delta x$ represent the changes in $z$, $\rho$, and $x$, respectively, employed to evaluate $j$ and $h$ from field data (all the other rel-

© Del documento, los autores. Digitalización realizada por ULPGC. Biblioteca Universitaria, 2009

evant quantities are derived from these two), while $\delta z$, $\delta\rho$, and $\delta x$ represent the field errors involved in measuring $\Delta z$, $\Delta\rho$, and $\Delta x$, respectively. Finally, $\delta h_a$ and $\delta h_i$ are the errors arising from ageostrophic isopycnal displacements and indirect errors, respectively.

The density error $\delta\rho$ will be the result of limitations in temperature resolution and variability in the $\theta$-$S$ relationship. The mean error due to variability in the $\theta$-$S$ relationship was estimated in section 4.1 as $0.007\,\sigma_\theta$ units. The error due to temperature resolution may be estimated using a linear approximation for density in terms of temperature and salinity and for salinity in terms of temperature. In this manner we obtain $\delta\rho = C\,\delta T$, with $C \simeq 0.3\,\sigma_\theta$ units °C$^{-1}$. The value for $\delta T$ is estimated by appreciating that this quantity appears only when calculating $\delta j$, so it refers to one single AXBT. For this reason we choose $\delta T$ as the resolution error for temperature readings when calculating $\rho$ (i.e., $\delta T = 0.01$ °C) and as twice this number when computing $\Delta\rho$, with the two factor arising because of the possible addition of errors when calculating differences; these would correspond to the first and third terms in the right-hand side of (9), respectively. The error involved in the last term of (9) is, however, the only potentially important error (it is larger than the first term by a factor $\rho/\Delta\rho$), and according to the previous approximations it is given by $\delta\rho \simeq 0.006\,\sigma_\theta$ units. The error due to the joint effect of temperature resolution and $\theta$-$S$ variability is simply calculated as the addition of the above individual estimates, resulting in $\delta\rho = 0.013\,\sigma_\theta$ units.

The depth error $\delta z$ will depend on the variable that is evaluated: $\delta j$ is calculated from one single AXBT data, while $\delta h$ is evaluated from data of two adjacent AXBTs. In the first case the error is estimated as $\delta z = 0.04\Delta z$. In the second case it is approximated by $\delta z = 0.04\bar{z} + 5$ m, where $\bar{z}$ is the mean depth (in meters) along an isopycnal for two adjacent AXBTs and 5 m corresponds to the mean isopycnal displacement caused by internal tides. In both cases the 0.04 coefficient corresponds to twice the accuracy in the probes' fall rate, again taking into account the possible addition of errors. We finally note that the position error is ~130 m, which causes $\delta x/\Delta x$ to be a small quantity, ~(130 m/12 km) $\simeq 0.01$.

After the above considerations we can write the following expressions for $\delta j$, $\delta Ri$, and the error in diapycnal shear ($\delta s$):

$$\begin{aligned}\delta j &= j\left(\frac{\delta\rho}{\rho} + \frac{\delta z}{\Delta z} + \frac{\delta\rho}{\Delta\rho}\right)\\ &\equiv \delta j_1 + \delta j_2 + \delta j_3\,, \qquad (12)\end{aligned}$$

$$\begin{aligned}\delta s &= s\left(\frac{\delta\rho}{\rho} + \frac{\delta z}{\Delta z} + \frac{\delta x}{\Delta x} + \frac{\delta\rho}{\Delta\rho}\right)\\ &\equiv \delta s_1 + \delta s_2 + \delta s_3 + \delta s_4\,, \qquad (13)\end{aligned}$$

$$\begin{aligned}\delta Ri &= Ri\left(\frac{\delta j}{j} + \frac{\delta\rho}{\rho} + \frac{2\,\delta s}{s}\right)\\ &\equiv \delta Ri_1 + \delta Ri_2 + \delta Ri_3\,, \qquad (14)\end{aligned}$$

where $\delta j_1 \equiv j\,\delta\rho/\rho < 10^{-5} j$, $\delta j_2 \equiv j\,\delta z/\Delta z \simeq 0.04 j$, $\delta j_3 \equiv j\,\delta\rho/\Delta\rho$, $\delta s_1 \equiv s\,\delta\rho/\rho < 10^{-5} s$, $\delta s_2 \equiv s\,\delta z/\Delta z \simeq 0.04\,s(\bar{z}/\Delta z + 0.1)$, $\delta s_3 \equiv s\,\delta x/\Delta x \simeq 0.01 s$, $\delta s_4 \equiv s\,\delta\rho/\Delta\rho$, $\delta Ri_1 \equiv Ri\,\delta j/j$, $\delta Ri_2 \equiv Ri\,\delta\rho/\rho$, and $\delta Ri_3 \equiv 2Ri\,\delta s/s$. The previous coefficients apply for all quantities in the MKS system.

The main contribution to $\delta j$ is $\delta j_3$, which arises from the $\delta\rho/\Delta\rho$ fraction. This fraction may be estimated as $(J\,\delta\rho)/\Delta z = (j\,\delta\rho)/(\rho\,\Delta z)$; choosing $\Delta z = 10$ m as the vertical distance over which AXBT data points are approximately independent, using $\delta\rho \simeq 0.01\,\sigma_\theta$ units, and having a typical $j$ value of $10^5$ m (section 5), we obtain a characteristic $\delta\rho/\Delta\rho$ value of ~0.1. The main contribution to $\delta s$ is $\delta s_2$, which is mostly related to possible errors in the probes' fall rate. Here $\delta s_2$ may be potentially important with increasing depth and for isopycnals of little slope because it depends on the fraction $(\bar{z}/\Delta z)$. The main potential contribution to $\delta Ri$ is $\delta Ri_3$, being twice the error in $s$.

We may summarize the above analysis by saying that the principal error source for $j$ is related to variability in the $\theta$-$S$ relation, while for both $s$ and $Ri$ the main error is related both to possible errors in the probes' fall rate and to $\theta$-$S$ variability. One additional consideration is that all $K_v$, $w_\rho$, and $\partial w_\rho/\partial\rho$ are functions of $Ri$ (in some instances, a high-order function), which causes their relative errors to be usually much larger. For example, in subcritical regions the error in the vertical density diffusivity will be $\delta K_v/K_v \simeq 9\,\delta Ri/Ri$ (equation (5)).

Besides the above errors, we have to keep in mind that there are intrinsic limitations related to the horizontal resolution and vertical smoothing of the data. For example, large station spacing and excesive vertical smoothing will usually lead to overestimates of the Richardson number. Another limitation is related to the uncertainties in the $K_v$ parameterization. Figure 1 shows only a few of many possible parameterizations but clearly illustrates that $K_v$ could change by as much as 1 order of magnitude depending on the selection. According to these considerations it is clear that our analysis of the distributions over a vertical section or an isopycnal surface must be mainly qualitative, looking at spatial and temporal patterns rather than at absolute numbers.

### 4.3. Monte Carlo Simulation

The above error propagation technique leads to estimates of maximum errors because it accumulates each individual error. In practice, however, some errors often will tend to compensate each other, and the final error will be much smaller. In this section we further pursue the issue of estimating errors, now through a Monte Carlo-style approach that produces more realistic values than those obtained with the error propagation technique.

The Monte Carlo method assumes that the measured variables indeed provide the true values, and it uses appropriate distributions that mimic the measurement errors in order to obtain a set of new simulated values [e.g., *Hammersley and Handscomb*, 1964]. The under-

© Del documento, los autores. Digitalización realizada por ULPGC. Biblioteca Universitaria, 2009

lying hypothesis is that the way in which the random errors contribute to the measured variable does not vary rapidly as a function of the true value, so the measured one is a reasonable surrogate.

In this analysis we have simulated, for every point in all $z$ and $j$ vertical sections, a sample set of 5000 values. This has been done both in the $(x, \rho)$ coordinates and in the $z$ and $j$ values using a uniform distribution within the following ranges: $\delta x = 130$ m, $\delta\rho = 0.01\sigma_\theta$, $\delta z = 0.04z$, and $\delta j = 0.1j$. For example, for every measured $z$ we have simulated 5000 new $z_i$ values within the range $z - \delta z < z_i < z + \delta z$. The ranges $\delta x$, $\delta\rho$, and $\delta z$ are those arising from the discussion in section 4.1, while the $\delta j$ range follows from the discussion in section 4.2.

Using the simulated values we have calculated at each point a sample of 5000 new values for both the diapycnal shear $\partial v/\partial\rho$ and the gradient Richardson number $Ri$. The error in each variable may be estimated as the standard deviation of the sample set generated at each point, and the relative error becomes the fraction between this standard deviation and the value initially calculated at that point. The results obtained with this method lead to errors considerably smaller than those obtained with the error propagation procedure, confirming that the propagation method provides a measure of the maximum errors arising from the data analysis.

## 5. Results

*Bane et al.* [1981, Figures 4 and 8] presented the surface temperature distribution for all five surveys as well as the temperature distribution at 100, 250, and 350 m for February 11. The temperature distributions clearly showed the progression of two large-amplitude meanders (which they called Bert and Ernie) through the region, with warm water filaments, or streamers, detaching from the crest of meanders into the cyclonic side of the stream. In these cases a dome of cold water, or a cold eddy, is formed between the filaments and the core of the Gulf Stream, usually at a trough of a meander. The filaments, however, are less evident with increasing depth and totally vanish at depths of ~250 m.

In Figure 4 we show the distribution of $\sigma_\theta$ at 200 m for all five surveys (the dots show the location of stations with water depth s 200 m). The filaments are not visible at this depth, and the meanders are considerably smoothed because of the compensating effect of salinity on density (in the western North Atlantic salinity decreases with depth) to the point where they are difficult to identify. A major meander, Ernie, is visible February 11, with its trough on section K and its crest between sections I and G; by February 14, Ernie's crest has propagated to somewhere between sections E and C. A more detailed description of this and other meanders will be given below.

Figures 5-9 show the distribution of several mixing properties, for all surveys, over the $\sigma_\theta = 26.34$ surface, with the dots showing the location of stations where water of this density is found. (Please note that in these and Figures 13-15 we have chosen to plot the logarithm distributions for the Richardson number, the density tendency, and the diapycnal convergence, because this greatly clarifies the plots, at the expense of some numerical smoothing in the maxima caused by the contouring routines.) Figures 5 and 6 show the distribution, for the February 11 and 17 surveys, of the following six quantities: depth $z$, separation index $j$, diapycnal shear $\partial v/\partial\rho$, gradient Richardson number $Ri$, density tendency $w_\rho$, and diapycnal convergence/divergence $\partial w_\rho/\partial\rho$. Figures 7-9, however, show the distribution of only two quantities ($j$ and $Ri$) for the remaining three surveys. The reason for showing a more complete set of quantities only for the February 11 and 17 surveys is for the sake of brevity and because they correspond to the two opposite situations that we want to compare: the presence of two large meanders February 11 versus no significant meander activity February 17.

The depth distribution of the $\sigma_\theta = 26.34$ isopycnal (Figures 5a and 6a) is also rather smooth in all stations. In Figure 5a (February 11) the meanders Bert and Ernie have their crests near sections C and I, respectively, while their troughs lie somewhere between sections E and G and near section K, respectively. The shallowing of this layer in the central portion of section K is indicative of a dome of cold water, while its deepening closer to the coast is indicative of a filament that emanated from the crest of meander Ernie. In Figure 6a, on the other hand, we may appreciate that on February 17 both meanders have traveled away from the region.

The distribution of the separation index $j$ over a shallow upper thermocline isopycnal (Figures 5b, 6b, 7a, 8a, and 9a) is a much better indicator of the meanders and filaments in the region: upwelling isopycnals are closely packed (relatively low $j$). An adequate threshold value showing the location of these rising isopycnals is $j = 20 \times 10^4$ m (surfaces separated by $0.1\sigma_\theta$ units are ~20 m apart), which is shown as a thick line in Figures 5b, 6b, 7a, 8a, and 9a (and as a thick broken line in the remaining parts of Figures 5-9). This isoline clearly follows the evolution of the meanders over the region. On February 9 the crest of Bert is near section K (Figure 7a), while by February 11 it has propagated to section C and the crest of Ernie is between sections I and G (Figure 5b). On February 14, Bert is already out of the region, while Ernie's crest has moved to between sections C and E (Figure 8a). On February 15 the crest of Ernie is located near section C (Figure 9a), while on February 17 it has finally left the region (Figure 6b). It is important to note that after the passage of these two meanders, there were still two small-amplitude oscillations going through the region: the crest of the first one propagated through sections K, G, and E February 14, 15, and 17, respectively, while the crest of the second one was located near section K on February 17 [see also *Bane et al.*, 1981, Figures 2 and 8].

The estimates for diapycnal shear, for the February

© Del documento, los autores. Digitalización realizada por ULPGC. Biblioteca Universitaria, 2009

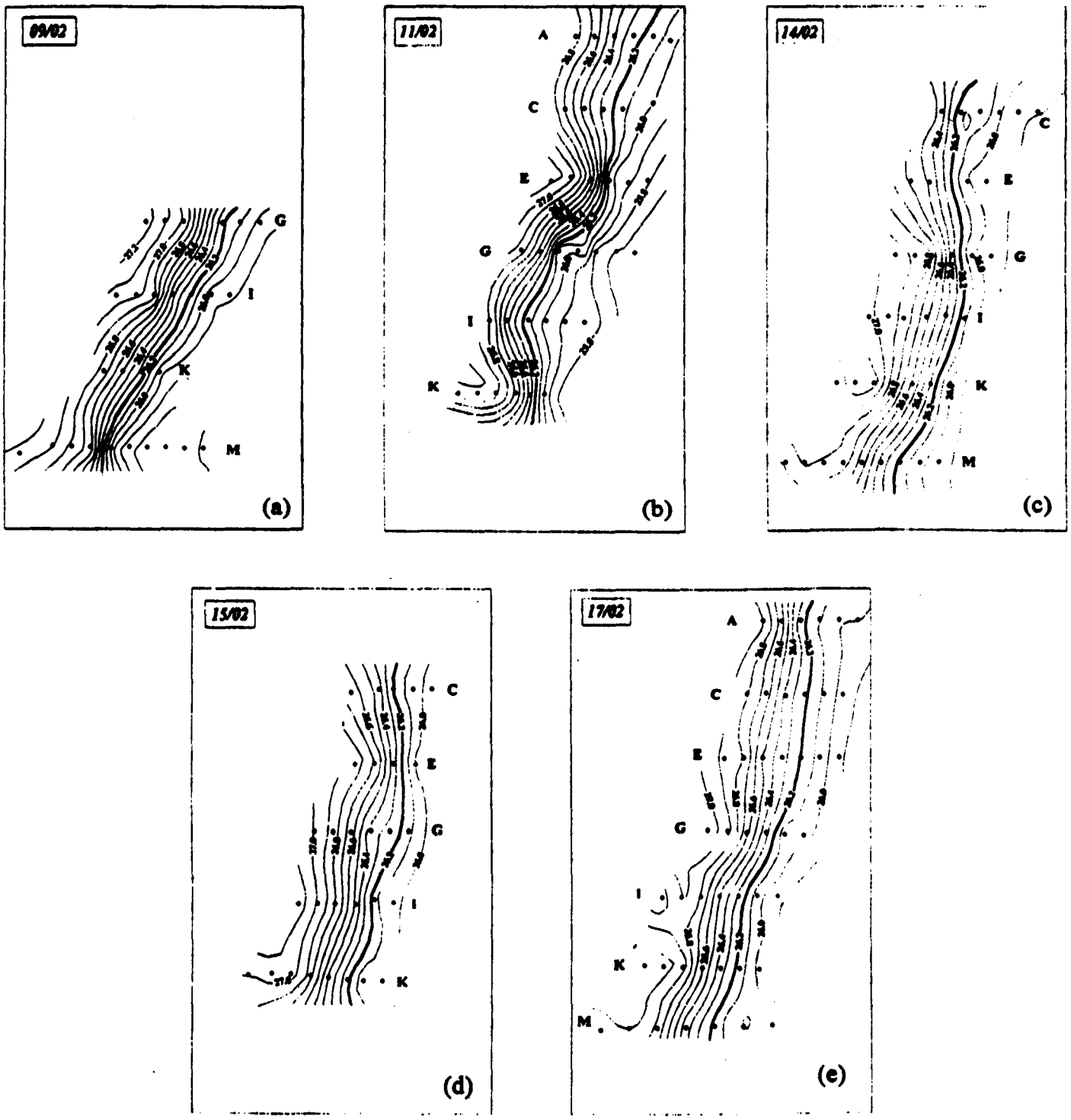


**Figure 4.** Sigma-theta $\sigma_\theta$ distribution at 200 m during February 1979, days (a) 9, (b) 11, (c) 14, (d) 15, and (e) 17.

11 and 17 surveys, are quite different (Figures 5c and 6c; the $\partial v/\partial \rho = 0.6$ m$^4$ kg$^{-1}$ s$^{-1}$ isoline is plotted there as a thick solid line). Figure 5c shows broad regions with relatively high diapycnal shear (maximum values of 1.2 m$^4$ kg$^{-1}$ s$^{-1}$), associated with the location of meanders, while Figure 6c shows that in the absence of large meanders these regions are much more restricted, and the maximum values are somewhat smaller (0.8 m$^4$ kg$^{-1}$ s$^{-1}$). Notice that these maxima mainly take place oceanward of the well packed isopycnals, i.e., in regions where $J$ is relatively large, because $\partial v/\partial \rho = J\, \partial v/\partial z$. Filaments may be associated with large vertical shear (*Brooks and Bane* [1983] reported countercurrents at the filaments as large as 0.5 m s$^{-1}$), but they spread over well-stratified regions (low $J$), and the corresponding diapycnal shear is moderate.

The main temporal and spatial patterns may be appreciated through the distribution of the gradient Richardson number (Figures 5d, 6d, 7b, 8b, and 9b). In many senses, Figures 5d, 6d, 7b, 8b, and 9b reflect the

© Del documento, los autores. Digitalización realizada por ULPGC. Biblioteca Universitaria, 2009

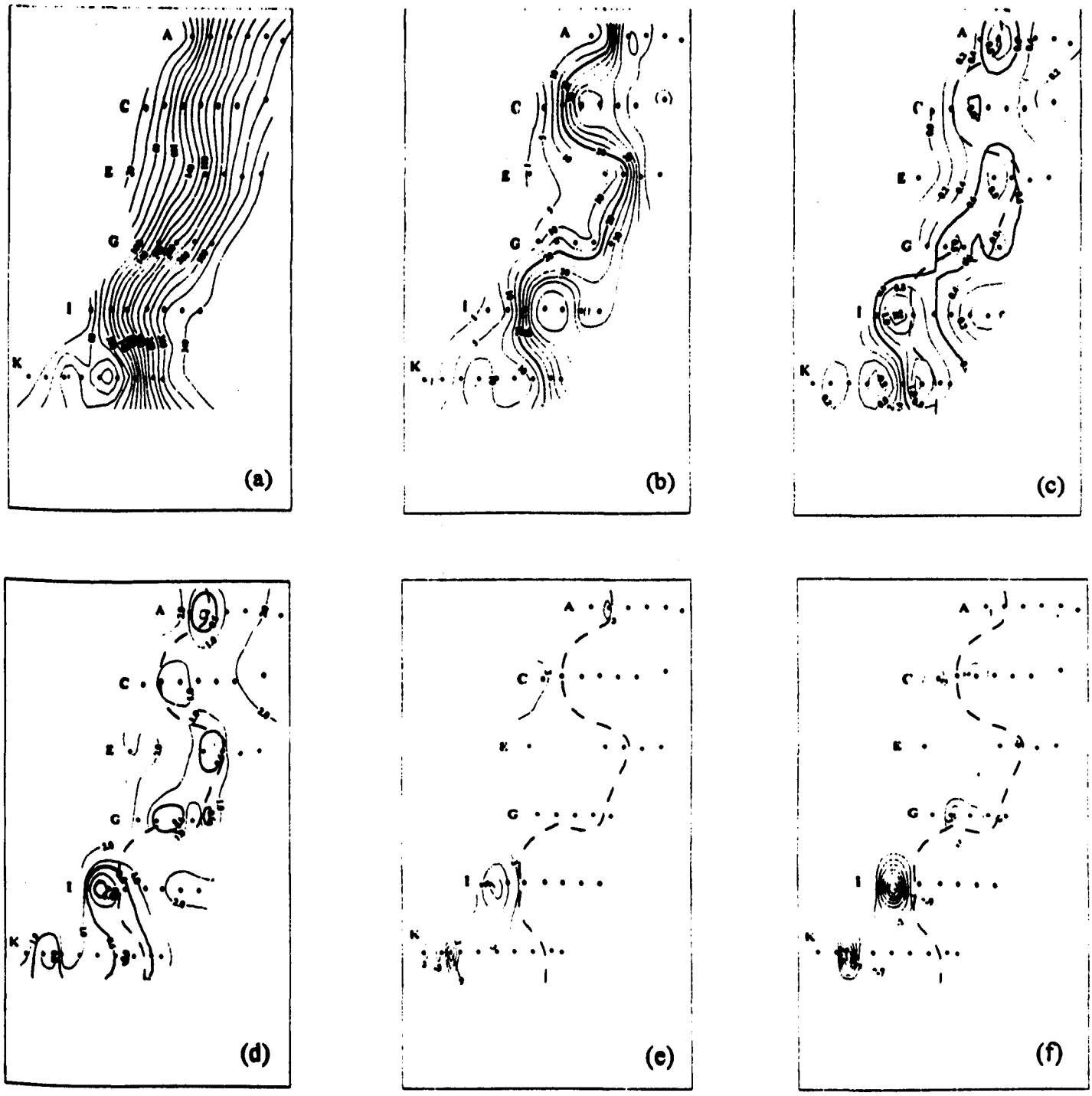


Figure 5. February 11 distribution over the $\sigma_\theta = 26.34$ surface of (a) depth $z$, (b) separation index $j$ ($10^4$ m), where the thick line corresponds to $j = 20 \times 10^4$ m, (c) diapycnal shear $\partial v/\partial \rho$ ($m^4\ kg^{-1}\ s^{-1}$), where the thick line corresponds to $\partial v/\partial \rho = 0.6\ m^4\ kg^{-1}\ s^{-1}$, (d) the logarithm of the Richardson number log $Ri$, where the thick line corresponds to log $Ri = 0.6$ ($Ri = 4$) and to log $Ri = -0.6$ ($Ri = 0.25$), (e) the logarithm of density tendency $w_\rho$ (units are such that log $w_\rho = n$ means $w_\rho = sgn(n)\, 10^{|n|-10}$ kg $m^{-3}\ s^{-1}$), and (f) the logarithm of diapycnal convergence/divergence $\partial w_\rho/\partial \rho$ (units are such that log $(\partial w_\rho/\partial \rho) = n$ means $\partial w_\rho/\partial \rho = sgn(n)\, 10^{|n|-8}$ $s^{-1}$). In Figures 5c, 5d, 5e, and 5f the $j = 20 \times 10^4$ m isoline is plotted as a thick broken line.

distribution of diapycnal shear because of the quadratic dependence of $Ri$ on $\partial v/\partial \rho$ (equation (4)), but they also illustrate the important role of the separation index. The logarithm values given by -0.6 ($Ri = 0.25$) and 0.6 ($Ri = 4$) are presented as thick solid lines to help visualize this evolution. Figures 5d and 7b show the existence of $Ri < 4$ over widespread areas, mainly over the crest and filament of meander Ernie but also at the trough of meander Bert. In particular, we may see that the absolute minimum, beyond subcritical ($Ri < 0.25$), is attained at Ernie's crest because of both low $j$ and high $\partial v/\partial \rho$. Figures 6c, 8b, and 9b suggest moder-

© Del documento, los autores. Digitalización realizada por ULPGC. Biblioteca Universitaria, 2009

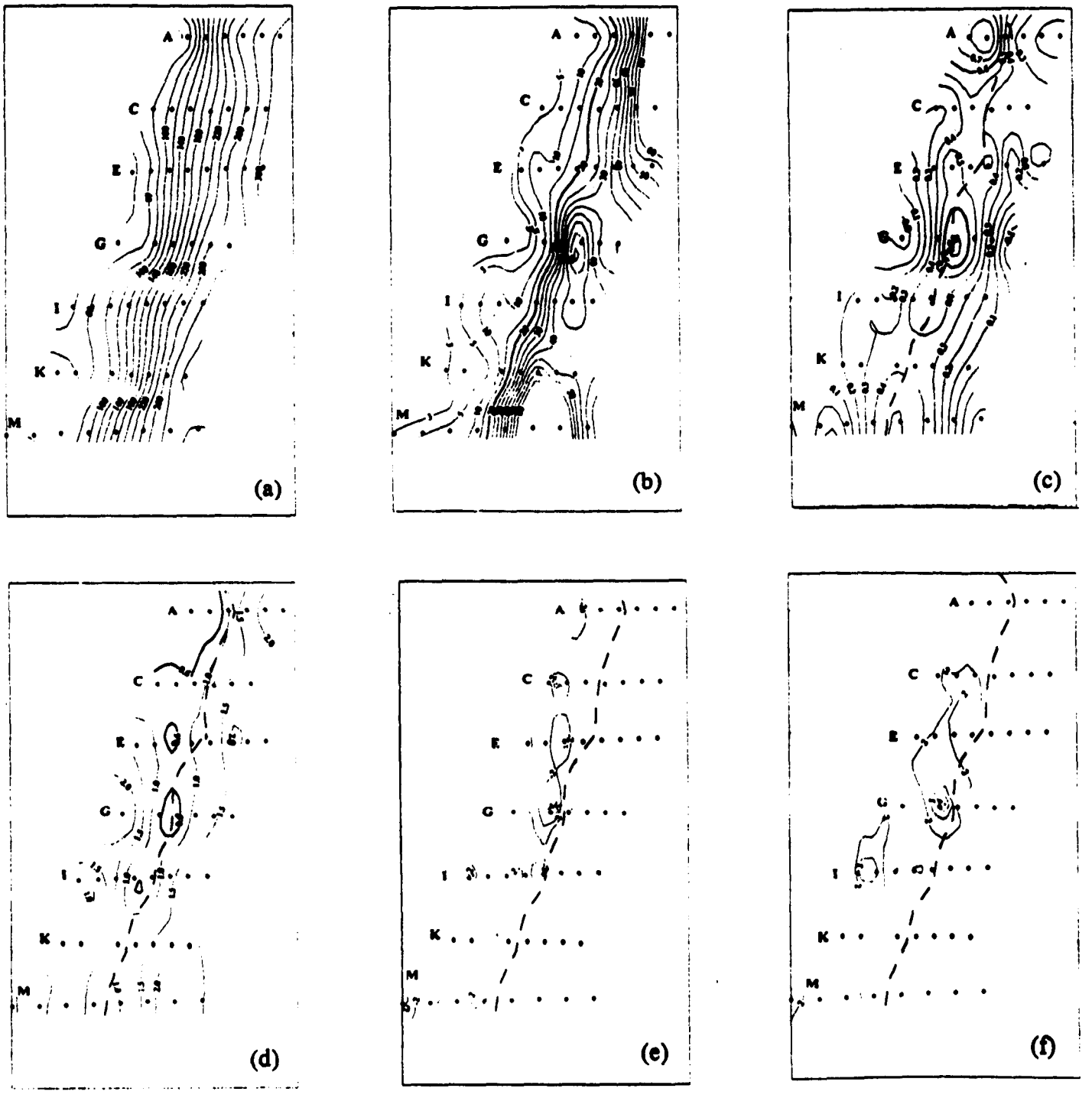


**Figure 6.** As in Figure 5 but for February 17.

ate dynamic stability, with $Ri$ typically ~10 and some scattered values below 4, possibly associated both with meander Ernie before it leaves the region and with the small-amplitude oscillations that are present in the area during February 14, 15, and 17.

Figure 10 presents the distribution of the maximum relative errors in diapycnal shear ($\delta s/s$) and the Richardson number ($\delta Ri/Ri$) over the $\sigma_\theta = 26.34$ surface for the February 11 survey. The error in the separation index ($\delta j$) is everywhere on this surface smaller than $0.3j$ and is not shown. Figure 10a shows that $\delta s$ ranges between $0.1s$ and $0.3s$ in most of the domain but reaches maximum values of $0.7s$ in the offshore regions, where the isopycnal surface is deep and rather flat. Figure 10b shows a similar picture for $\delta Ri$ but with values about twice as large ($0.2Ri$ to $0.6Ri$) in most of the domain. The $\delta Ri/Ri$ values over 0.6 are constrained to the deep offshore portion of the surface. Figure 11 presents the $\delta s/s$ and $\delta Ri/Ri$ distributions as calculated using the Monte Carlo method. Both methods lead to similar error patterns, with the Monte Carlo simulation leading to values about half those obtained with the propagation method. The main conclusion is that the errors are significant but should not affect the qualitative pat-

© Del documento, los autores. Digitalización realizada por ULPGC. Biblioteca Universitaria, 2009

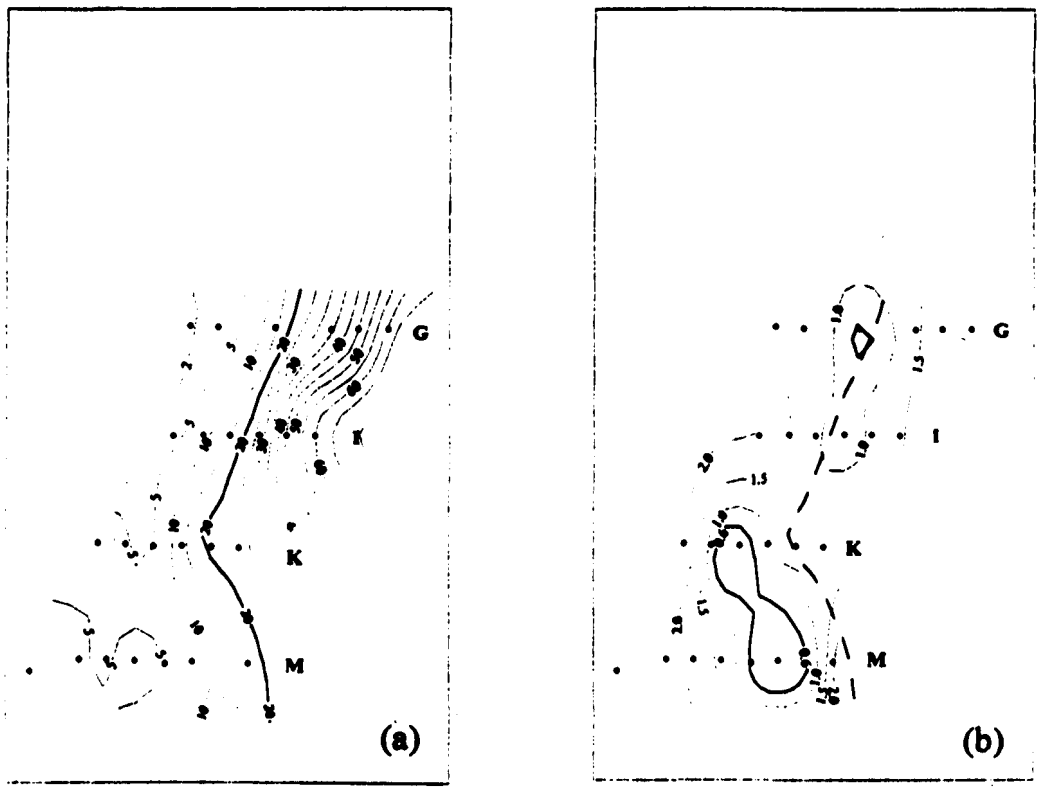


**Figure 7.** February 9 distribution over the $\sigma_\theta = 26.34$ surface of (a) the separation index $j$ ($10^4$ m) and (b) the logarithm of the Richardson number log $Ri$, where the thick line corresponds to log $Ri = 0.6$ ($Ri = 4$) and to log $Ri = -0.6$ ($Ri = 0.25$). The $j = 20 \times 10^4$ m isoline is plotted as a thick broken line.

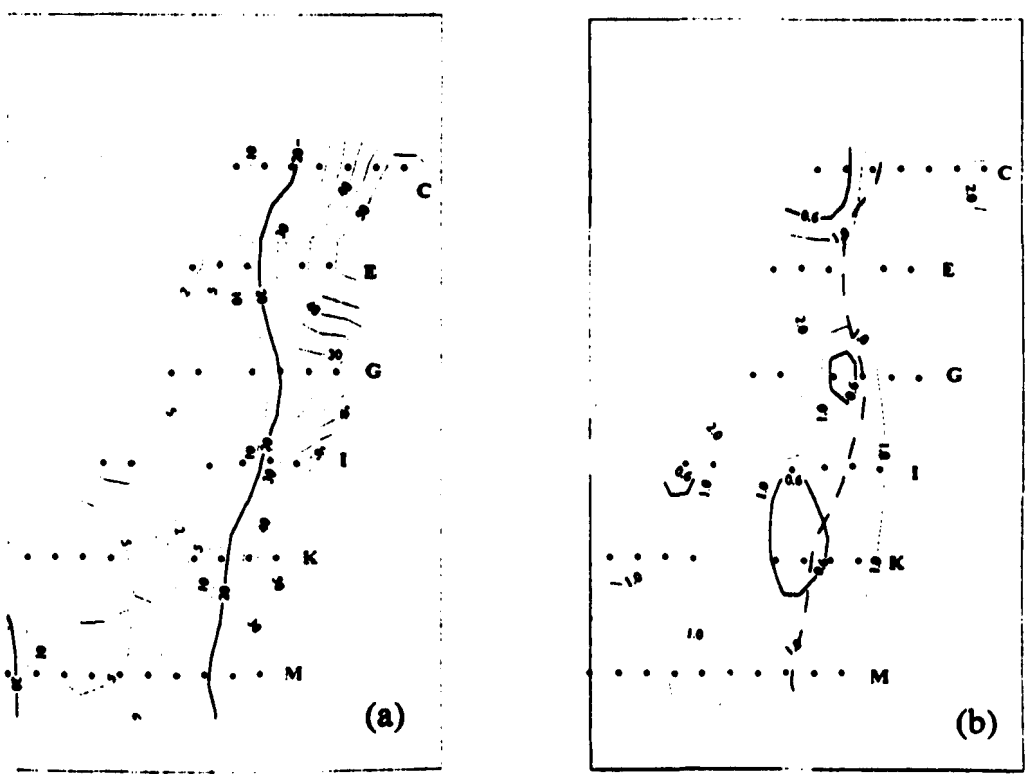


**Figure 8.** As in Figure 7 but for February 14.

© Del documento, los autores. Digitalización realizada por ULPGC. Biblioteca Universitaria, 2009

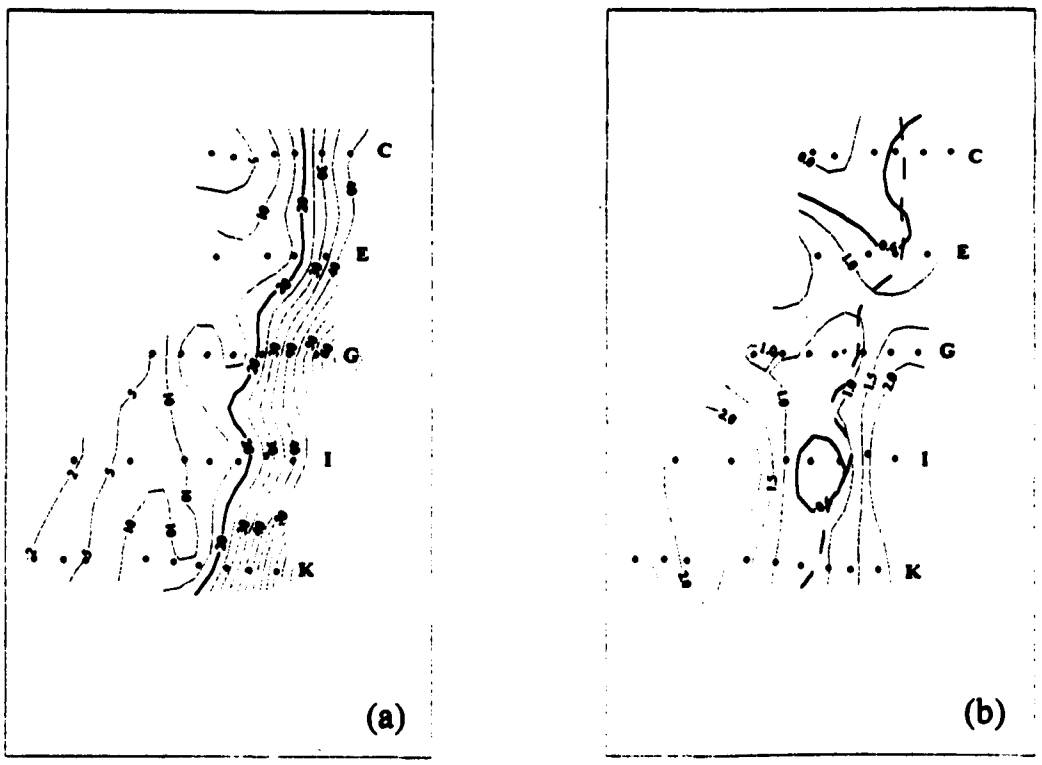


**Figure 9.** As in Figure 7 but for February 15.

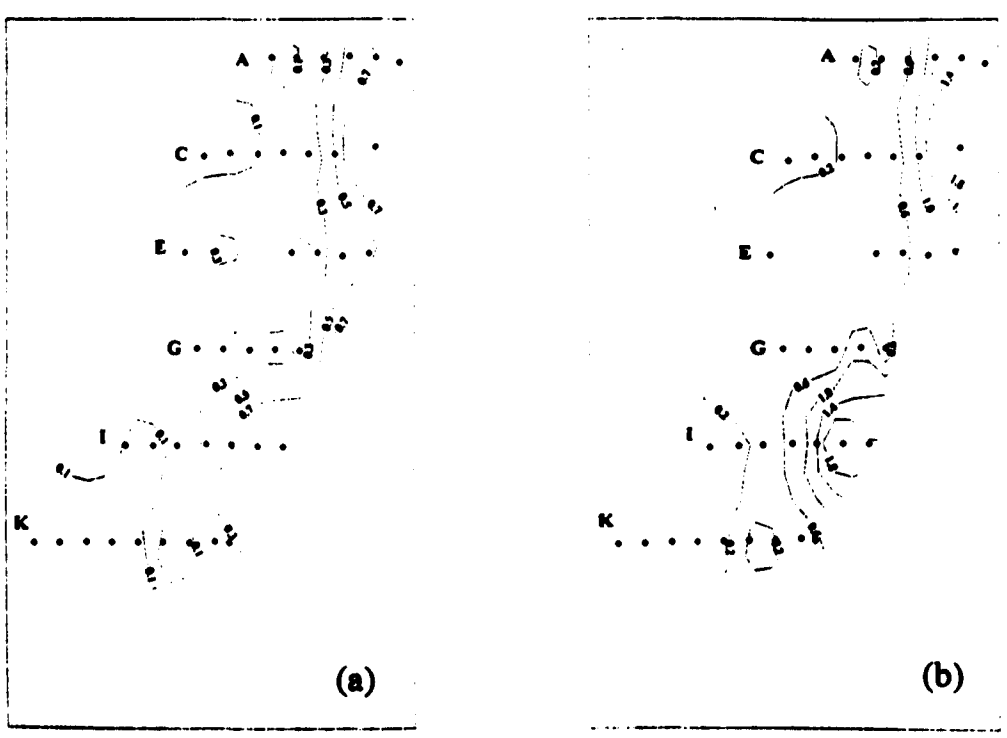


**Figure 10.** February 11 distribution over the $\sigma_\theta = 26.34$ surface of (a) maximum relative error in the diapycnal shear $\delta s/s$ and (b) maximum relative error in the Richardson number $\delta Ri/Ri$.

© Del documento, los autores. Digitalización realizada por ULPGC. Biblioteca Universitaria, 2009

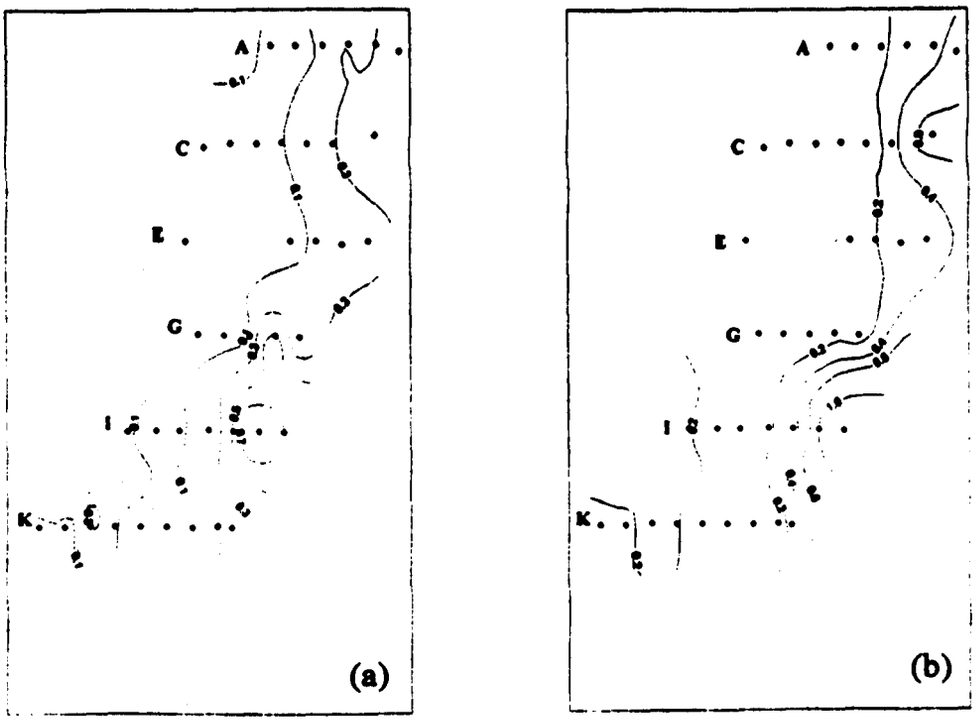


**Figure 11.** February 11 distribution over the $\sigma_\theta = 26.34$ surface of (a) relative error in the diapycnal shear $\delta s/s$ as obtained using the Monte Carlo method and (b) relative error in the Richardson number $\delta Ri/Ri$ as obtained using the Monte Carlo method.

terns extracted from the variable distributions, with the largest errors being found in the deepest regions and far away from meander activity.

The density tendency and diapycnal convergence are calculated using the parameterization described in section 2, and the results are presented in Figures 5e, 5f, 6e, and 6f. Maximum absolute values take place over Ernie's crest and its filament on February 11. The high values over the filament are related to the closely packed isopycnals near the continental shelf (recall the strong dependence of the density tendency with $J$ in (3)). The high values at the crest are clearly related to subcritical $Ri$ there.

The diapycnal (or entrainment) velocity is related to the density tendency by $w_d = Jw_\rho$ [*Pelegrí and Csanady*, 1994]. This implies that the diapycnal velocity, responsible for vertical mass and nutrient transfer, is further modulated by stratification. For example, the density tendencies are very high over both the crest and filament of a meander, but the diapycnal velocities may also be important in offshore upper thermocline layers where stratification is not so intense. Using the values in Figures 5 and 6 (but keeping in mind the note of caution expressed at the end of section 4.2), we may obtain diapycnal velocities as large as $10^{-2}$ m s$^{-1}$ over the crest and of order $10^{-5}$ m s$^{-1}$ farther offshore. At the filament the corresponding diapycnal velocities would be even larger, ~0.5 m s$^{-1}$. The accuracy of this very large values is questionable because the filament region has poor resolution in the density coordinate, but it is indicative of active mixing.

In Figures 12-15 we present the distribution of the mixing properties on three selected sections across the Gulf Stream. In Figure 12 we turn momentarily to the vertical coordinate system in order to show the $\sigma_\theta$ distribution for sections K and I during February 11 and for section K during February 17. In Figures 13, 14, and 15 we are back to the isopycnic system to show the distribution of $z$, $j$, $\partial v/\partial\rho$, $Ri$, $w_\rho$, and $\partial w_\rho/\partial\rho$ for these same sections. In order to ease intercomparison, Figures 12-15 are plotted to the same horizontal and vertical/isopycnic scales. The $j = 20 \times 10^4$ m isoline is presented in part b of Figures 12-15 as a thick solid line, while in parts c-f it is also plotted for reference as a thick broken line. In part c of Figures 12-15 the $\partial v/\partial\rho = 0.6$ m$^4$ kg$^{-1}$ s$^{-1}$ isoline is plotted as a thick solid line, while in part d of these same Figures the log $Ri = 0.6$ and -0.6 contours ($Ri = 4$ and 0.25, respectively) are also plotted as thick solid lines.

Figure 12a corresponds to section K, taken approximately across the trough of meander Ernie during February 11, while Figure 12b corresponds to section I, taken across the crest of meander Ernie that same day. Figure 12c shows the distribution on section K as characteristic of low meander activity during February 17. The frontogenetical character of the density structure associated with the meanders is clear as compared with much lower horizontal density gradients during the last day. Figures 13 and 14 correspond to the isopycnic distributions across sections K and I (trough and crest of meander Ernie, respectively) February 11. Figures 13 and 14 suggest some interesting features associated with the passage of meanders. On section K (Figure 13) the minimum (subcritical) $Ri$ values clearly correspond to the filament, where diapycnal shear is moderately low but the isopycnals are closely packed. A secondary

© Del documento, los autores. Digitalización realizada por ULPGC. Biblioteca Universitaria, 2009

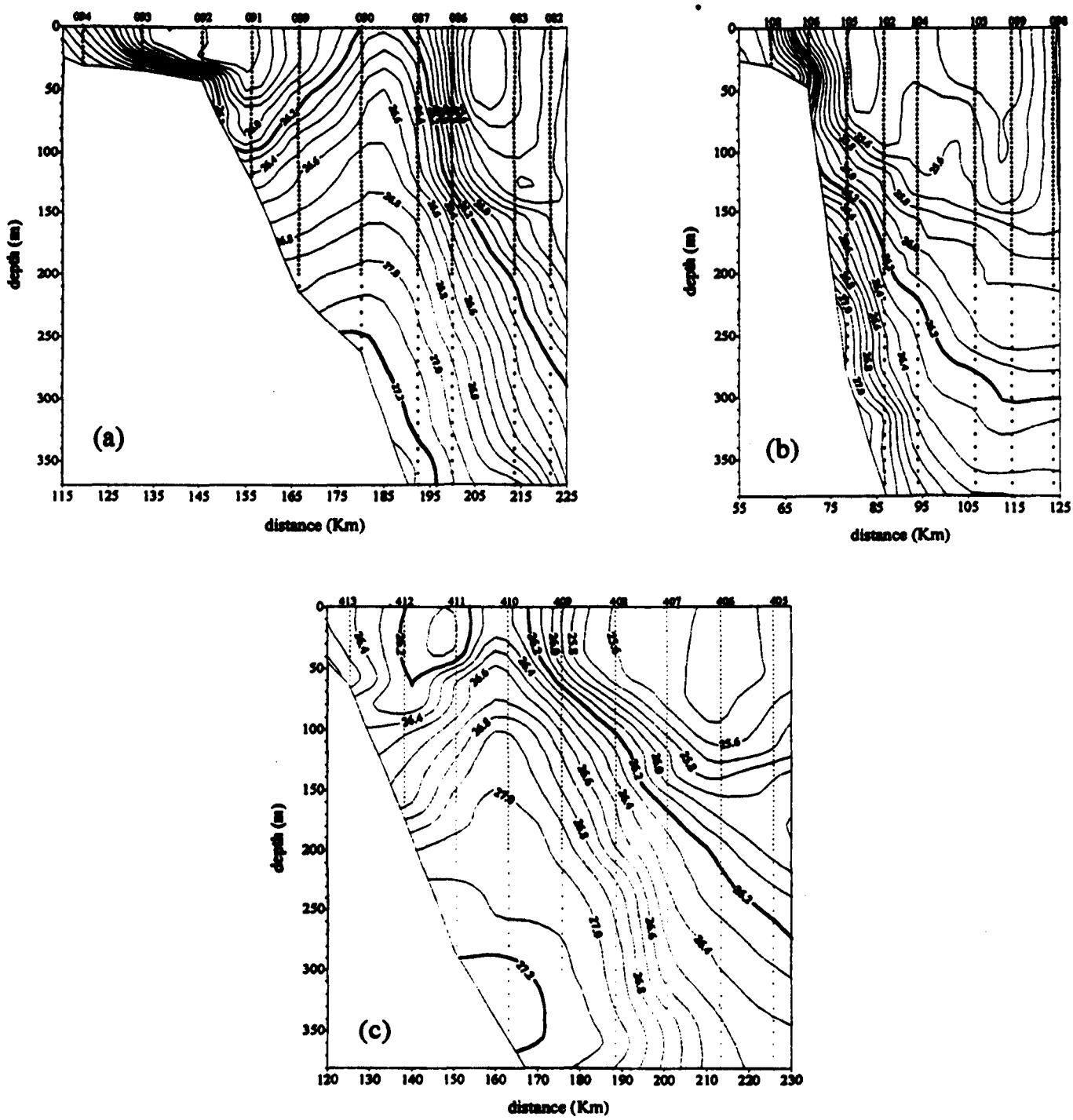


Figure 12. Potential density $\sigma_\theta$ distribution on (a) section K, February 11, (b) section I, February 11, and (c) section K, February 17.

minimum corresponds to the cyclonic side of the meander's trough, where the diapycnal shear is several times larger (1.5-2 $m^4\ kg^{-1}\ s^{-1}$) but $j$ is also ~20-30 times larger. In section I (Figure 14) the maximum diapycnal shear (almost 2 $m^4\ kg^{-1}\ s^{-1}$) totally overlies some of the smallest separation indexes in the cyclonic side of the meander's crest, causing an extensive area of subcritical $Ri$ values. Figure 15 corresponds to the isopycnic distribution across section K on February 17, in the absence of large meanders. In this case the maximum diapycnal shear is ~1 $m^4\ kg^{-1}\ s^{-1}$, i.e., only half the value found at Ernie's crest. Furthermore, this shear does not show good overlapping with regions of low $j$, and the corresponding $Ri$ values are nowhere subcritical.

Figures 16 and 17 present the relative errors for the diapycnal shear and the Richardson number, across section K on February 11, as calculated using both the error propagation and Monte Carlo methods, respectively. The errors become substantially large at some places but are relatively small in regions of low $Ri$ values, where mixing takes place. Furthermore, it is clear that the Monte Carlo method provides error estimates substantially smaller than the error propagation method.

The distributions of density tendency and diapycnal

© Del documento, los autores. Digitalización realizada por ULPGC. Biblioteca Universitaria, 2009

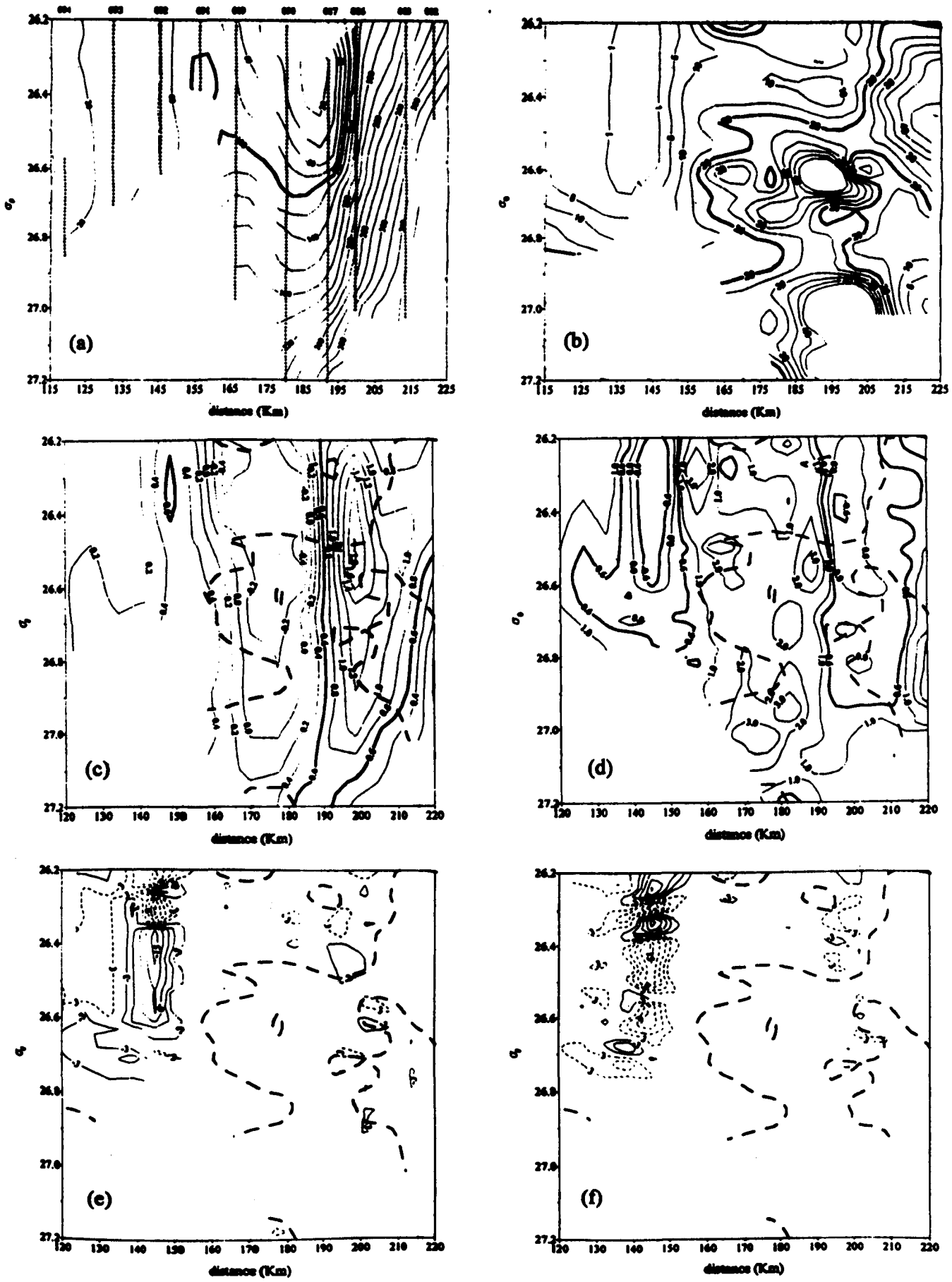


**Figure 13.** February 11 distribution over section K of (a) depth $z$, (b) separation index $j$ ($10^4$ m), (c) diapycnal shear $\partial v/\partial\rho$ (m $^4$ kg$^{-1}$ s$^{-1}$), the thick line corresponds to $\partial v/\partial\rho = 0.6$ m$^4$ kg$^{-1}$ s$^{-1}$, (d) the logarithm of the Richardson number log $Ri$, the thick line corresponds to log $Ri = 0.6$ ($Ri = 4$) and to log $Ri = -0.6$ ($Ri = 0.25$), (e) the logarithm of density tendency $w_\rho$ (units are such that log $w_\rho = n$ means $w_\rho = sgn(n)\,10^{|n|-10}$ kg m$^{-3}$ s$^{-1}$), and (f) the logarithm of diapycnal convergence/divergence $\partial w_\rho/\partial\rho$ (units are such that log $(\partial w_\rho/\partial\rho) = n$ means $\partial w_\rho/\partial\rho = sgn(n)\,10^{|n|-8}$ s$^{-1}$). In Figures 13c, 13d, 13e, and 13f the $j = 20\times10^4$ m isoline is plotted as a thick broken line.

© Del documento, los autores. Digitalización realizada por ULPGC. Biblioteca Universitaria, 2009

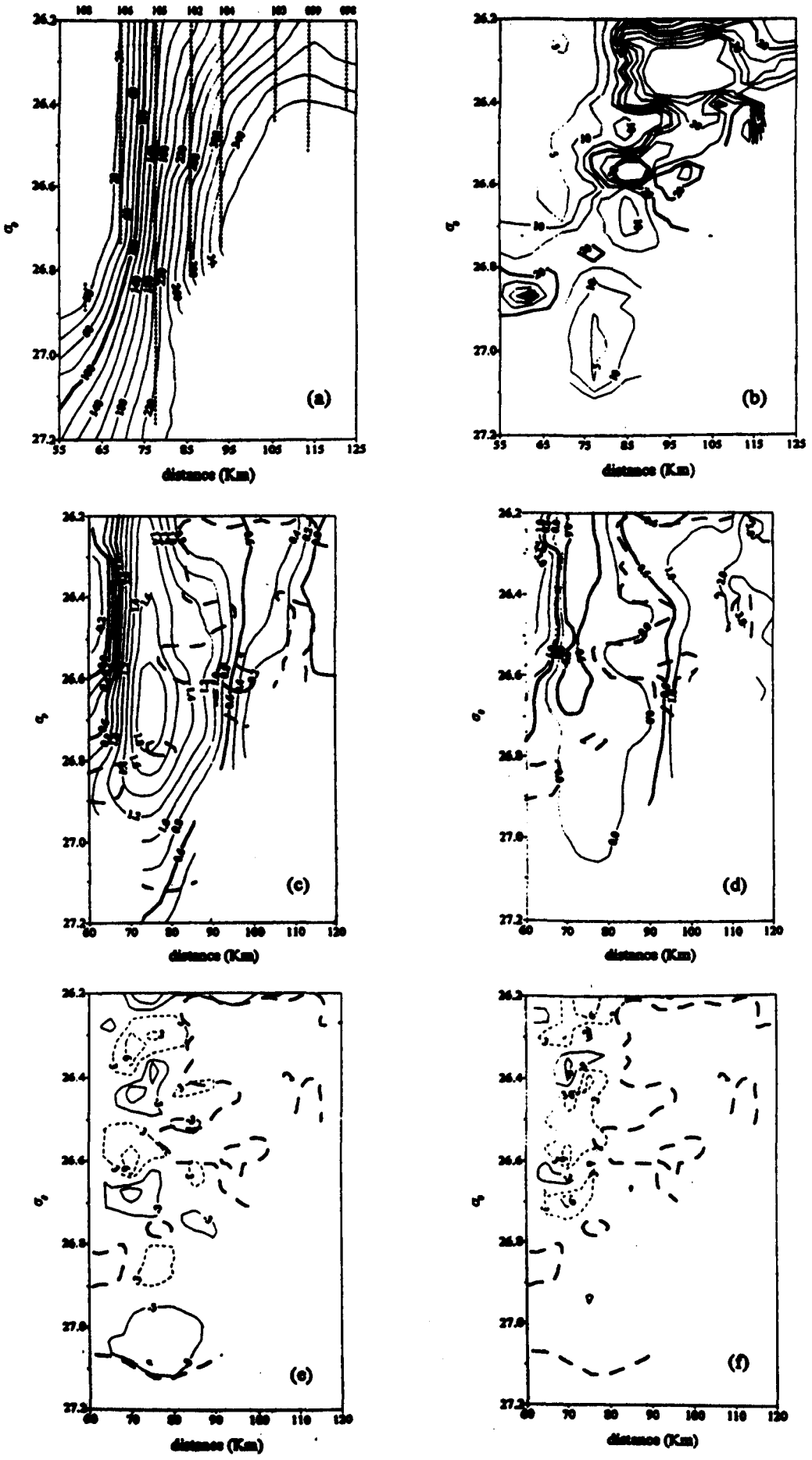


**Figure 14.** As in Figure 13 but for February 11, section I.

© Del documento, los autores. Digitalización realizada por ULPGC. Biblioteca Universitaria, 2009

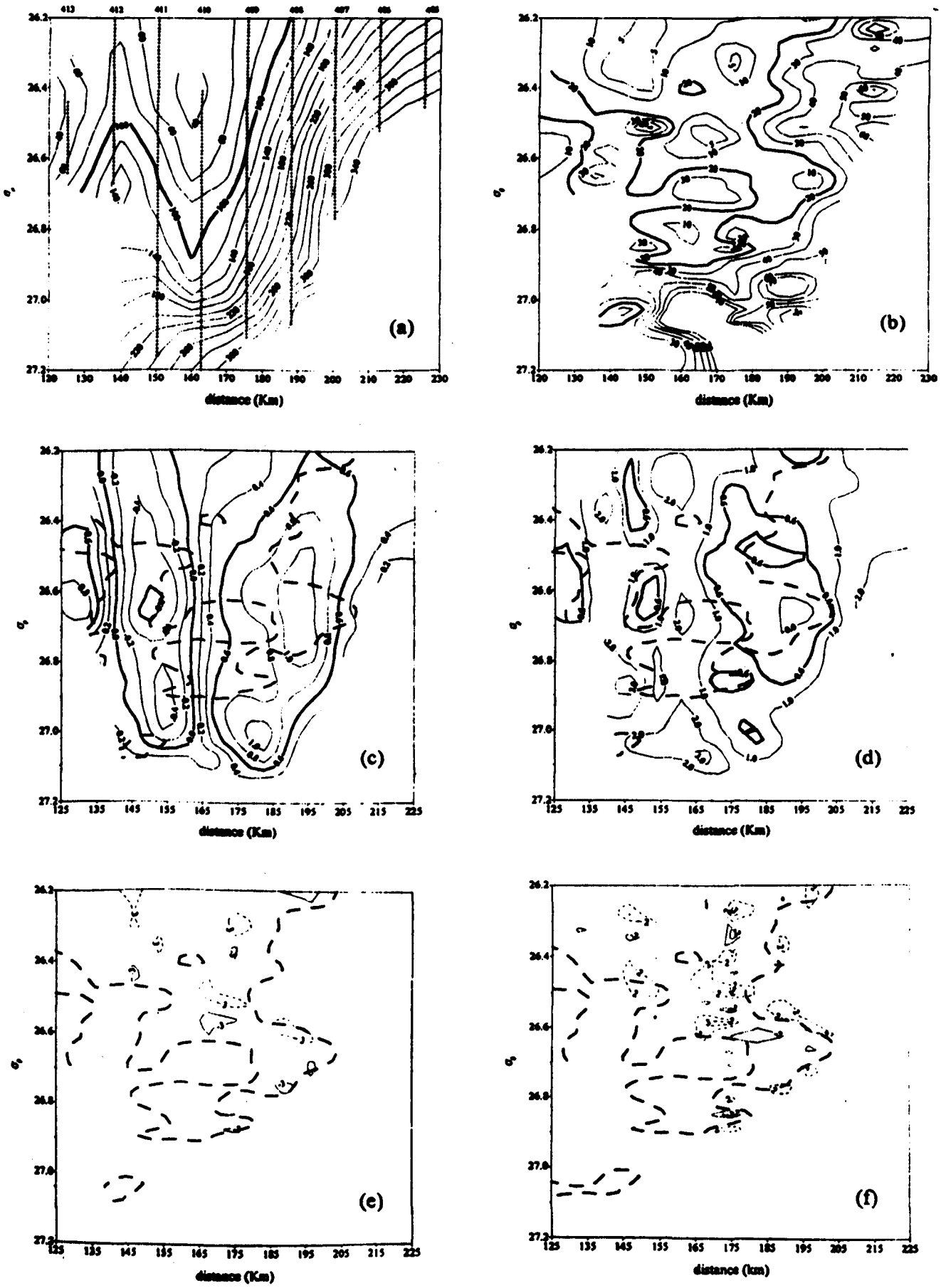


**Figure 15.** As in Figure 13 but for February 17, section K.

© Del documento, los autores. Digitalización realizada por ULPGC. Biblioteca Universitaria, 2009

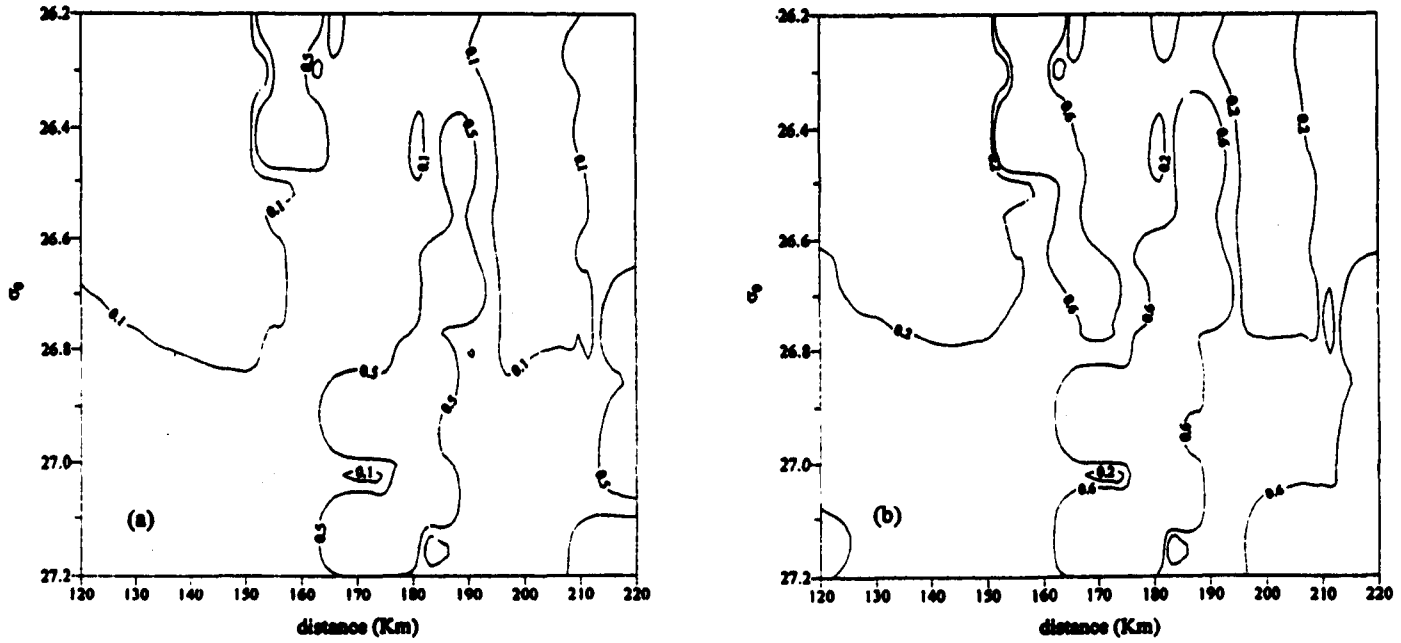


**Figure 16.** February 11 distribution over section K of (a) maximum relative error in the diapycnal shear $\delta s/s$ and (b) maximum relative error in the Richardson number $\delta Ri/Ri$.

convergence respond, as indicated by (3) and (7), to the distributions of $Ri$ and $j$. In general, small $Ri$ and $j$ values will guarantee large diapycnal mixing. Maximum activity corresponds to the closely packed filament and to the cyclonic side of the meander's crest (Figures 13 and 14). In the absence of large meanders the diapycnal mixing indicators attain much smaller values (Figure 15). A striking characteristic is the patchy character of the density tendency, with alternating positive and negative values (downward and upward diapycnal mass fluxes, respectively). The existence of several maxima (and/or minima) in density tendency causes the presence of patchy diapycnal convergence (negative values) and divergence (positive values).

## 6. Conclusions

Our calculations support the hypothesis of intense mixing in the surface and upper thermocline layers of the Gulf Stream, associated with frontogenetical stages taking place during meanders. During the passage of these meanders the maximum diapycnal shear $(\partial v/\partial \rho)$

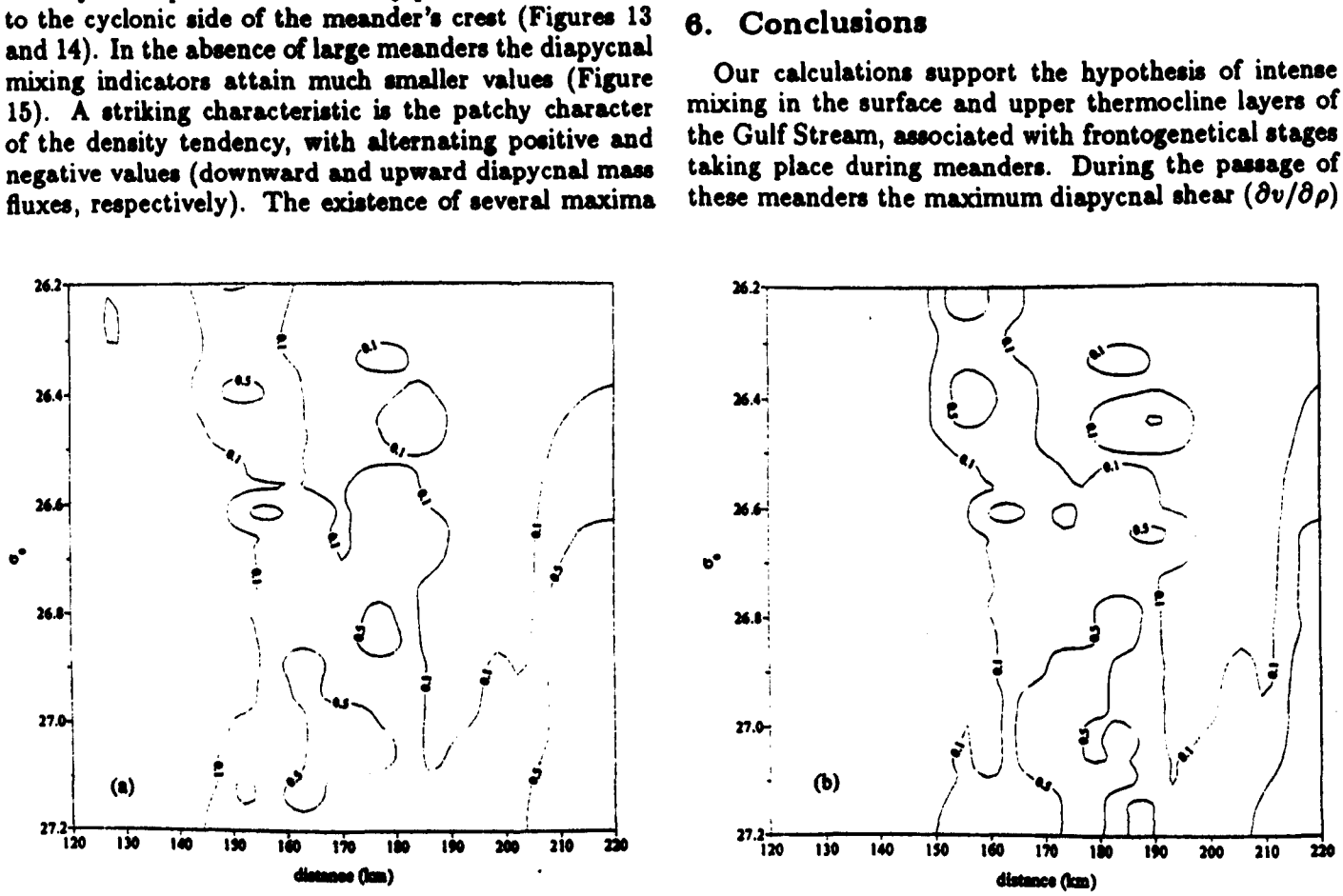


**Figure 17.** February 11 distribution over section K of (a) relative error in the diapycnal shear $\delta s/s$ as obtained using the Monte Carlo method and (b) relative error in the Richardson number $\delta Ri/Ri$ as obtained using the Monte Carlo method.

© Del documento, los autores. Digitalización realizada por ULPGC. Biblioteca Universitaria, 2009

shows a substantial increase as compared with situations with little meander activity. Furthermore, near the crest of the meanders the increase of diapycnal shear takes place in highly compressed regions (in Cartesian coordinates this would correspond to very high vertical shear), which causes these statically very stable regions to actually be dynamically unstable, characterized by near-critical and subcritical *Ri* numbers and large density tendencies and diapycnal convergence/divergence.

The presence of broad regions of low *Ri* values is probably related to the frontogenetical character of Gulf Stream meanders, which intensifies both the vertical stratification and the slope of the isopycnals (proportional to the diapycnal shear). This condition presumably also takes place in other unstable jets, such as the coastal upwelling jet, and may be the reason why in these systems the presence of near-critical *Ri* values is the rule rather than the exception [*Kundu and Beardsley*, 1991]. Our study has been limited to the production of shear-induced instabilities and mixing by the geostrophic flow field. The contribution to mixing by other sources, such as baroclinic tides and internal waves, may also be important but is beyond our scope.

Two points to note are, first, that the density tendency is directly related to the common entrainment equation through the Jacobian ($\partial z/\partial \rho$) but differs from the vertical epipycnal velocity which may be calculated from a dynamical meteorological tendency equation. Second, while it is true that we could have used the vertical coordinate system rather than the isopycnic coordinate system, we firmly believe that isopycnic thinking has some important conceptual and practical advantages. The main conceptual benefit is that it allows us to differentiate clearly between epipycnal and diapycnal mixing, two different physical processes, instead of simply comparing vertical and horizontal mixing. Some practical advantages are that we directly obtain estimates of density changes (the natural quantity to consider when discussing mixing) and diapycnal convergence/divergence (it is this quantity and not vertical convergence/divergence that controls the rate of separation of adjacent isopycnals).

The main limitation in our results comes from the intermittent and patchy character of the mixing processes, which requires very good temporal-spatial resolution and coverage. This character is probably associated with two factors: (1) frontogenesis taking place during the passage of meanders and (2) secondary frontogenesis being produced at the edges of the original mixing region. The data set we have used is probably adequate to deal with the vertical resolution but only marginally satisfactory to provide a good picture of the horizontal structure and temporal evolution of mixing. Another limitation arises from the accuracy of the AXBT data. Our results, however, clearly suggest that shear-induced diapycnal mixing is a principal process within Gulf Stream meanders.

As part of this study and motivated by some remarks from our reviewers, we have done a careful error analysis of the variables inferred from the AXBT data. A detailed discussion and application of two methods is presented in the paper: an error propagation method, which leads to the maximum possible errors resulting from cumulative errors in the analysis, and a Monte Carlo-type method, which generates an additional number of data sets that allow the computation of the standard deviations of the inferred values.

**Acknowledgments.** We would like to thank John Bane for kindly providing the AXBT data (obtained with funding from the Office of Naval Research and the National Science Foundation) and for a number of comments regarding the AXBT accuracy. We are also thankful to Larry Atkinson for gently providing the Blake Plateau CTD data (obtained with funding from the Minerals Management Service) and to our two reviewers for a number of very helpful comments. This work has been supported by the Spanish government through CICYT's project FRENTES (AMB95-0731) and by the European Union through MAST-3 project CANIGO (MAS3-CT96-0060).

## References

Armi, L., and N. A. Bray, A standard analytic curve of potential temperature versus salinity for the western North Atlantic, *J. Phys. Oceanogr.*, *12*, 384-387, 1982.

Atkinson, L. P., Distribution of Antarctic Intermediate Water over the Blake Plateau, *J. Geophys. Res.*, *88*, 4699-4704, 1983.

Bane, J. M., and M. H. Sessions, A field performance test of the Sippican deep aircraft-deployed expendable bathythermograph, *J. Geophys. Res.*, *89*, 3615-3621, 1984.

Bane, J. M., Jr. , D. A. Brooks, and K. R. Lorenson, Synoptic observations of the three-dimensional structure and propagation of Gulf Stream meanders along the Carolina continental margin, *J. Geophys. Res.*, *86*, 6411-6425, 1981.

Bower, A. S., Potential vorticity balances and horizontal divergence along particle trajectories in Gulf Stream meanders east of Cape Hatteras, *J. Phys. Oceanogr.*, *19*, 1669-1681, 1989.

Bower, A. S., and T. Rossby, Evidence of cross-frontal exchange processes in the Gulf Stream based on isopycnal RAFOS float data, *J. Phys. Oceanogr.*, *19*, 1177-1190, 1989.

Boyd, J. D., Improved depth and temperature conversion equations for Sippican AXBTs, *J. Atmos. Oceanic Technol.*, *4*, 545-551, 1987.

Boyd, J. D., and R. S. Linzell, Evaluation of the Sparton tight-tolerance AXBT, *J. Atmos. Oceanic Technol.*, *10*, 892-899, 1993.

Bower, S. A., H. T. Rossby, and J. L. Lillibridge, The Gulf Stream: Barrier or blender? *J. Phys. Oceanogr.*, *15*, 24-32, 1985.

Brooks, D. A., and J. M. Bane Jr., Gulf Stream fluctuations and meanders over the Onslow Bay upper continental slope, *J. Phys. Oceanogr.*, *11*, 247-256, 1981.

Brooks, D. A., and J. M. Bane Jr., Gulf Stream meanders off North Carolina during Winter and Summer 1979, *J. Geophys. Res.*, *88*, 4633-4650, 1983.

Bryden, H. L., New polynomials for thermal expansion, adiabatic temperature gradient and potential temperature of sea water, *Deep Sea Res. Oceanogr. Abstr.*, *20*, 401-408, 1973.

Chew, F., J. M. Bane Jr., and D. A. Brooks, On vertical motion, divergence, and the thermal wind balance in cold-dome meanders, a diagnostic study, *J. Geophys. Res.*, *90*, 3173-3183, 1985.

Churchill, J. H., E. R. Levine, D. N. Connors, and P. C. Cornillon, Mixing of shelf, slope and Gulf Stream water over the continental slope of the Middle Atlantic Bight, *Deep Sea Res., Part I*, *40*, 1063-1085, 1993.

© Del documento, los autores. Digitalización realizada por ULPGC. Biblioteca Universitaria, 2009

Csanady, G. T,. and P. Hamilton, Circulation of slopewater, *Cont. Shelf Res.*, *8*, 565-624, 1988.

Fisher, A., Entrainment of shelf water by the Gulf Stream northeast of Cape Hatteras, *J. Geophys. Res.*, *77*, 3248-3255, 1972.

Gregg, M. C., and T. B. Sanford, Signatures of mixing from the Bermuda Slope, the Sargasso Sea and the Gulf Stream, *J. Phys. Oceanogr.*, *10*, 105-127, 1980.

Hammersley, J. M., and D. C. Handscomb, *Monte Carlo Methods*, Monogr. Stat. Appl. Probab., Chapman and Hall, New York, 1964.

Hitchcock, G. L., T. Rossby, J. L. Lillibridge, E. J. Lessard, E. R. Levine, D. N. Connors, K. Y. Borsheim, and M. Mork, Signatures of stirring and mixing near the Gulf Stream front, *J. Mar. Res.*, *52*, 797-836, 1994.

Hood, C. A., and J. M. Bane Jr., Subsurface energetics in the Gulf Stream cyclonic frontal zone off Onslow Bay, North Carolina, *J. Geophys. Res*, *88*, 4651-4662, 1983.

Iselin, C.O'D., Some common characteristics of the Gulf Stream and the atmospheric jet stream, *Trans. N. Y. Acad. Sci., Ser. II*, *13*, 84-86, 1950.

Johns, E., D. R. Watts, and H. T. Rossby, A test of geostrophy in the Gulf Stream, *J. Geophys. Res.*, *94*, 3211-3222, 1989.

Keyser, D., and M. A. Shapiro, A review of the structure and dynamics of upper-level frontal zones, *Mon. Weather Rev.*, *114*, 452-499, 1986.

Kundu, P. K., and R. C. Beardsley, Evidence of a critical Richardson number in moored measurements during the upwelling season off northern California, *J. Geophys. Res.*, *96*, 4855-4868, 1991.

Lancaster, P., and K. Salkauskas, *Curve and Surface Fitting (An Introduction)*, Academic, San Diego, 1986.

Ledwell, J. R., A. J. Watson, and C. S. Law, Evidence for slow mixing across the pycnocline from an open-ocean tracer-release experiment, *Nature*, *364*, 701-703, 1993.

Lillibridge, J. L., G. Hitchcock, T. Rossby, E. Lessard, M. Mork, and L. Golmen, Entrainment and mixing of shelf/slope waters in the near-surface Gulf Stream, *J. Geophys. Res.*, *95*, 13,065-13,087, 1990.

Lohrenz, S. E., J. J. Cullen, D. A. Phinney, D. B. Olson, and C S. Yentsch, Distributions of pigments and primary production in a Gulf Stream meander, *J. Geophys. Res.*, *98*, 14,545-14,560, 1993.

Luther, M. A., and J. M. Bane Jr., Mixed instabilities in the Gulf Stream over the continental slope, *J. Phys. Oceanogr.*, *15*, 3-23, 1985.

Miller, J. L., and D. L. Evans, Density and velocity fine structure enhancement in oceanic eddies, *J. Geophys. Res.*, *90*, 4793-4806, 1985.

Munk, W. H., and E. R. Anderson, Notes on a theory of the thermocline, *J. Mar. Res.*, *7*, 276-295, 1948.

Newton, C. W., Synoptic comparison of jet stream and Gulf Stream systems, in *The Atmosphere and the Sea in Motion*, edited by B. Bolin, pp. 288-304, Rockefeller Inst. Press, New York, 1959.

Newton, C. W., Estimates of vertical motions and meridional heat exchange in Gulf Stream eddies and a comparison with atmospheric disturbances, *J. Geophys. Res.*, *66*, 853-870, 1961.

Newton, C. W., Fronts and wave disturbances in Gulf Stream and atmospheric jet stream, *J. Geophys. Res.*, *83*, 4697-4706, 1978.

Pacanowski, R. C., and S. G. H. Philander, Parameterization of vertical mixing in numerical models of tropical oceans, *J. Phys. Oceanogr.*, *11*, 1443-1451, 1981.

Padman, L., and I. S. Jones, Richardson number statistics in the seasonal thermocline, *J. Phys. Oceanogr.*, *15*, 844-854, 1985.

Palmén, E., and C. W. Newton, *Atmospheric Circulation Systems*, Academic, San Diego, 1969.

Park, Y., J. A. Whitehead, and A. Gnanadeskian, Turbulent mixing in stratified fluids: Layer formation and energetics, *J. Fluid Mech.*, *279*, 279-311, 1994.

Pelegrí, J. L., and G. T. Csanady, Nutrient transport and mixing in the Gulf Stream, *J. Geophys. Res.*, *96*, 2577-2583, 1991.

Pelegrí, J. L., and G. T. Csanady, Diapycnal mixing in western boundary currents, *J. Geophys. Res.*, *99*, 18,275-18,304, 1994.

Pelegrí, J. L., and J. G. Richman, On the role of shear mixing during transient coastal upwelling, *Cont. Shelf Res.*, *13*, 1363-1400, 1993.

Pelegrí, J. L., and J. G. Richman, Correction to "On the role of shear mixing during transient coastal upwelling," *Cont. Shelf Res.*, *14*, 1645-1646, 1994.

Pelegrí, J. L., and P. Sangrà, A mechanism for layer formation in stratified geophysical flows, *J. Geophys. Res.*, *103*, 30,679-30,693, 1998.

Pelegrí, J. L., G. T. Csanady, and A. Martins, The North Atlantic nutrient stream, *J. Oceanogr.*, *52*, 275-299, 1996.

Peters, H., M. C. Gregg, and J. M. Toole, On the parameterization of equatorial turbulence, *J. Geophys. Res.*, *93*, 1199-1218, 1988.

Phillips, O. M., Turbulence in a strongly stratified fluid: Is it unstable? *Deep Sea Res. Oceanogr. Abstr.*, *19*, 7-81, 1972.

Posmentier, E. S., The generation of salinity finestructure by vertical diffusion, *J. Phys. Oceanogr.*, *7*, 298-300, 1977.

Richards, F. A., and A. C. Redfield, Oxygen-density relationships in the western North Atlantic, *Deep Sea Res.*, *2*, 182-199, 1955.

Rossby, C. G., On the vertical and horizontal concentration of momentum in air and ocean currents, *Tellus*, *3*, 15-27, 1951.

Ruddick, B. R., and A. S. Bennett, Fine structure and mixing at the edge of a warm core ring, *J Geophys. Res.*, *90*, 8943-8951, 1985.

Ruddick, B. R., T. J. McDougall, and J. S. Turner, The formation of layers in a uniformly stirred density gradient, *Deep Sea Res., Part A*, *36*, 597-609, 1989.

Sánchez del Río, C., *Análisis de Errores*, Ediciones de la Univ. Complutense, Madrid, 1989.

Schmitt, R. W., R. G. Lueck, and T. M. Joyce, Fine- and microstructure at the edge of a warm-core ring, *Deep Sea Res., Part A*, *33*, 1665-1689, 1986.

Sessions, M. H., T. P. Barnett, and W. S. Wilson, The Airborne Expendable Bathythermograph, *Deep Sea Res. Oceanogr. Abstr.*, *23*, 779-782, 1976.

Stommel, H., *The Gulf Stream: A Physical and Dynamical Description*, 2nd ed., 248 pp., Univ. of Calif. Press, Berkeley, 1965.

Turner, J. S., Turbulent entrainment: The development of the entrainment assumption and its application to geophysical flows, *J. Fluid Mech.*, *173*, 431-471, 1986.

Ueda, H., S. Mitsumoto, and S. Komori, Buoyancy effects on the turbulent transport processes in the lower atmosphere, *Q. J. R. Meteorol. Soc.*, *107*, 561-578, 1981.

---

A. Marrero-Díaz, J. L. Pelegrí, A. Rodríguez-Santana, and P. Sangrà, Departamento de Física, Facultad de Ciencias del Mar, Universidad de Las Palmas de Gran Canaria, 35017 Las Palmas de Gran Canaria, Canary Islands, Spain. (e-mail: angel.rodriguez@fisica.ulpgc.es)

(Received February 13, 1996; revised May 28, 1999; accepted June 22, 1999.)

© Del documento, los autores. Digitalización realizada por ULPGC. Biblioteca Universitaria, 2009

ELSEVIER

Aquaculture 179 (1999) 499–512

Aquaculture

# Development of red porgy *Pagrus pagrus* visual system in relation with changes in the digestive tract and larval feeding habits

F.J. Roo [a,*], J. Socorro [a], M.S. Izquierdo [b], M.J. Caballero [b], C.M. Hernández-Cruz [b], A. Fernández [c], H. Fernández-Palacios [a]

[a] *Instituto Canario de Ciencias Marinas, Gobierno de Canarias, PO Box 56, E-35200 Telde, Las Palmas, Canary Islands, Spain*

[b] *Dpto. de Biología, Universidad de Las Palmas de Gran Canaria, PO Box 550, E-35017 Tafira Baja, Las Palmas, Canary Islands, Spain*

[c] *Dpto. de Morfología, Facultad de Veterinaria, Universidad de Las Palmas de Gran Canaria, Francisco Inglott Artiles, 12 35016-Las Palmas, Canary Islands, Spain*

**Abstract**

Red porgy larvae, like other sparids such as red seabream are visual feeders. The normal development of the visual system is essential for successful prey capture and predator avoidance, leading to increased larval growth and survival. The aim of this work is to characterise the development of visual organs in relation to changes in the digestive system and feeding habits. Twenty-five larvae from hatching to day 29 were daily collected from the rearing tank, fixed in formalin, embedded in paraffin, 5 μm sectioned and stained with haematoxylin and eosin (H&E) and Periodic Acid Shift Reactive-Haematoxiline (PAS-Hx). Light microscopy was used to study changes in ocular morphology with respect to digestive system development. At hatching, eye and digestive systems of *Pagrus pagrus* larvae have no function. However, at day 3 post-hatch, when the mouth opens, the larvae must be ready for prey capture and digestion. Despite this, few day 3 larvae had food in the digestive tract. At day 4 photoreceptors were well developed in the eye,

*Abbreviations:* A: Amacrine cells; B: Bipolar cells; C: Cornea; CR: Cartilaginous ring; DHA: Docosahexaenoic acid; EFA: Essential fatty acids; EPA: Eicosapentaenoic acid; G: Ganglion cell layer; HG: Hindgut; H: Horizontal cells; INL: Inner nuclear layer; IPL: Inner plexiform layer; ILCV: Ileocecal valve; LEC: Lens epithelial cells; L: Lens; LRM: Lens retractor muscle; MG: Midgut; ON: Optic nerve; ONL: Outer nuclear layer; OPL: Outer plexiform layer; P: Pigments; PN: Photoreceptor nuclei; PRES: Photoreceptors external segments; PRIS: Photoreceptors inner segments; RN: Rod nuclei

* Corresponding author. Tel.: +34-928132900/4; fax: +34-928132908; E-mail: jroo@iccm.rcanaria.es

0044-8486/99/$ - see front matter © 1999 Elsevier Science B.V. All rights reserved.
PII: S0044-8486(99)00183-0

© Del documento, los autores. Digitalización realizada por ULPGC. Biblioteca Universitaria, 2009

pigmentation pattern was complete and thus the visual system was completely ready for prey capture. This development coincided with detection of digestive activity in the midgut and most of larvae starting to take food. The results of this study suggest that adequate development of the visual system is important to establish the start of exogenous feeding. Besides, the appearance of rod cells increases larval photosensitivity and suggests that changes in lighting regimes could be necessary throughout the larval phase. © 1999 Elsevier Science B.V. All rights reserved.

*Keywords:* Red porgy; Larvae; Visual system; Digestive tract; Histology

## 1. Introduction

Red porgy is a species found on Eastern Atlantic coasts: Gibraltar Straits to 15°N (occasionally to 20°N) including Madeira and the Canary Islands; in the Mediterranean and northward to the British Isles (Bauchot, 1987; Bauchot and Hureau, 1990). It is found over hard (rock and rubble) or sandy bottoms (the young frequently found on seagrass beds) down to about 250 m depth, often above 150 m (Franquet and Brito, 1995). Red porgy is a characteristic pelagic spawner producing pelagic eggs ($1.00 \pm 0.02$ mm diameter). Spawning occurs between January and April, mainly when the water temperature reaches 18–22°C (Hernández-Cruz et al., 1990).

This species is being currently investigated as a potential aquaculture candidate (Kentouri et al., 1995; Stephanoun et al., 1995; Hernández-Cruz et al., 1997; Socorro et al., 1997).

At hatching, the larvae have a non-functional visual system, together with a poorly structured mouth and limited locomotion control similar to sea bream *Sparus aurata* (Blaxter, 1986). Larvae are hatched with relatively small yolk reserves and, as a result, they must start feeding soon after hatching. This requires the development of organs and systems involved in the capture and digestion of the food. Digestive and visual systems must be developed at the onset of feeding (Govoni et al., 1986).

Fish larvae are usually visual feeders, indicating that vision plays an important role in larval orientation at this stage (Blaxter, 1986). In sparids such as *Pagrus major* (Kawamura, 1984) and *Pagrus auratus* (Pankhurst, 1996) the most important changes in the eye structure occur in the lecitotrophic larvae as a preparation for prey capture. These changes should be coincident with digestive system development to start feeding as in *S. aurata* (Sarasquete et al., 1995; Hernández-Cruz et al., 1990). Other aspects of visual performance in relation to feeding have been investigated, especially the reception distance for food, which increases with body length (Blaxter, 1986).

This study aimed to shows the parallelism between the development of the digestive and visual system and the importance of both for the beginning of prey capture and predator avoidance. It has implications for hatchery management because an appropriate choice of prey size and lighting regimes will contribute to the success of larval rearing.

## 2. Materials and methods

The experiment was carried out from March 27th to April 26th at the Canary Institute of Marine Sciences.

© Del documento, los autores. Digitalización realizada por ULPGC. Biblioteca Universitaria, 2009

Eggs obtained from a wild stock of *Pagrus pagrus* by spontaneous spawning were distributed into 500-l fibreglass tank (100 eggs/l) filled with seawater. Larval development occurred between 20.5–21.8°C. Natural photoperiod of approximately 12 h light was used. Larvae were feed rotifers *Brachionus plicatilis* (S-1 strain) from day 4 after hatching, at a concentration of 10-rotifer $ml^{-1}$ in the larval culture tank. Rotifers were mass-cultured using bakers yeast and *Nannochloropsis* sp. (Eustigmatophycea). After day 20, *Artemia* nauplii were offered to larvae. Larval rearing procedure was as described by Hernández-Cruz et al. (1990).

Newly hatched larvae of 2.77 mm total length were reared up to 29 days and sampled daily. For that purpose, 20 larvae total length (TL), standard length (SL), head height (HH) and eye diameter (ED) were measured using a profile projector (Nikon V-12A).

### 2.1. Light microscopy

Another 25 red porgy larvae were fixed in 10% buffered formaldehyde for histological studies. All fish were sacrificed during the photophase so that the eyes were adapted to light at the time of fixation. Larvae were then dehydrated in an ethanol series, embedded in paraffin, serially sectioned at 4–5 μm, stained with haematoxylin and eosin (H&E) and Periodic Acid Shift Reactive-Haematoxylin (PAS-Hx) (García del Moral, 1993).

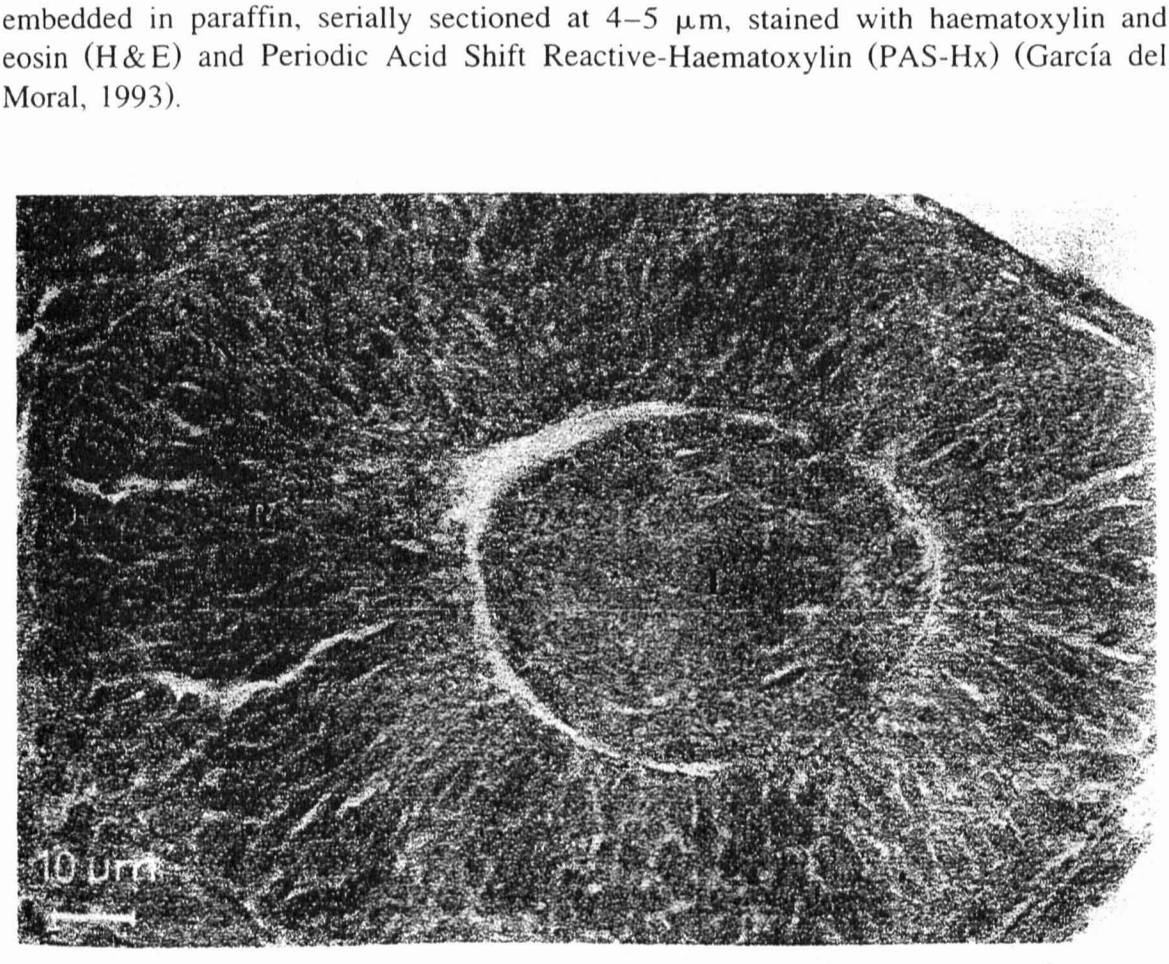


Plate I. Light micrograph of a longitudinal section through the eye of *P. pagrus* larvae at hatching (H&E). Eye lens (L) with undifferentiated cells. Retinal cells (R) on radial disposition. Precursors of the photoreceptors nuclei cells (PN) beginning to develop in the external part of the retina.

© Del documento, los autores. Digitalización realizada por ULPGC. Biblioteca Universitaria, 2009

BIBLIOTECA GENERAL

## 3. Results

At hatching, the eye lens (L) of *P. pagrus* showed undifferentiated cells having a spherical distribution. Retinal cells (R) are arranged radially and optic nerve were observed. At this stage, visual pigments were not present and some precursors of the photoreceptors nuclei cells (PN) were beginning to develop in the external part of the retina (Plate I). In the digestive tract, larvae had a simple undifferentiated straight gut linked to a non-structured mouth and anus.

The lens structure of one day old larva had two differentiated layers: an external layer of epithelial cells (LEC) surrounded by a non nucleated lens fibers layer formed by highly modified epithelial cells. On day 1 the retina also showed well defined layers, outer nuclear layer (ONL) composed by columnar nuclear bodies of photoreceptors, presumptive cones and an inner nuclear layer (INL) and a ganglion cell layer (G) formed by spherical nuclei of ganglion cells. Inner (IPL) and outer plexiform layers (OPL) showed the first signs of formation. At this stage several nuclei of pigment (P) cells were seen up the outer nuclear layer and a cartilaginous ring (CR) was present (Plate II). At this time in the foregut a short brush border was observed, with a digestive lumen being found in some larvae from the foregut to the hindgut.

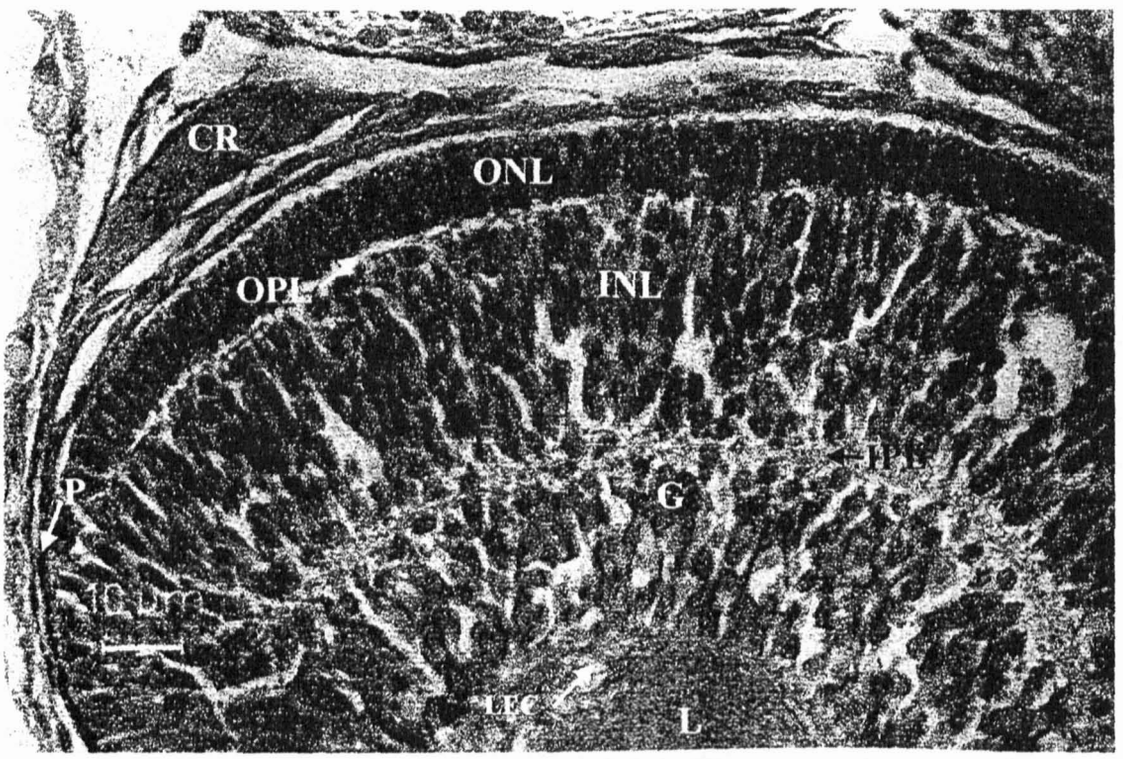


Plate II. Light micrograph of a longitudinal section through the eye of *P. pagrus* larvae at 1 day after hatching (3.65 mm TL). Retina differentiate into the outer nuclear layer (ONL), outer plexiform layer (OPL), inner nuclear layer (INL), inner plexiform layer (IPL), ganglion cell layer (G). Nuclei of pigment (P) cells were seen up the outer nuclear layer and cartilaginous ring (CR) was present. Bar equal to 10 µm (H&E).

© Del documento, los autores. Digitalización realizada por ULPGC. Biblioteca Universitaria, 2009

In two-day-old larvae, the nuclei photoreceptor in the outer nuclear layer increased in length. Inner and outer plexiform layers were well differentiated and a single layer of horizontal cells were present, down to the external plexiform layer. There was an increase in pigment contents. Lens retractor muscle was sketched and iris structure was better defined than days before. In the lens structure, there was an increase in the content of lens fibers and the lens epithelial cells were slender.

The digestive tract, initially straight, presented at this stage a small curvature in the last third of its length. The hindgut which was not pressured by the yolk sac, presented a clear digestive lumen. The brush border in the hindgut was less evident than in the foregut.

The third day after hatching the lens was well defined by a single epithelial cell layer with PAS affinity which covered the lens fibres. Photoreceptor cells were completely differentiated. Internal segment (PRIS) and external segment (PRES) contained visual pigments at this stage. Pigmented epithelial (PE) was well defined. Lens retractor muscle (LRM) was present and reached the lens, and the iris (I) was well defined (Plate III).

At day 3 post-hatch, the digestive system showed an increase in length at the anterior zone by a multiplication of the cell layers. In other parts of the digestive gut there was only a simple epithelium layer.

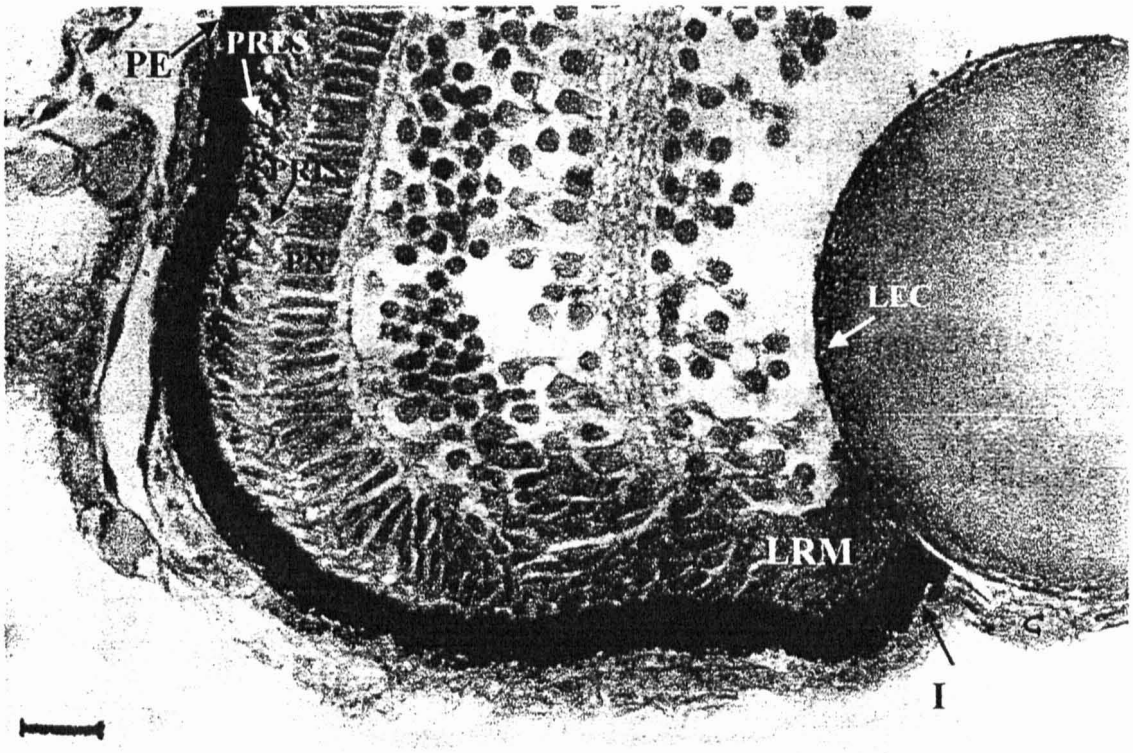


Plate III. Light micrograph of a longitudinal section through the eye of *P. pagrus* larvae at 3rd day after hatching (3.77 mm TL) (H&E). Pigmentation pattern was complete (PE), and the iris (I) was present, cornea (C) and lens epithelial cells (LEC) was well differentiated, lens retractor muscle (LRM) was patent.

© Del documento, los autores. Digitalización realizada por ULPGC. Biblioteca Universitaria, 2009

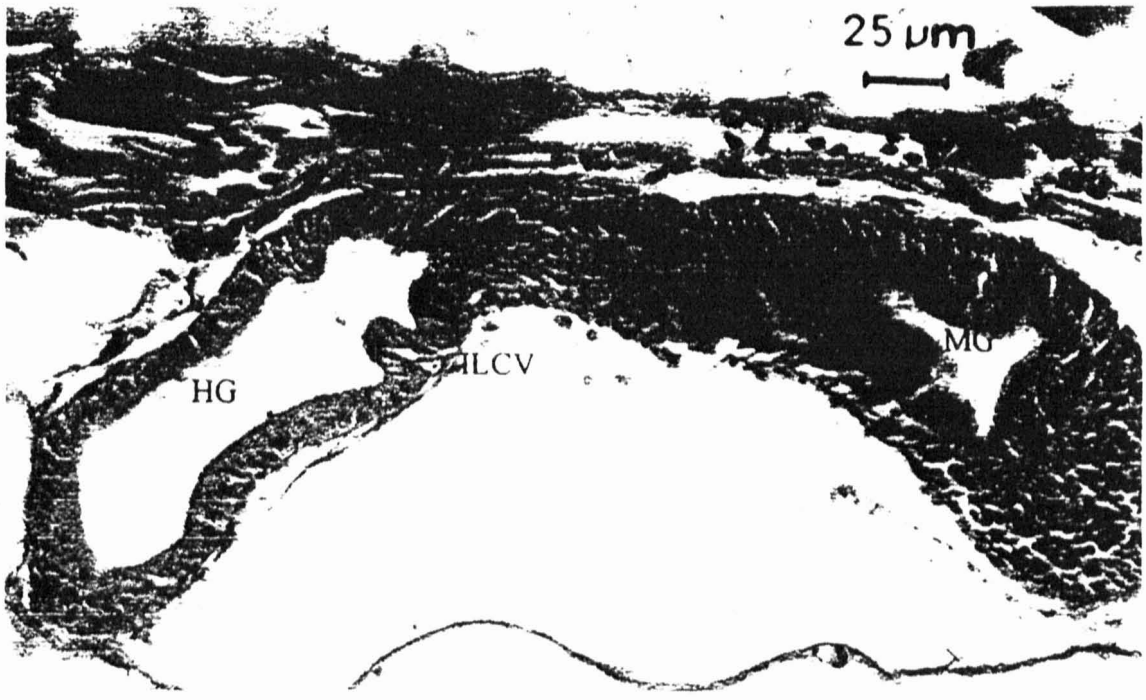


Plate IV. Light micrograph of a longitudinal section through the digestive system of *P. pagrus* larvae at 3rd day after hatching. Midgut (MG), ileocecal valve (ILCV), hindgut (HG), (3.77 mm TL) (H&E).

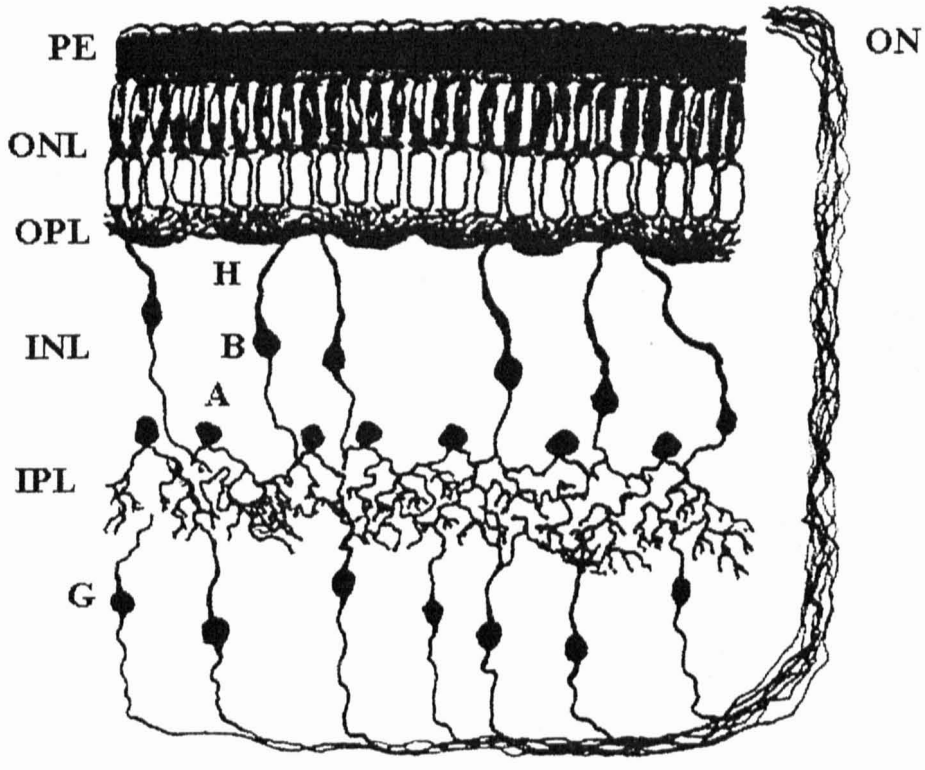


Plate V. Diagram of *P. pagrus* retina layers. Pigment epithelium layer (PE), outer nuclear layer (ONL), outer plexiform layer (OPL), inner nuclear layer (INL), horizontal cells (H), amacrine cells (A), bipolar cells (B), inner plexiform layer (IPL), ganglion cell layer (G), optic nerve (ON).

© Del documento, los autores. Digitalización realizada por ULPGC. Biblioteca Universitaria, 2009

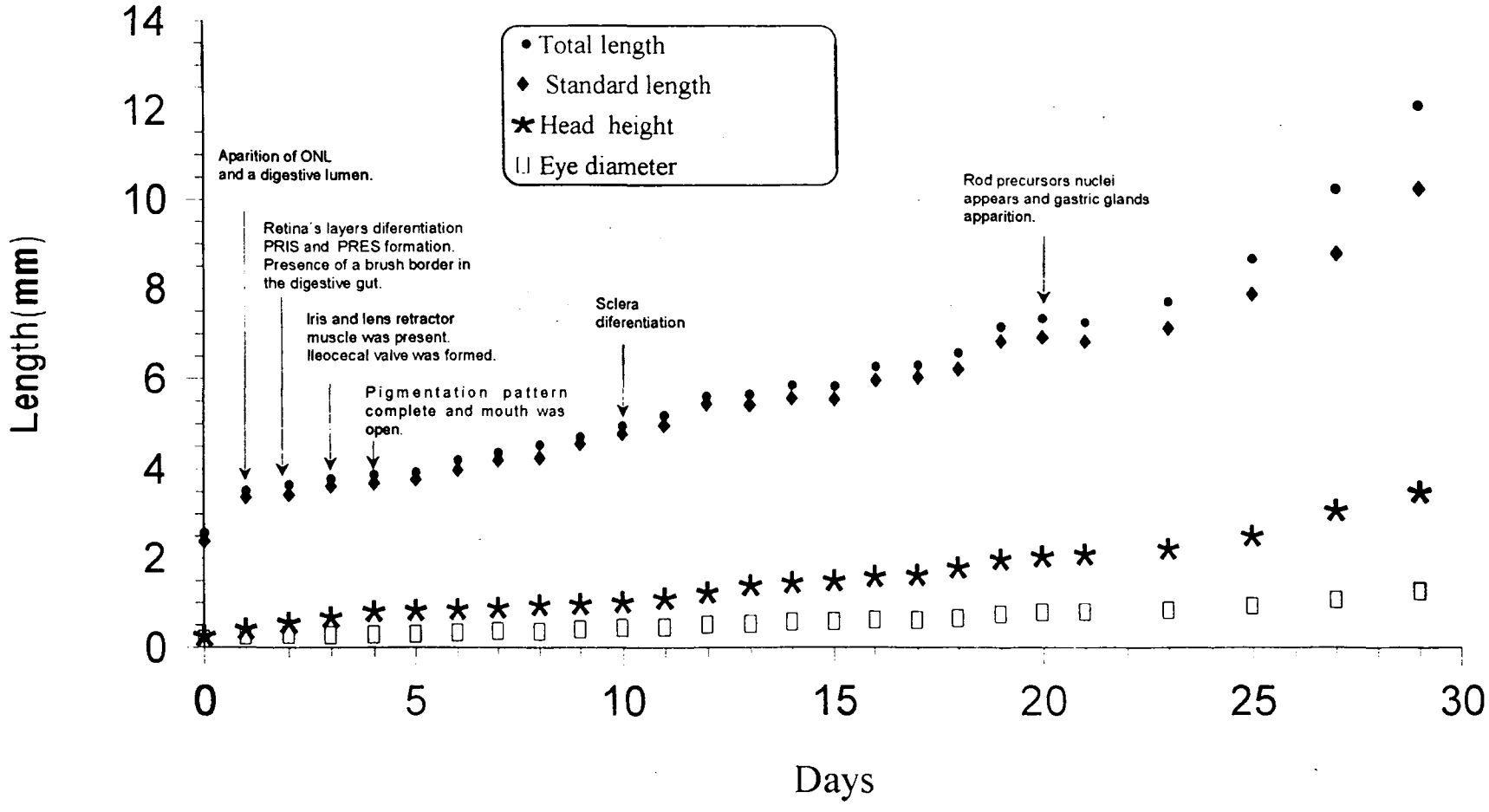


Fig. 1. Daily evolution of different morphological parameters, total length, standard length, head height and eye diameter in *P. pagrus* larvae.

© Del documento, los autores. Digitalización realizada por ULPGC. Biblioteca Universitaria, 2009

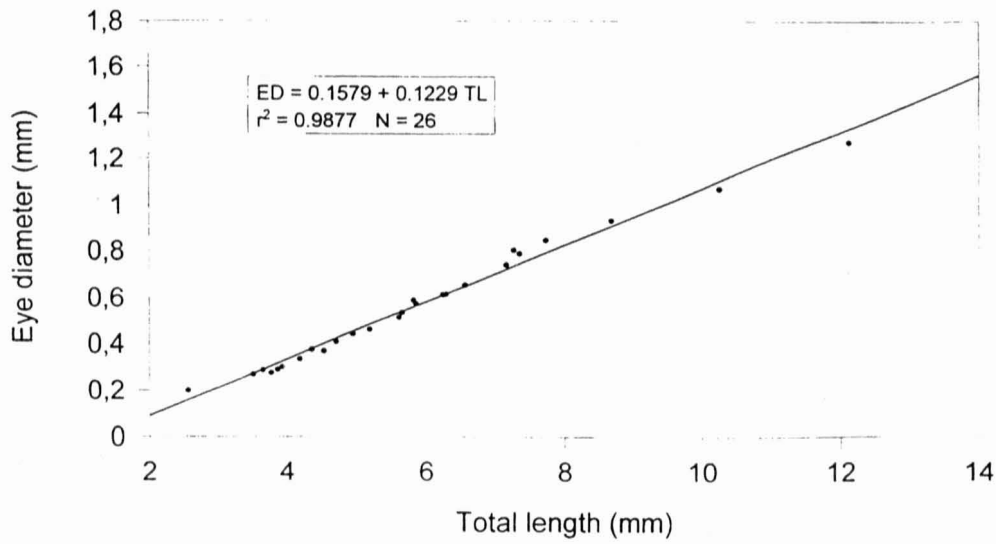


Fig. 2. Relationship between the total length (TL) and the eye diameter (DE) for *P. pagrus* larvae.

At this time, the ileocecal valve (ILCV) was formed, which separates midgut (MG) and hindgut (HG) (Plate IV).The brush border was seen from the most anterior part of foregut to the end of the intestinal tract. From day 3 post-hatch, the larval digestive tube could be divided into several parts: an oesophagus composed of a simple plane epithelium layer; a foregut formed by a simple cubical epithelium layer; a midgut where the epithelium layer was columnar, and a hindgut from the ileocecal valve composed of a columnar epithelium also.

By the fourth day, a clear differentiation of the retina layers was found. Pigmentation was completed and the eyes appeared like an adult fish eye (Plate V). The eye diameter

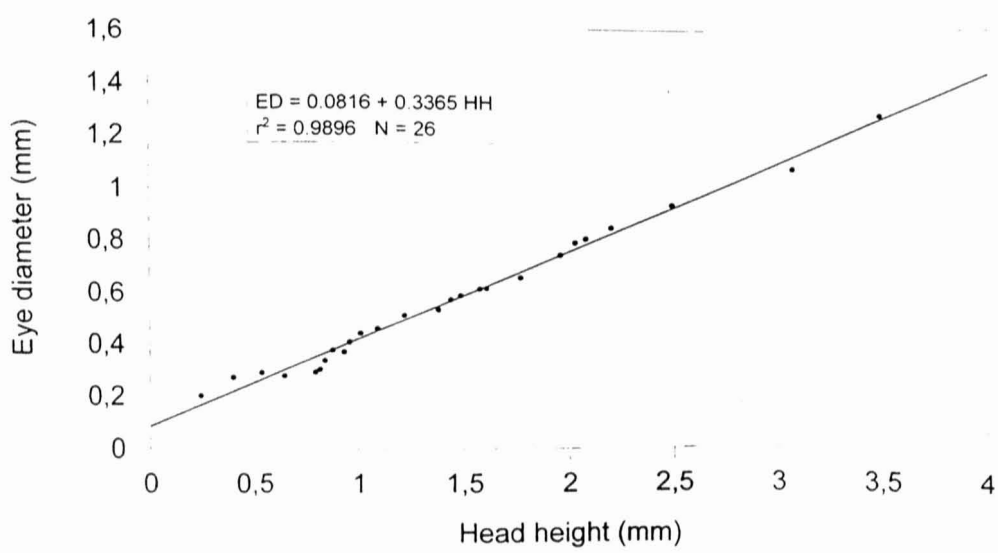


Fig. 3. Relationship between the head height (HH) and the eye diameter (DE) for *P. pagrus* larvae.

© Del documento, los autores. Digitalización realizada por ULPGC. Biblioteca Universitaria, 2009

of red porgy continued increasing in accordance with body size increment. In this way, during retinal growth, cones and other cell types were added concentrically at the retinal germinal margin. Horizontal and amacrine cells were clearly observed within the inner nuclear layer. There was an increase in length in the outer and inner segment of the photoreceptors.

On day 4, the digestive tract was developed and had several invaginations and an abundant brush border with columnar epithelium. The midgut of four old day larvae had digestive activity showing PAS affinity in the brush border. The ileocecal valve was better developed than on the third day. The larvae had started to ingest food and the anus was opened.

Food in the digestive tract was seen in most of the larvae at this time. During this time there was an increase in eye diameter which was significantly related to larval total length $r^2 = 0.987$ and head height $r^2 = 0.989$ (Figs. 1–3).

At day 10 after hatch, the sclera (S) started to differentiate but there were not significant changes in the retina.

Over the following days, an increase in length of the eye occurred but one important change in the visual system occurred at 20 days post-hatch. At this time spherical nuclei were seen in the basal zone of ONL, this type of cells were rod precursor nuclei (RN) which in the following days increased in number (Plate VI).

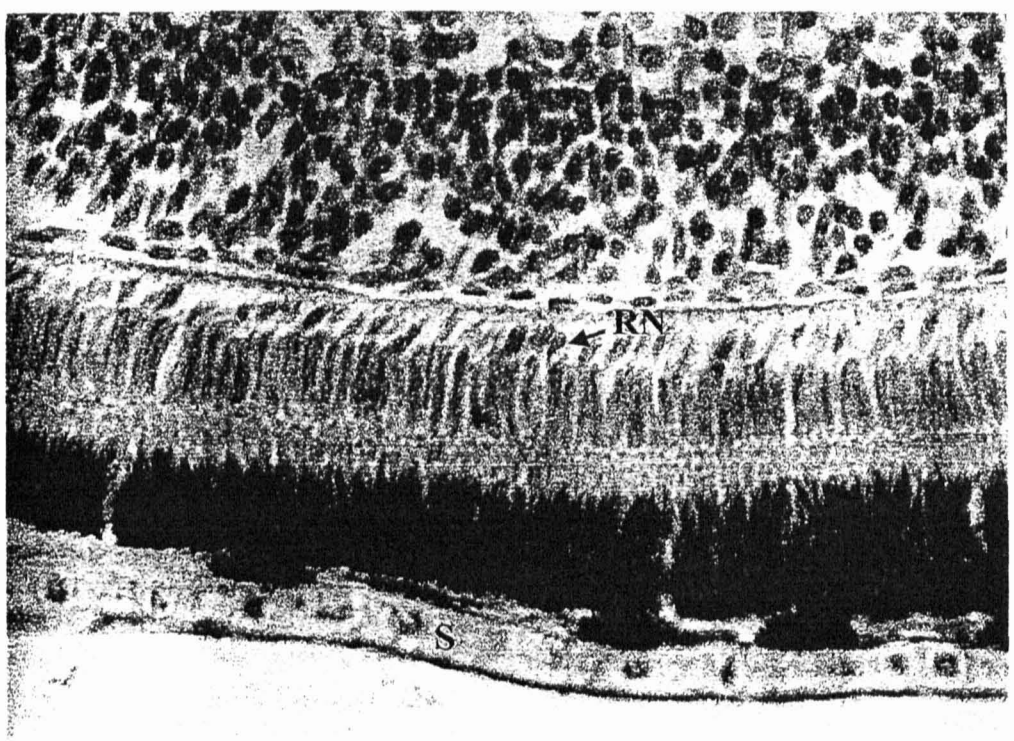


Plate VI. Light micrograph of a longitudinal section through the retina of *P. pagrus* larvae at day 20 after hatching (6.29 mm TL). In the retina at day 20 an spherical nuclei were seen added to the basal zone of ONL, this type cells were rod precursor nuclei (RN) and in following days increased in number, sclera was present also (S) (H&E).

© Del documento, los autores. Digitalización realizada por ULPGC. Biblioteca Universitaria, 2009

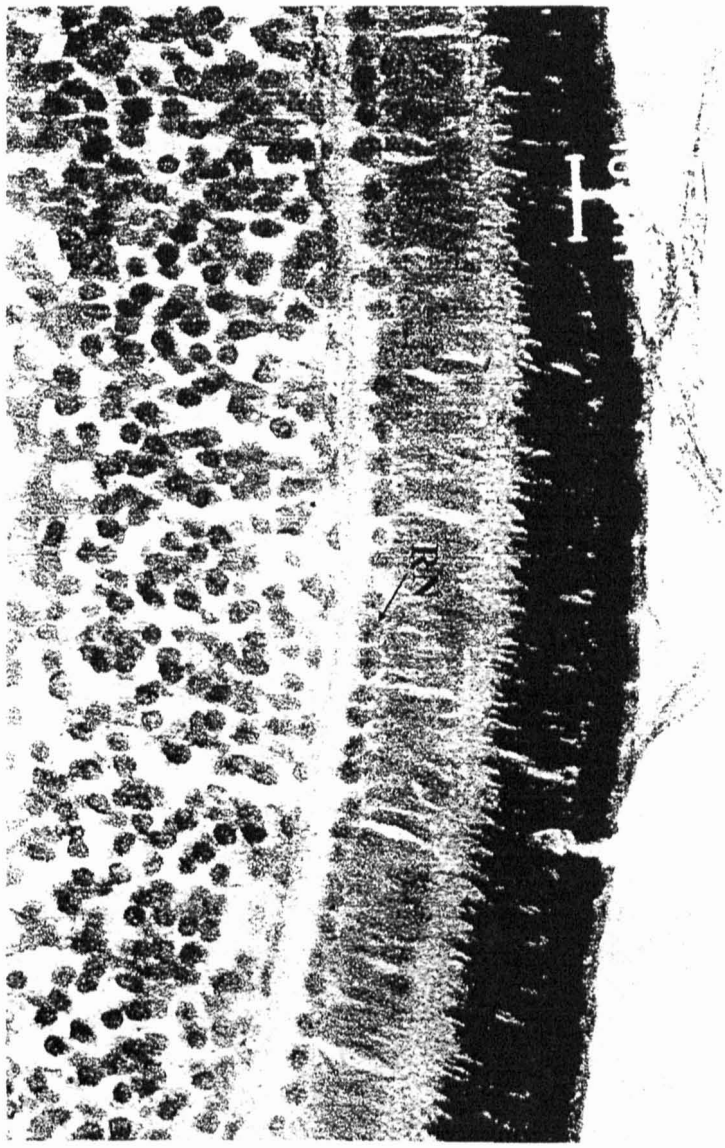


Plate VII. Light micrograph of a longitudinal section through the retina of *P. pagrus* larvae at day 25 after hatching (6.29 mm). Rod precursor nuclei layer (RN) (H&E).

At the same time, there were changes in the digestive tract with gastric glands appearing. On day 25 post-hatch, there was a clear increase in rods nuclei cells and a single layer of them were seen under the cones nuclear layer (Plate VII).

Cornea, sclera and iris were totally developed now. From day 25 post-hatch, there was an increase in length but no more changes in eye structure were observed.

## 4. Discussion

*P. pagrus* larvae had no functional eye and digestive system at hatching. As observed by Govoni et al. (1986) in other species, red porgy larvae had a simple undifferentiated straight gut linked to a non-structured mouth and anus.

© Del documento, los autores. Digitalización realizada por ULPGC. Biblioteca Universitaria, 2009

Red porgy eye structure was similar to those described by Kawamura (1984) for *P. major*, lens with undifferentiated cells disposed spherically, retinal cells on radial disposition and nerve optic cup were observed at this stage. The eye was not pigmented and some precursors of the photoreceptors nuclei cells were sketched in the external part of the retina.

One-day-old larvae had all the structural elements necessary for visual function, but most of them were not complete. This was an indication that the eye was about to be functional. Kawamura (1984) found that the visual system of *P. major* is functional at 36 h after hatch when visual cells and pigments are present and nerve optic fibres connect with the optic tectum. In red porgy, the visual system could not be functional at 28 h, principally because the pigmentation pattern, responsible for photon absorption was very sparse at this stage. The digestive system had started to differentiate.

The third day after hatching was one of the most important days for the larva which need to be ready for prey capture and digestion. Although histologically the larvae appears to be prepared and had their mouth opened, only a few of them had food in the digestive tract at this time. This fact could be due to a learning delay between the larvae.

At day 4 in the eye, presumptive cone photoreceptors were well developed, pigmentation pattern was complete and thus the visual system was completely ready for prey capture in coincidence with the digestive activity detected in the midgut. As a consequence most larvae started to feed. From this day, the larvae had good capacity for prey capture which was increased with body size.

Pure cone retina have been found in the earliest stages of many teleost larvae. At first feeding they are only equipped with simple cones, such as *P. major* (Kawamura, 1984) and *P. auratus* (Pankhurst, 1996) while rods and twin cones appear at metamorphosis (Blaxter and Staines, 1970).

Thus, in the studied species, on day 20 post-hatch spherical nuclei appeared in the basal zone of ONL, this cell type were rod precursor nuclei which in following days increased in number. From this moment, *P. pagrus* larvae had a duplex retina with cone and rods. These results agree with those found in other sparids. For instance, in *P. auratus* in which presumptive rod precursor cells appear at 18 days post hatch (Pankhurst, 1996) and in red seabream larvae single cones fused to form twin cones and first rods appear at 11 mm TL (Kawamura, 1984).

Rods provide a better vision under low light intensity levels (O'Connell, 1981; Kawamura, 1984; Pankhurst, 1996). Kawamura (1984) reported many changes in morphology as visual sensitivity increased. Behaviour changes like feeding habits and prey selection in wild fish occur in temporal association with its migration from the surface waters to benthic habitat. This is a common behavioural pattern in some sparids fish like *P. major*, *P. auratus* or *S. aurata* which have an early life stage in shallow waters and shift to deep waters later after metamorphosis (Franquet and Brito, 1995). Other species like Pacific salmon hatch at a more advanced stage and some rods are present (O'Connell, 1981). Northern anchovy have a pure rod-retina at hatch (O'Connell, 1981).

Normally, in culture conditions, daylight-type fluorescent tubes are used. Wild larvae migrate vertically to find the right illumination level according with its visual sensitivity, but in a culture tank, the correct illumination has to be provided (Huse, 1993).

© Del documento, los autores. Digitalización realizada por ULPGC. Biblioteca Universitaria, 2009

There were high correlations between different morphometric parameters like total length and head height with eye diameter. This means that the increase in length allows a better swim capacity and the increase in the eye diameter increased the visual capacity and prepare the larvae for the capture of larger prey sizes.

A good parallelism was seen between the development of visual system and digestive tract, until the larvae had no visual system ready, the digestive system was not ready either.

Before exogenous feeding the larva's eye was completely developed, and it was functional to provide a good vision level that let the larvae start to take food. Different studies attach great importance to docosahexaenoic acid. DHA is present at very high levels in the retina and neural tissues (Bell and Dick, 1993). In the lecitotrophic larvae, the development of all of its systems is from yolk reserves, this means that, the fish eggs should contain all the essential nutrients, like, essential fatty acids, glycerophospholipids and fat-soluble vitamins required for the development of the embryo and the growth of larvae (Izquierdo, 1996). N-3 highly unsaturated fatty acids (HUFA) are some of the main components of the lipids in fish eggs of several marine species such as red sea bream (Izquierdo et al., 1989a) and gilthead seabream (Mourente and Odriozola, 1990). Neuringer et al. (1988) has established a critical role for $n-3$ polyunsaturated fatty acids and docosahexaenoic acid DHA in neural and retinal tissue functions in mammals. Bell and Dick (1993) found that there is a high demand of DHA to form nerve membranes in fish larval stages.

Several authors have shown that the fatty acid composition of total lipids of the eggs reflects those of maternal diet (Watanabe et al., 1984, 1985; Mourente and Odriozola, 1990a; Fernández-Palacios et al., 1995). Thus, adequate feeding in the broodstock must provide the eggs with all the essential nutrients for correct development during this stage.

Both photoreceptors in the eye, rods and cones accumulate and selectively retain DHA in the external segments. Rods contain twice as much DHA as cones (Bell and Dick, 1993). Rods appear after the start of the exogenous feeding about 18th day after hatch, and important quantities of DHA will be necessary, consequently their requirements for $n-3$ HUFA should be satisfied by the diet. In nature different varieties of phytoplankton and zooplanckton supply $n-3$ HUFA requirements but in aquaculture these need to be supplemented in the diet.

In addition, the improvement of visual capacity associated with rod apparition occurs with an increase in photosensitivity, this fact could mean that different lighting regimes are required during this phase of larval development for correct development of the visual system. Inadequate lighting regimes may be another stress factor in larvae culture conditions and correct management can contribute to increased larval growth and survival and consequently better success in larval rearing.

## Acknowledgements

We are very grateful to D. Antonio Valencia for they invaluable contribution in the larval rearing.

© Del documento, los autores. Digitalización realizada por ULPGC. Biblioteca Universitaria, 2009

## References


Bauchot, M.L., 1987. Poissons Osseux. Sparidae. In: Fischer, W., Schneider, M., Bauchot, M.L. (Eds.), Fiches FAO d'identification des espèces pour les besoins de la pêche. (Révision 1). Méditerranée et mer Noire. Zone de pêche 37 Vol. 2: Vertebrés. FAO, Rome, pp. 1343–1376.

Bauchot, M.L., Hureau, J.C., 1990. Sparidae. In: Quéro, J.C., Hureau, J.C., Karrer, C., Post, A., Saldanha, L. (Eds.), Check-list of the Fishes of the Eastern Tropical Atlantic. Vol. 2. JNICT, Lisbon; SEI, Paris; and UNESCO, Paris, pp. 790–812.

Bell, M.V., Dick, J.R., 1993. The appearance of rods in the eyes of herring and increased di-docosahexaenoyl molecular species of phospholipids. J. Mar. Biol. Assoc. U.K. 73, 679–688.

Blaxter, J.H.S., 1986. Development of sense organs and behaviour of teleost larvae with special reference to feeding and predator avoidance. Trans. Am. Fish. Soc. 115, 98–114.

Blaxter, J.H.S., Staines, M., 1970. Pure cone retina and retinomotor responses in larval teleosts. J. Mar. Bio. Assoc. U.K. 50, 449–460.

Fernández-Palacios, H., Izquierdo, M.S., Robaina, L., Valencia, A., Salhi, M., Vergara, J., 1995. Effect of $n-3$ HUFA level in broodstock diets on eggs quality of gilthead seabream (*Sparus aurata* L.). Aquaculture 132, 325–337.

Franquet, F., Brito, A., 1995. Especies de interés pesquero de Canarias. Gobierno de Canarias.

García del Moral, R., 1993. Laboratorio de anatomía patológica. 1st edn. Interamericana. Mc Graw-Hill, Madrid, España.

Govoni, J.J., Boenhlert, G.W., Watanabe, Y., 1986. The physiology of digestion in fish larvae. Env. Biol. Fish. 16, 59–77.

Hernández-Cruz, C.M., Fernández-Palacios, H., Fernández-Palacios, J.E., 1990. Preliminary study on embrionary and larval development of red porgy, *Pagrus pagrus* (Pisces, Sparidae), under culture conditions. Vieraea 19, 215–224.

Hernández-Cruz, C.M., Salhi, M., Bessonart M., Fernández-Palacios, H., Valencia, A., Izquierdo, M.S., 1997. First experiences on larval culture of Red porgy Pagrus *pagrus* (Osteichthyes, Sparidae) In: Costa, J., Abellán, E., García, B., Ortega, A., Zamora, S. (Eds.), VI Congreso Nacional de Acuicultura. Cartagena, Spain, 9–11 July, 1997.

Huse, I., 1993. First feeding larval sensory perception and behavioural programming: Implications for systems and procedures in culture. In: Walther, B.T., Fyhn, H.J. (Eds.), Physiology and Biochemical Aspects of Fish Development. Bergen niv. Norway, Bergen, pp. 146–152.

Izquierdo, M.S., 1996. Review article: essential fatty acid requirements of cultured marine fish larvae. Aquacult. Nutri. 2, 183–191.

Izquierdo, M.S., Watanabe, T., Takeuchi, T., Arakawa, T., Kitajima, C., 1989a. Requirement of larval red seabream *Pagrus major* for essential fatty acids. Nippon Suisan Gakkaishi 55, 859–867.

Kawamura, G., 1984. The visual cell morphology of *Pagrus mayor* and its adaptative changes with shift from pelagic and benthic habitats. Bull. Jpn. Soc. Sci. Fish. 50, 1975–1980.

Kentouri, M., Pavlides, M., Papandroulakis, N., Divanach, P., 1995. Network on Technology of Aquaculture in the Mediterranean (TECAM). Nicosia (Cyprus), pp. 65–78.

Mourente, G., Odriozola, J.M., 1990. Effect of broodstock diets on lipid classes and their fatty acid composition in eggs of gilthead sea bream (*Sparus aurata* L.). Fish Physiol. Biochem. 8, 93–101.

Neuringer, M., Anderson, G.J., Connor, W.E., 1988. The essentiality of $n-3$ fatty acids for the development and function of the retina and brain. Annu. Rev. Nutr. 8, 517–541.

O'Connell, C.P., 1981. Development of organ systems in the Northern Anchovy, *Engraulis mordax*, and other teleosts. Am. Zool. 21, 429–446.

Pankhurst, P.M., 1996. Changes in visual morphology throughout life history stages of the New Zealand snapper, *Pagrus auratus*. New Zealand J. Mar. Freshwater Res. 30, 79–90.

Sarasquete, M.C., Polo, A., Yúfera, M., 1995. Histology and histochemistry of the development of the digestive system of larval gilthead seabream, *Sparus aurata* L. Aquaculture 130, 79–92.

Socorro, J.A., Oran, G., Izquierdo, M.S., Fernández, A., Caballero, M.J., Fernández-Palacios, H., 1997. First contributions to the osteological red porgy *Pagrus pagrus* and pink dentex *Dentex gibbosus*. In: Costa, J., Abellán, E., García, B., Ortega, A., Zamora, S. (Eds.), VI Congreso Nacional de Acuicultura. Cartagena, Spain, 9–11 July 1997.


© Del documento, los autores. Digitalización realizada por ULPGC. Biblioteca Universitaria, 2009

Stephanoun, D., Georgiou, G., Shourkri, E., 1995. Network on Technology of Aquaculture in the Mediterranean (TECAM). Nicosia (Cyprus), pp. 65–78.

Watanabe, T., Takeuchi, T., Saito, M., Nishimura, K., 1984. Effect of low protein-high calorie or essential fatty acid diet on reproduction of rainbow trout. Bull. Jpn. Soc. Sci. Fish. 50, 1207–1215.

Watanabe, T., Koizumi, T., Satoh, S., Takeuchi, T., Yoshida, N., Kitada, T., Tsukashima, Y., 1985. Improvement of quality of red seabream eggs by feeding broodstock on a diet containing cuttlefish meal on a raw krill shortly before spawning. Bull. Jpn. Soc. Sci. Fish. 51, 1511–1521.

© Del documento, los autores. Digitalización realizada por ULPGC. Biblioteca Universitaria, 2009

ELSEVIER

Aquaculture 179 (1999) 253–263

Aquaculture

# Effect of different dietary polar lipid levels and different $n-3$ HUFA content in polar lipids on gut and liver histological structure of gilthead seabream (*Sparus aurata*) larvae

M. Salhi [a,*], C.M. Hernández-Cruz [b], M. Bessonart [c], M.S. Izquierdo [b], H. Fernández-Palacios [a]

[a] *Instituto Canario de Ciencias Marinas, Gobierno de Canarias, PO Box 56, E-35200 Las Palmas, Spain*

[b] *Departamento de Biología, Universidad de Las Palmas de Gran Canaria, PO Box 550, E-35017 Las Palmas, Spain*

[c] *Instituto de Biología, Facultad de Ciencias, Universidad de la República, Iguá 4225, 11400 Montevideo, Uruguay*

**Abstract**

In a previous study feeding larval gilthead seabream on microdiets, an improved growth rate was observed when dietary $n-3$ HUFA ($n-3$ highly unsaturated fatty acids) were contained in the polar lipid fraction. A beneficial effect of dietary lecithin on $n-3$ HUFA incorporation to the larval polar lipids was also observed. To confirm those results and in order to obtain additional information on larval gut and liver histological structure, 11-day-old larvae were fed 4 microdiets differing in lipid composition. In diets N′ and NL′, the main sources of $n-3$ HUFA were neutral lipids, and polar lipids in diets P′ and PL′. Three lecithin levels were tested, being the highest in diet NL′ and the lowest in diet P′. The total $n-3$ HUFA level in diets N′ and NL′ was enough to meet the essential fatty acid requirement of larval gilthead seabream obtained in a previous study with a triacylglyceride based diet, while diets P′ and PL′ had a total $n-3$ HUFA level lower than the minimum determined. A reduction in the larval essential fatty acid requirement to 1.5% d.w. was obtained by feeding dietary $n-3$ HUFA present in the polar lipid fraction. Feeding larvae with microdiets with low polar lipid levels produced an accumulation of lipid droplets in the enterocytes and a high number of lipid vacuoles in the hepatocytes producing nuclear migration

* Corresponding author. Dpto. Fisiología, Facultad de Ciencias, Universidad de la República, Iguá 4225, 11400 Montevideo, Uruguay. Tel.: +598-2-5258618; fax: +598-2-5258617; E-mail: msalhi@fcien.edu.uy

0044-8486/99/$ - see front matter © 1999 Elsevier Science B.V. All rights reserved.
PII: S0044-8486(99)00194-5

© Del documento, los autores. Digitalización realizada por ULPGC. Biblioteca Universitaria, 2009

and suggesting a need of dietary polar lipid for lipid transport. © 1999 Elsevier Science B.V. All rights reserved.

*Keywords:* *Sparus aurata* larvae; Essential fatty acids; Phospholipids; Enterocytes; Hepatocytes

## 1. Introduction

Although, at present, live prey is more reliable for marine fish larvae production, development of microdiets would allow a reduction of cost production (Kissil, 1985). Development of well defined diets adapted to each species and larval age is needed. However, there is still a lack of knowledge on the nutritional needs of marine fish larvae, except those reported for essential fatty acids. Most of the nutritional requirement studies have been conducted using fatty acid enriched rotifers and *Artemia*, whose fatty acid composition can be modified by different enrichment methods (Imada et al., 1979; Watanabe et al., 1982). The use of microdiets to study the nutritional requirements of larvae allows for better control of the dietary composition and limits the influence of other unknown nutritional factors. In fact, during the past few years, several studies on nutritional requirements of fish larvae have been conducted by using microdiets: vitamins (Dabrowski, 1990; González et al., 1995, 1998a,b), fatty acids (Kanazawa et al., 1982; Salhi et al., 1994; Bessonart et al., 1998a,b); phospholipids (Kanazawa et al., 1981, 1983a,b, 1985; Geurden et al., 1995, 1997a; Salhi et al., 1995), proteins and amino acids (Kanazawa et al., 1989; López-Alvarado and Kanazawa, 1994).

Regarding the phospholipid requirement, it has been shown that the addition of polar lipids to artificial diets improved growth and survival of larval red seabream (Kanazawa et al., 1983a), ayu (Kanazawa et al., 1983b) and common carp (Geurden et al., 1995, 1997a), and also improved growth, but not survival, of European seabass and turbot juveniles (Geurden et al., 1997b). It has also been shown that by supplementing diets with phospholipids one observes an improved incorporation of oleic acid into tissue lipids (Koven et al., 1993) and a higher content of $n-3$ HUFA, mainly due to the DHA, in the polar lipids (Salhi et al., 1995) of gilthead seabream, as well as an increase in the $n-6$ and $n-3$ HUFAs in the total lipids of European seabass and turbot (Geurden et al., 1997b). Moreover, it has been observed that dietary $n-3$ HUFA in the polar lipid fraction improved the growth rate of gilthead seabream larvae (Salhi et al., 1995). The present work was conducted to confirm these results and to obtain additional information, from a histological study of liver and gut of larval gilthead seabream, on the effect of different dietary polar lipid levels with different $n-3$ HUFA content in microdiets.

## 2. Materials and methods

Eleven-day-old gilthead seabream (*Sparus aurata*) larvae ($4.57 \pm 0.29$ mm total length and $53.5 \pm 0.4$ μg dry weight) were fed four different microdiets (Table 1) for 16 days. In diets N′ and NL′ the main source of $n-3$ HUFA was neutral lipids, whereas in diets P′ and PL′ the main source was polar lipids. Three lecithin levels were tested, with

© Del documento, los autores. Digitalización realizada por ULPGC. Biblioteca Universitaria, 2009

Table 1
Formulation and lipid composition of the experimental microdiets

| Ingredients (g/100 g diet) | Diet N′ | Diet NL′ | Diet P′ | Diet PL′ |
|---|---|---|---|---|
| Squid powder[a] | 68.50 | 68.50 | 68.50 | 68.50 |
| Vitamin mixture[b] | 6.00 | 6.00 | 6.00 | 6.00 |
| Mineral mixture[c] | 4.50 | 4.50 | 4.50 | 4.50 |
| Attractant[d] | 3.00 | 3.00 | 3.00 | 3.00 |
| Gelatin | 3.00 | 3.00 | 3.00 | 3.00 |
| Soybean lecithin | 2.00 | 3.56 | – | 2.00 |
| Squid lipids[e] | – | – | 2.70 | 2.70 |
| Corn oil | 1.41 | – | 3.23 | 1.42 |
| Oleic acid | 3.04 | 3.10 | 3.65 | 3.73 |
| Palmitic acid | 3.82 | 3.61 | 3.85 | 3.58 |
| EPA 28[f] | 1.93 | 1.93 | 1.57 | 1.57 |
| DHA 27[f] | 2.80 | 2.80 | – | – |
| *Composition (%dry weight)* | | | | |
| Total lipids (TL) | 17.85 | 17.43 | 17.10 | 16.91 |
| Polar lipids (PL) | 2.37 | 2.84 | 2.80 | 3.60 |
| $n-3$ HUFA in TL | 1.78 | 1.86 | 1.51 | 1.52 |
| $n-3$ HUFA in PL | 0.38 | 0.33 | 1.04 | 0.99 |
| $n-3$ HUFA in NL | 1.43 | 1.41 | 0.52 | 0.54 |
| 20:5$n-3$/22:6$n-3$ in TL | 1/1.61 | 1/1.65 | 1/1.47 | 1/1.47 |

[a] Freeze-dried squid powder (lipid extracted 3 times with chloroform), Rieber & Son, Bergen, Norway.
[b] Kanazawa (1985).
[c] Teshima et al. (1982).
[d] Kanazawa et al. (1989).
[e] Lipids extracted from freeze-dried squid powder.
[f] Triacylglycerides containing 36% (DHA27) and 40% (EPA28) of $n-3$ HUFA, Nippon Chemical Feed, Tokyo, Japan.

the highest level in diet NL′ and the lowest level in diet P′. The total $n-3$ HUFA level in diets N′ and NL′ was enough to meet the essential fatty acid requirement of larval gilthead seabream (2% d.w. of $n-3$ HUFA with a EPA/DHA ratio of about 1/1.7) obtained in a previous study with a triacylglyceride based diet (Salhi, 1997), while diets P′ and PL′ had a total $n-3$ HUFA level lower than the minimum required.

The feeding trial was carried out in 100-l cylindrical tanks filled with 50 μm filtered seawater, provided with constant aeration and water flow (300–600 ml/min). Water flowed out through a 350 μm mesh to remove the non-ingested food. Water temperature ranged between 18.0–19.4°C. A photoperiod of 12 h artificial light was maintained during the experiment. No microalgae were added to the rearing tanks.

Larvae were divided into groups of 3000 fish and distributed into 12 tanks. During the next 16 days larvae were fed 2.0–2.7 g of the experimental microdiets per tank per day using automatic feeders. Larvae were also fed rotifers ($3.5 \times 10^5$ per tank twice a day) cultured on baker's yeast, which contained only $0.09 \pm 0.01\%$ $n-3$ HUFA (dry basis).

Larval growth was determined by measuring total length and dry weight of 28-day-old larvae (30 larvae per tank). Before ending the experiment, 24-day-old larvae were

© Del documento, los autores. Digitalización realizada por ULPGC. Biblioteca Universitaria, 2009

subjected to an activity test as an index of resistance to manipulation (Kitajima et al., 1980). This activity test consisted of keeping 15 larvae out of the water in a net for 15 s and determining the survival 24 h after returning the larvae to seawater. At the end of the experiment live larvae were individually counted to determine final survival. For the histological study 26 day-old larvae (10 larvae per tank) were anesthetized, fixed in 4% formaldehyde buffered with phosphate, and embedded in paraffin wax after dehydration. Sections (4 μm) were stained with haematoxylin-eosin and periodic acid Schiff haematoxylin (PAS). At the end of the feeding trial, larvae were individually counted for survival and sampled for lipid analysis. Lipids were extracted with a chloroform:methanol (2:1) mixture as described by Folch et al. (1957) and neutral and polar fractions were separated by adsorption chromatography on silica cartridges (Sep-pak, Waters, Milford, MA) as described by Juaneda and Rocquelin (1985). Fatty acid methyl esters of diets were obtained by transesterification with 1% sulfuric acid in methanol (Christie, 1992), and separated, identified and quantified by gas chromatography.

Statistical analysis of data was conducted using an ANOVA and Duncan test for multiple comparison of means with 5% significance level.

## 3. Results

No differences were found either in final larval survival nor in larval resistance to the activity test (Table 2) among larvae fed the different experimental diets.

The increase in polar lipid content in diet NL′ with respect to diet N′, increased larval growth up to a similar rate as that of larvae fed diet P′, although with no significant differences between larvae fed diet N′ and NL′ (Table 2). However, growth of larvae fed diet PL′ was lower than that obtained with diet P′, both diets contained the same level of $n-3$ HUFA in the polar lipid fraction.

Table 2
Survival (at the end of the experiment and after the activity test), growth (total length and dry weight), moisture, lipid content and histological observations of larvae fed the experimental microdiets

| | Initial | N′ | NL′ | P′ | PL′ |
|---|---|---|---|---|---|
| Final survival (%)[a] | | 13.8 ± 5.2 | 23.7 ± 7.8 | 20.7 ± 9.0 | 12.9 ± 3.5 |
| Activity test survival (%)[a] | | 71.1 ± 9.8 | 64.4 ± 10.2 | 60.7 ± 21.8 | 65.2 ± 16.9 |
| Total length (mm)[a] | 4.57 ± 0.29 | 5.61 ± 0.41a | 5.66 ± 0.43ab | 5.80 ± 0.49b | 5.53 ± 0.50a |
| Dry weight (μg)[a] | 53.5 ± 0.4 | 108.0 ± 3.3a | 116.4 ± 6.7ab | 132.0 ± 9.1b | 112.9 ± 8.5a |
| Moisture content (%) | 88.73 | 89.10 | 88.05 | 88.19 | 88.85 |
| Total lipid (% d.w.) | 16.03 | 24.05 | 17.32 | 18.21 | 26.28 |
| Neutral lipids (% d.w.) | 6.19 | 10.80 | 6.32 | 7.04 | 12.48 |
| Polar lipids (% d.w.) | 9.83 | 13.25 | 11.00 | 11.18 | 13.79 |
| Lipid droplets in the enterocytes[b] | | 24.3 | 15.2 | 14.1 | 4.1 |
| Hepatocyte vacuolization | | + + | + | + + | + + |
| PAS affinity | | + | + + | + + + | + |
| Zymogen granules | | + | + | + + | + + |

[a] Values having the same letter within each row were not significantly different ($P < 0.05$).
[b] Percentage of the examined larvae showing lipid droplets in the basal zone of the enterocytes.

© Del documento, los autores. Digitalización realizada por ULPGC. Biblioteca Universitaria, 2009

Fig. 1. Accumulation of lipid droplets in the basal zone of the enterocytes of larvae fed diet N′ (haematoxylin-eosin staining; Scale bar = 10 μm).

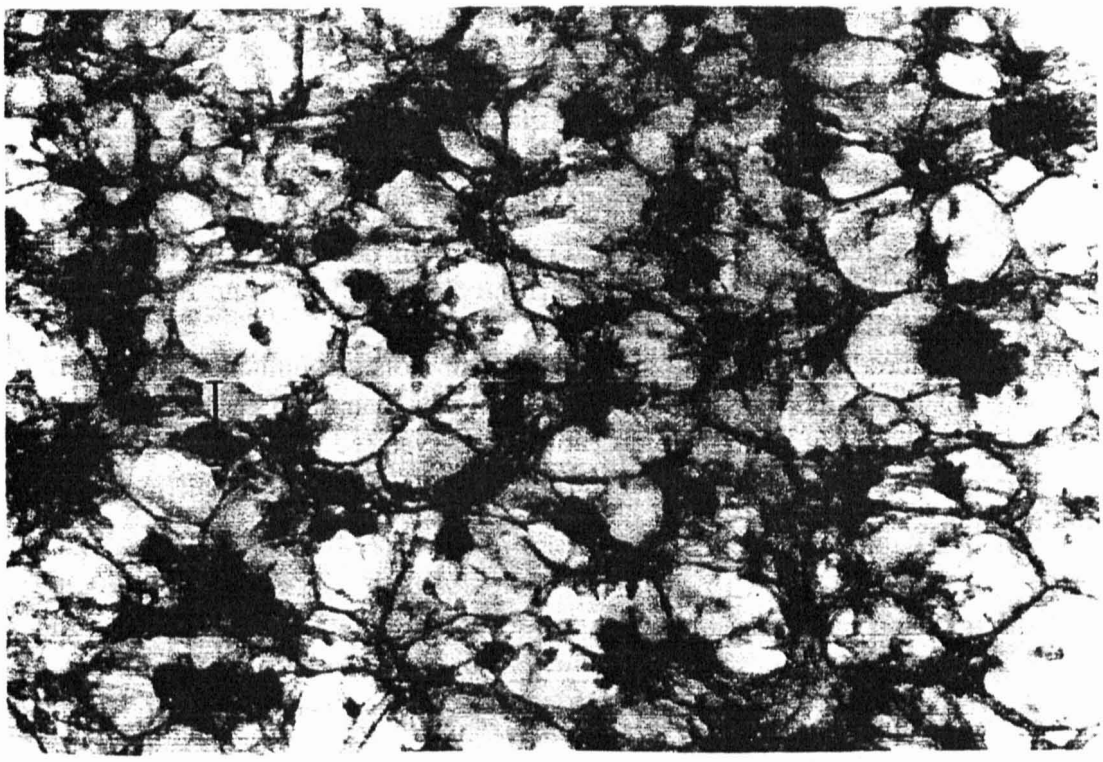

Fig. 2. Lipid vacuoles and nuclear migration in the hepatocytes of larvae fed diet N′ (PAS staining; scale bar = 10 μm).

© Del documento, los autores. Digitalización realizada por ULPGC. Biblioteca Universitaria, 2009

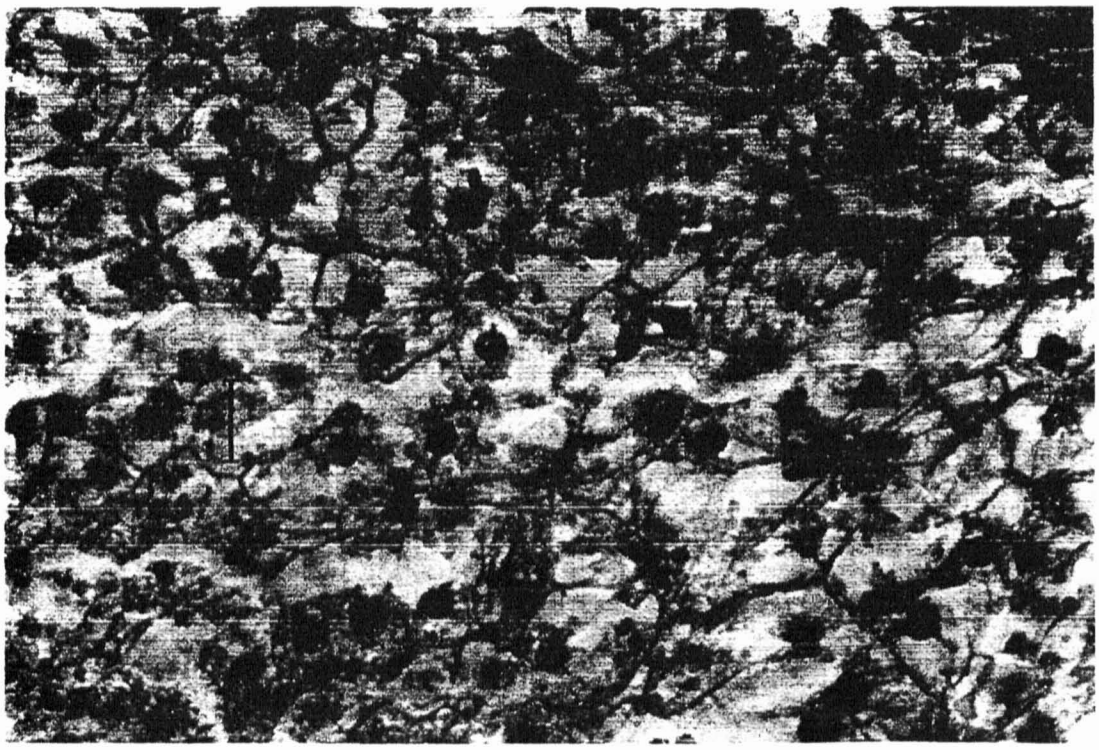

Fig. 3. Vacuolization in the hepatocytes of larvae fed diet NL′ (haematoxylin-eosin staining; scale bar = 10 μm).

In the anterior and middle part of the gut of larvae fed diet N′, a high number of the examined larvae showed a high lipid accumulation in the enterocytes (Table 2, Fig. 1). Regarding the histological structure of the liver, although differences in the hepatocyte size of the larvae were not observed, larvae fed diets N′, P′ and PL′ showed a higher hepatocyte vacuolization than those fed diet NL′ (Table 2, Figs. 2 and 3). The increased size of vacuoles in the hepatocytes on larvae fed diet N′ produced a migration of the liver cell nucleus (Fig. 2). Livers of larvae fed diets N′ and PL′ showed a lower PAS affinity than those fed diets NL′ and P′ (Table 2). In the pancreatic tissue, a higher number of zymogen granules was observed in larvae fed diets P′ and PL′ than in those fed diets N′ and NL′ (Table 2).

Initial and microdiet fed larvae showed similar moisture contents (Table 2). Total lipid content of larvae fed diets N′ and PL′ was higher than the other larvae, mainly due to a higher percentage of neutral lipid (Table 2). Larvae fed diets NL′ and P′ showed a total lipid content slightly higher than the initial larvae due to a small increase in the polar lipid portion (Table 2).

## 4. Discussion

In red seabream larvae, Kanazawa (1997) reported that supplementing microdiets with 3 and 5% soybean lecithin improved growth, total survival and survival to the air exposure test, compared to a soybean lecithin free diet. In the present work all diets

© Del documento, los autores. Digitalización realizada por ULPGC. Biblioteca Universitaria, 2009

contained polar lipid, with 2.37% being the lowest value. Higher dietary polar lipid levels and higher $n-3$ HUFA rich polar lipids did not improved total survival or survival following the activity test.

Regarding growth, although diet P′ had a lower $n-3$ HUFA content than diets N′ and NL′ and the same polar lipid level as diet NL′, larvae fed diet P′ showed a significantly better growth performance than larvae fed diet N′ and a similar growth rate as those fed diet NL′ (Table 2). This observation may suggest better utilization of dietary $n-3$ HUFA in the form of polar lipid than when they are supplied in the form of neutral lipid, as suggested previously (Kanazawa et al., 1983a; Izquierdo, 1988; Salhi et al., 1995). However, this hypothesis was not supported by growth of larvae fed diet PL′ which was lower than that obtained with diet P′, both diets contained the same amount of $n-3$ HUFA in the total and polar lipid fractions. Probably other factors than $n-3$ HUFA in polar lipids might be implicated.

Lipid vacuoles observed in the intestinal mucosa of larvae fed diet N′ (Fig. 1), suggest a reduction in the lipid transport rate from the enterocytes to the blood circulation. Some lipids may be stored in the epithelial cells (Bergot, 1981), but most of them are initially transported to the liver (Sargent et al., 1989). Lipid droplets observed in fish enterocytes probably represent lipid storage when the route of chylomicrons synthesis is saturated (Leger, 1985). These lipoproteins are constituted by tryacylglycerides, phospholipids and apoproteins, and their function is the transport of lipid from the enterocytes to the blood circulation. The low polar lipid level in diet N′ may be responsible for a low synthesis of chylomicrons, constituted in part by phospholipids, producing the accumulation of lipid droplets in the enterocytes of larvae fed this diet. Deplano et al. (1989) observed injuries in the intestinal mucosa of sea bass fed artificial diets associated with excess lipid droplets in epithelial cells. These authors suggested a lack of adaptation to the artificial food, both quantitative (excess of lipids) and/or qualitative (imbalanced dietary lipid, lack of lipotrope substances such as lecithins, choline or carnitine), as the responsible factor of this digestive pathology. Afterwards, Deplano et al. (1991) found that the lipid absorption in the enterocytes of sea bass larvae was no dependent on the type of diet (*Artemia* nauplii or artificial diet) and suggested that the lipids were stored as droplets due to the low ability of the enterocytes for lipoprotein synthesis in first feeding larvae. In gilthead seabream larvae, Díaz et al. (1997) suggested that the formation of large lipoproteins and of lipid droplets in the intestinal epithelium was closely related to the excess fat in immature enterocytes caused by the high fatty acid content of the prey (rotifers). From the present study, it seems that the increase in dietary polar lipids may improve lipid transport from the enterocytes to the blood, probably by enhancing chylomicron synthesis. Fontagné et al. (1998) suggested a specific function of phosphatidylcholine (PC) for the synthesis and secretion of chylomicrons or very low density lipoproteins (VLVL) and thus the prevention of intestinal steatosis. These authors found in common carp larvae fed polar lipid deficient diets an accumulation of fat droplets in the enterocytes of the anterior intestine that was prevented by using hydrogenated PC in the diet but not by feeding the larvae with a phosphatidylinositol enriched diet.

Larvae fed diets N′, P′ and PL′ showed a pronounced hepatocyte vacuolization (Table 2, Fig. 2). The low PAS affinity observed in larvae fed diets N′ and PL′, indicates a high

© Del documento, los autores. Digitalización realizada por ULPGC. Biblioteca Universitaria, 2009

lipid accumulation in the liver, producing, in the case of larvae fed diet N′ the migration of the hepatocyte nucleus (Fig. 2). The higher PAS positivity observed in larvae fed diet P′ suggests that the hepatocyte vacuolization was mainly due to glycogen storage. These results are in accordance with the higher total and neutral lipid content of larvae fed diets N′ and PL′ suggesting a lower lipid utilization by these larvae. Mosconi-Bac (1987) observed several disturbances in the liver of sea bass fed artificial diets, being important for the accumulation of lipid droplets in the hepatocytes, and suggested that such disturbances were probably reflecting hepatic disfunctions of nutritional origin possibly related to disorders in the lipid metabolism. In a previous study (Salhi, 1997), high lipid accumulation was found in the hepatocytes of gilthead seabream larvae fed low $n-3$ HUFA diets (1% d.w. $n-3$ HUFA in a triacylglyceride based microdiet), as has been observed in gilthead seabream juveniles fed $n-3$ HUFA deficient diets (Kalogeropoulos et al., 1992; Ibeas et al., 1994). Since diets N′ and NL′ had the same lipid and $n-3$ HUFA levels, the excess lipid accumulated in the hepatocytes of larvae fed diet N′ could be related to the lower polar lipid content of this diet, which may have affected the lipoprotein synthesis and consequently the transport of lipid from the liver to extrahepatic tissues. In fish, lipids from liver are transported to other tissues by mean of different types of lipoproteins: VLDL, LDL (low density lipoproteins) and HDL (high density lipoproteins) (Sheridan, 1988). HDL are the most abundant lipoproteins in teleost fish (Babin and Vernier, 1989) and contain a high amount of phospholipids (Santulli et al., 1993). Several authors (Kanazawa et al., 1985; Teshima et al., 1987) have suggested that fish larvae have a limited ability to synthesize phopholipids needed to produce lipoproteins and, as a result, require polar lipids in their diet.

The higher number of zymogen granules observed in larvae fed diets P′ and PL′ compared with those fed diets N′ and NL′ may be related to the higher content of $n-3$ HUFA in the polar lipid fraction of diets P′ and PL′, or with a higher consumption rate of these microdiets as observed in a previous experiment using similar diets (Salhi et al., 1998), although consumption of diet PL′ by the larvae was significantly higher than that of diet P′. Pedersen et al. (1987) observed a significant effect of prey density on the trypsinogen content in the pancreas of 15-day-old larval herring (*Clupea harengus*), the enzyme content being higher in larvae fed high prey density.

Regarding larvae fed diet PL′ (high polar lipid diet), the high lipid content in accordance with the presence of lipid vacuoles in the liver might be related to the higher microdiet ingestion found in these larvae, as previously mentioned (Salhi et al., 1998), resulting in a higher lipid intake but a lower lipid utilization by these larvae. However, the relation between the high polar lipid content of diet PL′ and the low growth rate obtained in larvae fed this diet compared with diet P′ remains unclear.

## 5. Conclusions

Feeding gilthead seabream larvae microdiets with a low polar lipid content, produced the appearance of lipid droplets in the enterocytes and a higher number of lipid vacuoles in the hepatocytes inducing nuclear migration. A relationship between the low larval

© Del documento, los autores. Digitalización realizada por ULPGC. Biblioteca Universitaria, 2009

growth and a high number of lipid vacuoles in the larval hepatocytes along with an elevated content of neutral lipids in the larval body was observed.

## Acknowledgements

We wish to thank Mr. Juan Antonio Socorro for the histological sample processing. This study was supported by a grant from the "Cabildo Insular de Gran Canaria".

## References

Babin, P.J., Vernier, J.M., 1989. Plasma lipoprotein in fish. J. Lipid Res. 30, 467–489.

Bergot, F., 1981. Fat absorption. In: Fontaine, M. (Ed.), Nutrition des Poissons. Actes du Colloque, CNERNA, Paris, pp. 123–129.

Bessonart, M., Izquierdo, M.S., Salhi, M., González, M., Hernández-Cruz, C.M., Fernández-Palacios, H., 1998a. Effect of different docosahexaenoic and eicosapentaenoic acid ratios in microdiets on growth of gilthead seabream larvae (*Sparus aurata* L.). Recent Advances in Finfish and Crustacean Nutrition, Abstracts VIII International Symposium on Nutrition and Feeding of Fish, 1998, Las Palmas, Spain, p. 214.

Bessonart, M., Izquierdo, M.S., Salhi, M., Hernández-Cruz, C.M., Fernández-Palacios, H., 1998b. Effect of arachidonic acid supplemented microdiets on growth and survival of gilthead seabream (*Sparus aurata* L.) larvae. Recent Advances in Finfish and Crustacean Nutrition, Abstracts VIII International Symposium on Nutrition and Feeding of Fish, Las Palmas, Spain, p. 215.

Christie, W.W., 1992. Lipid Analysis. Pergamon, Oxford, England.

Dabrowski, K., 1990. Ascorbic acid status in the early life of whitefish (*Coregonus lavaretus* L.). Aquaculture 84, 61–70.

Deplano, M., Connes, R., Díaz, J.P., Paris, J., 1989. Intestinal steatosis in the farm reared sea bass *Dicentrarchus labrax*. Dis. Aquat. Org. 6, 121–130.

Deplano, M., Díaz, J.P., Connes, R., Kentouri-Divanach, M., Cavalier, F., 1991. Appearance of lipid absorption capacities in larvae of sea bass *Dicentrarchus labrax* during transition to the exotrophic phase. Mar. Biol. 108, 361–371.

Díaz, J.P., Guyot, E., Vigier, S., Connes, R., 1997. First events in lipid absorption during post-embryonic development of the anterior intestine in gilt-head sea bream. J. Fish Biol. 51, 180–192.

Folch, J., Lees, M., Sloane Stanley, G.H., 1957. A simple method for the isolation and purification of total lipids from animal tissues. J. Biol. Chem. 226, 497–509.

Fontagné, S., Geurden, Y., Escaffre, A.M., Bergot, P., 1998. Histological changes induced by dietary phospholipids in intestine and liver of common carp (*Cyprinus carpio* L.) larvae. Aquaculture 161, 213–223.

Geurden, I., Radünz-Neto, J., Bergot, P., 1995. Essentiality of dietary phospholipids for carp (*Cyprinus carpio* L.) larvae. Aquaculture 131, 303–314.

Geurden, I., Charlon, N., Marion, D., Bergot, P., 1997a. Influence of purified soybean phospholipids on early development of common carp. Aquacult. Int. 5, 137–149.

Geurden, I., Coutteau, P., Sorgeloos, P., 1997b. Effect of dietary phospholipid supplementation on growth and fatty acid composition of European seabass (*Dicentrarchus labrax* L.) and turbot (*Scophthalmus maximus*) juveniles from weaning onwards. Fish Physiol. Biochem. 16, 259–272.

González, M.M., Izquierdo, M.S., Salhi, M., Hernández-Cruz, C.M., Fernández-Palacios, H., 1995. Dietary vitamin E for *Sparus aurata* larvae. In: Lavens, P., Jaspers, E., Roelants, Y. (Eds.), Proceedings of Larvi'95-Fish and Shellfish Larviculture Symposium, Gent, Belgium. European Aquacult. Soc. (Special Publ.) 24, 239–242.

González, M.M., Izquierdo, M.S., Christiansen, R., Torrisen, O.J., Valencia, A., Fernández-Palacios, H., 1998a. α-Tocopherol, vitamin A and carotenoid content during gilthead seabream (*Sparus aurata*) larval

© Del documento, los autores. Digitalización realizada por ULPGC. Biblioteca Universitaria, 2009

development. Recent Advances in Finfish and Crustacean Nutrition, Abstracts VIII International Symposium on Nutrition and Feeding of Fish, Las Palmas, Spain, p. 183.

González, M.M., Christiansen, R., Socorro, J.A., Izquierdo, M.S., Torrisen, O.J., Salhi, M., Hernández-Cruz, C.M., Bessonart, M., Fernández-Palacios, H., 1998b. The effect of inclusion of several levels of vitamin E and astaxanthin in microdiets for gilthead seabream (*Sparus aurata*) larvae. Recent Advances in Finfish and Crustacean Nutrition, Abstracts VIII International Symposium on Nutrition and Feeding of Fish, 1998, Las Palmas, Spain, p. 211.

Ibeas, C., Izquierdo, M.S., Lorenzo, A., 1994. Effect of different levels of n-3 highly unsaturated fatty acids on growth and fatty acid composition of juvenile gilthead seabream (*Sparus aurata*). Aquaculture 127, 177–188.

Imada, O., Kageyama, Y., Watanabe, T., Kitajima, C., Fujita, S., Yone, Y., 1979. Development of a new yeast as a culture medium for living feeds used in the production of fish seeds. Bull. Jpn. Soc. Sci. Fish. 45, 955–959.

Izquierdo, M.S., 1988. Estudio de los requerimientos de ácidos grasos esenciales en larvas de peces marinos. Modificación de la composición lipídica de las presas. PhD. Thesis, Universidad de la Laguna, Spain.

Juaneda, P., Rocquelin, G., 1985. Rapid and convenient separation of phospholipids from rat heart using silica cartridges. Lipids 20, 40–41.

Kalogeropoulos, N., Alexis, M.N., Henderson, R.J., 1992. Effect of dietary soybean and cod liver oil levels on growth and body composition of gilthead seabream (*Sparus aurata*). Aquaculture 104, 293–308.

Kanazawa, A., 1985. Nutritional requirement of larval fish. Saibaiken 14, 111–114, in Japanese.

Kanazawa, A., 1997. Effects of docosahexaenoic acid and phospholipids on stress tolerance of fish. Aquaculture 155, 129–134.

Kanazawa, A., Teshima, S., Inamori, S., Iwashita, T., Nagao, A., 1981. Effects of phospholipids on growth, survival rate and incidence of malformation in the larval ayu. Mem. Fac. Fish., Kagoshima Univ. 30, 301–309.

Kanazawa, A., Teshima, S., Sakamoto, S., 1982. Requirements of essential fatty acids for the larval ayu. Bull. Jpn. Soc. Sci. Fish. 48, 587–590.

Kanazawa, A., Teshima, S., Inamori, S., Matsubara, H., 1983a. Effects of dietary phospholipids on growth of the larval red seabream and knife jaw. Mem. Fac. Fish., Kagoshima Univ. 32, 109–114.

Kanazawa, A., Teshima, S., Kobayashi, T., Takae, M., Iwashita, T., Uehara, R., 1983b. Necessity of dietary phospholipids for growth of the larval ayu. Mem. Fac. Fish., Kagoshima Univ. 32, 115–120.

Kanazawa, A., Teshima, S., Sakamoto, M., 1985. Effects of dietary bonito-egg phospholipids and some phospholipids on growth and survival of the larval ayu, *Plecoglossus altivelis*. Z. Angew. Ichthyol. 4, 165–170.

Kanazawa, A., Koshio, S., Teshima, S., 1989. Growth and survival of larval red seabream *Pagrus major* and Japanese flounder *Paralichtys olivaceus* fed microbound diets. J. World Aquacult. Soc. 20, 31–37.

Kissil, G.Wm., 1985. Overview: rearing larval stages of marine fish on artificial diets. Isr. J. Zool. 33, 154–160.

Kitajima, C., Arakawa, T., Oowa, G., Fujita, S., Imada, O., Watanabe, T., Yone, Y., 1980. Dietary value for red saebream larvae of rotifer, *Brachionus plicatilis*, cultured with a new type of yeast. Bull. Jpn. Soc. Sci. Fish. 46, 43–46.

Koven, W.M., Kolkovski, S., Tandler, A., Kissil, G.Wm., Sklan, D., 1993. The effect of dietary lecithin and lipase, as a function of age, on n-9 fatty acid incorporation in the tissue lipids of *Sparus aurata* larvae. Fish Physiol. Biochem. 10, 357–364.

Leger, C., 1985. Digestion, absorption and transport of lipids. In: Cowey, C.B., Mackie, A.M., Bell, G.J. (Eds.), Nutrition and Feeding in Fish. Academic Press, London, pp. 299–331.

López-Alvarado, J., Kanazawa, A., 1994. Effect of dietary arginine levels on growth of red seabream larvae fed diets supplemented with crystalline amino acids. Fisheries Science 60, 435–439.

Mosconi-Bac, N., 1987. Hepatic disturbance induced by an artificial feed in the sea bass (*Dicentrarchus labrax*) during the first year of life. Aquaculture 67, 93–99.

Pedersen, B.H., Nilssen, E.M., Hjelmeland, K., 1987. Variation in the content of trypsin and trypsinogen in larval herring (*Clupea harengus*) digesting copepod nauplii. Mar. Biol. 94, 171–181.

Salhi, M., 1997. Estudio de los requerimientos lipídicos de larvas de dorada (*Sparus aurata*) alimentadas con microdietas. Ph.D. Thesis, Universidad de Las Palmas de Gran Canaria, Spain.

© Del documento, los autores. Digitalización realizada por ULPGC. Biblioteca Universitaria, 2009

Salhi, M., Izquierdo, M.S., Hernández-Cruz, C.M., González, M., Fernández-Palacios, H., 1994. Effect of lipid and n-3 HUFA levels in microdiets on growth, survival and fatty acid composition of larval gilthead seabream (*Sparus aurata*). Aquaculture 124, 275–282.

Salhi, M., Kolkovski, S., Izquierdo, M.S., Tandler, A., 1995. Inclusion of lecithin and polar or neutral lipids high in n-3 HUFA in microdiets for gilthead seabream (*Sparus aurata*) larvae. In: Lavens, P., Jaspers E., Roelants, I. (Eds.), Proceedings of Larvi'95-Fish and Shellfish Larviculture Symposium, Gent, Belgium. European Aquacult. Soc. (Special Publ.) 24, 184–187.

Salhi, M., Kolkovski, S., Izquierdo, M.S., Tandler, A., 1998. Incorporation of fatty acids from different lipid classes in larval gilthead seabream (*Sparus aurata*) fed on microdiets. Recent Advances in Finfish and Crustacean Nutrition, Abstracts VIII International Symposium on Nutrition and Feeding of Fish, Las Palmas, Spain, pp. 224.

Santulli, A., Modica, A. Cutatolo, A., D'Amelio, V., 1993. Lipid and apoprotein composition of lipoprotein of sea bass (*Dicentrarchus labrax* L.). Proceedings of World Aquaculture'93, from Discovery to Commercialization. Torremolinos, Spain. Eur. Aquacult. Soc. (Spec. Publ.) 19, 461.

Sargent, J.R., Henderson, R.J., Tocher, D.R., 1989. The lipids. In: Halver, J.E. (Ed.), Fish Nutrition. Academic Press, San Diego, pp. 153–218.

Sheridan, M.A., 1988. Lipid dynamics in fish: aspects on absorption, transportation, deposition and mobilization. Comp. Biochem. Physiol. 90B, 679–690.

Teshima, S., Kanazawa, A., Sakamoto, S., 1982. Microparticulate diets for the larvae of aquatic animals. Min. Rev. Data File Fish. Res. 2, 67–86.

Teshima, S., Kanazawa, A., Horinouchi, K., Yamasaki, S., Hirata, H., 1987. Phospholipids of the rotifers, prawn and larval fish. Nippon Suisan Gakkaishi 53, 609–615.

Watanabe, T., Ohta, M., Kitajima, C., Fujita, S., 1982. Improvement of the dietary value of brine shrimp *Artemia salina* for fish larvae by feeding them on 3 highly unsaturated fatty acids. Bull. Jpn. Soc. Sci. Fish. 48, 1775–1782.

© Del documento, los autores. Digitalización realizada por ULPGC. Biblioteca Universitaria, 2009

Third Conference
on Fluorescence Microscopy
and Fluorescent Probes

# FLUORESCENT STUDY OF ORGANIC COMPOUNDS OF ENVIRONMENTAL INTEREST IN ORGANIZED MOLECULAR SYSTEMS. ANALYTICAL APPLICATIONS

**J.J. Santana Rodríguez**

*Department of Chemistry, Faculty of Marine Sciences,*
*University of Las Palmas de G.C., 35017 Las Palmas de G.C., Spain*

## Introduction

At present, the environmental conservation is one of the most important subjects of social and scientific interest. In this respect, the determination and control of pollutants in the environment constitutes one of the principal aspects. Because of this, in the last years important effort has been expended to optimize new and more sensitive and selective analytical methods for the determination of contaminants in environmental samples. Three important groups of these pollutants are polychlorinated biphenyls (PCBs), arochlors and polychlorinated dibenzofurans (PCDBs).

Polychlorinated biphenyls and arochlors (commercial mixtures of PCBs) are families of compounds produced commercially by the direct chlorination of biphenyl. These compounds have found application in a wide variety of industrial uses due to their chemical and thermal stability. Since their discovery in environmental samples in 1966 (1), it has been generally accepted that they are ubiquitous in every component of the global ecosystem (2-5).

It has been shown that the toxicity of PCBs varies with the degree of chlorination and the substitution pattern. The structure-activity relationships of the PCBs have shown that the most biologically active congeners have chlorine substitution of the biphenyl rings in both *para* positions, in two or more of the four *meta* positions, and in one or none of the four *ortho* positions (6).

Polychlorinated dibenzofurans are chlorinated tricyclic aromatic compounds and are emitted into the environment as unwanted by-products of anthropogenic processes. PCDBs have been globally distributed and are found in all environmental media. They are chemically stable, have low solubilities in water, and have been shown to accumulate in the foodchain. It is well known that the PCDBs with chlorines substituted in the 2,3,7,8 positions are thought to pose a risk to human health due to their toxicity, carcinogenic potential and potential effects on animal reproductive and inmunological systems (7-9)

© Del documento, los autores. Digitalización realizada por ULPGC. Biblioteca Universitaria, 2009

Because of these environmental problems, the identification and quantification of these compounds is a matter of great concern for many analysts. In this work, we present new analytical methods for the determination of these organochlorinated compounds based on their fluorescent characteristics in the presence of different organized molecular systems. A systematic study of fluorescent behavior of PCBs, arochlors and PCDBs in the presence of cationic, anionic and non-ionic surfactants has been carried out. Variables, such as surfactant concentration, organic solvent concentration and temperature, were optimized and analytical parameters, such as linear dynamic range, reproducibility and detection limit, were established. The proposed methods have been applied to the determination of these pollutants in real enviromental samples.

In addition to the above mentioned studies and using the fluorescent characteristics of PCBs and PCDBs in the presence of different surfactants, we report also on the determination of these compounds by high performace liquid chromatography with fluorescent detection combined with "cloud point" methodology.

## Results and Discussion

### 1. Fluorescence determination of organochlorinated compounds in the presence of micellar media

The use of organized media (aqueous and reverse micelles, bilayers, microemulsions, vesicles and liposomes) has been common practice in all fields of analytical chemistry for the modification on the reactivity between analytes and reagents and to improve the analytical procedures. Micellar systems can produce an increase in fluorescence intensity of organic compounds compared to that obtained in aqueous medium under identical instrumental conditions. This has led to the use of different micellar media to improve the sensitivity and selectivity of many fluorescent determinations (10-14).

We have carried out a systematic study of the following PCBs, arochlors and PCDBs: biphenyl, 4-chlorobiphenyl (4-PCB), 4,4′-dicholorobiphenyl (4,4′-PCB), 3,4,4′-tricholorobiphenyl (3,4,4′-PCB), 2,2′,5,5′-tetracholobiphenyl (2,2′,5,5′-PCB), 3,3′,4,4′-tetrachlorobiphenyl (3,3′,4,4′-PCB), 2,2′,4,5,5′-pentachlorobiphenyl (2,2′,4,5,5′-PCB), 3,3′,4,4′,5-pentachlorobiphenyl (3,3′,4,4′,5-PCB), 2,3,3′,4,4′,5-hexachlorobiphenyl (2,3,3′,4,4′,5-PCB) 2,2′,4,4′,5,5′-hexachlorobiphenyl (2,2′,4,4′,5,5′-PCB), 3,3′,4,4′,5,5′-hexachlorobihenyl (3,3′,4,4′,5,5′-PCB), 2,2′,3,3′,4,4′,5,5′-octachlorobihenyl (2,2′,3,3′,4,4′,5,5′-PCB); Arochlor 1016, Arochlor 1221, Arochlor 1232, Arochlor 1242, Arochlor 1248, Arochlor 1254, Arochlor 1268, dibenzofuran, 4-chlorodibenzofuran (4-PCDB), 2,8-dichlorodibenzofuran (2,8-PCDB), 2,4,6-trichlorodibenzofuran (2,4,6-PCDB), 2,3,7,8-tetrachlorodibenzofuran (2,3,7,8-PCDB), 2,3,4,7,8-pentachlorodibenzofuran (2,3,4,7,8-PCDB) and 2,3,4,5,7,8-PCDB), in the presence of hexadecyltrimethylammonium bromide (HDTAB), benzyldimethylhexadecylammonium chloride (BDMHDAC), cetylpyridinium bromide (CPB), sodium dodecyl-

© Del documento, los autores. Digitalización realizada por ULPGC. Biblioteca Universitaria, 2009

benzenosulfonate (NaDDBS), sodium lauryl sulfate (NaLS), polyoxyethylene(10)lauryl ether (POLE), polyoxyethylene(10)oleyl ether (Brij-96) and isooctylphenoxypolyethoxyethanol (Tx-100) as surfactants.

### *1.1. Fluorescence characteristics*

Generally, the excitation wavelengths of polychlorinated compounds present similar values in organized and aqueous (2 % ethanol) media; however, in the emision wavelengths a different behavior is observed. Thus, while for arochlors no shift is observed in emision maxima in micellar and aqueous media, for PCBs and PCDBs a shift to shorter wavelengths is observed in organized medium respect to aqueous medium (15, 16, 17).

In aqueous medium the polychlorinated compounds present a decrease of the relative intensity of fluorescence with the number of chlorine atoms on the molecule of dibenzofuran. The enhancement of fluorescence, with respect to aqueous medium, in the presence of surfactants depends on the position of the chlorine atoms: PCBs with chlorine atoms in *ortho* position do not fluoresce; however, for PCBs with chlorine atoms in other than *ortho* position, the enhancement of fluorescence increases with the number of chlorine atoms up to 3,3′,4,4′-PCB, which presents maximum fluorescence, or arochlors with 40 % chlorine. PCBs with a higher number of chlorine atoms, the relative fluorescence intensity decreases and the enhancement of fluorescence is very low. Polychlorinated dibenzofurans present a similar behavior to PCBs.

According to the results obtained, polyoxyethylene(10)lauryl ether produces the maximum enhacement of fluorescence for all compounds studied.

### *1.2. Optimization of variables*

The influence of surfactant concentration, percentage of organic solvent, temperature and stability with time was studied for 3,4,4′-PCB, 3,3′,4,4′-PCB, 2,8-PCDB and 2,3,7,8-PCDB in the presence of POLE.

For all the compounds studied, the relative fluorescence intensity increases sharply with POLE concentration up to concentrations next to critical micelle concentration (c.m.c.). At higher surfactant concentrations, the fluorescence of polychlorinated compounds remains practically constant (Fig. 1).

The total amount of ethanol in the solution of a micellar medium of POLE affects to the fluorescence of PCBs, but no influence is observed for PCDBs. In the case of PCBs in the presence of POLE, a decrease of the relative fluorescence intensity is observed from 30 % (*V/V*) of ethanol, obtaining similar values to those obtained in aqueous medium, when high percentages of ethanol are used (Fig. 2 and 3).

The influence of temperature on fluorescence of all compounds was studied, obtaining a linear decrease between 15 and 75 °C (Fig. 4). This effect can be due to a high number of collisions between fluorophor molecules and to a decrease of solute-micelle interactions. Also, a stability of at least one hour was obtained for all compounds to the different temperatures studied.

© Del documento, los autores. Digitalización realizada por ULPGC. Biblioteca Universitaria, 2009

### *1.3. Fluorimetric determination of 3,4,4'-PCB, 3,3',4,4'-PCB, 2,8-PCDB and 2,3,7,8-PCDB*

After optimization of conditions, new methods were proposed for the determination of 3,4,4'-PCB, 3,3',4,4'-PCB, 2,8-PCDB and 2,3,7,8-PCDB in the presence of POLE. These studies included calibration curves, reproducibility of the methods, detection limits, as well as a study of the possible interference by other compounds of environmental interest. According to the data obtained, these methods can be considered accurate and precise. The detection limits obtained, 4.9 ng/ml for 3,4,4'-PCB, 1.4 ng/ml for 3,3',4,4'-PCB, 1.1 ng/ml for 2,8-PCDB and 1.3 ng/ml for 2,3,7,8-PCDB are values much lower than those obtained in aqueous medium.

Due to the high environmental interest of the compounds studied, the methods established were applied to the determination of these compounds in sea water samples, obtaining very satisfactory recovery percentages.

### *1.4. Synchronous fluorescence determination of 3,3',4,4'-PCB and 2,3,7,8-PCDB*

3,3',4,4'-PCB and 2,3,7,8-PCDB are highly toxic compounds that are normally found normally together in the environment. Because of this we tried the simultaneous determination of these compounds using their synchronous fluorescence characteristics in the presence of POLE. Hovewer, a high overlapping was observed on the corresponding synchronous spectra, using a range of $\Delta\lambda$ between 1 and 100 nm (18).

A study of second-derivative synchronous fluorescence spectra of 3,3',4,4'-PCB and 2,3,7,8-PCDB indicates that both compounds can be determined simultaneously using $\Delta\lambda$ of 48 nm (Fig. 5), obtaining a detection limit of 5.3 ng/ml for 3,3',4,4'-PCB and 2.7 ng/ml for 2,3,7,8-PCDB. This method was applied satisfactorily to the resolution of mixtures of both compounds in sea water samples.

### *1.5. Fluorescence quenching determination of 4-PCB and Arochlor 1221*

4-PCB and Arochlor 1221 are compounds with similar percentage of chlorine and their fluorescence signal is not enhanced for none of surfactants studied. Hovewer, the presence of cetylpiridinium bromide produces a fluorescence quenching effect in these organochlorinated compounds, wich can be used from an analytical point of view (Fig. 6) (19). This quenching effect is described for the Stern-Volmer equation, the constant of which depends on fluorophor concentration (Table 1).

© Del documento, los autores. Digitalización realizada por ULPGC. Biblioteca Universitaria, 2009

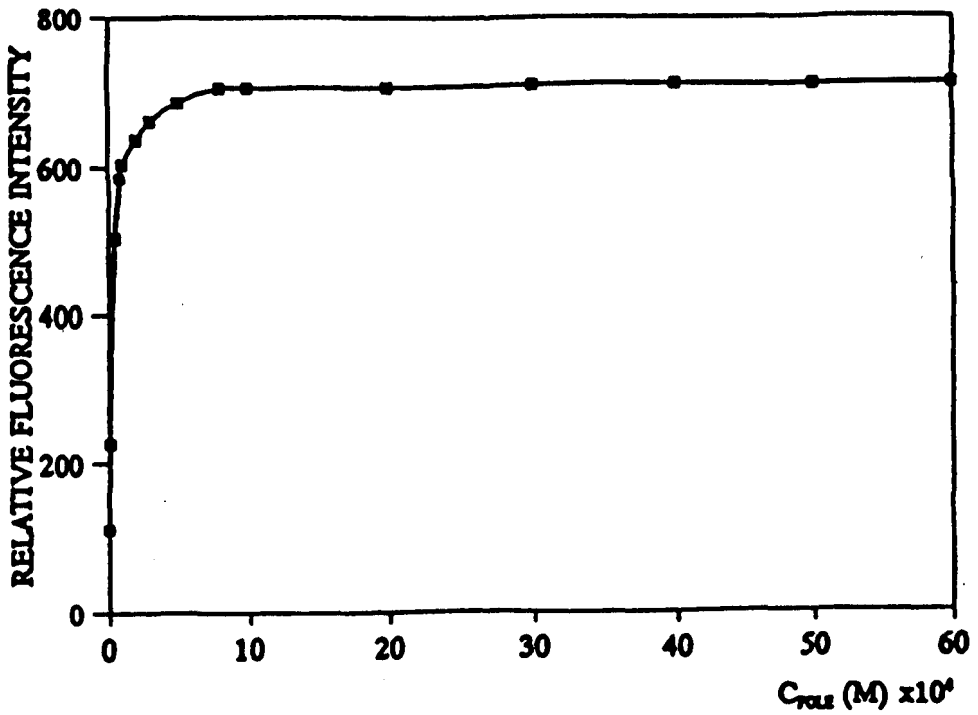


**Fig. 1.** Effect of POLE concentration on the fluorescence intensity of 3,4,4′-PCB in 2 % (*V/V*) ethanol-water. $c_{PCB}$ = 1 μM.

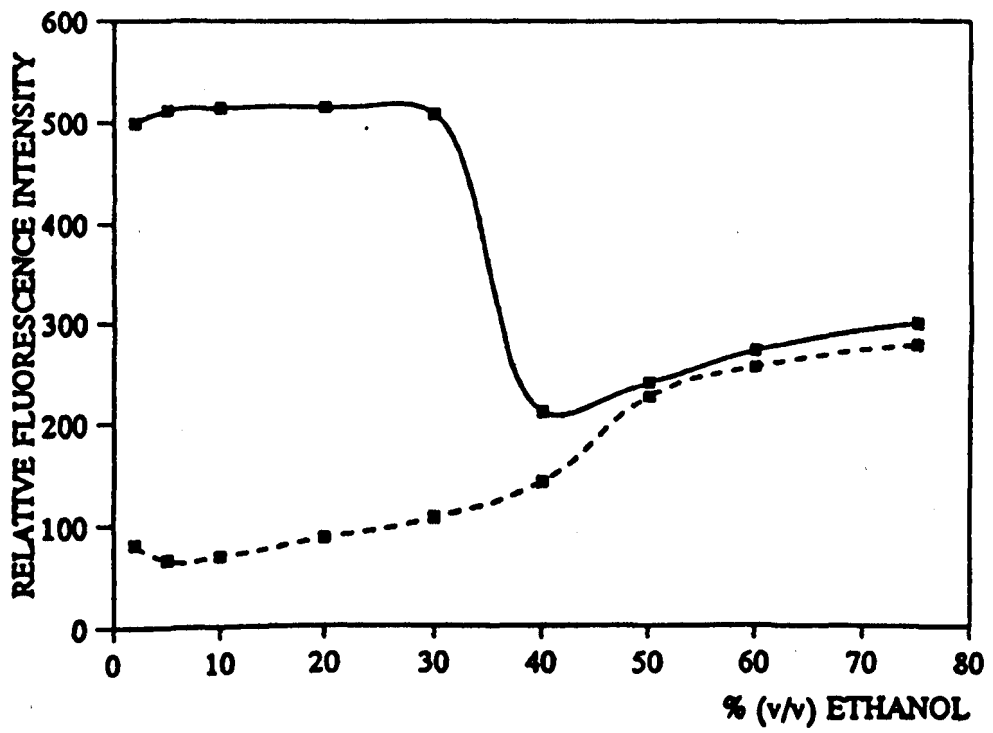


**Fig. 2.** Effect of ethanol on the fluorescence intensity of 3,3′,4,4′-PCB in micellar medium (solid curve) and in aqueous medium (dashed curve). $c_{PCB}$ = 1 μM; $c_{POLE}$ = 2 mM.

© Del documento, los autores. Digitalización realizada por ULPGC. Biblioteca Universitaria, 2009

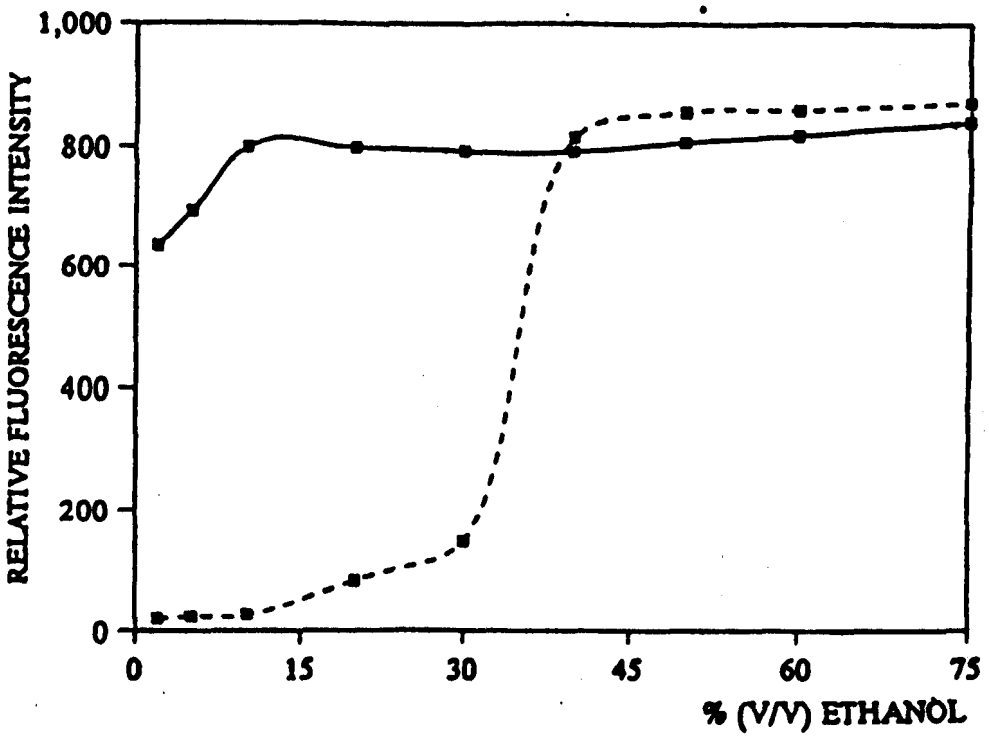


**Fig. 3.** Effect of ethanol on fluorescence intensity of 2,3,7,8-PCDB in micellar (solid curve) and aqueous (dashed curve) media. $c_{PCDB}$ = 1 μM; $c_{POLE}$ = 2 mM

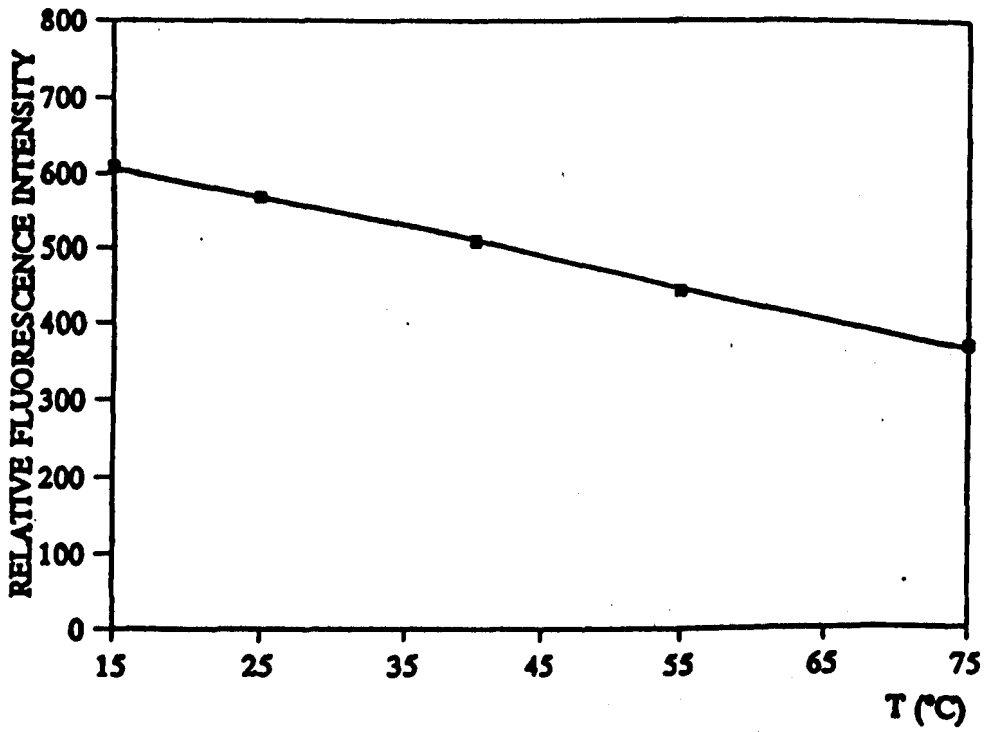


**Fig. 4.** Effect of temperature on fluorescence intensity of 3,4,4′-PCB in micellar medium. $c_{PCB}$ = 1 μM; $c_{POLE}$ = 2 mM.

© Del documento, los autores. Digitalización realizada por ULPGC. Biblioteca Universitaria, 2009

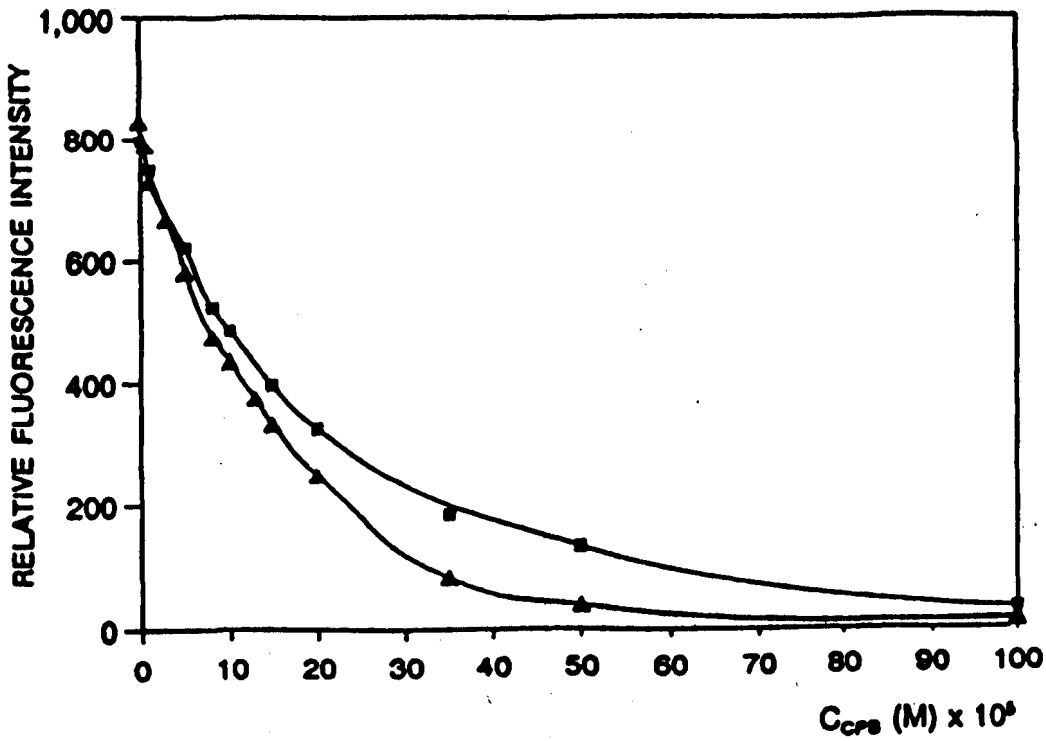


**Fig. 5.** Influence of concentration of CPB on the fluorescence intensity of 4-PCB (lower curve) and Arochlor 1221 (upper curve).

**Table 1.** Variation of Stern-Volmer constant ($K_{SV}$) with 4-PCB and Arochlor 1221 concentration

| 4-PCB | | Arochlor 1221 | |
|---|---|---|---|
| **Concentration ng/ml** | $K_{SV}$ | **Concentration ng/ml** | $K_{SV}$ |
| 3.2 | 2985.9 | 5.0 | 1219.0 |
| 5.3 | 3928 | 8.0 | 3856.3 |
| 10.6 | 4772.1 | 13.6 | 4223.9 |
| 31.7 | 8951.0 | 25.0 | 4705.9 |
| 52.8 | 11056.3 | 50.0 | 4837.4 |
| 79.2 | 12142.4 | 60.0 | 5974.7 |
| 105.6 | 10345.2 | 80.0 | 5513.8 |
| 150.2 | 9158.0 | 90.0 | 5100.3 |
| 200.0 | 6985.9 | 100.0 | 4219.0 |

After optimization of variables, such as percentage of organic solvent, temperature and surfactant concentration, as well as a study of the possible interference of other polychlorinated biphenyls and arochlors, a new analytical method was established to estimate these compounds, using the quenching ef-

© Del documento, los autores. Digitalización realizada por ULPGC. Biblioteca Universitaria, 2009

fect produced by CPB. High recovery percentages were obtained when the method was applied to sea- water samples.

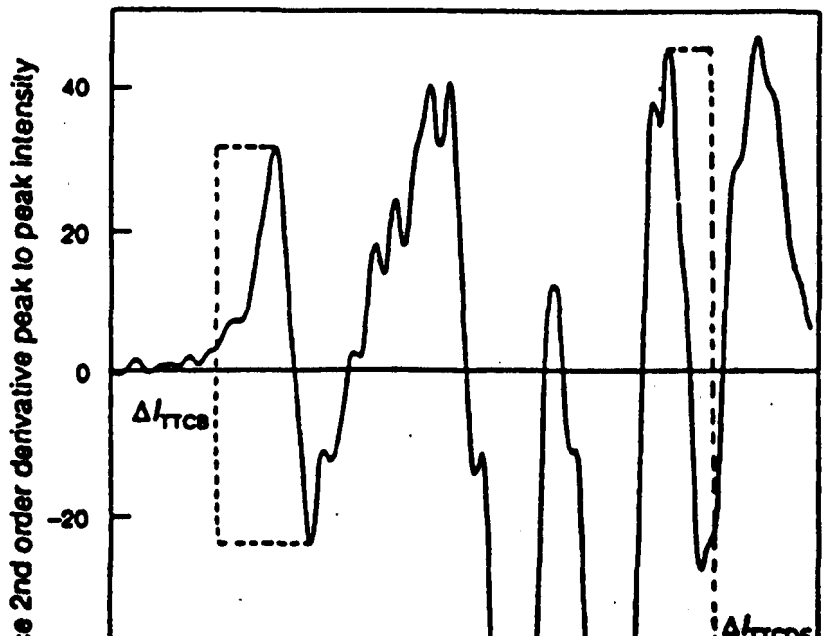


**Fig. 6.** Second-derivative synchronbous fluorescence spectrum of a binary mixture of TTCB (3,3′,4,4′-PCB) and TTCDF (2,3,7,8-PCDB) in micellar medium. $c_{TTCB}$ = 0.4 μM; $c_{TTCDF}$ = 0.1 μM; $c_{POLE}$ = 2 mM.

## 2. Use of organized molecular systems on the extraction/preconcentration of organo-chlorinated compounds and their determination by high-performance liquid chromatography with fluorescence detection

Separation procedures based on the peculiar properties of aqueous non-ionic and zwitterionic surfactant solutions have been also proposed as an alternative to the use of traditional organic solvent. Efficient preconcentrations of organic solutes have been obtained using the cloud-point phase separation phenomena (20-22). The analytical potential of the cloud-point-phenomenon-mediated phase separations, cloud- point extraction (CPE), has been discussed by several authors (23-26). The small volume of the surfactant-rich phase allows us to preconcentrate

© Del documento, los autores. Digitalización realizada por ULPGC. Biblioteca Universitaria, 2009

and extract the analytes in one step, prior to gas- or liquid-chromatographic analysis. Moreover, the surfactant-rich phase is compatible with the micellar and aqueous-organic mobile phase in liquid chromatography, which facilitates the application of this analytical method, with the obvious benefits.

In this part of the work, we report the results of a study of the experimental parameters which affect the extraction efficiency and preconcentration factor of the CPE process of a series of PCBs and PCDBs previous to their determination by high performance liquid chromatography, using four non-ionic surfactants, Oligoethylene glycol monoalkyl ether (Genapol X-080), polyoxy-ethylene(10)lauryl ether (Brij-30), polyoxyethylene(10)cetyl ether (Brij 56) and polyoxyethylene(10)oleyl ether (Brij-97). This CPE methodology was applied to the analysis of mixtures of PCBs and PCDBs in sea water samples.

### 2.1. *Phase diagrams*

When we plot cloud-point values against the percentage (*W/V*) of surfactant in solution, the figure shows a co-solution curve, above which the two phases appear (Fig. 7). The behavior is similar for the four surfactants used, the first showing a sharp drop in temperature up to a concentration of 2 % (*W/V*) above which the cloud-point temperature is fairly constant. According to the results obtained, the critical temperature of the cloud-point for Genapol X-080, Brij-30, Brij-56 and Brij-97 was 80 ± 1 °C, 95 ± 1 °C, 90 ± 1 °C and 85 ± 1 °C, respectively (27, 28).

### 2.2. *Optimization of the preconcentration factor*

There are different factors that can alter the extraction process and it is very important to optimize them in order to obtain good recovery factors: concentration and volume of surfactant, equilibration time, ionic strength and analyte concentration (29).

#### 2.2.1. *Concentration and volume of surfactant*

For the PCBs studied, when the concentration of surfactant changes between 0.05- and 5 % (*W/V*), keeping the volume constant, the ratio $V_w/V_s$ (volume of aqueous phase/volume of surfactant phase) decreases with the concentration of surfactant, being practically constant from 1 % (*W/V*). When the volume of surfactant changes, keeping concentration constant, $V_w/V_s$ remains constant for Genapol X-080 and Brij-56, and decreases linearly for Brij-30 and Brij-97. For PCDBs, these two variables do not influence the extraction process.

#### 2.2.2. *Equilibration time*

The behavior of PCBs is different, depending on the surfactant. In the case of Genapol X-080, the recovery percentages of PCBs increase up to a maximum value of 15 min, decreasing after that; for Brij-30, the behavior is similar to Genapol X-080 but the recovery percentages increase again for times higher than 20 min; in the case of Brij-97, the recovery percentages decrease lightly up

© Del documento, los autores. Digitalización realizada por ULPGC. Biblioteca Universitaria, 2009

to 15 min, remaining practically constant after that; for Brij-56, the time neccesary to obtain the highest recovery percentages decreases with the number of chlorine atoms on the molecule.

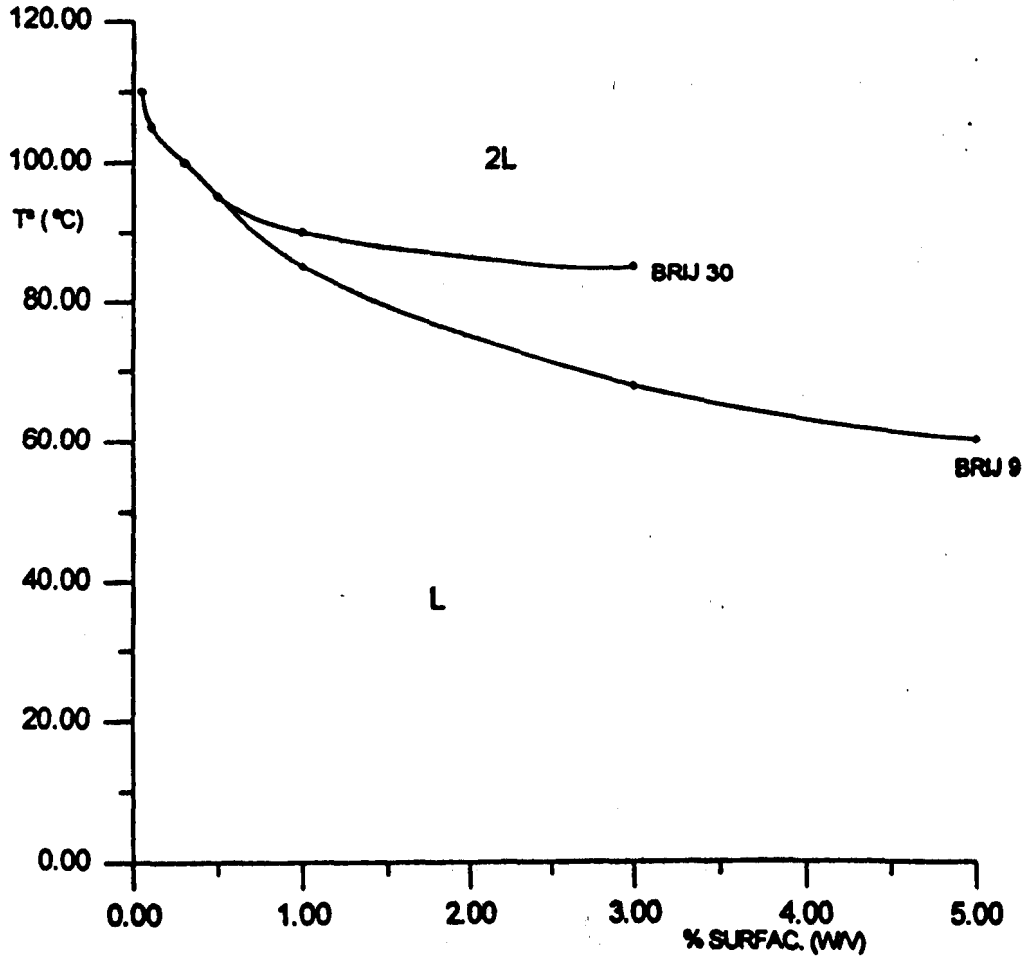


Fig. 7. Phase diagram for Brij 30 and Brij 97. The region above the cosolution curve is a two-phase region.

In the case of PCDBs, using Genapol X-080, we observed that 4-PCDB shows a similar behavior to the PCDB with an even number of chlorine atoms. The recovery percentages of these compounds decrease with time to 13 min, increasing to 15 min (maximum recovery percentage) and going down again for longer times. In the case of PCDB with odd numbers of chlorine atoms, recovery percentages increase with time to 13 min, decreasing for 15 min and increasing for longer periods. Using Brij-56, the recovery percentages decrease sharply for all the PCDB with time up to 13 min, but with longer periods two behaviors could be observed: for PCDB with even numbers of chlorine atoms, the recovery percentage increases up to 20 min, decreasing gradually over longer periods; the rest of the PCDB presents low recovery percentages for 20 min, increasing to 25 min.

© Del documento, los autores. Digitalización realizada por ULPGC. Biblioteca Universitaria, 2009

### 2.2.3. *Ionic strength*

The presence of salt in the solution can be important for the extraction process and in the extracted volume of surfactant-rich phase. The study of the influence of this parameter was carried out by adding different percentages of $KNO_3$ (1–10 % *W/V*) to the solution. The results indicated that the addition of salt does not affect the extracted volume of surfactant-rich phase or the recovery percentages of all analytes studied. But the addition of inert salt increases the density of the bulk aqueous phase and facilitates the separation process of the two phases. These results are in accordance with those obtained by other authors (30).

### 2.2.4. *Analyte concentration*

To determine the effect of analyte concentration, solutions containig different concentrations of PCBs and PCDBs were subjected to the CPE procedure. The results obtained indicated that for PCBs, using Genapol X-080, Brij-30 and Brij-97, the extraction process is not affected in the concentration intervals studied; for PCDBs, neither Genapol X-080 nor Brij-56 influence the recovery percentages of these analytes.

## 2.3. *Cloud-point preconcentration and liquid chromatographic analysis*

Another important step in these studies is the optimization of the chromatographic conditions for the separation and determination of the organochlorinated compounds. When chromatography is used as a separation technique, it is necesary to obtain good relationship between the analysis time and analyte separation. The results indicated as best chromatographic conditions a mobile phase of 85:15 (*V/V*) methanol:water and a flow rate of 1 ml/min. Using these conditions and the characteristic excitation and emission wavelengths, the corresponding chromatograms indicated a satisfactory separation of all compounds (Fig. 8 and 9). After the establishment of the calibration curves and reproducibility of the methods, the detection limits (31) were calculated (Tables 2 and 3).

**Table 2.** Detection limits (ng/ml) for PCBs

| PCB | Brij-30 | Brij-97 |
|---|---|---|
| Biphenyl | 1.54 | 0.70 |
| 4-PCB | 1.89 | 0.94 |
| 4,4'-PCB | 2.23 | 1.10 |
| 3,4,4'-PCB | 7.71 | 2.57 |
| 3,3'4,4'-PCB | 2.92 | 2.92 |
| 3,3'4,4',5-PCB | 16.30 | 16.30 |
| 3,3'4,4'5,5'-PCB | 10.82 | 18.04 |

© Del documento, los autores. Digitalización realizada por ULPGC. Biblioteca Universitaria, 2009

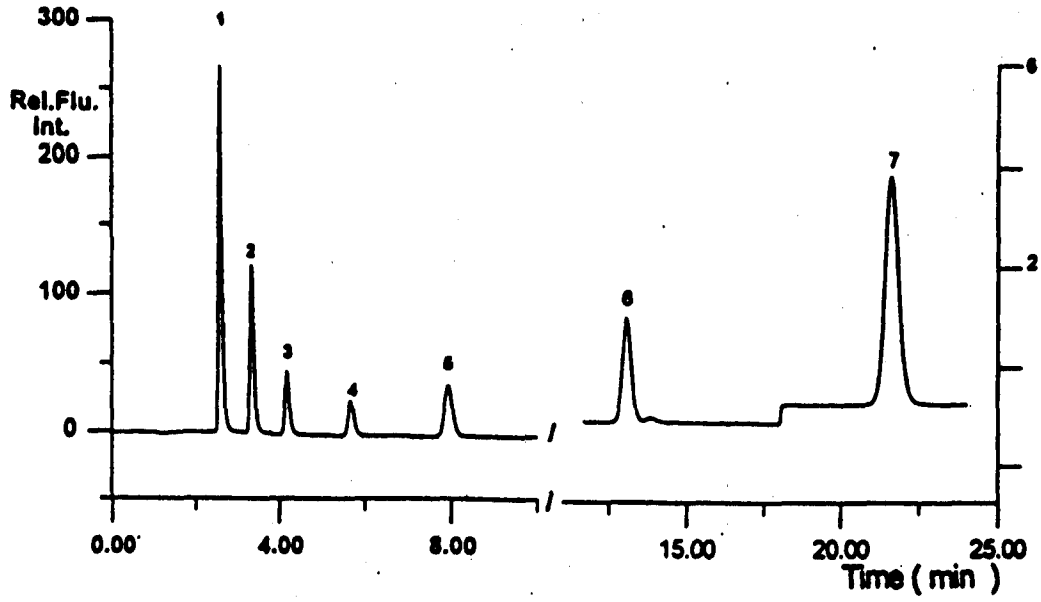


**Fig. 8.** Elution of a mixture of seven PCBs using 2 % (*W/V*) Brij 30 as preconcentrant. 1 - biphenyl, 2 - 4-PCB, 3 - 4,4'-PCB, 4 - 3,4,4'-PCB, 5 - 3,3',4,4'-PCB, 6 - 3,3',4,4',5-PCB, 7 - 3,3',4,4',5,5'-PCB. Concentration 500 ng/ml; eluent was methanol-water 85:15), flow rate 1 ml/min.

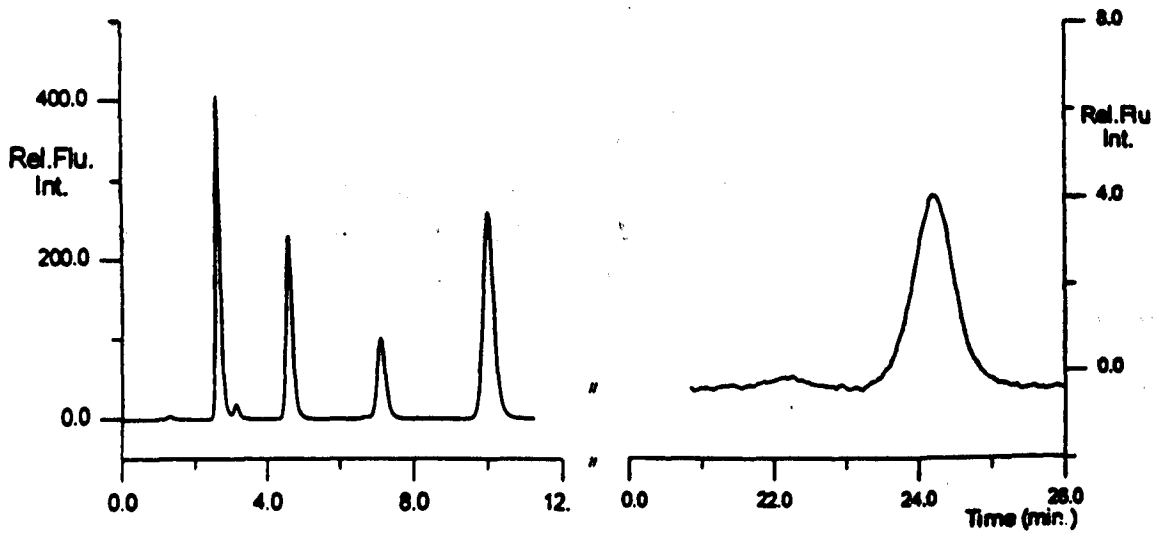


**Fig. 9.** Elution of a mixture of six PCBs using 2 % (*W/V*) Genapol X-080 as preconcentrant. 1 - dibenzofuran, 2 - 4-PCDB, 3 - 2,8-PCDB, 4 - 2,4,8-PCDB, 5 - 2,3,7,8-PCDB, 6 - 1,2,3,4,8-PCDB. Concentration 500 ng/ml; eluent was methanol-water 85:15), flow rate 1 ml/min.

© Del documento, los autores. Digitalización realizada por ULPGC. Biblioteca Universitaria, 2009

### 2.4. *Analytical applications*

Once optimized, the proposed methods were applied to the determination of PCBs and PCDBs in sea-water samples from different Spanish areas (Arinaga and Agaete, Canary Islands and Elantxobe, Vizcaya), previously spiked with suitable amounts of PCBs and PCDBs. The results indicated recovery between 84 and 106 %.

**Table 3.** Detection Limits for PCDBs using Genapol X-080 and Brij-56

| PCDB | Detection limit ng/ml |
|---|---|
| Dibenzofuran | 0.5 |
| 4-PCDB | 17.6 |
| 2,8-PCDB | 13.3 |
| 2,4,8-PCDB | 4.9 |
| 2,3,7,8-PCDB | 0.7 |
| 1,2,3,4,8-PCDB | 27.5 |

## References


1. Jensen, S., *New. Sci.*, 1966, **32**, 612
2. Hutzinger, O., Safe, S. and Zitko, V., *The Chemistry of PCBs*, CRC Press, Cleveland, OH, 1974, pp. 249-251
3. Erickson, M.D., *Analytical Chemistry of PCBs*, Erickson M.D. Ed., Ann Arbor Science, Ann Arbor, MI 1986, pp.24-34
4. Paasivirta, J., Mantykoski, K., Paukker, R., Piilola, T., Vihonen, H., Sarkka, J. and Grauberg, K., *Aqua Fenn.*, 1986, **16**, 17
5. Waid, J.S., *PCBs and the Environment*, CRC Press, Boca Raton, Fl, 1986
6. Bandiera, S., Safe, S. and Okey, A.B., *Chem. Biol. Inter. Acta*, 1982, **39**, 259
7. Fletcher, C. L. and McKay, W. A., *Chemosphere*, 1993, **26**, 1041
8. Broman, D., Näf, C., Rolff, C. and Zebühr, Y., *Environ. Sci. Technol.*, 1991, **25**, 1850.
9. Clement, R.E., *Anal. Chem.*, 1991, **63**, 1130
10. Hinze, W.L., Singh, H.N., Baba, Y. and Harvey, N.G., *Trends. Anal. Chem.*, 1984, **3**, 193
11. Howard, J.H. and Fazio, T., *J. Assoc. Anal. Chem.*, 1980, **63**, 1077
12. Pelizzetti, E. and Pramauro, E., *Anal. Chim. Acta*, 1985, **169**, 1
13. Santana Rodríguez, J.J., Sosa Ferrera, Z., Afonso Perera, A. and González Díaz, V., *Anal. Chim. Acta*, 1991, **255**, 107
14. Von Wandruszka, R., *Critical Reviews in Anal. Chem.*, 1992, **23**, 187
15. J.Hernández García, J.R.Betancort Rodríguez, A.J.Bermejo Martín-Lázaro and J.J.Santana Rodríguez, *Anal.Chim.Acta*, 1994, **290**, 146
16. J.Hernández García, A.J.Bermejo Martín-Lázaro, Z.Sosa Ferrera and J.J.Santana Rodríguez, *Anal.Letters*, 1994, **27**, 1355.
17. J.Hernández García, A.J.Bermejo Martín-Lázaro, Z.Sosa Ferrera and J.J.Santana Rodríguez, *Mikrochim.Acta*, 1995, **118**, 185


© Del documento, los autores. Digitalización realizada por ULPGC. Biblioteca Universitaria, 2009

18. J.J.Santana Rodríguez, Z.Sosa Ferrera, J.Hernández García and A.J.Bermejo Martín-Lázaro, *The Analyst,* 1994, **119,** 2241
19. J.J.Santana Rodríguez, J.Hernández García, Z.Sosa Ferrera, and A.J.Bermejo Martín-Lázaro, *Fresenius J.Anal.Chem,* 1996, **354,** 221
20. R.G. Laughrin, in G.H. Brown (Editor), *Advances in Liquid Crystals*, Academic Press:New York, 1978, Vol. 3, p. 41,76,106
21. H. Watanabe, in K.L. Mittal, E.J. Fendler ( Editors) *Solution Behavior of Surfactants*, Plenum Press, New York, 1982
22. W.L. Hinze and E.Pramauro, *Crit. Rev. Anal. Chem.*, **24**,113 (1993)
23. W.L. Hinze, *Ann. Chim.*, 1987, **77**,167
24. N.D.Gullickson, J.F. Scamehorn, J.H. Harwell, in J.F. Scamehorn, J.H. Harwell (Editors) *Surfactant-Based Separation Processes*, Marcel Dekker, New York, 1989
25. H. Hoshino, T. Saitoh, H. Taketoni, T. Yotsuyanagi, H. Watanabe, K. Tachikawa, *Anal. Chim. Acta,* 1983, **147,** 339
26. T. Saitoh, W.L. Hinze, *Talanta,* 1995, **42,** 119
27. A. Eiguren Fernández, Z. Sosa Ferrera and J.J. Santana Rodríquez, *Quím. Anal.*, 1997, **16**, *2*, 283
28. A. Eiguren Fernández, Z. Sosa Ferrera and J.J. Santana Rodríquez, *Anal. Chim. Acta,* 1998, **358,**145
29. A. Eiguren Fernández, Z. Sosa Ferrera and J.J. Santana Rodríquez, *The Analyst,* 1999, **124,** 487
30. E.Minati and D.Zanette, *Colloids Surf. A,* 1996, **113**, 237
31. S.Lindsay, in *High Performance Liquid Chromatography,* Wiley, New York, 1992, pp.71,72.

© Del documento, los autores. Digitalización realizada por ULPGC. Biblioteca Universitaria, 2009

# El acceso a los recursos genéticos en el Convenio sobre Diversidad Biológica

Pedro Sosa Henríquez

*Departamento de Biología. Universidad de Las Palmas de Gran Canaria.*

Uno de los aspectos más comprometidos y polémicos del Convenio sobre Diversidad Biológica (CDB), firmado durante la Conferencia de Naciones Unidas sobre Medio Ambiente y Desarrollo, celebrada en Río de Janerio en junio de 1992, es el acceso y el reparto equitativo de los beneficios derivados del uso de los recursos genéticos (artículo 15).

El CDB es el primer acuerdo mundial integral que abarca todos los aspectos de la diversidad biológica, y se estableció con el fin de conocer y conservar la biodiversidad en sus tres formas o niveles establecidos: genes, especies y ecosistemas, proponiendo como herramientas básicas, además de las medidas expresas de conservación necesarias, el uso racional y sostenible de los recursos biológicos. Pero el Convenio ha tenido también como objetivo redefinir el hecho histórico de que los recursos genéticos eran patrimonio común de la humanidad y, por lo tanto, se encontraban a la libre disposición de todos. Este libre intercambio de los recursos no obligaba a las instituciones o empresas que los empleaban a compartir los beneficios obtenidos de su uso con el país de origen de los recursos. El resultado se traducía en una explotación gratuita de la biodiversidad, y consecuentemente en la inexistencia de incentivos económicos adicionales para su conservación por parte del país de origen.

Cresta de gallo *(Isoplexis canariensis)*. Archivo.



© Del documento, los autores. Digitalización realizada por ULPGC. Biblioteca Universitaria, 2009

El artículo 15 del Convenio establece claramente como una novedad la autoridad y responsabilidad de los países y sus Gobiernos como soberanos en la determinación del acceso a los recursos genéticos en aquellas áreas que se encuentren dentro de su jurisdicción. También insta a tomar medidas apropiadas que regulen el acceso a los recursos naturales mediante el sometimiento a la legislación nacional. Así, muchos países ricos en biodiversidad y celosos de sus propios recursos genéticos han querido poner rápidamente coto a su expolio, explotación o sustracción gratuita, limitando drásticamente los accesos a tales recursos.

Filipinas fue el primero en adoptar una legislación de acceso en concordancia con el CDB en la forma de Orden Ejecutiva Presidencial (mayo 1995) al que han seguido otros como Malasia, Brasil, Costa Rica, Australia o Fiji. También Perú, Colombia, Venezuela, Bolivia y Ecuador firmaron en julio de 1996 el Pacto Andino, (legislación conocida como el Acuerdo de Cartagena), y que representa el primer esfuerzo en establecer una legislación de acceso conjunta en una región biogeográfica.

Los países más desarrollados, preocupados a su vez por mantener el nivel de acceso a la diversidad biológica y recursos genéticos bajo soberanía de otros países y presionados por las industrias, empresas, investigadores y otros sectores de su economía, se esfuerzan en demostrar que a partir de ahora van a establecer un sistema de beneficios compartidos, justo y equitativo, en concordancia con el Convenio. Muchos países de la Unión Europea se encuentran en este caso. Existen también países que, por el momento, se preocupan poco o nada por este problema, porque piensan que de una manera u otra van a seguir teniendo acceso a cualquier recurso genético y componente de la diversidad biológica del planeta, se encuentre donde se encuentre. Estados Unidos parece ser el más claro representante de este comportamiento. Hay que recordar que EEUU no ha firmado aún el CDB debido, entre otras razones, a las presiones que ejercieron en su momento las grandes compañías del sector biotecnológico y farmacéutico.

La importancia que está cobrando la regulación de acceso a los recursos genéticos y los beneficios compartidos se pone claramente de manifiesto en la Estrategia sobre Biodiversidad de la Unión Europea promovido por la DGXI, así como en la Estrategia Española para la conservación y el uso sostenible de la diversidad biológica. Ambos documentos consideran los beneficios compartidos derivados del uso de los recursos genéticos como fundamental para su desarrollo, así como uno de los cinco temas clave de su redacción. En este sentido, hay que señalar que se ha firmado un convenio de colaboración entre el Ministerio de Medio Ambiente y la Universidad de Las Palmas de Gran Canaria con el fin de establecer y analizar la situación de los recursos genéticos en España.

Malva del Risco *(Lavatera acerifolia)*. Archivo

## Canarias, rica en recursos genéticos

Canarias es una región muy rica en recursos genéticos, que actúa como permanente donante de biodiversidad en muy diversas direcciones, especialmente en lo que ha recursos fitogenéticos se refiere. El archipiélago dispone de más de 4.200 endemismos, muchos de los cuales son paleoendemismos, es decir, estirpes muy antiguas que, en cierto modo, encierran en su genoma valiosa información sobre el pasado y, por lo tanto, podrían constituirse como recursos genéticos de gran valor no sólo evolutivo, sino económico.

Conviene recordar que muchas especies (especialmente vegetales) son fuentes de principios activos empleados para la producción de insecticidas, productos farmacéuticos, cosméticos o en la alimentación. Según datos de la Organización Mundial de la Salud (OMS), en los países industrializados el 25% de las medicinas vendidas en las farmacias es de origen vegetal, mientras que otro 25% contienen principios vegetales modificados químicamente. Además, la revolución biotecnológica y la genética molecular abren aún más el abanico de posibilidades en la aplicación y uso de nuevos productos, así como en la explotación de los recursos genéticos. De este modo, las multinacionales del fármaco han puesto en marcha en la última década programas de investigación sobre las plantas medicinales procedentes de países en desarrollo ricos en biodiversidad. Estos programas y proyectos de prospección biológica (bioprospección) consisten en la exploración sistemática de plantas, animales o microorganismos con el fin de encontrar en la naturaleza recursos genéticos y bioquímicos que resulten económicamente valiosos.



© Del documento, los autores. Digitalización realizada por ULPGC. Biblioteca Universitaria, 2009

Los Institutos Nacionales de Salud destinaron más de 60 millones de dólares a la investigación relacionada con la biodiversidad y productos médicos provenientes del mundo natural. El Instituto Nacional del Cáncer, en busca de productos naturales para tratar esta enfermedad y el SIDA, ya ha recolectado más de 50.000 muestras derivadas de plantas, microorganismos y diversidad genética marina proveniente de 30 países tropicales. El principal acuerdo contractual para este acceso reconoce la necesidad de compensar a las organizaciones y comunidades del país de origen en caso de comercializarse un fármaco desarrollado a partir de un organismo recogido dentro de sus fronteras, pero no establece la cuantía. También en Canarias han existido diversos casos de prospección biológica. Por ejemplo, en el año 1995 se firmó un convenio de investigación entre el Instituto de Algología Aplicada de la Universidad de Las Palmas de Gran Canaria y la empresa Merck España, mediante el que se analizó la capacidad antibacteriana de diversos extractos obtenidos de más de 80 especies de macroalgas del litoral canario después de mantenerlas en diversas condiciones de cultivo. Sin embargo, en el convenio establecido, la empresa farmacéutica retuvo los derechos de la posible explotación de los productos obtenidos sin considerar el reparto de beneficios.

## Legislar el acceso a los recursos genéticos

Al hilo de lo comentado, podemos vislumbrar la importancia y la necesidad de establecer una legislación de acceso a los recursos genéticos. No sólo debido a los beneficios que puede reportar sino, tal y como contempla el Convenio, a que puede constituir una medida eficaz de conservación de la biodiversidad. Sin embargo, no es difícil prever los problemas prácticos que están surgiendo y que con toda seguridad seguirán apareciendo a partir de la ratificación del Convenio y de la aparición de leyes de acceso y beneficios compartidos. Cualquier ley que establezca procedimientos de acceso excesivamente burocratizantes y un control extremadamente centralizado tenderá a imponer restricciones al intercambio de recursos genéticos, lo que puede implicar graves impedimentos al desarrollo científico y tecnológico para aquellas áreas dependientes de éstos. La gran descentralización en competencias medioambientales existente en España, y también en Canarias, podría dificultar al mismo tiempo la puesta en marcha de estos procedimientos.

En las diversas reuniones y mesas de trabajo que ya se están celebrando en todo el mundo con respecto al acceso a los recursos, se pone de manifiesto la necesidad de incluir elementos básicos en los contratos de cooperación, pero también se concluye en la inexistencia de un único modelo contractual para todas las ocasiones y para todos los recursos. Además, la industria prospectora requiere sobre todo interlocutores atractivos en los países de origen, con competencias y potestad para negociar todos los aspectos del contrato, al mismo tiempo que con suficiente capacidad de manejo e investigación para llevar a buen término la labor pactada. Esto podría significar la creación de puestos de trabajo, además de una fuente de ingresos alternativa, pero también será necesario formar técnicos y especialistas en estas áreas de la conservación y explotación biológica. Existe un gran vacío político, legal y técnico en torno a este tema, y aún es prematuro señalar en qué dirección se va a mover. Además, la ambigüedad de la Convención sobre la Diversidad Biológica en los derechos de la propiedad intelectual y física, así como los arreglos de compensación que se deben aplicar en las transacciones, refleja un estado de transición sin precedentes, que al mismo tiempo está conduciendo a fuertes debates en el seno de la Secretaría de la Convención y en la Conferencia de las partes (órgano de seguimiento del CDB).

Indudablemente, será necesario activar y desarrollar nuevos protocolos internacionales, nacionales y locales más específicos que puedan paliar las deficiencias que ya se detectan. También es necesario revisar el marco legislativo español y autonómico relacionado con el acceso a los recursos genéticos de forma que se consiga establecer competencias claras en este área y unificar los procedimientos de acceso, al mismo tiempo que realizar un esfuerzo de planteamiento interno considerando el papel que las autonomías, municipios y cabildos pueden tener en el mismo. Hay que determinar la capacidad técnica, administrativa y financiera de las instituciones canarias para supervisar y gestionar el cumplimiento de la ley; qué instituciones tendrán la capacidad de informar, autorizar y negociar el acceso; establecer modelos adecuados de contrato según la naturaleza de los recursos; clarificar cuestiones relacionadas con la propiedad (física e intelectual) o el papel de las patentes como mecanismos de control, y será esencial realizar un análisis de la demanda potencial de los recursos genéticos por sectores, así como una valoración de los mismos. Además, muchos recursos genéticos son compartidos, no sólo por más de un país sino por diferentes especies, por lo que en el proceso de planificación se deberían establecer acuerdos multilaterales (como los establecidos en el Pacto Andino) con otros Estados o zonas biogeográficas próximas con los mismos recursos genéticos (caso de la Región Macaronésica). En este sentido, Canarias, no sólo por su situación geográfica sino por su potencial científico y tecnológico, podría constituirse como centro de actuación en esta región biogeográfica.



© Del documento, los autores. Digitalización realizada por ULPGC. Biblioteca Universitaria, 2009

# Review

# Isozymes in macroalgae (seaweeds): genetic differentiation, genetic variability and applications in systematics

PEDRO A. SOSA[1] AND SANDRA C. LINDSTROM[2]

[1] Department of Biology, University of Las Palmas, Campus Universitario de Tafira, 35017 Las Palmas, Canary Islands, Spain
[2] Department of Botany, #3529–6270 University Blvd., University of British Columbia, Vancouver, B.C., Canada V6T 1Z4

(Received 10 May 1999; accepted 15 August 1999)

Use of isozymes (including allozymes) in studies of population genetics and systematics of seaweeds has increased sufficiently in the last decade to allow some generalization. Only a single locus has been observed for about half the enzymes analysed in seaweeds, compared with 29% in vascular plants. Compared with higher plants, macroalgal species generally have low amounts of electrophoretically detectable genetic variation; the lowest levels of genetic variation found in natural populations are those reported for seaweeds. Nonetheless, seaweeds show an association between levels of genetic diversity as revealed by isozymes and species-specific attributes, such as mating system and predominance of asexual versus sexual reproduction. In systematic studies, isozymes have revealed cryptic species and identified pairs of sibling taxa. The quaternary structure of enzymes appears to be conserved at the phylum level. With the current availability of improved techniques for enzyme electrophoresis and for data interpretation, we expect future studies utilizing isozyme electrophoresis to provide further insight into population and evolutionary processes in seaweeds.

Key words: allozymes, electrophoresis, genetic identity, genetic structure, genetic variability, isozymes, population genetics, seaweeds, systematics

## Introduction

Prior to Cheney's (1985) compilation of procedures for isozyme gel electrophoresis in macroalgae, there were few published papers applying this technique to seaweeds (Sosa & Garcia-Reina, 1991*a*). Sufficient electrophoretic data for seaweeds have now accumulated that a meaningful synthesis is possible. Here, we review the current application of isozyme analysis to macroalgae. Practical aspects of isozyme electrophoresis are not included, since electrophoretic techniques for algae usually involve only minor modifications of procedures published for other organisms, and they have been described for macroalgae in detail elsewhere (Cheney, 1985; Lindstrom & South, 1989; Sosa & Garcia-Reina, 1991*b*). However, some general genetic concepts commonly used in isozyme analysis will be reviewed in order to explain or emphasize the utility and importance of these techniques.

Hunter & Markert (1957) were the first to apply specific enzyme histochemical stains to detect bands on a gel. Markert & Möller (1959) called them 'isozymes,' indicating multiple forms of an enzyme with the same catalytic specificity but with different kinetic properties and different migration rates on a gel. Since then, the term isozyme has been used in a variety of ways, to refer both to the total number of bands observed, without any genetic interpretation, and to the products of different loci exclusively (Kephart, 1990). Some authors differentiate the gene locus and the isozyme product more effectively by invoking 'isozyme locus' instead of isozyme.

Nowadays, usage of the term isozyme, or isoenzyme, has shifted in accordance with recommendations of the Nomenclature Committee of the International Union of Biochemistry (Kephart, 1990). In practice, two forms of protein data can be gathered simultaneously using electrophoresis (Murphy *et al.*, 1996). One is derived from isozymes, which are all functionally similar forms of enzymes, produced by different gene loci. The other data set consists of allozymes, a subset of isozymes, which are variants of polypeptides representing different allelic alternatives of the same gene locus. In phycological studies, the term isozyme has often been used, even when the products of only a single locus are considered. We follow this broader usage here, recognizing nevertheless that in many cases the term allozyme would be more appropriate.

Isozymes are employed to investigate a variety of interesting and significant problems. At present, the use of isozymes still represents one of the best techniques for analysing and studying large numbers of genes and alleles of different individuals and populations at one time.

Correspondence to: P. A. Sosa. Fax: +34 928.45.29.22. e-mail: pedro.sosa@biologia.ulpgc.es

© Del documento, los autores. Digitalización realizada por ULPGC. Biblioteca Universitaria, 2009

Multiple enzyme systems can be surveyed with standard electrophoretic techniques to determine levels of genetic differentiation, to detect distributional patterns of genotypes, and to estimate the degree of outcrossing or inbreeding within populations, or to detect cryptic species (the genotypes of which have diverged but which remain morphologically indistinguishable).

In macroalgae, isozyme studies are still uncommon. Technical difficulties associated with polysaccharides, especially in some red and brown algae, the tendency of phycologists to prefer more traditional approaches in systematics and, conversely, the current tendency of phycologists to utilize DNA-based molecular techniques employing the polymerase chain reaction (PCR) for population or phylogenetic purposes, are some of the reasons so few studies of seaweeds have examined isozymes. The application and advantages of electrophoresis of isozymes and the limitations of the technique have been discussed in detail elsewhere (Gottlieb, 1981; Tanksley & Orton, 1983; Soltis & Soltis, 1989a; May, 1992; Murphy *et al.*, 1996), and although direct DNA studies are increasing, there has not been a commensurate reduction in investigations using isozymes. In fact, DNA techniques and enzyme electrophoresis can provide complementary information (van Oppen *et al.*, 1995). It is clear that isozymes deserve a wider application than they have thus far seen (van der Meer, 1986).

## Genetic interpretation

The genetic interpretation of banding patterns constitutes one of the most important aspects of isozyme electrophoresis. Electrophoretic data can contain significantly more information than simply relative mobility or presence and absence of bands. Moreover, the possibility of non-homologous or even artefactual bands can lead to erroneous conclusions if genetic interpretation is foregone (Gottlieb, 1977; Wendel & Weeden, 1989; Murphy *et al.*, 1996).

Although genetic control of banding differences can be established by formal genetic analysis using breeding studies, such tests may be impossible or impractical due to difficulties in culturing seaweeds or in inducing sexuality. As allozymes are usually co-dominantly inherited, crosses between individuals with different electromorphs should result in F1 progeny that display both parental bands. To date, however, isozyme analysis and breeding studies have not been carried out together. Thus, the genetic basis and inheritance of isozymes in seaweeds is an area of research yet to be broached experimentally. Until such studies are made, assumptions regarding Mendelian inheritance and conclusions based on these assumptions are tentative and warrant caution.

In the absence of breeding studies, other important factors for appropriate interpretation of enzyme banding patterns are: (1) the number of coding genes, (2) the ploidy of the individual, (3) the quaternary structure of the enzyme, (4) the subcellular localization of the enzyme, and (5) artefacts. These factors are discussed below.

## Number of genes

The number of loci coding an enzyme system affects the interpretation of bands. Obviously, the more genes, the more bands, and the more complex the banding pattern. In seaweeds, the number of genes observed depends on both the enzyme and the species analysed. To date, only a single locus has been identified for about half of the enzyme systems analysed in seaweeds (Table 1). In vascular plants, 29% of enzymes are coded by a single gene; most are coded by two or more loci (Weeden & Wendel, 1989). Although the low percentage of multilocus genes found in seaweeds has facilitated genetic interpretation, it has also limited the utility of this technique in analysing genetic variation in natural populations (Neefus *et al.*, 1993). The relatively high proportion of single-locus enzymes in algae is especially striking for enzymes assayed with artificial substrates, such as phosphatases, esterases, peroxidases and superoxide dismutases. In vascular plants and animals, these multiple-substrate enzymes almost always display many bands for an individual. Because these bands are usually derived from heterogeneous enzymes, coded by more than one locus, their interpretation can be difficult (Innes, 1984). In land plants, peroxidase is often represented by many loci, whereas in seaweeds only one gene has been encountered (Table 1). For esterase, the maximum number of loci is three in macroalgae (Table 1), whereas more than 10 loci have been observed for many land plant species (Weeden & Wendel, 1989).

In macroalgae, four or more loci have been recognized for only three enzyme systems, all of them enzymes detected by non-natural substrates: acid phosphatase, superoxide dismutase and diaphorase (Table 1). Superoxide dismutase (SOD) activity has been described for some peroxidase enzymes (Kiang & Gorman, 1983), which could indicate that some SOD loci correspond to peroxidase enzymes. Also, a diverse group of flavoproteins is capable of using reduced pyridine co-factors to reduce acceptor substrates, and these stains may have little specificity; therefore, diaphorase stains may also reveal a heterogeneous group of enzymes. In the same way, seaweeds can contain a variety of enzymes with phosphatase activity, some of which may have broad and overlapping substrate specificity *in vitro*.

In contrast to vascular plants, where conservation is particularly striking with respect to enzymes of glycolysis and the pentose phosphate pathway, a variable number of loci has been described for these pathways in seaweeds. Thus, a maximum of two loci has been described for triose phosphate isomerase (TPI) and phosphoglucomutase (PGM), whereas between one and three loci have been observed for malate dehydrogenase (MDH) and glucose phosphate isomerase (GPI), depending on the species or genus (Table 1).

© Del documento, los autores. Digitalización realizada por ULPGC. Biblioteca Universitaria, 2009

**Table 1.** Number of isozyme loci described or inferred for macroalgae using electrophoresis

| Enzyme | Abbreviation | No. of loci | Reference |
|---|---|---|---|
| Acid phosphatase[a] | ACP | 2 | O |
| | | 3–6 | B |
| Aconitase | ACO | 1 | R |
| Alanine peptidase | ALAP | 1 | L |
| Alanine aminotransferase | ALT | 1 | T |
| Aldolase | ALD | 1 | J, K, L, M, R, T |
| Alkaline phosphatase[a] | ALP | 1 | O, U, V, W |
| Amylase | AMY | 1 | H |
| Aspartate aminotransferase | AAT/GOT | 1 | A, C, E, F, D, G, L, M, R, X |
| | | 2 | H, J, K, L, M |
| Catalase[a] | CAT | 1 | O, P, Q, C, D, E, F, G |
| Diaphorase[a] | DIA | 1 | A, C, D, G, E |
| | | 2 | O, W |
| | | 4 | U, V |
| Esterase[a] | EST | 1 | L |
| | | 2 | W |
| | | 3 | U, V |
| Formate dehydrogenase | FDH | 1 | R |
| Fructose biphosphatase | FBF | 1 | T |
| Glucose dehydrogenase | GD | 1 | I |
| Glucose-6-phosphate dehydrogenase | G6PDH | 1 | C, D, E, F, I, M, J, K, L, O, R |
| Glutamate dehydrogenase[b] | GDH | 1 | D, E, F, G, L, M, J, K, S, P, Q, W |
| 6-Phosphogluconic dehydrogenase | 6PGD | 1 | A,C, D, G, E, F, L, J, K, M, I, R |
| | | 2 | A |
| Glyceraldehyde-3-phosphate dehydrogenase | G3PDH | 1 | I, R |
| Isocitrate dehydrogenase | IDH | 1 | C, D, G, J, K, M, N, Q, Y |
| | | 2 | T |
| | | 3 | R |
| Hexokinase | HEX | 2 | T |
| Lactate dehydrogenase | LDH | 1 | I, J, K |
| Leucine aminopeptidase | LAP | 1 | P, C |
| L-Leucylglycine peptidase | PEP | 1 | O |
| Leucyltyrosine peptidase | LT | 1–2 | A |
| Malate dehydrogenase | MDH | 1 | A, D, E, F, G, I, N, P, Q, R, Y |
| | | 2 | A, B, C, O, U, V |
| | | 3 | A, B, W |
| Malic enzyme | ME | 1 | A, J, K, M, Y |
| | | 2 | A |
| | | 3 | R |
| Mannose phosphate isomerase | MPI | 1 | C, D, E, F, G, I, R |
| Peptidase | PEP | 2 | I |
| Peroxidase[a] | PER | 1 | J, K, P |
| | | 2 | R |
| Phosphoglucoisomerase | PGI/GPI | 1 | A, B, D, E, F, G, J, K, L, N, Q, R, S, X |
| | | 2 | C, I, O, P, Y |
| | | 3 | U, V, W |
| Phosphoglucomutase | PGM | 1 | B, C, D, E, F, G, H, I, J, L, M, N, Q, S, U, V, W, X, Y |
| | | 2 | J, K, M |
| Ribulose-biphosphate carboxylase | RBC | 2 | T |
| Shikimic dehydrogenase | SKDH | 1 | J, K, M |
| | | 2 | J, K, R |
| Superoxide dismutase[a] | SOD/IPO | 1 | B, C, D, E, F, G, H, I, K, L, O, P |
| | | 2 | K, L |
| | | 3 | W |
| | | 5 | V |
| | | 6 | U |
| Triosephosphate isomerase | TPI | 1 | N, R, Y |
| | | 2 | X, T |

A, Benzie *et al.* (1997); B, Cheney & Babbel (1978); C, Fujio *et al.* (1985); D, Fujio *et al.* (1987); E, Gil-Kodaka *et al.* (1988); F, Gil-Kodaka *et al.* (1990); G, Hara *et al.* (1986); H, Innes & Yarish (1984); I, Intasuwan *et al.* (1993); J, Lindstrom & Cole (1990*a*); K, Lindstrom & Cole (1992*a*–*c*); L, Lindstrom & South (1989); M, Lindstrom (1993*a*); N, Lu & Williams (1994); O, Malinowski (1974); P, Miura *et al.* (1978*a*); Q, Miura *et al.* (1979); R, Neefus *et al.* (1993); S, Okumura & Fujino (1986); T, Pearson & Murray (1997); U, Sosa & Garcia-Reina (1992); V, Sosa & Garcia-Reina (1993); W, Sosa *et al.* (1996); X, van Oppen *et al.* (1995); Y, Williams & Di Fiori (1996).

[a] Multiple substrate enzymes.

[b] NAD- and NADP-dependent

© Del documento, los autores. Digitalización realizada por ULPGC. Biblioteca Universitaria, 2009

These results appear to indicate that the number of loci coding proteins is lower in macroalgae compared with vascular plants, where new loci have been incorporated by duplication and mutation during evolution. One of us believes this difference is real, and one of us believes it is artefactual due to technical difficulties associated with electrophoresis of proteins in seaweeds. The capacity of polysaccharides found in most seaweeds to bind to proteins (especially in brown algae) can influence directly the number of bands and, therefore, the number of loci observed. Most authors have described bands with uninterpretable variation or with inconsistent staining, which they omitted from their analyses; such bands may represent the missing loci.

## Ploidy and life-history phase

Seaweeds exhibit a diversity of life histories; these may be monophasic, biphasic or even triphasic (DeWreede & Klinger, 1988). Different phases may exist simultaneously as free-living haploid and diploid thalli, and these phases may be isomorphic or heteromorphic. Seaweeds are therefore good biological models to analyse isozyme variation among individuals with different ploidy levels. Data obtained by pooling thalli with unknown ploidy levels should be avoided because differences observed in such pooled data may simply reflect different proportions of the haploid and diploid stages in the sample rather than true genetic differences (Innes, 1984).

An assumption regarding banding patterns is that they are simpler in haploid thalli. In haploid individuals only one allele is present for each locus, so consequently each band corresponds to just one locus. Thus, hybrid bands between products of different alleles of the same locus cannot occur as they can for diploid individuals. For example, in species of *Porphyra*, in which only the haploid macroscopic gametophyte has been sampled, each band has been interpreted as the product of a single gene, and multiple bands would necessarily have to be the products of different loci (however, see Fujio *et al.*, 1988, for an exception). In contrast, in other genera, species may be polyploid in origin, and this multigenicity complicates the interpretation of the zymograms. Complex banding patterns for several enzyme systems in individuals of *Caulerpa peltata* suggest that this species is polyploid (Benzie *et al.*, 1997). This hypothesis could be verified by inheritance studies.

In very few species have both haploid and diploid life-cycle stages been analysed. In the two phases of *Gelidium arbuscula* and *G. canariensis*, which are isomorphic, no differential expression of alleles was detected (Sosa & Garcia-Reina, 1992, 1993). Thus, the haploid gametophyte banding pattern was used as a tool in interpreting the zymograms genetically. No consistent differences in banding patterns between thalli identified as male (haploid) and those known to be tetrasporophytes (diploid) were seen in other red algae with isomorphic life histories (Cheney & Babbel, 1978; Lindstrom & South, 1989; Pearson & Murray, 1997). Because species with a heteromorphic life cycle have two phases with very different morphologies, seasonalities, and even habitats, it would be very interesting to compare and to analyse the enzyme loci of the two phases. Only Abo *et al.* (1996) have observed isozymes in both phases of heteromorphic species (*Porphyra tenera* and *P. yezoensis*). These authors did not report using controls or replicates nor did they interpret their data genetically. Thus, further studies on the two phases of heteromorphic species are warranted.

## Quaternary structure

Many proteins contain more than one polypeptide chain (subunit) bound together by hydrogen bonds, van der Waals forces, ionic bonds, disulphide bridges and/or hydrophobic interactions. Proteins having more than one polypeptide are said to have a quaternary structure. Proteins with only one polypeptide chain are called *monomers*. A *dimer* is formed by two subunits, each consisting of a single polypeptide chain; an enzyme is a *tetramer* if four subunits are required to form the active protein. The identification of the quaternary structure of an enzyme by electrophoresis can be determined from the number of bands obtained from heterozygous diploid individuals (Wendel & Weeden, 1989; Kephart, 1990; May, 1992; Murphy *et al.*, 1996): two bands for a monomer, three for a dimer, and five for a tetramer.

For most enzymes in vascular plants, genetic inferences can be made from gel banding patterns, because the quaternary structure of most enzymes is highly conserved in biochemical evolution at the level of class, especially for enzymes with known natural substrates. Thus, for vascular plants, enzymes such as PGM and ACO are monomers, whereas ADH, MDH, PGI and TPI are dimers (Weeden & Wendel, 1989; Kephart, 1990).

In seaweeds, inferences regarding quaternary structure have been made directly from electrophoretic banding patterns (Table 2). From results to date, it seems that quaternary structure is also evolutionarily conserved in seaweeds. For example, PGI (described as a dimer in vascular plants) has been interpreted as a monomer in *Silvetia compressa* (as *Pelvetia fastigiata*) and *Macrocystis pyrifera* (Phaeophyceae), but as a dimer in *Gelidium canariensis*, *G. arbuscula*, *Gracilaria cervicornis* and *Porphyra yezoensis* (Rhodophyta) (Table 2). Similar results have been observed for the enzymes MDH, PGM, GOT and SOD. For example, MDH is considered dimeric in all red and brown seaweeds analysed so far but is monomeric in *Codium fragile* (Chlorophyta) (Table 2). However, more studies, especially formal crossing analyses, are required to determine with certainty the quaternary structure of isozymes in seaweeds and to confirm evolutionary conservation within phyla.

© Del documento, los autores. Digitalización realizada por ULPGC. Biblioteca Universitaria, 2009

**Table 2.** Quaternary structure of enzymes described or inferred for macroalgae using isozyme gel electrophoresis

| Enzyme | Structure | Species | Reference |
|---|---|---|---|
| ACP | Monomer | *Eucheuma isiforme* var. *denudatum*[a]; *E. isiforme* var. *isiforme*; *Meristiella gelidium*[b] | Cheney & Babbel (1978) |
| ALP | Monomer | *Gelidium arbuscula* | Sosa & Garcia-Reina (1992) |
| | | *Gelidium canariensis* | Sosa & Garcia-Reina (1993) |
| AMY | Monomer | *Enteromorpha linza* | Innes & Yarish (1984) |
| CAT | Monomer | *Codium fragile* | Malinowski (1974) |
| DIA | Monomer | *Gelidium arbuscula* | Sosa & Garcia-Reina (1992) |
| | | *Gelidium canariensis* | Sosa & Garcia-Reina (1993) |
| EST | Monomer | *Gelidium arbuscula* | Sosa & Garcia-Reina (1992) |
| | | *Gelidium canariensis* | Sosa & Garcia-Reina (1993) |
| | | *Gracilaria cervicornis* | Sosa *et al.* (1996) |
| GDH | Monomer | *Gelidium arbuscula* | Sosa & Garcia-Reina (1992) |
| GOT | Dimer | *Enteromorpha linza* | Innes & Yarish (1984) |
| MDH | Monomer | *Codium fragile* | Malinowski (1974) |
| | Dimer | *Halidrys dioica* | Lu & Williams (1994) |
| | | *Gelidium arbuscula* | Sosa & Garcia-Reina (1992) |
| | | *Gelidium canariensis* | Sosa & Garcia-Reina (1993) |
| | | *Porphyra yezoensis* | Fujio *et al.* (1985) |
| | | *Porphyra* sp. | Fujio *et al.* (1988) |
| MPI | Monomer | *Porphyra* sp. | Fujio *et al.* (1988) |
| PEP | Monomer | *Codium fragile* | Malinowski (1974) |
| PGI/GPI | Monomer | *Silvetia compressa*[c], *Macrocystis pyrifera* | Williams & Di Fiori (1996) |
| | Dimer | *Gelidium arbuscula* | Sosa & Garcia-Reina (1992) |
| | | *Gelidium canariensis* | Sosa & Garcia-Reina (1993) |
| | | *Gracilaria cervicornis* | Sosa *et al.* (1996) |
| | | *Porphyra yezoensis* | Fujio *et al.* (1985) |
| PGM | Monomer | *Halidrys dioica* | Lu & Williams (1994) |
| | Dimer | *Enteromorpha linza* | Innes & Yarish (1984) |
| SOD | Monomer | *Eucheuma isiforme* var. *isiforme*, *E. isiforme* var. *denudatum* | Cheney & Babbel (1978) |
| | Dimer | *Enteromorpha linza* | Innes & Yarish (1984) |
| TPI | Dimer | *Halidrys dioica* | Lu & Williams (1994) |

[a] As *Eucheuma nudum*.
[b] As *Eucheuma gelidium* and *E. acanthocladum*.
[c] As *Pelvetia fastigiata*.

## Subcellular distribution

In vascular plants, many routinely examined isozymes have chloroplast, mitochondrial, microbody and cytosolic forms (Weeden & Wendel, 1989). Generally, such isozymes, coded by different loci, are unable to associate into active enzymes, and therefore they form no intergenic heteromultimers (there are exceptions). Thus, band phenotypes may be simplified by subcellular compartmentalization of isozymes but no research on compartmentalization of electrophoretically interesting enzymes in seaweeds has been published, although its existence has been suggested. Malinowski (1974), comparing patterns obtained for chloroplast and whole plant extracts, established that the GOT-1 locus was localized in the chloroplasts of *Codium fragile*. Lindstrom (1993*a*) reported occasional faint secondary bands for several enzymes in species of *Porphyra*, which she thought could represent isozymes from different subcellular locations.

## Artefacts and null alleles

Artefacts from extraction, electrophoresis and staining of seaweed enzymes have also been observed on gels. Most of these can be dismissed by proper experimental controls or testing. Description and discussion of artefacts and their control can be found elsewhere (Oelshlegel & Stahman, 1973; Cheney; 1985; Kephart, 1990; May, 1992; Murphy *et al.*, 1996). Finally, alleles that are no longer transcribed or that code for defective polypeptides lacking enzymatic activity are generally referred to as 'null' or 'silent' alleles. These variants often remain undetected because their presence is masked in the heterozygous condition. As yet, no null alleles have been described in seaweeds.

## Genetic variation

The detection of genetic variability in seaweed populations is a function of sample size and number of loci analysed. Sufficient numbers of individuals and enzymes are essential for meaningful results. Surveys of 10 or more loci in several hundred diploid individuals are often reported in animal and higher plant studies. These numbers of loci and individuals can be difficult to achieve in seaweeds, and the optimal sampling design will depend on the specific purpose of the study and the nature of the populations.

© Del documento, los autores. Digitalización realizada por ULPGC. Biblioteca Universitaria, 2009

**Table 3. Measures of genetic variability in natural populations of seaweeds averaged across those populations**

| Species | S | NP | NL | A | P | H | Reference |
|---|---|---|---|---|---|---|---|
| CHLOROPHYTA | | | | | | | |
| *Caulerpa cupressoides* (d) | 12–15 | 2 | 13 | 1·10 | 7·7 | 0·013 | Benzie *et al.* (1997) |
| *C. lentillifera* (d) | 14 | 1 | 8 | 1·00 | 0·0 | 0·000 | Benzie *et al.* (1997) |
| *C. racemosa* var. *imbricata* (d) | 7 | 1 | 10 | 1·40 | 30·0 | 0·129 | Benzie *et al.* (1997) |
| *C. racemosa* var. *laetevirens* (d) | 2–21 | 7 | 9 | 1·30 | 30·1 | 0·122 | Benzie *et al.* (1997) |
| *C. racemosa* var. *racemosa* (d) | 16–20 | 3 | 9 | 1·06 | 7·4 | 0·023 | Benzie *et al.* (1997) |
| *Caulerpa* sp. (d) | 8 | 1 | 12 | 1·30 | 25·0 | 0·091 | Benzie *et al.* (1997) |
| *C. serrulata* (d) | 5–22 | 3 | 14 | 1·10 | 9·5 | 0·036 | Benzie *et al.* (1997) |
| *C. sertularoides* (d) | 21 | 1 | 8 | 1·00 | 0·0 | 0·000 | Benzie *et al.* (1997) |
| *C. taxifolia* (d) | 7–25 | 7 | 11 | 1·30 | 14·3 | 0·067 | Benzie *et al.* (1997) |
| *Codium fragile* (d) | 10–100 | 14 | 14 | 1·36 | 31·0 | 0·150 | Malinowski (1974) |
| *Enteromorpha linza* (d) | 47–479 | 4 | 5 | 1·90 | 100 | 0·180 | Innes & Yarish (1984) |
| Average | | 4·0 | 10·3 | 1·26 | 23·2 | 0·074 | |
| Average (excluding *E. linza*) | | 4·0 | 10·8 | 1·19 | 15·5 | 0·063 | |
| PHAEOPHYCEAE | | | | | | | |
| *Halidrys dioica* (d) | 55–72 | 5 | 5 | 1·83 | 50·0 | 0·193 | Lu & Williams (1994) |
| *Silvetia compressa*[a] (d) | 30–60 | 5 | 7 | 1·14 | 10·0 | 0·014 | Williams & Di Fiori (1996) |
| *Agarum cribrosum* (d) | 20–50 | 3 | 8 | 1·00 | 0·00 | 0·000 | Neefus *et al.* (1993) |
| *Halosiphon tomentosus*[b] (d) | 30 | 2 | 5 | 1·00 | 0·00 | 0·000 | Neefus *et al.* (1993) |
| *Laminaria digitata* (d) | 10–74 | 5 | 11 | 1·00 | 0·00 | 0·000 | Neefus *et al.* (1993) |
| *Laminaria groenlandica* (d) | 60 | 1 | 11 | 1·36 | 36·0 | 0·120 | Neefus *et al.* (1993) |
| *Macrocystis pyrifera* (d) | 50 | 2 | 8 | 1·00 | 0·00 | 0·000 | Neefus *et al.* (1993) |
| Average | | 3·3 | 7·9 | 1·19 | 13·7 | 0·047 | |
| Average (excluding invariate kelps) | | 3·7 | 7·7 | 1·44 | 32·0 | 0·109 | |
| RHODOPHYTA | | | | | | | |
| *Eucheuma isiforme* var. *isiforme* (h, d) | 24–56 | 3 | 11 | 1·36 | 36·4 | – | Cheney & Babbel (1978) |
| *E. isiforme* var. *denudatum*[c] (h, d) | 50–58 | 3 | 11 | 1·31 | 31·3 | – | Cheney & Babbel (1978) |
| *Gelidium arbuscula* (d, h) | 11–49 | 3 | 22 | 1·15 | 13·6 | 0·044 | Sosa & Garcia-Reina (1992) |
| *G. canariensis* (d, h) | 11–50 | 3 | 22 | 1·14 | 13·6 | 0·041 | Sosa & Garcia-Reina (1993) |
| *Gracilaria cervicornis* (h) | 22–63 | 3 | 16 | 1·06 | 5·9 | 0·082 | Sosa *et al.* (1996) |
| *G. chilensis* (d) | Ca 20 | 17 | 14 | – | 2·5 | 0·007 | Intasuwan *et al.* (1993) |
| *Lithothrix aspergillum* (d) | 53–75 | 5 | 16 | 1·38 | 35·0 | 0·131 | Pearson & Murray (1997) |
| *Meristiella gelidium*[d] (h, d) | 12–29 | 2 | 8 | 1·27 | 26·8 | – | Cheney & Babbel (1978) |
| *Palmaria palmata* (d) | 24–31 | 2 | 10 | 1·20 | 10·0 | 0·036 | Lindstrom & South (1989) |
| *Phycodrys rubens* (d) | 2–33 | 18 | 3 | 1·00 | 0·0 | 0·000 | van Oppen *et al.* (1995) |
| *Porphyra abbottae* (h) | 46 | 1 | 15 | 1·00 | 0·0 | 0·000 | Lindstrom (1993*a*) |
| *P. fallax* (h) | 60 | 1 | 16 | 1·06 | 6·3 | 0·032 | Lindstrom (1993*a*) |
| *P. kanakaensis* (h) | 45 | 1 | 18 | 1·06 | 5·6 | 0·029 | Lindstrom (1993*a*) |
| *P. mumfordii* (h) | 30–99 | 2 | 17 | 1·56 | 26·5 | 0·104 | Lindstrom (1993*a*) |
| *P. perforata* (h) | 75 | 1 | 17 | 1·00 | 0·0 | 0·000 | Lindstrom (1993*a*) |
| *P. pseudolanceolata* (h) | 55–104 | 2 | 16 | 1·59 | 25·1 | 0·087 | Lindstrom (1993*a*) |
| *P. pseudolinearis* (h) | 45 | 1 | 11 | 1·54 | 54·5 | 0·068 | Gil-Kodaka & Fujio (1990) |
| *Porphyra* sp. (h) | 60 | 1 | 11 | 1·36 | 27·3 | 0·111 | Gil-Kodaka & Fujio (1990) |
| *P. torta* (h) | 32–105 | 2 | 16 | 1·22 | 6·3 | 0·029 | Lindstrom (1993*a*) |
| *P. yezoensis*[e] (h) | 12–224 | 11 | 8 | 1·50 | 39·8 | 0·152 | Miura *et al.* (1979) |
| *P. yezoensis* (h) | 21–228 | 3 | 12 | 1·64 | 33·3 | 0·127 | Fujio *et al.* (1985) |
| *P. yezoensis* (h) | 78–319 | 1 | 12 | 3·08 | 91·7 | 0·210 | Hara *et al.* (1986) |
| *P. yezoensis* (h) | 23–111 | 11 | 12 | 2·29 | 58·3 | 0·197 | Fujio *et al.* (1987) |
| *P. yezoensis*[f] (h) | 5–125 | 3 | 11 | 1·99 | 78·8 | 0·239 | Gil-Kodaka *et al.* (1988) |
| *P. yezoensis* (h) | 91–105 | 1 | 11 | 1·91 | 63·6 | 0·160 | Gil-Kodaka & Fujio (1990) |
| Average | | 4·0 | 13·4 | 1·44 | 27·7 | 0·086 | |
| Average (excluding *P. yezoensis*) | | 3·7 | 14·2 | 1·24 | 17·2 | 0·050 | |
| AVERAGES | | | | | | | |
| Seaweeds | | 3·9 | 11·7 | 1·35 | 24·2 | 0·076 | This study |
| Seaweeds (excluding *E. linza*, *P. yezoensis* and invariate kelps) | | 3·8 | 12·5 | 1·24 | 18·1 | 0·061 | |
| Bryophytes | | | | 1·43 | 28·4 | 0·098 | Wyatt *et al.* (1989) |
| Pteridophytes | | | | 1·60 | 37·8 | 0·121 | Soltis & Soltis (1989*b*) |
| Higher plants | | | | 2·00 | 54·4 | 0·152 | Frankel *et al.* (1995) |

S, numbers of individuals sampled per population; NP, numbers of populations or subpopulations sampled; NL, numbers of loci; A, average number of alleles per locus; P, average polymorphism; H, average coefficient of gene diversity (expected heterozygosity); – not available; (h), haploid individuals; (d), diploid individuals.

[a] As *Pelvetia fastigiata*.

[b] As *Chorda tomentosa*.

[c] As *Eucheuma nudum*.

[d] As *Eucheuma acanthocladum* and *E. gelidium*.

[e] Cultured populations not included.

© Del documento, los autores. Digitalización realizada por ULPGC. Biblioteca Universitaria, 2009

From 3 to 22 loci have been investigated in seaweed populations (Table 3). In most cases, a low number of loci is a consequence of undetectable enzyme activity and not lack of effort on the part of the researcher. However, conclusions based on few polymorphic loci should be accepted with caution.

Table 3 summarizes several measures of genetic variability for natural populations of 38 macroalgal taxa. Numbers of individuals sampled per population ranged from 2 to 479, with most in the minimally acceptable range of 30–60 for adequate population sampling. The data in Table 3 constitute mean values of all populations.

Table 3 reveals that species of seaweeds differ greatly in their levels and patterns of genetic variation. Some species, such as *Porphyra yezoensis* and *Enteromorpha linza*, seem replete with genetic diversity (however, see caveats below). In contrast, others, including species of *Porphyra* (Lindstrom, 1993*a*) and other red algae such as *Phycodrys rubens* (van Oppen *et al.*, 1995), are genetically depauperate. (Some of these results are a consequence of data for only selected loci being reported; for example, Innes & Yarish (1984) analysed only polymorphic loci in *Enteromorpha linza*.)

Overall, macroalgal species maintain relatively low amounts of electrophoretically detectable genetic variation compared with other plants (Table 3). On average, seaweeds are polymorphic (P) at only about 25% of their loci with an average (A) of 1·39 alleles per locus and a mean expected heterozygosity (H) of 0·074. Since these values are skewed by the high variability reported for *Enteromorpha linza* and *Porphyra yezoensis*, we also calculated averages without these taxa, reducing these values even further (Table 3). Thus, the lowest levels of genetic variation found in any natural populations are those reported for seaweeds.

There is no compelling evidence in Table 3 that isozyme variation is related to phylum. Species in the three phyla (Chlorophyta, Heterokontophyta and Rhodophyta) do not differ significantly in their genetic variation, all phyla showing a similar range and average of genetic variability among their populations (Table 3). However, the scarcity of these kinds of studies means that this conclusion is preliminary.

It is also apparent in Table 3 that species in which the haploid phase is dominant maintain as much genetic variability as species with only a diploid phase or with both haploid and diploid phases. Thus, average genetic variability for haploid individuals is P = 30.0%, A = 1·50 and H = 0·093, and the average for diploid individuals is P = 17·6%, A = 1·22 and H = 0·059 (the values for haploid individuals are skewed by the unusually high levels reported for *Porphyra yezoensis*). Sosa & Garcia-Reina (1992, 1993) described a lower genetic variability for the haploid phase compared with the diploid phase for two *Gelidium* species, but the number of haploid individuals analysed was sufficiently lower than the number of tetrasporophytes to account for the discrepancy (Sosa *et al.*, 1998). The figures given here for the amount of genetic variability in the haploid phase of seaweeds are biased because most of the haploid individuals analysed belong to species of *Porphyra*. The generalization of no difference in diversity in species with different life history patterns requires studies across a broader spectrum of taxa in all seaweed phyla, and interpretation in light of the functionality of haploidy and diploidy in seaweeds (Valero *et al.*, 1992).

Both species-specific attributes (the biological properties of the species) and abiotic ecological factors have a significant influence on the level and distribution of genetic variation in natural populations (Frankel *et al.*, 1995). These factors influence the genetic composition of populations in both a directed and a stochastic fashion through natural selection and random events: in the ways in which new variants arise (mutation) or are sorted into genotypes (recombination), and in the ways in which the gametes are brought together (mating system) or new propagules move to new sites (gene flow/migration). The results of physical factors acting on populations, i.e. genetic differentiation in response to environmental variation, are well established in seaweed ecology. These responses can be recognized in morphological or physiological ecotypes (Russell, 1986). Spatial or temporal organization of genetic variation is another response. Isozyme analysis is especially useful in revealing the latter.

## Natural selection

Very little is known about how natural selection affects genetic variation in seaweed populations. Populations that are subjected to selection are expected to show distinct spatial patterns in relation to the environmental variables producing selection pressure. Some researchers have reported a correlation between isozyme loci in seaweeds and environmental or physiological factors (Miura *et al.*, 1978*a,b*; Okumura & Fujino, 1986; Innes, 1987, 1988; Intasuwan *et al.*, 1993). However, a positive correlation by itself cannot prove causality, and the possibility of different taxa being sampled cannot be ruled out. Williams & Di Fiori (1996) found a highly structured spatial distribution of PGI alleles in *Silvetia compressa* (as *Pelvetia fastigiata*) on three different reefs. It was highly improbable that the observed pattern was due to chance, suggesting that natural selection was maintaining the distribution of alleles, but no specific abiotic factor was implicated. Thus, microgeographic differentiation may play a crucial role in structuring natural populations of seaweeds. As discussed by Linhart & Grant (1996), genetic differentiation over short distances (a few metres) can be as great as that over several to tens of kilometres.

## Genetic drift

In the absence of selection, genetic drift can lead to a loss of genetic variation within populations, exhibited as a loss of heterozygosity and eventual fixation of alleles. The

© Del documento, los autores. Digitalización realizada por ULPGC. Biblioteca Universitaria, 2009

effects of genetic drift arising from bottlenecks have been estimated to result ultimately in a 75% reduction in heterozygosity (Frankel *et al.*, 1995) and a simultaneous reduction in the average number of alleles per locus (Sytsma & Schaal, 1985). Population size is the most important determinant of genetic drift, with small populations being more strongly affected than large ones. The magnitude of random drift can be estimated from the effective size of a population. This is defined as the size of an ideal population whose genetic make-up is affected by random drift to the same degree as is the make-up of the real population under study. A sudden decline in population size can affect the mating process. Fewer individuals are available to participate in mating and, therefore, the next generation will consist of individuals that are more closely related than were individuals in the previous generation. Reduced genetic variability results from such inbreeding.

Neefus *et al.* (1993) suggested that low levels of genetic variation observed among eight species of Laminariales were a reflection of the relatively recent evolution of the group, or due to a bottleneck as populations arose from very small numbers of individuals after the last ice age. Relatively recent colonization following the last glaciation has also been suggested to explain the lack of enzyme diversity in many species of *Porphyra* in British Columbia and adjacent waters (Lindstrom, 1993*a*). The effect of genetic drift following a bottleneck can be so dramatic that genetic variation not only decreases but undergoes a genetic revolution, as exemplified by differentiation of northern European populations of *Phycodrys rubens* into two distinct genetic groups (van Oppen *et al.*, 1995).

Malinowski (1974) found that all *Codium fragile* subsp. *tomentosoides* individuals within a population were genetically identical. Ten of 14 loci analysed were monomorphic at all ten sites in Long Island Sound and southeastern Massachusetts. The remaining four loci showed identical allele frequencies in all individuals (thus accounting for the high heterozygosity detected in this species) (Table 3). The most plausible explanation was that the entire Western Atlantic population was founded by only a few colonizers of identical genotype. An asexual reproductive strategy of these colonizers (Carlton & Scanlon, 1985) coupled with high dispersibility of the flagellated parthenogenetic gametes yielded a clone. Additional samples from Maine, California, British Columbia and England revealed some genotypic diversity, and the pattern of genetic differentiation grouped the California and British Columbia samples together, with the remaining samples forming a second group, suggesting that Europe was the source of introduction of this species to eastern North America (Malinowski, 1974).

## Gene flow

Non-random distribution of genetic variation is often referred to as the genetic structure of a population (Loveless & Hamrick, 1984). In the absence of strong selection, gene flow is the primary determinant of genetic differentiation within and among populations (Futuyma, 1986; Lacy, 1987; Neigel, 1997; Hartl & Clark, 1997). Gene flow is defined as the movement of genes from one location to another, and thus it includes all movements of gametes, propagules and individuals that are effective in changing the spatial distributions of genes (Slatkin, 1985; Neigel, 1997). Gene flow tends to homogenize populations and eliminate local differences. In contrast, the consequence of limited gene flow is to produce structured populations composed of patches of genetically similar individuals. Moreover, if gene flow is sufficiently restricted, even large continuously distributed assemblages of conspecifics may come to consist of many small breeding units, where deviations from random mating among the units will favour genetic divergence. If gene flow is the only factor operating (i.e. if population sizes are so large that genetic drift may be ignored and if the alleles are selectively neutral), all the populations will homogenize to the same allele frequency. However, if population sizes are sufficiently small, homogenization of gene frequencies by gene flow is counteracted by random divergence caused by genetic drift.

The estimation of gene flow from the distribution of genetic markers in populations requires an indirect approach and remains an area of great interest and discussion (Neigel, 1997). We will not attempt to summarize the large literature on this topic but instead refer the reader to reviews by Slatkin (1985, 1987, 1993), Futuyma (1986), Weir (1996), Hartl & Clark (1997) and Neigel (1997). A useful method is Wright's statistic for estimating the standardized variance in allele frequencies among different populations ($F_{ST}$). $F_{ST}$ can be interpreted as an index of genetic differentiation (Hartl & Clark, 1997); ideally, it has a theoretical minimum of 0 (indicating no genetic divergence) and a theoretical maximum of 1 (indicating fixation for alternative alleles in different populations). Wright suggested qualitative guidelines for the interpretation of $F_{ST}$ (Hartl & Clark, 1997). Thus, a range from 0 to 0·05 is considered to indicate little genetic differentiation, and values above of 0·25 to indicate a great deal of genetic differentiation.

Estimates of $F_{ST}$ for natural populations of seaweeds vary widely (Table 4), presumably because $F_{ST}$ is influenced by the size of the populations, by the amount and pattern of migration, and by other factors. However, estimates of $F_{ST}$ values are expected to be similar across loci (if each locus studied is neutral). A high discrepancy between loci can be explained by the occurrence of artefacts, by problems in the interpretation of the loci, or by selection at one of the loci studied. This problem can easily be overcome when many loci are studied. Some species, such as *Caulerpa peltata* (Benzie *et al.*, 1997) and *Halidrys dioica* (Lu & Williams, 1994), exhibit little genetic differentiation (low $F_{ST}$ values), even over very large geographical areas, while other species, such as *Silvetia compressa* (as *Pelvetia fastigiata*) (Williams & Di Fiori, 1996), are highly differentiated (Table 4).

© Del documento, los autores. Digitalización realizada por ULPGC. Biblioteca Universitaria, 2009

**Table 4.** Indices of genetic differentiation ($F_{ST}$ value) and approximated geographic distance (GD) described in natural populations of seaweed

| Species | NP | $F_{ST}$ | GD (km) | Reference |
|---|---|---|---|---|
| *Caulerpa cupressoides* (d) | 2 | 0·912 | 15 | Benzie *et al.* (1997) |
| *Caulerpa peltata* | 1 | 0·000 | 35 | Benzie *et al.* (1997) |
| *C. racemosa* var. *laetevirens* (d) | 5 | 0·266 | – | Benzie *et al.* (1997) |
| *C. racemosa* var. *racemosa* (d) | 2 | 0·886 | 0·3–600 | Benzie *et al.* (1997) |
| *C. serrulata* (d) | 5 | 0·635 | 0·3–600 | Benzie *et al.* (1997) |
| *C. taxifolia* (d) | 7 | 0·418 | 15 | Benzie *et al.* (1997) |
| *Halidrys dioica* (d) | 3 | 0·039 | 1 | Lu & Williams (1994) |
| | | 0·018 | 4 | |
| | | 0·194 | 90 | |
| *Silvetia compressa* (as *Pelvetia fastigiata*) (d) | 2 | 0·005 | 0·003–0·64 | Williams & Di Fiori (1996) |
| | | 0·806 | 80–130 | |
| *Gelidium arbuscula* (d) | 7 | 0·280 | 30–120 | Sosa *et al.* (1998) |
| *G. canariensis* (d) | 5 | 0·130 | 30–120 | Sosa *et al.* (1998) |
| *Gracilaria cervicornis* (h) | 2 | 0·009 | 20 | Sosa *et al.* (1996) |
| | | 0·186 | > 130 | |
| *Lithothrix aspergillum* (d) | 8–11 | 0·004 | 0·03 | Pearson & Murray (1997) |
| | | 0·03 | 5·5 | |
| | | 0·398 | 70 | |
| | | 0·618 | > 750 | |
| *Porphyra yezoensis* (h) | 8 | 0·472 | – | Miura *et al.* (1979) in Fujio *et al.* (1985) |
| *Porphyra yezoensis* (h) | 6 | 0·623 | – | Fujio *et al.* (1985) |
| *Porphyra yezoensis* (h) | 11 | 0·125 | 0·003–0·6 | Fujio *et al.* (1987) |

NP, number of polymorphic loci used to calculate $F_{ST}$; (d), diploid; (h), haploid; –, not available.

Mating systems and dispersal capabilities influence gene flow, and therefore they are excellent predictors of genetic diversity and population structuring. In higher plants, genetic differentiation is far more extensive in selfing and asexual species (with low mobility) than in preferentially outcrossing species (Hamrick, 1989; Linhart & Grant, 1996), and some reviews have focused on correlations between life-history traits and genetic differentiation among populations (Hamrick *et al.*, 1979, 1991; Hamrick & Godt, 1997). Although it is still premature to conclude that life-history characteristics are good predictors of genetic variation in natural populations of seaweeds (Lu & Williams, 1994), available isozyme data suggest a correlation between genetic variation or differentiation in populations or species and the reproductive strategy of the species. For example, Pearson & Murray (1997) found a clear relationship between genetic differentiation and geographic distance in Californian populations of *Lithothrix aspergillum*. The $F_{ST}$ values were very low ($F_{ST}$ = 0·004 and 0·030) over a spatial scale of 30 m and 5·5 km, but these values increased to 0·583–0·683 for populations separated by more than 700 km, which agrees well with the limited long-distance dispersal of the species (Pearson & Murray, 1997; Table 4). Lu & Williams (1994) analysed five loci of *Halidrys dioica* from five localities in southern California. This species is dioecious, perennial, and has buoyant reproductive fronds that confer on it the capacity for high gene flow between populations, especially over short distances. Lu & Williams found very high genetic variation within populations, and moderate population differentiation ($F_{ST}$ = 0·194) over considerable geographic distances (90 km; Table 4). Conversely, Benzie *et al.* (1997) found a strong spatial differentiation (highly significant $F_{ST}$ values) for populations of *Caulerpa* spp. from Australia (Table 4). These values suggest that gene flow among populations of *Caulerpa* spp. is low, although most of the *Caulerpa* species are thought to be outcrossing. Most analysed populations approached conditions of random mating. Thus, the bulk of the populations were outbreeding, but geographical isolation led to differences in gene frequencies between sites (Benzie *et al.*, 1997). Such high $F_{ST}$ values for conspecific populations warrant caution: these could be due to the low number of polymorphic loci analysed.

In *Porphyra*, Hwang *et al.* (1998) and Lindstrom (1993*b*, unpublished; Table 5) observed significantly higher average expected heterozygosity among species that are dioecious or sectored compared with species with the sexes intermixed on the thallus. Significantly higher average heterozygosity was also the case for species with a narrower geographic range and species occurring higher in the intertidal. There were no significant differences between levels of population differentiation based on season of appearance or persistence of the thalli.

Most seaweed species reproduce asexually during at least part of their life cycle. Reduced genetic diversity is an expected consequence of this type of reproduction. Asexual reproduction causes many individuals within a population to be genetically identical (van Oppen *et al.*, 1995). From the viewpoint of the population dynamics of genes, asexual reproduction transmits the whole set of genes of an individual to its offspring. Since recombination of genes is absent, alleles at different loci are fixed, and the genotypes in the populations do not change. Therefore,

© Del documento, los autores. Digitalización realizada por ULPGC. Biblioteca Universitaria, 2009

**Table 5.** Comparison of mean levels of population differentiation in species of *Porphyra* with different ecological, phenological and other attributes

| Attribute | Mean heterozygosity | Per cent polymorphic loci | Species |
|---|---|---|---|
| *Geographic range* | * | NS | |
| 1000–3500 km | 0·077 ± 0·041 | 0·272 ± 0·202 | Pe(2), Pf, Pk, Pm(2) |
| 5000–8500 km | 0·018 ± 0·021 | 0·078 ± 0·094 | Pa, Pp, Pt(2) |
| *Habitat* | * | * | |
| High intertidal | 0·072 ± 0·039 | 0·270 ± 0·176 | Pe(2), Pf, Pm(2), Pt(2) |
| Mid-intertidal | 0·010 ± 0·017 | 0·019 ± 0·032 | Pa, Pk, Pp |
| *Season* | NS | NS | |
| Winter | 0·063 ± 0·045 | 0·236 ± 0·189 | Pe(2), Pf, Pm(2), Pp, Pt(2) |
| Spring (and summer) | 0·015 ± 0·021 | 0·028 ± 0·040 | Pa, Pk |
| *Mating system* | ** | ** | |
| Sexes mixed | 0·022 ± 0·017 | 0·072 ± 0·073 | Pa, Pf, Pk, Pp, Pt(2) |
| Sexes separate | 0·101 ± 0·024 | 0·378 ± 0·151 | Pe(2), Pm(2) |
| *Persistence* | NS | NS | |
| ≤ Four months | 0·073 ± 0·066 | 0·274 ± 0·296 | Pa, Pf, Pm(2) |
| ≥ Five months | 0·045 ± 0·036 | 0·160 ± 0·140 | Pe(2), Pk, Pp, Pt(2) |

Data from Lindstrom (1993*a*, *b*). Significant differences were determined using the Tukey HSD test.
*$0·01 < p < 0·05$; **$0·001 < p < 0·005$; NS, not significant.
Species abbreviations: Pa, *P. abbottae*; Pe, *P. pseudolanceolata*; Pf, *P. fallax*; Pk, *P. kanakaensis*; Pm, *P. mumfordii*; Pp, *P. perforata*; Pt, *P. torta*. (2) indicates that data from two different populations were used.

effective population size is probably small for many algal species although the number of individuals may be large, and genetic drift is more efficient.

## Reproductive strategy

Asexual reproduction may explain the lack of genetic variation in some species. Cheney & Babbel (1978) observed that most new individuals in Florida populations of *Eucheuma* were found in proximity to parent plants, which implied limited dispersal. Vegetative reproduction in these populations probably accounted for the observed heterozygote deficiency. Innes & Yarish (1984) observed only 13 out of a possible 5400 multi-locus phenotypes in more than 1000 individuals of *Enteromorpha linza* from Long Island Sound and suggested that this was due to asexual reproduction. Genetic variation in New Zealand *Gracilaria chilensis* was also very low (Intasuwan *et al.*, 1993; Table 3), with most alleles in a population being fixed. Asexual reproduction by vegetative fragmentation, which occurs in this species, could account for such low genetic variation. Similarly, Sosa *et al.* (1996) concluded that asexual reproduction was the most important factor responsible for low genetic variation in three Canary Island populations of *Gracilaria cervicornis*, although a low effective population size could not be discarded as an explanation; fertile tetrasporophytes were not detected in two of the three populations over several years, supporting the notion that these populations are clonal.

As discussed by Hunter (1993), locally adapted clones may propagate asexually and become dominant through competitive advantage in stable habitats, thereby minimizing the availability of unoccupied substratum and limiting opportunity for recruitment of new genotypes. Populations such as these are expected to be almost wholly structured by the processes of clonal replication. Genetic drift is more efficient in a species characterized by asexual reproduction and a reduced population size (Sosa *et al.*, 1998), and therefore species with vegetative reproduction are expected to exhibit a higher level of differentiation among populations. Thus, Pearson & Murray (1997) observed high genetic differentiation between southern and northern California populations of *Lithothrix aspergillum*. The southern populations reproduced sexually and exhibited relatively high genetic diversity for red algae. The northern population, isolated from a previously continuous population (bottleneck event) or introduced through a founder event, persisted by vegetative propagation, perennation and asexual bispore reproduction and showed no genetic diversity.

There are exceptions to the generalization that asexual reproduction is correlated with low levels of within-population genetic diversity and high levels of population differentiation. If an asexual species is characterized by a high migration rate, however, gene flow could compensate for the genetic drift, and a higher level of genetic diversity would occur. Other exceptions have been reported. *Porphyra mumfordii*, which is monoecious but sectored and probably selfed at least some of the time, is as polymorphic as *P. pseudolanceolata* and *P. pseudolinearis*, which are dioecious obligate outcrossers (Lindstrom & Cole, 1992*c*; Lindstrom, 1993*a*). *Porphyra yezoensis*, which is also monoecious and reportedly largely selfed (Shin & Miura, 1990), has one of the highest levels of genetic variation described in seaweeds (Table 3; Hwang *et al.*, 1998). Genetic variation in *P. yezoensis* may indeed be as high as

© Del documento, los autores. Digitalización realizada por ULPGC. Biblioteca Universitaria, 2009

studies indicate. Japan and Korea were not glaciated during the Pleistocene and have rather steep environmental gradients, particularly of temperature. These ecological fluctuations may have provided conditions conducive to the development of high levels of polymorphism without accompanying speciation. However, such high genetic diversity led Lindstrom (1993*a*) to question whether Japanese researchers had confused morphologically similar but genetically distinct species. Reported morphological and phenological differences (Miura *et al.*, 1978*b*) and linkages of seven polymorphic enzymes (Fujio *et al.*, 1987) provide evidence for cryptic species rather than genetic differentiation within a single species. Not surprisingly, cultured populations of *Porphyra yezoensis* showed little genetic differentiation (Miura *et al.*, 1979; Gil-Kodaka *et al.*, 1988).

The relationship between reproductive strategy and genetic variation can also be analysed by determining deviation of the genotype from Hardy-Weinberg equilibrium or by F-statistics (Weir & Cockerham, 1984; Weir, 1996; Hartl & Clark, 1997). In a strictly sexually reproducing species, the distribution of genotype frequencies at a locus should approximate Hardy-Weinberg proportions (Hartl & Clark, 1997). In contrast, a population of asexually reproducing individuals is expected to show large deviations from Hardy-Weinberg equilibrium, non-random association among loci and reduced genotypic diversity compared with a population of sexually reproducing individuals. Deviations from this equilibrium have been shown in several species of seaweeds with primarily asexual reproduction. Innes & Yarish (1984) thought that asexual reproduction was responsible for a non-random association of genotypes and a significant deviation from Hardy-Weinberg equilibrium for five loci in *Enteromorpha linza*. Similar observations have been made in *Eucheuma nudum* (= *E. isiforme* var. *denudatum*) and *E. isiforme* (Cheney & Babbel, 1978), *Gelidium arbuscula* (Sosa & Garcia-Reina, 1992; Sosa *et al.*, 1998), *Caulerpa taxifolia* (Benzie *et al.*, 1997) and *Lithothrix aspergillum* (Pearson & Murray, 1997). In contrast, most loci analysed in the obligate outcrosser *Halidrys dioica* (Lu & Williams, 1994) and several outcrossing *Caulerpa* species (Benzie *et al.*, 1997) exhibited Hardy-Weinberg equilibrium.

Assumptions required for Hardy-Weinberg equilibrium are rarely met in most seaweed populations (Pearson & Murray, 1997), because of non-random mating and asexual reproduction, without regard to natural selection. Moreover, deviations of gene frequencies from Hardy-Weinberg equilibrium can result from the Wahlund effect, i.e. two genetically different populations being sampled and pooled (Hartl & Clark, 1997). This latter problem can be avoided by using a hierarchical and stratified sampling strategy to determine more accurately spatial-scale factors influencing within-population structure and to discriminate between heterozygote deficiencies due to breeding behaviour of a species (e.g. inbreeding) and deficits due to the Wahlund effect (Goudet *et al.*, 1994). Since most authors have not used an appropriate sampling strategy for discriminating among causes of the observed population structure, conclusions about Hardy-Weinberg equilibrium should be accepted with caution (Benzie *et al.*, 1997; Sosa *et al.*, 1998).

## Use of isozymes in systematics

Isozymes are particularly useful as taxonomic characters because they are relatively easily observed, provide reliable data, and have the power to discriminate among taxa. They provide a valuable source of data because of the direct connection between the enzymes, as revealed in zymograms, and the genome. However, like other forms of systematic data, isozyme characters are also subject to certain limitations. Not all data will be useful for all taxa: enzymes useful for one group of species may be useless for another. For maximum value, comparisons need to be made between closely related taxa, where perceived similarities are most likely due to homology and not to convergence.

Mallery & Richardson (1972) were the first to apply protein electrophoresis to look for relationships among seaweeds. They compared zymograms for three multisubstrate enzymes (acid phosphatase, esterase and aminopeptidase) for 11 genera across the Rhodophyta. Although the resulting complex banding patterns could not be interpreted genetically, the authors nonetheless opened the door to the application of isozymes as a systematic tool for macroalgae.

As in population studies, allelic frequencies provide the basis for comparisons among species in systematic approaches. A number of coefficients have been developed that summarize these frequencies into indices that measure the degree of identity or the converse, distance, between pairs of populations or species. The three most commonly used indices are Nei's genetic identity (Nei, 1972), the distance measure of Rogers (Rogers, 1972) and Hedrick's genotypic identity (Hedrick, 1971). All indices equal 1 when pairs of populations or species share the same alleles in exactly the same proportions, i.e. the distance between populations or species is zero when they are identical. Likewise, all identities equal zero when the populations or species being compared share no alleles. All indices utilize data from all loci, not just the polymorphic loci. Both Nei's and Roger's coefficients are skewed by within-taxon heterozygosity, and a correction has been proposed (Hillis, 1984). Innes (1987) has suggested that Hedrick's identity provides a better measure of similarity than coefficients based on allelic frequencies for populations not in Hardy-Weinberg equilibrium, as is often the case for asexually reproducing seaweeds. This is so because two populations with the same allelic frequencies may have different genotype frequencies. Although there is merit to this idea, the lack of genetic interpretation of the banding patterns limits the usefulness of Hedrick's measure, and its values cannot be compared between life-cycle stages with different ploidy levels. Hedrick's identity has been used by

© Del documento, los autores. Digitalización realizada por ULPGC. Biblioteca Universitaria, 2009

**Table 6.** Mean genetic identities (I) and distances (D, in parentheses) (Nei, 1972) among conspecific populations of seaweeds

| Species | I (D) | I Range | Reference |
|---|---|---|---|
| CHLOROPHYTA | | | |
| *Caulerpa cupressoides* | 1·000 (0·000) | – | Benzie *et al.* (1997)* |
| *C. racemosa* var. *laetevirens* | 0·913 (0·091) | 0·808–1·000 | Benzie *et al.* (1997)* |
| *Caulerpa racemosa* var. *racemosa* | 0·897 (0·109) | 0·845–1·000 | Benzie *et al.* (1997)* |
| *Caulerpa serrulata* | 1·000 (0·000) | – | Benzie *et al.* (1997)* |
| *Caulerpa taxifolia* | 0·873 (0·136) | 0·795–0·958 | Benzie *et al.* (1997)* |
| *Codium fragile* | 0·927 (0·076) | 0·623–1·000 | Malinowski (1974) |
| *Enteromorpha linza* | 0·908 (0·097) | 0·695–0·999 | Innes & Yarish (1984)* |
| PHAEOPHYCEAE | | | |
| *Halidrys dioica* | 0·924 (0·079) | 0·823–0·999 | Lu & Williams (1994)* |
| *Laminaria saccharina*[a] | 0·998 (0·002) | – | Neefus *et al.* (1993)* |
| *Silvetia compressa*[b] | 0·944 (0·058) | 0·863–0·999 | Williams & Di Fiori (1996)* |
| RHODOPHYTA | | | |
| *Eucheuma isiforme* var. *isiforme* | 0·996 (0·004) | 0·993–0·998 | Cheney & Babbel (1978) |
| *E. isiforme* var. *denudatum*[c] | 0·895 (0·111) | 0·830–0·952 | Cheney & Babbel (1978) |
| *Gelidium arbuscula* | 0·983 (0·017) | 0·954–0·991 | Sosa & Garcia-Reina (1992) |
| *Gelidium canariensis* | 0·972 (0·028) | 0·960–0·997 | Sosa & Garcia-Reina (1993) |
| *Gracilaria cervicornis* | 0·991 (0·009) | 0·985–0·999 | Sosa *et al.* (1996) |
| *Gracilaria chilensis* | – | 0·650–1·000 | Intasuwan *et al.* (1993) |
| *Lithothrix aspergillum* | 0·820 (0·198) | 0·714–0·999 | Pearson & Murray (1997) |
| *Meristiella gelidium*[d] | 0·857 (0·154) | – | Cheney & Babbel (1978) |
| *Palmaria palmata* | 0·886 (0·121) | – | Lindstrom & South (1989) |
| *Porphyra abbottae* | – | 0·933–1·000 | Lindstrom & Cole (1992*c*) |
| *Porphyra smithii* | – | 0·938–1·000 | Lindstrom (1993*b*) |
| *Porphyra yezoensis* | 0·898 (0·107) | 0·667–1·000 | Miura *et al.* (1979) |
| *Porphyra yezoensis* | 0·919 (0·084) | 0·785–0·998 | Fujio *et al.* (1987)* |
| Average | 0·936 (0·066) | 0·836–0·993 | |
| Self-fertilizing plants | 0·975 (0·025) | | Gottlieb (1981) |
| Outcrosser plants | 0·956 (0·045) | | Gottlieb (1981) |
| Bryophytes | 0·900 (0·105) | | Wyatt *et al.* (1989) |
| Pteridophytes | 0·911 (0·093) | | Soltis & Soltis (1989*b*) |

Values are from original authors, or were calculated from allelic frequencies provided by authors (*).

[a] As *Laminaria longicruris* and *L. saccharina*.

[b] As *Pelvetia fastigiata*.

[c] As *Eucheuma nudum*.

[d] As *Eucheuma gelidium* and *E. acanthocladum*.

Cheney & Babbel (1978), Cheney & Mathieson (1979) and Blair *et al.* (1982).

Table 6 presents mean genetic identities and distances using Nei's measure for conspecific populations of seaweeds. These identity values are generally high and are comparable to those reported for higher plants. Overall, values average above 0·90, and are similar in all three algal phyla. Instances where values dipped just below this level may represent cases of incipient speciation. For example, the two populations of *Palmaria palmata* sampled by Lindstrom & South (1989), with an identity of 0·886, came from opposite sides of the North Atlantic; van der Meer (1987) reported abnormal meiosis in crosses between *P. palmata* populations from the eastern and western Atlantic, suggesting that speciation is in progress for these disjunct populations. Not included in the table are the data of Blair *et al.* (1982) for *Chaetomorpha* spp.; they obtained phenotypic identities of 0·84 and 0·87 between two pairs of species that have since been considered conspecific. Also not included are the recently published data for Korean species of *Porphyra* for which Hwang *et al.* (1998) observed phenotypic identities between populations of the same species to range from 0·529 to 0·998. Values below 0·80 may represent comparisons of cryptic species rather than populations of a single species. For example, the low values observed by Malinowski (1974) in *Codium fragile* were between northeast Pacific and northwest Atlantic populations, which are currently recognized to represent different subspecies if not species (Carlton & Scanlon, 1985; Goff *et al.*, 1992). Similar, low values among populations of *Enteromorpha linza*, *Gracilaria chilensis* and *Porphyra yezoensis* suggest that more than one species may have been involved in those studies.

These examples highlight one of the strengths of isozyme electrophoresis: its ability to call into question specific or even generic identification of taxa based on levels of similarity of their genotypes. Lindstrom & Cole (1990*a*) used isozymes to confirm the distinctness of a suite of species that had earlier been included in *Porphyra perforata*; based on distinct zymograms as well as other characters, they identified and described one additional species that previously had not been segregated from the complex (Lindstrom & Cole, 1990*b*). Among specimens that had been included earlier in *P. lanceolata* or *P.*

© Del documento, los autores. Digitalización realizada por ULPGC. Biblioteca Universitaria, 2009

**Table 7.** Mean genetic identities (I) and distances (D) (Nei, 1972) among congeneric species of seaweeds

| Species | I (D) | Reference |
|---|---|---|
| CHLOROPHYTA | | |
| *Caulerpa cupressoides–C. racemosa* var. *imbricata* | 0·600 (0·511) | Benzie *et al.* (1997)* |
| *Caulerpa cupressoides–Caulerpa* sp. | 0·800 (0·223) | Benzie *et al.* (1997)* |
| *Caulerpa cupressoides–Caulerpa serrulata* | 0·600 (0·511) | Benzie *et al.* (1997)* |
| *Caulerpa cupressoides–C. sertularioides* | 0·800 (0·223) | Benzie *et al.* (1997)* |
| *Caulerpa racemosa* var. *imbricata–C. racemosa* var. *laetevirens* | 0·383 (0·958) | Benzie *et al.* (1997)* |
| *Caulerpa racemosa* var. *imbricata–Caulerpa* sp. | 0·600 (0·511) | Benzie *et al.* (1997)* |
| *Caulerpa racemosa* var. *imbricata–C. serrulata* | 0·400 (0·916) | Benzie *et al.* (1997)* |
| *Caulerpa racemosa* var. *imbricata–C. sertularioides* | 0·600 (0·511) | Benzie *et al.* (1997)* |
| *Caulerpa racemosa* var. *imbricata–C. taxifolia* | 0·402 (0·911) | Benzie *et al.* (1997)* |
| *Caulerpa racemosa* var. *laetevirens–Caulerpa* sp. | 0·398 (0·921) | Benzie *et al.* (1997)* |
| *Caulerpa racemosa* var. *laetevirens–C. serrulata* | 0·563 (0·574) | Benzie *et al.* (1997)* |
| *Caulerpa racemosa* var. *laetevirens–C. taxifolia* | 0·441 (0·819) | Benzie *et al.* (1997)* |
| *Caulerpa* sp.–*C. serrulata* | 0·782 (0·246) | Benzie *et al.* (1997)* |
| *Caulerpa* sp.–*C. sertularioides* | 0·982 (0·018) | Benzie *et al.* (1997)* |
| *Caulerpa serrulata–C. sertularioides* | 0·800 (0·223) | Benzie *et al.* (1997)* |
| PHAEOPHYCEAE | | |
| *Laminaria digitata–L. 'groenlandica'* | 0·399 (0·919) | Neefus *et al.* (1993)* |
| *Laminaria digitata–L. longicruris* | 0·562 (0·576) | Neefus *et al.* (1993)* |
| *Laminaria digitata–L. saccharina* | 0·600 (0·511) | Neefus *et al.* (1993)* |
| *Laminaria 'groenlandica'–L. longicruris* | 0·500 (0·693) | Neefus *et al.* (1993)* |
| *Laminaria 'groenlandica'–L. saccharina* | 0·500 (0·693) | Neefus *et al.* (1993)* |
| RHODOPHYTA | | |
| *Gelidium arbuscula–G. canariensis* | 0·848 (0·165) | Sosa *et al.* (1998) |
| *Palmaria hecatensis–P. callophylloides* | 0·400 (0·916) | Lindstrom & South (1989) |
| *Palmaria mollis–P. callophylloides* | 0·391 (0·938) | Lindstrom & South (1989) |
| *Porphyra abbottae–P. torta* | 0.469 (0·757) | Lindstrom & Cole (1993) |
| *Porphyra amplissima–P. cuneiformis* | 0·692 (0·368) | Lindstrom & Cole (1993) |
| *Porphyra brumalis–P. kurogii* | 0·467 (0·761) | Lindstrom & Cole (1993) |
| *Porphyra fallax–P. fallax* subsp. *comonyae* | 0·745 (0·294) | Lindstrom & Cole (1993) |
| *Porphyra kurogii–P. linearis* | 0·599 (0·512) | Lindstrom & Cole (1993) |
| *Porphyra kurogii–P. pseudolinearis* | 0·531 (0·633) | Lindstrom & Cole (1993)' |
| *Porphyra kurogii–P. 'purpurea'* | 0·600 (0·511) | Lindstrom & Cole (1993) |
| *Porphyra 'leucosticta'–P. fucicola* | 0·436 (0·830) | Lindstrom & Cole (1993) |
| *Porphyra linearis–P. pseudolinearis* | 0·433 (0·837) | Lindstrom & Cole (1993) |
| *Porphyra linearis–P. 'purpurea'* | 0·439 (0·823) | Lindstrom & Cole (1993) |
| *Porphyra miniata–P. variegata* | 0·385 (0·955) | Lindstrom & Cole (1993) |
| *Porphyra pseudolinearis–P. 'purpurea'* | 0·600 (0·511) | Lindstrom & Cole (1993) |
| *Porphyra 'umbilicalis'–P. 'umbilicalis'* | 0·457 (0·783) | Lindstrom & Cole (1993) |
| *Porphyra yezoensis–Porphyra* sp. | 0·886 (0·121) | Gil-Kodaka & Fujio (1990) |
| *Porphyra yezoensis–P. pseudolinearis* | 0·377 (0·974) | Gil-Kodaka & Fujio (1990) |
| *Porphyra* sp.–*P. pseudolinearis* | 0·408 (0·896) | Gil-Kodaka & Fujio (1990) |

Values are from original authors, or are calculated from allelic frequencies provided by authors (*).

*pseudolanceolata*. Lindstrom & Cole (1992*b*) recognized three new species using isozymes in addition to morphological, ecological and chromosome characters. Van Oppen *et al.* (1995) interpreted fixed allelic differences at three of four loci as indicating specific differences between samples all originally identified as *Phycodrys rubens*. A low level of similarity ($I_p$ = 0·372) between pairs of *Eucheuma* spp. (Cheney & Babbel, 1978) provided part of the evidence for including one of the pairs of species in a new genus of Solieriaceae, *Meristiella* (Gabrielson & Cheney, 1987).

The converse is also true: isozymes appear especially well suited to recognizing conspecific and closely related species. Lindstrom & Cole (1990*a*) used lack of differences in zymograms to synonymize the asexual *Porphyra sanjuanensis* with the sexual *P. perforata*. Later, they used isozymes, morphology and chromosomes to identify pairs of disjunct sibling species of *Porphyra* occurring in the northeast Pacific and northwest Atlantic (Lindstrom & Cole, 1992*a*). Nei's identities for these species pairs ranged from 0·385 to 0·692 (Table 7). Subsequently, they reported three additional pairs of sibling species, two of which were restricted to the northeast Pacific: two of the three pairs had identities of 0·457 and 0·469, whereas the third, recognized at the rank of subspecies, had an identity of 0·745 (Lindstrom & Cole, 1993). In contrast to animals and higher plants, macroalgal sibling species tend to display fixation for different alleles rather than different allelic frequencies. These alleles can be considered diagnostic for identifying the species. Allelic fixation has been observed in species of *Palmaria* (Lindstrom & South, 1989), *Porphyra* (Lindstrom & Cole, 1992*a*, 1993), *Gracilaria* (Intasuwan *et*

© Del documento, los autores. Digitalización realizada por ULPGC. Biblioteca Universitaria, 2009

*al.*, 1993) and *Phycodrys* (van Oppen *et al.*, 1995) in the Rhodophyta, for species of *Ulva* (Doi *et al.*, 1993) and *Caulerpa* (Benzie *et al.*, 1997) in the Chlorophyta, and for species of *Laminaria* (Neefus *et al.*, 1993) in the Phaeophyta.

Nei's genetic identities for species pairs for which genetic identity or allelic frequency data have been published are given in Table 7. Since, as a rule of thumb, if $D_N > 1{\cdot}0$ ($I_N < 0{\cdot}37$), divergence has probably exceeded the resolution of the technique because of the masking effect of parallel or back mutations (Nei, 1987), we have included only pairs with identities exceeding 0·37. This cut-off value may in fact have some meaning in seaweeds: all of Lindstrom & Cole's (1992*a*, 1993) sibling species had values exceeding this level; Cheney & Babbel's (1978) species that were eventually segregated into different genera had an identity at just this level.

Isozymes can serve as the first approach to identifying species in morphologically difficult genera. Brostoff & Gordon (1997) examined allozyme variation in *Porphyra* specimens from 27 sites around the coast of New Zealand and concluded that more species existed than were previously reported. Their study was too preliminary to delimit taxa clearly, however. Their results are especially cautionary for population biologists, who need to remain open to the possibility that variation in isozymes in the seaweeds they are studying may be a reflection of interspecific rather than intraspecific differences. This is particularly important for genera or species with few distinctive morphological features. Moreover, generalities that have emerged from studies of isozymes in other groups of organisms may not be appropriate for seaweeds. For example, seaweeds have a relatively large number of enzymes that are coded at only one locus observable with current techniques (Table 1), and monomorphism is common in populations and species of seaweeds whereas polymorphism is low relative to other groups of organisms (Table 3).

As with measures of population parameters, one must keep in mind the sensitivity of genetic identities and distances to the numbers and kinds of loci on which the indices are based: the more individuals per population or species and the more single substrate enzymes sampled, the stronger the data. Difficulties with techniques or interpretations that hampered earlier studies (Richardson & Mallery, 1973; Kemp *et al.*, 1980; Küppers & Weidner, 1980; Marsden *et al.*, 1981, 1984*a*,*b*; Matlock & Romeo, 1981; Mohammad & Shaalan, 1985, 1991; Shaalan & Mohammad, 1985, 1986; Penniman, 1987; Rice & Crowden, 1987; Shaalan, 1991, 1992) are being overcome, and we expect future studies utilizing isozyme electrophoresis to provide insight into important population and evolutionary processes in seaweeds. Understanding patterns of genetic variability and population structure within a species using molecular markers is of fundamental importance to studies of ecology and evolution, and isozyme (including allozyme) loci provide one of the most useful genetic markers for obtaining these data.

## References


Abo, K., Ecoshi, K. & Noda, H. (1996). Isozyme from conchocelis and leafy thalli of *Porphyra* species. *Fish. Sci.*, **62**: 367–371.

Benzie, J.A.H., Price, I.R. & Ballment, E. (1997). Population genetics and taxonomy of *Caulerpa* (Chlorophyta) from the Great Barrier Reef, Australia. *J. Phycol.*, **33**: 491–504.

Blair, S., Mathieson, A.C. & Cheney, D.P. (1982). Morphological and electrophoretic investigations of selected species of *Chaetomorpha* (Chlorophyta, Cladophorales). *Phycologia*, **21**: 164–172.

Brostoff, W.N. & Gordon, M.E. (1997). Allozyme variation in New Zealand *Porphyra* (Rhodophyta). *N.Z.J. Bot.*, **35**: 203–220.

Carlton, J.T. & Scanlon, J.A. (1985). Progression and dispersal of an introduced alga: *Codium fragile* ssp. *tomentosoides* (Chlorophyta) on the Atlantic Coast of North America. *Bot. Mar.*, **28**: 155–165.

Cheney, D.P. (1985). Electrophoresis. In *Handbook of Phycological Methods. Ecological Field Methods: Macroalgae* (Littler, M.N. & Littler, D.S., editors) 87–119. Cambridge University Press, Cambridge.

Cheney, D.P. & Babbel, G.R. (1978). Biosystematic studies of the red algal genus *Eucheuma*. I. Electrophoretic variation among Florida populations. *Mar. Biol.*, **47**: 251–264.

Cheney, D.P. & Mathieson, A.C. (1979). Population differentiation in the seaweed *Chondrus crispus*: preliminary results. *Isozyme Bull.*, **12**: 5[illegible]

De Wreede, R.E. & Klinger, T. (1988). Reproductive strategies in algae. In *Plant Reproductive Ecology* (Doust, J.L. & Doust, L.L., editors), 267–284. Oxford University Press, New York.

Doi, K., Kamiya, M., Hara, Y. & Chihara, M. (1993). Taxonomic studies on *Ulva pertusa* (Ulvophyceae). II. Preliminary isozyme analysis. *Jpn. J. Phycol.*, **41**: 199–206.

Frankel, O.H., Brown, A.H.D. & Burdon, J.J. (1995). *The Conservation of Plant Biodiversity*. Cambridge University Press, Cambridge.

Fujio, Y., Kodaka, P.L.G. & Hara, M. (1985). Genetic differentiation and amount of genetic variability in natural populations of the haploid laver *Porphyra yezoensis*. *Jpn. J. Genet.*, **60**: 347–354.

Fujio, Y., Tanaka, M.Y., Hara, M. & Akiyama, K. (1987). Enzyme polymorphism and population structure of the haploid laver *Porphyra yezoensis*. *Nippon Suisan Gakkaishi*, **53**: 357–362.

Fujio, Y., Kodaka, P.L.G., Hara, M. & Akiyama, K. (1988). Electrophoretic variants characteristic of heterozygotes in haploid laver *Porphyra* sp. *Nippon Suisan Gakkaishi*, **54**: 969–974.

Futuyma, D.J. (1986). *Evolutionary Biology*. Sinauer Associates, Sunderland, MA.

Gabrielson, P.W. & Cheney, D.P. (1987). Morphology and taxonomy of *Meristiella* gen. nov. (Solieriaceae, Rhodophyta). *J. Phycol.*, **23**: 481–493.

Gil-Kodaka, P.L. & Fujio, Y. (1990). Genetic similarity and distance among 3 species of *Porphyra*. *Fish. Genet. Breeding Sci.*, **15**: 31–34.

Gil-Kodaka, P.L., Hara, M., Akiyama, K. & Fujio, Y. (1988). Genetic differences between natural and cultured populations of *Porphyra yezoensis*. *Tohoku J. Agric. Res.*, **38**: 27–34.

Goff, L.J., Liddle, L., Silva, P.C., Voytek, M. & Coleman, A.W. (1992). Tracing species invasions in *Codium*, a siphonous green alga, using molecular tools. *Am. J. Bot.*, **79**: 1279–1285.

Gottlieb, L.D. (1977). Electrophoretic evidence and plant systematics. *Ann. Mo. Bot. Gdn.*, **64**: 161–180.

Gottlieb, L.D. (1981). Electrophoretic evidence and plant populations. *Prog. Phytochem.*, **7**: 1–46.

Goudet, J., De Meüs, T., Day, A.J. & Guinon, C. (1994). The different levels of population structuring of dogwhelks, *Nucella lapillus*, along the south Devon coast. In *Genetics and Evolution of Aquatic Organisms* (Beaumont, A., editor), 81–95. Chapman & Hall, London.

Hamrick, J.L. (1989). Isozymes are the analysis of genetic structure in plant populations. In *Isozymes in Plant Biology* (Soltis, D.E., Soltis, P.S., editors) 87–105. Dioscorides Press, Portland, OR.

Hamrick, J.L., Linhart, Y.B. & Mitton, B. (1979). Relationships between life history characteristics and electrophoretically detectable genetic variation in plants. *Annu. Rev. Ecol. Syst.*, **10**: 173–200.

Hamrick, J.L., Godt, M.J.W., Murawski, D.A. & Loveless, M.D. (1991). Correlations between species traits and allozyme diversity: implications for conservation biology. In *Genetics and Conservation of Rare Plants* (Falk, D.A., Holsinger, K.E., editors) 75–86. Oxford University Press, Oxford.

Hamrick, J.L. & Godt, M.J.W. (1997). Effects of life history traits on genetic diversity in plant species. In *Plant Life Histories: Ecology, Phylogeny and*


© Del documento, los autores. Digitalización realizada por ULPGC. Biblioteca Universitaria, 2009

*Evolution* (Silverstown, J., Franco, M. & Harper, J.L., editors), 102–118. The Royal Society/Cambridge University Press, London/Cambridge.

Hara, M., Tanaka, M.Y. & Fujio, Y. (1986). Linkage of an additional isozyme genes in *Porphyra yezoensis*. *Fish Genet. Breeding Sci.*, **11**: 25–28. (In Japanese.)

Hartl, D.L. & Clark, A.G. (1997). *Principles of Population Genetics*, 3rd edition. Sinauer Associates, Sunderland, MA.

Hedrick, P.W. (1971). A new approach to measuring genetic similarity. *Evolution*, **25**: 276–280.

Hillis, D.M. (1984). Misuse and modification of Nei's genetic distance. *Syst. Zool.*, **33**: 238–240.

Hunter, C.L. (1993). Genotypic variation and clonal structure in coral populations with different disturbance histories. *Evolution*, **47**: 1213–1228

Hunter, R.L. & Markert, C.L. (1957). Histochemical demonstration of enzymes separated by zone electrophoresis in starch gels. *Science*, **125** 1294–1295

Hwang, M.S., Han, M. & Lee, I.K. (1998). Allozyme variation and species relationships in the genus *Porphyra* (Bangiales, Rhodophyta) from Korea. *Algae*, **13**: 447–459.

Innes, D.J. (1984). Genetic differentiation among populations of marine algae. *Helgoländer Meeresunters.*, **38**: 401–417.

Innes, D.J. (1987) Genetic structure of asexually reproducing *Enteromorpha linza* (Ulvales: Chlorophyta) in Long Island Sound. *Mar. Biol.*, **94** 459–467.

Innes, D.J. (1988). Genetic differentiation in the intertidal zone in populations of the alga *Enteromorpha linza* (Ulvales: Chlorophyta). *Mar. Biol.*, **97**: 9–16.

Innes, D.J. & Yarish, C. (1984). Genetic evidence for the occurrence of asexual reproduction in populations of *Enteromorpha linza* (Chlorophyta) from Long Island Sound. *Phycologia*, **23**: 311–320.

Intasuwan, S., Gordon, M.E., Daugherty, C.H. & Lindsay, G.C. (1993). Assessment of allozyme variation among New Zealand populations of *Gracilaria chilensis* (Gracilariales, Rhodophyta) using starch gel electrophoresis. *Hydrobiologia*, **260/261** (*Proc. Int. Seaweed Symp.*, **14**): 159–165.

Kemp, L., Riabowol, R. & Druehl, L. (1980). Isoenzyme variation in *Macrocystis integrifolia* Bory. *J. Phycol.*, **16** (Suppl.): 23.

Kephart, S.R. (1990). Starch gel electrophoresis of plant isozymes: a comparative analysis of techniques. *Am. J. Bot.*, **77**: 693–712.

Kiang, Y.T. & Gorman, M.B. (1983). Soybean. In *Isozymes in Plant Genetics and Breeding*, part B (Tanksley, S. & Orton, T.J., editors). 295–328. Elsevier, Amsterdam.

Küppers, U. & Weidner, M. (1980). Seasonal variation of enzyme activities in *Laminaria hyperborea*. *Planta*, **148**: 222–230.

Lacy, R.C. (1987) Loss of genetic diversity from managed populations. Interacting effects of drift, mutation, immigration, selection, and population subdivision. *Conserv. Biol.*, **1**: 143–158.

Lindstrom, S.C. (1993*a*). Intraspecific and interspecific genetic variation in species of *Porphyra* (Rhodophyta, Bangiales) from British Columbia and adjacent waters. *J. Appl. Phycol.*, **5**: 53–62.

Lindstrom, S.C. (1993*b*). Intra- and interpopulation genetic variation in species of *Porphyra* (Rhodophyta: Bangiales) from British Columbia and adjacent areas. In *Program & Abstracts, Western Society of Naturalists, 73rd Annual Meeting*. Newport, Oregon, 7–10 Jan. 1993

Lindstrom, S.C. & Cole, K.M. (1990*a*). An evaluation of species relationships in the *Porphyra perforata* complex (Bangiales, Rhodophyta) using starch gel electrophoresis. *Hydrobiologia*, **204/205** (*Proc. Int. Seaweed Symp.*, **13**): 179–183.

Lindstrom, S.C. & Cole, K.M. (1990*b*). *Porphyra tuilax*, a new species of Rhodophyta from British Columbia and northern Washington. *Jpn. J. Phycol.*, **38**: 371–376.

Lindstrom, S.C. & Cole, K.M. (1992*a*). Relationships between some North Atlantic and North Pacific species of *Porphyra* (Bangiales, Rhodophyta): evidence from isozymes, morphology, and chromosomes. *Can. J. Bot.*, **70** 1355–1363

Lindstrom, S.C. & Cole, K.M. (1992*b*). The *Porphyra lanceolata*-*P. pseudolanceolata* (Bangiales, Rhodophyta) complex unmasked: recognition of new species based on isozymes, morphology, chromosomes and distributions. *Phycologia*, **31**: 431–448.

Lindstrom, S.C. & Cole, K.M. (1992*c*). A revision of the species of *Porphyra* (Rhodophyta: Bangiales) occurring in British Columbia and adjacent waters. *Can. J. Bot.*, **70**: 2066–2075.

Lindstrom, S.C. & Cole, K.M. (1993). The systematics of *Porphyra*: character evolution in closely related species. *Hydrobiologia*, **260/261** (*Proc. Int. Seaweed Symp.*, **14**): 151–157.

Lindstrom, S.C. & South, G.R. (1989). Evidence of species relationships in the Palmariaceae (Palmariales, Rhodophyta) based on starch gel electrophoresis. *Crypt. Bot.*, **1**: 32–41.

Linhart, Y.B. & Grant, M.C. (1996). Evolutionary significance of local genetic differentiation in plants. *Annu. Rev. Ecol. Syst.*, **27**: 237–277.

Loveless, M.D. & Hamrick, J.L. (1984). Ecological determinants of genetic structure in plant populations. *Annu. Rev. Ecol. Syst.*, **15**: 65–95.

Lu, T.T. & Williams, S.L. (1994). Genetic diversity and genetic structure in the brown alga *Halidrys dioica* (Fucales: Cystoseiraceae) in Southern California. *Mar. Biol.*, **121**: 363–371.

Malinowski, K. (1974). '*Codium fragile*': the ecology and population biology of a colonizing species. PhD dissertation, Yale University, New Haven, CN.

Mallery, C. & Richardson, N. (1972). Disc gel electrophoresis of proteins of Rhodophyta. In *Proceedings of the Seventh International Seaweed Symposium* (Nishizawa, K., editor), 292–300. University of Tokyo Press, Japan.

Markert, C.L. & Möller, F. (1959). Multiple forms of enzymes: tissue, ontogenetic and species specific patterns. *Proc. Natl. Acad. Sci. USA*, **45**: 753–763.

Marsden, W.J.N., Callow, J.A. & Evans, L.V. (1981). A novel and comprehensive approach to the extraction of enzymes from brown algae and their separation by polyacrylamide gel electrophoresis. *Mar. Biol. Lett.*, **2**: 353–362.

Marsden, W.J.N., Callow, J.A. & Evans, L.V. (1984*a*). A preliminary investigation of the electrophoretic characteristics of enzymes from a range of macroscopic brown algae. *Bot. Mar.*, **27**: 521–526.

Marsden, W.J.N., Evans, L.V., Callow, J.A. & Keen, J.N. (1984*b*). A preliminary electrophoretic comparison of *Fucus serratus* and *Fucus vesiculosus*. *Bot. Mar.*, **27**: 79–83.

Matlock, D.B. & Rombo, C. (1981). Interspecific variability within the genus *Gracilaria* (Rhodophyta) on Guam. *Proc. 4th Int. Coral Reef Symp.*, **2**: 415–417.

May, B. (1992). Starch gel electrophoresis of allozymes. In *Molecular Genetic Analysis of Populations: a Practical Approach* (Hoelzel, A.R., editor), 1–28. IRL Press, Boca Raton, FL.

Miura, W., Fujio, Y. & Suto, S. (1978*a*). Isozymes from individual thallus of *Porphyra* species. *Jpn. J. Phycol.*, **26**: 139–143. (In Japanese.)

Miura, W., Fujio, Y. & Suto, S. (1978*b*). Polymorphism of catalase isozyme in *Porphyra*. *Tohoku J. Agric. Res.*, **29**: 159–166.

Miura, W., Fujio, Y. & Suto, S. (1979). Genetic differentiation between the wild and cultured populations of *Porphyra yezoensis*. *Tohoku J. Agric. Res.*, **30**: 114–125.

Mohammad, Y.A. & Shaalan, S.H. (1985). Electrophoretic studies of isoenzymes in some Rhodophycean marine algae from Alexandria. *Bull. Fac. Sci., Alex. Univ.*, **25**: 10–22.

Mohammad, Y.A. & Shaalan, S.H. (1991). Classical and biochemical taxonomy of some *Sargassum* species from the seashore of Alexandria, Egypt. *Bull. Fac. Sci., Alex. Univ.*, **31**: 118–141.

Murphy, R.W., Sites, J.W. Jr, Buth, D.G. & Haufler, C.H. (1990). Proteins: isozyme electrophoresis. In *Molecular Systematics*, 2nd edition (Hillis, D.M., Moritz, C. & Mable, B.K., editors), 51–120. Sinauer Associates, Sunderland, MA.

Neefus, C.D., Allen, B.P., Baldwin, H.P., Mathieson, A.C., Eckert, R.T., Yarish, C. & Miller, M.A. (1993). An examination of the population genetics of *Laminaria* and other brown algae in the Laminariales using starch gel electrophoresis. *Hydrobiologia*, **260/261** (*Proc. Int. Seaweed Symp.*, **14**): 67–79.

Nei, M. (1972). Genetic distance between populations. *Am. Nat.*, **106** 283–292.

Nei, M. (1987). *Molecular Evolutionary Genetics*. Columbia University Press, New York.

Neigel, J.E. (1997). A comparison of alternative strategies for estimating gene flow from genetic markers. *Annu. Rev. Ecol. Syst.*, **28** 105–128.

Oelshlegel, F.J. & Stahman, M.A. (1973). The electrophoretic technique: a practical guide for its application. *Bull. Torr. Bot. Club*, **100** 260–271.

© Del documento, los autores. Digitalización realizada por ULPGC. Biblioteca Universitaria, 2009

Okumura, S. & Fujino, K. (1986). Thermostability of variations of enzymes in sea algae. *Bull. Jpn. Soc. Sci. Fish.*, **52**: 37–40.

Pearson, E.A. & Murray, S.N. (1997). Patterns of reproduction, genetic diversity and genetic differentiation in California populations of the geniculate coralline alga *Lithothrix aspergillum* (Rhodophyta). *J. Phycol.*, **33**: 753–763.

Penniman, C.A. (1987). Application of isozyme electrophoresis to systematic and genetic studies of marine macroalgae. *J. Phycol.*, **23** (suppl.): 12.

Rice, E.L. & Crowden, R.K. (1987). An improved method for the extraction and electrophoresis of proteins and active enzymes from fucalean macroalgae (Phaeophyta). *Phycologia*, **26**: 235–246.

Richardson, N. & Mallery, C.H. (1973). Some chemosystematic aspects of the *Audouinella* (*Acrochaetium*-*Rhodochorton*) complex. *Am. J. Bot.*, **60**: 1051–1056.

Rogers, J.S. (1972). Measures of genetic similarity and genetic distance. In *Studies in Genetics VII*. 145–153. University of Texas, Austin, TX.

Russell, G. (1986). Variation and natural selection in marine macroalgae. *Oceanogr. Mar. Biol. Annu. Rev.*, **24**: 309–377.

Shaalan, S.H. (1991). A collective taxonomic study of Eusiphonidae (Chlorophycophyta) from the Mediterranean seashore of Alexandria, Egypt. *Bull. Fac. Sci., Alex. Univ.*, **31**: 194–217.

Shaalan, S.H. (1992). Taxonomic studies of some Bryopsidophycean marine algae from the Mediterranean seashore of Alexandria: a cumulative approach. *Algol. Stud.*, **67**: 45–67.

Shaalan, S.H. & Mohammad, Y.A. (1985). Chemotaxonomy of some marine algae belonging to family Ulvaceae from Alexandria sea shore. *J. Fac. Mar. Sci.*, **4**: 183–191.

Shaalan, S.H. & Mohammad, Y.A. (1986). Biochemical taxonomy of some *Codium* species from Alexandria sea shore. *J. Univ. Kuwait Sci.*, **13**: 101–108.

Shin, J.A. & Miura, A. (1990). Estimation of the degree of self-fertilisation in *Porphyra yezoensis* (Bangiales, Rhodophyta). *Hydrobiologia*, **204/205** (*Proc. Int. Seaweed Symp.*, **13**): 397–400.

Slatkin, M. (1985). Gene flow in natural populations. *Annu. Rev. Ecol. Syst.*, **16**: 393–430.

Slatkin, M. (1987). Gene flow and the geographic structure of natural populations. *Science*, **236**: 787–792.

Slatkin, M. (1993). Isolation by distance in equilibrium and non-equilibrium populations. *Evolution*, **47**: 264–279.

Soltis, D.E. & Soltis, P.S. (Editors) (1989a). *Isozymes in Plant Population Biology*. Dioscorides Press, Portland, OR.

Soltis, D.E. & Soltis, P.S. (1989b). Ploidy, breeding systems, and genetic differentiation in homosporous pteridophytes. In *Isozymes in Plant Population Biology* (Soltis, D.E. & Soltis, P.S., editors). 241–258. Dioscorides Press, Portland, OR.

Sosa, P.A. & Garcia-Reina, G. (1991a). Isozymes in seaweeds. In *Seaweed Cellular Biotechnology. Physiology and Intensive Cultivation* (Garcia Reina, G. & Pedersén, M., editors). 257–264. COST-48, University of Las Palmas de Gran Canaria, Las Palmas.

Sosa, P.A. & Garcia-Reina, G. (1991b). Suggestion for analysing isoenzymes in agarophytes by starch electrophoresis. In *Seaweed Cellular Biotechnology. Physiology and Intensive Cultivation* (Garcia Reina, G. & Pedersén, M., editors). 309–312. COST-48, University of Las Palmas de Gran Canaria, Las Palmas.

Sosa, P.A. & Garcia-Reina, G. (1992). Genetic variability and differentiation of sporophytes and gametophytes in populations of *Gelidium arbuscula* (Gelidaceae: Rhodophyta) determined by isozyme electrophoresis. *Mar. Biol.*, **113**: 679–688.

Sosa, P.A. & Garcia-Reina, G. (1993). Genetic variability of *Gelidium canariensis* determined by isozyme electrophoresis. *J. Phycol.*, **29**: 118–124.

Sosa, P.A., Cabrera-Pérez, M.A. & Garcia-Reina, G. (1996). Genetic variation of *Gracilaria cervicornis* (Rhodophyta) gametophytes from the Canary Islands. *Eur. J. Phycol.*, **31**: 143–147.

Sosa, P.A., Valero, M., Batista, F. & Gonzalez-Perez, M.A. (1998). Genetic structure of natural populations of *Gelidium* species: a re-evaluation of results. *J. Appl. Phycol.*, **10**: 279–284.

Sytsma, K. & Schaal, B. (1985). Genetic variation, differentiation, and evolution in a species complex of tropical shrubs based on isozymic data. *Evolution*, **39**: 582–593.

Tanksley, S.D. & Orton, T.J. (1983). *Isozymes in Plant Genetics and Breeding*, parts A and B. Elsevier, Amsterdam.

Valero, M., Richerd, S., Perrot, V. & Destombe, C. (1992). Evolution of alternation of haploid and diploid phases in life cycles. *Trends Ecol. Evol.*, **7**: 25–29.

van der Meer, J.P. (1986). Genetic contributions to research on seaweeds. *Prog. Phycol. Res.*, **4**: 1–35.

van der Meer, J.P. (1987). Experimental hybridization of *Palmaria palmata* (Rhodophyta) from the northeast and northwest Atlantic Ocean. *Can. J. Bot.*, **65**: 1451–1458.

van Oppen, M.J.H., Olsen, J.L. & Stam, W.T. (1995). Genetic variation within and among North Atlantic and Baltic populations of the benthic alga *Phycodrys rubens* (Rhodophyta). *Eur. J. Phycol.*, **30**: 251–260.

Weeden, N. & Wendel, J. (1989). Genetics of plant isozymes. In *Isozymes in Plant Biology* (Soltis, D. & Soltis, P., editors). 46–72. Dioscorides Press, Portland, OR.

Weir, B.S. (1990). Genetic Data Analysis II. Methods for Discrete Population Genetic Data. Sinauer Associates, Sunderland, MA.

Weir, B.S. & Cockerham, C.C. (1984). Estimating the *F*-statistics for the analysis of population structure. *Evolution*, **38**: 1358–1370.

Wendel, J. & Weeden, N.F. (1989). Visualization and interpretation of plant isozymes. In *Isozymes in Plant Biology* (Soltis, D. & Soltis, P., editors). 5–43. Dioscorides Press, Portland, OR.

Williams, S.L. & Di Fiori, R.E. (1996). Genetic diversity and structure in *Pelvetia fastigiata* (Phaeophyta: Fucales): does a small effective neighborhood size explain fine-scale genetic structure? *Mar. Biol.*, **126**: 371–382.

Wyatt, R., Stoneburner, A. & Odrzykoski, I.O. (1989). Bryophyte isozymes: systematic and evolutionary implications. In *Isozymes in Plant Biology*. (Soltis, D.E. & Soltis, P.S., editors). 221–240. Dioscorides Press, Portland, OR.

© Del documento, los autores. Digitalización realizada por ULPGC. Biblioteca Universitaria, 2009

ELSEVIER

Journal of Volcanology and Geothermal Research 94 (1999) 305–321

Journal of volcanology and geothermal research

www.elsevier.com/locate/jvolgeores

# Fluid flow from pore pressure measurements off La Palma, Canary Islands

Roger Urgeles [a,*], Miquel Canals [a,1], John Roberts [b,2], SNV "Las Palmas" Shipboard Party [3]

[a] GRC Geociències Marines, Dept. d'Estratigrafia i Paleontologia, Facultat de Geologia, Universitat de Barcelona, Campus de Pedralbes, E-08071 Barcelona, Spain

[b] GEOTEK, Unit 3 Faraday Close, Drayton Fields, Daventry, Northamptonshire, NN11 5RD, UK

Received 10 May 1999

**Abstract**

In situ subseafloor pore pressure results from the western flank of the island of La Palma, Canary Islands, are presented. The data, obtained with a Pop Up Pore Pressure Instrument (PUPPI), provide constraints on the fluid circulation and its causes in a very special context: The sediment piles near an intraplate oceanic island built on the continental rise of the Northwest African Margin. The ambient pore pressures estimated from 2- to 4-days-long records are negative in almost all cases with values, at depths of a few meters below sea floor, usually on the order of −10 to −70 Pa. Excess pore pressures develop only in the distalmost areas. The permeabilities and compressibilities, obtained respectively from the decay of the insertion pressures and the amplitude of the tidally induced pore pressure variations, range between $2.5 \times 10^{-18}$ and $6.6 \times 10^{-16}$ m$^2$, and $6.2 \times 10^{-9}$ and $1.5 \times 10^{-7}$ Pa$^{-1}$. According to these permeabilities fluid flow is estimated to be mostly downward and usually on the range between 0 and −0.3 mm yr$^{-1}$. However, from the excess pore pressure profile a complex pattern of fluid circulation is inferred where horizontal fluid motion cannot be neglected. Horizontal flow is probably controlled by significant contrasts in the permeability of the different layers. The prevailing downward fluid flow is abnormal for a classical passive margin. We thus interpret these results as the superposition to the loss of fluids by sediment compaction (on the continental rise), of a large-scale flow system stimulated by thermal buoyancy (100 km wide) related to the volcanic activity on the island of La Palma. © 1999 Elsevier Science B.V. All rights reserved.

*Keywords:* pore pressure; piezometer; hydrothermal processes; Canary Islands

## 1. Introduction

In recent years, in situ pore pressure measurements have been made in a wide variety of environments, such as ridge crests (Davis et al., 1991) and ridge flanks (Davis et al., 1986, 1991; Langseth et al., 1992; Fang et al., 1993), but also on river deltas (Hirst and Richards, 1976; Benett et al., 1982),

* Corresponding author. Tel.: +34-3-4021375; fax: +34-3-4021340; e-mail: roger@beagle.geo.ub.es

[1] Tel.: +34-3-4021360; fax: +34-3-4021340; e-mail: miquel@natura.geo.ub.es.

[2] Tel.: +44-1327-311666; fax: +44-1327-311555; e-mail: roberts@geotek.co.uk.

[3] SNV "Las Palmas" Shipboard Party: Belén Alonso, Ignacio Alonso, Jesús Baraza and Peter Schultheiss.

0377-0273/99/$ - see front matter © 1999 Elsevier Science B.V. All rights reserved.
PII: S0377-0273(99)00109-2

© Del documento, los autores. Digitalización realizada por ULPGC. Biblioteca Universitaria, 2009

coastal areas (Benett et al., 1996), deep lakes (Harvey et al., 1998) and abyssal plains (Schultheiss and Noel, 1987). These measurements have been mainly carried out to study hydrothermal circulation in the oceanic crust (e.g., Davis et al., 1991) or to estimate in situ geotechnical properties of marine sediments (e.g., Benett et al., 1982). Little is known, however, of the role of pore pressure and fluid flow on deep-sea sediment accumulations adjacent to hot spot oceanic islands. In the Hawaiian chain, for instance, significant rates of hydrothermal fluid flow have been hypothesised (Garven and McNutt, 1995) to explain the apparent lack of a heat-flow anomaly over the Hawaiian flexural moat (Von Herzen et al., 1989).

A special situation exists where intraplate oceanic islands develop over or near a passive margin, as in the region of the Canary Islands — NW African Margin. The sediment piles that accumulate on the continental margin can be thick enough to heat organic constituents and produce oil and gas. Fluid flow would, in principle, occur upwards as a result of positive buoyancy of these products and by compaction of the thick layers of sediment (Working Group 3, 1987). It should also be expected that the load associated with massive volcanoes, as is the case in the study area, would further compact the sediments and promote dewatering and upward fluid flow.

The pore pressure is also an important soil parameter that can only be measured in situ (Baligh, 1986; Schultheiss, 1990a), and which has a fundamental effect on the stability of sediments (Bea et al., 1975; Benett et al., 1982; Schultheiss, 1990a). Over-pressured sediments will have lower shear strength and will therefore be less stable as the effective stress is thereby reduced.

In November–December, 1995 and May–June, 1996, two cruises were carried out on board the *RRS*

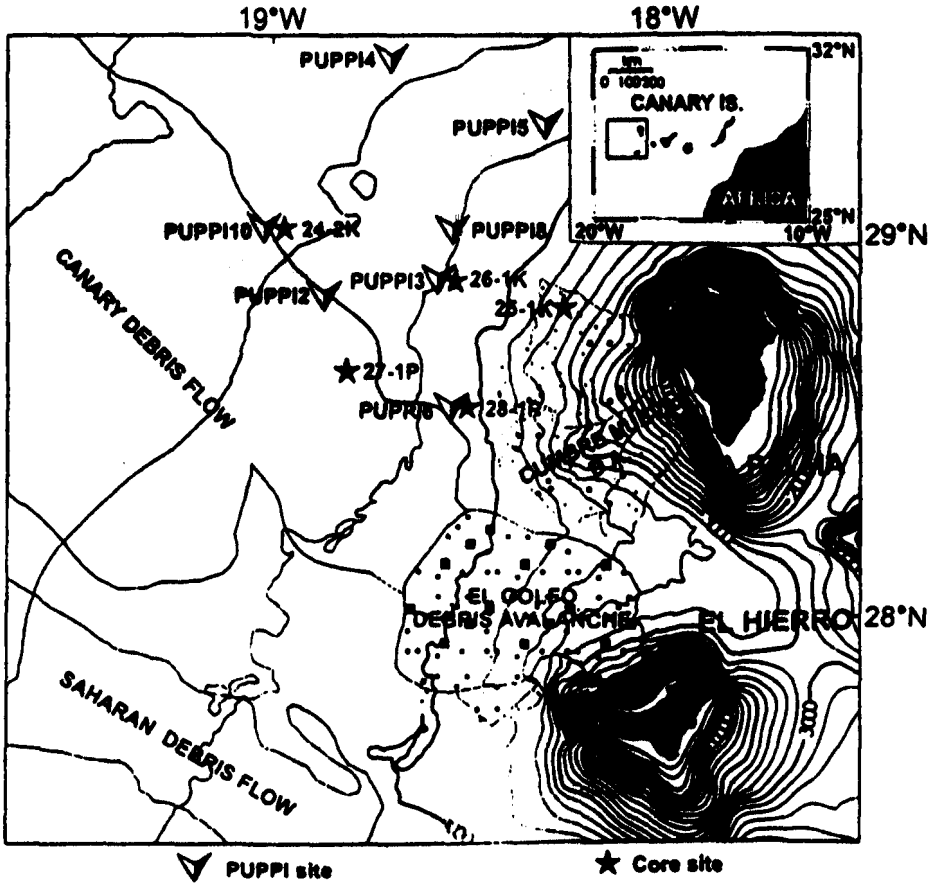


Fig. 1. Bathymetry of the study area and schematic facies mapping (modified from Masson, 1996 and Urgeles et al., 1997, 1999) with the location of the PUPPI deployments, and cores discussed in Roberts and Camp (1996). Contour interval is 200 m.

© Del documento, los autores. Digitalización realizada por ULPGC. Biblioteca Universitaria, 2009

Table 1
PUPPI deployment data summary

| Station number | Latitude (N) | Longitude (W) | Water depth (m) | Nearby core | Sediment field |
|---|---|---|---|---|---|
| PUPPI 2 | 28°50′ | 18°51.9′ | 4350 | | Undisturbed sediment on the north-eastern edge of the CDF |
| PUPPI 3 | 28°52.075′ | 18°32.142′ | 4110 | CD56-26 | Downslope side of sediment wave |
| PUPPI 4 | 29°25.647′ | 18°42.02′ | 4400 | | Downslope end of a sediment wave |
| PUPPI 5 | 29°14.958′ | 18°18.471′ | 4125 | | Sediment wave |
| PUPPI 6 | 28°33.1′ | 18°31.3′ | 4075 | CD56-28 | Undisturbed sediment on the eastern edge of the CDF |
| PUPPI 10 | 28°59.92′ | 19°00.02′ | 4410 | CD56-24 | Undisturbed sediment on the north-eastern edge of the CDF |

*Discovery* and the *SNV Las Palmas*. During these cruises 11 Pop Up Pore Pressure Instruments (PUPPI) were deployed on the western reaches of La Palma between 4000 and 4500 m water depth. Six of the PUPPIs provided useful high-resolution records of the in situ pore pressure of sediment north of a large debris flow known as the Canary Debris Flow (Fig. 1, Table 1).

The objective of this study is to quantify the fluid flow through the seafloor sediments west of La Palma to better understand the hydrodynamic fluid circulation near ocean islands. Hydrothermal flow may induce abnormal pore water pressures in the flanks of the islands that may enhance, in turn, volcanic landslides. This process may be relevant on the island of La Palma, where the southern volcanic ridge is thought to be at the early stage of giant landslide initiation (Bonelli Rubio, 1950; Carracedo, 1994). It is also proposed that estimates of "in situ" properties from the piezometer data, such as pore water pressure and shear strength, will also allow to assess the role of these properties in sediment stability west of the island.

## 2. Geological setting

The Canary Islands form an ~500-km-long volcanic lineament of oceanic islands seaward of the Northwest African Margin. The islands are built over the continental slope and rise and hold a large history of volcanic activity expanding, at least, from the Middle Miocene to present day (Hoernle and Schmincke, 1993). Seismic reflection studies west of the islands of La Palma and El Hierro suggest that the top of the oceanic basement is buried beneath 1–2 km of sediment (Ranero et al., 1995), with the lower values close to the islands (Urgeles et al., 1998). These studies suggest that there exists a depth-to-basement anomaly that is estimated to be about 500 m after correction for sediment loading (Ranero et al., 1995). In addition, gravity modelling indicates a lithospheric thinning in the vicinities of El Hierro and La Palma that has been interpreted as a sign of reheating of the old Mesozoic lithosphere beneath the Canary Basin (Ranero et al., 1995). The data of Urgeles et al. (1998) suggest that the sediments in the area where the PUPPIs were deployed are mainly made of silty volcaniclastic turbidites with interbedded hemipelagites.

The Canary Islands have been reported to suffer from large lateral collapses that affect both the subaerial and submarine slopes of the islands (Holcomb and Searle, 1991; Ancochea et al., 1994; Watts and Masson, 1995; Masson, 1996; Teide Group, 1997; Urgeles et al., 1997, 1999). These lateral collapses generate large debris avalanches that deposit on the lower slopes of the islands, thereby loading the hemipelagic sediments and triggering, in turn, huge debris flows and turbidity currents (Masson, 1996; Roberts and Cramp, 1996; Masson et al., 1998).

West of the islands of La Palma and El Hierro several studies have been carried out to characterise the sedimentary processes and resulting deposits (Kidd et al., 1985; Simm et al., 1991; Masson et al., 1992, 1998; Masson, 1996; Urgeles et al., 1997). These include using a variety of mapping techniques such as deep-towed high-resolution side-scan sonar

© Del documento, los autores. Digitalización realizada por ULPGC. Biblioteca Universitaria, 2009

(TOBI), swath bathymetry and high- and ultrahigh-resolution seismic reflection profiling. These data have been validated by coring at different sites and geotechnical studies have been carried out on core samples to assess slope stability west of El Hierro and La Palma (Roberts and Cramp, 1996).

The most striking feature shown by those studies is the Canary Debris Flow (Masson et al., 1992), which develops immediately west and downslope of debris avalanche lobes in the western flanks of both islands (Masson, 1996; Urgeles et al., 1999) (Fig. 1). The single debris avalanche resulting from the collapse of the northern flank of the island of El Hierro and the Canary Debris Flow are two closely related events dated at about 15 ka (Masson, 1996) and have been estimated to account for a total volume of 580 km$^3$ (Masson et al., 1992; Urgeles et al., 1997).

## 3. Methods

### 3.1. Pore pressure measurements

The Pop Up Pore Pressure Instrument (PUPPI) (Fig. 2), originally developed at the Institute of Oceanographic Sciences (Schultheiss and McPhail, 1986; Schultheiss and Noel, 1987), is designed and constructed to make accurate in situ measurements of the vertical pore pressure gradient in the seafloor. The PUPPI measures differential pore pressures at ports on a lance, with a resolution of about 5 Pa. It is a free-fall instrument that can be ballasted with lead or steel weights to penetrate a range of sediment types in water depths of up to 6000 m. The length of lance that can be used depends on the sediment stiffness. Typically, a 4-m lance can be used successfully in soft hemipelagic sediments, although 6-m-long lances have also been used with success in deep-sea pelagic muds. During our cruises we used two types of PUPPI lances with ports at 2, 3 and 4 mbsf and 1.5, 2.25 and 3 mbsf, respectively (Fig. 2). The probes were left on the sea floor for a period ranging from 50 to 90 h until insertion pressures were dissipated (Fig. 3).

Pore pressures are measured relative to hydrostatic at the porous ports on the lance using specially designed differential pressure transducers connected

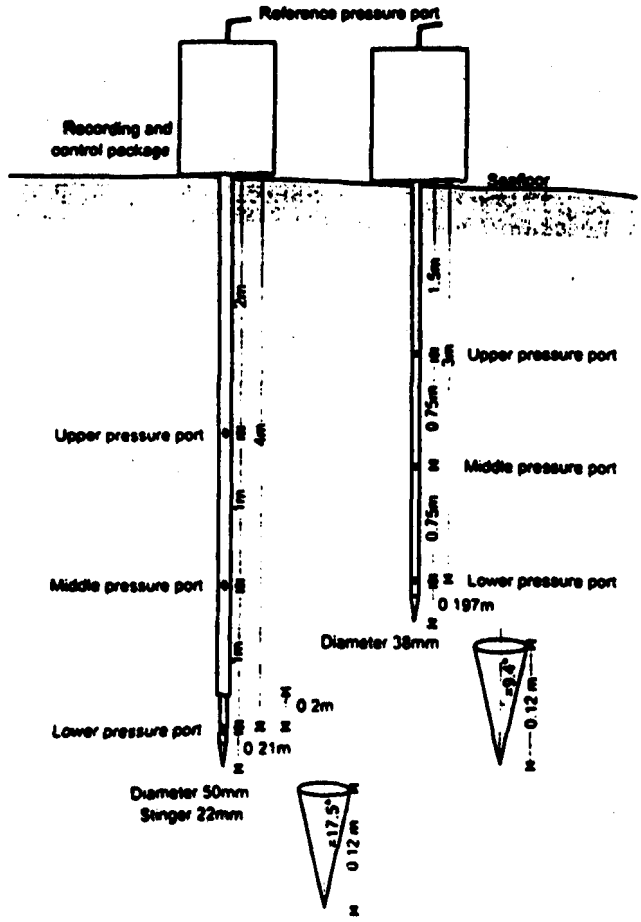


Fig. 2. Technical characteristics and dimensions of the PUPPI apparatus.

to the pressure ports and the open sea water. A microprocessor-based data logger is used to record the data. Sampling rates are preprogrammed being normally rapid during the early part of the deployment (insertion and initial decay) but need only to be slow during the later stages when pressures are only changing slowly.

Whilst it is possible to calibrate the transducers for temperature and absolute pressure with a reasonable degree of accuracy, they cannot be calibrated for mechanical creep effects. These may be significant as the transducers are cycled through important changes in absolute pressure. Consequently, during our cruise a new motorised valve was used, which can be programmed to operate at any time during the measurement period. The valve closes and isolates the pressure ports on the lance whilst opening the differential pressure transducers to seawater. In this

© Del documento, los autores. Digitalización realizada por ULPGC. Biblioteca Universitaria, 2009

way reference zero pressures can be obtained at any time during the deployment and hence any drift monitored by regular zero measurements. Likewise, the valve can be used to enable a single pressure transducer to monitor more than one pressure port. Accordingly, one of the two transducers was set to sporadically monitor the third middle port.

Just prior to recovery an acoustic command is normally sent to the instrument to activate the pre-release pipe cutter. This opens both sides of each differential pressure transducer to the open seawater, hence providing an in situ zero pressure calibration just before recovery. Recovery is accomplished using an acoustic command, which activates a release mechanism severing the disposable from recoverable parts; the lance and ballast weight assembly is left on the seafloor while the buoyant instrument package ascends to the surface for recovery (Fig. 2). In addition to the acoustic command for release, the instrument also houses a back-up release timer that can be set to release the instrument at any required time.

### 3.2. Analysis of the data

In addition to the ambient pore pressure ($u_e$), the pore pressure transients produced by the penetration of the PUPPI probe and by tidally induced pressure variations on the seafloor also provide information of hydrogeological and geotechnical interest. The maximum insertion pressure ($u_{max}$) is indicative of the shear strength ($S_u$), whilst modelling of the decay curve and tidally induced signals can provide estimates of the permeability ($K$) and confined frame compressibility ($m_v$) of the sediments (Schultheiss, 1990b; Fang et al., 1993; Wang and Davis, 1996; Wang et al., 1998).

At low penetration rates a spherical pore pressure distribution develops in the vicinity of the tip, whereas along the shaft the distribution tends to be more radial. At higher penetration rates this spherical distribution around the tip becomes more oblate or radial in nature and similar to that generated along the shaft (Elsworth, 1991). Therefore, estimates of the value of $K$ can be obtained by modelling in two dimensions the expansion of a cylindrical cavity for undrained distributions of pore pressures at both, the upper and lower ports. Benett et al. (1985) used the solutions of Soderberg (1962) and Randolph et al. (1979) to predict the permeability from the time taken for 50% of $u_{max}$ to dissipate ($t_{50}$):

$$K = \mu m_v r_0^2 \tau_{50} / t_{50} \quad (1)$$

in which $\mu$ is the viscosity of seawater ($1.656 \times 10^{-3}$ Pa s), $m_v$ is the sediment confined frame compressibility as obtained from Eq. (2) (see below), $r_0$ is the radius of the probe, $t_{50}$ is the time for pore pressure to fall to 50% of its initial value, and $\tau_{50}$ is the $t_{50}$ related dimensionless time factor. Several studies (Benett et al., 1985; Schultheiss and Noel, 1987; Schultheiss, 1990b; Davis et al., 1991) assumed the value of $\tau_{50}$ to be unity based, but more recently Fang et al. (1993) indicated that this could cause the value of $K$ to be in error by 1 order of magnitude. Fang (1995) shows that more suitable values for $\tau_{50}$ are 3.93 at the ports on the probe shaft and 4.65 at the lower port. The middle port is only seldom monitored and can not provide values of $t_{50}$. It is to be noted that this analysis provides property estimates in the horizontal dimension, while physical properties measured in the laboratory are generally derived from vertical samples. However, in clay-rich sediments anisotropic conditions may exist. In sediments with a random soil fabric (as might be expected for deep marine mud) nearly isotropic conditions generally exist (Benett et al., 1982). This must be accounted for when expressions involve both types of parameters. Eq. (1) also assumes that insertion of the probe does not change the permeability of the sediment, and that the sediment–probe interface does not act as a channel with permeability higher than that of the sediments (Fang, 1995).

In addition, to the insertion pressure, small oscillations of the pore pressure induced by ocean tides can be observed on the PUPPI records (Fig. 3). Ocean tides generate oscillations of water pressure at the sea bottom. Deformation of the sediment as well as fluid flow is simultaneously induced in response to the tidal pressure variations since the sediment behaves as a porous medium. Fang et al. (1993) gave simplified formulae allowing to estimate the confined frame compressibility ($m_v$) from the amplitude of the tidally induced pore pressure variations ($u_t$).

© Del documento, los autores. Digitalización realizada por ULPGC. Biblioteca Universitaria, 2009

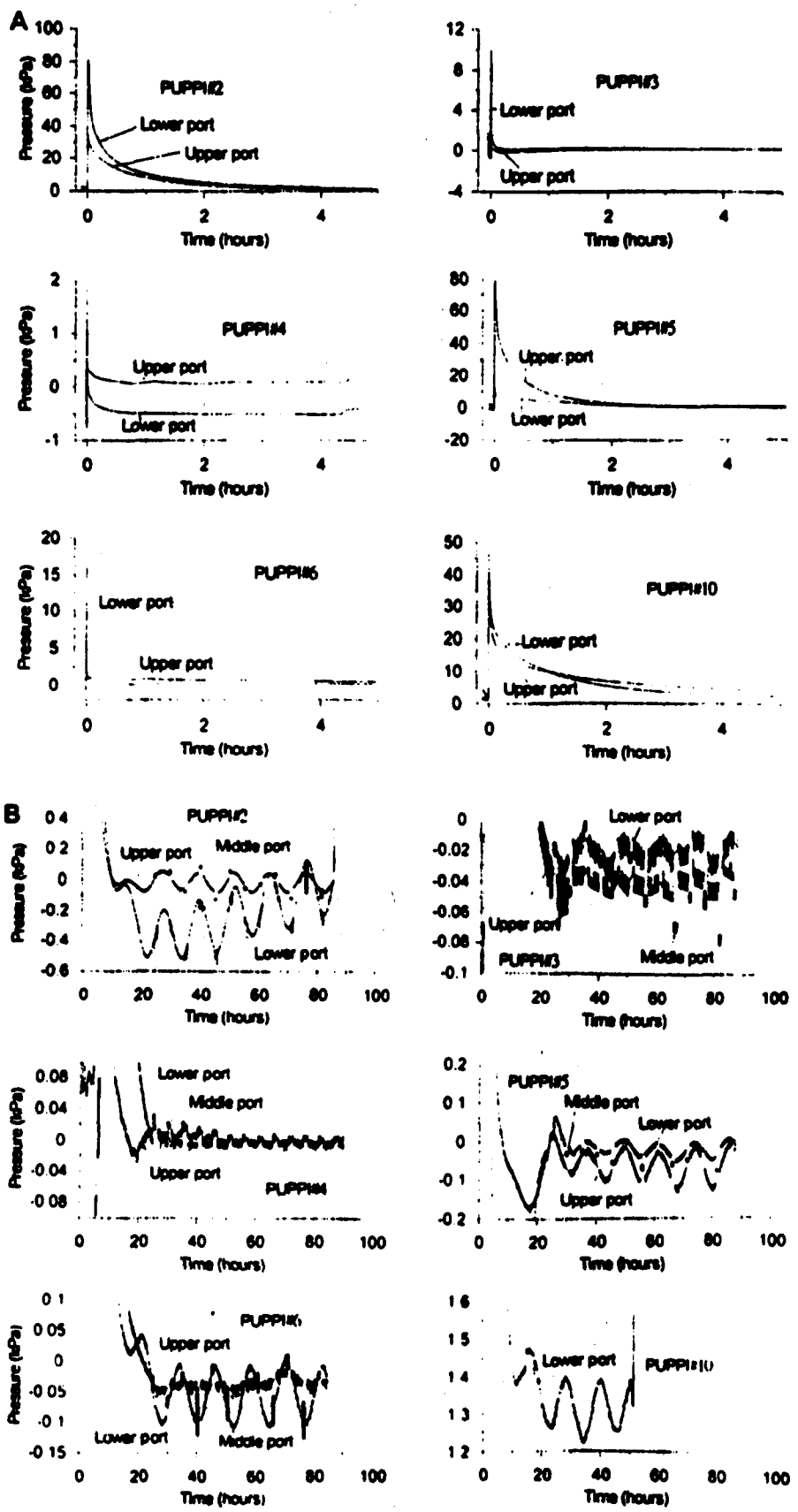


© Del documento, los autores. Digitalización realizada por ULPGC. Biblioteca Universitaria, 2009

The formula modified according to Wang and Davis (1996) is:

$$\mu_t \cong Q\frac{n\beta_f}{n\beta_f + m_v} \quad (2)$$

where $Q$ is the amplitude of the seafloor pressure variation (6.5 kPa), $n$ is the fractional porosity as determined by Roberts and Cramp (1996) (0.7) and $\beta_f$ is the compressibility of the pore fluid, seawater ($4.54 \times 10^{-10}$ Pa$^{-1}$).

Direct in situ measurements of pore pressure gradients in seafloor sediments is also one of the primary ways to detect and quantify fluid flow through the seafloor and to estimate the subseafloor pressures at greater depths. The rates of pore fluid flow are related to the pore pressure gradient through Darcy's law, i.e., the flux of pore fluid is proportional to the pore pressure gradient times the permeability. Thus the seepage velocity ($v$) of an element of water in the soil can be expressed as:

$$v = Ku_e/\mu z n \quad (3)$$

where $z$ is the depth of the port measuring the pore pressure.

The pore pressure data was also used in combination with sediment core data from Roberts and Cramp (1996) to assess the effect of nonhydrostatic pore pressures on sediment stability under cyclic loading. To this purpose we reexamined the results of Roberts and Cramp (1996) with the newly obtained pore pressure measurements. In their study, they estimate a horizontal ground acceleration expressed as a fraction of gravity, $k$, from the normalised strength parameter ($S$) and the maximum past stress ($\sigma'_{vm}$) (Lee and Edwards, 1986):

$$k = \frac{\gamma'}{\gamma}\left[A_c A_r U S\left(\frac{\sigma'_{vm}}{\sigma'_v}\right)^m - \sin\alpha\right] \quad (4)$$

where $A_c$ is a correction for anisotropic consolidation, $A_r$ is a correction for cyclic loading, $m$ is a sediment parameter typically about 0.8, $\gamma'$ is the effective sediment unit weight, $\gamma$ is the total wet sediment unit weight, $\sigma'_v$ is the overburden pressure, which in turn can be expressed as a function of depth in sediment ($\sigma'_v = \gamma' z - u_e$), and $U$ is the ratio $\sigma'_v$ to $\gamma' z$. The ratio $\sigma'_{vm}/\sigma'_v$ is also designated as the overconsolidation ratio (OCR).

## 4. Results

### 4.1. Ambient pore pressures

At the end of the recording period at all PUPPI deployments, pore pressures were close to equilibrium but still slightly descending. To avoid the influence of the high initial insertion pressures we estimated the equilibrium pressure by plotting the pressure record from 25 h after penetration until recovery vs. the reciprocal of time and extrapolating to 1/time = 0 (Fig. 4), a technique suggested by Davis et al. (1991) and Fang et al. (1993).

The ambient pore pressures estimated for the lower ports of all deployments are usually higher than those estimated for the middle and upper ports (except for PUPPI 6) (Fig. 5). The lower port of the westernmost deployment (PUPPI 10), at the edge of the Canary Debris Flow, shows the only evidences of substantial excess pore pressures that reach 1322 Pa. This suggests that excess pore pressures might have played an important role in the past in triggering the Canary Debris Flow (see further discussion).

In general all the deployments show that the ambient pore pressures within the first 4 m of the sediment column are negative (Table 2). This is always the case for ambient pore pressures in the upper and middle ports, with values ranging from 0 Pa at the lower port of deployment 2 to −72 Pa recorded at the middle port of deployment 3. The deployments do not show a single trend of pore water pressure increase or decrease that could be interpreted as a downward constant pressure gradient. In general the middle ports show more negative values (from −11 to −72 Pa) than those at the upper (from −9 to −85 Pa) and lower ports (1322 to −46 Pa). The exception is deployment number 5.

Fig. 3. Record of all PUPPI deployments where the initial high insertion pressures (A) and decay to ambient pore pressures with superimposed tidal cycles (B) can be observed.

© Del documento, los autores. Digitalización realizada por ULPGC. Biblioteca Universitaria, 2009

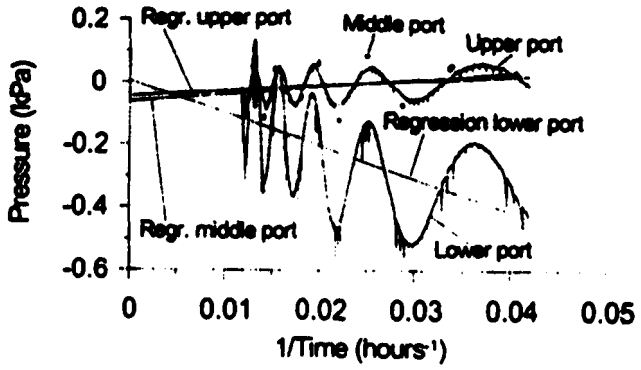


Fig. 4. Extrapolation of the last hours of the pore pressure decay vs. the reciprocal of time for PUPPI 2. At 1/time = 0 (i.e., time = ∞) the pore pressure is assumed to be the ambient or equilibrium pore pressure.

with an upper value of −85 Pa and a middle value of −64 Pa (Fig. 5). This is clearly shown by the total and between ports pressure gradients in Table 2. In most of the cases, the total pressure gradients are negative but, in contrast, the pressure gradient between the middle and lower ports is always positive.

The distribution of pore pressures can be explained by the model of Fig. 6 in which the negative pore pressures appear closer to the island of La Palma and the positive pore pressures off the island flanks. It can also be observed that the negative pore pressures display, overall, a wedge thickening towards the island of La Palma (Fig. 6).

### 4.2. Maximum insertion pressures and half decay times

The maximum insertion pressures of the sediments recorded by the probes are highly variable. This is an important point since they are directly related to the shear strength of the sediment. The maximum insertion pressures range from 81 611 Pa

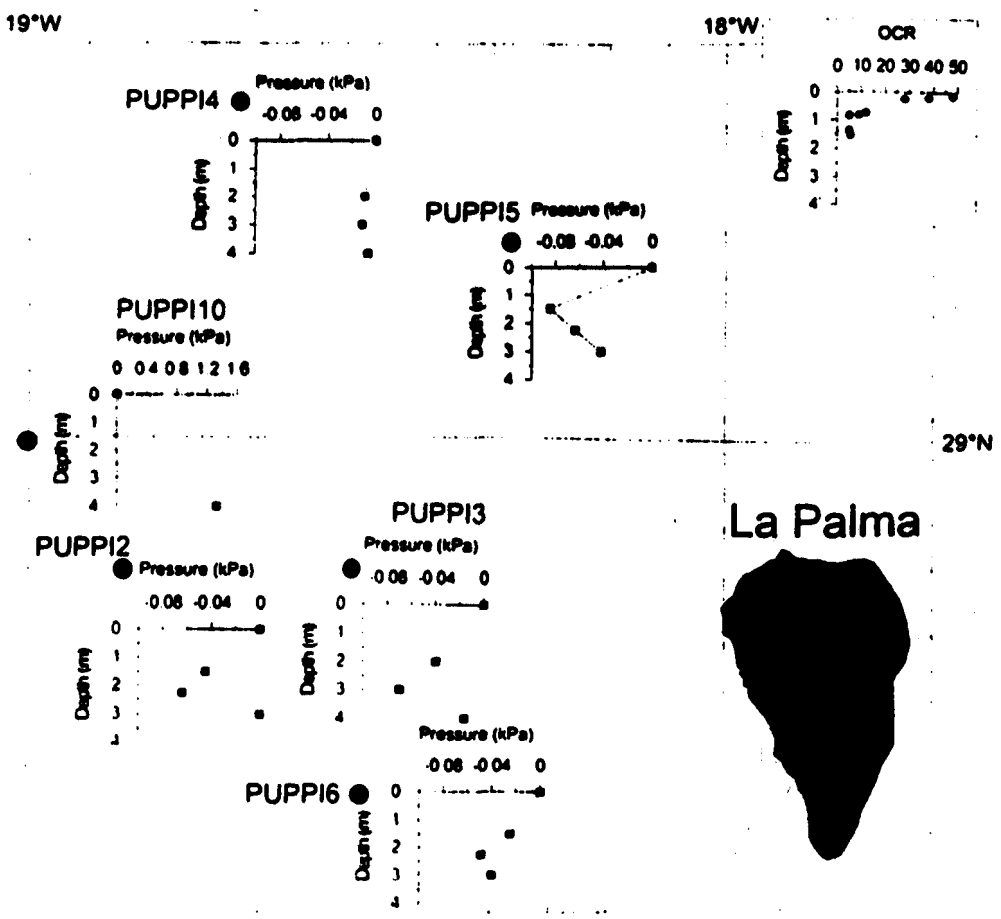


Fig. 5. Excess pore pressure (kPa) vs. depth in z-axis (meters) located geographically. PUPPI 10 is shown with a dashed line since only the record of the lower port is available. Note that the z-axis is not drawn at the same scale in all the deployments. An exponential fit plot of OCR vs. depth as depicted from the data (circles) of Roberts and Cramp (1996) is also shown on the upper right corner. This shows the maximum depth to which the equilibrium pressure estimates might be influenced by overconsolidation.

© Del documento, los autores. Digitalización realizada por ULPGC. Biblioteca Universitaria, 2009

Table 2
PUPPI-recorded data summary

| Station number | | Depth of port (m) | Equilibrium pressure (kPa) | Maximum insertion pressure (kPa) | $t_{50}$ (s) | Pressure gradient (kPa/m) | | Tidal cycle amplitude (kPa) |
|---|---|---|---|---|---|---|---|---|
| | | | | | | Total | Between ports | |
| PUPPI 2 | Upper port | 1.5 | −0.045 | 35.917 | 355.32 | −0.030 | | 0.12 |
| | Middle port | 2.25 | −0.064 | | | −0.028 | −0.025 | 0.207 |
| | Lower port | 3 | ≈0 | 81.611 | 31.32 | 0 | 0.085 | 0.32 |
| PUPPI 3 | Upper port | 2 | −0.040 | 0.463 | 101.16 | −0.020 | | 0.014 |
| | Middle port | 3 | −0.072 | | | −0.024 | −0.032 | 0.038 |
| | Lower port | 4 | −0.016 | 10.317 | 4.295 | −0.004 | 0.056 | 0.029 |
| PUPPI 4 | Upper port | 2 | −0.009 | 0.341 | 658.8 | −0.004 | | |
| | Middle port | 3 | −0.011 | | | −0.004 | 0.002 | |
| | Lower port | 4 | −0.006 | 0.447 | 18 | −0.001 | 0.005 | |
| PUPPI 5 | Upper port | 1.5 | −0.085 | 80.369 | 352.8 | 0.056 | | 0.071 |
| | Middle port | 2.25 | −0.064 | | | −0.028 | 0.028 | 0.046 |
| | Lower port | 3 | −0.042 | 23.334 | 34.92 | 0.014 | 0.029 | 0.038 |
| PUPPI 6 | Upper port | 1.5 | −0.025 | 1.053 | 17 734.68 | 0.016 | | 0.015 |
| | Middle port | 2.25 | −0.049 | | | 0.021 | −0.032 | 0.077 |
| | Lower port | 3 | 0.040 | 19.146 | 10.2 | 0.013 | 0.012 | 0.090 |
| PUPPI 10 | Upper port | 2 | | 46.703 | 175.32 | | | |
| | Lower port | 4 | 1.322 | 41.962 | 571.32 | 0.331 | | 0.152 |

recorded at the lower port of PUPPI 2 to 340 Pa recorded at the upper port of PUPPI 4. In fact, at some sites the insertion pressures were very small (Table 2)(PUPPI 3 upper port, PUPPI 4 and PUPPI 6 upper port). There are three possible reasons for this: (1) the decay rate is too great for the sampling rate (6 s); and thus the maximum insertion pressure was not recorded; (2) there was little or no penetration, or (3) the sediments have a very low shear strength.

Where low insertion pressures were recorded $t_{50}$ shows generally low values and tidal cycles have low amplitudes or are not present in the record. These two factors suggest that the sediments have high permeability (i.e., the peak insertion pressures were not recorded) and low shear strengths (see Table 3). An exception to this is PUPPI site 6 where the upper port recorded a low insertion pressure but $t_{50}$ is 17 734 s, probably anomalous due to an unsampled higher insertion pressure (note the $t_{50}$ of 10.2 s at the lower port).

### 4.3. Estimated compressibility and permeability

Compared with the core data reported by Roberts and Cramp (1996) the permeability estimates derived from the pore pressure data are generally one order of magnitude lower. Estimates of permeability from dissipation data (Eq. (1)) are highly variable and range between $2.5 \times 10^{-18}$ to $6.6 \times 10^{-16}$ m$^2$. The average estimated permeabilities from each site show a graded distribution from proximal to distal consequent with their relative location to the detrital source areas. The confined frame compressibilities (Eq. (2)) range between $6.2 \times 10^{-9}$ and $1.5 \times 10^{-7}$ Pa$^{-1}$ and, in the same manner as permeability, are about one order of magnitude less than the mean determined from core data (Roberts and Cramp, 1996). Compressibilities and, in turn, permeabilities can be underestimated since we are using the confined frame compressibility derived from the unloading/reloading curves, while in consolidation models it is generally used the compressibility derived from the virgin loading curve (Fang et al., 1993).

Table 3 shows that, at most sites, the permeability is lower for the upper port than for the lower port, while compressibility is higher at the upper port than at the lower port. This suggests that the sediments might be overconsolidated in the first two metres of the sediment column. This is in agreement with data from Roberts and Cramp (1996) that show that the

© Del documento, los autores. Digitalización realizada por ULPGC. Biblioteca Universitaria, 2009

first meter of sediment is overconsolidated (see also Fig. 5). It is known from several studies that the typical overcompaction of deep-sea sediments may be due to various causes including erosion, ageing, initial cementation, sediment reworking and bioturbation. Induced tidal pressure oscillations, which are observed in almost all deployments, is the most likely cause of sediment overcompaction.

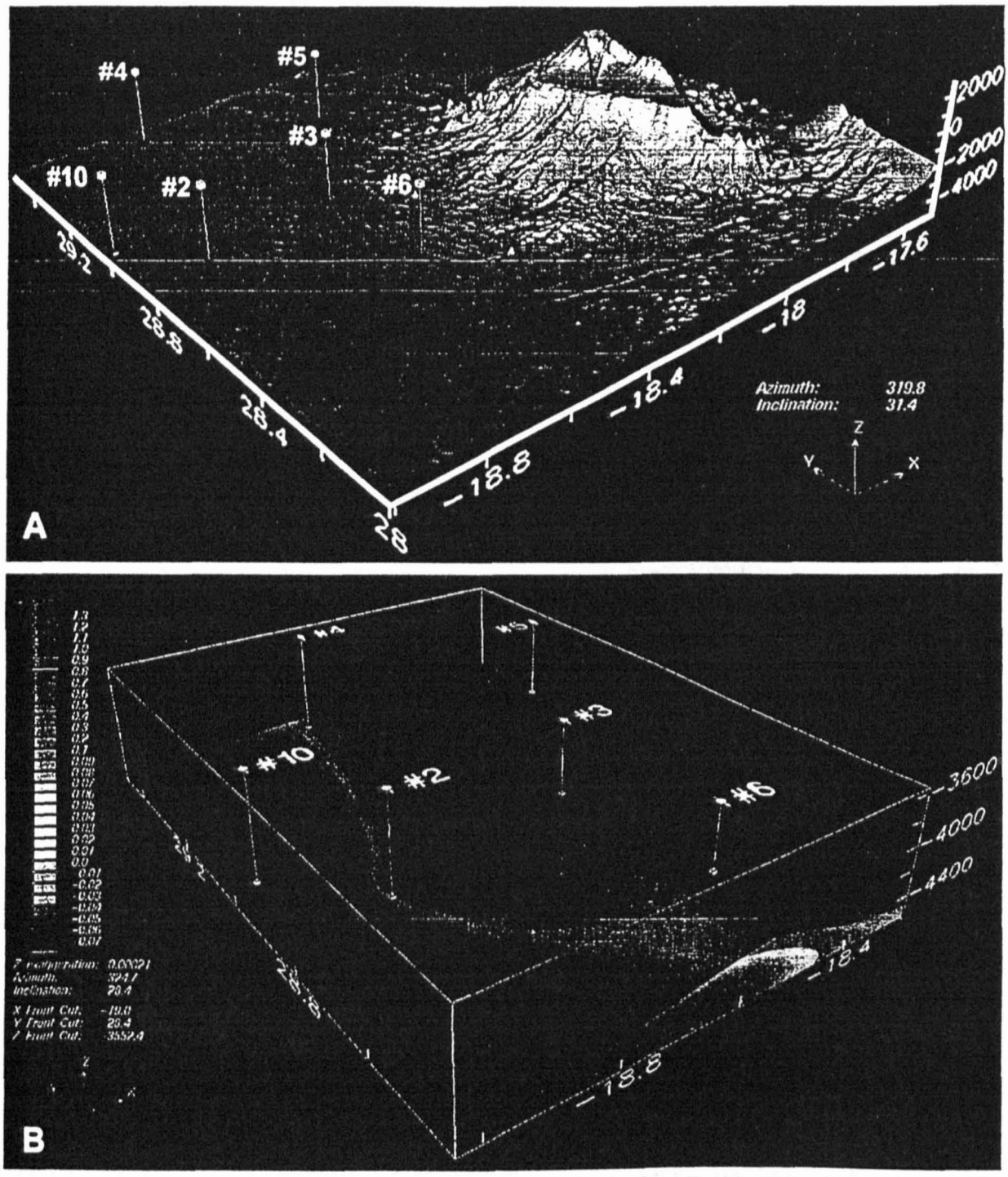


Fig. 6. Perspective view of the Island of La Palma from swath bathymetry and digitised on land contours (data from Urgeles et al., 1999) with location of the PUPPI sites (A), and 3-D model view showing the bathymetry of the area surveyed with the PUPPIs and the distribution of pore pressures within the first 5 m of sediment (B). Vertical scale is magnified 50 times and the interval with pore pressure records is magnified 20 times with respect to the topographic scale.

© Del documento, los autores. Digitalización realizada por ULPGC. Biblioteca Universitaria, 2009

Table 3
Estimated permeability, confined frame compressibility, seepage velocity and shear strength

| Station number | | Compressibility ($m_v$) × $10^{-8}$ ($Pa^{-1}$) | Permeability[a] ($K$) × $10^{-17}$ ($m^2$) | Seepage velocity[b] ($v$) (mm $yr^{-1}$) | Shear strength[c] ($S_u$) (kPa) |
|---|---|---|---|---|---|
| PUPPI 2 | Upper | 3.54 | 2.70 | −0.0221 | 13.60 |
| | Lower | 0.62 | 3.57 | 0 | 5.98 |
| PUPPI 3 | Upper | 14.95 | 66.54 | −0.3620 | 0.07 |
| | Lower | 7.20 | 1.01 | −0.0011 | 1.71 |
| PUPPI 4 | Upper | – | 2.54 | −0.0031 | 0.05 |
| | Lower | – | 5.47 | −0.0022 | 0.07 |
| PUPPI 5 | Upper | 2.92 | 4.90 | −0.0755 | 13.39 |
| | Lower | 5.49 | 17.85 | −0.0679 | 3.88 |
| PUPPI 6 | Upper | 13.95 | 0.25 | −0.0011 | 0.17 |
| | Lower | 2.29 | 39.32 | −0.1426 | 3.19 |
| PUPPI 10 | Upper | – | 1.83 | – | 7.78 |
| | Lower | 1.35 | 1.65 | 0.1487 | 6.99 |

[a]Permeabilities at sites where tidal oscillations are not observed were estimated from the mean $m_v$.
[b]Seepage velocities are calculated with respect to the total pressure gradient.
[c]Inferred from the empirical relation $S_u = u_{imax}/6$.

### 4.4. Slope stability analysis

The slope stability analysis was performed according to the method of Lee and Edwards (1986) (see Eq. (4)), that assess the stability of a slope undergoing seismic load. The values for the sediment density ($\gamma$), friction angle ($\Phi$), normalised strength parameter ($S$) and past overburden pressure ($\sigma'_{vm}$) were obtained from Roberts and Cramp (1996). Two of the selected PUPPI sites (3 and 10) correspond to core sites from Roberts and Cramp (1996) (Fig. 1), and thus, the results here presented can be directly compared to the geotechnical measurements made on these cores.

It is also to be noted that the excess pore pressures are mainly negative (Table 2 or Table 4) and, thus, this parameter will reinforce sediment stability instead of favouring failure. Only PUPPI 10, located at the edge of the Canary Debris Flow, shows positive excess pore pressures in such amount that would be able to reduce significantly (6%) the value of $k$.

We observe that the method of Lee and Edwards (1986) is also quite influenced by the overconsolidation ratio (OCR). If we assume that the values of OCR are actual and present at depth, the values of $k$ range between 0.832 and 0.2. If the overconsolidation is apparent and the sediments are normally consolidated (OCR = 1), as deduced west of La

Table 4
Reassessment of the slope stability

| Core number | Depth (m) | Pressure gradient (Pa/m) | Estimated excess pore pressure(Pa) | $\gamma_w$ ($N/m^3$) | $\gamma$ ($N/m^3$) | $\alpha$ (deg) | $S$ | Induced OCR | $k$ | $k$ if $u_e = 0$ | %[a] |
|---|---|---|---|---|---|---|---|---|---|---|---|
| CD56-24 | 0.14 | | 46.27 | | | | 0.74 | 1 | 0.187 | 0.199 | |
| | 0.83 | 330.5 | 274.31 | | 15.535 | 0.25 | 0.53 | 1 | 0.133 | 0.142 | 6.3 |
| | 1.39 | (PUPPI 10) | 459.39 | 10.253 | | | 0.57 | 1 | 0.143 | 0.153 | |
| CD56-26 | 0.23 | −20 | −4.60 | | 15.774 | 0.8 | 0.66 | 1 | 0.180 | 0.179 | −0.37 |
| | 0.85 | (PUPPI 3) | −17.00 | | | | 0.54 | 1 | 0.146 | 0.146 | |

[a]Negative percentages indicate increase in the value of $k$.

© Del documento, los autores. Digitalización realizada por ULPGC. Biblioteca Universitaria, 2009

Palma by Roberts and Cramp (1996) and other settings (Baraza et al., 1990), then the values of $k$ range between 0.187 and 0.133. The effects of excess pore pressure are much more significant when the sediments are normally consolidated inducing variations in the value of $k$ in excess of 6%.

## 5. Discussion

### 5.1. Fluid flow and seepage velocities

From our data, it is evident that the ambient pore pressures found on the sediments on the western flank of La Palma are not typically what one should expect on a passive margin (i.e., mainly excess pore pressures generated by fluid expulsion due to sediment compaction). In this setting, it would have been reasonable to expect that sediment loading by volcanic material produced by ocean island growth would contribute to enhance this effect. There is not however, a clear trend on the pore pressure profiles on Fig. 5. Although all of the measurements show negative pore pressures at all ports with the given exception of the westernmost deployment, the gradients between ports clearly show that there is not a simple constant pressure gradient with depth (Table 2). Likewise, it is known that an increase in shear stress, such as the probe penetration, may induce a dilatancy in overconsolidated clays (Imai and Xie, 1990). This is usually accompanied by the generation of transient negative pore pressures such as those of PUPPI 5 (Fig. 3B) but the length of the measurement period as well as the extrapolation to time = ∞ should neutralise this effect. In addition, the data of Roberts and Cramp (1996) indicate that overconsolidation does not extends deeper than 2 m while the lower ports recording negative pressures are 4 m below the sea floor (Fig. 5).

A possible explanation for the opposed between-ports gradient is that lateral advection occurs, taking advantage of more permeable media such as volcaniclastic turbidite sands. It is normally assumed that in deep marine conditions fluid flow would occur vertically in the lowly permeable sediment section and laterally through the highly permeable oceanic basement. Nevertheless, the turbidite layers that are interbedded with the hemipelagic sediments may act as minor inflow layers (compared to the oceanic basement).

Although flow regimes might be quite different, analogies can be found in continental sedimentary basins. In these settings, cross flow might be present that may even lead to opposite fluid flow regimes in low-permeability formations (Alexander et al., 1987). A revision of the literature where data from pore pressure probes was analysed (Hirst and Richards, 1976; Benett et al., 1982, 1996; Davis et al., 1986, 1991; Schultheiss and Noel, 1987; Langseth et al., 1992; Fang et al., 1993; Harvey et al., 1998) shows that only one or two pressure ports where used in estimating pore fluid pressures. The data from those probes will always provide a single pressure gradient trend. However, using several ports would have probably shown a more complex pattern of fluid circulation in which different permeability layers also influence the fluid circulation.

As a general rule, we observe that the fluid flow occurs downward (Table 3). The exception is PUPPI 10, which is the distalmost deployment. Conceiving the causes of such a distribution of pore pressures is not easy if thermal effects associated to the volcanic activity in the island of La Palma are not taken into account. We think that the "anomalous" results observed off La Palma could be due to the effect of a hot spot-related hydrothermal cell superimposed to the typical expulsion of fluids on a passive margin (Fig. 7). This is consequent with the data presented on the 3-D model of Fig. 6, where a wedge of negative pore pressures, indicating downward fluid flow, thickens towards La Palma. Such a hydrothermal cell would extend for about 100 km, which can be compared to those of other hot spots such as the Marquesas or the Hawaiian ones, with cells extending 150 and 25 km, respectively (Garven and McNutt, 1995). It remains unclear, however, whether the hydrothermal cell is associated with the volcanism on the La Palma edifice alone or to a broader thermal anomaly related to the hot spot. It is also important to remark that evidence of hydrothermal activity has been found offshore midplate ocean islands, where hydrothermal vents are also present (Malahoff et al., 1982; Cheminée et al., 1991). The excess pore pressures, typical of a passive margin, are then to be found away from the island flanks as shown in Fig. 7, but positive pore pressures are also

© Del documento, los autores. Digitalización realizada por ULPGC. Biblioteca Universitaria, 2009

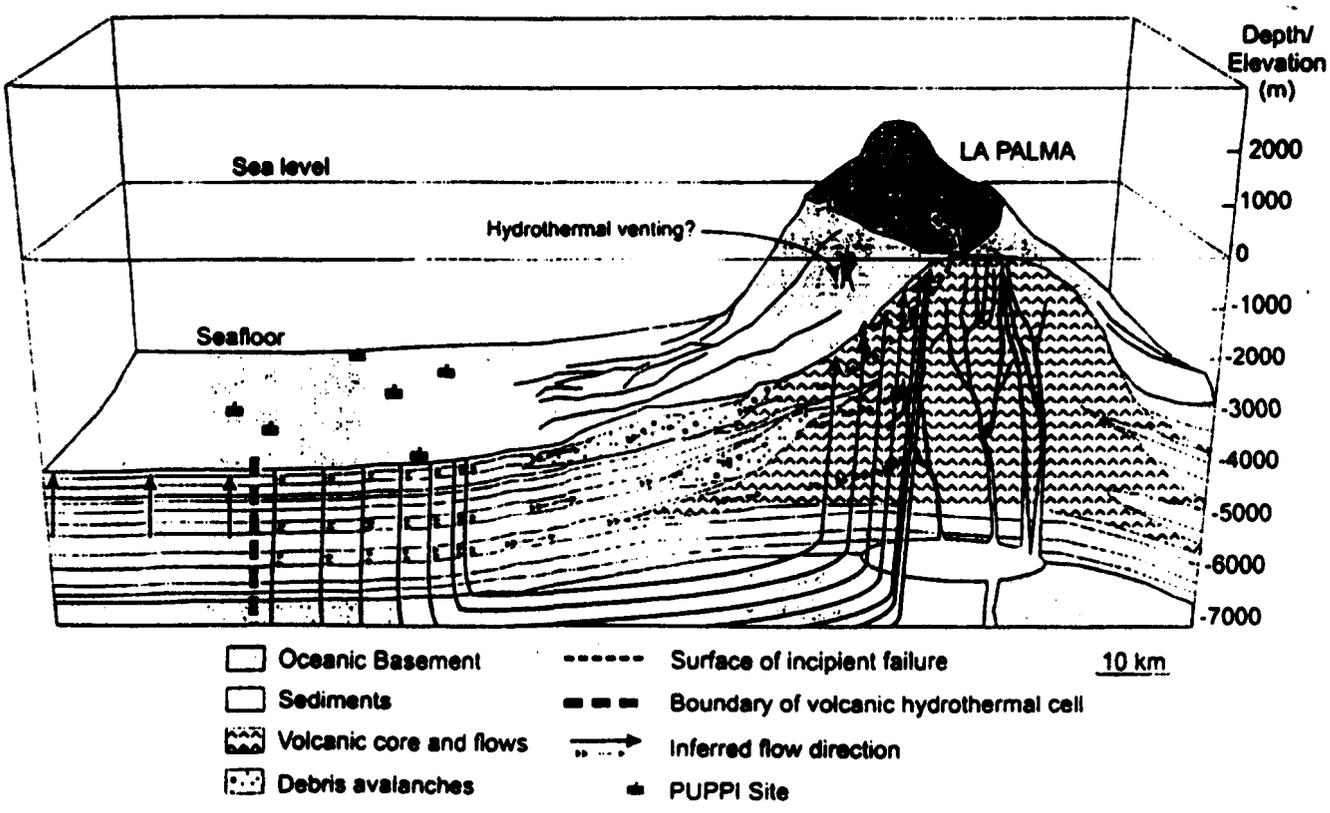


Fig. 7. Model of fluid flow path on the flanks of an oceanic island as shown by the distribution of ambient pore pressures recorded by the PUPPI apparatus. Depth of shallow magma chambers as inferred from Kluegel et al. (1997), with uplifted basement inferred from Urgeles et al. (1998).

expected in the more proximal areas driven by the thermal anomalies.

Estimates of the flow seepage velocities ($v$) were obtained following Darcy's law (Eq. (3)). Permeabilities from insertion pressure dissipation times indicate that the downward seepage velocities range between −0.001 and −0.3 mm yr$^{-1}$, respectively. These numbers would imply greater fluid flow than those found from PUPPI results in the Madeira Abyssal Plain, which shows almost no flow (Schultheiss and Noel, 1987). On the other hand, the rates of fluid flow are lower than those encountered in the sediment fields near mid-ocean ridges with downward velocities ranging between −2 and −7 mm yr$^{-1}$ (Fang et al., 1993) and upward velocities of 15 mm yr$^{-1}$ (Davis et al., 1991). Although the calculated flow velocities can be considered very low, a strong thermal anomaly must be present to induce hydrothermal circulation in sediments exceeding 1 km in thickness.

At the westernmost PUPPI 10 the measured upward fluid flow can not be maintained alone by typical sedimentation rates in the study area, currently averaging 60 m Ma$^{-1}$. However, when loading by the adjacent islands of El Hierro and La Palma is considered, then the upward fluid flow can be easily accounted for.

### 5.2. *Implications of a hot spot-related hydrothermal cell*

The intersection of a hydrothermal cell with the seafloor surface implies both a zone where fluids flow downwards and a zone, usually more concentrated (e.g., hydrothermal vents), where fluid flows upwards. Since, within the hypothetical hydrothermal cell, the data presented in this study only show evidence for downward fluid flow, we presume that upward flow should occur somewhere in the more proximal island flanks. It is known that very characteristic hydrothermal vents, in terms of compositional and thermal differences, may occur in ocean islands (Malahoff et al., 1982) but very few observations have been done in islands other than Hawaii.

© Del documento, los autores. Digitalización realizada por ULPGC. Biblioteca Universitaria, 2009

Thus, the submarine ridges around La Palma, an island where the last subaerial eruption occurred in 1971 (Carracedo, 1994), could be one of the primary targets worldwide, for searching for such hydrothermal vents.

It is also worth remarking that the upward fluid flow that might be occurring in the more proximal island flanks will reduce the shear strength of the volcanic materials and therefore could be one of the primary factors enhancing the trigger of giant volcanic landslides and debris avalanches. Again, La Palma is a good example for that, since the fissures that opened during the 1949 eruption on the southern Cumbre Nueva Ridge (Bonelli Rubio, 1950) are believed to correspond to the initial stage of one of these giant landslides (Carracedo, 1994).

### 5.3. The role of pore pressure in triggering sediment landslides

It is known that the region surveyed with the PUPPIs has undergone large sediment failures such as the Canary Debris Flow, involving volumes of up to 400 $km^3$ (Masson et al., 1992). However, from the slope stability results it is clear that the sediment wave field west of the island of La Palma is at present a stable feature. For that reason we need to invoke external factors to generate such increments of pore pressure that allow the triggering of these huge debris flows. Roberts and Cramp (1996) propose that the Canary Debris Flow could have been triggered by loading of the slope by the El Golfo Debris Avalanche, a deposit related to the lateral collapse of the northern flank of the edifice of El Hierro.

It is also important to admit that the pore pressure may not have remained constant over time. There have been important reorganisations of the volcanism within the rift system in La Palma (Carracedo et al., 1997), which might have altered hydrothermal circulation. For example, since about 7 ka, the distribution of volcanic vents in the southern rift has changed completely and activity has concentrated along the north–south rift, which has extended northwards (Carracedo et al., 1997). Such reorganisations may consequently induce radical changes of the associated hydrothermal cell ranging from a simple redistribution to the complete disappearance of the cell in periods of magmatic quiescence. For that reason, in some periods the pore pressures could have been much higher than nowadays, being more favourable to trigger landslides in the sedimentary piles adjacent to the volcanic flanks. This implies that in this area the thermal diffusivity is larger than the hydraulic diffusivity, which is plausible given the permeabilities of the sedimentary materials, the overall sediment thickness and the extent of the hydrothermal cell.

### 5.4. Further developments and studies

Along with this study we have presented a pore pressure model (Fig. 6) that fits the data observed in six probes. The model is simplistic since the data, which are costly to obtain, are scarce. Thus, the development of longer pore pressure probes, able to achieve more rapidly the dissipation of the excess pore pressures would enhance the possibility for a greater number of deployments while giving data from deeper horizons. This would also allow dissipating some doubts concerning the nature of the negative pore pressures in relation to sediment consolidation risen in this article.

Pursuing the study of fluid flow and effects of pore pressure on the stability of island flanks requires the deployment of more probes around oceanic islands. Heat flow measurements may also help us to understand fluid circulation in this context as well as the role of such process in creating excess pore pressures. Future studies should include the use of instrumented sleds and submersibles searching for hydrothermal vents, with the aim to increase understanding of the thermal and hydrologic regimes in and around hot spot-related oceanic islands.

## 6. Conclusions

The PUPPI instrument has proven to be of great value for obtaining in situ high-quality pore pressure data and permeabilities, as well as to assess fluid flow and sediment stability. The ambient pore pressures recorded off west La Palma are negative in most of the cases, generally on the order of 0 to −85 Pa. Excess pore pressures are only present in the most distal areas.

© Del documento, los autores. Digitalización realizada por ULPGC. Biblioteca Universitaria, 2009

The compressibilities estimated from the amplitude of the pore pressure variation induced by tides range between $6.2 \times 10^{-9}$ and $1.5 \times 10^{-7}$ $Pa^{-1}$. The permeabilities estimated from the dissipation data and the above compressibilities range between $2.5 \times 10^{-18}$ and $6.6 \times 10^{-16}$ $m^2$. The estimated permeabilities are usually higher for the lower port suggesting that the first 2 m of sediment might be overconsolidated.

Reassessment of the stability according to the data in Roberts and Cramp (1996) and to the PUPPI data presented in this paper shows that the sediment field on the western flank of La Palma is a stable feature. Induced accelerations on the seafloor of the range 0.187–0.133 g (if normal consolidation of the sediments is assumed) are needed to trigger new sediment landslides. The ambient pore pressures encountered in the study area have shown to favour stability and only deployment 10 shows excess pore pressures in such amount to be able to reduce the critical acceleration factor by 6%.

The data presented in this paper shows that fluid flow recorded by the PUPPIs is, in most of the cases, abnormal for a classical passive margin where we would expect an upwards flow instead of downwards. This is interpreted as the superposition to the release of pore fluids by compaction on the continental rise, of a 100-km-wide hydrothermal cell, related to the volcanic activity on the island of La Palma.

Estimates of seepage velocity range between 0 and $-0.3$ mm $yr^{-1}$ for the downward fluid flow related to the hydrothermal cell, and of 0.14 mm $yr^{-1}$ for estimates of fluid flow outside the area of thermal influence.

The occurrence of such convective cell related to the volcanic activity could generate excess pore pressures on the proximal flanks of the island that would significantly enhance the triggering of giant volcanic landslides.

## 7. Data accessibility

Pore pressure data recorded by all deployments is accessible upon request to Miquel Canals (miquel@natura.geo.ub.es).

## Acknowledgements

This work was supported by the projects MAR98-0347 (GRANDES) and AMB94-0323 (CRESCENT), funded by the Spanish National Agency for Science and Technology (CICYT), the European Union MAST-II Programme, project number MAS2-CT94-0083 (STEAM), and the "Comissionat per a Universitats i Recerca" (C.U.R.) of the "Generalitat de Catalunya", project 1997SGR-80. R. Urgeles held a fellowship of the C.U.R. We particularly thank Derek Elsworth, Kelin Wang, Marcel Hürlimann and Mark Randolph for their help while writing this manuscript. Critical reviews by D. Abbott, P. Cochonat, E.E. Davis, R.P. von Herzen and an anonymous reviewer are also acknowledged. Special thanks are given to Julio Robert, master of the *SNV Las Palmas*, whose enthusiasm and dedication allowed the campaign to take place. Thanks are also due to the master of the *RRS Discovery* and crews of the two vessels for their efficiency and cooperation.

## Appendix A. List of symbols

| | |
|---|---|
| $A_a$ | correction for anisotropic consolidation (dimensionless) |
| $A_c$ | correction for cyclic loading (dimensionless) |
| $\alpha$ | slope angle (°) |
| $\beta_f$ | compressibility of the pore fluid ($Pa^{-1}$) |
| $g$ | acceleration due to gravity ($m/s^2$) |
| $\gamma$ | total wet sediment unit weight ($\rho g$) ($N/m^3$) |
| $\gamma'$ | effective sediment unit weight ($\gamma - \gamma_w$) ($N/m^3$) |
| $\gamma_w$ | unit weight of seawater ($N/m^3$) |
| $k$ | fraction of $g$ (critical earthquake acceleration) required for sediment failure (dimensionless) |
| $K$ | permeability ($m^2$) |
| $m$ | sediment parameter typically about 0.8 (dimensionless) |
| $m_v$ | confined frame compressibility ($Pa^{-1}$) |
| $n$ | fractional porosity (dimensionless) |
| $\mu$ | viscosity of seawater (Pa s) |
| OCR | Overconsolidation ratio (dimensionless) |

© Del documento, los autores. Digitalización realizada por ULPGC. Biblioteca Universitaria, 2009

| | |
|---|---|
| $Q$ | amplitude of the seafloor pressure variation (Pa) |
| $S$ | normalised strength parameter (dimensionless) |
| $S_u$ | shear strength (Pa) |
| $\sigma_v'$ | overburden pressure (Pa) |
| $\sigma_{vm}'$ | past overburden pressure (Pa) |
| $U$ | ratio of $\sigma_v'$ to $\gamma z'$ (dimensionless) |
| $u_{max}$ | maximum insertion pressure (Pa) |
| $u_e$ | ambient equilibrium pore pressure (Pa) |
| $u_t$ | amplitude of the tidally induced pore pressure variations (Pa) |
| $t_{50}$ | half decay time (s) |
| $T_{50}$ | dimensionless time factor for pore pressure to fall to 50% of its initial value (dimensionless) |
| $v$ | seepage velocity (m/s) |
| $z$ | depth in sediment (m) |

## References


Alexander, J., Black, J.H., Brightman, M.A., 1987. The role of low-permeability rocks in regional flow. In: Goff, J.C., Williams, B.P.J. (Eds.), Fluid Flow in Sedimentary Basins and Aquifers. Geol. Soc. London, Spec. Publ. No. 34, pp. 173–183.

Ancochea, E., Hernán, F., Cendrero, A., Cantagrel, J.M., Fúster, J.M., Ibarrola, E., Coello, J., 1994. Constructive and destructive episodes in the building of a young oceanic island, La Palma, Canary Islands, and the genesis of the Caldera de Taburiente. J. Volcanol. Geotherm. Res. 60, 243–262.

Baligh, M.M., 1986. Undrained deep penetration: II. Pore pressures. Géotechnique 36, 487–501.

Baraza, J., Lee, J.I., Kayen, R.E., Hampton, M.A., 1990. Geotechnical characteristics and slope stability on the Ebro margin, western Mediterranean. Mar. Geol. 95, 379–393.

Bea, R.G., Bernard, H.A., Arnold, P., Doyle, E.H., 1975. Soil movements and forces developed by wave-induced slides in the Mississippi Delta. J. Pet. Technol. 27, 500–514.

Benett, R.H., Burns, J.T., Clarke, T.L., Faris, J.R., Forde, E.B., Richards, A.F., 1982. Piezometer probes for assessing effective stress and stability in submarine sediments. In: Saxov, S., Nieuwenhuis, J.K. (Eds.), Marine Slides and Other Mass Movements. Plenum, New York, pp. 129–161.

Benett, R.H., Hulbert, M.H., Meyer, M.M., Lavoie, D.M., Briggs, K.B., Lavoie, D.L., Baerwald, R.J., Chiou, W.A., 1996. Fundamental response of pore-water pressure to microfabric and permeability characteristics Eckernförde Bay. Geo-Mar. Lett. 16, 182–188.

Bonelli Rubio, J.M., 1950. Contribución al estudio de la erupción del Nambroque o San Juan (Isla de la Palma). Instituto Geográfico y Catastral, Madrid, Spain.

Carracedo, J.C., 1994. The Canary Islands: an example of structural control on the growth of large oceanic-islands volcanoes. J. Volcanol. Geotherm. Res. 60, 225–241.

Carracedo, J.C., Day, S.J., Guillou, H., 1997. Late (Quaternary) shield-stage volcanism in La Palma and El Hierro, Canary Islands, International Workshop on Volcanism and Volcanic Hazards in Immature Intraplate Oceanic Islands. Estación Volcanológica de Canarias, La Palma, Canary Islands, Spain, pp. 59–66.

Cheminée, J.-L., Stoffers, P., McMurtry, G., Richnow, H., Puteanus, D., Sedwick, P., 1991. Gas-rich submarine exhalations during the 1989 eruption of Macdonald Seamount. Earth Planet. Sci. Lett. 107, 318–327.

Davis, E.E., Goodfellow, W.D., Bornhold, B.D., Adshead, J., Blaise, H., Villinger, H., Le Cheminant, G.M., 1986. Massive sulfides in a sedimented rift valley, northern Juan de Fuca Ridge. Earth Planet. Sci. Lett. 82, 49–61.

Davis, E.E., Horel, G.C., MacDonald, R.D., 1991. Pore pressures and permeabilities measured in marine sediments with a tethered probe. J. Geophys. Res. 96, 5975–5984.

Elsworth, D., 1991. Dislocation analysis of penetration in saturated porous media. J. Eng. Mech. 117, 391–408.

Fang, W.W., 1995. Fluid flow in upper oceanic crust: in situ measurement and numerical modelling. PhD thesis, Columbia University, New York, USA.

Fang, W.W., Langseth, M.G., Schultheiss, P.J., 1993. Analysis and application of in situ pore pressure measurements in marine sediments. J. Geophys. Res. 98, 7921–7938.

Garven, G., McNutt, M.K., 1995. Hydrogeologic modeling of archipelagic aprons. Geol. Soc. Am. Abstr. Programs 27, 429.

Harvey, F.E., Rudolph, D.L., Frape, S.K., 1998. Measurement of hydraulic properties in deep lake sediments using a tethered pore pressure probe: applications in the Hamilton Harbour, western Lake Ontario. Water Resour. Res. 33, 1917–1928.

Hirst, T.J., Richards, A.F., 1976. Excess pore pressure in Mississipi Delta sediments: initial report. Mar. Geotechnol. 1, 337–344.

Hoernle, K.A., Schmincke, H.-U., 1993. The role of partial melting in the 15-Ma geochemical evolution of Gran Canaria: a blob model for the Canary Hot Spot. J. Petrol. 34, 594–626.

Holcomb, R.T., Searle, R.C., 1991. Large landslides from oceanic volcanoes. Mar. Geotechnol. 10, 19–32.

Imai, G., Xie, C., 1990. An endochronic constitutive law for static shear behaviour of overconsolidated clays. Soils Foundations 30, 65–75.

Kidd, R.B., Simm, R.W., Searle, R.C., 1985. Sonar acoustic facies and sediment distribution on an area of deep ocean floor. Mar. Pet. Geol. 2, 210–221.

Kluegel, A., Hansteen, T.H., Schmincke, H.-U., 1997. Rates of magma ascent and depths of magma reservoir beneath La Palma (Canary Islands) International Workshop on Volcanism and Volcanic Hazards in Immature Intraplate Oceanic Islands. Estación Volcanológica de Canarias, La Palma, Canary Islands, Spain, pp. 29–30.

Langseth, M.G., Becker, K., von Herzen, R.P., Schultheiss, P.J., 1992. Heat and fluid flux through sediment on the western flank of the Mid-Atlantic Ridge: a hydrogeological study of North Pond. Geophys. Res. Lett. 19, 517–520.


© Del documento, los autores. Digitalización realizada por ULPGC. Biblioteca Universitaria, 2009

Lee, H.J., Edwards, B.D., 1986. Regional method to assess offshore slope stability. J. Geotech. Eng. 112, 489–509.

Malahoff, A., McMurtry, G.M., Wiltshire, J.C., Yeh, H.W., 1982. Geology and chemistry of hydrothermal deposits from active submarine volcano Loihi, Hawaii. Nature 298, 234–239.

Masson, D.G., 1996. Catastrophic collapse of the volcanic island of Hierro 15 ka ago. Geology 24, 231–234.

Masson, D.G., Canals, M., Alonso, B., Urgeles, R., Huhnerbach, V., 1998. The Canary Debris Flow: source area morphology and failure mechanisms. Sedimentology 45, 411–432.

Masson, D.G., Hugget, Q.J., Weaver, P.P.E., Brunsden, D., Kidd, R.B., 1992. The Saharan and Canary debris flows offshore Northwest Africa. Landslide News 6, 9–12.

Ranero, C.R., Torne, M., Banda, E., 1995. Gravity and multichannel seismic reflection constraints on the lithospheric structure of the Canary Swell. Mar. Geophys. Res. 17, 519–534.

Roberts, J.A., Cramp, A., 1996. Sediment stability on the western flanks of the Canary Islands. Mar. Geol. 134, 13–30.

Schultheiss, P.J., 1990a. In-situ pore-pressure for a detailed geotechnical assessment of marine sediments: state of the art. In: Demars, K.R., Chaney, R.C., (Eds.), Geotechnical Engineering of Ocean Waste Disposal. ASTM STP 1087. American Society for Testing and Materials, Philadelphia, USA, pp. 190–205.

Schultheiss, P.J., 1990b. Pore pressures in marine sediments: an overview of measurement techniques and some geological and engineering applications. Mar. Geophys. Res. 12, 153–168.

Schultheiss, P.J., McPhail, S.D., 1986. Direct indication of pore water advection from pore pressure measurements in the Madeira Abyssal Plain sediments. Nature 320, 348–350.

Schultheiss, P.J., Noel, M., 1987. Evidence of pore-water advection in the Madeira Abyssal Plain from pore-pressure and temperature measurements. In: Weaver, P.P.E., Thomson, J. (Eds.), Geology and Geochemistry of Abyssal Plains. Geological Society Special Publication No. 31, London, pp. 113–129.

Simm, R.W., Weaver, P.P.E., Kidd, R.B., Jones, E.J.W., 1991. Late Quaternary mass movement on the lower continental rise and abyssal plain off Western Sahara. Sedimentology 38, 27–40.

Teide Group, 1997. Morphometric interpretation of the Northwest and south-east slopes of Tenerife, Canary Islands. J. Geophys. Res. 102, 20325–20342.

Urgeles, R., Canals, M., Baraza, J., Alonso, B., Masson, D.G., 1997. The most recent megalandslides on the Canary Islands: the "El Golfo" debris avalanche and the Canary debris flow, west Hierro Island. J. Geophys. Res. 102, 20305–20323.

Urgeles, R., Canals, M., Baraza, J., Alonso, B., 1998. Seismostratigraphy of the western flanks of Hierro and La Palma (Canary Islands): a record of the Canary Islands volcanism. Mar. Geol. 146, 225–241.

Urgeles, R., Masson, D.G., Canals, M., Watts, A.B., Le Bas, T., 1999. Recurrent giant landslides on the west flank of La Palma, Canary Islands. J. Geophys. Res. 104, 25331–25348.

Von Herzen, R.P., Cordery, M.J., Detrick, R.S., Fang, C., 1989. Heat flow and the thermal origin of hot spot swells: the Hawaiian Swell revisited. J. Geophys. Res. 94, 13783–13799.

Wang, K., Davis, E.E., 1996. Theory for the propagation of tidally induced pore pressure variations in layered subseafloor formations. J. Geophys. Res. 101, 11483–11495.

Wang, K., Davis, E.E., van der Kamp, G., 1998. Theory for the effects of free gas in subsea formations on tidal pore pressure variations and seafloor displacements. J. Geophys. Res. 103, 12339–12353.

Watts, A.B., Masson, D.G., 1995. A giant landslide on the north flank of Tenerife, Canary Islands. J. Geophys. Res. 100, 24487–24498.

Working Group 3, 1987. Fluid circulation in the crust and Global Geochemical Budget. Report of the Second Conference on Scientific Ocean Drilling (COSOD II), European Science Foundation, Strasbourg, France, pp. 67–86.

© Del documento, los autores. Digitalización realizada por ULPGC. Biblioteca Universitaria, 2009

© Del documento, los autores. Digitalización realizada por ULPGC. Biblioteca Universitaria, 2009

ELSEVIER

Aquaculture 179 (1999) 35–44

Aquaculture

# Growth, feed utilization and body lipid content of gilthead seabream (*Sparus aurata*) fed increasing lipid levels and fish meals of different quality

J.M. Vergara [a,*], G. López-Calero [b], L. Robaina [a], M.J. Caballero [b], D. Montero [a], M.S. Izquierdo [a], A. Aksnes [c]

[a] *Departamento de Biología, Universidad de Las Palmas de Gran Canaria, Campus Universitario de Tafira, 35017 Las Palmas de Gran Canaria, Canary Island, Spain*

[b] *Instituto Canario de Ciencias Marinas, Gobierno de Canarias, P.O. Box 56, 35200 Telde, Las Palmas de Gran Canaria, Canary Island, Spain*

[c] *Norwegian Herring Oil and Meal Research Institute, N-5033 Bergen, Norway*

**Abstract**

The present study shows the effects of feeding gilthead seabream, 70 to 400 g, with nine diets containing three different lipid levels (15, 22 and 28% on a dry weight basis), combined with two types of fish meal of different quality. In addition, feed processing effects (extruded vs. pelletized) were also compared for the diet containing 22% lipid. The diets prepared with the high quality fish meal promoted better growth than those prepared with the low quality one. Protein utilization was enhanced by a sparing effect of dietary lipid at 22%. This lipid level needed to be increased up to 28% with low quality meal to effectively spare dietary protein. A significant increase in fish growth with higher dietary lipid levels, in both high and low quality fish meal diets, was only related to a significant increase in total body lipid content in high quality fish meal diets, and an excess of lipid may have been the cause of hepatocyte abnormalities in fish fed the highest lipid levels. The effect of pellet processing was apparent in low quality fish meal diets, where a significantly better growth performance was obtained in fish fed the extruded diet. There were no significant differences among all treatments in feed intake, and values were similar to those suggested by commercial fish feed producers, for similar fish size and water temperatures. Values for feed conversion ratio (FCR) were lower than 1.6 for all diets. © 1999 Elsevier Science B.V. All rights reserved.

*Keywords:* Gilthead seabream; Dietary lipids; Feed quality; Growth; Body lipid

* Corresponding author. Instituto Canario de Ciencias Marinas, Gobierno de Canarias, P.O. Box 56, 35200 Telde, Las Palmas de Gran Canaria, Canary Island, Spain. Tel.: +34-928-132900; fax: +34-928-132908; E-mail: vergara@iccm.rcanaria.es

0044-8486/99/$ - see front matter © 1999 Elsevier Science B.V. All rights reserved.
PII: S0044-8486(99)00150-7

© Del documento, los autores. Digitalización realizada por ULPGC. Biblioteca Universitaria, 2009

## 1. Introduction

The current trend in fish feed production is to increase the lipid content in diets to spare proteins, to improve feed conversion and to decrease the amount of waste produced by the fish. Most of the research in this area has been done with salmonid species (Hillestad and Johnsen, 1994; Weatherup et al., 1997; Helland and Grisdale-Helland, 1998), whereas less information exists on warmwater marine species (Ballestrazzi and Lanari, 1996; Tibaldi et al., 1996; Pérez et al., 1997) and seabream in particular (Vergara et al., 1996). Optimal dietary lipid levels will also depend on the available digestible energy of the ingredients used, and in particular of fish meal being the main ingredient in carnivorous fish feeds. Different fish meal quality may affect feed intake and digestibility and consequently have an impact on growth performance and aquaculture waste (Aksnes and Mundheim, 1997). Fish meal quality may vary greatly due both to the freshness of the raw material and to the processing conditions (i.e., temperature). Protein digestibility, measured in mink has been shown to be a good indicator for differences in protein digestibility due to processing conditions (Mundheim and Opstvedt, 1989; Romero et al., 1994) and shows significantly reduced values with increased processing temperatures (Aksnes and Mundheim, 1997).

In several works, high quality fish meals were shown to improve the growth performance for various species of fish. Thus, growth and feed efficiency were affected by fish meal quality in salmon (Anderson et al., 1993), wolffish (Moksness et al., 1995) and turbot (Danielssen et al., 1989) and more recently feed efficiency was shown to be improved by fish meal quality in seabream (Aksnes et al., 1997).

The aim of the present work was to investigate the effect of varying the dietary lipid level in combination with the quality of fish meal in practical diets fed to gilthead seabream from juvenile to market size. Comparison was also made between cold pelleted and extruded diets.

## 2. Material and methods

### 2.1. Diets and experimental design

Experimental diets were prepared in order to obtain three different dietary lipid levels (15, 22 and 28% on a dry weight basis) and a fixed protein content of 48%, using a 'standard quality' fish meal or a 'low temperature (LT)' fish meal (Norse-LT 94$^{00}$) for each of the three dietary lipid levels. In addition to the six resulting diets, processed by extrusion, two more diets containing 48% protein and 22% lipid were produced with the two fish meals, but pelleted. Both fish meals were obtained from Norsildmel, Norway. The quality of the fish meals was evaluated according to chemical analyses and protein digestibility as measured by mink (Skrede, 1979) using four animals per sample. Data for fish meals are given in Table 1.

The diet compositions were based on a commercial blend. Data for ingredient composition and chemical compositions are given in Table 2. Diets 1 and 2 contained 15% lipid, Diets 3, 4, 5, and 6 contained 22% lipid and Diets 7 and 8, 28% lipid. 'Good'

© Del documento, los autores. Digitalización realizada por ULPGC. Biblioteca Universitaria, 2009

quality, Norse-LT 94 fish meal was used in Diets 1, 3, 5 and 7, and 'Standard' quality fish meal was used in Diets 2, 4, 6 and 8. Diets 1, 2, 3, 4, 7 and 8 were extruded to 2.5 mm pellets (BM 52, Wenger, USA) and dried in a heated air dryer. Diets 5 and 6 were produced by cold compression in a Simon-Heesen monoroll laboratory pellet mill. All blends were mixed to contain 11% lipid and the remaining oil was added by coating in a rotating cement mixer after pelleting.

### 2.2. *Fish and experimental conditions*

Gilthead seabream (*Sparus aurata*) of 68–73 g initial body weight were anaesthetized (chlorobutanol 200 mg $l^{-1}$), weighed and randomly stocked in 500-l fiberglass tanks in duplicate groups of 60 fish. After 2 months of feeding, fish were transferred to 1000-l tanks. All tanks were supplied with a continuous flow of natural seawater (20.7–24.4°C), which was increased from 4 to 10 l $min^{-1}$ along the experimental period. Fish were fed 'ad libitum', three times a day, 6 days a week. At the start of the experiment, 12 fish were killed by an overdose of chlorobutanol and stored at −20°C for subsequent chemical analysis. At the end of the experiment three fish per tank were sampled in the same way. At subsequent monthly intervals and at the end of the experiment, fish were individually weighed. The trial was continued for 6 months.

### 2.3. *Chemical analyses*

Dry matter and ash in feeds were determined gravimetrically after drying for 12 h at 105°C and after combustion for 12 h at 450°C, respectively. Crude protein content (N × 6.25) was determined by the Kjeldahl method (Association of Analytical Chemists, 1985) and total lipid by petroleum ether extraction (Soxhlet technique). Water soluble protein was determined as for crude protein after extraction with boiling water and filtration using black bond filter. The results are given as the percentage of total crude protein. Cadaverine and histamine were measured by HPLC according to Mietz and Karmas (1978). Dry matter and total lipid in fish were determined as described above.

Table 1
Analyses of fish meals (g $kg^{-1}$ or specified)

| Fish meal | 'Standard' | Norse-LT 94 [a] |
|---|---|---|
| Crude protein (N×6.25) | 719 | 716 |
| Lipid (Soxhlet) | 100 | 80 |
| Ash | 111 | 136 |
| Dry matter | 928 | 917 |
| Water soluble protein (percentage of total protein) | 29.9 | 25.9 |
| Cadaverine | 1.50 | 0.50 |
| Histamine | 0.24 | 0.20 |
| True protein digestibility — mink[a] (%) | 85.0 ± 1.2 | 91.6 ± 0.5 |

[a] Determined with mink as the test animal.

© Del documento, los autores. Digitalización realizada por ULPGC. Biblioteca Universitaria, 2009

### 2.4. Statistical analysis

One-way analysis of variance (ANOVA), Duncan's multiple range test and Student's test were employed to compare data (Zar, 1984).

## 3. Results

All diets were well accepted by the fish, and there were no differences among treatments in the monthly average feed intake, although there was a similar and continuous decrease for all diets as fish grew. Values ranged between 2.19 and 1.7, and they were similar to those suggested by commercial fish feed producers, for similar fish

Table 2
Ingredient and chemical composition of the experimental diets

| | Diet no. | | | | | | | | |
|---|---|---|---|---|---|---|---|---|---|
| | Extruded | | | | Pelleted | | Extruded | | |
| | 1 | 2 | 3 | 4 | 5 | 6 | 7 | 8 | commercial |
| *Ingredients (g kg$^{-1}$)* | | | | | | | | | |
| Fish meal — Norse-LT 94 | 446 | 0 | 486 | 0 | 486 | 0 | 526 | 0 | |
| Fish meal — standard | 0 | 456 | 0 | 497 | 0 | 497 | 0 | 537 | |
| Fish oil | 74 | 64 | 134 | 123 | 134 | 123 | 194 | 183 | |
| Soy lecitin[a] | 5 | 5 | 5 | 5 | 5 | 5 | 5 | 5 | |
| Bread crumbles | 220 | 220 | 170 | 170 | 170 | 170 | 120 | 120 | |
| Soybean meal | 220 | 220 | 170 | 170 | 170 | 170 | 120 | 120 | |
| Wheat grain | 20 | 20 | 20 | 20 | 20 | 20 | 20 | 20 | |
| Vitamin mix.[b] | 10 | 10 | 10 | 10 | 10 | 10 | 10 | 10 | |
| Mineral mix.[c] | 5 | 5 | 5 | 5 | 5 | 5 | 5 | 5 | |
| *Chemical composition (g kg$^{-1}$ dry matter)* | | | | | | | | | |
| Crude protein (N × 6.25) | 477 | 517 | 475 | 498 | 479 | 480 | 483 | 497 | 465 |
| Lipid | 151 | 160 | 228 | 241 | 237 | 229 | 270 | 291 | 279 |
| Ash | 90 | 74 | 85 | 113 | 90 | 80 | 92 | 77 | 85 |
| Carbohydrate[d] | 282 | 249 | 212 | 148 | 194 | 211 | 155 | 156 | 171 |
| Gross energy (MJ kg$^{-1}$)[e] | 22.1 | 22.8 | 23.9 | 23.9 | 24.1 | 24.1 | 24.8 | 25.1 | 25.0 |

[a]Soy lecitin obtained from Denota, Norway.
[b]Provides per kg feed: vitamin A, 3000 IU (Rovimix A 500P); vitamin $D_3$, 1600 IU (Rovimix D3 500); vitamin E, 160 mg (Rovimix E50 SD); thiamin, 12 mg (thiamin mononitrate); riboflavin, 24 mg (Rovimix B280 SD); pyridoxine, 12 mg (pyridoxine HCL); vitamin C, 60 mg (Rovimix Stay-C25); vitamin $B_{12}$, 0.024 mg (B12 1% FG); pantothenic acid, 48 mg (Rovimix Calpan); niacin, 120 mg (Rovimix Niacin); folic acid, 6 mg (Rovimix Folic 80 SD); biotin, 0.6 mg (Rovimix H2); menadione bisulphite, 12 mg; choline, 3.4 g. The vitamins were obtained from F. Hoffmann-La Roche, Switzerland.
[c]Provides per kg feed: $MnSO_4 \cdot H_2O$, 10 mg; $MgHPO_4 \cdot 3H_2O$, 500 mg; $FeSO_4 \cdot 2H_2O$, 50 mg; $ZnSO_4 \cdot H_2O$, 80 mg; $CuSO_4 \cdot 5H_2O$, 5 mg; $KH_2PO_4$, 400 mg; $K_2CO_3$, 400 mg; $CaCO_3$, 18.89 mg.
[d]Carbohydrate = NFE + fibre = 1000 − protein − lipid − ash.
[e]Gross energy = (23.6 MJ kg$^{-1}$ × % protein + 39.8 MJ kg$^{-1}$ × % lipid + 17.2 MJ kg$^{-1}$ × % carbohydrate)/100.

© Del documento, los autores. Digitalización realizada por ULPGC. Biblioteca Universitaria, 2009

size and water temperatures. No loss of fish occurred during the experiment, growth and feed efficiency were generally very high.

The two fish meals had different true protein digestibility as measured in mink and freshness of raw material used for the fish meal processing as evaluated by the content of cadaverine (Table 1).

Growth was comparable to that observed under normal conditions with commercial diets. When comparing extruded diets prepared with good quality meal, the final weight was significantly higher with 22% dietary lipids than with 15%. However, the increase up to 28% was not able to further promote growth. On the other hand, the comparison of extruded diets, prepared with standard quality meal, showed that 22% lipid in the diet was not enough to improve growth significantly, and only 28% dietary lipid level produced a significant increase in fish growth with respect to the other two diets (Fig. 1).

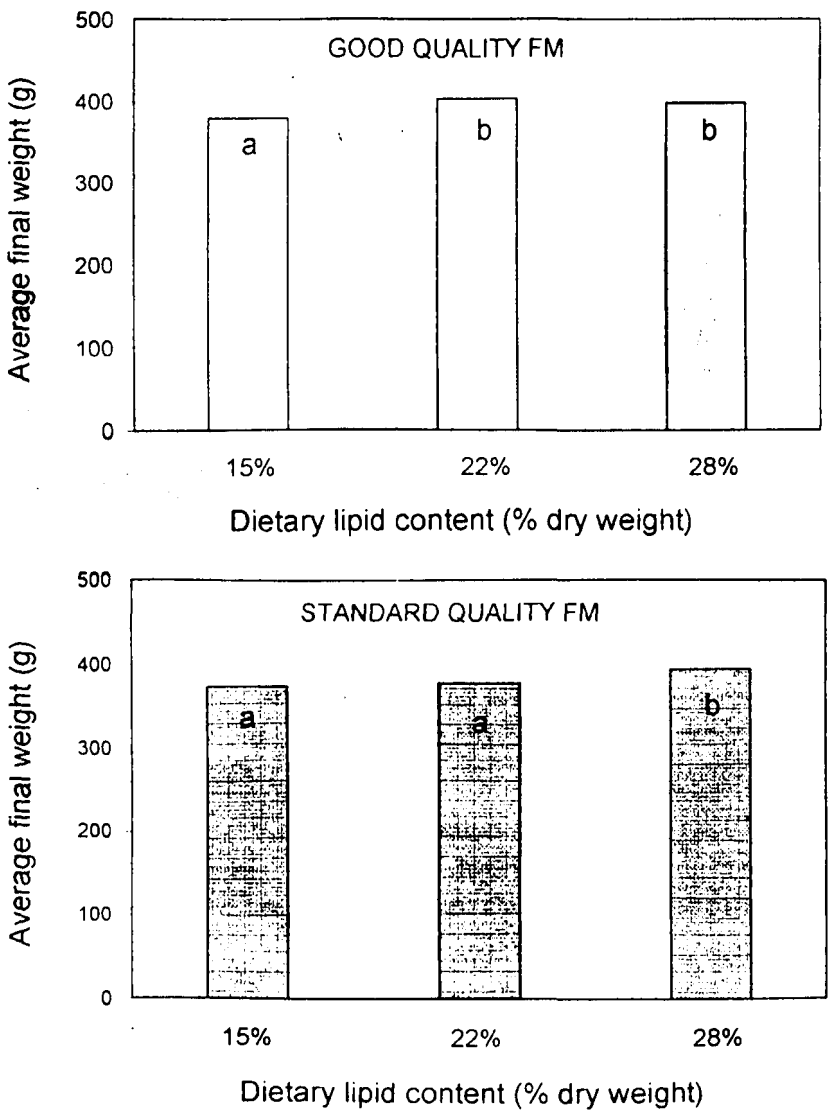


Fig. 1. Effect of extruded diets containing different lipid levels on gilthead seabream growth after 6 months of feeding. Good and standard quality fish meal (FM) diets are compared separately with one-way ANOVA and Duncan's range test. Bars with same letters are not significantly different ($P < 0.05$).

© Del documento, los autores. Digitalización realizada por ULPGC. Biblioteca Universitaria, 2009

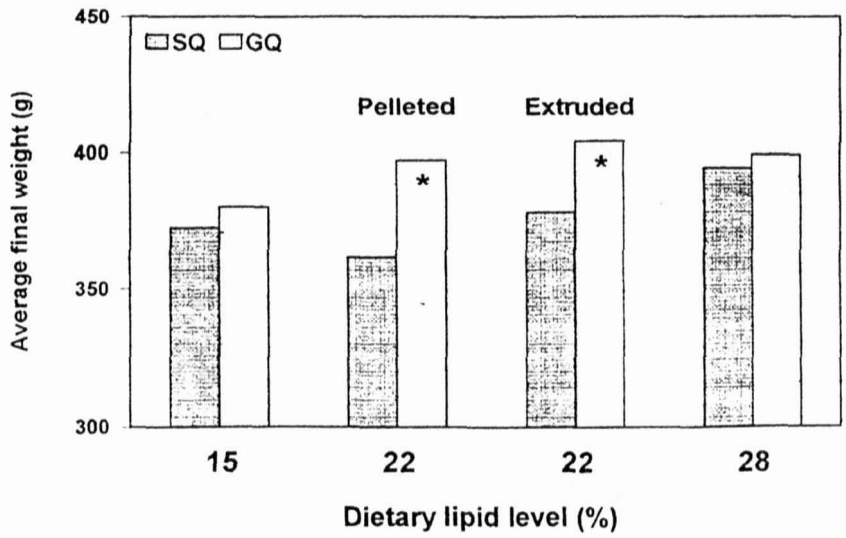


Fig. 2. Effect of fish meal quality on gilthead seabream growth after 6 months of feeding. Each dietary lipid level (15, 22 and 28%) is considered separately and fish meal quality compared using the Student's test. SQ, standard quality fish meal; GQ, good quality fish meal. Asterisks denote significant differences ($P < 0.05$).

Fish meal quality did not show any significant effect on growth for diets with 15% lipid, although there was a trend towards improvement with the better quality meal. The comparison of diets with 22% lipid level showed that good quality fish meal enhanced fish growth significantly, both in pelleted and extruded forms, while in diets with 28% lipid level, the effect of meal quality on growth was not significant (Fig. 2).

The effect of pellet type was apparent in standard quality fish meal diets, where a significantly better growth performance was obtained in fish fed the extruded diet (Fig. 3).

Values for feed conversion ratio (FCR) were statistically similar for all treatments, ranging between 1.41 and 1.54.

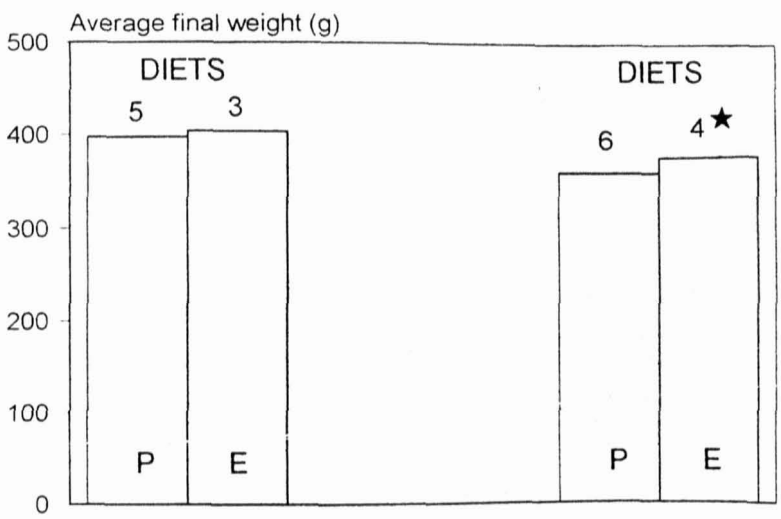


Fig. 3. Effect of pellet type on gilthead seabream growth after 6 months of feeding. Asterisks denote significant differences ($P < 0.05$). Diets 5 and 3 include good quality fish meal, and diets 6 and 4 include standard quality fish meal; P, pelleted diets; E, extruded diets.

© Del documento, los autores. Digitalización realizada por ULPGC. Biblioteca Universitaria, 2009

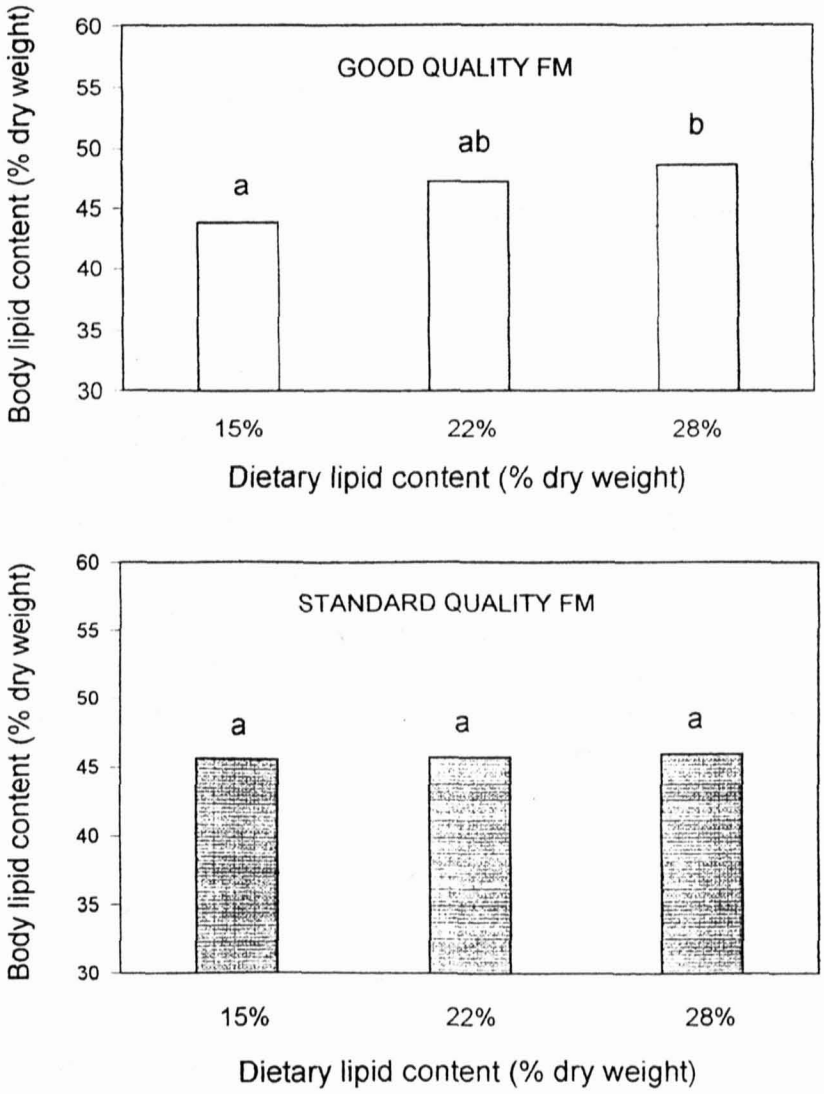


Fig. 4. Effect of extruded diets containing different lipid levels on gilthead seabream body lipid content after 6 months of feeding. Good and standard quality fish meal (FM) diets are compared separately with one-way ANOVA and Duncan's range test. Bars with same letters are not significantly different ($P < 0.05$).

Average whole body lipid content of fish after 6 months of trial showed little correlation with fish size ($r^2 = 31.78$), and values were significantly higher as dietary lipid levels increased, for good quality fish meals. On the contrary, in fish fed the standard quality fish meals, the body lipid content was similar for all dietary lipid levels (Fig. 4).

## 4. Discussion

Most commercial diets available for gilthead seabream include a the range of 17 to 28% lipid. However, most of the recent studies on the nutrition of this species report dietary lipid levels around 12% or below (Aksnes et al., 1997; Deguara, 1997; Guinea

© Del documento, los autores. Digitalización realizada por ULPGC. Biblioteca Universitaria, 2009

and Fernández, 1997), and up to 15% when studying the protein-sparing effect of dietary lipids (Vergara et al., 1996). As in other fish species (Bromley, 1980; Shimeno et al., 1980; Weatherup et al., 1997), an increase in dietary lipid levels generally results in an increased body lipid deposition (Vergara et al., 1996), an effect that is becoming also apparent in commercially produced animals. However, little research work is being done on the long-term effects of these high energy diets, thus resembling commercial situations.

Previous reports have not shown a clear effect of fish meal quality on growth of seabream (Aksnes et al., 1997; Deguara, 1997), although in halibut growth was positively correlated with the quality of fish meal used (Aksnes and Mundheim, 1997). However, fish meal of good quality supported significantly better feed efficiency in gilthead seabream when compared to a poorer quality one (Aksnes et al., 1997). On the other hand, Deguara (1997) found that extruded diets produced significantly better growth, feed and protein efficiency in this species when compared to pelleted diets.

Quality differences in commercial fish meals are usually due to differences in both protein digestibility and the freshness of the raw material used for processing (measured by the content of biogenic amines). In the present comparison, the content of cadaverine differed significantly (1.50 and 0.50 mg $kg^{-1}$ for Norse-LT 94 and 'Standard' fish meal, respectively) as did the protein digestibility as measured with mink (91.6 and 85.0% for Norse-LT 94 and 'Standard' fish meal, respectively). Protein digestibility has been reported to be increased for seabream when extruded diets were used, compared to pelleted diets (Aksnes et al., 1997; Deguara, 1997).

In the present study, the use of good quality fish meal produced an enhancement of protein utilization by a sparing effect of dietary lipids at the 22% level. This can be considered as the optimum dietary lipid level, since an excess of energy in the diets did not promote further protein sparing at 28% lipid. On the other hand, only 28% dietary lipid level increased lipid availability for sparing in standard quality fish meal diets, while 22% lipid in the diet was not enough to promote this sparing effect, due probably to insufficient protein quality and digestibility. In addition, different processing techniques may have an effect on the quality of lipid in the fish meal.

Comparison of fish meal quality at any dietary lipid level suggests that 15% was an insufficient lipid level to met the energy requirements, leading to a subsequent utilization of dietary protein for this purpose, thus with no effect on fish growth. On the other hand, a combined effect of meal quality and better lipid utilization (sparing effect) could be the cause of an enhancement of fish growth, both in pelletized and extruded forms in 22% lipid diets. In diets with 28% lipid level, only the effect of meal quality was shown, although not significant, and probably an excess in energy was not able to promote further protein sparing and significant better growth.

Similar values in the monthly average feed intake for all groups could be due to the fact that the range of gross energy content for the different diets was quite narrow (22–25 MJ $kg^{-1}$).

In this work, a higher body lipid content corresponding to increased dietary lipid levels was apparent in fish fed the good quality fish meal compared to those fed the standard quality one. However, neither muscle nor total body lipid content in this species were affected by the quality of the fish meal in previous studies (Aksnes et al.,

© Del documento, los autores. Digitalización realizada por ULPGC. Biblioteca Universitaria, 2009

1997; Deguara, 1997), when fish were assayed for shorter periods (3–4 months). On the other hand, pellet type has been reported to influence both muscle and total body lipid composition in this species, extruded diets usually leading to increased fat content (Aksnes et al., 1997; Deguara, 1997).

A significant improvement in growth performance due to the sparing effect of lipid on dietary protein has been reported for similar fish species and the gilthead seabream (Takeuchi et al., 1991; Vergara et al., 1996). The body lipid contents observed in this work (particularly for the diets with the lower dietary lipid content) are higher than those reported for this species in previous works (Vergara et al., 1996; Aksnes et al., 1997; Deguara, 1997). This difference may be due to the different duration of the experimental periods, and also to the different fish sizes.

A significant increase in fish growth with higher dietary lipid levels, in both good and standard quality fish meal diets, agrees with reported results for other fish species and gilthead seabream (Hillestad and Johnsen, 1994; Tibaldi et al., 1996; Vergara et al., 1996; Pérez et al., 1997; Weatherup et al., 1997), and this was not related to a significant increase in total body lipid contents, while such positive correlation has been observed in most of the fish species investigated to date (Shearer, 1994). Again, this difference may be due to different duration of the experimental periods and different fish sizes. In addition, the increase of dietary lipid in this work resulted in an increase in lipid in hepatocytes (Caballero, personal communication), which in the case of diets with the highest level and good quality meal produced focal swelling of hepatocytes, suggesting hepatic disturbances in the fat metabolism (fatty degeneration or steatosis) as a result of nutritional imbalance.

The present study has shown the importance of high quality fish meal in diets for gilthead seabream, suggesting an optimum dietary lipid level of 22% for diets based on such meal. The elevation of dietary lipid levels up to 28% is needed to promote best growth when standard quality fish meal is utilized. Finally, extruded diets support better growth than pelleted ones when standard quality fish meal is used, the effect of pellet type being less apparent for diets based on high quality fish meal.

## Acknowledgements

The authors wish to thank the private farm 'ADSA' (Castillo del Romeral, Gran Canaria Island) for supplying the experimental fish.

## References

Aksnes, A., Mundheim, H., 1997. The impact of raw material freshness and processing temperature for fish meal on growth, feed efficiency and chemical composition of Atlantic halibut (*Hippoglossus hippoglossus*). Aquaculture 149, 87–106.

Aksnes, A., Izquierdo, M.S., Robaina, L., Vergara, J.M., Montero, D., 1997. Influence of fish meal quality and feed pellet on growth, feed efficiency and muscle composition in gilthead seabream (*Sparus aurata*). Aquaculture 153, 251–261.

© Del documento, los autores. Digitalización realizada por ULPGC. Biblioteca Universitaria, 2009

Anderson, J.S., Lall, S.P., Anderson, D.M., McNiven, M.A., 1993. Evaluation of protein quality in fish meals by chemical and biological assays. Aquaculture 115, 305–325.

Association of Analytical Chemists, 1985. Official Methods of Analysis, 14th edn. Washington.

Ballestrazzi, R., Lanari, D., 1996. Growth, body composition and nutrient retention efficiency of growing sea bass (*Dicentrarchus labrax* L.) fed fish oil or fatty acid Ca salts. Aquaculture 139, 101–108.

Bromley, P.J., 1980. Effect of dietary protein, lipid and energy content on the growth of turbot (*Scophthalmus maximus*). Aquaculture 19, 359–369.

Danielssen, D.S., Gulbrandsen, K.E., Hjertnes, T., 1989. Fish meal quality in dry feed for turbot (*Scophthalmus maximus* L.). EAS Spec. Publ. no. 10, pp. 83–84.

Deguara, S., 1997. Evaluation of different pressed and extruded fish meal based diets on the growth of gilthead sea bream, *Sparus aurata* L. Cashier Options Méditerraneé 22, 123–139.

Guinea, J., Fernández, F., 1997. Effect of feeding frequency, feeding level and temperature on energy metabolism in *Sparus aurata*. Aquaculture 148, 125–142.

Helland, S.J., Grisdale-Helland, B., 1998. The influence of replacing fish meal in the diet with fish oil on growth, feed utilization and body composition of Atlantic salmon (*Salmo salar*) during the smoltification period. Aquaculture 162, 1–10.

Hillestad, M., Johnsen, F., 1994. High-energy/low-protein diets for Atlantic salmon: effects on growth, nutrient retention and slaughter quality. Aquaculture 124, 109–116.

Mietz, J.L., Karmas, E., 1978. Polyamine and histamine content of rockfish, salmon, lobster and shrimp as an indicator of decomposition. Journal of the Association of Official Agricultural Chemists 61, 139–145.

Moksness, E., Rosenlund, G., Lie, Ø., 1995. Effect of fish meal quality on growth of juvenile wolffish, *Anarhichas lupus*. Aquacult. Res. 26, 109–115.

Mundheim, H., Opstvedt, O., 1989. Effect of dietary level of protein and fiber on apparent protein digestibility in the rainbow trout (*Oncorhynchus mykiss*) and salmon (*Salmo salar*) and comparison of protein digestibility in mink (*Mustela vison*), rainbow trout and salmon. In: Takeda, M., Watanabe, T. (Eds.), The Current Status of Fish Nutrition in Aquaculture. Laboratory of Fish Nutrition, Tokyo, pp. 195–200.

Pérez, L., González, H., Jover, M., Fernández-Carmona, J., 1997. Growth of European sea bass fingerlings (*Dicentrarchus labrax*) fed extruded diets containing varying levels of protein, lipid and carbohydrate. Aquaculture 156, 183–193.

Romero, J.J., Castro, E., Diaz, A.M., Reveco, M., Zaldivar, J., 1994. Evaluation of methods to certify the 'premium' quality of Chilean fish meals. Aquaculture 124, 351–358.

Shearer, K.D., 1994. Factors affecting the proximate composition of cultured fishes with emphasis on salmonids. Aquaculture 119, 63–88.

Shimeno, S., Hosokawa, H., Takeda, M., Kajiyama, H., 1980. Effects of calorie to protein ratios in formulated diet on the growth, feed conversion and body composition of young yellowtail. Nippon Suisan Gakkaishi 46, 1083–1087.

Skrede, A., 1979. Utilization of fish and animal byproducts in mink nutrition: IV. Fecal excretion and digestibility of nitrogen and amino acids in mink fed cod fillet or meat- and bone-meal. Acta Agric. Scand. 29, 241–257.

Takeuchi, T., Shina, Y., Watanabe, T., 1991. Suitable protein and lipid levels in diets for fingerlings of red sea bream (*Pagrus major*). Nippon Suisan Gakkaishi 57, 293–299.

Tibaldi, E., Beraldo, P., Volpelli, L.A., Pinosa, M., 1996. Growth response of juvenile dentex (*Dentex dentex* L.) to varying protein level and protein to lipid ratio in practical diets. Aquaculture 139, 91–99.

Vergara, J.M., Robaina, L., Izquierdo, M.S., De la Higuera, M., 1996. Protein sparing effect of lipids in diets for fingerlings of gilthead seabream. Fish. Sci. 62, 624–628.

Weatherup, R.N., Mccracken, K.J., Foy, R., Rice, D., McKendry, J., Mairs, R.J., Hoey, R., 1997. The effects of dietary fat content on performance and body composition of farmed rainbow trout (*Oncorhynchus mykiss*). Aquaculture 151, 173–184.

Zar, J.H., 1984. Biostatistical Analysis, 2nd edn. Prentice-Hall, NJ.

© Del documento, los autores. Digitalización realizada por ULPGC. Biblioteca Universitaria, 2009

© Del documento, los autores. Digitalización realizada por ULPGC. Biblioteca Universitaria, 2009

© Del documento, los autores. Digitalización realizada por ULPGC. Biblioteca Universitaria, 2009

© Del documento, los autores. Digitalización realizada por ULPGC. Biblioteca Universitaria, 2009

ULPGC Biblioteca Universitaria
*622968*
BIB. 574.3 GOZ pol

© Del documento, los autores. Digitalización realizada por ULPGC. Biblioteca Universitaria, 2009